METABOLIC INTERACTIONS BETWEEN BACTERIA AND PHYTOPLANKTON

EDITED BY: Xavier Mayali, Sonya Dyhrman and Chris Francis

PUBLISHED IN: Frontiers in Microbiology and Frontiers in Marine Science

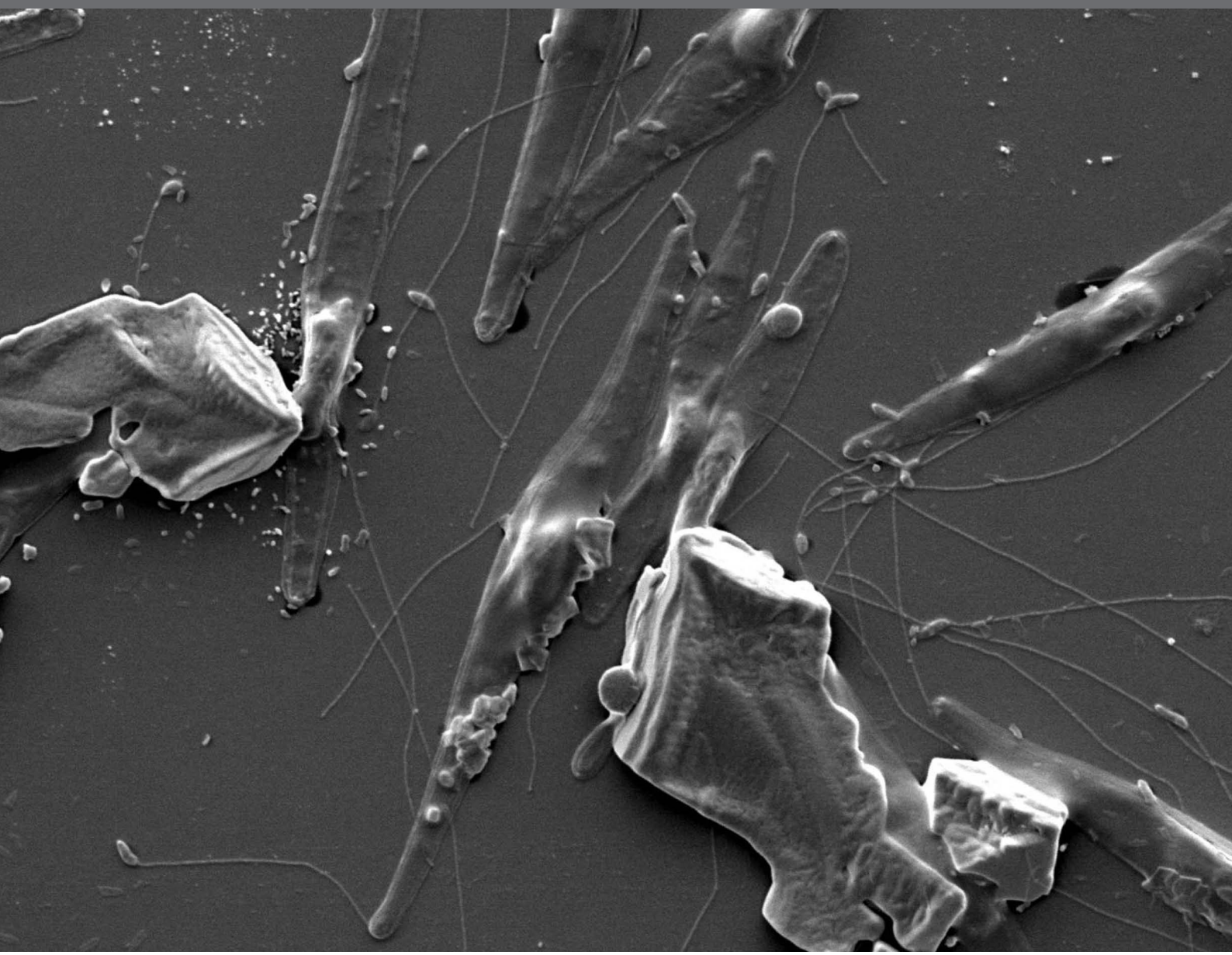

frontiers Research Topics

ISSN 1664-8714
ISBN 978-2-88945-495-2
DOI 10.3389/978-2-88945-495-2

About Frontiers

Frontiers is more than just an open-access publisher of scholarly articles: it is a pioneering approach to the world of academia, radically improving the way scholarly research is managed. The grand vision of Frontiers is a world where all people have an equal opportunity to seek, share and generate knowledge. Frontiers provides immediate and permanent online open access to all its publications, but this alone is not enough to realize our grand goals.

Frontiers Journal Series

The Frontiers Journal Series is a multi-tier and interdisciplinary set of open-access, online journals, promising a paradigm shift from the current review, selection and dissemination processes in academic publishing. All Frontiers journals are driven by researchers for researchers; therefore, they constitute a service to the scholarly community. At the same time, the Frontiers Journal Series operates on a revolutionary invention, the tiered publishing system, initially addressing specific communities of scholars, and gradually climbing up to broader public understanding, thus serving the interests of the lay society, too.

Dedication to quality

Each Frontiers article is a landmark of the highest quality, thanks to genuinely collaborative interactions between authors and review editors, who include some of the world's best academicians. Research must be certified by peers before entering a stream of knowledge that may eventually reach the public - and shape society; therefore, Frontiers only applies the most rigorous and unbiased reviews.
Frontiers revolutionizes research publishing by freely delivering the most outstanding research, evaluated with no bias from both the academic and social point of view. By applying the most advanced information technologies, Frontiers is catapulting scholarly publishing into a new generation.

What are Frontiers Research Topics?

Frontiers Research Topics are very popular trademarks of the Frontiers Journals Series: they are collections of at least ten articles, all centered on a particular subject. With their unique mix of varied contributions from Original Research to Review Articles, Frontiers Research Topics unify the most influential researchers, the latest key findings and historical advances in a hot research area! Find out more on how to host your own Frontiers Research Topic or contribute to one as an author by contacting the Frontiers Editorial Office: researchtopics@frontiersin.org

METABOLIC INTERACTIONS BETWEEN BACTERIA AND PHYTOPLANKTON

Topic Editors:
Xavier Mayali, Lawrence Livermore National Laboratory (DOE), United States
Sonya Dyhrman, Columbia University, United States
Chris Francis, Stanford University, United States

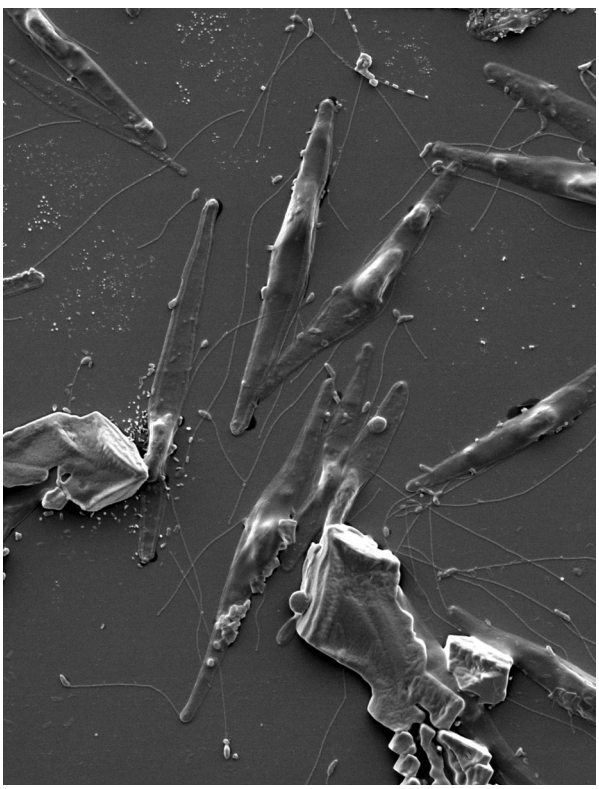

Scanning electron micrograph of laboratory cultures of the diatom Phaeodactylum tricornutum and its microbiome. Image: Ty Samo.

The cycling of energy and elements in aquatic environments is controlled by the interaction of autotrophic and heterotrophic processes. In surface waters of lakes, rivers, and oceans, photosynthetic microalgae and cyanobacteria fix carbon dioxide into organic matter that is then metabolized by heterotrophic bacteria (and perhaps archaea). Nutrients are remineralized by heterotrophic processes and subsequently

enable phototrophs to grow. The organisms that comprise these two major ecological guilds are numerous in both numbers and in their genetic diversity, leading to a vast array of physiological and chemical responses to their environment and to each other. Interactions between bacteria and phytoplankton range from obligate to facultative, as well as from mutualistic to parasitic, and can be mediated by cell-to-cell attachment or through the release of chemicals.

The contributions to this Research Topic investigate direct or indirect interactions between bacteria and phytoplankton using chemical, physiological, and/or genetic approaches. Topics include nutrient and vitamin acquisition, algal pathogenesis, microbial community structure during algal blooms or in algal aquaculture ponds, cell-cell interactions, chemical exudation, signaling molecules, and nitrogen exchange. These studies span true symbiosis where the interaction is evolutionarily derived, as well as those of indirect interactions such as bacterial incorporation of phytoplankton-produced organic matter and man-made synthetic symbiosis/synthetic mutualism.

Citation: Mayali, X., Dyhrman, S., Francis, C., eds. (2018). Metabolic Interactions Between Bacteria and Phytoplankton. Lausanne: Frontiers Media.
doi: 10.3389/978-2-88945-495-2

Table of Contents

frontiers in Microbiology

EDITORIAL
published: 10 April 2018
doi: 10.3389/fmicb.2018.00727

Editorial: Metabolic Interactions Between Bacteria and Phytoplankton

*Xavier Mayali**

Lawrence Livermore National Laboratory (DOE), Livermore, CA, United States

Keywords: microalgae, bacteria, metabolites, 16S rRNA gene, roseobacter

Editorial on the Research Topic

Metabolic Interactions Between Bacteria and Phytoplankton

INTRODUCTION

Gone are the days when bacteria (and archaea) were largely ignored by oceanographers and limnologists. The study of microbes now dominates the aquatic sciences, as microbes do in activity and sometimes biomass, in most of earth's biomes (Whitman et al., 1998). Current efforts to better understand the impact of the human microbiome on our health (Cho and Blaser, 2012) underlie the major attitude change that we have had about the impact of microbial life on the rest of the world, from either unimportant or disease-causing to instrumental in maintaining a healthy ecosystem. In sunlit aquatic ecosystems (lakes, streams, estuaries, and the surface ocean), we know that bacteria processes on average 50% of the carbon fixed by photosynthesis (Azam and Malfatti, 2007), remineralizing CO_2 and inorganic nutrients in the process. As such, the interactions between primary producing photoautotrophs (microalgae and cyanobacteria) and the secondary consuming and nutrient recycling heterotrophs (bacteria and archaea) are critical to understand ecosystem level processes, and it could be argued that these organisms should be studied together rather than in isolation.

Studies of bacterial-algal interactions, while becoming more common, have been undertaken for decades. In particular, some seminal papers paved the way for the recent papers that can utilize modern techniques to try to tackle old, still unanswered questions. For example, the term "phycosphere" was defined in 1972 (Bell and Mitchell, 1972) as the zone surrounding an algal cell analogous to the plant root rhizosphere, where the concentration of algal-derived molecules is thought to be higher than the bulk water. Due to methodological limitations, the phycosphere still has not been directly measured or quantified, though it has been modeled (Seymour et al., 2017), and this area is still ripe for study. Another seminal paper (Pomeroy, 1974) first suggested that bacteria were responsible for processing the majority of phytoplankton-fixed C in the ocean; this was later termed the microbial loop (Azam et al., 1983). Now decades later, bacteria are still not included in most biogeochemical models (Evans and Fasham, 2013), and in the rare case that they are, they are lumped into one black box, even if we know that not all bacteria are created equal. Clearly, more research on interactions between these two major guilds of organisms is needed.

This research topic presents 15 articles related to interactions between phytoplankton and bacteria, grouped into the following categories: (i) growth impact of bacteria on dinoflagellates, (ii) algicidal bacteria, (iii) algal-bacterial associations inferred from environmental surveys, (iv) chemical signaling, (v) competition for nitrogen and (vi) mesocosm manipulations. In addition, one final article reviews a type of metabolic modeling approach that may be useful to predict the impact of algal-bacterial interaction on ecosystem processes.

OPEN ACCESS

Edited by:
Alison Buchan,
University of Tennessee, Knoxville, United States

Reviewed by:
Assaf Vardi,
Weizmann Institute of Science, Israel
Shady A. Amin,
New York University Abu Dhabi, United Arab Emirates

***Correspondence:**
Xavier Mayali
mayali1@llnl.gov

Specialty section:
This article was submitted to Aquatic Microbiology, a section of the journal Frontiers in Microbiology

Received: *18 December 2017*
Accepted: *28 March 2018*
Published: *10 April 2018*

Citation:
Mayali X (2018) Editorial: Metabolic Interactions Between Bacteria and Phytoplankton. Front. Microbiol. 9:727. doi: 10.3389/fmicb.2018.00727

GROWTH IMPACT OF BACTERIA ON DINOFLAGELLATES

Phycologists long ago realized that removing bacteria from dinoflagellate laboratory cultures was difficult (Guillard and Keller, 1984) and many dinoflagellate species in fact cannot grow without bacteria. Such is the case with *Gymnodinium catenatum*, a harmful algal bloom causing species. Bolch et al. established laboratory batch co-cultures of this dinoflagellate with combinations of 1, 2, or 3 bacterial species and compared their growth, finding that bacteria can exert growth effects as strong as those of light and temperature. The 3 different bacterial strains, either alone or in the presence of others, exerted different growth effects on *G. catenatum*; in particular, a *Roseobacter* strain inhibited growth rate, led to lower maximum algal cell yield, and increased algal death rate. This effect was decreased but not completely eliminated by the presence of other bacteria, showing that bacterial competition can impact the interactions between algae and bacteria, as shown previously (Mayali and Doucette, 2002). In another study in this special topic, Cruz-Lopez examined the ability of bacteria to provide vitamins to the dinoflagellate *Lingulodinium polyedrum*. The authors first were able to render their algal culture axenic, then established bacterial enrichment cultures by adding 0.8 micron seawater filtrates. These cultures were maintained with or without additions of vitamins B_1, B_7, and B_{12}. The authors showed that *L. polyedrum* is auxotrophic for B_1 and B_{12}, and that seawater bacteria can provide enough of those vitamins for long term culture growth. Interestingly, bacterial community taxonomy was not significantly different between cultures grown with and without added vitamins, suggesting that vitamin exchange is not a major factor in controlling which bacteria grow in the presence of the dinoflagellate.

ALGICIDAL BACTERIA

The effect of bacteria that kill algae (so-called algicidal bacteria) has been studied for decades (reviewed by Mayali and Azam, 2004). The large number of such studies is likely explained by, on the one hand, the need to mitigate harmful algal blooms (HABs) and understand the natural demise of these events in coastal zones, and on the other, by preventing algal pond crashes when algae are grown for aquaculture or other valuable products. Related to the latter, Ganuza et al. investigated the possibility of water treatment, through decreased *pH* for 15 min in the presence of acetate, to alleviate bacterial infection of the green alga *Chlorella* by the parasitic bacteria *Vampirovibrio*. The treatment was successful in prolonging algal cultivation, and the algicidal bacterium appears to be unable to build up immunity to this treatment (the impact on other bacteria was not characterized). Bagwell et al. also investigated the possibility of preventing *Vampirovibrio* infection of *Chlorella* cultures, in their case by inducing the production of bioactive small peptides and glycosides by *Chlorella* under iron limitation, which prevented *Vampirovibrio* infection. In another algal system, Mayers et al. investigated the interactions between the coccolithophore *Emiliania huxleyii* and a bacterial strain from the *Ruegeria* genus (Rhodobacteriaceae), finding that the bacterium is an opportunistic pathogen that kills certain *E. huxleyii* cell types only at higher temperatures.

ASSOCIATIONS INFERRED FROM ENVIRONMENTAL SURVEYS

Moving from the laboratory to natural samples, three articles aim to link specific bacterial taxa with specific algal species. Sison-Mangus et al. examined the bacterial community structure at a coastal site over time through a number of blooms of the diatom genus *Pseudo-nitzschia*. They found that total bacterial diversity was lower when the bloom was dominated by *P. australis* that produce high amounts of the algal toxin domoic acid, and the communities were dominated by *Firmicutes* bacteria. Bloom samples from low toxin producing *P. fraudulenta* had higher diversity and were dominated by *Vibrio* bacteria. These results suggest that algal toxins potentially play a role in regulating bacterial community structure, although effects other than toxin production are also likely to be involved. At the same location, Farnelid et al. used flow cytometric cell sorting of photosynthetic picoeukaryotes followed by 16S rRNA sequencing to examine the bacterial communities physically-associated with these cells. These communities included both commonly-found free-living taxa, suggesting the eukaryotes potentially ingested these bacteria, as well as taxa not found free-living, suggesting symbiosis with specialized taxa (either intra or extracellular). Bunse et al. also aimed to correlate specific bacterial taxa with particular phytoplankton by sampling across the spring diatom bloom in the Baltic Sea. They found that numerically dominant bacterial taxa did not correlate well with algal bloom-related variables. On the other hand, several less-abundant bacterial taxa showed strong associations with algal bloom dynamics, including different *Bacteroidetes* taxa being associated with genetic subgroups of the dominant diatom.

CHEMICAL SIGNALING

Indole 3 acetic acid (IAA) production from tryptophan has been previously identified as a metabolite involved in algal growth enhancement by bacteria (De-Bashan et al., 2008), and detected in the ocean (Amin et al., 2015; Segev et al., 2016). Labeeuw et al. investigated a different potential role of IAA as a signaling molecule among algal cells. They found that one type of axenic *E. huxleyi* cells produced IAA after tryptophan addition. *E. huxleyi* cultures co-incubated with a *Ruegeria* strain previously found to produce IAA from tryptophan were found to produce less IAA than the axenic cultures, which suggested to the authors that IAA is potentially not involved in bacterial-algal interactions between these organisms. This remains a controversial topic, as another possibility is that the IAA in the co-culture was incorporated more than in the algal monoculture. Regarding signaling molecules that inhibit growth, Harvey et al. identified the quorum sensing molecule 2-heptyl-4-quinolone (HHQ) as

the compound responsible for growth inhibition of *E. huxleyi* when grown with the bacterium *Pseudoalteromonas piscicida*. This compound may be specific to *E. huxleyi* as it did not have any growth-inhibiting effects on two other algal strains, but the latter were not axenic cultures, suggesting bacteria-bacteria interactions may also play a role in this interaction.

COMPETITION FOR NITROGEN

Two submissions to the research topic involved the examination of nitrogen cycling between microalgae and bacteria. First, Le Chevanton et al. used ammonium-limited chemostats to examine the impact of a strain of *Alteromonas* previously shown to increase the growth of *Dunaliella* in non-limiting batch cultures. Surprisingly, the presence of the bacterium led to a decrease in algal growth under these limiting conditions, and the bacterium did not remineralize organic nitrogen for algal uptake. This study demonstrates another example of an interaction between algae and bacteria that can change depending on the environment, going from mutualistic under ammonium replete to competitive under ammonium deplete conditions. In the same realm, Diner et al. examined competition for nitrate between another *Alteromonas* strain and the diatom *Phaeodactylum tricornutum*. They showed that under conditions without external inputs of organic carbon, the bacterium did not compete for nitrate and exhibited mutualistic effects, but with extra carbon in the form of pyruvate, it led to algal growth inhibition. Taking it one step further with genetic tests with mutants of both algae and bacteria, they showed that nitrate reductase-deficient bacteria did not inhibit algal growth in the presence of pyruvate and that wild-type bacteria could rescue growth of *P. tricornutum* nitrate reductase-deficient with nitrate as the sole N source, demonstrating direct mutualism: the algae provide organic C to the bacterium and the bacterium provides N back to the algae, in a form other than nitrate.

MESOCOSM MANIPULATIONS

A type of study that is intermediate between laboratory and field involves bringing nature into the lab (or bringing the lab into nature) through the use of micro- or mesocosms. Russo et al. used a metaproteomic analysis to examine the succession of autotrophs (microalgae and cyanobacteria) and heterotrophic bacteria in freshwater mesocosms incubated under oligotrophic and eutrophic conditions. They found that *Bacteroidetes* expressed extracellular hydrolases and Ton-B dependent receptors to degrade and transport high molecular weight compounds in oligotrophic conditions, and that *Alpha-* and *Beta-proteobacteria* captured different substrates from algal exudate (carbohydrates and amino acids, respectively). They also found strong evidence of bacterial mixotrophy (either chemoautotrophy or photoheterotrophy), suggesting the division of algae and bacteria into autotrophs and heterotrophs may be outdated. Geng et al. followed the bacterial community structure of indoor microcosms associated with the saltwater microalga *Nannochloropsis salina* in the presence of antibiotics and signaling compounds. Using a network analysis of correlations, they found that a few bacterial taxa from the *Alteromonadaceae* and *Rhodobacteriaceae* were driving the community dynamics by being strongly associated with community "modules" that changed drastically across treatments. Further, they showed that tropodithietic acid, an antibiotic produced by members of the *Rhodobacteriaceae* (Wang et al., 2016), drastically changes bacterial community structure within a short timeframe, leading to the hypothesis that this and other compounds may be responsible for community structure dynamics.

CONCLUSIONS

In order to better understand the impact of algal-bacterial interactions on processes of interest such as biogeochemical cycling, production of valuable or noxious compounds, and ecosystem impacts, it is becoming clear that experimental data must be used to better inform models that eventually hope to be predictive. One modeling approach discussed by Perez-Garcia et al., Stoichiometric Metabolic Network (SMN), can incorporate a variety of experimental data such as community structure, functional gene information (i.e., "omics data") to mathematically represent cell biogeochemistry to quantify metabolic rates. Metabolic modeling of this type (e.g., Flux Balance Analysis, and similar) have been applied mostly to single species or very simple communities, but efforts will continue to investigate microbial interactions in more complex ecosystems, which may necessitate new modeling approaches.

In combination with new modeling approaches, experimental data, such as those published under this special topic, will need to continue to be collected if we are to take significant steps forward in our understanding of algal-bacterial interactions. The post-genomic era now enables cheap and fast generation of DNA, RNA, protein, and metabolite data, and new imaging methods are being developed to probe cell-cell interactions. I would argue that it is imperative to utilize these great tools in combination with well-designed experiments with environmentally-appropriate model systems or manipulations of natural samples incubated under relevant conditions, when specific effects can be directly tested. One challenge in this endeavor is that algal-bacterial interactions exist at the single cell scale, and an algal-dominated ecosystem is comprised of billions of single algal cells interacting with hundreds of different bacterial species. How can we determine which microscale algal-bacterial interactions have ecosystem-level consequences? What approaches can we take to apply what we learn from laboratory co-culture experiments to understand what occurs in the more complex natural environment? These are questions that future studies on algal-bacterial interactions should aim to address.

AUTHOR CONTRIBUTIONS

The author confirms being the sole contributor of this work and approved it for publication.

ACKNOWLEDGMENTS

Funding was provided by the DOE-OBER-funded Biofuels Science Focus Area Grant SCW1039. Work was performed under the auspices of the US Department of Energy at the Lawrence Livermore National Laboratory under Contract DE-AC52-07NA27344.

REFERENCES

Amin, S. A., Hmelo, L. R., Van Tol, H. M., Durham, B. P., Carlson, L. T., Heal, K. R., et al. (2015). Interaction and signalling between a cosmopolitan phytoplankton and associated bacteria. *Nature* 522, 98–101. doi: 10.1038/nature14488

Azam, F., Fenchel, T., Field, J. G., Gray, J. S., Meyer Reil, L.A., and Thingstad, F. (1983). The ecological role of water-column microbes in the sea. *Mar. Ecol. Prog. Ser.* 10, 257–263. doi: 10.3354/meps010257

Azam, F., and Malfatti, F. (2007). Microbial structuring of marine ecosystems. *Nat. Rev. Microbiol.* 5, 782–791. doi: 10.1038/nrmicro1747

Bell, W., and Mitchell, R. (1972). Chemotactic and growth responses of marine bacteria to algal extracellular products. *Biol. Bull.* 143, 265–277. doi: 10.2307/1540052

Cho, I., and Blaser, M. J. (2012). The Human Microbiome: at the interface of health and disease. *Nat. Rev. Genet.* 13, 260–270. doi: 10.1038/nrg3182

De-Bashan, L.E., Antoun, H., and Bashan, Y. (2008). Involvement of indole-3-acetic acid produced by the growth-promoting bacterium azospirillum spp. In promoting growth of *Chlorella vulgaris*. *J. Phycol.* 44, 938–947. doi: 10.1111/j.1529-8817.2008.00533.x

Evans, G. T., and Fasham, M. J. R. (2013). *Towards a Model of Ocean Biogeochemical Processes.* Berlin: Springer Science & Business Media.

Guillard, R. R. L., and Keller, M. D. (1984). Culturing dinoflagellates. *Dinoflagellates* 1, 391–442. doi: 10.1016/B978-0-12-656520-1.50016-X

Mayali, X., and Azam, F. (2004). Algicidal bacteria in the sea and their impact on algal blooms. *J. Eukaryot. Microbiol.* 51, 139–144. doi: 10.1111/j.1550-7408.2004.tb00538.x

Mayali, X., and Doucette, G.J. (2002). Microbial community interactions and population dynamics of an algicidal bacterium active against *Karenia brevis* (Dinophyceae). *Harmful Algae* 1, 277–293. doi: 10.1016/S1568-9883(02)00032-X

Pomeroy, L.R. (1974). The ocean's food web, a changing paradigm. *Bioscience* 24, 499–504. doi: 10.2307/1296885

Segev, E., Wyche, T. P., Kim, K. H., Petersen, J., Ellebrandt, C., Vlamakis, H., et al. (2016). Dynamic metabolic exchange governs a marine algal-bacterial interaction. *eLife* 5:e17473. doi: 10.7554/eLife.17473

Seymour, J. R., Amin, S. A., Raina, J.-B., and Stocker, R. (2017). Zooming in on the phycosphere: the ecological interface for phytoplankton–bacteria relationships. *Nat. Microbiol.* 2:17065. doi: 10.1038/nmicrobiol.2017.65

Wang, R, Gallant, É., and Seyedsayamdost, M. R. (2016). Investigation of the genetics and biochemistry of roseobacticide production in the roseobacter clade bacterium Phaeobacter inhibens. *Bio* 016:e02118-5. doi: 10.1128/mBio.02118-15

Whitman, W. B., Coleman, D. C., and Wiebe, W. J. (1998). Prokaryotes: the unseen majority. *Proc. Natl. Acad. Sci. U.S.A.* 95, 6578–6583. doi: 10.1073/pnas.95.12.6578

Conflict of Interest Statement: The author declares that the research was conducted in the absence of any commercial or financial relationships that could be construed as a potential conflict of interest.

frontiers in Microbiology

ORIGINAL RESEARCH
published: 19 April 2017
doi: 10.3389/fmicb.2017.00670

Bacterial Associates Modify Growth Dynamics of the Dinoflagellate *Gymnodinium catenatum*

Christopher J. S. Bolch[1], Thaila A. Bejoy[1†] and David H. Green[2]*

[1] Institute for Marine and Antarctic Studies, University of Tasmania, Launceston, TAS, Australia, [2] Scottish Association for Marine Science, Scottish Marine Institute, Oban, UK

Marine phytoplankton cells grow in close association with a complex microbial associate community known to affect the growth, behavior, and physiology of the algal host. The relative scale and importance these effects compared to other major factors governing algal cell growth remain unclear. Using algal-bacteria co-culture models based on the toxic dinoflagellate *Gymnodinium catenatum*, we tested the hypothesis that associate bacteria exert an independent effect on host algal cell growth. Batch co-cultures of *G. catenatum* were grown under identical environmental conditions with simplified bacterial communities composed of one-, two-, or three-bacterial associates. Modification of the associate community membership and complexity induced up to four-fold changes in dinoflagellate growth rate, equivalent to the effect of a 5°C change in temperature or an almost six-fold change in light intensity (20–115 moles photons PAR m^{-2} s^{-1}). Almost three-fold changes in both stationary phase cell concentration and death rate were also observed. Co-culture with *Roseobacter* sp. DG874 reduced dinoflagellate exponential growth rate and led to a more rapid death rate compared with mixed associate community controls or co-culture with either *Marinobacter* sp. DG879, *Alcanivorax* sp. DG881. In contrast, associate bacteria concentration was positively correlated with dinoflagellate cell concentration during the exponential growth phase, indicating growth was limited by supply of dinoflagellate-derived carbon. Bacterial growth increased rapidly at the onset of declining and stationary phases due to either increasing availability of algal-derived carbon induced by nutrient stress and autolysis, or at mid-log phase in *Roseobacter* co-cultures potentially due to the onset of bacterial-mediated cell lysis. Co-cultures with the three bacterial associates resulted in dinoflagellate and bacterial growth dynamics very similar to more complex mixed bacterial community controls, suggesting that three-way co-cultures are sufficient to model interaction and growth dynamics of more complex communities. This study demonstrates that algal associate bacteria independently modify the growth of the host cell under non-limiting growth conditions and supports the concept that algal–bacterial interactions are an important structuring mechanism in phytoplankton communities.

Keywords: dinoflagellate, bacteria, interaction, model, *Gymnodinium catenatum*, growth

OPEN ACCESS

Edited by:
Xavier Mayali, Lawrence Livermore National Laboratory (DOE), USA

Reviewed by:
Tatiana A. Rynearson, University of Rhode Island, USA
Hongbin Liu, Hong Kong University of Science and Technology, Hong Kong

****Correspondence:***
Christopher J. S. Bolch
chris.bolch@utas.edu.au

†Present address:
Thaila A. Bejoy, School of Public Health, Curtin University, Bentley, WA, Australia

Specialty section:
This article was submitted to Aquatic Microbiology, a section of the journal Frontiers in Microbiology

Received: *16 February 2016*
Accepted: *31 March 2017*
Published: *19 April 2017*

Citation:
Bolch CJS, Bejoy TA and Green DH (2017) Bacterial Associates Modify Growth Dynamics of the Dinoflagellate Gymnodinium catenatum. Front. Microbiol. 8:670. doi: 10.3389/fmicb.2017.00670

INTRODUCTION

In natural aquatic systems marine microalgae grow in close association with a complex microbial community (associates) that form an intrinsic component of phytoplankton physiology and ecology (Cole, 1982). Considerable research from a diversity of species indicate that interactions between the associate community and phytoplankton (host) cells are ubiquitous in marine and freshwater systems (Doucette et al., 1998; Amin et al., 2012; Ramanan et al., 2015), play important roles in algal bloom initiation, growth and termination (Azam, 1998; Doucette et al., 1998), and moderate the lifecycle and behavior of algal cells (Adachi et al., 2003; Mayali et al., 2007). Interactions vary from highly specific symbiont/host relationships (e.g., Amin et al., 2015) to commensal/mutualist relationships (e.g., Grossart, 1999; Amin et al., 2009) or parasitic/algicidal behavior (e.g., Fukami et al., 1992; Iwata et al., 2004; Wang et al., 2015), to less-specific interactions such as nutrient competition/modification (Danger et al., 2007). Interactions among associates and the algal host also directly or indirectly alter the behavior, and physiology of both the algal and bacterial partners. For example, phytoplankton stimulate bacteria by supplying much of the organic matter for bacterial growth (e.g., Lau et al., 2007) or produce antibiotics limiting bacterial growth (Cole, 1982). Bacteria produce growth factors such as vitamins and essential nutrients (Croft et al., 2005), increase availability of iron (Amin et al., 2009), or can even modify phycotoxin content and production by diatoms and dinoflagellates (e.g., Osada and Stewart, 1997; Hold et al., 2001; Albinsson et al., 2014).

The composition and structure of associate bacterial communities is broadly similar across different species. For example, among the dinoflagellates, Alphaproteobacteria (Rhodobacteraceae) are the dominant phylotype associated with *Pfiesteria* sp. (Alavi et al., 2001), *Alexandrium tamarense* and *Scrippsiella trochoidea* cultures (Hold et al., 2001). Similarly, members of Gammaproteobacteria belonging to Alteromonadaceae (*Marinobacter* sp. and *Alteromonas* sp.) are associated with a wide variety of dinoflagellates (Alavi et al., 2001; Hold et al., 2001; Seibold et al., 2001; Ferrier et al., 2002; Jasti et al., 2005). Despite the similarities, several studies also indicate that phylogenetically related associates of different phytoplankton species are genetically/functionally different and engage in species-specific interactions (Bolch et al., 2004; Green et al., 2006; Amin et al., 2009).

Associate communities of uni-algal cultures are composed of potentially 1000s of bacterial genotypes; even carefully washed and isolated single cells result in non-axenic cultures with upward of 20–50 bacterial types (Alavi et al., 2001; Hold et al., 2001; Green et al., 2010). This diversity results in potentially 1000s of bacteria–bacteria and bacterial–algal interactions that confound controlled experiments to examine interactions. To address this problem we have developed simplified co-culture experimental models for three dinoflagellate genera (*Scrippsiella*, *Lingulodinium,* and *Gymnodinium*) that contain a dinoflagellate host and one to three cultured bacterial associates of the dinoflagellate (Bolch et al., 2011). The models provide not only a tractable tool to investigate mechanisms of interaction, but also enable controlled testing of specific hypotheses to gain insight into the function and importance algal–bacterial interactions in complex natural systems.

Despite evidence from culture-based research and evidence of linkages between bacterioplankton and phytoplankton production in nature (Prieto et al., 2015), we have limited knowledge of the relative scale and importance of microbial effects on phytoplankton growth. Models of phytoplankton growth currently include only bottom–up physical factors of light and temperature (Thompson, 1999), availability and uptake of major (C, N, P, and Si) and minor nutrients (Morel and Hudson, 1985), and top-down controls of predation and loss due to sinking (Turner et al., 1998). Here we use the *Gymnodinium catenatum* co-culture model to examine the relative scale and effect of associate bacteria community membership and complexity on dinoflagellate growth dynamics. Our culture experiments indicate that changes in the bacterioplankton community can be as significant for growth of dinoflagellates as changes induced by seasonal changes in light and temperature.

MATERIALS AND METHODS

Bacterial Cultures

Associate bacteria for co-culture experiments were isolated from *G. catenatum* cultures and characterized as detailed in earlier studies (Green et al., 2004, 2010). Three bacterial associates used for co-culture experiments, *Alcanivorax* cf. *borkumensis* DG881, *Marinobacter* sp. DG879 and *Roseobacter* sp. DG874, were selected for experiments based on their ability to support *G. catenatum* growth in uni-bacterial cultures (data not shown). Bacterial cultures were maintained on either Zobell's marine agar (ZM1) prepared in 75% filtered seawater (26 ppt), or the same medium prepared at 1/10 concentration of nutrients (ZM/10). ZM1 medium contained 5 g L^{-1} of bacterial peptone, 1 g L^{-1} of yeast extract and was solidified with 15 g L^{-1} of Difco-Bacto^{TM} Agar. Both media were supplemented with filter-sterilized trace elements and vitamins (Green et al., 2004). The medium was supplemented with 1% (w/v) sodium acetate as a carbon source when used for *Alcanivorax* DG881 (Green et al., 2004).

Establishment of Controlled Associate Co-cultures *G. catenatum*

Cultures of *G. catenatum* with specific bacterial associate communities were established following the approach described in detail by Bolch et al. (2011) using resting cysts produced by sexually compatible crosses of *G. catenatum* strains GCHU11 and GCDE08 (hereafter HU11 and DE08 respectively). Briefly, resting cysts of *G. catenatum* were harvested by centrifugation and surface-sterilized by resuspension in 0.5% hydrogen peroxide for 1 h. Batches of 30–40 surface-sterile resting cysts were then aseptically transferred to sterile 36 mm Petri dishes containing 1.9 mL of sterile GSe algal culture medium, a medium based on sterile natural seawater (28 ppt) supplemented with nitrate, phosphate, trace metals, and vitamins (Blackburn et al., 1989). Associate bacterium additions used in the experiments are shown in **Table 1**. Cultures of each associate bacterium were grown

TABLE 1 | Cultures and bacterial additions used to establish controlled bacterial associate communities.

Culture identifier	Bacterial treatment of resting cysts
M	*Marinobacter* sp. DG879 added to cysts at 10^5 cells mL^{-1}
A	*Alcanivorax* sp. DG881 added to cysts at 10^5 cells mL^{-1}
R	*Roseobacter* sp. DG874 added to cysts at 10^5 cells mL^{-1}
MA	*Marinobacter* sp. DG879 and *Alcanivorax* sp. DG881 in equal proportions; added to cysts at a total concentration of 10^5 cells mL^{-1}
AR	*Alcanivorax* sp. DG881 and *Roseobacter* sp. DG 874 in equal proportions; added to cysts at a total concentration of 10^5 cells mL^{-1}
MR	*Marinobacter* sp. DG879 and *Roseobacter* sp. DG874 in equal proportions; added to cysts at a total concentration of 10^5 cells mL^{-1}
MAR	*Marinobacter* sp. DG879, *Alcanivorax* sp. DG881 and *Roseobacter* sp. DG874 in equal proportions; added to cysts at a total concentration of 10^5 cells mL^{-1}
DEHU	100 μL of 8 μm filtrate from mid-log phase parent cultures GCDE08 and GCHU11; added to cysts undiluted
DE08	Clonal non-axenic parent strain GCDE08 for comparison
HU11	Clonal non-axenic parent strain GCHU11 for comparison

All cultures were established from 30 to 40 surface-sterilized Gymnodinium catenatum resting cysts (GCDE08 × HU11 crosses), germinated and grown for 30 days, transferred to 150 mL Erlenmeyer flasks prior to growth experiments. All culture treatments carried out in duplicate.

overnight in ZM10 medium (Green et al., 2004) and immediately added to dishes of sterile resting cysts in single, pairwise or three-way combinations at a total bacterial concentration of 10^5 CFU mL^{-1}. All bacterial additions were established as independent triplicates. Dishes were sealed with parafilm^{TM} and incubated at $19 \pm 2°C$ at a light intensity of 90 ± 10 μmoles m^{-2} s^{-1} with a 12L:12D photoperiod to allow for resting cyst germination.

From previous studies (Bolch et al., 2004, 2011; Albinsson et al., 2014), cases of co-culture contamination by non-associate bacteria were detectable during the establishment phase using sterile medium-only controls and in each case resulted from contaminated algal growth medium. To minimize the risk of systematic contamination, all algal culture media was prepared from autoclave-sterilized stock reagents where possible. To control aerial/casual contamination, all co-culture flasks used steristoppers with double-layer foil dust caps and all culture manipulation and transfers were carried out in a class 2 laminar flow cabinet using standard aseptic microbiological techniques. Medium sterility (growth medium only) and cyst sterility controls (cysts with no bacteria added) and mixed parental bacterial community controls were used in all experiments. Sterility controls were assessed for accidental or systematic failure of sterilization or contamination spread plating of multiple undiluted sub-samples onto ZM1 and ZM10 medium (Green et al., 2004). Plates were incubated at 20°C for 7 days, assessed for evidence of bacterial growth by direct visual inspection and 5–60x magnification using a Leica Z9.5 stereomicroscope. If contamination was detected in media-only controls then the experiment was terminated and re-established. If contamination was detected in cyst sterility controls, all cultures derived from the contaminated cyst batch were discarded.

All treatments and control dishes containing resting cysts were examined using a Leica Z9.5 stereomicroscope every 3 days after germination. Cyst quality was monitored by recording final germination (%) and motile dinoflagellate cells by direct examination at 20–63x using a stereomicroscope. After 30 days, two replicates from treatments and positive controls were transferred to sterile 150 mL Erlenmeyer flasks containing 100 mL of sterile GSe medium, stoppered with sterile dust caps to limit aerial or other casual contamination, and grown at $19 \pm 2°C$ under a light intensity of 90 ± 10 μmoles m^{-2} s^{-1} (12L: 12D). Negative control cultures (no added bacteria) resulted in death of *G. catenatum* after germination (see Bolch et al., 2011) and could not be included in further growth studies.

For growth experiments, the established 100 mL cultures were aseptically transferred to 150 ml flasks of sterile GSe medium and grown under the light and temperature conditions described above. Dinoflagellate cell concentration was determined every 4 days from triplicate sub-samples using a Sedgwick-Rafter counting chamber (Guillard, 1973) and by *in vivo* fluorometry (Kiefer, 1973). Bacterial concentration (CFU mL^{-1}) was determined every 4 days from triplicate sub-samples and serial dilution spread-plating (Buck and Cleverdon, 1960) onto ZM1 agar. Colony morphology of the associate bacteria used was not sufficiently distinct for reliable differentiation during cell counts therefore total bacterial community counts were undertaken. Bacterial colony morphology on plates was routinely examined for evidence of contamination by non-associate bacteria.

Statistical Analysis

Growth phases were derived from visual inspection of growth curves, and exponential growth/death rates calculated according to Guillard (1973). Differences in dinoflagellate exponential growth and death rates, maximum cell concentration (cells mL^{-1}) were compared by one-way ANOVA with significant differences determined by Tukey's *post hoc* tests, using SPSS ver. 19 (LEAD Technologies, Chicago, IL, USA). Overall similarity of dinoflagellate batch culture dynamics was compared by principal component analysis (PCA) using the software package PRIMER 6. Seven variables were derived from growth curves of each replicate culture for each treatment: exponential growth and death rate (**Figures 1A,B**); maximum cell concentration (**Figure 1C**); and the duration of four batch culture growth phases indicated in **Figures 2**, **3**. Variables were normalized prior to analysis (subtraction of variable means, division by variable standard deviation) to account for order of magnitude differences in value ranges (Clarke and Gorley, 2006). The correlation matrix was used for a two-dimensional PCA, and the principal components displayed as an ordination plot.

RESULTS

Germination, Sterility, and Negative Controls

No culturable bacteria were detected by dilution spread plating of growth media from sterility controls (medium only) and negative

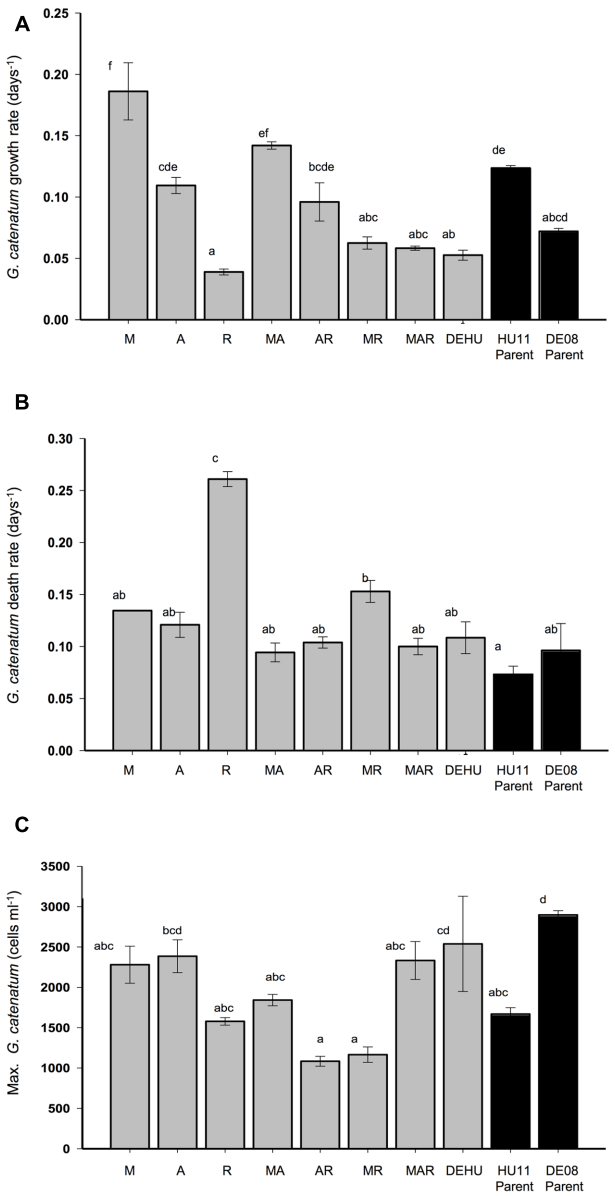

FIGURE 1 | Exponential growth rate (A), death rate **(B)**, and maximum cell density **(C)** (±SE) of *Gymnodinium catenatum* cultures grown with single, pairwise and three-way combinations of bacterial associates compared to mixed culture community (DEHU) and parental non-axenic cultures (GCHU11 and GCDE08). M, *Marinobacter* DG879; A, *Alcanivorax* DG881; R, *Roseobacter* DG874. See **Table 1** for culture codes and additional details. Letters (a–f) indicate significant differences ($p = < 0.05$).

controls (cysts with no bacteria added) indicating that surface-sterilization was effective at removing bacteria and there was low probability of incidental or systematic contamination of media or from airborne sources. Negative controls containing cysts with no bacterial addition showed poor germination rates (15%) and dinoflagellate cells died within the 30 day initial observation period. Long-term culture was not possible and these treatments were not included in the study. All cultures receiving bacterial associate additions exhibited germination rates typical of non-sterilized cysts from earlier studies (54%, Bolch et al., 2002) and similar to the mixed community positive control (DEHU, $p > 0.066$) with the exception of reduced germination in uni-bacterial *Roseobacter* sp. DG874 co-cultures (25%, $p = 0.013$). No significant difference was observed in dinoflagellate cell number per cyst at day 30 post-germination ($f = 4.422$; df = 8, 18; $p > 0.982$).

Growth Dynamics in Batch Culture

All controlled associate co-cultures were grown successfully to 150 ml flask scale, aseptically transferred, and grown through an extended batch culture cycle over a period of 68 days. Growth curves and rates derived from cell counts were not substantially different to that calculated from *in vivo* fluorescence data (not shown). As fluorescence-based estimates are potentially unreliable outside logarithmic-phase (Falkowski and Kiefer, 1985; Cullen et al., 1988), only cell count data were used for further analysis. Presence or concentration of non-cultured bacteria could not be determined in our experiment, however, routine observation of colony morphology on dilution plates did not detect evidence of contamination by culturable non-associate bacteria in experimental cultures.

Marked differences in dinoflagellate growth rate, death rate, maximum cell concentration (**Figure 1**) and batch culture dynamics were evident between *G. catenatum* cultures grown with different bacterial associate communities (**Figures 2**, **3**). No distinct lag-phase was evident, but the exponential growth phase was longer and the stationary phase shorter in cultures containing *Roseobacter* sp., either alone or in combination with other bacteria. Cultures grown with *Marinobacter* sp. or *Alcanivorax* sp. exhibited higher exponential growth rates than mixed associate controls ($f = 23.99$; df = 9,10; $p = 0.000$, 0.033) or cultures containing only *Roseobacter* sp. ($p < 0.008$). Cultures grown with *Roseobacter* sp. showed the slowest exponential growth rate (**Figure 1**) and did not reach stationary phase till day 40–44 (**Figure 2**, R). These co-cultures also exhibited a more rapid decline in death phase than cultures grown with *Marinobacter* sp. ($f = 19.301$; df = 9, 10; $p = 0.001$) or *Alcanivorax* sp. ($f = 19.301$; df = 9, 10; $p = 0.000$) (**Figure 1**).

Co-cultures grown with pair-wise combinations of bacteria exhibited growth curves with a mix of features of the respective uni-bacterial cultures (**Figure 2**, MA, AR, and MR). Co-cultures with *Marinobacter* sp. and *Alcanivorax* sp. showed a short rapid exponential growth period (days 0–12) similar to cultures grown only with *Marinobacter* sp., but a more gradual death phase similar to co-cultures containing only *Alcanivorax* sp. Similar "hybrid" growth curves were evident in the cultures grown with both *Alcanivorax* sp. and *Roseobacter* sp., however, cultures grown with *Marinobacter* sp. and *Roseobacter* sp. showed growth curves similar to co-cultures grown with *Roseobacter* sp. (compare **Figures 2**, MR and R). Mean growth rates of pairwise combinations were intermediate between that of the corresponding uni-bacterial cultures in all cases (**Figure 1**). Mean maximum cell concentrations in two-bacterium co-cultures containing *Roseobacter* sp. achieved a lower maximum cell concentration than mixed community controls ($f = 6.804$;

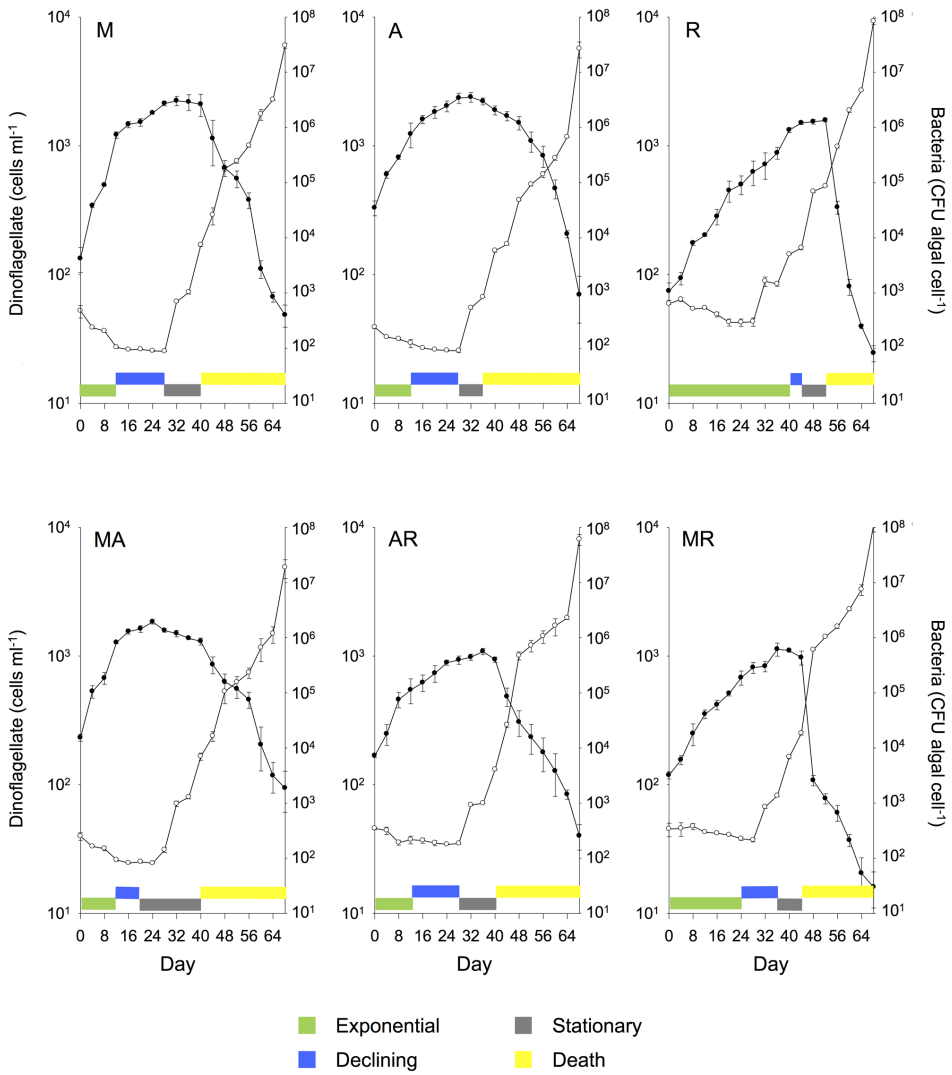

FIGURE 2 | Mean (± SE) batch culture growth curves of *G. catenatum* (closed circles) and total bacteria (CFU algal cell^{-1}, open circles) from duplicate cultures grown with single and pairwise combinations of bacterial associates (M, *Marinobacter* DG879; A, *Alcanivorax* DG881; R, *Roseobacter* DG874; MA, *Marinobacter* DG879 and *Alcanivorax* DG881; AR, *Alcanivorax* DG881 and *Roseobacter* DG874; MR, *Marinobacter* DG879 and *Roseobacter* DG874). See **Table 1** for culture codes and additional details.

df = 9,10; $p < 0.01$). A sharp decline after day 44 was evident in cultures grown with *Marinobacter* sp. and *Roseobacter* sp., however, the overall rate of decline to day 68 was not different from other two-bacterium combinations.

Cultures grown with communities composed of three bacterial strains (MAR) exhibited batch culture dynamics most similar to those of the mixed associate control (DEHU) containing log-phase bacterial communities from cultures HU11 and DE08 (**Figure 3**). Exponential growth rate, maximum cell concentration and death rates were almost identical (**Figure 1**) and only small differences were noted in the onset and length of batch culture phases (see **Figures 2**, **3**). The three-way combination cultures (MAR) exhibited a lower exponential growth rate ($f = 23.99$; df = 9, 10; $p = 0.041$) than either parent crossing strain DE08 and or HU11 (**Figure 1**).

The two-dimensional PCA of dinoflagellate growth curve parameters separated cultures grown with *Roseobacter* sp. versus *Alcanivorax* sp. and *Marinobacter* sp. along the PC1 axis, primarily due to increased exponential phase duration and increased death rate (**Figure 4**). Pairwise combinations of associates were placed midway between the relevant two uni-bacterial associate cultures. Cultures grown with a three-way associate combination (MAR) and mixed parental associate communities (DEHU) were displaced negatively along the PC2 axis, primarily due to higher maximum cell concentrations and an extended duration of death phase.

Bacterial Abundance and Growth

Similar patterns of bacterial abundance were observed across all cultures. Bacteria per dinoflagellate cell (CFU dinoflagellate

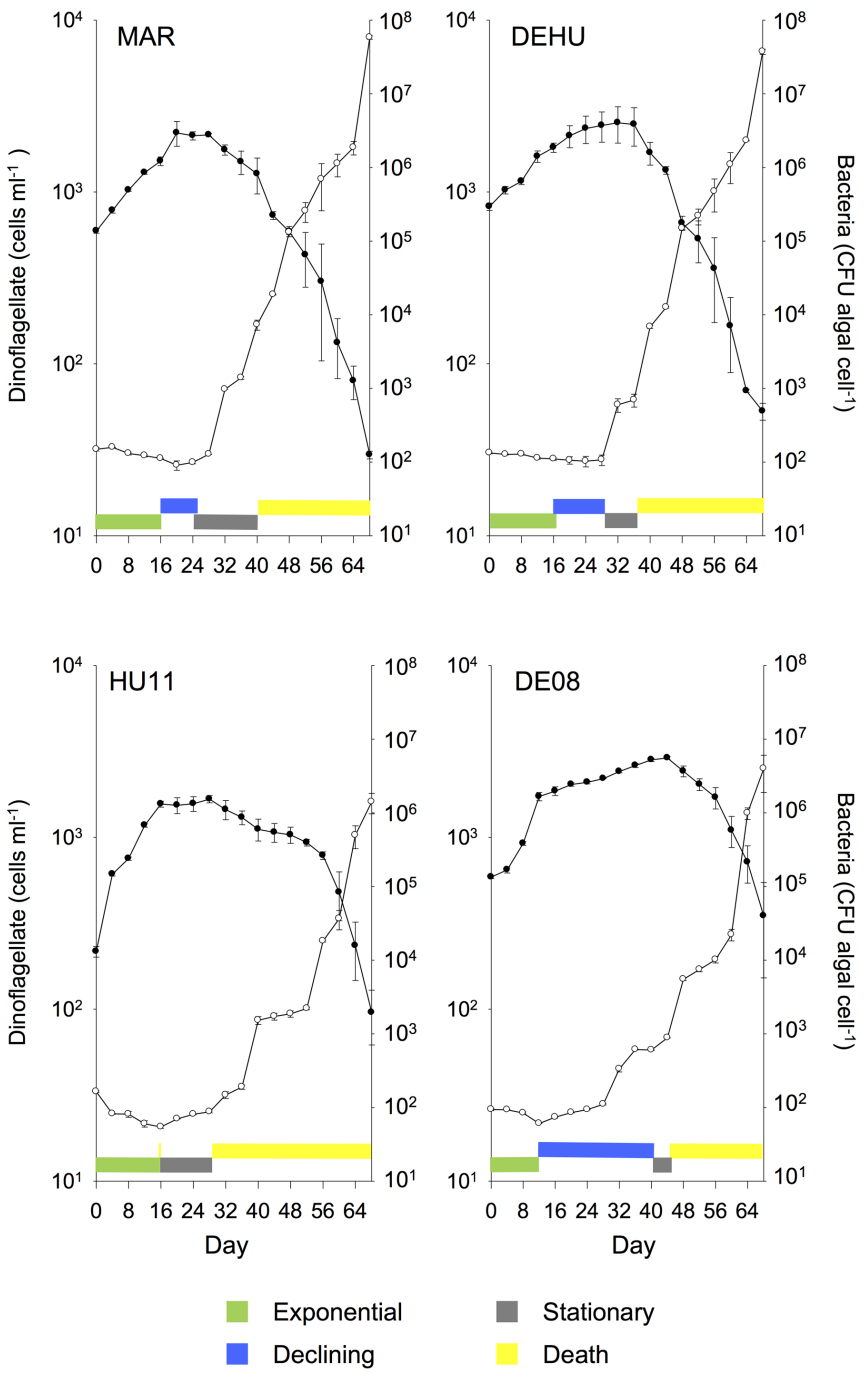

FIGURE 3 | Mean (± SE) batch culture growth curves of *G. catenatum* (closed circles) and total bacteria (CFU algal cell^{-1}, open circles) from duplicate cultures grown with three-way combinations of bacterial associates compared to mixed culture community co-cultures and parent cultures (MAR, *Marinobacter* DG879, *Alcanivorax* DG881 and *Roseobacter* DG874; DEHU, mixed bacterial community from non-axenic GCHU11 and GCDE08 parent cultures; GCDE08, GCHU11, clonal non-axenic parent cultures). See **Table 1** for culture codes and additional details.

cell^{-1}), remained relatively constant during dinoflagellate exponential phase in most cultures, beginning between 100 and 200 bacteria cell^{-1}, decreasing to approximately 100 bacteria cell^{-1} by day 24–28 in most cases (see **Figures 2**, **3**). Bacteria increased sharply at or near the end of dinoflagellate logarithmic-phase to approximately10^7–10^8 bacteria cell^{-1} by day 68 when the experiment was terminated.

Changes in bacterial versus dinoflagellate abundance were strongly associated with dinoflagellate growth phase (**Figures 5**, **6**) and followed similar trajectories over the

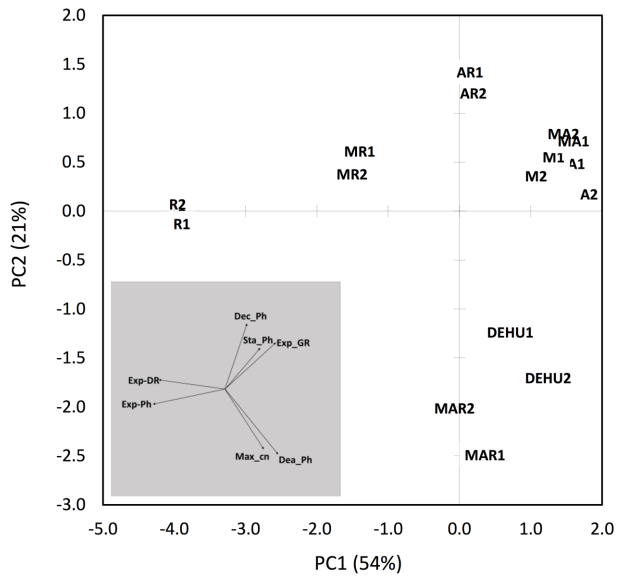

FIGURE 4 | Two-dimensional principal component analysis (PCA) of dinoflagellate batch growth dynamics of *G. catenatum* cultures grown with different associate bacterial communities. Variables were normalized prior to analysis and included exponential growth and death rate, maximum cell concentration, and batch growth phase durations indicated by colored bars in **Figures 2**, **3**. Replicate co-cultures are indicated by number suffix (1 or 2). See **Table 1** for culture codes and additional detail (M, *Marinobacter* DG879; A, *Alcanivorax* DG881; R, *Roseobacter* DG874; MA, *Marinobacter* DG879 and *Alcanivorax* DG881; AR, *Alcanivorax* DG881 and *Roseobacter* DG874; MR, *Marinobacter* DG879 and *Roseobacter* DG874; MAR, *Marinobacter* DG879, *Alcanivorax* DG881 and *Roseobacter* DG874; DEHU, mixed bacterial community from non-axenic GCHU11 and GCDE08 parent cultures). Vectors of original batch curve variables used in the analysis are shown in the shaded plot. Variables: Dea_Ph, length of death phase in days; Dec_Ph, length of declining phase in days; Exp_DR, death rate (μ) during death phase; Exp_GR, growth rate (μ) during log-phase; Exp_Ph, length of dinoflagellate log-phase in days; Max_cn, maximum dinoflagellate cell concentration (cells ml^{-1}); Sta_Ph, length of stationary phase in days.

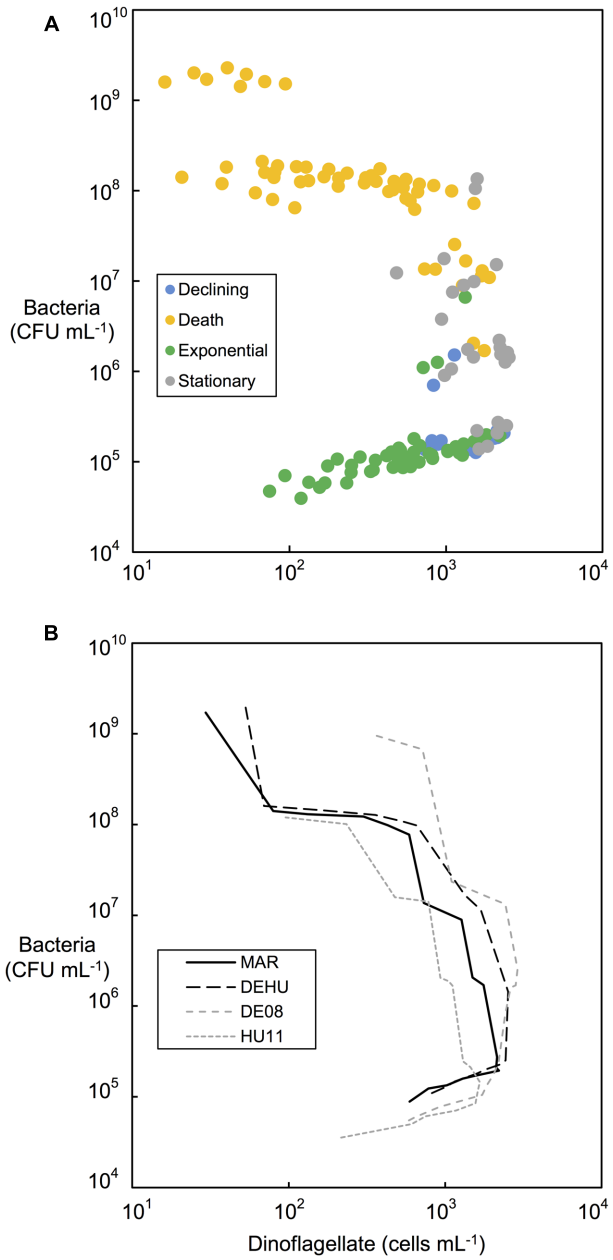

FIGURE 5 | Bacterial and dinoflagellate cell concentrations (cells mL^{-1}) during different phases of dinoflagellate culture growth. **(A)** All replicate controlled associate community cultures categorized according to dinoflagellate growth phases indicated by colored bars in **Figures 2**, **3**. **(B)** Comparison of mean bacterial and dinoflagellate concentrations from replicate cultures (n = 2) of three-way combination (MAR) compared to a mixed community (DEHU) and each parental non-axenic culture (GCDE08 and GCHU11). See **Table 1** for culture codes and additional detail.

course of the experiment (**Figure 5A**). Bacterial abundance increased with dinoflagellate concentration during dinoflagellate exponential phase, increased rapidly during dinoflagellate stationary phase, and remaining high during culture death phase. Mean abundance patterns differed among treatments, most evident when comparing parental cultures GCDE08 and GCHU11 with the mixed community control (DEHU) and the three-way combination of associates (MAR) which exhibited a similar intermediate microbial-dinoflagellate abundance pattern (**Figure 5B**). Total bacterial community growth rate ranged from 0.03 to 0.075 days^{-1} during dinoflagellate exponential phase and was positively correlated with dinoflagellate growth rate ($r^2 = 0.46$, df $= 18$, $p < 0.001$; **Figure 6**). From day 28, total bacterial growth rate increased dramatically in all cultures (0.16–0.23 days^{-1}), coinciding with onset of stationary phase except in co-cultures with *Roseobacter* sp. and two-way co-cultures containing *Marinobacter* sp. and *Roseobacter* sp. where increased bacterial growth rate coincided with mid- and late-log to declining phase respectively.

DISCUSSION

Our experiments demonstrate that associate bacterial communities modify dinoflagellate growth independent of

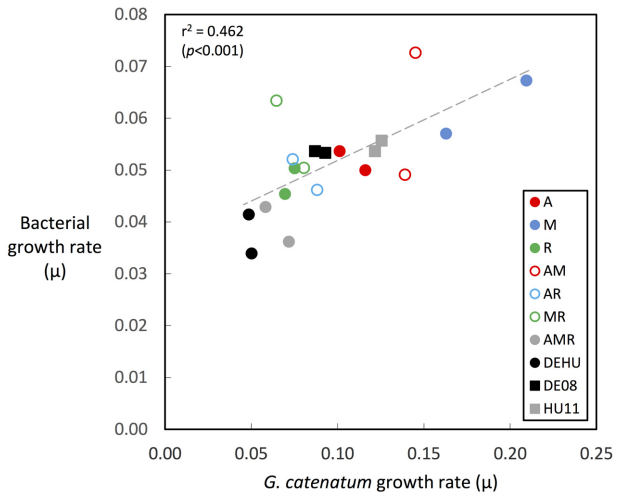

FIGURE 6 | Correlation of bacterial associate and dinoflagellate growth rates during dinoflagellate exponential phase. Growth rates were calculated over exponential phase period in each culture as indicated by green-colored bars in **Figures 2**, **3** (circles = co-cultures, squares = parent cultures; see **Table 1** for culture codes and additional detail).

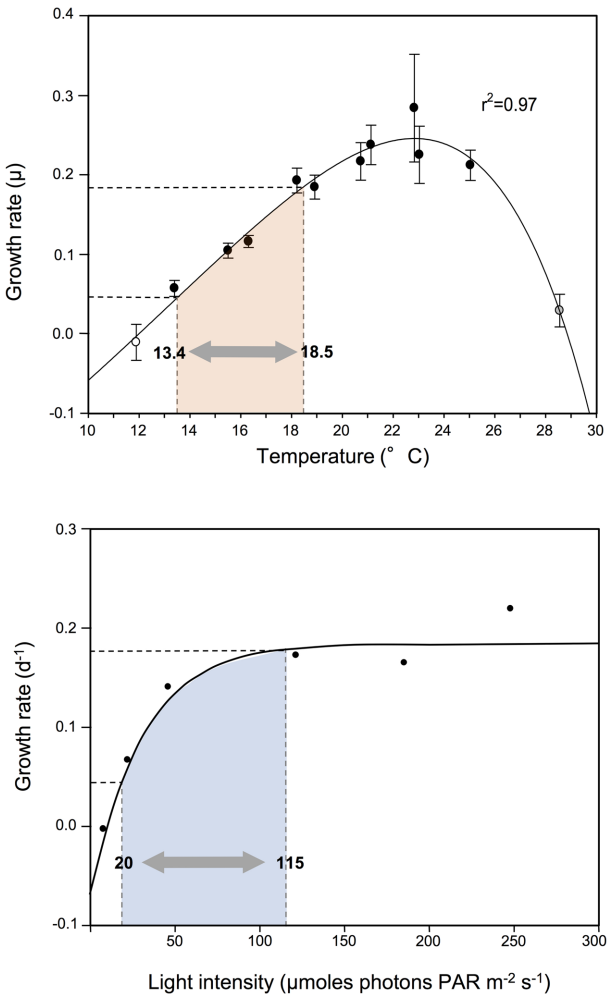

FIGURE 7 | Changes in exponential growth rate of *G. catenatum* strains due to modified associate bacteria compared to responses to light and temperature. Range of growth rate change observed due to associate microbial indicated by shaded area within dashed lines; equivalent temperature and light ranges shaded in pink and blue respectively. Temperature and light response of *G. catenatum* at 19°C (equivalent to the present study) were adapted from Armstrong (2010).

other environmental factors considered to control growth of phytoplankton. Co-cultures were grown under identical conditions, in nutrient-replete medium (including vitamins) at saturating light intensity (90–100 μmoles photons PAR m^{-2} s^{-1} at 19°C; Armstrong, 2010), and in the middle of the optimal temperature for *G. catenatum* in both lab culture (12–25°C; Blackburn et al., 1989) and nature (12–20°C; Hallegraeff et al., 2012). The significant observed differences in algal growth dynamics support the concept that the associate bacterial interactions are an important factor in algal population dynamics even under optimal and non-limiting conditions. The scale of change in growth rates was surprisingly large (>four-fold) and equivalent to that typically observed for *G. catenatum* over a five degree temperature range, or an almost six-fold increase/decrease in light intensity (**Figure 7**). Environmental changes of this magnitude are of similar scale to those experienced over an annual cycle in mid-latitude coastal waters of southern Tasmania where *G. catenatum* forms seasonal bloom populations (Hallegraeff et al., 2012), indicating that the influence of bacterial associates is potentially as important for *G. catenatum* population dynamics as light and temperature.

Changes in phytoplankton growth due to modification of bacterial communities are described from a range of phytoplankton species. For example, co-culture with a Flavobacterium increases maximum cell density, growth rate and length of stationary phase of axenic cultures of the diatom, *Chaetoceros gracilis*, and haptophytes *Isochrysis galbana* and *Pavlova lutheri* (Suminto and Hirayama, 1997). Harvestable biomass of the green alga *Botryococcus braunii* increases by 50% when grown in co-culture with a cultured alphaproteobacterial associate (Tanabe et al., 2015). Supplementation with four different associates resulted in a doubling of growth rate and an almost three-fold increase in biomass of *Chlorella vulgaris* (Cho et al., 2015). These findings indicate that bacterial associate interactions are likely to be important for most phytoplankton species.

We observed significant changes in batch culture dynamics, included changes in stationary phase length and cell concentration, and substantial changes in death rate, particularly evident in co-culture with *Roseobacter* sp. DG874. In particular *Roseobacter* co-cultures differed in exhibiting rapidly increasing bacterial concentration from mid-log phase rather than at the onset of stationary phase. The underlying cause or mechanism driving the different growth dynamics is difficult to determine from our data. It may be caused by *G. catenatum* autolysis, or nutrient competition (Wheeler and Kirchman, 1986;

Jumars et al., 1989), or alternatively, it may result from a Jekyll-and Hyde interaction where the associate bacterium switches from supportive to algicidal (Seyedsayamdost et al., 2011). Members of the *Roseobacter* clade often dominate the microbial communities associated with phytoplankton and are known to switch from growth promotion to algilytic activity (Geng and Belas, 2010). For example, *Phaeobacter gallaceiencis* produces selective, potent algicides roeseobacticide A and B that lyse *Emiliania huxleyi* (Seyedsayamdost et al., 2011), and *Dinoroseobacter shibae* exhibits similar supportive/algicidal behavior in co-culture with *Prorocentrum minimum* (Wang et al., 2014). The *Roseobacter* in our experiments may also switch to algicidal mode during log-phase dinoflagellate growth, resulting in increased cell lysis that counteracts growth from cell division. This would explain the reduction in net growth rate during mid-log phase and ultimately the 1.5-fold reduction in dinoflagellate concentration at stationary phase. In our models, the mid-log reduction in dinoflagellate growth becomes evident at *Roseobacter* concentrations of 1.5×10^5 cells ml^{-1} (day 20–24), much lower than onset of lysis by *D. shibae* in co-culture models of *P. minimum* (Wang et al., 2014). However, massive cell lysis and steep death phase occurs at similar *Roseobacter* sp. concentrations (10^8 cells ml^{-1}) to that observed in the *Prorocentrum*/*D. shibae* model. Alternatively, the reduction in net-growth rate may be entirely due to *G. catenatum* autolysis (Berges and Falkowski, 1998). The dinoflagellate cannot be grown axenically (Bolch et al., 2011) so we cannot easily determine the extent of autolysis in the absence of bacteria, however there is little evidence of reduced dinoflagellate net growth rate in co-cultures without *Roseobacter* sp., suggesting that autolysis is not the main cause.

Similar promotion/lysis patterns were observed in uni- and mixed-bacterial co-cultures with *Marinobacter* and *Alcanivorax*, however dinoflagellate lysis and decline occurred on or after declining growth phase. In these cultures, cell lysis was more probably stimulated by cell autolysis caused by onset of nutrient stress (Veldhuis et al., 2001) with bacterial algilytic activity perhaps contributing during the subsequent death phase. Previous studies indicate that algicidal activity is cell density-dependent and may be mediated by acetylated homoserine lactones (AHL)-dependent quorum-sensing mechanisms (Paul and Pohnert, 2011; Egan et al., 2013) that up-regulate algilytic compound pathways. Our preliminary analyses of *Marinobacter* genome data indicate that most strains produce either short (C4) or medium (C6-8) AHLs but do not possess a conventional quorum-sensing system (Green, unpublished data). However, it is also possible that algilytic activity is be mediated via other quorum-sensing systems (Bassler, 1999).

We practiced rigorous media preparation processes, careful aseptic technique and sub-sampling to minimize risk of subsequent aerial or other contamination. We did not detect random or systematic contamination of the experiment by culturable non-associate bacteria, but we cannot rule out the presence of uncultured bacteria in our co-cultures. However, the consistency of replicates and clear differences between the associate treatments suggest that if present the effect of uncultured bacteria was either not significant or consistent across the experiment. Studies using the same models/methods described here (Bolch et al., 2004, 2011) indicate that rare instances of co-culture contamination are detectable during the germination and establishment phase and the cultures removed from further experimentation. These studies also cultured associate communities at the end-point of the experiments. Sequencing 16S rDNA of randomly selected isolates routinely recovered only the expected added associates (Bolch et al., 2011).

While *G. catenatum* is considered autotrophic, mixotrophy appears common among photosynthetic dinoflagellates (Jeong et al., 2005) and both intracellular bacteria and bacterial uptake has been reported for this species (Seong et al., 2006). However, bacterial ingestion is estimated to contribute less than 2% to total carbon acquisition by dinoflagellates of similar size to *G. catenatum* (Seong et al., 2006) and is unlikely to have contributed significantly to growth in our co-culture models. Additionally, capacity to support growth in uni-bacterial cultures is limited to only a few bacterial associates and is highly strain/species specific (Bolch et al., 2004). Even closely related bacterial associates to those used here (<0.5% seq. divergence at the 16S rDNA) are unable to support growth in uni-bacterial co-culture (Bolch et al., 2004). Bacterivory cannot explain this high level of specificity. Other experiments indicate that after germination, *G. catenatum* growth can be maintained without bacterial associates at similar growth rates by repeated addition 0.2 μm filtrates from non-axenic log-phase *G. catenatum* cultures (Matsumoto and Bolch, unpublished data). Yet removal of associates from late-log phase co-cultures using antibiotics leads to cessation of growth and ultimately death of the dinoflagellate culture (Bolch et al., 2011). Taken together, these observations indicate that the essential growth factor/s are dissolved or colloidal extracellular products produced by associate bacteria.

The consistent patterns of total bacterial and dinoflagellate concentration, the low bacterial growth rates observed, and the correlated growth rates during dinoflagellate exponential phase indicate that bacterial associate growth was limited by algal-derived organic carbon in our models. During exponential growth, phytoplankton tend to release only a few percent of their photosynthetic products directly (Wiebe and Pomeroy, 1999) therefore supply of organic carbon would logically limit bacterial growth in the co-culture models. This is supported by the low bacterial growth rates we observed during dinoflagellate exponential phase (<0.1 day^{-1}) which are 1–2 orders of magnitude lower than associate bacterial taxa grown in organically enriched medium (3.6–8.0 day^{-1} for *Marinobacter* spp.; Guo et al., 2007). Even the fastest bacterial community growth rates observed during dinoflagellate stationary/death phase (0.36–0.42 day^{-1}) are at least 10-fold less, suggesting that organic carbon limits associate growth throughout the batch growth cycle.

The uncoupling of bacterial and dinoflagellate growth rates during dinoflagellate stationary and death phases is likely due to onset of algal cell autolysis, resulting in increased supply of organic carbon for bacterial growth and perhaps increased bacterial competition for inorganic nutrients

(Bratbak and Thingstad, 1985), further hastening the decline of the dinoflagellate. The stepwise increases in bacterial abundance during these phases have been noted in earlier studies (Bolch et al., 2011) and results from the use of a 12:12 day night cycle which induces synchronous cell division in *G. catenatum* ranging from 4 to 13 days div^{-1} across our experiment. When combined with a 4 day sampling frequency, bacterial growth proceeds in most cultures as a series of rapid increases during/after each semi-synchronous dinoflagellate division. We hypothesize that each division results in quantum increases in host dinoflagellate biomass and exuded organic carbon, which in turn provides substrate for short periods of unconstrained bacterial growth until organic carbon limitation is re-established. The stepwise patterns of total bacterial growth were also remarkably consistent in uni-bacterial and two- and three-way combination models, indicating the same organic carbon limitations and dynamics govern patterns of total abundance of more complex associate communities. We did not track abundance of each bacterial type or assess unculturable bacteria, but other experiments indicate that associates dynamics and behavior in two-way co-culture models can be quite complex. Both the relative proportions of each associate and attachment to algal cell surfaces change markedly over the dinoflagellate growth cycle (Albinsson et al., unpublished), and different associates may interact in different ways during different dinoflagellate growth phases.

Our two- and three-way combination models generally displayed dinoflagellate and bacterial dynamics intermediate of the respective uni-bacterial co-cultures (**Figure 4**). Increasing associate community complexity to three bacteria resulted in dinoflagellate growth dynamics very similar to the more complex mixed-associate controls (DEHU), indicating that our three-way model is sufficient to model interaction and growth dynamics of more complex associate communities. Interestingly, onset of rapid bacterial growth in our MAR co-cultures only occurred in stationary phase, suggesting that the presence of both *Marinobacter* and *Alcanivorax* may moderate the proposed lytic effects of *Roseobacter* sp. DG874. Similar antagonistic interactions among culture associates protect the dinoflagellate *Karenia brevis* from lysis by an algicidal Bacteroidetes bacterium, either through release of specific antibiotic activity, or resource competition stopping the bacterium achieving sufficient concentration for lytic activity (Mayali and Doucette, 2002).

Our previous studies show that *Roseobacter* (including DG874) dominate (85%) the associate community of GCDE08, with *Marinobacter* as sub-dominant (13%) and *Alcanivorax* being relatively uncommon (<1%) (Green et al., 2010). The *Roseobacter*-dominated community may thus explain the distinctive two-phase exponential growth pattern of GCDE08 cultures, also evident to varying degree in other *Roseobacter* co-cultures in this work (**Figures 2**, **3**; AR and MR). By logical extension, differing associate community composition may also explain a component of within-species variation in growth/performance commonly observed in algal culture studies. Such observations are usually explained as genetic diversity or uncontrolled/random variance, however, our model indicates that *Roseobacter* dominated associate communities can lead to reduced growth rate and culture yield. The averaging effect seen in combined co-cultures suggest associate-related effects may be moderated when there is sufficient associate diversity/redundancy, but standard phytoplankton isolation techniques involve several cell-washing steps that reduce associate community diversity. As an example, the total number of associate taxa in parent *G. catenatum* cultures in our models differ substantially; seven associate taxa in strain GCHU11 versus 17 in GCDE08 (Green et al., 2010). This is sufficiently low for associate effects to be a significant contributor to strain variation and a confounding factor in culture-based algal growth studies.

The importance and contribution of microbial interactions in phytoplankton population decline and nutrient cycling have been recognized for some time but our study shows that associate microbial interactions are of potential equal importance to the physical factors traditionally thought to moderate phytoplankton growth and primary production in the world's aquatic ecosystems. Studies of coastal plankton communities have recently shown that phytoplankton production is reliant on a metabolically active heterotrophic bacterial community even when sufficient inorganic nutrients are available for growth (Prieto et al., 2015), demonstrating that the bacterioplankton can be essential for phytoplankton production in nature. Culture-based studies with models like those used here describe a range of mechanisms that may mediate these processes. For example, a metabolically active bacterioplankton community may be essential for phytoplankton trace metal uptake via an interaction process known as Iron-Carbon mutualism (Amin et al., 2009). Algal-associates of the genus *Marinobacter* produce the photo-labile iron siderophore, Vibrioferrin (VF), that is released into the algal cell boundary layer. Photolysis of VF leads to release of soluble Fe^{3+} near the algal cell surface that is rapidly taken up by the algal cell, increasing algal iron uptake rate by almost 20-fold (Amin et al., 2009). The capacity for photo-labile siderophore production is widespread in the natural marine bacterial populations, but estimated to be present in perhaps only 1–2% of the total microbial community (Gardes et al., 2013), as one might expect if this capacity is associated predominantly with the low abundance algal-associate community. The challenge is now to understand the specific conditions under which these interactive mechanisms alter/modify growth and primary production, and the level of functional redundancy that exists in both the associate and background free-living bacterial communities.

AUTHOR CONTRIBUTIONS

Authors CB and DG were responsible for the concepts and experimental plan, design of experiments, and the provision of research material including isolation of bacterial strains, and supply of algal strains for the study. Experimental data collection, and analysis was carried out by TB and CB. Drafts of the manuscript, figures and tables were completed by TB with input

from CB. The final manuscript and figures were revised by CB with input from DG.

FUNDING

This work was supported by University of Tasmania Internal Research Grant Scheme B0015641 awarded to CB.

ACKNOWLEDGMENTS

The authors thank Dr. Susan Blackburn (CSIRO Marine and Atmospheric Research) for providing *G. catenatum* cultures GCHU11 and GCDE08. The authors also thank Prof. Rosa Martinez (University of Cantabria, Spain) for helpful comments on early drafts of this manuscript. We also thank the reviewers for numerous valuable suggestions to improve the manuscript.

REFERENCES

Adachi, M., Kanno, T., Okamoto, R., Itakura, S., Yamaguchi, M., and Nishijima, T. (2003). Population structure of *Alexandrium* (Dinophyceae) cyst formation-promoting bacteria in Hiroshima Bay, Japan. *Appl. Environ. Microbiol.* 69, 6560–6568. doi: 10.1128/AEM.69.11.6560-6568.2003

Alavi, M., Miller, T., Erlandson, K., Schneider, R., and Belas, R. (2001). Bacterial community associated with *Pfiesteria*-like dinoflagellate cultures. *Environ. Microbiol.* 3, 380–396. doi: 10.1046/j.1462-2920.2001.00207.x

Albinsson, M. A., Negri, A. P., Blackburn, S. I., and Bolch, C. J. S. (2014). Microbial influences on the toxicity of the dinoflagellate *Gymnodinium catenatum*. *PLoS ONE* 9:e104623. doi: 10.1371/journal.pone.0104623

Amin, S. A., Green, D. H., Hart, M. C., Küpper, F. C., Sunda, W. G., and Carrano, C. J. (2009). Photolysis of iron-siderophore chelates promotes bacterial-algal mutualism. *Proc. Natl. Acad. Sci. U.S.A.* 106, 17071–17076. doi: 10.1073/pnas.0905512106

Amin, S. A., Hmelo, L. R., van Tol, H. M., Durham, B. P., Carlson, L. T., Heal, K. R., et al. (2015). Interaction and signalling between a cosmopolitan phytoplankton and associated bacteria. *Nature* 522, 98–101. doi: 10.1038/nature14488

Amin, S. A., Parker, M. S., and Armbrust, E. V. (2012). Interactions between diatoms and bacteria. *Microbiol. Mol. Biol. Rev.* 76, 667–684. doi: 10.1128/MMBR.00007-12

Armstrong, P. B. (2010). *Nitrogen Uptake by Phytoplankton in the Huon Estuary: With Special Reference to the Physiology of the Toxic Dinoflagellate Gymnodinium catenatum*. Ph.D. thesis, University of Tasmania, Hobart TAS.

Azam, F. (1998). Microbial control of oceanic carbon flux: the plot thickens. *Science* 280, 694–696. doi: 10.1126/science.280.5364.694

Bassler, B. L. (1999). How bacteria talk to each other: regulation of gene expression by quorum sensing. *Curr. Opin. Microbiol.* 2, 582–587. doi: 10.1016/S1369-5274(99)00025-9

Berges, J. A., and Falkowski, P. G. (1998). Physiological stress and cell death in marine phytoplankton: induction of proteases in response to nitrogen and light limitation. *Limnol. Oceanogr.* 43, 129–135. doi: 10.4319/lo.1998.43.1.0129

Blackburn, S. I., Hallegraeff, G. M., and Bolch, C. J. (1989). Vegetative reproduction and sexual life cycle of the toxic dinoflagellate *Gymnodinium catenatum* from Tasmania, Australia. *J. Phycol.* 25, 577–590. doi: 10.1111/j.1529-8817.1989.tb00264.x

Bolch, C. J., Negri, A. P., Blackburn, S. I., and Green, D. H. (2002). "Lifecycle variation in PST content and cell toxicity in PST-producing dinoflagellates," in *Proceedings of the Life History of Microalgal Species Causing Harmful Blooms: Report of a European Workshop*, eds E. Garcés, A. Zingone, M. Montresor, B. Reguera, and B. Dale (Brussels: European Commission), 37–42.

Bolch, C. J. S., Subramanian, T., and Green, D. H. (2011). The toxic dinoflagellate *Gymnodinium catenatum* (Dinophyceae) requires marine bacteria for growth. *J. Phycol.* 47, 1009–1022. doi: 10.1111/j.1529-8817.2011.01043.x

Bolch, C. J. S., Vincent, B., Blackburn, S. I., and Green, D. H. (2004). "Host-symbiont range of growth stimulating bacteria associated with *Gymnodinium catenatum*," in *Proceedings of the Abstract and Programme of the 11th International Conference on Harmful Algae*, Capetown.

Bratbak, G., and Thingstad, T. F. (1985). Phytoplankton-bacteria interactions: an apparent paradox? Analysis of a model system with both competition and commensalism. *Mar. Ecol. Prog. Ser.* 25, 23–30. doi: 10.3354/meps025023

Buck, J. D., and Cleverdon, R. C. (1960). The spread plate as a method for the enumeration of marine bacteria. *Limnol. Oceanogr.* 5, 78–80. doi: 10.4319/lo.1960.5.1.0078

Cho, D.-H., Ramanan, R., Jina Heo, J., Lee, J., Kim, B.-H., Oh, H.-M., et al. (2015). Enhancing microalgal biomass productivity by engineering a microalgal bacterial community. *Bioresour. Technol.* 175, 578–585. doi: 10.1016/j.biortech.2014.10.159)

Clarke, R. N., and Gorley, R. N. (2006). *PRIMER v6*. Plymouth: Plymouth Marine Laboratory, 190.

Cole, J. J. (1982). Interactions between bacteria and algae in aquatic ecosystems. *Annu. Rev. Ecol. Syst.* 13, 291–314. doi: 10.1146/annurev.es.13.110182.001451

Croft, M. T., Lawrence, A. D., Raux-Deery, E., Warren, M. J., and Smith, A. G. (2005). Algae acquire vitamin B12 through a symbiotic relationship with bacteria. *Nature* 438, 90–93. doi: 10.1038/nature04056

Cullen, J. J., Yentsch, C. M., Cuccr, T. L., and MacIntyre, H. L. (1988). Autofluorescence and other optical properties as tools in biological oceanography. *SPIE* 925, 149–156.

Danger, M., Oumarou, C., Benest, D., and Lacroix, G. (2007). Bacteria can control stoichiometry and nutrient limitation of phytoplankton. *Funct. Ecol.* 21, 202–210. doi: 10.1111/j.1365-2435.2006.01222.x

Doucette, G. J., Kodama, M., Franca, S., and Gallacher, S. (1998). "Bacterial interactions with harmful algal bloom species: bloom ecology, toxigenesis, and cytology," in *Physiological Ecology of Harmful Algal Blooms*, eds D. M. Anderson, A. D. Cembella, and G. M. Hallegraeff (Berlin: Springer-Verlag), 619.

Egan, S., Harder, T., Burke, C., Steinberg, P., Kjelleberg, S., and Thomas, T. (2013). The seaweed holobiont: understanding seaweed–bacteria interactions. *FEMS Microbiol. Rev.* 37, 462–476. doi: 10.1111/1574-6976.12011

Falkowski, P., and Kiefer, D. A. (1985). Chlorophyll a fluorescence in phytoplankton: relationship to photosynthesis and biomass. *J. Plankton Res.* 7, 715–731. doi: 10.1093/plankt/7.5.715

Ferrier, M., Martin, J. L., and Rooney-Varga, J. N. (2002). Stimulation of *Alexandrium fundyense* growth by bacterial assemblages from the Bay of Fundy. *J. Appl. Microbiol.* 92, 706–716. doi: 10.1046/j.1365-2672.2002.01576.x

Fukami, K., Yuzawa, A., Nishijima, T., and Hata, Y. (1992). Isolation and properties of a bacterium inhibiting the growth of *Gymnodinium nagasakiense*. *Nippon Suisan Gakkaishi* 58, 1073–1077. doi: 10.2331/suisan.58.1073

Gardes, A., Triana, C., Amin, S. A., Green, D. H., Romano, A., Trimble, L., et al. (2013). Detection of photoactive siderophore biosynthetic genes in the marine environment. *Biometals* 26, 507–516. doi: 10.1007/s10534-013-9635-1

Geng, H., and Belas, R. (2010). Molecular mechanisms underlying *Roseobacter*-phytoplankton symbioses. *Curr. Opin. Biotechnol.* 21, 332–338. doi: 10.1016/j.copbio.2010.03.013

Green, D. H., Bowman, J. P., Smith, E. A., Gutierrez, T., and Bolch C. J. S. (2006). *Marinobacter algicola* sp. nov., isolated from laboratory cultures of paralytic shellfish toxin-producing dinoflagellates. *Int. J. Syst. Evol. Microbiol.* 56, 523–527. doi: 10.1099/ijs.0.63447-0

Green, D. H., Hart, M. C., Blackburn, S. I., and Bolch, C. J. S. (2010). Bacterial diversity of *Gymnodinium catenatum* and the relationship to dinoflagellate toxicity. *Aquat. Microb. Ecol.* 61, 73–87. doi: 10.3354/ame01437

Green, D. H., Llewellyn, L. E., Negri, A. P., Blackburn, S. I., and Bolch, C. J. S. (2004). Phylogenetic and functional diversity of the cultivable bacterial community associated with the paralytic shellfish poisoning dinoflagellate *Gymnodinium catenatum*. *FEMS Microbiol. Ecol.* 47, 345–357. doi: 10.1016/S0168-6496(03)00298-8

Grossart, H. P. (1999). Interactions between marine bacteria and axenic diatoms (*Cylindrotheca fusiformis*, *Nitzschia laevis*, and *Thalassiosira weissflogii*) incubated under various conditions in the lab. *Aquat. Microb. Ecol.* 19, 1–11. doi: 10.3354/ame019001

Guillard, R. R. L. (1973). "Division rates," in *Handbook of Phycological Methods: Culture Methods and Growth Measurements*, ed. J. R. Stein (London: Cambridge University), 289–312.

Guo, B., Gu, J., Ye, Y. G., Tan, Y. Q., Kida, K., and Wu, X. L. (2007). *Marinobacter segnicrescens* sp nov. a moderate halophile isolated from benthic sediment of the South China Sea. *Int. J. Syst. Evol. Microbiol.* 57, 1970–1974. doi: 10.1099/ijs.0.65030-0

Hallegraeff, G. M., Blackburn, S. I., Doblin, M. A., and Bolch, C. J. S. (2012). Global toxicology, ecophysiology and population relationships of the chainforming PST dinoflagellate *Gymnodinium catenatum*. *Harmful Algae* 14, 130–143. doi: 10.1016/j.hal.2011.10.018

Hold, G. L., Smith, E. A., Birkbeck, T. H., and Gallacher, S. (2001). Comparison of paralytic shellfish toxin (PST) production by the dinoflagellates *Alexandrium lusitanicum* NEPCC 253 and *Alexandrium tamarense* NEPCC 407 in the presence and absence of bacteria. *FEMS Microbiol. Ecol.* 36, 223–234. doi: 10.1111/j.1574-6941.2001.tb00843.x

Iwata, Y., Sugahara, I., Kimura, T., Kowa, H., Matsumoto, A., and Noritake, K. (2004). Properties of an algicidal bacterium (*Flavobacterium* sp.) against *Karenia mikimotoi* isolated from Ise Bay, Japan. *Nippon Suisan Gakkaishi* 70, 537–541. doi: 10.2331/suisan.70.537

Jasti, S., Sieracki, M. E., Poulton, N. J., Giewat, M. W., and Rooney-Varga, J. N. (2005). Phylogenetic diversity and specificity of bacteria closely associated with *Alexandrium* sp. and other phytoplankton. *Appl. Environ. Microbiol.* 71, 3483–3494. doi: 10.1128/AEM.71.7.3483-3494.2005

Jeong, H. J., Yoo, Y. D., Park, J. Y., Song, J. Y., Kim, S. T., Lee, S. H., et al. (2005). Feeding by the phototrophic red-tide dinoflagellates: five species newly revealed and six species previously known to be mixotrophic. *Aquat. Microb. Ecol.* 40, 133–155. doi: 10.3354/ame040133

Jumars, P. A., Penry, D. L., Baross, J. A., Perry, M. J., and Frost, B. W. (1989). Closing the microbial loop: dissolved carbon pathway to heterotrophic bacteria from incomplete ingestion, digestion and absorption in animals. *Deep Sea Res.* 36, 483-495. doi: 10.1016/0198-0149(89)90001-0

Kiefer, D. A. (1973). Chlorophyll a fluorescence in marine centric diatoms: responses of chloroplasts to light and nutrient stress. *Mar. Biol.* 23, 39–46. doi: 10.1007/BF00394110

Lau, W. W. Y., Keil, R. G., and Armbrust, E. V. (2007). Succession and diel transcriptional response of the glycolate-utilizing component of the bacterial community during a spring phytoplankton bloom. *Appl. Environ. Microbiol.* 73, 2440–2450. doi: 10.1128/AEM.01965-06

Mayali, X., and Doucette, G. J. (2002). Microbial community interactions and population dynamics of an algicidal bacterium active against *Karenia brevis* (Dinophyceae). *Harmful Algae* 1, 277–293. doi: 10.1016/S1568-9883(02)00032-X

Mayali, X., Franks, P. J. S., and Azam, F. (2007). Bacterial induction of temporary cyst formation by the dinoflagellate *Lingulodinium polyedrum*. *Aquat. Microb. Ecol.* 50, 51–62. doi: 10.3354/ame01143

Morel, F., and Hudson, R. (1985). "Geobiological cycle of trace elements in aquatic systems: redfield revisited," in *Chemical Processes in Lakes*, ed. W. Stumm (New York, NY: John Wiley and Sons), 251–281.

Osada, M., and Stewart, J. E. (1997). Gluconic acid gluconolactone: physiological influences on domoic acid production by bacteria associated with *Pseudo-nitzschia multiseries*. *Aquat. Microb. Ecol.* 12, 203–209. doi: 10.3354/ame012203

Paul, C., and Pohnert, G. (2011). Interactions of the algicidal bacterium *Kordia algicida* with diatoms: regulated protease excretion for specific algal lysis. *PLoS ONE* 6:e21032. doi: 10.1371/journal.pone.0021032

Prieto, A., Barber-Lluch, E., Haernandez-Ruiz, M., Martinez-Garcia, S., Fernandez, E., and Tiera, E. (2015). Assessing the role of phytoplankton-bacterioplankton coupling in response the response of microbial plankton to nutrient additions. *J. Plankton Res.* 38, 55–63. doi: 10.1093/plankt/fbv101

Ramanan, R., Kim, B.-H., Cho, D.-H., Oh, H.-M., and Kim, H.-S. (2015). Algae–bacteria interactions: evolution, ecology and emerging applications. *Biotechnol. Adv.* 34, 14–29. doi: 10.1016/j.biotechadv.2015.12.003

Seibold, A., Wichels, A., and Schütt, C. (2001). Diversity of endocytic bacteria in the dinoflagellate *Noctiluca scintillans*. *Aquat. Microb. Ecol.* 25, 229–235. doi: 10.3354/ame025229

Seong, K. A., Jeong, H. J., Kim, S., Kim, G. H., and Kang, J. H. (2006). Bacterivory by co-occurring red-tide algae, heterotrophic nanoflagellates, and ciliates. *Mar. Ecol. Prog. Ser.* 322, 85–97. doi: 10.3354/meps322085

Seyedsayamdost, M. R., Case, R. J., Kolter, R., and Clardy, J. (2011). The Jekyll–and–Hyde chemistry of *Phaeobacter gallaeciensis*. *Nat. Chem.* 3, 331–335. doi: 10.1038/nchem.1002

Suminto, S., and Hirayama, K. (1997). Application of a growth promoting bacteria for stable mass culture of three marine microalgae. *Hydrobiologia* 358, 223–230. doi: 10.1023/A:1003109503745

Tanabe, Y., Okazaki, Y., Yoshida, M., Matsuura, H., Kai, A., Shiratori, T., et al. (2015). A novel alphaproteobacterial ectosymbiont promotes the growth of the hydrocarbon-rich green alga *Botryococcus braunii*. *Sci. Rep.* 5:10467. doi: 10.1038/srep10467

Thompson, P. (1999). Response of growth and biochemical composition to variations in daylength, temperature, and irradiance in the marine diatom *Thalassiosira pseudonana* (Bacillariophyceae). *J. Phycol.* 35, 1215–1223. doi: 10.1046/j.1529-8817.1999.3561215.x

Turner, J. T., Tester, P. A., and Hansen, P. J. (1998). "Intertactions between toxic marine phytoplanktion and metazoan and protistan grazers," in *Physiological Ecology of Harmful Algal Blooms*, eds D. M. Anderson, A. D. Cembella, and G. M. Hallegraeff (Berlin: Springer- Veralag), 453–474.

Veldhuis, M. J. W., Kraay, G. W., and Timmermans, K. R. (2001). Cell death in phytoplankton: correlation between changes in membrane permeability, photosynthetic activity, pigmentation and growth. *Eur. J. Phycol.* 36, 167–177. doi: 10.1080/09670260110001735318

Wang, H., Tomasch, J., Jarek, M., and Wagner-Döbler, I. (2014). A dual-species co-cultivation system to study the interactions between *Roseobacter*s and dinoflagellates. *Front. Microbiol.* 5:311. doi: 10.3389/fmicb.2014.00311

Wang, H., Tomasch, J., Michael, V., Bhuju, S., Jarek, M., Petersen, J., et al. (2015). Identification of genetic modules mediating the Jekyll and Hyde interaction of *Dinoroseobacter shibae* with the dinoflagellate *Prorocentrum minimum*. *Front. Microbiol.* 6:1262. doi: 10.3389/fmicb.2015.01262

Wheeler, P. A., and Kirchman, D. L. (1986). Utilization of inorganic and organic nitrogen by bacteria in marine systems. *Limnol. Oceanogr.* 31, 998–1009. doi: 10.4319/lo.1986.31.5.0998

Wiebe, W. J., and Pomeroy, L. R. (1999). "The temperature-substrate controversy resolved?," in *Microbial Biosystems: New Frontiers, Proceedings of the 8th International Symposium on Microbial Ecology*, eds C. R. Bell, M. J. Brylinsky, and P. Johnson-Green (Halifax, NS).

Conflict of Interest Statement: The authors declare that the research was conducted in the absence of any commercial or financial relationships that could be construed as a potential conflict of interest.

frontiers in Microbiology

ORIGINAL RESEARCH
published: 06 May 2016
doi: 10.3389/fmicb.2016.00560

The Vitamin B_1 and B_{12} Required by the Marine Dinoflagellate *Lingulodinium polyedrum* Can Be Provided by Its Associated Bacterial Community in Culture

Ricardo Cruz-López and Helmut Maske*

Oceanografía Biológica, Centro de Investigación Científica y de Educación Superior de Ensenada, Ensenada, Mexico

In this study we established the B_1 and B_{12} vitamin requirement of the dinoflagellate *Lingulodinium polyedrum* and the vitamin supply by its associated bacterial community. In previous field studies the B_1 and B_{12} demand of this species was suggested but not experimentally verified. When the axenic vitamin un-supplemented culture (B-ns) of *L. polyedrum* was inoculated with a coastal bacterial community, the dinoflagellate's vitamin growth limitation was overcome, reaching the same growth rates as the culture growing in vitamin $B_1B_7B_{12}$-supplemented (B-s) medium. Measured B_{12} concentrations in the B-s and B-ns cultures were both higher than typical coastal concentrations and B_{12} in the B-s culture was higher than in the B-ns culture. In both B-s and B-ns cultures, the probability of dinoflagellate cells having bacteria attached to the cell surface was similar and in both cultures an average of six bacteria were attached to each dinoflagellate cell. In the B-ns culture the free bacterial community showed significantly higher cell abundance suggesting that unattached bacteria supplied the vitamins. The fluorescence *in situ* hybridization (FISH) protocol allowed the quantification and identification of three bacterial groups in the same samples of the free and attached epibiotic bacteria for both treatments. The relative composition of these groups was not significantly different and was dominated by Alphaproteobacteria (>89%). To complement the FISH counts, 16S rDNA sequencing targeting the V3–V4 regions was performed using Illumina-MiSeq technology. For both vitamin amendments, the dominant group found was Alphaproteobacteria similar to FISH, but the percentage of Alphaproteobacteria varied between 50 and 95%. Alphaproteobacteria were mainly represented by *Marivita* sp., a member of the *Roseobacter* clade, followed by the Gammaproteobacterium *Marinobacter flavimaris*. Our results show that *L. polyedrum* is a B_1 and B_{12} auxotroph, and acquire both vitamins from the associated bacterial community in sufficient quantity to sustain the maximum growth rate.

Keywords: B vitamin auxotrophy, dinoflagellate–bacteria interactions, fluorescence *in situ* hybridization (FISH), 16S rDNA, Illumina-MiSeq sequencing

OPEN ACCESS

Edited by:
Xavier Mayali, Lawrence Livermore National Laboratory, USA

Reviewed by:
Laura Gomez-Consarnau, University of Southern California, USA
David H. Green, Scottish Association for Marine Science, UK

****Correspondence:***
Ricardo Cruz-López
ricardo.crlp@gmail.com

Specialty section:
This article was submitted to Aquatic Microbiology, a section of the journal Frontiers in Microbiology

Received: *14 January 2016*
Accepted: *04 April 2016*
Published: *06 May 2016*

Citation:
Cruz-López R and Maske H (2016) The Vitamin B_1 and B_{12} Required by the Marine Dinoflagellate Lingulodinium polyedrum Can Be Provided by Its Associated Bacterial Community in Culture. Front. Microbiol. 7:560. doi: 10.3389/fmicb.2016.00560

INTRODUCTION

Culture-based (Tang et al., 2010) and field studies (Bertrand et al., 2007; Gobler et al., 2007; Koch et al., 2011, 2012) have supported long standing hypothesis that vitamin availability can have an impact on phytoplankton growth and community composition (Droop, 2007). A majority of eukaryotic phytoplankton requires exogenous B vitamins, hence being B vitamin auxotroph. They are lacking the biosynthetic pathways to produce them or alternative pathways to bypass the need for the vitamin as in the case of B_{12}. Of the examined species 54% required vitamin B_{12} (cobalamin; hereafter B_{12}), 27% required vitamin B_1 (thiamine; hereafter B_1) and 8% required vitamin B_7 (biotin; hereafter B_7) (Tang et al., 2010). B_{12} is essential for the synthesis of amino acids, deoxyriboses, and the reduction and transfer of single carbon fragments in many biochemical pathways. B_1 plays a pivotal role in intermediary carbon metabolism and is a cofactor for a number of enzymes involved in primary carbohydrate and branched-chain amino acid metabolism. B_7 is a cofactor for several essential carboxylase enzymes, including acetyl coenzyme A (CoA) carboxylase, which is involved in fatty acid synthesis, and so is universally required (Croft et al., 2006; Tang et al., 2010).

Dinoflagellates are among the most abundant eukaryotic phytoplankton in freshwater and coastal systems (Moustafa et al., 2010). Of the 45 examined dinoflagellate species, those species involved in harmful algal bloom events, 100% required B_{12}, 78% B_1 and 32% B_7 (Tang et al., 2010). Available genomic data indicate that some heterotrophic bacteria and archaea, as well marine cyanobacteria are vitamin producers (Bonnet et al., 2010; Sañudo-Wilhelmy et al., 2014). Many dinoflagellates are mixotrophs (Burkholder et al., 2008), therefore they could acquire their B vitamins from the environment either through phagotrophy (Jeong et al., 2005), active uptake from the soluble fraction (Bertrand et al., 2007; Kazamia et al., 2012) or through episymbiosis (Croft et al., 2005; Wagner-Döbler et al., 2010; Kazamia et al., 2012; Kuo and Lin, 2013; Xie et al., 2013). The relative contribution of these different mechanisms to vitamin acquisition of dinoflagellates is not known but could help in the understanding of dinoflagellate ecology and the possible role of vitamins in bloom development.

Lingulodinium polyedrum is a dinoflagellate with a mixotrophic lifestyle (Jeong et al., 2005) that is recurrently forming blooms along the coast of southern California and northern Baja California (Peña-Manjarrez et al., 2005). Although its physiology (Hastings, 2007; Beauchemin et al., 2012) and microbial ecology (Mayali et al., 2008, 2010, 2011) have been previously studied, its vitamin auxotrophy has only been inferred from oceanographic observations (Carlucci, 1970), but has not been experimentally established. Here we investigate the role of vitamins and bacteria in the autecology of *L. polyedrum*, using axenic and non-axenic cultures of *L. polyedrum* under different combinations of multiple and single vitamin limitation.

To document the association of a natural bacterial community in *L. polyedrum* cultures under $B_1B_7B_{12}$-supplemented (hereafter B-s) and $B_1B_7B_{12}$-not supplemented (hereafter B-ns) cultures, we employed a FISH and digital imaging approach to quantify free and attached bacteria, and 16S rDNA sequencing targeting V3–V4 regions looking for phylogenetic composition. To complement the information on the B_{12} synthesis, we quantified the B_{12} in both vitamin amendments.

MATERIALS AND METHODS

Strain and Growth Conditions

Coastal seawater was collected off Ensenada (31.671° N, 116.693° W; Ensenada, México) treated with activated charcoal, filtered through GF/F, and 0.22-mm pore-size cartridge filter (Pall corporation) and stored in the dark at room temperature to age for at least 2 months. Aged seawater was sparged with CO_2 (5 min per 1 L of seawater), autoclaved for 15 min and then equilibrated with air. Non-axenic *L. polyedrum* HJ culture (Latz Laboratory, UCSD-SIO) was grown in L1 medium (National Center for Marine Algae and Microbiota, Boothbay, ME, USA) prepared with aged oceanic water under 12:12 h light/dark cycle at an irradiance level of 100 μmol m^2 s^{-1} and a temperature of 20°C. To make the culture axenic, *L. polyedrum* cultures were incubated with 1 ml of antibiotic solution (Penicillin, 5,000 U; Streptomycin, 5 mg ml^{-1}; Neomycin, 10 mg ml^{-1}. Sigma–Aldrich, P4083-100ML) for 50 ml of culture during 24 h, rinsed with L1 medium, and repeated three times each step. Bacterial presence in the *L. polyedrum* culture was checked by staining with the nucleic acid-specific stain 4′,6-diamino-2-phenylindole (DAPI,1 μg ml^{-1}) and quantification using epifluorescence microscopy (Axioskope II plus, Carl Zeiss, Oberkochen, Germany) connected by liquid light guide to a 175 W xenon arc lamp (Lambda LS, Sutter), with optical filtering (Excitation, 360 nm/Dichroic, 395 nm / Emission, >397 nm; Semrock and Zeiss) under X100 objective lens (Plan-Apochromat, Carl Zeiss). The axenic status was declared when after three antibiotic rounds and sterile medium washes we could not detect bacteria in the culture through epifluorescence microscopy. Semi-continuous cultures were transferred approximately weekly using 10 × dilutions.

Qualitative Assessment of B_1, B_7, and B_{12} Dinoflagellate Auxotrophy

Bacteria are a potential source of B_1, B_7, and B_{12}, making it necessary to establish axenic cultures before testing vitamin auxotrophy. To test the vitamin auxotrophic status of *L. polyedrum*, cultures ($n = 3$) were grown semi-continuously in 15 ml glass test tubes with silicon stoppers. Cultures were acclimated by five semi-continuous transfers during 5 weeks. The medium for *L. polyedrum* axenic cultures was supplemented either with the L1 vitamin mix (B_1, 296000; B_7, 2050; B_{12}, 370; pmol L^{-1}), or with the following combinations of vitamins, B_1+B_{12}, B_1+B_7, and B_7+B_{12} at the same concentration (B_1, Sigma–Aldrich; B_7, Sigma–Aldrich; B_{12}, Sigma–Aldrich). Cell growth rate was monitored by mixing first the cultures with an inclined rotating test tube holder (10 rpm) before measuring *in vivo* chlorophyll *a* fluorescence using a Turner Designs 10-000 fluorometer at the midpoint of the light phase. The specific growth rate (μ) was estimated according to the

equation $\mu = \ln(N2/N1)/(t2–t1)$: where N1 and N2 was *in vivo* chlorophyll *a* fluorescence in relative units (r. u.) at time 1 (t1) and time 2 (t2) respectively. Vitamin auxotrophy was declared when a culture ceased to grow in the absence of vitamins while growth persisted in parallel control treatments with added vitamin.

Qualitative Assessment of B_1 and B_{12} Synthesis from the Bacterial Community

The axenic *L. polyedrum* culture ($n = 3$) was inoculated with a prokaryotic community obtained by filtering (0.8 μm polycarbonate filter) rocky intertidal seawater (31.861755 °N, 116.668097°W; Ensenada, México). *L. polyedrum* culture lines were divided into B-s and B-ns cultures, and acclimated by culture transfer for 6 months to ensure depletion of the initial vitamin present and to be sure that the persisting microbial community had the potential to synthesize vitamins. The specific growth rate was monitored as described above, taking the day eight as t2 and day zero as t1.

Cell Fixation, Immobilization, and Embedding

Five mililiter of *L. polyedrum* cells from B-s and B-ns cultures were harvested at lag, exponential and stationary phase and fixed with paraformaldehyde-PBS at a final concentration of 1% for 12 h at 4°C. For attached bacteria, fixed cells were immobilized onto an 8.0 μm pore size, 25 μm-diameter Nucleopore filter (Whatman International, Ltd., Maidstone, England) using a pressure difference of <3.3 kPa to avoid cell disintegration, and rinsed with phosphate-buffered saline (PBS,0.1 M NaCl, 2 mM KCl, 4 mM Na_2HPO_4, pH 8.1; Palacios and Marín, 2008). For free-living bacteria, the fraction which passed through 8.0 μm pore size filter was collected on 0.2 μm pore size, 25 mm-diameter Nucleopore filter (Whatman International, Ltd., Maidstone, England) and rinsed with PBS. The cells collected on the 8.0 μm filter were covered with 13 μl of low-melting point agarose (0.05%, LMA) (BioRad, 161-3111) at 55°C, dried for 15 min at 37°C, then LMA was added again and the filter dried as previously.

Fluorescence *In Situ* Hybridization

All *in situ* hybridizations were performed as described in Cruz-López and Maske (2014). In brief, before hybridization, bacterial cells were partially digested with 400,000 U ml^{-1} lysozyme (Sigma, L6876) dissolved in buffer containing 100 mM Tris-HCl, 50 mM EDTA, pH 8.0 for 1 h at 37°C. The enzyme reaction was stopped by rinsing the filter three times with 5 ml sterile water for 1 min at 4°C. Fixed and embedded samples were hybridized with a buffer containing 900 mM NaCl, 20 mM Tris-HCl, 0.02% SDS, pH 8.0. When probes with different stringency optima were applied to the same sample, sequential hybridization was performed, beginning with the probes requiring the most stringent conditions. Probes and hybridization conditions are listed in **Table 1**. Hybridizations containing 1 μl of probe for every 20 μl of buffer (final probe concentration = 25 ng μl^{-1}) were performed at 46°C for 2 h. After this, filters were washed with pre-warmed (48°C) buffer (900 mM NaCl, 20 mM Tris-HCl, 0.02% SDS, 5 μM EDTA) for 15 min and rinsed for 5 min in distilled H_2O. To be able to localize the theca and bacterial cells, we used Calcofluor (Sigma-Aldrich, México City, México) (1 μg ml^{-1}) and for DNA staining 4,6-diamino-2-phenylindole (DAPI Molecular Probes) (1 μl ml^{-1}), incubating 5 min in the dark at room temperature. Filters were rinsed twice with sterile H_2O for 5 min, dried and mounted in antifade reagent (Patel et al., 2007) and covered with cover slip.

Visualization

The epifluorescence microscope (Axioskope II plus, Carl Zeiss, Oberkochen, Germany; oil immersion X100 objective, Plan-Apochromat, Carl Zeiss; 175 W xenon arc lamp; Lambda LS, Sutter connected through a liquid light guide) was used with a triple Sedat filter, a dichroic filter with three transmission bands. Excitation and emission spectra were controlled by filter wheels (Lambda 10-3, Sutter). Images were captured with a cooled CCD camera (Clara E, Andor) with 10 ms integration time. Optical stacks, 2.0 μm focal distance between images, were acquired with a computer controlled focusing stage (Focus Drive, Ludl Electronic Products, Hawthorne, NY, USA) and Micro-Manager (version 1.3.40, Vale Lab, UCSF) that controlled filter selection and the focusing stage. The images were processed in ImageJ (Schneider et al., 2012). For each spectral channel a summary image was composed by selecting the pixels of maximum intensity within the stack, and using the 'Find Edges' and 'Despeckle' functions to reduce images noise (Cruz-López and Maske, 2014).

16S rRNA Gene Amplicon Sequencing

The free and attached bacterial communities from B-s and B-ns cultures were characterized and compared using barcoded high-throughput amplicon sequencing of the bacterial 16S rDNA. Four samples with no replicates were sequenced: (1) 50 ml of *L. polyedrum* cells from B-s and B-ns cultures were harvested at mid-exponential phase, and pre-filtered with (a) 8.0 μm pore size, 47 mm-diameter Nucleopore filter (Whatman International, Ltd., Maidstone, England) using a pressure difference of <3.3 kPa to avoid cell disintegration, with a second filtration step with (b) 0.4 μm pore size, 47 mm-diameter polycarbonate filter (Whatman International, Ltd., Maidstone, England) to recover the free-bacterial fraction, and (2) The first filter (a) containing the dinoflagellate cells were treated with 10 mM *N*-acetyl cysteine (NAC; Sigma) (PBS – 0.2 μM calcium chloride, 0.5 mM magnesium chloride, 15 mM glucose) for 1 h with agitation (70 rpm) at room temperature to detach adhered bacteria (Barr et al., 2013). The detached bacterial cells were collected onto a 0.4 μm pore size, 47 mm-diameter polycarbonate filter. Filters containing both free and detached bacterial communities were processed by the Research and Testing Laboratory (RTL, Lubbock, TX, USA), including DNA extraction. The bacterial hypervariable regions V3-V4 of the 16S rRNA gene were PCR amplified using the forward 341F (CCTACGGGNGGCWGCAG) and the reverse 805R (GACTACHVGGGTATCTAATCC) primers set (Herlemann et al., 2011) followed by sequencing on the MiSeq

TABLE 1 | Oligonucleotide probes used in this study.

Probe	Target group	Sequence (5′-3′)	Target site[a]	% Formamide in ISH[b] buffer	Reference
EUB338	Bacteria	GCTGCCTCCCGTAGGAGT	16S (338–355)[c]	0–50	Amann et al., 1990
NON338	Negative control	ACTCCTACGGGAGGCAGC	16S (338–355)[c]		Amann et al., 1990
ALF968	Alphaproteobacteria	GGTAAGGTTCTGCGCGTT	16S (968–986)[e]	20	Glöckner et al., 1999
CF319a	Bacteroidetes	TGGTCCGTGTCTCAGTAC	16S (319–336)[d]	35	Manz et al., 1996
GAM42a	Gammaproteobacteria	GCCTTCCCACATCGTTT	23S (1027–1043)[c]	35	Glöckner et al., 1999

[a]*E. coli* numbering; [b]*In situ* hybridization; [c]Cy3; [d]ATTO425; [e]Alexa594.

platform (Illumina Inc., USA). MiSeq reads were quality checked and paired reads joined using PEAR (Zhang et al., 2013), dereplicated using USEARCH (Edgar, 2010), OTU selected using UPARSE (Edgar, 2013) and chimera checked using UCHIME (Edgar et al., 2011) executed in *de novo* mode. Generated sequences then were run against the RDP classifier employing the NCBI database. All downstream analysis were done in the RTL facility using their standard pipeline. The MiSeq reads have been deposited in the NCBI Sequence Read Archive with accession number SRP071004.

Dissolved B_{12} Quantification

B_{12} was quantified during the mid-exponential phase in non-axenic B-s and B-ns cultures. Twenty mililiter of *L. polyedrum* cultures were harvested, and pre-filtered with 8.0 μm pore size, followed by a filtration step with 0.45 μm pore size, both 47 mm-diameter Nucleopore filter (Whatman International, Ltd., Maidstone, England) using a pressure difference of <3.3 kPa to avoid cell disintegration. B_{12} was pre-concentrated by solid phase (RP-C18) extraction according to Okbamichael and Sañudo-Wilhelmy (2004), the column was eluted with 5 ml methanol, the methanol was evaporated at 60°C with vacuum, and 50 μl of the concentrate was injected into the ELISA well plate for quantification (Immunolab GmbH, B12-E01. Kassel, Germany) according to Zhu et al. (2011).

Statistical Analysis

One-way ANOVA was used to compare growth rate curves of *L. polyedrum* under B-s and B-ns cultures, and to compare the B_{12} synthesis from both bacterial communities. Since the distribution of the number of attached bacteria per dinoflagellate cell was not normal, a Kruskal–Wallis test was used to assess the significance ($\alpha = 0.05$) in the number of attached bacterial during the *L. polyedrum* growth curve. All analysis were performed using the STATISTICA 7.1v software (Stat Soft Inc., USA).

RESULTS

Lingulodinium polyedrum Auxotrophy for B Vitamins

Lingulodinium polyedrum was grown axenically with (B-s) and without (B-ns) adding the L1 vitamin mix. B-s cultures continued growing after five subcultures, B-ns cultures started to show slower growth rates after one transfer, but only after the third transfer, the B-ns cultures stopped growing. To establish which B vitamins were limiting the growth of *L. polyedrum* we prepared cultures containing ($B_1B_7B_{12}$), (B_1B_{12}), (B_1B_7) and (B_7B_{12}). Under $B_1B_7B_{12}$-s condition, cultures continued growing after five subcultures. In the B_1B_{12}-s condition cultures showed the same growth rate as the $B_1B_7B_{12}$-s condition, whereas in B_1B_7-s and B_7B_{12}-s condition, the cultures ceased to grow. These experiments were repeated three times with the same result (**Figure 1**).

Co-Culture of *L. polyedrum* with a Natural Bacterial Community

Non-axenic *L. polyedrum* culture in B-ns condition could maintain growth through more than five culture transfers at growth rates similar ($p > 0.05$) to the axenic and the non-axenic, B-s cultures (**Figure 2**). These results suggest that the bacteria in the non-axenic culture could provide sufficient amounts of vitamins to sustain *L. polyedrum* growth. In the non-axenic cultures the concentration of freely suspended bacteria in the B-ns culture was significantly higher than in the B-s culture ($p < 0.05$; **Figure 3A**, **Supplementary Figure S1**). The mean number of attached bacteria ranged from 1 to 6 in B-s culture and from 1 to 12 in B-ns culture; in both types of non-axenic cultures the probability of *L. polyedrum* cells to have bacteria attached or the average number of bacteria attached to *L. polyedrum* cells were not significantly different ($p > 0.05$; **Figure 3B**).

Free and Attached Bacterial Community by FISH

A multiprobe FISH protocol was used to identify the major bacterial groups in *L. polyedrum* cultures that were either freely suspended or attached to the host cells (Cruz-López and Maske, 2014). These results showed that Alphaproteobacteria were abundant in the free and attached fractions of B-s and B-ns cultures. In both vitamin treatments Alphaproteobacteria comprised on average 80% of the bacterial community, while Gammaproteobacteria and Bacteroidetes were scarcely detected (**Figures 4A,B**). As stated in Biegala et al. (2002) when working with phytoplankton it is critical to use group-specific probes to discriminate the false positives coming from the plastids. In our samples we could discriminate the eubacterial probe (EUB338) from the group-specific probes this allowed us to confirm the group specific probes with bacteria attached to *L. polyedrum* cells.

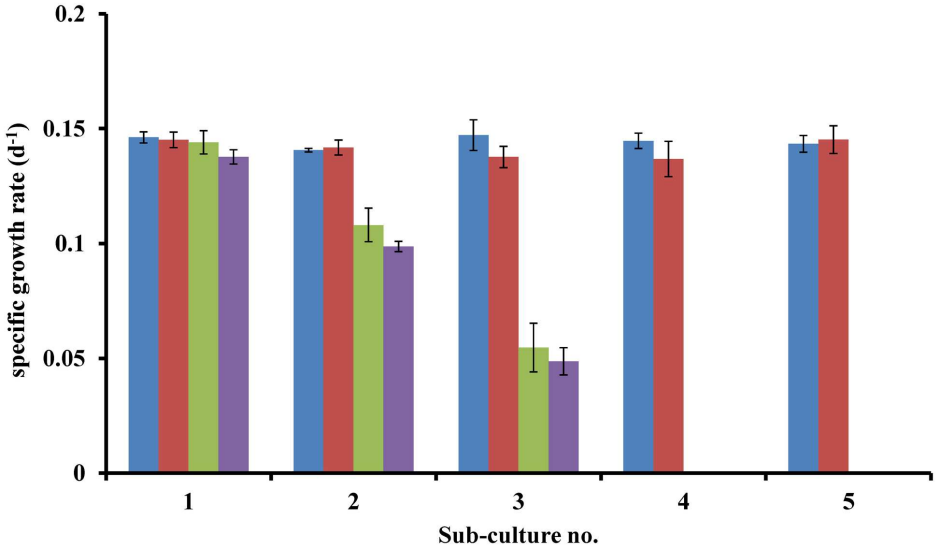

FIGURE 1 | Specific growth rates of axenic *L. polyedrum* grown in: (■) $B_1B_7B_{12}$-s; (■) B_1B_{12}-s; (■) B_1B_7-s; (■) B_7B_{12}-s cultures.

Free and Attached Bacterial Community by 16S Amplicons

We assessed the relative abundance of bacterial taxa at the level of phylum, class, genus and species for each sample. Four samples with no replicates were sequenced: the attached and the free living bacterial community of B-s and B-ns cultures.

In the B-s culture, most of the free-bacterial community reads were assigned to the class Alphaproteobacteria (49.6%), with *Marivita* sp. as the dominant species (35.8%), followed by *Maricaulis* sp. (6.5%) and *Pelagibaca* sp. (5.4%). The class Gammaproteobacteria represented 35.8%, with *Marinobacter flavimaris* as the dominant species (33.2%). Other phyla presented were Actinobacteria, Planctomycetes, Cyanobacteria and Firmicutes representing the 2.76%, while the unclassified reads represented the 9.64% (**Figure 5**).

In the B-ns culture, most of the free-bacterial community reads were assigned to the class Alphaproteobacteria comprising 93.6% of the detected sequences, with *Marivita* sp. as the dominant species in the sample (74.9%) followed by *Pelagibaca* sp. (9.1%), *Maricaulis* sp. (7.1%). The class Gammaproteobacteria represented 5.1%, dominated by *Marinobacter flavimaris* (4.8%). Other phyla presented were Actinobacteria, Planctomycetes, Cyanobacteria and Firmicutes representing less than 1%, while the unclassified reads represented the 1.4% (**Figure 5**)

In the B-s culture, even though the attached bacterial community was dominated by the Alphaproteobacteria (51.2%), the dominant species was the Bacteroidetes *Flaviicola* sp. (26.8%), followed by the Alphaproteobacteria *Marivita* sp. (20.3%), *Maricaulis* sp. (18.3%), *Erythrobacter* sp. (6.7%), *Pelagibaca* sp. (4.3%), and the Gammaproteobacteria *Marinobacter flavimaris* (8.6%). Other phyla presented were Planctomycetes, Actinobacteria, Firmicutes and Cyanobacteria representing 5.11% of the reads, while the unclassified reads represented 9.6% (**Figure 5**).

In the B-ns culture, the attached community was dominated by the class Alphaproteobacteria (66.3%), the dominant observed species were the Alphaproteobacteria *Marivita* sp. (45.7%), the Gammaproteobacteria *Marinobacter flavimaris* (16.3%), and the Bacteroidetes *Flaviicola* sp. (13.5%) (**Figure 5**) followed by the alphaproteobacterial species *Maricaulis* sp. (11.4%) and *Pelagibaca* sp. (8.2%) (**Figure 5**). Other phyla presented were Planctomycetes, Actinobacteria, Firmicutes and Cyanobacteria representing 1.58% of the reads, while the unclassified reads represented 2.9% (**Figure 5**).

Dissolved B_{12} Quantification

After 5 days during the mid-exponential phase, we quantified B_{12} in B-s and B-ns cultures; our results show that the synthesis of B_{12} from the microbial community varies between conditions. The initial B_{12} concentration in the L1 medium is 370 pmol L^{-1} (Guillard, 1975). In our cultures, we quantified the B_{12} during the exponential phase, in the B-s culture, the B_{12} was 26.3 ± 2.8 pmol L^{-1} ($n = 3$), and in the B-ns culture was 14.4 ± 7.6 pmol L^{-1} ($n = 3$).

In both cases, the differences of B_{12} in the cultures ($p < 0.05$) are the balance between the consumption of the *L. polyedrum* population and the synthesis and excretion from the microbial community. The vitamin mix of the L1 medium includes B_1 and B_7, and below we only discuss B_{12} because we could quantify its concentration.

DISCUSSION

Lingulodinium polyedrum and Vitamin Auxotrophy

Phytoplankton vitamin B auxotrophy has been previously observed in cultures (reviewed by Droop, 2007) and in natural

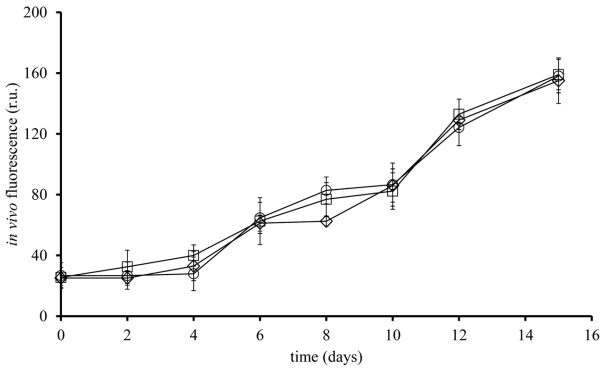

FIGURE 2 | Growth curve of *L. polyedrum*, axenic or in co-culture with a natural marine bacterial community. (□) axenic, B-s; (○) non-axenic, B-ns; (◊) non-axenic, B-ns. Each curve is the results of three culture replicates with the standard deviation indicated by vertical bars.

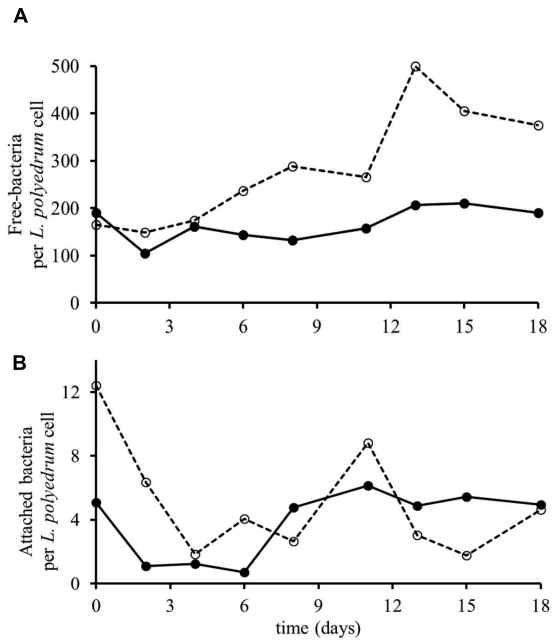

FIGURE 3 | Growth of *L. polyedrum* and associated bacteria culture under B-s (-●-) and B-ns (-○-) conditions. (A) Ratio of freely suspended bacteria to *L. polyedrum* cells. **(B)** Average number of bacteria attached to those *L. polyedrum* cells that had at least one bacteria attached. $n = 50$ dinoflagellate cells.

phytoplankton assemblages in coastal areas (Sañudo-Wilhelmy et al., 2006: Gobler et al., 2007; Koch et al., 2012). Here we address vitamin auxotrophy of *L. polyedrum* and its vitamin supply by natural bacterial communities. *L. polyedrum* was chosen because it forms coastal red tides and because previous studies had demonstrated high bacterial abundance and diversity of attached bacteria (Fandino et al., 2001; Mayali et al., 2011). Carlucci (1970) interpreted phytoplankton and B_{12} data from coastal waters of S. California and concluded that *L. polyedrum* was B_{12} auxotroph, but *L. polyedrum* vitamin B auxotrophy has not been previously tested experimentally. In our axenic cultures the sequential transfer into vitamin B free media led to a continuous reduction in growth rates until growth stopped. The continued growth of the first subcultures was probably supported by the vitamin present in the inoculum used for culture transfer, either in the medium or intracellularly. Further culture experiments demonstrated B_1 and B_{12} auxotrophy of *L. polyedrum* (**Figure 1**) similar to what has been reported for other dinoflagellate species (Tang et al., 2010). B_1 and B_{12} behaved like independent limiting factors, both vitamins were necessary to support growth.

Lingulodinium polyedrum is expected to be mixotrophic, potentially allowing for different modes of vitamin uptake; through osmotrophy, phagotrophy (Jeong et al., 2005) or through the episymbiosis with heterotrophic bacteria attached to cells (Croft et al., 2005). In our cultures the probability of bacterial attachment to *L. polyedrum* cells and the number of attached bacteria was not significantly different in B-ns and B-s cultures of *L. polyedrum* which argues against episymbiosis. The ratio of freely suspended bacteria to *L. polyedrum* cells did significantly increase in B-ns cultures, suggesting that vitamins for *L. polyedrum* growth were provided by part of the free bacterial community and then the dissolved vitamin was taken up by *L. polyedrum* and the auxotrophic part of the bacterial community.

The measured concentration of B_{12} in the B-ns non axenic culture was close to 50% lower than the B-s culture, but despite that, both concentrations are in the range of highly productive coastal systems (reviewed in Sañudo-Wilhelmy et al., 2014), Because culture concentrations were similar its seems probable that the B_{12} concentrations did not limit the *L. polyedrum* growth rate in culture. The concentrations in the culture without vitamin added were measured during exponential phase and represent the equilibrium concentration between the continuous supply from the bacterial consortium and the uptake by the dinoflagellate. In this case the bacterial consortium includes B_{12} producers and consumers with an overall B_{12} overproduction. It should be considered that the B-s culture received not only B_{12} but in addition B_1 and B_7. Because *L. polyedrum* is B_1 auxotroph the addition of this vitamin might influence the outcome of the equilibrium B_{12} concentration.

Although we found no increase in bacteria attached to *L. polyedrum*, the interaction between the free-bacterial community and *L. polyedrum* still constitute a form of symbiosis between vitamin producing bacteria in suspension and *L. polyedrum* where the latter provides the labile organics to the media to sustain the growth of the suspended bacteria. We did not measure dissolved organic carbon (DOC) in the culture medium but the medium was prepared from aged seawater and no DOC was added by us. Our data do not exclude the possibility of vitamin acquisition by either episymbiosis or phagocytosis, but we found no microscopic evidence for phagocytosis. We considered episymbiosis to be unlikely because of similar numbers and phylogenetic composition of attached bacteria, but attached epibionts could still contribute to the B_{12} supply (Wagner-Döbler et al., 2010).

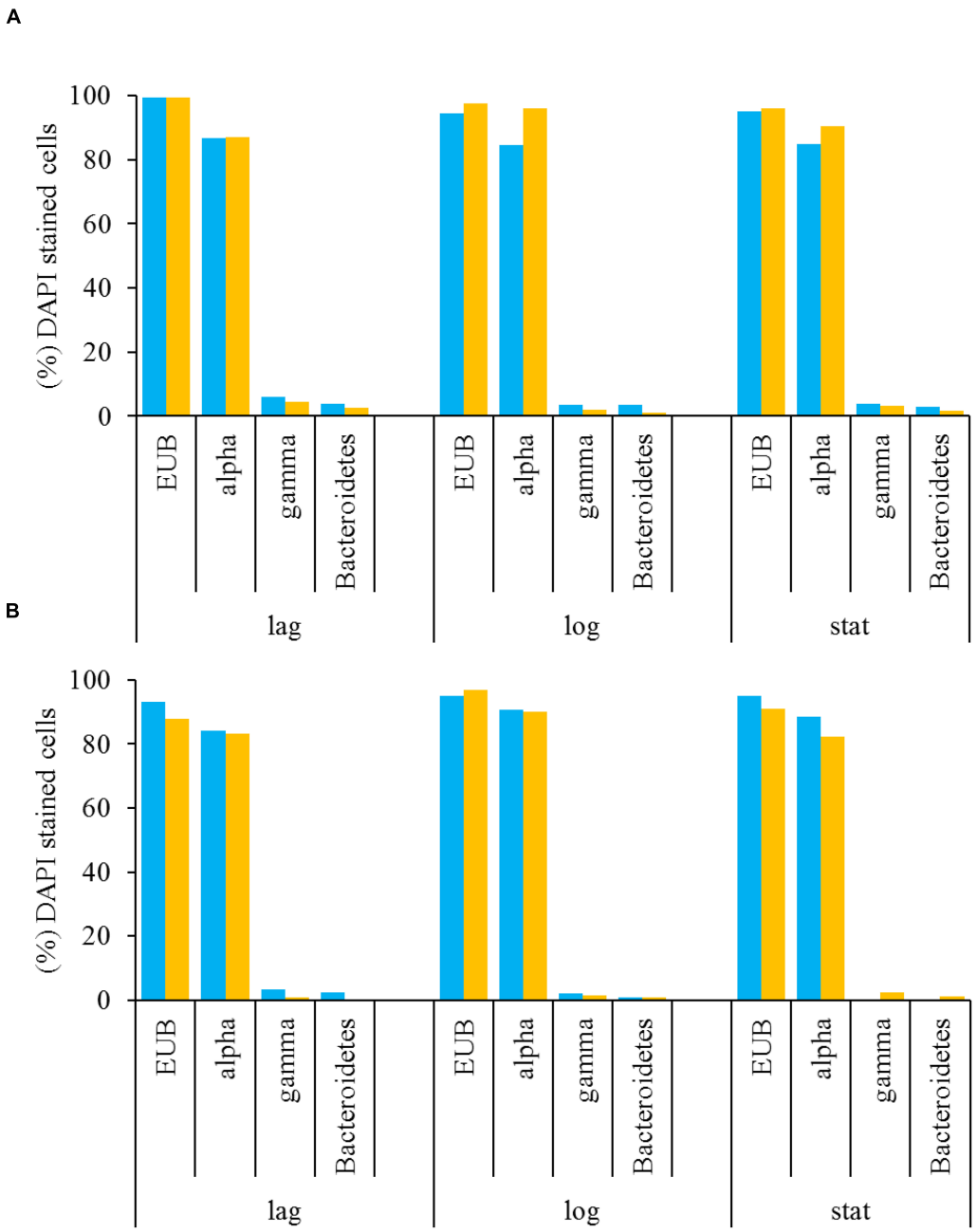

FIGURE 4 | Free-living (A) and attached (B) bacteria associated with *L. polyedrum* in B-ns (■) and B-s (■) cultures during different culture phases (lag, mid-exponential and stationary phases) given in percentages of the total number of DAPI-stained cells. Specific bacterial groups were quantified by FISH hybridized with the four probes listed in **Table 1**.

Free and Attached Bacterial Community by FISH

The selected probes used for FISH analysis were based on available probes for bacteria associated with dinoflagellates. This method identified Alphaproteobacteria as the dominant bacterial group in the attached and freely suspended bacterial community in B-s and B-ns cultures (**Figures 4A,B**). It is difficult to relate the dominance observed in this study to particular functional phenotypes, because the Alphaproteobacteria are metabolically diverse (Luo and Moran, 2014). However, recent evidence indicates that the Alphaproteobacteria could contribute with B_1 and B_{12} to their dinoflagellate host (Wagner-Döbler et al., 2010). The *Roseobacter* clade is an important marine Alphaproteobacteria lineage associated with dinoflagellates (Fandino et al., 2001; Hasegawa et al., 2007; Mayali et al., 2008, 2011) and includes species that produce B_1 and B_{12}

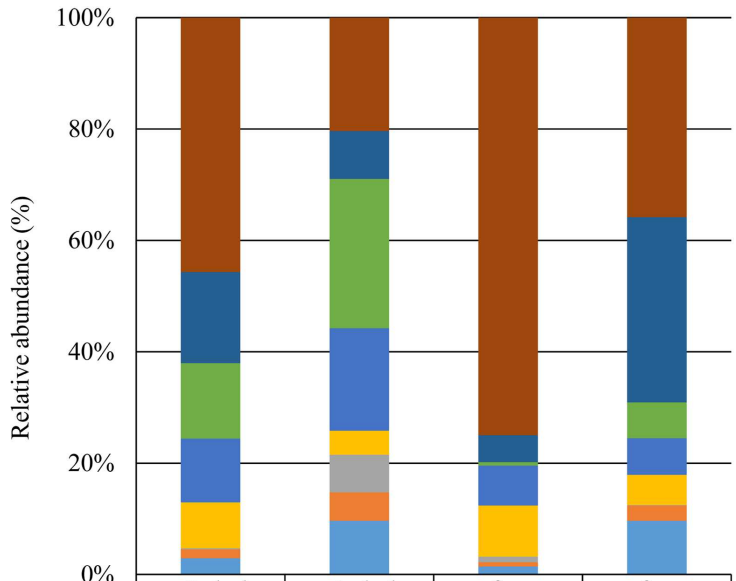

	attached (B-ns)	attached (B-s)	free (B-ns)	free (B-s)
Marivita sp.	45.70	20.34	74.98	35.81
Marinobacter flavimaris	16.34	8.64	4.82	33.27
Fluviicola sp.	13.56	26.82	0.63	6.46
Maricaulis sp.	11.45	18.37	7.19	6.57
Pelagibaca sp.	8.25	4.34	9.18	5.45
Erythrobacter sp.	0.18	6.73	0.99	0.04
Others	1.58	5.11	0.80	2.76
Unclassified	2.93	9.66	1.41	9.64

FIGURE 5 | Taxonomic classification of bacterial 16S rDNA (V3–V4) Illumina reads at species level.

(Wagner-Döbler et al., 2010). Bacteria within this clade are known to be epibionts of dinoflagellates, including *L. polyedrum* (Mayali et al., 2011) and can represent the most abundant group within the bacterial assemblages associated with phytoplankton cultures and during bloom conditions (Fandino et al., 2001; Hasegawa et al., 2007).

We also identified Gammaproteobacteria and Bacteroidetes as less frequent epibionts. Gammaproteobacteria and Bacteroidetes have been found previously in natural samples during bloom conditions (Fandino et al., 2001; Garcés et al., 2007; Mayali et al., 2011), their low attachment frequency in our cultures is in agreement with their low abundances reported in culture and field samples (Garcés et al., 2007). Genomic data about these two groups confirm that most Gammaproteobacteria have the metabolic potential to produce B_1 and B_{12}, whereas only some Bacteroidetes possess the pathway for B_1 but not for B_{12} (Sañudo-Wilhelmy et al., 2014).

The stable communities observed by FISH counts during the course of the culture (**Figures 4A,B**) suggest that Alphaproteobacteria and possibly *Roseobacter* clade species are an integral part of the epiphytic community of *L. polyedrum*. The similarity of probe frequency in attached and suspended fractions and in both vitamin amendments, suggests that bacteria of the different phylogenetic groups could move between both forms, thus, the bacterial community composition seemed more influenced by the host-specificity rather than the capacity to produce vitamins.

Free and Attached Bacterial Community by 16S Amplicons

Overall, the phylogenetic composition of the four samples was restricted to the Alphaproteobacteria and Gammaproteobacteria classes and Bacteroidetes phylum. The Alphaproteobacteria class dominated in the free and attached bacterial fraction.

In this study, *Marivita* sp. was more abundant in the B-ns culture in comparison with the B-s culture, suggesting a functional association with *L. polyedrum* for example as B vitamin producer, or potentially as suggested in Green et al. (2015) as a growth-promoter. Wagner-Döbler et al. (2010) and Durham et al. (2015) observed other members of the *Roseobacter* clade to be associated with phytoplankton such as *Dinoroseobacter shibae* and *Ruegeria pomeroyi* respectively.

The second most abundant species in our samples was *Marinobacter flavimaris*. *Marinobacter* genus has been reported in association with dinoflagellates in culture (Green et al., 2004, 2006, 2015; Hatton et al., 2012). This genus is known for having a mutualistic relationship with phytoplankton as an iron siderophore producer or as a growth promoter

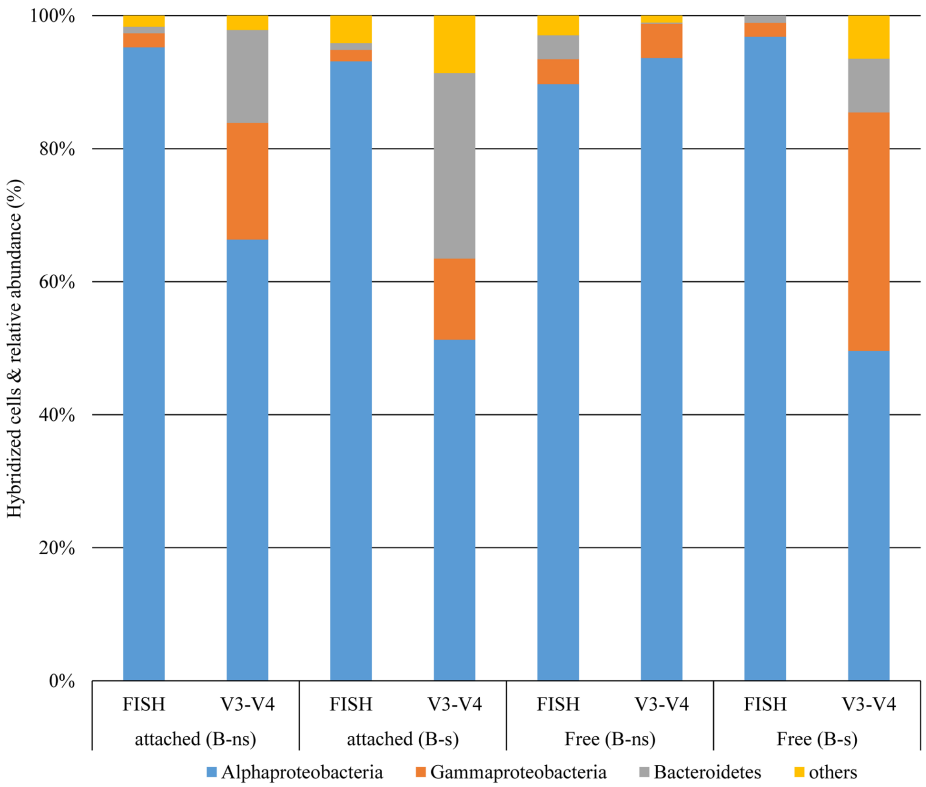

FIGURE 6 | Comparison of taxonomic classification of bacterial groups at phylum and class levels from 16 rDNA-FISH hybridization and 16S rDNA (V3–V4) Illumina reads.

(Amin et al., 2009; Bolch et al., 2011). During an iron-siderophore survey, *M. flavimaris* was isolated from different dinoflagellates species in culture but not from *L. polyedrum* (Amin et al., 2009). This species is phylogenetically related to *M. algicola, M. adhaerens,* and *M. aquaeolei* based on 16S rRNA sequence (Gärdes et al., 2010), however, its metabolic potential is expected to be rather different since *M. algicola* is known for siderophore production, *M. adhaerens* for the induction of marine organic matter aggregation and *M. aquaeolei* for its capacity to consume hydrocarbons. These different physiological profiles make it difficult to assume a metabolic potential for *M. flavimaris* based on the 16S rRNA gene.

In a recent study, Green et al. (2015) reported the co-occurrence of *Marivita* sp. and *Marinobacter* sp. in cultures of the coccolithophorids *Emiliania huxleyi* and *Coccolithus pelagicus* f. *braarudii*. In our data we have a similar co-occurrence of *Marivita* sp. and *Marinobacter flavimaris*; in the attached fraction, in the B-ns, the ratios were *Marivita* sp.: *M. flavimaris* 2.7:1, while in the B-s were 2.3:1. In the free-bacterial fraction, this ratio changed from 15.5:1 for the B-ns, to 1:1 for the B-s. Since iron was in replete conditions, our data suggest that this co-occurrence is more related to the vitamin supply.

The third most abundant species was from the phylum *Bacteroidetes*. This phylum has been recognized as specialist for the degradation of macromolecules, having a preference for growth attached to particles, surfaces or algal cells (Fernández-Gómez et al., 2013; Mann et al., 2013). Our data follow this pattern, since the attached fraction in B-s and B-ns cultures was enriched with member of this group. In the B-s condition, the *Bacteroidetes* accounted for 27%, mainly represented by *Fluviicola* sp., whereas in the B-ns culture, *Fluviicola* sp. represented 13.5% (**Figure 5**). This bacterial species has been previously reported during a *L. polyedrum* bloom, exhibiting its highest peak during the middle bloom stage, and a second peak at the end of the bloom, mainly clustered with other *Flavobacteria* species (Mayali et al., 2010, 2011).

Other alphaproteobacterial species were detected in the samples. *Maricaulis* sp. has been detected associated with toxic and non-toxic dinoflagellates in culture (Hold et al., 2001; Strömpl et al., 2003) but its relation to dinoflagellate ecophysiology is not known. Another species was *Pelagibaca* sp., and despite its enrichment in the B-ns amendment, its closest relative, *Pelagibaca bermudensis* HTCC2601 has only been detected with a free-living lifestyle (Slightom and Buchan, 2009), although some members of the *Roseobacter* clade, are known to have the potential to synthesize cobalamin, thiamine and iron siderophores (Newton et al., 2010). *Erythrobacter* sp. was an infrequent species but showed >1% in the B-s attached fraction. *Erythrobacter* sp., a marine aerobic anoxygenic phototroph like *Dinoroseobacter shibae* (Koblížek et al., 2003; Wagner-Döbler et al., 2010), is known for its free-living

lifestyle that is scarcely detected in dinoflagellate cultures (Green et al., 2015). Although FISH counts showed that the phylum Bacteroidetes was numerically less abundant in all dinoflagellate growth phases than other groups, the Illumina data showed that their contribution during exponential phase accounted for 13.98% of the attached bacteria (FISH 0.9%) for B-ns, and 27.8% (FISH 1%) in B-s; and for free-bacteria 0.1% (FISH 3.6%) for B-ns, and 8% (FISH 1%) for B-s (**Figure 6**).

The community composition obtained using FISH counts differed from the 16S rDNA amplicon reads (**Figure 6**). This type of difference has been observed before (Dawson et al., 2012; Lenchi et al., 2013). There are different possible explanations for these differences: FISH probe hybridization efficiency or the relative amount of inactive cells that could not be visualized by FISH were probably not responsible for the difference because the FISH count were checked against the eubacterial probe EUB338 and DAPI staining showing that most prokaryotes were stained by FISH (**Figures 4A,B**). Another explanation for the difference might have been the low coverage of the probe for the represented groups in the culture, given that probe ALF968 covers approximately 81% of the class Alphaproteobacteria, probe GAM42a covers approximately 76% of the class Gammaproteobacteria, and CF319a covers approximately 38% of the phylum Bacteroidetes (Amann and Fuchs, 2008). Because we were working with probes previously used in research related to the bacterial diversity associated with dinoflagellates (Alavi et al., 2001; Alverca et al., 2002; Biegala et al., 2002; Garcés et al., 2007; Cruz-López and Maske, 2014) we did not confirm the selected probes targeted sequences in our Illumina data set before FISH experiments. One simple reason for the difference could be that the primers used to target the V3-V4 region (V3 338-533, V4 576-682; *Escherichia coli* 16S SSU rDNA numbering) and the FISH probes covered different regions or even the 23S rDNA subunit (**Table 1**) did not allow us to make a direct correlation between the two techniques. Dawson et al. (2012) and Lenchi et al. (2013), suggested different explanations for the difference, the underrepresentation of some phyla, PCR primer or gene copy number bias in the 16S rRNA sequencing, or the possibility of bacterial groups not being properly covered by the probe combination used, and the low relative abundance arguments that we would reject for reasons mentioned above.

Dissolved B_{12} Synthesis from the Microbial Community

Our results show that although the concentration of B_{12} in the B-s culture was higher than in the B-ns culture, this difference should be the result of the initial supplemented concentration from L1. The B-s culture medium contained initially 370 pmol L^{-1} of B_{12} that was reduced to 26 pmol L^{-1} during culture growth, close to twice the concentration in the exponential phase B-ns culture of 14.4 pmol L^{-1}. The high consumption of B_{12} in the B-s culture might be due not only to *L. polyedrum* but also to the bacterial community. Neither of the culture concentrations was expected to be limiting the growth rate of *L. polyedrum* because these concentrations were as high as in very productive coastal waters. In the case of the B-ns culture the source of B_{12} was the microbial community maintaining the exponential growth phase of *L. polyedrum* while being supported by organic substrate provided by the phototroph host. The *L. polyedrum* biomass in B-ns and B-s cultures during vitamin sampling was similar. If we assume that the vitamin consumption is proportional to *L. polyedrum* biomass, neglecting B_{12} luxury uptake by *L. polyedrum*, consumption by bacteria or the production by bacteria in the B-s culture. From this we can roughly estimate that 370 -26 pmol L^{-1} of B_{12} was produced by the bacterial community during B-ns culture development to support the growth 8×10^6 *L. polyedrum* cells L^{-1} (**Supplementary Figure S1**), which amounts to 4×10^{-17} mol B_{12} $cell^{-1}$. This high potential of B_{12} production while being supported by organics provided by the auxotrophic *L. polyedrum* suggests an easy capacity for the bacterial community to supply the oceanic auxotrophs phototrophs with B_{12} as long as no other controls limit the bacterial development. Our data suggest that B_{12} synthesis in the *L. polyedrum*/bacterial community respond to changes in B_{12} concentration, and that the supply may depend on the extent of B_1 and B_{12} limitation, which in turn selects the bacterial community structure and it B_1 and B_{12} synthesis capacity. The next step to study the contribution of all players within this type of system would be the use of metatranscriptomics combined with mass-spectrometry for the quantification of gene expression levels and its products, to estimate the contribution of eukaryotic DOC exudation and bacterial products.

CONCLUSION

In this work we have shown that *L. polyedrum* is a B_1 and B_{12} auxotroph. Non-axenic cultures of *L. polyedrum* can acquire both vitamins from the associated bacterial community in sufficient quantity to sustain the maximum growth rate defined by culture conditions. The growth of the associated heterotrophic bacterial community was sustained by substrates provided by *L. polyedrum* because the culture medium was not amended with organic substrates.

Previous studies have shown B_{12} auxotrophy of dinoflagellates and diatoms species and the acquisition of B_{12} from a bacterial partner, however, is its known that, phytoplankton such as dinoflagellates not only require B_{12}, but also B_1, and they naturally interact with bacterial and archaeal communities, rather than with single bacterial species.

A small portion of the associated bacterial community was attached to the *L. polyedrum* cells; with or without vitamin addition to the culture medium the statistics of attachment, the proportion of *L. polyedrum* cells with bacteria attached or the number of bacteria attached to *L. polyedrum* cells did not change, but the abundance of freely suspended bacteria was significantly higher in B-ns culture. Using the same bacterial community inoculum, we showed that a characteristic bacterial community emerges even under contrasting vitamin amendments. We

demonstrate that by association, the microbial community in the B-ns culture was able to synthesize and excrete sufficient B_1 and B_{12} quantities to sustain the growth of its dinoflagellate host while being supported by organic substrates supplied by the host.

AUTHOR CONTRIBUTIONS

All authors listed, have made substantial, direct and intellectual contribution to the work, and approved it for publication.

FUNDING

This work was supported by the National Council of Science and Technology (CONACyT) project CB-2008-01 106003 (to HM) and a Ph.D. fellowship (to RC-L).

ACKNOWLEDGMENTS

We would like to thank the reviewers for constructive comments and suggestions. Professor Michael Latz (UCSD-Scripps Institution of Oceanography) kindly provided us with the *L. polyedrum* HJ strain.

SUPPLEMENTARY MATERIAL

The Supplementary Material for this article can be found online at: http://journal.frontiersin.org/article/10.3389/fmicb.2016.00560

FIGURE S1 | Growth of *L. polyedrum* and associated bacteria culture under B-s (-●-) and B-ns (-○-) conditions. (A) *L. polyedrum* abundance. **(B)** Free-bacteria abundance. **(C)** Percent of *L. polyedrum* cells colonized by bacteria.

REFERENCES

Alavi, M., Miller, T., Erlandson, K., Schneider, R., and Belas, R. (2001). Bacterial community associated with Pfiesteria-like dinoflagellate cultures. *Environ. Microbiol.* 3, 380–396. doi: 10.1046/j.1462-2920.2001.00207.x

Alverca, E., Biegala, I. C., Kennaway, G. M., Lewis, J., and Franca, S. (2002). In situ identification and localization of bacteria associated with *Gyrodinium instriatum* (Gymnodiniales, Dinophyceae) by electron and confocal microscopy. *Eur. J. Phycol.* 37, 523–530. doi: 10.1017/S0967026202003955

Amann, R., and Fuchs, B. M. (2008). Single-cell identification in microbial communities by improved fluorescence in situ hybridization techniques. *Nat. Rev. Microbiol.* 6, 339–348. doi: 10.1038/nrmicro1888

Amann, R. I., Binder, B. J., Olson, R. J., Chisholm, S. W., Devereux, R., and Stahl, D. A. (1990). Combination of 16S rRNA-targeted oligonucleotide probes with flow cytometry for analyzing mixed microbial populations. *Appl. Environ. Microbiol.* 56, 1919–1925.

Amin, S. A., Green, D. H., Hart, M. C., Küpper, F. C., Sunda, W. G., and Carrano, C. J. (2009). Photolysis of iron-siderophore chelates promotes bacterial-algal mutualism. *Proc. Natl. Acad. Sci. U.S.A.* 106, 17071–17076. doi: 10.1073/pnas.0905512106

Barr, J., Auro, R., Furlan, M., Whiteson, K. L., Erb, M. L., Pogliano, J., et al. (2013). Bacteriophage adhering to mucus provide a non-host-derived immunity. *Proc. Natl. Acad. Sci. U.S.A.* 110, 10771–10776. doi: 10.1073/pnas.1305923110

Beauchemin, M., Roy, S., Daoust, P., Dagenais-Bellefeuille, S., Bertomeu, T., Letourneau, L., et al. (2012). Dinoflagellate tandem array gene transcripts are highly conserved and not polycistronic. *Proc. Natl. Acad. Sci. U.S.A.* 109, 15793–15798. doi: 10.1073/pnas.1206683109

Bertrand, E. M., Saito, M. A., Rose, J. M., Riesselman, C. R., Lohan, M. C., Noble, A. E., et al. (2007). Vitamin B12 and iron co-limitation of phytoplankton growth in the Ross Sea. *Limnol. Oceanogr.* 52, 1079–1093. doi: 10.4319/lo.2007.52.3.1079

Biegala, I. C., Kennaway, G., Alverca, E., Lennon, J. F., Vaulot, D., and Simon, N. (2002). Identification of bacteria associated with dinoflagellates (Dinophyceae) *Alexandrium* spp. using tyramide signal amplification-fluorescence in situ hybridization and confocal microscopy. *J. Phycol.* 38, 404–411. doi: 10.1046/j.1529-8817.2002.01045.x

Bolch, C. J. S., Subramanian, T. A., and Green, D. H. (2011). The toxic dinoflagellate *Gymnodinium catenatum* (Dinophyceae) requires marine bacteria for growth. *J. Phycol.* 47, 1009–1022. doi: 10.1111/j.1529-8817.2011.01043.x

Bonnet, S., Webb, E. A., Panzeca, C., Karl, D., Capone, D. G., and Sañudo-Wilhelmy, S. A. (2010). Vitamin B12 excretion by cultures of the marine cyanobacteria *Crocosphaera* and *Synechococcus*. *Limnol. Oceanogr.* 55, 1959–1964. doi: 10.4319/lo.2010.55.4.1959

Burkholder, J. M., Glibert, P. M., and Skelton, H. M. (2008). Mixotrophy, a major mode of nutrition for harmful algal species in eutrophic waters. *Harm. Alg.* 8, 77–93. doi: 10.1016/j.hal.2008.08.010

Carlucci, A. F. (1970). "Part II. Vitamin B12, thiamine, biotin," in *The Ecology of the Phytoplankton Off La Jolla*, ed. J. D. H. Strickland (Berkeley: University of California Press), 23–31.

Croft, M. T., Lawrence, A. D., Raux-Deery, E., Warren, M. J., and Smith, A. G. (2005). Algae acquire vitamin B12 through a symbiotic relationship with bacteria. *Nature* 438, 90–93. doi: 10.1038/nature04056

Croft, M. T., Warren, M. J., and Smith, A. G. (2006). Algae need their vitamins. *Euk. Cell* 5, 1175–1183. doi: 10.1128/EC.00097-06

Cruz-López, R., and Maske, H. (2014). A non-amplified FISH protocol to identify simultaneously different bacterial groups attached to eukaryotic phytoplankton. *J. Appl. Phycol.* 27, 797–804. doi: 10.1007/s10811-014-0379-2

Dawson, K. S., Strapoć, D., Huizinga, B., Lidstrom, U., Ashby, M., and Macalady, J. L. (2012). Quantitative fluorescence in situ hybridization analysis of microbial consortia from a biogenic gas field in Alaska's Cook Inlet basin. *Appl. Environ. Microbiol.* 78, 3599–3605. doi: 10.1128/AEM.07122-11

Droop, M. M. (2007). Vitamins, phytoplankton and bacteria: symbiosis or scavenging? *J. Plankton Res.* 29, 107–113. doi: 10.1093/plankt/fbm009

Durham, B. P., Sharma, S., Luo, H., Smith, C. B., Amin, S. A., Bender, S. J., et al. (2015). Cryptic carbon and sulfur cycling between surface ocean plankton. *Proc. Natl. Acad. Sci. U.S.A.* 112, 453–457. doi: 10.1073/pnas.1413137112

Edgar, R. C. (2010). Search and clustering orders of magnitude faster than BLAST. *Bioinformatics* 26, 2460–2461. doi: 10.1093/bioinformatics/btq461

Edgar, R. C. (2013). UPARSE: highly accurate OTU sequences from microbial amplicon reads. *Nat. Methods* 10, 996–998. doi: 10.1038/nmeth.2604

Edgar, R. C., Haas, B. J., Clemente, J. C., Quince, C., and Night, R. (2011). UCHIME improves sensitivity and speed of chimera detection. *Bioinformatics* 27, 2194–2200. doi: 10.1093/bioinformatics/btr381

Fandino, L. B., Riemann, L., Steward, G. F., Long, R. A., and Azam, F. (2001). Variations in the bacterial community structure during a dinoflagellate bloom analyzed by DGGE and 16S rDNA sequencing. *Aquat. Microbiol. Ecol.* 23, 119–130. doi: 10.3354/ame023119

Fernández-Gómez, B., Richter, M., Schüler, M., Pinhassi, J., Acinas, S. G., González, J. M., et al. (2013). Ecology of marine Bacteroidetes: a comparative genomics approach. *ISME J.* 7, 1026–1037. doi: 10.1038/ismej.2012.169

Garcés, E., Vila, M., Reñé, A., Alonso-Sáez, L., Angles, S., Luglie, A., et al. (2007). Natural bacterioplankton assemblage composition during blooms of *Alexandrium* spp. (Dinophyceae) in NW Mediterranean coastal waters. *Aquat. Microb. Ecol.* 46, 55–70. doi: 10.3354/ame046055

Gärdes, A., Kaeppel, E., Shehzas, A., Seebah, S., Teeling, H., Yarza, P., et al. (2010). Complete genome sequence of *Marinobacter adhaerens* type strain (HP15), a diatom-interacting marine microorganism. *Stand. Genom. Sci.* 3, 97–107. doi: 10.1073/pnas.0905512106

Glöckner, F. O., Fuchs, B. M., and Amann, R. (1999). Bacterioplankton compositions of lakes and oceans: a first comparison based on fluorescence in situ hybridization. *Appl. Environ. Microbiol.* 65, 3721–3726.

Gobler, C. J., Norman, C., Panzeca, C., Taylor, G. T., and Sañudo-Wilhelmy, S. A. (2007). Effect of B-vitamins (B1, B12) and inorganic nutrients on algal bloom dynamics in a coastal ecosystem. *Aquat. Microbiol. Ecol.* 49, 181–194. doi: 10.3354/ame01132

Green, D. H., Bowman, J. P., Smith, E. A., Gutierrez, T., and Bolch, C. J. (2006). *Marinobacter algicola* sp. nov., isolated from laboratory cultures of paralytic shellfish toxin-producing dinoflagellates. *Int. J. Syst. Evol. Microbiol.* 56, 523–527. doi: 10.1099/ijs.0.63447-0

Green, D. H., Echavarri-Bravo, V., Brennan, D., and Hart, M. C. (2015). Bacterial Diversity associated with the *Coccolithophorid algae Emiliania huxleyi* and *Coccolithus pelagicus* f. braarudii. *Biomed. Res. Int.* 2015:194540. doi: 10.1155/2015/194540

Green, D. H., Llewellyn, L. E., Negri, A. P., Blackburn, S. I., and Bolch, C. J. S. (2004). Phylogenetic and functional diversity of the cultivable bacterial community associated with the paralytic shellfish poisoning dinoflagellate Gymnodinium catenatum. *FEMS. Microbiol. Ecol.* 46, 345–357. doi: 10.1016/S0168-6496(03)00298-8

Guillard, R. R. L. (1975). "Culture of phytoplankton for feeding marine invertebrates," in *Culture of Marine Invertebrate Animals*, eds W. L. Smith and M. H. Chanley (New York, NY: Plenum Press), 26–60.

Hasegawa, Y., Martin, J. L., Le Gresley, M., Burke, T., and Rooney-Varga, J. N. (2007). Microbial community diversity in the phycosphere of natural populations of the toxic alga, *Alexandrium fundyense*. *Environ. Microbiol.* 9, 3108–3121. doi: 10.1111/j.1462-2920.2007.01421.x

Hastings, J. W. (2007). The Gonyaulax clock at 50: translational control of circadian expression. *Cold Spring Harb. Symp. Quant. Biol.* 72, 141–144. doi: 10.1101/sqb.2007.72.026

Hatton, A. D., Shenoy, D. M., Hart, M. C., Mogg, A., and Green, D. H. (2012). Metabolism of DMSP, DMS and DMSO by the cultivable bacterial community associated with the DMSP-producing dinoflagellate *Scrippsiella trochoidea*. *Biogeochemistry* 110, 131–146. doi: 10.1007/s10533-012-9702-7

Herlemann, D. P., Labrenz, M., Jürgens, K., Bertilsson, S., Waniek, J. J., and Andersson, A. F. (2011). Transition in bacterial communities along the 2000 km salinity gradient of the Baltic Sea. *ISME J.* 5, 1571–1579. doi: 10.1038/ismej.2011.41

Hold, G. L., Smith, E. A., Rappé, M. S., Maas, E. W., Moore, E. R. B., Stroempl, C., et al. (2001). Characterization of bacterial communities associated with toxic and non-toxic dinoflagellates: *Alexandrium* spp. and *Scrippsiella trochoidea*. *FEMS Microbiol. Ecol.* 37, 161–173. doi: 10.1111/j.1574-6941.2001.tb00864.x

Jeong, H. J., Yoo, Y. D., Park, J. Y., Song, J. Y., Kim, S. T., Lee, S. H., et al. (2005). Feeding by phototrophic red-tide dinoflagellates: five species newly revealed and six species previously known to be mixotrophic. *Aquat. Microb. Ecol.* 40, 133–150. doi: 10.3354/ame040133

Kazamia, E., Czesnick, H., Nguyen, T. T., Croft, M. T., Sherwood, E., Sasso, S., et al. (2012). Mutualistic interactions between vitamin B (12)-dependent algae and heterotrophic bacteria exhibit regulation. *Environ. Microbiol.* 14, 1466–1476. doi: 10.1111/j.1462-2920.2012.02733.x

Koblížek, M., Béjà, O., Bidigare, R. R., Christensen, S., Benitez-Nelson, B., Vetriani, C., et al. (2003). Isolation and characterization of *Erythrobacter* sp. strains from the upper ocean. *Arch. Microbiol.* 180, 327–338. doi: 10.1007/s00203-003-0596-6

Koch, F., Hattenrath-Lehmann, T. K., Goleski, J. A., Sañudo-Wilhelmy, S., Fisher, N. S., and Gobler, C. J. (2012). Vitamin B1 and B12 uptake and cycling by plankton communities in coastal ecosystems. *Front. Microbiol.* 3:363. doi: 10.3389/fmicb.2012.00363

Koch, F., Marcoval, A., Panzeca, C., Bruland, K. W., Sañudo-Wilhelmy, S. A., and Gobler, C. J. (2011). The effects of vitamin B12 on phytoplankton growth and community structure in the Gulf of Alaska. *Limnol. Oceanogr.* 3, 1023–1034. doi: 10.4319/lo.2011.56.3.1023

Kuo, R. C., and Lin, S. (2013). Ectobiotic and endobiotic bacteria associated with *Eutreptiella* sp. Isolated from Long Island sound. *Protist* 164, 60–74. doi: 10.1016/j.protis.2012.08.004

Lenchi, N., Inceoğlu, O., Kebbouche-Gana, S., Gana, M. L., Llirós, M., Servais, P., et al. (2013). Diversity of microbial communites in production and injection waters of algerian oilfields revealed by 16S rRNA gene amplicon 454 pyrosequencing. *PLoS ONE* 8:e66588. doi: 10.1371/journal.pone.0066588

Luo, H., and Moran, M. A. (2014). Evolutionary ecology of the marine *Roseobacter* clade. *Microbiol. Mol. Biol. Biol. Rev.* 78, 573–587. doi: 10.1128/MMBR.00020-14

Mann, A. J., Hahnke, R. L., Huang, S., Werner, J., Xing, P., Barbeyron, T., et al. (2013). The genome of the alga-associated marine flavobacterium Formosa agariphila KMM 3901T reveals a broad potential for degradation of algal polysaccharides. *Appl. Environ. Microbiol.* 79, 6813–6822. doi: 10.1128/AEM.01937-13

Manz, W., Amann, R., Ludwing, W., Vancanneyt, M., and Schleifer, K.-H. (1996). Application of a suite of 16S rRNA-specific oligonucleotide probes designed to investigate bacteria of the phylum cytophaga-flavobacter-*bacteroides* in the natural environment. *Microbiology* 142, 1097–1106. doi: 10.1099/13500872-142-5-1097

Mayali, X., Franks, P. J. S., and Azam, F. (2008). Cultivation and ecosystem role of marine RCA cluster bacteria. *Appl. Environ. Microbiol.* 74, 2595–2603. doi: 10.1128/AEM.02191-07

Mayali, X., Franks, P. J. S., and Burton, R. S. (2011). Temporal attachment dynamics by distinct bacterial taxa during a dinoflagellate bloom. *Aquat. Microb. Ecol.* 63, 111–122. doi: 10.3354/ame01483

Mayali, X., Palenik, B., and Burton, R. S. (2010). Dynamics of marine bacterial and phytoplankton populations using multiplex liquid bead array technology. *Environ. Microbiol.* 12, 975–989. doi: 10.1111/j.1462-2920.2004.02142.x

Moustafa, A., Evans, A. N., Kulis, D. M., Hackett, J. D., Erdner, D. L., Anderson, D. M., et al. (2010). Transcriptome profiling of a toxic dinoflagellate reveals a gene-rich protist and a potential impact on gene expression due to bacterial presence. *PLoS ONE* 5:e9688. doi: 10.1371/journal.pone.0009688

Newton, R. J., Griffin, L. E., Bowles, K. M., Meile, C., Gifford, S., Gvens, C. E., et al. (2010). Genome characteristics of a generalist marine bacterial lineage. *ISME J.* 4, 784–798. doi: 10.1038/ismej.2009.150

Okbamichael, M., and Sañudo-Wilhelmy, S. A. (2004). A new method for the determination of vitamin B12 in seawater. *Anal. Chim. Acta* 517, 33–38. doi: 10.1016/j.aca.2004.05.020

Palacios, L., and Marín, M. (2008). Enzymatic permeabilization of the thecate dinoflagellate *Alexandrium minutum* (Dinophyceae) yields detection of intracellularly associated bacteria via catalyzed reporter deposition-fluorescence in situ hybridization. *Appl. Environ. Microbiol.* 74, 2244–2247. doi: 10.1128/AEM.01144-07

Patel, A. R., Nobel, T., Steele, J. A., Schwalbach, M. S., Hewson, I., and Fuhrman, J. A. (2007). Virus and prokaryote enumeration from planktonic marine environments. Epifluorescence microscopy with SYBR Green I. *Nat. Prot.* 2, 269–276. doi: 10.1038/nprot.2007.6

Peña-Manjarrez, J. L., Helenes, J., Gaxiola-Castro, G., and Orellana-Cepeda, E. (2005). Dinoflagellate cysts and Bloom events at Todos Santos Bay, Baja California, México, 1999–2000. *Cont. Shelf Res.* 25, 1375–1393. doi: 10.1016/j.csr.2005.02.002

Sañudo-Wilhelmy, S. A., Gobler, C. J., Okbamichael, M., and Taylor, G. T. (2006). Regulation of phytoplankton dynamics by vitamin B12. *Geophys. Res. Lett.* 33:L04604. doi: 10.1029/2005GL025046

Sañudo-Wilhelmy, S. A., Gómez-Consarnau, L., Suffridge, C., and Webb, E. A. (2014). The role of B vitamins in marine biogeochemistry. *Annu. Rev. Mar. Sci.* 6, 14.1–14.29. doi: 10.1146/annurev-marine-120710-100912

Schneider, C. A., Rasband, W. S., and Eliceiri, K. W. (2012). NIH Image to ImageJ: 25 years of image analysis. *Nat. Methods* 9, 671–675. doi: 10.1038/nmeth.2089

Slightom, R. N., and Buchan, A. (2009). Surface colonization by marine *Roseobacters*: integrating genotype and phenotype. *App. Environ. Microbiol.* 75, 6027–6037. doi: 10.1128/AEM.01508-09

Strömpl, C., Hold, G. L., Lünsdorf, H., Graham, J., Gallacher, S., Abraham, W.-R., et al. (2003). *Oceanicaulis alexandrii* gen. nov., sp. nov., a novel stalked bacterium isolated from a culture of the dinoflagellate *Alexandrium tamarense* (Lebour) Balech. *Int. J. Syst. Evol. Microbiol.* 53, 1901–1906. doi: 10.1099/ijs.0.02635-0

Tang, Y. Z., Koch, F., and Gobler, C. J. (2010). Most harmful algal bloom species are vitamin B1 and B12 auxotrophs. *Proc. Natl. Acad. Sci. U.S.A.* 107, 20756–20761. doi: 10.1073/pnas.1009566107

Wagner-Döbler, I., Ballhausen, B., Berger, M., Brinkhoff, T., Buchholz, I., Bunk, B., et al. (2010). The complete genome sequence of the algal symbiont Dinoroseobacter shibae: a hitchhiker's guide to life in the sea. *ISME J.* 4, 61–77. doi: 10.1038/ismej.2009.94

Xie, B., Bishop, S., Stessman, D., Wright, D., Spalding, M. H., and Halverson, L. J. (2013). *Chlamydomonas reinhardtii* thermal tolerance enhancement mediated by a mutualistic interaction with vitamin B12-producing bacteria. *ISME J.* 7, 1544–1555. doi: 10.1038/ismej.2013.43

Zhang, J., Kobert, K., Flouri, T., and Stamatakis, A. (2013). PEAR: a fast and accurate Illumina Paired-End read merger. *Bioinformatics* 30, 614–620. doi: 10.1093/bioinformatics/btt593

Zhu, Q., Aller, R. C., and Kaushik, A. (2011). Analysis of vitamin B12 in seawater and marine sediment porewater using ELISA. *Limnol. Oceanogr. Methods* 9, 515–523. doi: 10.4319/lom.2011.9.515

Conflict of Interest Statement: The authors declare that the research was conducted in the absence of any commercial or financial relationships that could be construed as a potential conflict of interest.

frontiers in Microbiology

ORIGINAL RESEARCH
published: 20 June 2016
doi: 10.3389/fmicb.2016.00848

A Novel Treatment Protects *Chlorella* at Commercial Scale from the Predatory Bacterium *Vampirovibrio chlorellavorus*

Eneko Ganuza[1], Charles E. Sellers[1], Braden W. Bennett[2], Eric M. Lyons[1] and Laura T. Carney[2]*

[1] Microbiology Group, Heliae Development, LLC, Gilbert, AZ, USA, [2] Molecular Ecology Group, Heliae Development, LLC, Gilbert, AZ, USA

The predatory bacterium, *Vampirovibrio chlorellavorus*, can destroy a *Chlorella* culture in just a few days, rendering an otherwise robust algal crop into a discolored suspension of empty cell walls. *Chlorella* is used as a benchmark for open pond cultivation due to its fast growth. In nature, *V. chlorellavorus* plays an ecological role by controlling this widespread terrestrial and freshwater microalga, but it can have a devastating effect when it attacks large commercial ponds. We discovered that *V. chlorellavorus* was associated with the collapse of four pilot commercial-scale (130,000 L volume) open-pond reactors. Routine microscopy revealed the distinctive pattern of *V. chlorellavorus* attachment to the algal cells, followed by algal cell clumping, culture discoloration and ultimately, growth decline. The "crash" of the algal culture coincided with increasing proportions of 16s rRNA sequencing reads assigned to *V. chlorellavorus*. We designed a qPCR assay to predict an impending culture crash and developed a novel treatment to control the bacterium. We found that (1) *Chlorella* growth was not affected by a 15 min exposure to pH 3.5 in the presence of 0.5 g/L acetate, when titrated with hydrochloric acid and (2) this treatment had a bactericidal effect on the culture (2-log decrease in aerobic counts). Therefore, when qPCR results indicated a rise in *V. chlorellavorus* amplicons, we found that the pH-shock treatment prevented the culture crash and doubled the productive longevity of the culture. Furthermore, the treatment could be repeatedly applied to the same culture, at the beginning of at least two sequential batch cycles. In this case, the treatment was applied preventively, further increasing the longevity of the open pond culture. In summary, the treatment reversed the infection of *V. chlorellavorus* as confirmed by observations of bacterial attachment to *Chlorella* cells and by detection of *V. chlorellavorus* by 16s rRNA sequencing and qPCR assay. The pH-shock treatment is highly selective against prokaryotes, and it is a cost-effective treatment that can be used throughout the scale up and production process. To our knowledge, the treatment described here is the first effective control of *V. chlorellavorus* and will be an important tool for the microalgal industry and biofuel research.

Keywords: algae industry, *Chlorella*, crop protection, *Micractinium inermum*, pH-shock, predatory bacterium, *Vampirovibrio chlorellavorus*

OPEN ACCESS

Edited by:
Yoav Bashan,
The Bashan Institute of Science, USA

Reviewed by:
Kathleen Scott,
University of South Florida, USA
Qiang Wang,
Chinese Academy of Sciences, China

****Correspondence:***
Eneko Ganuza
enekoganuza@gmail.com

Specialty section:
This article was submitted to Aquatic Microbiology, a section of the journal Frontiers in Microbiology

Received: *01 February 2016*
Accepted: *22 May 2016*
Published: *20 June 2016*

Citation:
Ganuza E, Sellers CE, Bennett BW, Lyons EM and Carney LT (2016) A Novel Treatment Protects Chlorella at Commercial Scale from the Predatory Bacterium Vampirovibrio chlorellavorus. Front. Microbiol. 7:848. doi: 10.3389/fmicb.2016.00848

INTRODUCTION

Vampirovibrio chlorellavorus is a non-photosynthetic cyanobacterium (*Melainabacteria*; Soo et al., 2014) with a predatory lifestyle that targets a variety of *Chlorella* species (Coder and Starr, 1978). This predator only feeds on living algae cells and is unable to grow in liquid or agar media unless co-cultured with the alga. Electron microscopy-based studies (Coder and Goff, 1986; Mamkaeva and Rybal'chenko, 1979) have shown that *V. chlorellavorus* uses a flagellum to reach its prey and attach to the surface of the alga through fibril appendages. The attached cells remain epibiotic contrary to other predatory bacteria belonging to *Bdellovibrio* or *Daptobacter* (Guerrero et al., 1986). The unique predation mechanisms of *V. chlorellavorous* are exquisitely regulated. The bacterial cell secretes a path that connects with the alga, breaches through the parent cell wall and if necessary also through the daughter cell wall (Coder and Goff, 1986). Recent metagenomic analyses suggest that plasmid DNA and hydrolytic enzymes are transferred to the prey cells via the T4SS secretion system where they apparently degrade the algal cell contents (Soo et al., 2015). As the *Chlorella* cell is digested, the color changes from dark green to yellow brown, and empty or "ghost" *Chlorella* cells accumulate in the culture. If left unabated, the majority of *Chlorella* cells are destroyed and the culture develops a granular texture due to progressive clumping of algal cells visible to the naked eye (Coder and Starr, 1978).

Early detection by optical microscopy is difficult due to the pleomorphic shape and the small size of *V. chlorellavorus* ($<1\ \mu m^3$; ultramicrobacterium; Coder and Starr, 1978). Other bacterial epiphytes may be mistaken for *V. chlorellavorus*; however, the infection becomes more apparent with the rapid increase in the proportion of *Chlorella* cells with attached bacteria and the development of a clear zone that spreads through the infected cell from the site of attachment (Coder and Goff, 1986). Using electron microscopy, *V. chlorellavorus* was first described in freshwater samples from a reservoir in Ukraine (Gromov and Mamkaeva, 1972) and later in freshwater anuran amphibian ponds in Brighton, UK (Wong et al., 1994). However, traditional detection tools have failed to provide a definitive diagnosis, and it is likely that the incidence of *V. chlorellavorous* infection has been overlooked. For example, only a few original papers have been published since this predator was first described (Gromov and Mamkaeva, 1972). Recently, molecular tools have targeted this predator across diverse systems. For example, *V. chlorellavorous* was identified in soil samples from Anhui, China (Shi et al., 2015), in bovine rumen samples from Nagaland, India (Das et al., 2014) and from open pond cultures of *Chlorella* at three different universities in the southwestern USA which suffered repeated *V. chlorellavorus* infections (personal communication from Drs. P. Lammers, J. Brown, and M. Sommerfeld).

In recent years it has become apparent that algal crop protection is one of the most important challenges facing the algal industry (Carney and Lane, 2014; McBride et al., 2016). *Chlorella* was the first eukaryotic microalgae to be grown in pure culture (Beijerinck, 1890) and today it is arguably the most common alga grown by the microalgal industry. Its high productivity and robustness allows a wide range of applications including food, feed, fertilizer, wastewater remediation, CO_2 capture, and biodiesel production (Safi et al., 2014). *V. chlorellavorus* attacks this alga whether it is growing photoautotrophically (Coder and Goff, 1986), heterotrophically (Wong et al., 1994), or as described here, mixotrophically. Therefore, the lack of treatment to control *V. chlorellavorus* is a major challenge for the industry. Here, we report the development of tools for early detection and treatment of *V. chlorellavorous*.

MATERIALS AND METHODS

Chlorella Culture Conditions

Identification of the Algae

Chlorella HS26 was isolated from soil samples in the Sonoran Desert of Arizona, USA and privately deposited in the Culture Collection of Algae at the University of Cologne (Germany). Total genomic DNA was extracted and purified using the DNeasy Plant Mini Kit (Qiagen, Hilden Germany) and the nuclear-encoded rRNA-operon was amplified by polymerase chain reaction (PCR) using DreamTaq™ DNA Polymerase (Fermentas, St. Leon-Rot, Germany). The DNA was sequenced for 18S, ITS1, 5.8S, ITS2, 28S regions using universal eukaryotic primers (see Marin et al., 2003; Marin, 2012). The following PCR protocol was used: an initial denaturation step (95°C for 180 min) was followed by 30 cycles including denaturation (95°C for 45 min), annealing (55°C for 60 min), and elongation (72°C for 180 min). PCR products which showed single clear bands by gel electrophoresis were purified using the Dynabeads M-280 Streptavidin system (Holmberg et al., 2005). For sequencing the SequiTherm EXCEL II Long Read DNA Sequencing Kit (Biozym Diagnostik, Germany) and fluorochrome-labeled primer combinations were used. Two partial and overlapping sequences of each strand were read out with a LI-COR IR2 DNA Sequencer (LI-COR Biosciences, Lincoln, NE, USA) and assembled to the complete rDNA sequence using the program AlignIR™ 2.0 (LI-COR Biosciences, Lincoln, NE, USA). Sequences were aligned manually on the basis of conserved rRNA secondary structures using SeaView 4.3.0 software and only unambiguously aligned sequences were used for phylogenetic analysis. The sequences were compared with existing sequences on the NCBI GenBank database via BLAST. The closest BLAST hits had at least 99 % similarity to *Chlorella* sp. NIES2171 (accession number AB731604) and *Chlorella vulgaris* CCAP/79 (FR865683), consequently the species was preliminary identified as *Chlorella* sp. HS26. It should be noted that recently, the two reference species were proposed as *Micractinium inermum* NIES2171 (Hoshina and Fujiwara, 2013) and *Micractinium* sp. CCAP 211/79 (Germond et al., 2013), respectively. The new sequences for the strain used in this work were deposited in the NCBI database under the accession number KU641127.

Laboratory Culture Conditions

Small-scale testing of *Chlorella* was performed in duplicate using baffled experimental Erlenmeyer flasks (100 ml volume), incubated at 25°C, and shaken at 100 rpm. The cultures were inoculated at 10% v/v from an axenic 2–3-day-old exponentially

growing autotrophic flask culture using BG-11 medium. The experimental flasks were illuminated with LED lights at an intensity of 100 μmol photons/m/s, and sodium acetate trihydrate (2.5 g/L) was added daily to support mixotrophic conditions. The pH was maintained between 7 and 8, and the flasks were maintained in a CO_2 enriched (2 %) atmosphere inside a chamber. For each flask experiment, we tested for a treatment effect, a time effect, and a treatment by time interactions using linear mixed models. Treatment and time were modeled as fixed effects, and we included a first-order autoregressive error structure (AR1) to account for temporally autocorrelated measures. Models were fit using the package lme4 (Bates et al., 2015) in R version 3.0.2 (R Core Team, 2016).

Open Pond Culture Conditions

The pH treatment validation was performed outdoors in open pond raceways (1000 L running volume) measuring 3.5 m long, 1.75 m wide and 19 ± 1 cm depth cultures. The mixotrophic cultures were fed acetic acid on demand through a pH-auxostat feedback control system. The culture was maintained at pH 7.4 ± 0.05 and residual acetic acid (0.2–1 g/L) and nitrate (0.2–0.5 g/L) were maintained at constant concentrations throughout the batch cycle using a feedstock solution of acetic acid (40% v/v) and $NaNO_3$ (40 g/L) as titrants. The initial BG-11 medium was modified to contain (in g/L): sodium acetate (0.5), NaNO3 (0.5), K_2HPO_4 $3H_2O$ (0.04), $MgSO_4$ $7H_2O$ (0.075), CaCl $2H_2O$ (0.036), citric acid (0.006), ferric ammonium citrate (0.006), $MgNa_2EDTA$ H_2O (0.001), and 1 ml/L of a trace metal solution. The trace metal solution contained (in g/L): H_3BO_3 (2.86), $MnCl_2$ $4H_2O$ (1.81), $ZnSO_4$ $7H_2O$ (0.22), $CuSO_4$ $5H_2O$ (0.079), Na_2MoO_4 $2H_2O$ (0.391), $Co(NO_3)_2$ $6H_2O$ (0.0494). The medium was prepared using reverse osmosis water and initial pH was corrected to 7.5 using HCl (1 M). The raceways were inoculated with 10% v/v of outdoor open cultures that had previously been exposed to *Vampirovibrio chlorellavorus*. Temperature was maintained at 24 ± 2°C using a 6 m long stainless steel heat exchange coil. Mixing was applied with a paddlewheel at 1 m/s tip speed. The cultures were aerated (0.05 vol air/vol culture per min) using a 6 m long porous hose and evaporation was corrected daily using reverse osmosis water. Culture conditions above were scaled up to a pilot (60,000 L) and commercial reactor (130,000 L) according to (Tonkovich et al., 2014, International Patent No 2014/144270 A1).

Growth Assessment

Cell Dry Weight

Cell dry weight samples (10 ml) were collected in duplicates daily from the cultures and vacuum filtered with glass microfiber filter papers designed to retain particles of 1.1 μm (Ahlstrom™ Grade 161). The filtrate was washed twice with 10 ml of ammonium bicarbonate 0.5 M solution and placed in an oven (105°C) until weight was stable.

Residual Nutrients

Culture samples (2 mL) were centrifuged (17,000 × *g* for 7 min) and the supernatant was removed and diluted 20-fold. Acetate in the medium was analyzed by HPLC according to the Association of Official Agricultural Chemists Official Method 986.13. The nitrates were analyzed using a Latchat Quickchem™ 8500 and the UV-method 10049 (Hach, Milwaukee, WI, USA).

Culture Longevity

Culture longevity of *Chlorella* was determined based on the total productive days in the target reactor. *Chlorella* cultures operated in sequential batch cycles. The new batch started from the previous batch before this reached stationary phase. Thus, those days with stable or declining dry weights indicated the end of the life of that culture and were excluded from the longevity calculations. The longevity within our commercial reactors (130,000 L) was compared between treated ($n = 9$) and untreated ($n = 8$) runs using a student's *t*-test (JMP®, Version 12.1 SAS Institute Inc., Cary, NC, USA).

Contamination Assessment

Total Aerobic Bacterial Counts

Total aerobic bacterial counts were determined in duplicates using 3M Petrifilm™ Aerobic Count Plates. The plates were incubated for 3 days at 35°C and counts were read using the 3M™ Petrifilm™ Plate Reader and associated image analysis software.

The Percentage of *Chlorella* with Attached Bacteria

The percentage of *Chlorella* with attached bacteria was determined with phase contrast light microscopy using oil immersion objective lens (100×; Olympus DP72). Algal cells with one or more bacteria on their surface were recorded as positive infection. Overall, 50–100 algal cells were used to calculate the percentage. The standard deviation for the method was below 10%.

Determination of Bacterial Community Structure

Samples (2 mL) were collected daily from outdoor *Chlorella* cultures and prepared for small subunit rDNA sequencing as follows. For total DNA extraction, the biomass was concentrated by centrifugation (10,000 × *g* for 10 min) and DNA was purified using the ZR Fungal/Bacterial DNA mini prep kit (Zymo Research, Irvine, CA, USA). To isolate microbiome DNA that was only associated with the phycosphere, biomass was concentrated using slow speed centrifugation (1000 × *g* for 7 min), the supernatant containing unattached bacteria was discarded, the pellet was washed by resuspension in sterile water three times, and the final pellet was collected using high speed centrifugation (17,000 × *g* for 7 min). To isolate DNA from the whole culture portion, biomass was collected using high speed centrifugation (17,000 × *g* for 7 min). For all samples, DNA purity and quantity was determined via 260/280 nm readings then normalized to 10 ng/μL. PCR was conducted on the normalized gDNA using chloroplast excluding 16S rDNA primer set 799F/U1492R (Chelius and Triplett, 2001). The following PCR protocol was used: an initial denaturation step (98°C for 30 s), followed by 35 cycles of denaturation (98°C for 10 s), annealing (53°C for 30 s) and elongation (72°C for 60 s). The PCR cycle was ended with a 72°C final elongation for 10 min. The resulting PCR product was visualized on agarose gels for confirmation of expected bands

(~700 bp) and then cloned using Zero Blunt Topo PCR cloning kits (Invitrogen, Carlsbad, CA, USA). 16S rDNA clone library inserts were sequenced with the T7 vector primer using an ABI 3730xl DNA Analyzer.

The resulting 16S rDNA sequences were aligned and trimmed of primer and vector sequences using the built-in trimming tool in the Geneious 8.1.5 software suite (Biomatters, Ltd, New Zealand) with vector trimming against the NCBI UniVec database[1]. Sequences with an HQ % quality score below 30% were excluded from analysis. Sequences were then aligned to the NCBI "nr" database for taxonomic assignment using BLAST (Altschul et al., 1990). Best BLAST hits had ≥98% similarity to the query sequence picked for taxonomic assignment. For verification of assignments, the trimmed sequences were also aligned and classified using the SINA online alignment tool against the SILVA 119 database [lc1] (Pruesse et al., 2012). Although these methods involved two different reference databases and alignment algorithms, the taxonomic assignments were in agreement at >98–99% sequence similarity (data not shown).

[1]ftp://ftp.ncbi.nlm.nih.gov/pub/UniVec/

Heatmaps of bacterial relative abundance were generated using the phyloseq R package (McMurdie and Holmes, 2013).

Predator Identification and Tracking Using qPCR Assay

A proprietary 6-carboxyfluorescein based (FAM) qPCR assay was designed for *V. chlorellavorous* consisting of forward and reverse primers and a species specific probe. The assay is not publically available at this time; however, the information may be made available by contacting Heliae and agreeing to confidentiality terms. The assay was designed using a clone insert bacterial 16S rRNA sequence from an infected pond (Accession number KU570459). The clone exhibited >99% similarity (692/695 nucleotide match) to a GenBank 16S gene sequence (Accession number HM038000) from the *V. chlorellavorous* type culture that was deposited by Coder and Starr (1978) and sequenced by the American Type Culture Collection (ATCC29753). DNA collected from the phycosphere-enriched fraction of the same culture was used as a positive control template. Pond samples (2 mL) were lysed by bead beating using 0.5 mm beads at 3400 rpm for 2 min and centrifuged at 10000 × *g* for 1 min to remove cellular debris.

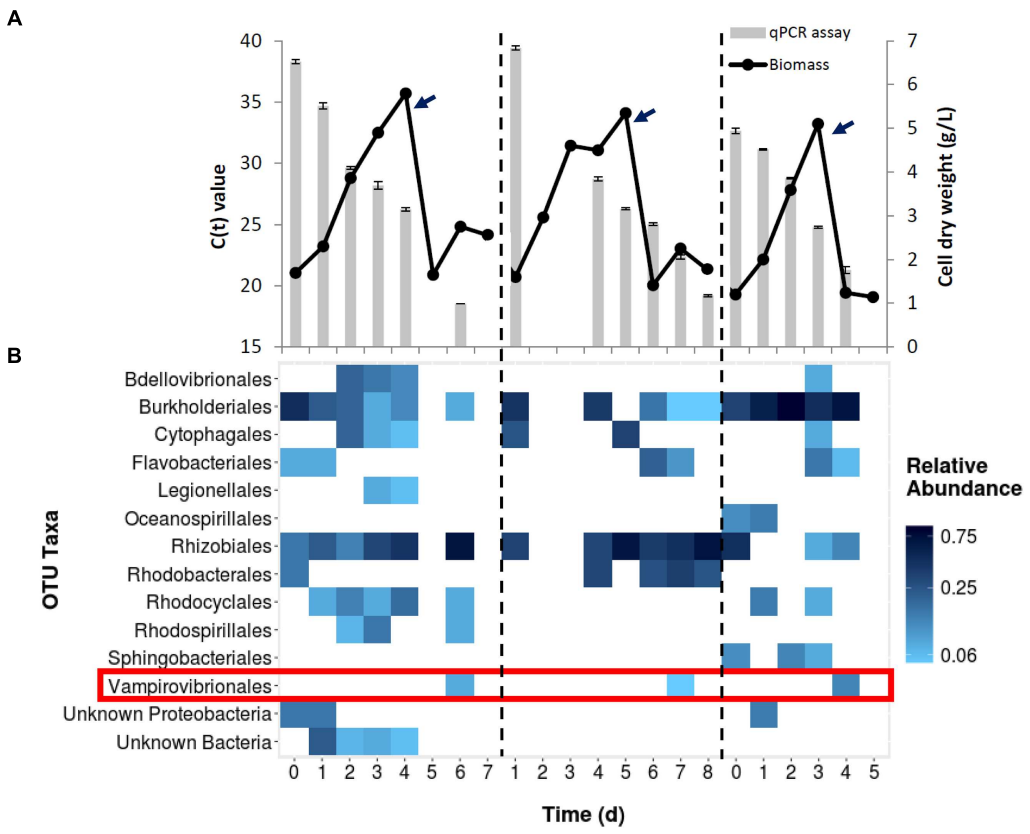

FIGURE 1 | (A) Growth of *Chlorella* culture during three different scale up cycles in outdoor mixotrophic commercial reactors. Each cycle (divided by the dash line) represents the seed production (60,000 L) and transfer (denoted by arrows) to a commercial-scale reactor (130,000 L volume). Bars represent *Vampirovibrio chlorellavorus* infection as detected by qPCR assay in each cycle. The C_t value, or cycle threshold, decreases as the target abundance increases. **(B)** Bacterial community structure from whole culture samples of same three runs based on 16s rRNA gene sequencing. The detection of *V. chlorellavorus* sequences coincide with a decline or arrest in the growth of *Chlorella* shown in **(A)**.

The aqueous supernatant (1 μL) from the lysate was used as a template for the qPCR assay in 10 uL total volume reactions. The following qPCR protocol was used: an initial denaturation step (98°C for 3 min), followed by 40 cycles of denaturation at 95°C for 5 s, and annealing at 60°C for 30 s. The total run time for the assay was 120 min. The assay showed specificity only to the *V. chlorellavorous* assigned clone insert and tested negative ($C_t = 0$) against purified 16S sequences from various bacterial isolates representing multiple genera (*Shewanella* sp., *Acinetobacter* sp., *Ochrobactrum* sp., *Pseudochrobactrum* sp., *Bacillus* sp., *Stenotrophomonas* sp., *Clostridium* sp., *Azospirillum* sp., *Gemmobacter* sp., *Pseudomonas*

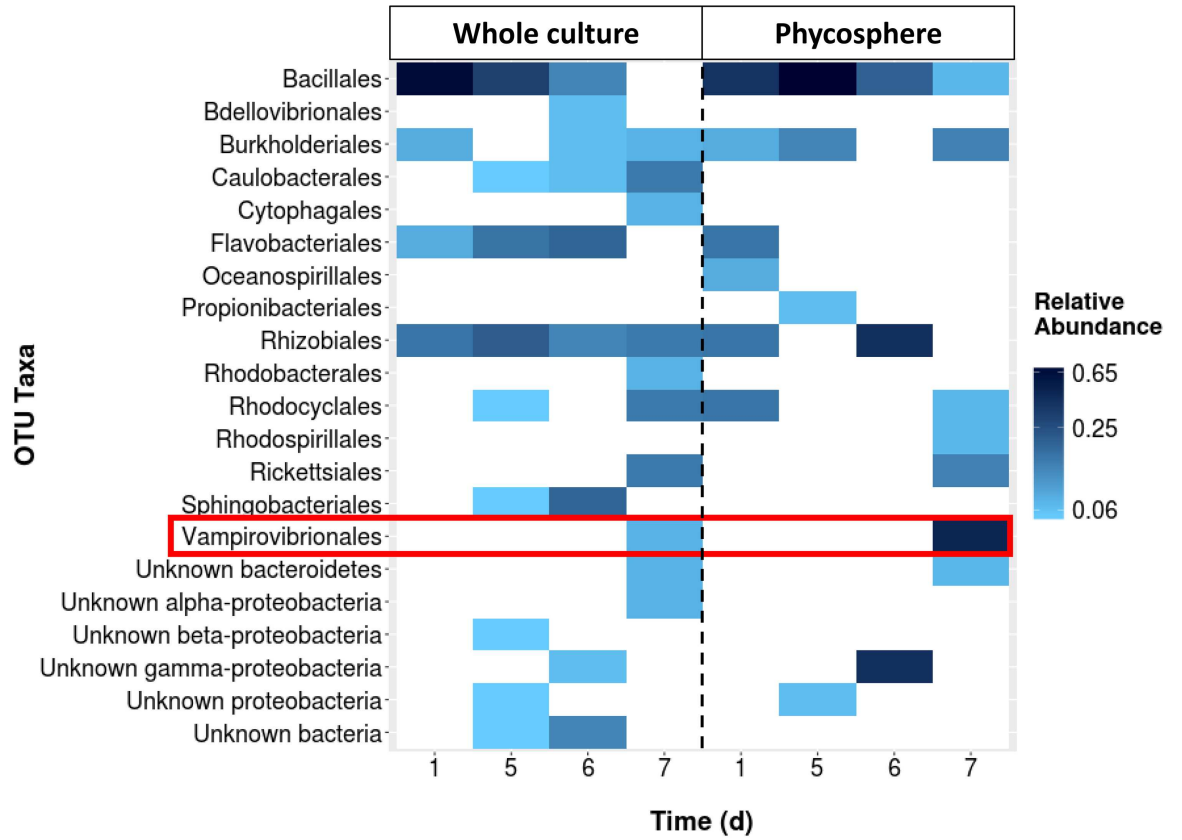

FIGURE 2 | The comparison between the whole culture bacterial community structure (16s rRNA gene sequencing assay) of a batch culture of *Chlorella* and the corresponding phycosphere portion. Sequencing data was not available for days 2–4.

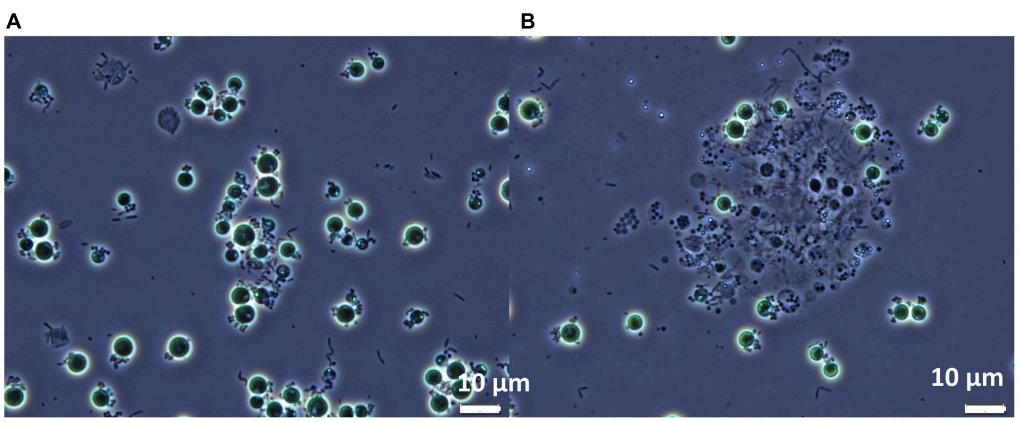

FIGURE 3 | Phase contrast micrographs of *Chlorella* commercial cultures heavily infested with *Vampirovibrio*-like cells at two different stages (A) Appearance of the first empty or ghost cells. (B) Culture clumping. Micrographs produced by R. A. Andersen.

sp., *Pedobacter* sp., *Pannonibacter* sp., *Rheinheimera* sp. *Azoarcus* sp., *Cloacibacterium* sp., and *Comamonas* sp.).

Predator Treatment Development

Literature Review on Cytoplasmic pH Regulation by Microalgae

Literature review on cytoplasmic pH regulation by microalgae was performed to compare the response of Cyanophyta and Chlorophyta to the medium pH. The review included peer-reviewed articles that analyzed the cytosolic pH of algae at two or more medium pH set points. Cytosolic pH was analyzed using either 5,5-dimethoxazolidine-2,4-dione (DMO), ^{31}P-NMR spectroscopy, or fluorochrome methods. Mean pH values were easily transcribed either from a data table or a detailed line graph reported in those articles. Means and standard deviations were calculated based on data from 3 to 7 different strains. Acidophilic microalgae, with an optimum growth at a pH below 5, were excluded from this review. Most cyanobacteria stopped growing at medium pH below 6 and cytosolic pH data could not be retrieved for those data points.

The pH-Shock Treatment

The pH-shock treatment was applied by adding hydrochloric acid (HCl; 34% v/v) to well mixed algae culture until the pH decreased from 7.5 to 3.5. The pH of the algae culture was maintained at pH 3.5 for 15 min in the presence of 0.5 g/L residual acetate. The pH was then returned to pH 7.5 using sodium hydroxide (2 M). More details on the method and method variants are provided by Ganuza and Tonkovich (2015, U.S. Patent No 9,181,523).

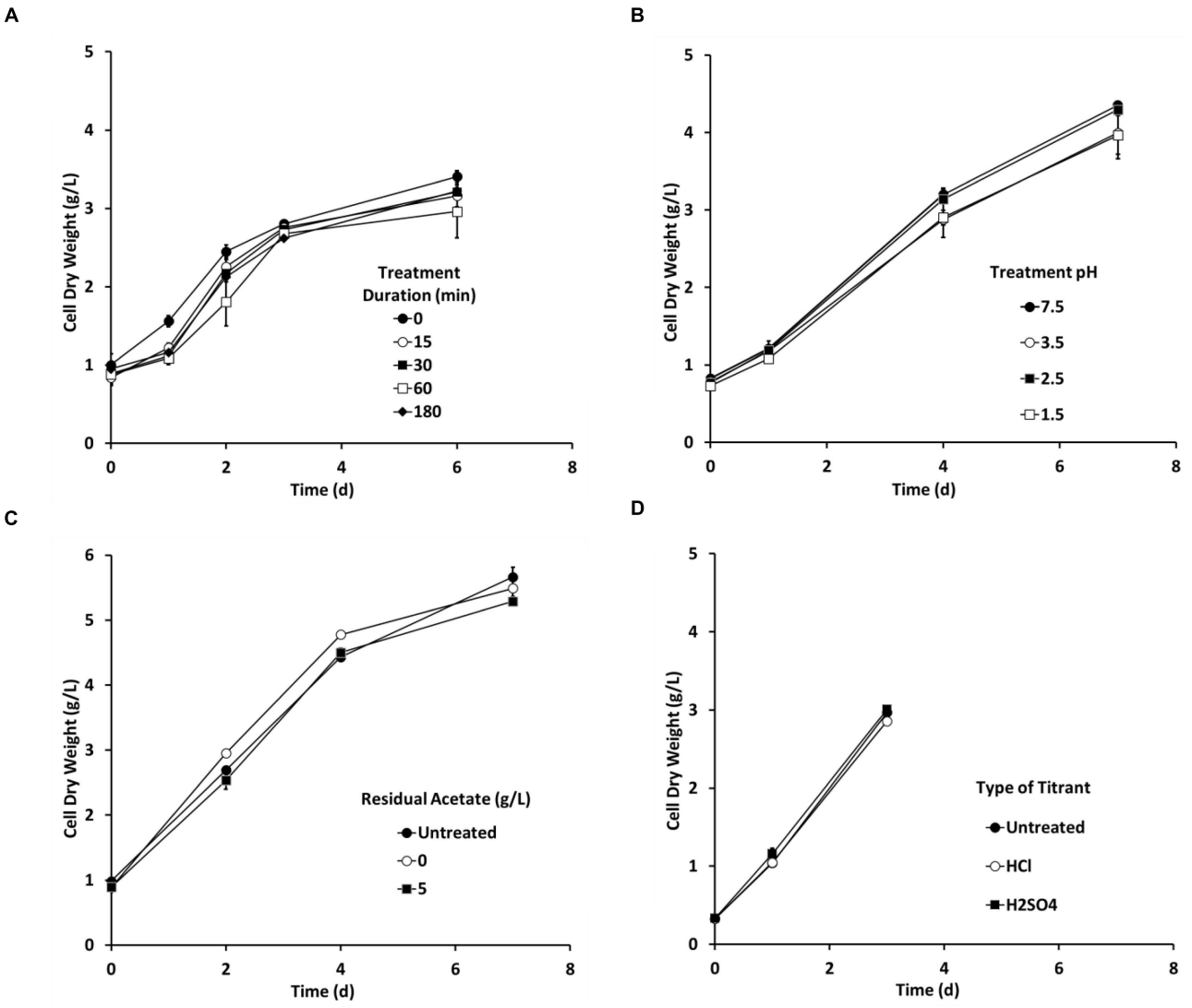

FIGURE 4 | The pH-shock treatment (A) duration, (B) pH level, (C) residual acetate concentration, and (D) type of titrant did not affect *Chlorella* growth in flasks (250 mL, $n = 2$). Unless stated otherwise the pH treatment was conducted using hydrochloric acid (HCL) to reduce pH to 3.5 for 15 min in the presence of 0.5 g/L acetate and then inoculated aseptically into the *Chlorella* culture. Error bars represent 1 standard deviation.

RESULTS

Predator Identification

Three data sets are presented as representative examples (**Figure 1**). Cultures grown in 60,000 L bioreactors showed initial *Chlorella* growth as measured by biomass increase. After transferring the cultures to the 130,000 L reactor (arrows; **Figure 1A**), biomass declined in 2–3 days. When identifying *V. chlorellavorus* using 16S rRNA sequences, the bacterium was not detected until day 6, at which time the culture was crashing. In addition to *V. chlorellavorus*, other bacterial taxa were present throughout the experiments (**Figure 1B**). When quantifying *V. chlorellavorus* using the qPCR assay the progress of the infection was observed in anticipation of the crashing of the culture (**Figure 1A**).

A fourth 130,000 L reactor was investigated using only 16S rRNA sequences and the proportion of *V. chlorellavorus* from the whole pond community was compared to the community associated with the phycosphere (**Figure 2**). While *V. chlorellavorus* was present in both whole pond and phycosphere samples on day 7, the proportion of reads assigned to this predatory bacterium was much more abundant in the phycosphere sample (0.47 versus 0.07).

When viewed microscopically, the *Chlorella* culture was heavily infested with *Vampirovibrio*-like cells (**Figure 3**). Initially, a single *V. chlorellavorus* cell attached to the outside of a *Chlorella* cell, but this quickly developed into a chain and then a cluster of bacterial cells. As the predation proceeded, numerous bacterial cells formed and then were released, eventually leaving empty or ghost algal cells (**Figure 3A**). Finally, as the predation

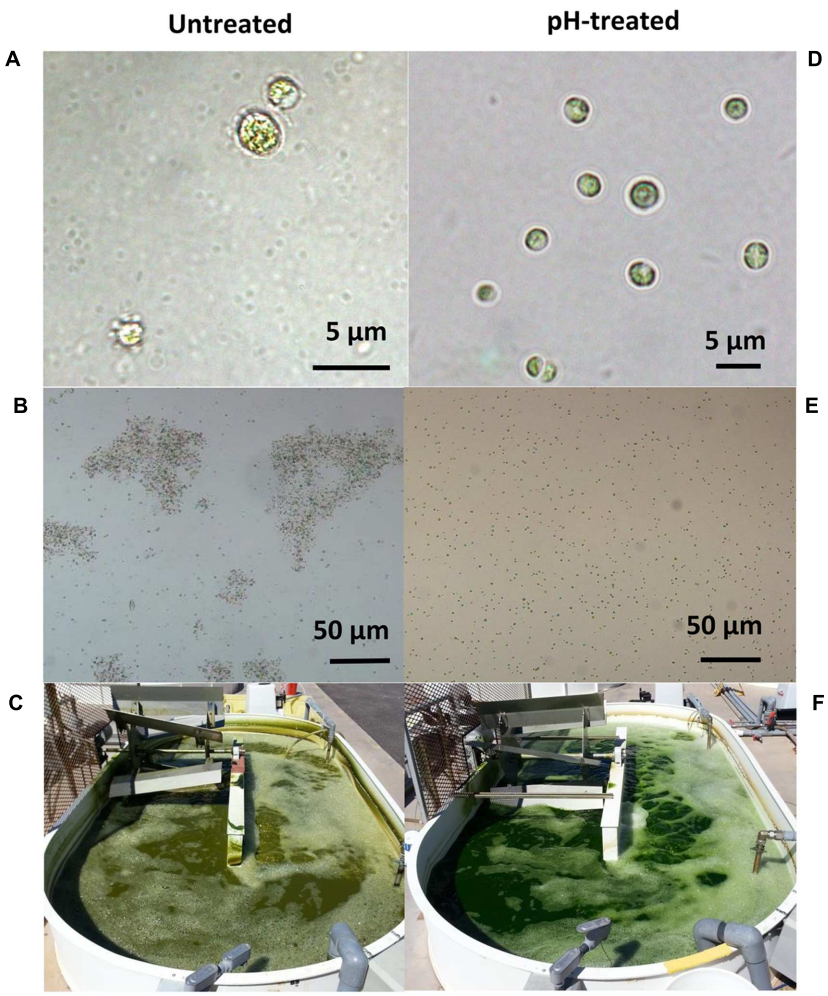

FIGURE 5 | The symptoms associated with *Vampirovibrio chlorellavorus* infection such as (A) bacterial attachment to the algae (B), clumping of algae cells and (C) change in the coloration of the culture (C) were reverted by the pH-shock treatment (D–F, respectively). Pictures and micrographs correspond to a simultaneous side by side comparison of raceways (1000 L, **C,F**) containing untreated (left) or pH-treated (right) culture derived from an industrial scale reactor (130,000 L). Micrograph 5A was produced by J. Wilkenfeld.

event neared completion, the *Chlorella* cells began clumping, apparently held together by a bacterial matrix (**Figure 3B**).

Predator Treatment Development in Laboratory

Preliminary flask experiments showed that *Chlorella* tolerated a pH-shock (pH 3.5) up to at least 2 h (**Figure 4A**). *Chlorella* also tolerated a 15 min pH-shock as low as pH 1.5 (**Figure 4B**), and cells tolerated the pH-shock even in the presence of up to 5 g/L acetate (**Figure 4C**). Lastly, *Chlorella* tolerated treatments using either sulfuric acid or HCls as titrants (**Figure 4D**). No significant differences were observed between any of the treatments tested during these four experiments according to the Generalized Linear Model analysis ($P > 0.1$).

Predator Treatment Development in Open Ponds

Based on positive results from laboratory experiments, the pH-shock treatment was tested outdoors on mixotrophic cultures growing in small raceways (1000 L). A contaminated culture (70% *Chlorella* cells having attached bacteria) was removed from a large reactor (130,000 L) and used to inoculate two small raceways. One raceway was pH-treated as follows: (1) the pH was decreased from 7.5 to 3.5 using HCl, (2) the pH was maintained at pH 3.5 for 15 min in the presence of 0.5 g L^{-1} residual acetate, and (3) the pH was then returned to pH 7.5 using sodium hydroxide (Ganuza and Tonkovich, 2015, U.S. Patent No 9,181,523). The second raceway was left untreated. The visual symptoms associated with *V. chlorellavorus* predation (i.e., bacterial attachment to the algae, clumping of algae cells, and change in culture color)

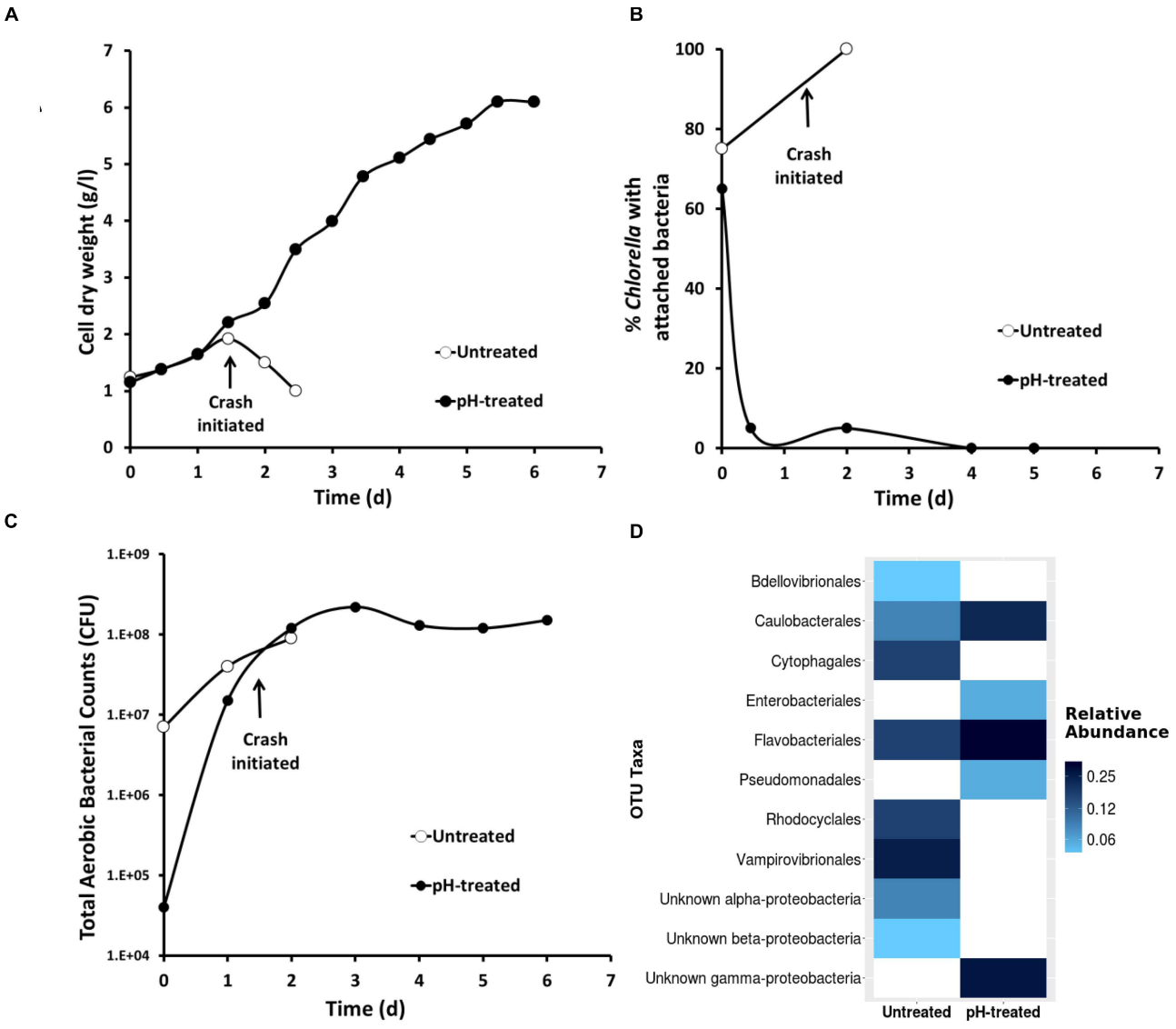

FIGURE 6 | The impact of pH-shock treatment (close circles) on (A) *Chlorella* growth (B) bacterial attachment to the algae phycosphere (C) total aerobic bacterial count and (D) 16s rRNA *Vampirovibrio chlorellavorus* sequencing. Data correspond to a simultaneous side by side comparison in raceways (1000 L, $n = 1$) of pH-treated and untreated culture originated from in an industrial scale reactor (130,000 L).

were only observed in the untreated raceway (**Figures 5A–C**), and this culture crashed within 2 days. In the pH treated culture, the symptoms of infection were reversed and a culture crash was prevented (**Figures 5D–F**). The pH-treated culture remained healthy, reaching a cell density of 6 g/L within 6 days (**Figure 6A**). Bacterial attachment to the algal cells was reversed and eliminated within 12 h of treatment (**Figure 6B**) and a two-log decrease in total aerobic plate counts (day 0, treated vs. untreated) demonstrated the bactericidal effect of the treatment (**Figure 6C**). Analyses based on16s rRNA sequencing showed suggested that the pH treatment was effective at eliminating *V. chlorellavorus*, i.e., *V. chlorellavorus* reads were not detected in the pH-treated reactor 2 days after treatment but *V. chlorellavorus* comprised 25% of the bacterial community in the untreated reactor (**Figure 6D**).

A second outdoor pH treatment experiment used the more sensitive and timely qPCR analysis to track infection (**Figure 7**). A mildly contaminated culture (20% bacterial attachment) removed from an open pond raceway (1000 L) was used to inoculate two additional 1000 L raceways that were operating mixotrophically. One raceway was left untreated while the other received a pH-shock treatment. Bacterial attachment in the untreated reactor dramatically increased to 100% within 3 days and cell dry weight declined and crashed within 3–5 days (**Figures 7A,B**). These changes followed an increase in detection of *V. chlorellavorus* in the untreated

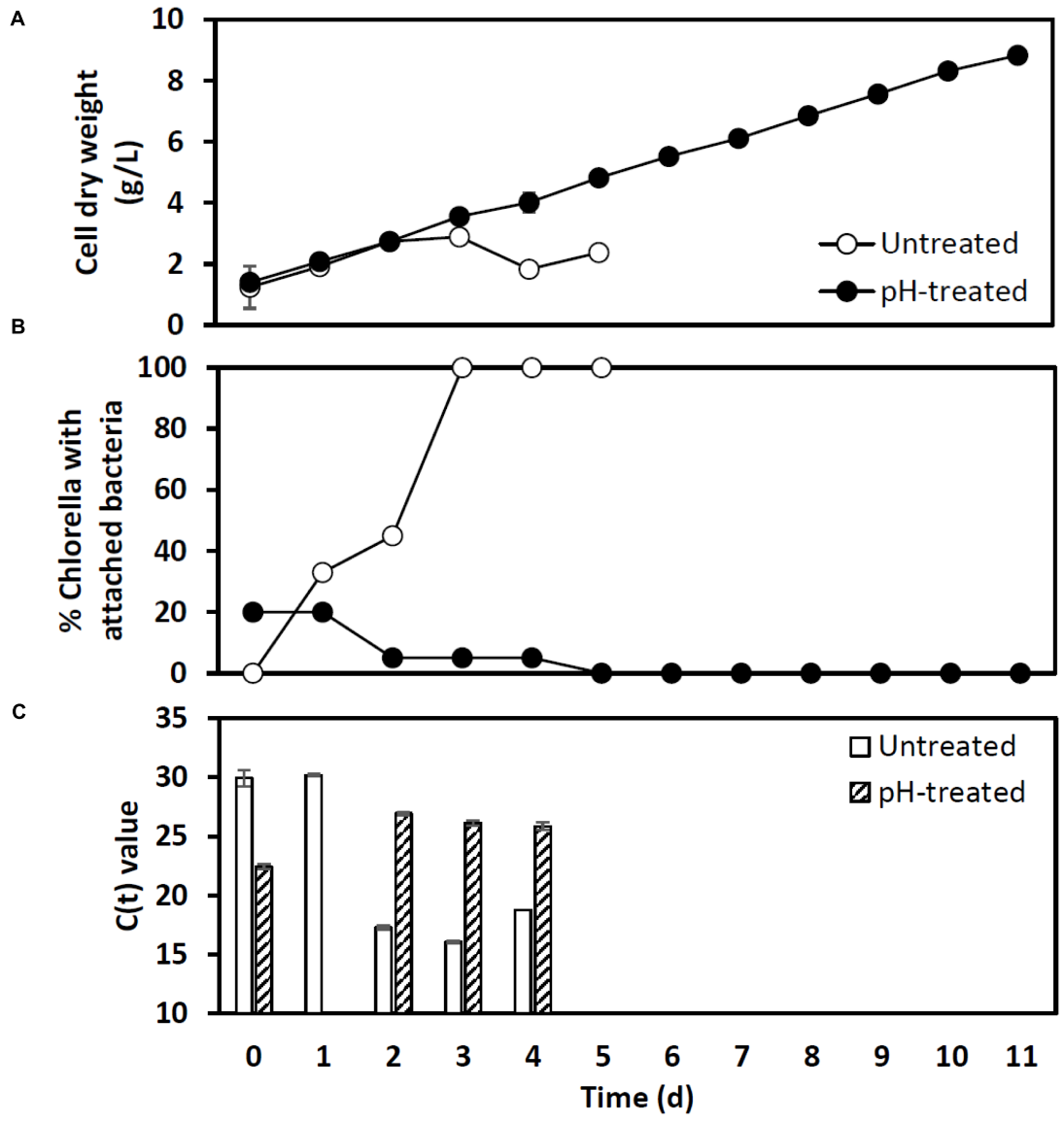

FIGURE 7 | Impact of the pH-shock treatment on (A) *Chlorella* cell dry weight, (B) bacterial attachment, and (C) qPCR assay C_t values for *Vampirovibrio chlorellavorous* from outdoor pilot scale reactors (1000 L, $n = 1$) inoculated with a contaminated *Chlorella* culture. The C_t value, or cycle threshold, in **(C)** decreases as the target abundance increases. Lysates prepared for qPCR on day 1 from the pH treated reactor failed to amplify.

reactor via qPCR on day 2 when attachment was at 40% (**Figure 7B**). If this had been a single commercial scale reactor run, qPCR would have provided a 3-day warning that the culture was headed for a crash and crop protection strategies could have been initiated. *V. chlorellavorus* detection in the pH-treated culture remained stable, while attachment was reduced to 5% and cell dry weights continued to increase for 11 days to 8.5 g/L (**Figure 7**). This response confirmed the efficacy of the pH treatment against this previously fatal *V. chlorellavorus* predator in outdoor ponds used to grow *Chlorella*.

To date, we have confirmed the efficacy of the pH-shock treatment at commercial-scale (130,000 L running volume) during nine additional reactor runs that were compared to untreated control cultures. The longevity of the pH treated ponds (12.7 ± 2.7 days [mean ± 1 SD]) was significantly higher (*t*-test; $t(1) = 4.47$, $P < 0.01$) than the longevity of the untreated ponds (7.0 ± 2.7 days [mean ± 1 SD]), increasing the total harvested biomass. Additionally, we found that for a typical batch operation involving scaling up and transferring cultures every 6 days between outdoor reactors, *Chlorella* could be treated right before transfer for at least two sequential transfers; this treatment schedule resulted in an increased culture longevity from eight to over twenty consecutive days (**Figure 8**).

DISCUSSION

Microalgae are among the few species in industrial microbiology that are grown in open ponds. Consequently, as in agriculture, crop protection is one of the most important challenges facing the microalgal industry, and it has been recognized as a chief limiting factor for microalgal production at commercial scale (Carney and Lane, 2014; McBride et al., 2016). Previously, pests encountered in commercial microalgal systems were not widely reported, and even minimized in an effort to make the microalgal industry appear more promising. Today, a diverse assemblage of zooplankton, fungi, bacteria, and viruses are known to attack microalgal cultures, and their impacts range from chronically reduced production to swift and irreversible culture crashes (Carney et al., 2014; Gong et al., 2015; Touloupakis et al., 2015; White and Ryan, 2015). Despite a more open acknowledgment of pests and the more frequent use of molecular diagnostic techniques for predator and pathogen detection (Carney et al., 2016), there are still very few detailed descriptions of crop protection strategies. Reports of treatments have included commercial fungicides (McBride et al., 2014) and hydrogen peroxide (Carney and Sorensen, 2015, U.S. Patent No 9,113,607) for fungal pathogens, pH transitions for rotifers (Zmora and Richmond, 2004), hyperchlorite (Zmora and Richmond, 2004), and size selective pulsed electric fields (Rego et al., 2015) for protozoa; see McBride et al. (2016) for a detailed review of reactive and preventative strategies.

Our study identified the causative organism that was apparently impacting our commercial *Chlorella* ponds. During infection, a larger proportion of *V. chlorellavorous* sequence reads were present in the region immediately surrounding the algal cells (i.e., the phycosphere) compared to bacteria free-living in the supernatant (**Figure 2**). This observation is in agreement with reports describing the epibiotic lifestyle of this predator (Coder and Star, 1978). Although *V. chlorellavorous* was originally identified as the potential causative crash agent

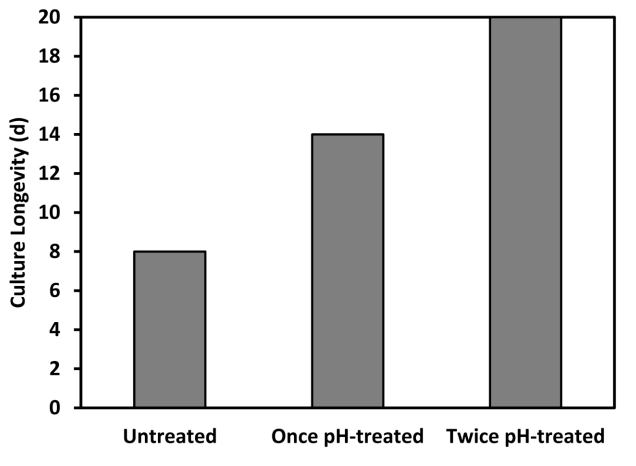

FIGURE 8 | Longevity of a *Chlorella* culture was prolonged by applying the pH treatment repeatedly to the same culture upon transfer, at the beginning of at least two consecutive batch cycles.

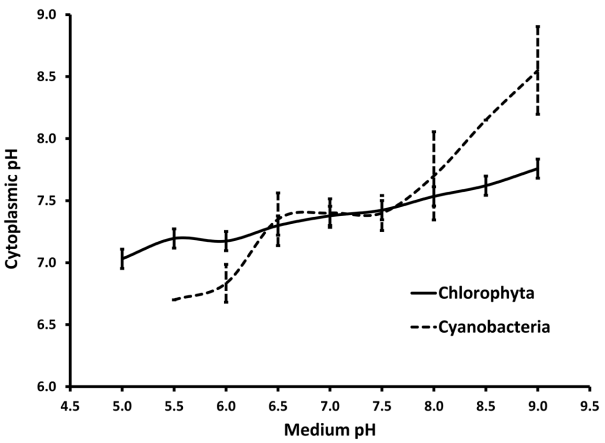

FIGURE 9 | Summary of cytoplasmic pH regulation in response to the pH in the surrounding media for members of phylum Chlorophyta and Cyanobacteria reported in the literature (seven and four members, respectively). Chlorophyta includes *Chlorella kessleri* (El-Ansari and Colman, 2015), *Chlorella pyrenoidosa* and *Scenedesmus quadricauda* (Lane and Burris, 1981), *Chlorella saccharophila* (Gehl and Colman, 1985), *Chlorella vulgaris* and *Chlorella fusca* (Küsel et al., 1990) and *Dunaliella parva* (Gimmler et al., 1988). Cyanobacteria include *Agmenellum quadruplicatum* and *Gloeobacter violaceus* (Belkin et al., 1987), *Anacystis nidulans*, (Falkner and Horner, 1976) and *Synechococcus* sp. (Kallas and Castenholz, 1982). Note that only one Cyanobacterium (*A. quadruplicatrum*) did grow at a pH below 6.0. All other data points are expressed as mean values with error bars representing 1 standard deviation.

via 16s rRNA sequencing (**Figures 1** and **2**), qPCR was relied upon for advanced warning of a culture crash via increasing *V. chlorellavorous* abundance (**Figure 7C**). In general, detection of *V. chlorellavorous* via qPCR preceded visual observations of an impending crash, including an increase in the percent of *Chlorella* cells with attached bacteria (> 20%; **Figures 6B** and **7B**), algal cell clumping and the culture changing color from dark green to yellowish brown (**Figure 5**). The analytical techniques developed and utilized here (i.e., *V. chlorellavorus*-specific qPCR assay, % bacterial attachment to *Chlorella* cells) proved important for determining timing and success of treatment applications.

Although largely unaccounted for in the literature, *V. chlorellavorus* is known as a devastating predator of *Chlorella*. We have experienced first-hand how this cyanobacterium can induce culture crashes in a matter of days. Likewise, other *Chlorella* ponds in the southwestern USA have suffered similar crises from this predator (personal communication from Drs. P. Lammers, J. Brown, and M. Sommerfeld). Molecular reports available in the NCBI GenBank database suggest that this predator is widespread globally and therefore could potentially affect *Chlorella* cultures regardless of their location. In this context, the development of a treatment against *V. chlorellavorus* is especially significant because (1) there was no treatment available prior and (2) *Chlorella*-like microalgae are among the most commonly produced crops by the industry. In addition, the treatment was opportunistically validated in outdoor mixotrophic cultures, which are one order of magnitude more productive than traditional photoautotrophic cultures (Ganuza et al., 2015; Ganuza and Tonkovich, 2016, U.S. Patent No 2015/0118735 A1).

The crop protection strategy demonstrated here is straightforward and can be inexpensively applied at commercial scale (∼USD $100 for a 130,000 L reactor). The treatment has a low risk of failure given the broad tolerance of *Chlorella* to low pH. The pH-shock is highly selective against prokaryotes, as illustrated by the two log decrease in the total aerobic counts. Indeed, green microalgae (Chlorophyta) are better prepared than cyanobacteria to regulate internal pH relative to low external pH (relevant studies are summarized in **Figure 9**). Previously, the use of pH-shock treatment has been used to control lactic acid bacterial contamination from anaerobic yeast cultures in the Brazilian bioethanol industry (Basso et al., 2011). In microalgae, the transition to moderately low pH (6) has been used to control diatoms (Zmora and Richmond, 2004), while the transition to high pH (9–10) has been used to promote the growth of cyanobacteria over green microalgae (Vonshak et al., 1983; Touloupakis et al., 2015). Because the pH-shock treatment against *V. chlorellavorus* is applied for a discrete amount of time (15 min), resistance is less likely to develop than if applied continuously to the culture. To date, there is no indication that *V. chlorellavorus* has developed a tolerance to the treatment in our growth systems.

Successful rescue of actively infected algae culture heading for a crash is typically rare and attempts to circumvent a crash generally end in total loss when the culture is discarded. Total culture losses due to infections can greatly impact productivity, not to mention provide ample pathways to infect other ponds in the area during operation and take-down (reviewed by Carney and Lane, 2014; White and Ryan, 2015). The pH-shock treatment we have described here is capable of completely reversing high infection rates (>70% attachment) of a predatory bacterium, doubling *Chlorella* culture longevity and increasing the total harvested biomass from a commercial scale production platform. This treatment is now a routine component of our company mixotrophic operation.

AUTHOR CONTRIBUTIONS

EG and EL studied and reviewed the pH regulation in microalgae. EG and CS planned, designed, acquired, analyzed, and interpreted the data leading to the pH treatment development. LC and BB developed molecular assays and analyzed and interpreted the molecular data leading to the identification and monitoring of *V. chlorellavorus*. All authors drafted, read, critically revised and approved the final manuscript.

ACKNOWLEDGMENTS

We would like to thank the GP2 team (M. Lamont, A. Sitek, J. Lloyd-Randolfi, K. Boyd, B. Alderson, S. Ventre, R. Vannela, and L. Cizek) for helping to develop our mixotrophic platform, K. Sorensen for assistance with molecular work, J. Kniep for pushing the patenting process leading to the publishing of this paper, S. Qin and J. Wilkenfeld for monitoring our cultures, Dr. Gherardi for his advice on statistics, the two anonymous reviewers for their helpful comments/suggestions and B. Melkonian and M. Melkonian for the molecular work on HS26. Lastly, we would like to thank R. A. Andersen for his microscopy work and his invaluable suggestions that greatly improved this manuscript.

REFERENCES

Altschul, S. F., Gish, W., Miller, W., Myers, E. W., and Lipman, D. J. (1990). Basic local alignment search tool. *J. Mol. Biol.* 215, 403–410. doi: 10.1016/S0022-2836(05)80360-2

Basso, L., Basso, T., and Rocha, S. (2011). "Ethanol production in Brazil: The industrial process and its impact on yeast fermentation," in *Biofuel Production-Recent Developments and Prospects*, ed. M. A. S. Bernardes (Rijeka: InTech Open Access Publisher), 85–100.

Bates, L., Maechler, M., Bolker, B., and Walker, S. (2015). Fitting linear mixed-effects models using lme4. *J. Stat. Softw.* 67, 1–48. doi: 10.18637/jss.v067.i01

Beijerinck, M. (1890). Kulturversuche mit Zoochlorellen, Lichenengonidien und anderen niederen Algen. *Bot. Ztg.* 48, 729.

Belkin, S., Mehlhorn, R. J., and Packer, L. (1987). Proton gradients in intact cyanobacteria. *Plant Physiol.* 84, 25–30. doi: 10.1104/pp.84.1.25

Carney, L. T., and Lane, T. W. (2014). Parasites in algae mass culture. *Front. Microbiol.* 5:278. doi: 10.3389/fmicb.2014.00278

Carney, L. T., McBride, R. C., Smith, V. H., and Lane, T. W. (2016). "Molecular diagnostic solutions in algal cultivation systems," in *Micro-Algal Production for Biomass and High-Value Products*, eds S. P. Slocombe and J. R. Benemann (Boca Raton, FL: CRC Press).

Carney, L. T., Reinsch, S. S., Lane, P. D., Solberg, O. D., Jansen, L. S., Williams, K. P., et al. (2014). Microbiome analysis of a microalgal mass culture growing in municipal wastewater in a prototype OMEGA photobioreactor. *Algal Res.* 4, 52–61. doi: 10.1016/j.algal.2013.11.006

Carney, L. T., and Sorensen, K. (2015). *Methods for Treating a Culture of Haematococcus pluvialis for Contamination Using Hydrogen Peroxide. U.S. Patent No 9,113,607*. Washington, DC: U.S. Patent and Trademark Office.

Chelius, M. K., and Triplett, E. W. (2001). The diversity of archaea and bacteria in association with the roots of *Zea mays* L. *Microb. Ecol.* 41, 252–263. doi: 10.1007/s002480000087

Coder, D., and Goff, L. (1986). The host range of the chlorellavorus bacterium ("*Vampirovibrio chlorellavorus*"). *J. Phycol.* 46, 543–547. doi: 10.1111/j.1529-8817.1986.tb02499.x

Coder, D. M., and Starr, M. P. (1978). Antagonistic association of the chlorellavorus bacterium ("*Bdellovibrio*" chlorellavorus) with *Chlorella vulgaris*. *Curr. Microbiol.* 1, 59–64. doi: 10.1007/BF02601710

Das, K. C., Paul, S. S., Sahoo, L., Baruah, K. K., Subudhi, P. K., Ltu, K., et al. (2014). Bacterial diversity in the rumen of mithun (*Bos frontalis*) fed on mixed tree leaves and rice straw based diet. *Afr. J Microbiol. Res.* 8, 1426–1433. doi: 10.5897/AJMR2013.6507

El-Ansari, O., and Colman, B. (2015). Inorganic carbon acquisition in the acid-tolerant alga *Chlorella kessleri*. *Physiol. Plant.* 153, 175–182. doi: 10.1111/ppl.12228

Falkner, G., and Horner, F. (1976). pH Changes in the Cytoplasm of the Blue-Green Alga *Anacystis nidulans* Caused by Light-dependent Proton Flux into the Thylakoid Space. *Plant Physiol.* 58, 717–718. doi: 10.1104/pp.58.6.717

Ganuza, E., and Tonkovich, A. L. (2015). *Method of Treating Bacterial Contamination in a Microalgae Culture with pH shock. U.S. Patent No 9,181,523*. Washington, DC: U.S. Patent and Trademark Office.

Ganuza, E., and Tonkovich, A. L. (2016). "Heliae Development, LLC: an industrial approach to mixotrophy in microalgae," in *Industrial biorenewables: a practical viewpoint*, ed. P. Dominguez de Maria (New York, NY: Wiley), 616.

Ganuza, E., Tonkovich, A. L., and Licamele, J. D. (2015). *Method of Culturing Microorganisms in Non-Axenic Mixotrophic Conditions. 41. U.S. Patent No 2015/0118735 A1*. Washington, DC: U.S. Patent and Trademark Office.

Gehl, K. A., and Colman, B. (1985). Effect of external pH on the internal pH of *Chlorella saccharophila*. *Plant Physiol.* 77, 917–921. doi: 10.1104/pp.77.4.917

Germond, A., Hata, H., Fujikawa, Y., and Nakajima, T. (2013). The phylogenetic position and phenotypic changes of a chlorella-like alga during 5-year microcosm culture. *Eur. J. Phycol.* 48, 485–496. doi: 10.1080/09670262.2013.860482

Gimmler, H., Kugel, H., Leibfritz, D., and Mayer, A. (1988). Cytoplasmic pH of *Dunaliella parva* and *Dunaliella acidophila* as monitored by in vivo ^{31}P-NMR spectroscopy and the DMO method. *Physiol. Plant.* 74, 521–530. doi: 10.1111/j.1399-3054.1988.tb02013.x

Gong, Y., Patterson, D. J., Li, Y., Hu, Z., Sommerfeld, M., Chen, Y., et al. (2015). *Vernalophrys algivore* gen. nov., sp. nov. (Rhizaria: Cercozoa: Vampyrellida), a new algal predator isolated from outdoor mass culture of *Scenedesmus dimorphus*. *Appl. Environ. Microbiol.* 81, 3900–3913. doi: 10.1128/AEM.00160-15

Gromov, B. V., and Mamkaeva, K. A. (1972). Electron microscopic study of parasitism by *Bdellovibrio chlorellavorus* bacteria on cells of the green alga *Chlorella vulgaris*. *Tsitologiia* 14, 256–260.

Guerrero, R., Pedros-Alio, C., Esteve, I., Mas, J., Chase, D., and Margulis, L. (1986). Predatory prokaryotes: predation and primary consumption evolved in bacteria. *Proc. Natl. Acad. Sci. U.S.A.* 83, 2138–2142. doi: 10.1073/pnas.83.7.2138

Holmberg, A., Blomstergren, A., Nord, O., Lukacs, M., Lundeberg, J., and Uhlén, M. (2005). The biotin-Streptavidin interaction can be reversibly broken using water at elevated temperatures. *Electrophoresis* 26, 501–510. doi: 10.1002/elps.200410070

Hoshina, R., and Fujiwara, Y. (2013). Molecular characterization of chlorella cultures of the national institute for environmental studies culture collection with description of *Micractinium inermum* sp. nov., *Didymogenes sphaerica* sp. nov., and *Didymogenes soliella* sp. nov. (Chlorellaceae, Trebouxiphyceae). *Phycol. Res.* 61, 124–132.

Kallas, T., and Castenholz, R. W. (1982). Rapid transient growth at low pH in the cyanobacterium *Synechococcus* sp. *J. Bacteriol.* 149, 237–246.

Küsel, A. C., Sianoudis, J., Leibfritz, D., Grimme, L. H., and Mayer, A. (1990). The dependence of the cytoplasmic pH in aerobic and anaerobic cells of the green algae *Chlorella fusca* and *Chlorella vulgaris* on the pH of the medium as determined by ^{31}P in vivo NMR spectroscopy. *Arch. Microbiol.* 153, 254–258. doi: 10.1007/BF00249077

Lane, A. E., and Burris, J. E. (1981). Effects of environmental pH on the internal pH of *Chlorella pyrenoidosa*, *Scenedesmus quadricauda*, and *Euglena mutabilis*. *Plant Physiol.* 68, 439–442. doi: 10.1104/pp.68.2.439

Mamkaeva, K. A., and Rybal'chenko, O. V. (1979). Ultrastructural characteristics of *Bdellovibrio chlorellavorus*. *Mikrobiologiia* 48, 159–161.

Marin, B. (2012). Nested in the chlorellales or independent class? Phylogeny and classification of the Pedinophyceae (Viridiplantae) revealed by molecular phylogenetic analyses of complete nuclear and plastid-encoded rRNA operons. *Protist* 163, 778–805. doi: 10.1016/j.protis.2011.11.004

Marin, B., Palm, A., Klingberg, M., and Melkonian, M. (2003). Phylogeny and taxonomic revision of plastid-containing euglenophytes based on SSU rDNA sequence comparisons and synapomorphic signatures in the SSU rRNA secondary structure. *Protist.* 154, 99–145. doi: 10.1078/143446103764928521

McBride, R. C., Lopez, S., Meenach, C., Burnett, M., Lee, P. A., Nohilly, F., et al. (2014). Contamination management in low cost open algae ponds for biofuels production. *Ind. Biotechnol.* 10, 221–227. doi: 10.1089/ind.2013.1614

McBride, R. C., Smith, V. H., Carney, L. T., and Lane, W. T. (2016). "Crop protection in open ponds," in *Micro-Algal Production for Biomass and High-Value Products*, eds S. P. Slocombe and J. R. Benemann (Boca Raton, FL: CRC Press).

McMurdie, P. J., and Holmes, S. (2013). Phyloseq: an R package for reproducible interactive analysis and graphics of microbiome census data. *PLoS ONE* 8:e61217. doi: 10.1371/journal.pone.0061217

Pruesse, E., Peplies, J., and Glöckner, F. O. (2012). SINA: accurate high-throughput multiple sequence alignment of ribosomal RNA genes. *Bioinformatics* 28, 1823–1829. doi: 10.1093/bioinformatics/bts252

R Core Team (2016). *R: Language and Enviroment for Statistical Computing*. Vienna: R Foundation for Statistical Computing. Available at: http://www.R-project.org/

Rego, D., Redondo, L. M., Geraldes, V., Costa, L., Navalho, J., and Pereira, M. T. (2015). Control of predators in industrial scale microalgae cultures with Pulsed Electric Fields. *Bioelectrochemistry* 103, 60–64. doi: 10.1016/j.bioelechem.2014.08.004

Safi, C., Zebib, B., Merah, O., Pontalier, P.-Y., and Vaca-Garcia, C. (2014). Morphology, composition, production, processing and applications of *Chlorella vulgaris*: a review. *Renew. Sustain. Energy Rev.* 35, 265–278. doi: 10.1016/j.rser.2014.04.007

Shi, C., Wang, C., Xu, X., Huang, B., Wu, L., and Yang, D. (2015). Comparison of bacterial communities in soil between nematode-infected and nematode-uninfected *Pinus massoniana* pinewood forest. *Appl. Soil Ecol.* 85, 11–20. doi: 10.1016/j.apsoil.2014.08.008

Soo, R. M., Skennerton, C. T., Sekiguchi, Y., Imelfort, M., Paech, S. J., Dennis, P. G., et al. (2014). An expanded genomic representation of the phylum Cyanobacteria. *Genome Biol. Evol.* 6, 1031–1045. doi: 10.1093/gbe/evu073

Soo, R. M., Woodcroft, B. J., Parks, D. H., Tyson, G. W., and Hugenholtz, P. (2015). Back from the dead; the curious tale of the predatory cyanobacterium *Vampirovibrio chlorellavorus*. *PeerJ.* 3:e968. doi: 10.7717/peerj.968

Tonkovich, A. L., Ganuza, E., Licamele, J. D., Galvez, A., Sullivan, T. J., Adame, T., et al. (2014). *Large Scale Mixotrophic Systems. WO. Patent No 2014/144270 A1*. Geneva: World Intellectual property Organization.

Touloupakis, E., Cicchi, B., Benavides, A. M. S., and Torzillo, G. (2015). Effect of high pH on growth of *Synechocystis* sp. *PCC* 6803 cultures and their contamination by golden algae (*Poterioochromonas* sp.). *Appl. Microbiol. Biotechnol.* 100, 1333–1341.

Vonshak, A., Boussiba, S., Abeliovich, A., and Richmond, A. (1983). Production of Spirulina biomass: maintenance of monoalgal culture outdoors. *Biotechnol. Bioeng.* 25, 341–349.

White, R. L., and Ryan, R. A. (2015). Long-term cultivation of algae in open-raceway ponds: messons from the field. *Ind. Biotechol.* 11, 213–220. doi: 10.1089/ind.2015.0006

Wong, A. L. C., Beebee, T. J. C., and Griffiths, R. A. (1994). Factors affecting the distribution and abundance of an unpigmented heterotrophic alga *Prototheca richardsi*. *Freshw. Biol.* 32, 33–38. doi: 10.1111/j.1365-2427.1994.tb00863.x

Zmora, O., and Richmond, A. (2004). "Microalgae for aquaculture: microalgae production for aquaculture," in *Handbook of Microalgal Culture*, ed. A. Richmond (Oxford: Blackwell Publishing Ltd), 365–379.

Conflict of Interest Statement: The authors declare that the research was conducted in the absence of any commercial or financial relationships that could be construed as a potential conflict of interest.

Heliae holds patents relevant to this work, all of which have been cited in this article.

frontiers in Microbiology

ORIGINAL RESEARCH
published: 18 April 2016
doi: 10.3389/fmicb.2016.00516

Discovery of Bioactive Metabolites in Biofuel Microalgae That Offer Protection against Predatory Bacteria

Christopher E. Bagwell[1], Amanda Abernathy[1], Remy Barnwell[1], Charles E. Milliken[1], Peter A. Noble[2], Taraka Dale[3], Kevin R. Beauchesne[4] and Peter D. R. Moeller[4]*

[1] Environmental Sciences and Biotechnology, Savannah River National Laboratory, Aiken, SC, USA, [2] Department of Biological Sciences, Alabama State University, Montgomery, AL, USA, [3] Bioscience Division, Los Alamos National Laboratory, Los Alamos, NM, USA, [4] National Oceanic and Atmospheric Administration/National Centers for Coastal Ocean Science's Center for Human Health Research Hollings Marine Laboratory, Charleston, SC, USA

OPEN ACCESS

Edited by:
Xavier Mayali, Lawrence Livermore National Laboratory, USA

Reviewed by:
Ding He, University of Georgia, USA
Tilmann Harder, University of Bremen, Germany

***Correspondence:**
Christopher E. Bagwell
christopher.bagwell@srnl.doe.gov

Specialty section:
This article was submitted to Aquatic Microbiology, a section of the journal Frontiers in Microbiology

Received: *15 January 2016*
Accepted: *29 March 2016*
Published: *18 April 2016*

Citation:
Bagwell CE, Abernathy A, Barnwell R, Milliken CE, Noble PA, Dale T, Beauchesne KR and Moeller PDR (2016) Discovery of Bioactive Metabolites in Biofuel Microalgae That Offer Protection against Predatory Bacteria. Front. Microbiol. 7:516. doi: 10.3389/fmicb.2016.00516

Microalgae could become an important resource for addressing increasing global demand for food, energy, and commodities while helping to reduce atmospheric greenhouse gasses. Even though *Chlorophytes* are generally regarded safe for human consumption, there is still much we do not understand about the metabolic and biochemical potential of microscopic algae. The aim of this study was to evaluate biofuel candidate strains of *Chlorella* and *Scenedesmus* for the potential to produce bioactive metabolites when grown under nutrient depletion regimes intended to stimulate production of triacylglycerides. Strain specific combinations of macro- and micro-nutrient restricted growth media did stimulate neutral lipid accumulation by microalgal cultures. However, cultures that were restricted for iron consistently and reliably tested positive for cytotoxicity by *in vivo* bioassays. The addition of iron back to these cultures resulted in the disappearance of the bioactive components by LC/MS fingerprinting and loss of cytotoxicity by *in vivo* bioassay. Incomplete NMR characterization of the most abundant cytotoxic fractions suggested that small molecular weight peptides and glycosides could be responsible for *Chlorella* cytotoxicity. Experiments were conducted to determine if the bioactive metabolites induced by Fe-limitation in *Chlorella* sp. cultures would elicit protection against *Vampirovibrio chlorellavorus*, an obligate predator of *Chlorella.* Introduction of *V. chlorellavorus* resulted in a 72% decrease in algal biomass in the experimental controls after 7 days. Conversely, only slight losses of algal biomass were measured for the iron limited *Chlorella* cultures (0–9%). This study demonstrates a causal linkage between iron bioavailability and bioactive metabolite production in strains of *Chlorella* and *Scenedesmus.* Further study of this phenomenon could contribute to the development of new strategies to extend algal production cycles in open, outdoor systems while ensuring the protection of biomass from predatory losses.

Keywords: microalgae, bioactive metabolites, iron, crop protection, predation

INTRODUCTION

Microscopic algae offer tremendous potential as a renewable source of clean burning liquid fuels, industrial chemicals, and high value commodities (Hannon et al., 2010; Sander and Murthy, 2010). Microalgae grow by capturing solar energy to power the conversion of carbon dioxide and inorganic nutrients into valued biochemicals, such as hydrocarbon substrates that can be readily converted to liquid transportation fuels. The sustainability and economic viability of large scale production of microalgal fuels and products, though, will require scientific and engineering advancements to improve our understanding of algal physiology, specifically carbon and energy flows to allow for controlled expression and maximum output of valued commodities (Brennan and Owende, 2010; Hannon et al., 2010; Fields et al., 2014).

Open, outdoor systems (i.e., ponds, raceways) are likely to be the most economical growth format for producing the vast quantities of algal biomass that would be required to meet the renewable fuels targets set forth by the U.S. Department of Energy [USDOE] (2010). Microalgal feedstocks will impose significant demands on nutrient and water resources for continuous operation (Pate et al., 2011; Bazilian et al., 2013). Site selection models are being applied to best match feedstock requirements to resource availability (Wigmosta et al., 2011; Venteris et al., 2014); for example, priority sites may permit access to effluent streams from industry, agriculture, or wastewater treatment facilities to satisfy growth rate potentials. However, these resource inputs and the large surface area required for open pond designs make them highly susceptible to biological contamination. Biological contamination will have important impacts on the sustainability of algal production as well as the efficiency of downstream fuel conversion processes (Ugwu et al., 2008; Gao et al., 2012; Letcher et al., 2013; Smith and Crews, 2014). The lack of crop protection options and practical solutions to control biological contamination is a major obstacle in algal biofuels production.

Bacteria, cyanobacteria, and regional algae can be introduced into an open pond growth system via the water supply and/or resource streams, as well as by atmospheric deposition. These organisms will compete with the intended algal 'crop' for habitat, light, and nutrients. The potential for growth of nuisance strains or toxin producing species must also be considered as many cyanobacteria and microalgae are prolific producers of potent toxins and bioactive metabolites (Leflaive and Ten-Hage, 2007; Berry et al., 2008; Gademann and Portmann, 2008; Bertin et al., 2012a,b; de Morais et al., 2015) which could inadvertently impact the usage of harvested biomass for food or feed preparations, for example. Furthermore, viruses, fungi, and micro zooplankton grazers and predators can significantly and consistently reduce biomass and/or commodity yields (Letcher et al., 2013; Gong et al., 2015). Once established, herbivorous consumers can effectively destroy an algal crop in as little as a few days (Carney and Lane, 2014; Smith and Crews, 2014; Van Ginkel et al., 2015). Integrated pest management entailing selective application of chemical herbicides and pesticides has been successfully demonstrated (McBride et al., 2014; Xu et al., 2015), however, reliance on these treatments will increase operational costs and prolonged use could select for resistance in pest populations. Additional options that have been discussed in the literature include ecological engineering of aquatic communities to promote beneficial biological and/or chemical interactions (de-Bashan et al., 2004; Leão et al., 2010; Mendes and Vermelho, 2013; Bagwell et al., 2014; Carney and Lane, 2014; Kazamia et al., 2014; Smith and Crews, 2014), as well as the development of new biotechnologies to enable genetic and metabolic engineering for trait or strain development (Henley et al., 2013; Rasala et al., 2014). This area of research is receiving tremendous attention because the future success of algal derived fuels and commodities hinges on our ability to manage and control the biology of these engineered ecosystems.

Resource competition and predator – prey interactions play a pivotal role in shaping planktonic community composition and productivity, and these trophic dynamics that will likely be intensified in engineered systems intended for high density production of microalgae. Microalgae, though, have a variety of inducible defenses and adaptations that can be used to gain a competitive advantage or increase survivorship (Legrand et al., 2003; Pohnert et al., 2007; Granéli et al., 2008). For example, specific chemicals released by *Daphnia* during feeding induce colony formation in *Scenedesmus* spp.; these cell aggregates are too large to be consumed by the predator (Zhu et al., 2015). Other inducible defenses are chemically mediated, including the production of protective or deterrent secondary metabolites (i.e., allelochemicals), infochemicals, or toxins (Ianora et al., 2006). Allelopathy in planktonic systems has been known for some time and describes the production of bioactive metabolites by one organism to specifically influence the growth, survival, or reproduction of a target organism(s). Approximately 40 allelopathic species of microalgae have been described and the production of chemical defenses is enhanced by stress conditions; including nutrient limitation (most typically described for N and P), changes in pH and temperature, community composition and abundance, as well as grazing pressure (Wolfe, 2000; Legrand et al., 2003; Tillmann, 2003; Ianora et al., 2006; Granéli et al., 2008; Macías et al., 2008; Van Donk et al., 2011). Bioactive metabolite production by toxic algae is a compelling defensive strategy thought to inhibit the growth of competitors and deter grazers during a 'bloom' of rapid growth and high cell densities (Tillmann, 2004; Granéli et al., 2008). The production of allelochemicals by biofuel candidate strains of microalgae has not been systematically investigated, but the potential for allelopathic interactions to naturally influence, or to be used to intentionally control, the biotic structure of open pond systems is intriguing.

The aim of this study was to conduct a preliminary evaluation of selected biofuel candidate strains of unicellular green algae for innate predatory defenses that may hold promise for exploitation in the development of algal crop protection strategies. This investigation specifically examined the response of dense algal cultures to typical stress scenarios used to trigger triacylglycerides (TAG) biosynthesis (i.e., substrate for biofuel conversion) in algae. This study emphasizes a link between nutrient availability

and bioactive metabolite production in microalgae, and while more work is needed to better understand the physiology and mechanisms involved; inducible defenses and allelochemicals should be examined as part of an overall strategy for achieving the true production potential of algae.

MATERIALS AND METHODS

Strain and Culture Conditions

Scenedesmus sp. (strain 18B) and *Chlorella* sp. (strain 15) were obtained from a regional culture collection (Bagwell et al., 2014) and selected for this investigation based on prior performance in laboratory growth studies. The strains were grown to high density in nutrient replete M8 medium (10 L) with 18 h full spectrum white light/6 h dark cycling and continuous air bubbling. Once stationary phase was reached (as indicated by stabilization in total cell densities), biomass (∼5 g wet wt algae) was harvested by centrifugation (6,000 × *g*, 10 min, 15°C) and directly transferred to independent, 10 L glass column photobioreactors (custom built) containing modified growth medium devised to limit biomass for various macro- and/or micro-nutrients. Unmodified M8 medium is formulated to maximize biomass capacity and served as the nutrient replete experimental control (Mandalam and Palsson, 1998). Growth medium modifications (i.e., treatments) employed in this study are as follows. Treatment 1 was modified M8 medium having only ½ total PO_4 (370 mg/L KH_2PO_4, 130 mg/L Na_2HPO_4*$2H_2O$) and a 1000x increase in Cu ∼0.1 mg/L $CuSO_4$*$5H_2O$ (calculated final concentration, 0.5 μM). Copper sulfate is a commonly used algaecide and it was reasoned that low level applications might lend additional stress to microalgae cultures during production. Treatment 2 was N8 medium which is purported to limit algal biomass for N, Mg, S, and Fe (Mandalam and Palsson, 1998). Treatment 3 was modified M8 medium which contained 1/100th KNO_3 (30 mg/L). Treatment 4 was modified M8 medium which contained 1/10th total iron (1 mg/L Fe(III)-EDTA, 13 mg/L Fe(II)SO_4*$7H_2O$), and Treatment 5 was also modified M8 medium which contained 1/100th total iron (0.1 mg/L Fe(III)-EDTA, 1.3 mg/L Fe(II)SO_4*$7H_2O$). Cultures were grown for 3 weeks before being submitted for cytotoxicity screening. These medium formulations were selected for laboratory experimentation with high density microalgal cultures and thus, are not expected to be strain optimized or necessarily nutrient limiting for practical applications.

Flow Cytometry

Samples of *Scenedesmus* sp. (strain 18B) and *Chlorella* sp. (strain 15) cultures were shipped overnight to Los Alamos National Laboratory (LANL) on blue ice for analysis by flow cytometry. Multi-parameter flow cytometry measurements were obtained using a BD Accuri™ C6 flow cytometer fitted with a 96-well plate autosampler. Prior to sample analysis, instrumentation fluidics were calibrated to a 250 μl volume in a 96-well round bottom deep well plate. Algal samples were diluted in the appropriate medium designated for each treatment to ensure a count rate of 1,000–10,000 events/second. All samples were independently run three times, each in duplicate, thereby giving six analytical replicates per treatment. Counts were collected at a set event value of 10,000 on the slow fluidics setting.

Algae cells were gated based on a dot-plot of side light scatter versus forward light scatter. Chlorophyll autofluorescence per cell was determined in the same experiment by using the 488 nm excitation laser and a 670 nm long pass emission filter in the flow cytometer. The green fluorescence intensity (488 nm ex, 530/30 nm em) of each event was also measured on these samples. These data was used as the unstained, background fluorescence intensity, to be subtracted from the BODIPY® (505/515) stained replicates (below).

Neutral lipid content, specifically TAG, for *Scenedesmus* and *Chlorella* samples was examined by flow cytometry, using the green fluorescent neutral lipid stain, BODIPY® (505/515; Life Technologies, D-3921). Briefly, samples were diluted in triplicate in appropriate medium, as described above. Samples were stained by adding a working stock of 400 μM BODIPY® in 50% DMSO to a final concentration of 22.6 μM BODIPY®. Stained samples were incubated at RT in the dark for at least 30 min and analyzed within 3 h. 10,000 count events were collected per well, on the slow fluidics setting. Green fluorescence intensity (488nm excitation, 530/30 nm emission) was measured for each event. The arithmetic mean of the fluorescence intensity for the stained samples was subtracted from the arithmetic mean of the fluorescence intensity of the unstained samples and plotted in GraphPad Prism.

Fluorescence Microscopy

BODIPY® (505/515) stained cultures (8 μl) were also individually examined using a Zeiss Axioplan epifluorescence microscope fitted with a Zeiss 100x objective lens. Images were captured using a Nikon D7000 digital camera and Nikon Camera Control Pro 2 software. Fluorescence was observed using a 450–490 nm excitation laser and a 520 nm long pass emission filter, permitting the collection of BODIPY® (505/515) and chlorophyll fluorescence in the same image.

Cytotoxicity Assay

Cell mass and production media were separated by centrifugation (6,000 × *g*, 15 min, 15°C) and samples (5 g wet weight algae and 1 L production medium/treatment) were lyophilized for cytotoxicity bioassays conducted at the NOAA laboratory in Charleston, SC, USA. Briefly, elutropic solvent extractions (dichloromethane, methanol, and water) were performed on every sample; yielding partitioned samples having corresponding differences in polarity. Partitioned samples were dried under a nitrogen gas stream and recovered in 100 μL of methanol as the carrier solvent for cytotoxicity assay against two immortalized mammalian cell lines in a high throughput process. Assays utilized the rat pituitary GH_4 C1 cell line (ATCC CCL-82.2) and the mouse neuroblastoma Neuro 2A (N2A) cell line (ATCC CCL-131) in a conventional MTT (3-(4,5-Dimethylthiazol-2-yl)-2,5-diphenyltetrazolium bromide) colorimetric reaction to establish cytotoxicity of algal or produced water samples (Mosmann, 1983). Briefly, mammalian cells were transferred to a 96-well culture plate at a concentration of 2.8×10^3 cells/mL (100 μl

per well) and incubated at 37°C in 5% CO_2 for at least 4 h before use in the MTT assay. Fractionated algal samples were added to sample wells in triplicate at 4, 2, 1 μl as to inform of cytotoxic compound potency or relative quantity. Methanol was used as a negative vehicle control and chloroform was used as a positive cytotoxic control (4 μl/well). All reaction wells received MTT (15 μL), and plates were then incubated for 24 h at 37°C in 5% CO_2. Assays were stopped by adding 100 μl of a 0.01% HCl (v/v), 10% SDS (w/v) solution to the reaction wells and color formation was measured using a plate reader at 570 nm. Samples that assayed as 'bioactive' were subsequently fractionated by liquid chromatography and base level characterization of bioactive components (compound tagging) was performed by LC/MS. Bioactive methanol fractions were then loaded on a long glass column (1″id × 2.5′ long) containing 50 g of Amino packing (Sepra NH2 50 μm, 65A, Phenomenex). The packing was charged with 100% ethyl acetate (EtoAC) and the sample(s) was loaded in EtoAC. A series of elutions were performed with 100% methanol, 95% methanol/water, 90% methanol/water, 85% methanol/water. Fractions were collected separately, dried, and then tested for cytotoxicity as described above. The 90% methanol fraction was the most active and subsequently carried to the next step of semi-preparative HPLC purification.

Liquid Chromatography/Mass Spectroscopy (LC/MS)

Bioactive fractions (100 μl; produced as described above) were semi-purified on a Waters® HPLC system equipped with a Luna C18 (3 μm) column (Phenomenex Corporation, Torrance, CA, USA) by isothermal (35°C) gradient elution (97% H_2O/3% Acetonitrile to 100% Acetonitrile) at a 1.0 mL/min flow rate with a photodiode array detector. Molecular mass determinations were made with a Waters® 1525 system equipped with a 2767 sample manager and Micromass ZQ Mass Spectrometer. Spectra were analyzed using the MassLynx™ software system.

Nuclear Magnetic Resonance (NMR)

Semi-preparative HPLC purified bioactive components were structurally analyzed by nuclear spectroscopy using a 700 MHz NMR Spectrometer Bruker AVANCE™ III HD equipped with a Bruker CryoProbe™. One-dimensional proton (^{1}H) and carbon (^{13}C) experiments were conducted using the Bruker ZG NMR pulse sequence and the Bruker ZGDC pulse sequence, respectively. Spectral analyses utilized the TopSpin™ software (Bruker) to structurally characterize the partitioned samples.

Elemental Analysis of Microalgal Biomass

Microalgal biomass (1 g wet weight) was prepared for elemental analysis according to Bagwell et al. (2008) in order to remove loosely sorbed metals from extracellular matrices. Aqua regia dissolution was performed by digesting algal biomass with 3:1 (v:v) mixture of HCl and HNO_3 for 30 min. Samples were diluted to 10 ml in deionized water and analyzed on an Agilent 730 ES Simultaneous Inductively Coupled Plasma – Atomic Emission Spectrometer (ICP-AES). Yttrium was used as an internal standard and instrument calibration was performed with a NIST traceable elemental standard.

Statistical Analyses

Orthogonal transformation of the elements to their principal components (PC) was performed in JMP® (SAS). Pearson correlation coefficient was used to measure the linear correlation between elements. Principal component analysis (PCA) was determined using the matrix of distances, D, and Euclidean distance. To investigate and visualize differences between the elements, the first two principal components (PC1 and PC2) of the distance matrix D were retained and a projection of each sample time was calculated onto the (PC1, PC2) plane as a bi-plot. Projecting sample time on the ordination plot reveals the relative contribution of time to the ordination of the elements.

Predation Studies

Vampirovibrio chlorellavorus cultures were maintained as co-cultures with *Chlorella sorokiniana* (strain DOE 1412) in standard formulation BG-11 growth medium. Prior to experimentation, a working stock culture of *V. chlorellavorus* was prepared by recovering the aqueous phase (30 mL) of gravity settled (10 min) *C. sorokiniana* co-cultures. *V. chlorellavorus* cells were harvested by centrifugation (10,000 × *g* for 5 min) and the bacterial pellet was re-suspended in freshly prepared M8 medium (15 mL) containing no added iron. C*hlorella* sp. (strain 15) stock cultures were prepared under iron limited growth conditions corresponding to Treatments 4 and 5 as described above, and cultures grown in unmodified M8 medium were designated as controls. Cytotoxicity bioassays were performed on *Chlorella* sp. (strain 15) biomass harvested from all treatments, as described above, to confirm cytotoxicity for the Fe-limited cultures (Treatments 4 and 5) and no-reactivity for the control culture. Aliquots (24 mL) from each of the primary cultures (10^6 cells/mL) were transferred in triplicate to sterile snap cap tubes with the predator *V. chlorellavorus* (1 mL) or without (1 mL sterile M8 medium). Experimental co-cultures were held at 28°C in the dark for 7 days. Viable algal cell counts that were determined microscopically (60× objective) using a hemocytometer.

RESULTS AND DISCUSSION

Culture Screening for Cytotoxicity and TAG

A conceptual illustration of the experimental design and analyses performed for bioactive metabolite induction, detection, and recovery from microalgae is summarized in **Figure 1**. *Scenedesmus* sp. (strain 18B) and *Chlorella* sp. (strain 15) cultures were grown in a variety of medium formulations intended to restrict biomass for macro- or micro-nutrients to simulate conditions that could be encountered during algal biomass production for biofuels or other high value commodities. Neutral lipid production, chiefly as TAG, is a well characterized

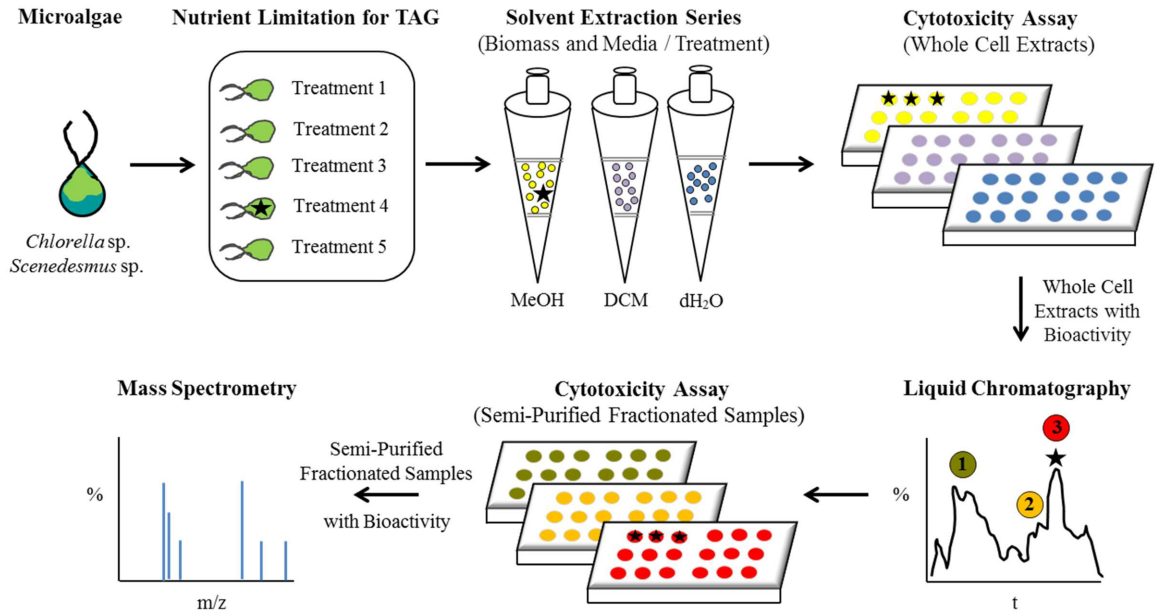

FIGURE 1 | Flow diagram illustrating the experimental design and analytical characterization of bioactive metabolites from microalgae.

response to nutrient limitation or environmental stress in diverse microalgae, including *Scenedesmus* and *Chlorella* strains, yet their ability to synthesize potentially beneficial bioactive metabolites in response to these stressors has not been investigated (e.g., Kellam et al., 1988). Interestingly, when iron was a limited nutrient, both strains yielded solvent fractionated samples that exhibited cytotoxicity when presented to mammalian cells (**Table 1**). Corresponding liquid chromatographs and total ion current plots for these solvent fractionated whole cell preparations are provided as Supplementary Figures S1–S6.

Plots of the mean fluorescence intensity for TAGs (BODIPY 505/515 staining) and chlorophyll autofluorescence of *Scenedesmus* sp. (strain 18B) cultures, as measured by flow cytometry, between treatments are shown in **Figure 2A**. Treatment 1 resulted in high cell to cell variability as fluorescence signals for TAG (BODIPY®) and chlorophyll were both equally high. Cultures from Treatments 2, 3, and 5 showed low TAG accumulation as indicated by BODIPY® fluorescence relative to significantly higher chlorophyll content. Finally, Treatment 4 produced a highly chlorotic culture as indicated by the very low chlorophyll auto-fluorescence signal. The TAG induction response for Treatment 4, though, was strong and unanimous among cells in the culture, large lipid bodies were observed by microscopy.

TABLE 1 | Cytotoxicity demonstrated for freshwater green algae in response to nutrient limitation.

Strain	Revised medium formulation	Elutropic solvent series		
		DCM	MeOH	H_20
***Scenedesmus* sp. (Strain 18B)**	Treatment 1 ($^1/_2$ PO_4, 1000x Cu^{2+})	–	–	–
	Treatment 2 (N8: Limited N, Mg, S, Fe)	–	$+^{N2A}$	–
	Treatment 3 ($^1/_{100}$ NO_3)	–	–	–
	Treatment 4 ($^1/_{10}$ total iron)	$+^{GH4C1/N2A}$	$++^{GH4C1/N2A}$	$++^{GH4/N2A}$
	Treatment 5 ($^1/_{100}$ total iron)	ND	ND	ND
***Chlorella* sp. (Strain 15)**	Treatment 1 ($^1/_2$ PO_4, 1000x Cu^{2+})	–	–	–
	Treatment 2 (N8: Limited N, Mg, S, Fe)	–	–	–
	Treatment 3 ($^1/_{100}$ NO_3)	–	–	–
	Treatment 4 ($^1/_{10}$ total iron)	–	$+++^{GH4C1/N2A}$	–
	Treatment 5 ($^1/_{100}$ total iron)	–	$+++^{GH4C1/N2A}$	–

The potency of algal cell extracts to the mammalian cells was inferred from the bioassay volume resulting in cell death; thus, 1 µl = +++, 2 µl = ++, and 4 µl = +. Cytotoxic activity is inferred from the immortalized mammalian cell lines GH4C1 and N2A which exhibit predominantly Ca^{2+} channel activity and Na^+ channel activity, respectively. Bioassay results where no cytotoxicity was detected is indicated by '–' and 'ND' indicates bioassays could not be performed because of poor growth and insufficient biomass.

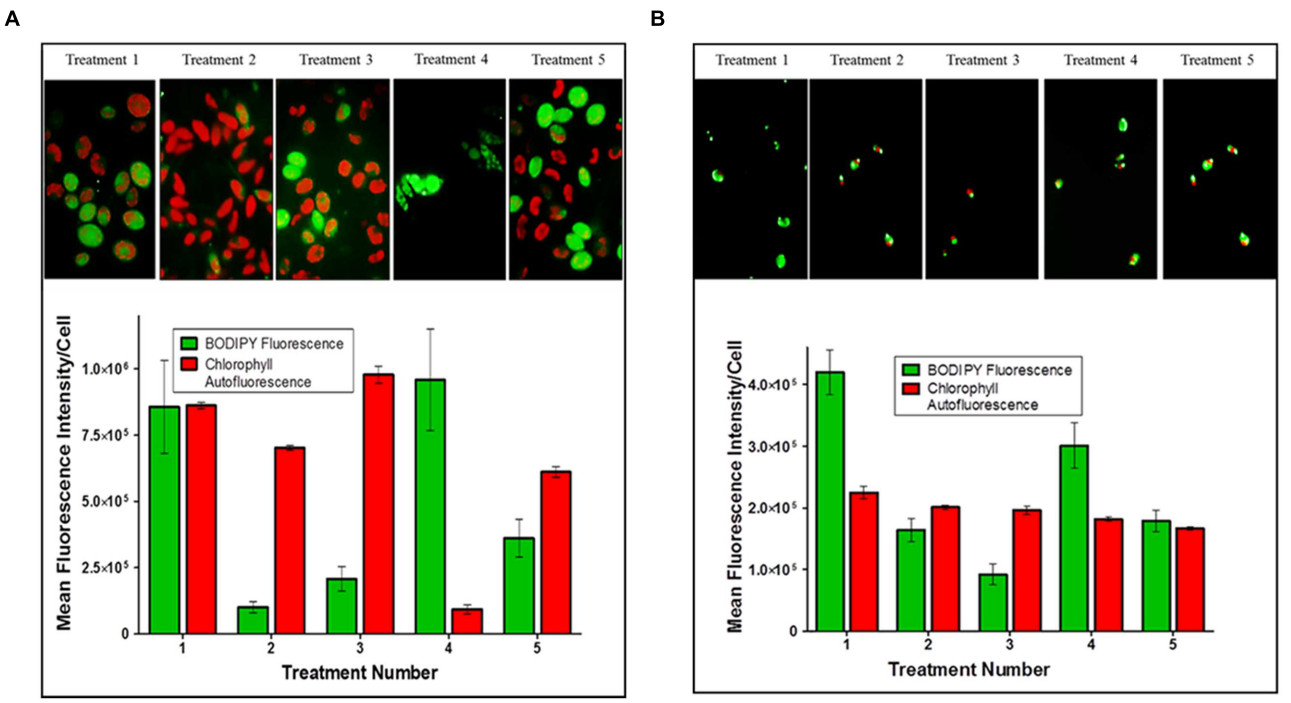

FIGURE 2 | triacylglycerides (TAG) induction in microalgal cultures. The arithmetic mean and standard deviation ($n = 6$) in fluorescence intensity per cell for **(A)** *Scenedesmus* sp. (strain 18B) and **(B)** *Chlorella* sp. (strain 15) treatment populations analyzed by multi-parameter flow cytometry. Cells were stained with BODIPY® 505/515 for TAG accumulation and auto-fluorescence was measured for chlorophyll content.

Bioactivity was measured from all three extraction phases performed on *Scenedesmus* Treatment 4 biomass, though relative activity appeared to trend with solvent polarity (DCM < MeOH = H_2O; **Table 1**). Biomass yields in Treatment 5 were too low to perform a valid cytotoxicity assay, no results are provided for this treatment. Cytotoxicity was also measured for *Scenedesmus* Treatment 2 biomass though the bioassay reaction was weak and inhibitory to only 1 of the mammalian cell lines.

Iron levels in N8 medium (Treatment 2) are comparable to those in Treatment 4 (10 mg/L and 14 mg/L, respectively), however, N8 medium is intended to also limit cell growth for N, Mg, and S (Mandalam and Palsson, 1998). *Scendesmus* sp. (strain 18B) was quite sensitive to iron limitation, compared to *Chlorella* sp. (strain 15) described below, suggesting possible differences between cultures in their physiological requirement for iron or their ability to efficiently transport iron into the cell. *Scenedesmus* cultures were quick to undergo chlorosis in response to iron limitation and growth yields were exceptionally low (<1 g/L wet weight); still, potent cytotoxic metabolites could be extracted. Because of the severe constraints in *Scenedesmus* biomass production in response to nutrient limitation, however, we could not pursue the *Scenedesmus* sp. (strain 18B) culture in any meaningful way. These results are significant, however, because *Scenedesmus* strains are being actively pursued for large scale production of biofuels and commodities (Fields et al., 2014; Hamed and Klöck, 2014; McBride et al., 2014), and this study provides an interesting starting point for future investigations of better performing strains that may also elicit production of bioactive metabolites under similar treatments.

Chlorella sp. (strain 15) cultures proved to be generally robust and insensitive to macro- or micro-nutrient limitation as assessed by growth yields, which typically exceeded 5 g/L (wet weight), and microscopic inspection by auto-fluorescence. Plots of the mean relative fluorescence (BODIPY® and chlorophyll) of *Chlorella* cultures between treatments are shown in **Figure 2B**. Treatments 1 and 4 both induced TAG accumulation as indicated by BODIPY® fluorescence in these cultures relative to the auto-fluorescence of chlorophyll. TAG induction in Treatment 1 was clearly the strongest, and while the measured BODIPY® signal response for Treatment 4 was modest; relative to chlorophyll auto-fluoresce and by comparison to other treatments, we can conclude that iron depletion prescribed by this treatment did induce TAG accumulation. Conversely, high cell to cell variability measured for Treatments 2, 3, and 5 indicate physiological asynchrony among cells at different stages of growth and TAG accumulation. As performed, these treatments failed to produce a demonstrable TAG induction signal in *Chlorella* sp. (strain 15) as indicated by BODIPY® fluorescence.

Cytotoxic activity was consistently high for the methanol soluble fractions obtained from *Chlorella* biomass harvested from Treatments 4 and 5 (**Table 1**). The strength of the cytotoxicity response was unaffected by a 4x dilution of the algal extracts, which we interpreted to signify a high abundance or potency (reactivity) of the bioactive metabolites present in those extracts.

The experimental design (i.e., medium formulations, growth/incubation time) was not optimized for maximum TAG production by these microalgal strains. Analysis by flow cytometry clearly showed a pronounced stress response imposed by a few treatments (*Scenedesmus* Treatment 4 and *Chlorella* Treatments 1 and 4) as reflected by BODIPY® fluorescence for TAG relative to chlorophyll autofluorescence (**Figure 2**). All other treatments failed to impose a strong induction response for TAG biosynthesis within the time frame permitted for these experiments. Low BODIPY® fluorescence relative to high or equal intensity chlorophyll autofluorescence implies these cultures had yet to fully transition out of photoautotrophic growth. Still, we are encouraged by the initial results that suggest the possibility of coordinating TAG biosynthesis and bioactive metabolite production in these microalgal strains.

The cytotoxicity outcomes were independently confirmed in three different growth studies. When both cultures were grown in iron depleted medium, we were able to consistently and reproducibly extract methanol soluble cytotoxic fractions from both strains. Based on these preliminary results, we hypothesize that either iron is an important trigger for induction of cytotoxic metabolite production in these green microalgae strains, or iron itself represents a critical chemical component whereby complexation with organic metabolites modulates compound reactivity (e.g., Oppenheimer et al., 1979; Gademann and Portmann, 2008). Iron has been implicated as important trigger for the production of chemical defenses in algae and dinoflagellates (Moeller et al., 2007; Gademann and Portmann, 2008; Bertin et al., 2012b); however, the inherent chemical and biological complexity of natural systems and the synergistic effects of nutrients has complicated mechanistic deduction of pathways that regulate cellular toxicity (e.g., Silva, 1990; Plumley, 1997; Larsen and Bryant, 1998; Kuffner and Paul, 2001; Anderson et al., 2002; Leflaive and Ten-Hage, 2007; Hardison et al., 2013).

Correlation between Iron and Cytotoxicity

In order to test this hypothesis a series of experiments were performed in which iron was added back to *Chlorella* sp. (strain 15) cultures once cytotoxicity was established. If our supposition is correct, that iron depletion is a trigger for bioactive metabolite production, supplementation with new iron should reduce the cytotoxicity of the algal biomass in a time and/or concentration dependent manner. Again, *Chlorella* cultures (10 L) were limited for iron as prescribed in Treatment 4 (1/10 total iron) and Treatment 5 (1/100 total iron) to induce cytotoxicity (start of the experiment, $T = 0$), which was confirmed by *in vivo* bioassay and LC-MS fingerprinting of the methanol soluble cell fractions. Once cytotoxicity was confirmed, iron levels were fully restored for Treatment 4 *Chlorella* cultures; i.e., 0.1 mg/L Fe(III)-EDTA and 1.3 mg/L $Fe(II)SO_4 \times 7H_2O$ was added to the cultures. Iron-replete conditions were established for the Treatment 5 *Chlorella* cultures; i.e., 40 mg/L Fe(III)-EDTA and 520 mg/L $Fe(II)SO_4 \times 7H_2O$ was added to the cultures. Upon the addition of iron, deep green pigmentation was restored to cultures of both treatments, signifying a shift from a chlorotic state to chlorophyll biosynthesis.

Figure 3 shows the elemental responses of *Chlorella* sp. (strain 15) cultures following the addition of iron as a function of time. Relative cytotoxicological activity responded in a time dependent manner in all cultures for both treatments following the addition to iron. Cytotoxicity in Treatment 4 (**Figure 3A**) cultures was just detectable after 7 days and no activity could be detected at 14 days. Interestingly, ordination plots of elements revealed that cellular contents of potassium (K), sulfur (S), and phosphorous (P) most strongly distinguished these time dependent samples, and that time had the greatest effect on S and P concentration, not K, at 14 days.

For the Treatment 5 cultures, only weak cytotoxicological activity could be measured at 7 days. Again, ordination plots suggest a time dependent response in elemental composition of microalgal cultures (**Figure 3B**). Samples taken at the start of the experiment, time = 0, were distinguished by sulfur (S) and potassium (K) concentration. Conversely, phosphorous (P) and iron (Fe) were more affected by time than the other elements included in the analysis, with Fe being the most responsive.

These results combined imply decreased potency (inactivation) or turnover of the cytotoxic metabolites in response to added iron. However, it remains unclear whether iron itself is the cue for bioactive metabolite production or turnover, or if the condition restricts cells for other nutrients (i.e., K, S, and P) which then triggers bioactive metabolite production. In fact, the production of allelochemicals and toxins by microalgae in response to co-limiting or unbalanced concentrations of nitrogen (N), phosphorous (P), and iron (Fe) are well documented (Granéli et al., 2008; Van Donk et al., 2011; Xu et al., 2013). Over the course of this experiment, algal cell numbers were statistically invariant ($p = 0.33$) between treatments, thus the changes in phenotype observed were due to a metabolic response(s) to available iron and were not an indirect consequence of changes in cell densities.

All living organisms require iron but this micronutrient is often in limited supply or chemically unavailable in many aquatic environments (Martin et al., 1994; Wilhelm, 1995; Hecky and Kilham, 1988; Boyd et al., 2007; Lis et al., 2015). In response to iron limitation many eubacteria, cyanobacteria, fungi, and algae will synthesize iron chelating metabolites, modulate virulence, and in some cases, release toxins or other bioactive metabolites to gain a competitive advantage for limited iron supplies (Loper and Buyer, 1991; Buysens et al., 1996; Mey et al., 2005; Paulsen et al., 2005; Gademann and Portmann, 2008; Ding et al., 2014). For example, *Anabaena flos-aquae* releases metal chelating siderophores as well as allelopathic chemicals to suppress the growth of competitors (Matz et al., 2004; Granéli et al., 2008). Additionally, the biosynthesis of authentic marine toxins domoic acid (produced by *Pseudo-nitzschia*; Mos, 2001) and microcystins (produced by *Microcystis aeruginosa*; Lukač and Aegerter, 1993) has been shown to be directly linked to iron bioavailability. To be clear, we are not suggesting that *Chlorella* and *Scenedesmus* are authentic toxin producers or that

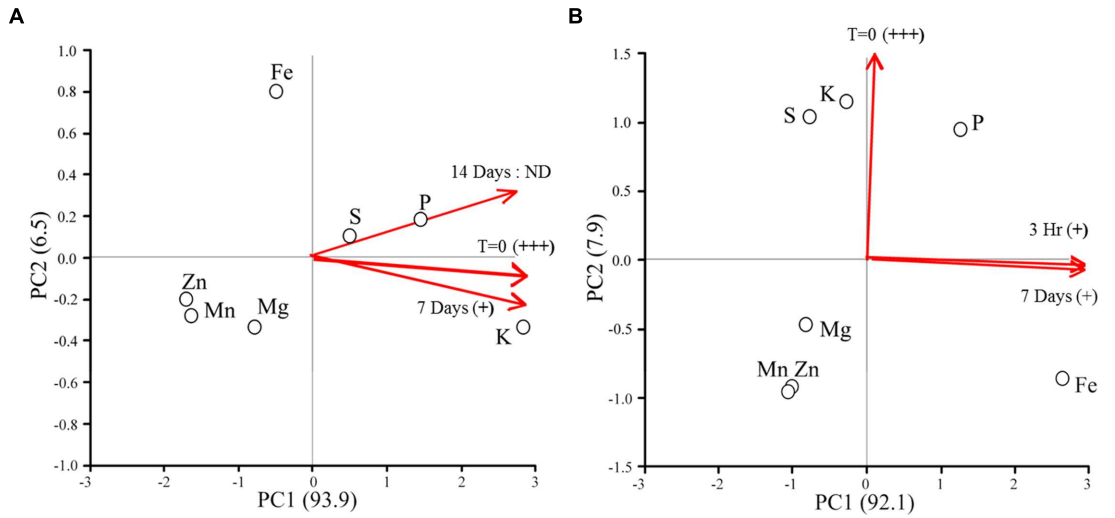

FIGURE 3 | Ordination plots of elements for cytotoxic *Chlorella* sp. (strain 15) cultures responding to the addition of new iron. Red lines indicate the relative contribution of sampling time to the positioning of the elements in the ordination. Iron levels were fully restored for Treatment 4 *Chlorella* cultures **(A)**; i.e., 0.1 mg/L Fe(III)-EDTA and 1.3 mg/L $Fe(II)SO_4 \times 7H_2O$ was added to the cultures. Iron-replete conditions were established for the Treatment 5 *Chlorella* cultures **(B)**; i.e., 40 mg/L Fe(III)-EDTA and 520 mg/L $Fe(II)SO_4 \times 7H_2O$ was added to the cultures. Relative cytotoxic activity was inferred by *in vivo* bioassay and is denoted as highly active (+++), low level of activity (+), and no activity detected (ND).

these compounds are necessarily hazardous. Many microalgae, including biofuel candidate strains, are known to synthesize bioactive metabolites and allelochemicals that act as a defense or a deterrent against competitors, predators and grazers (Tanaka et al., 1986; Ianora et al., 2006; Adolf et al., 2007; Leflaive and Ten-Hage, 2007; Gademann and Portmann, 2008; de Morais et al., 2015).

Culture Susceptibility to Predation

Experiments were performed to determine if the bioactive metabolites induced by iron limitation in *Chlorella* sp. (strain 15) would elicit protection against a specific predator. *V. chlorellavorus* was selected for these experiments because this bacterium has been shown to be a particularly problematic threat in the outdoor cultivation of algae. This bacterium is an obligate predator of green algae with a host range restricted to *Chlorella* (Coder and Starr, 1978; Coder and Goff, 1986; Soo et al., 2015). Recently, *V. chlorellavorus* was identified in water samples collected during scaled up growth studies in outdoor greenhouses and raceways and most importantly, was determined to be responsible, or at least complicit, in crashes of *C. sorokiniana* cultures (Judith Brown, personal communication). The sequenced genome of *V. chlorellavorus* is consistent with an obligate predatory lifestyle which includes discrete phases of attachment to the *Chlorella* host, penetration into the host cell using a type IV secretion apparatus, consumption of leaked metabolites, cell division, and release (Soo et al., 2015).

Chlorella biomass was prepared under iron limited conditions and methanol soluble fractions were assayed for cytotoxicity as described previously. Treatment 4 biomass (1/10 total iron), again, consistently generated highly bioactive preparations; fourfold dilution of the extract did not decrease cytotoxicity. Treatment 5 biomass, however, elicited a weak but detectable response only when bioassays were conducted with full strength (4 µl) preparations. Iron limited (cytotoxicity confirmed) and control *Chlorella* cultures were then incubated with the predator in the dark to suspend photoautotrophic growth of the host alga. Additionally, cultures were maintained in the depleted growth medium to preserve the physiological state (cytotoxic phenotype) of the host cultures for the duration of the experiment. Predation by *V. chlorellavorus* effectively destroyed the control cultures (**Figure 4**); viable cell counts were reduced on average by 72% in 7 days. Remarkably, no detectable cell loss was measured for Treatment 4 cultures (high level of relative cytotoxicity), and averaged viable cell loss for Treatment 5 cultures (low level of relative cytotoxicity) was only 9%. In a parallel experiment, iron was reintroduced by transferring the cytotoxic cultures to fresh M8 medium. Predatory losses for these cultures averaged 0 and 57% for Treatments 4 and 5, respectively. Standard deviation around the averaged cell counts did not exceed 15% for any of these experimental treatments. These results reinforce the postulated linkage between iron availability and the synthesis and potency of bioactive metabolites in this *Chlorella* strain. Importantly, the bioactive metabolites induced by iron limitation protected *Chlorella* biomass against epibiotic predation by *V. chlorellavorus*.

Preliminary Characterization of Bioactive Metabolites

Approximately 450 g (wet weight) of viable *Chlorella* sp. (strain 15) biomass was produced under iron limiting conditions, as described for Treatment 4. Cytotoxic metabolites were captured

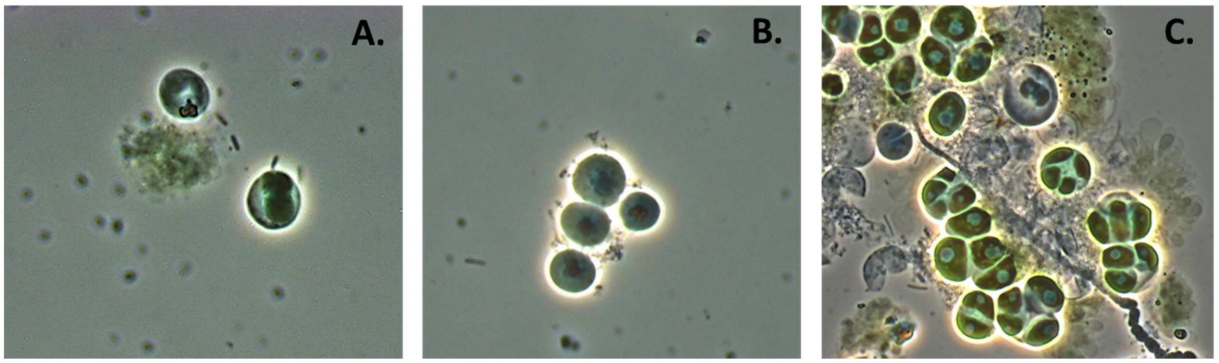

FIGURE 4 | *Chlorella* culture under attack by *Vampirovibrio chlorellavorus*. **(A)** Shows *V. chlorellavorus* (rods) seeking out and contacting algal cells. **(B)** Shows epibionts (coccoids) attached to host cells. **(C)** Shows the aftermath of lysed and degraded algal cells.

by HPLC separation and fraction collection, and individual fractions were re-assayed for bioactivity (Supplementary Figures S5 and S6). Partial characterization of the most abundant bioactive sample by NMR provided spectra demonstrating the presence of diagnostic anomeric carbon resonances between 90 and 102 ppm (Supplementary Figure S7). These resonances coupled to oxygenated carbons found in the 68–85 ppm range are indicative of a glycosidic compound. It should be noted that these preparations for NMR were not of absolute purity and despite relatively high activity; chromatographic purification yielded only 50 μg of material which is insufficient for full structural characterization. For comparison, the complete characterization of the infochemicals released by grazing *Daphnia* which induce morphological defense in microalgae required 10 kg of starting material because the active compounds, aliphatic sulfates, were present in such low concentration (Yasumoto et al., 2008). In fact, the majority of allelopathic chemicals known to be produced by microalgae have not been formally characterized because of the technical limitations inherent to the study of molecules that are produced intermittently in response to unknown stimuli at sub - ng/L quantities (Legrand et al., 2003; Ianora et al., 2006; Leflaive and Ten-Hage, 2007; Granéli et al., 2008). Furthermore, several peaks observed by ^{13}C NMR in the 50–70 ppm range could signify the presence of low molecular weight peptides. While the sugar signals were much stronger by comparison in these samples, we cannot definitively credit the observed activity strictly to a glycoside, nor can we discard the possibility of a synergistic mode of action.

CONCLUSION

It is now evident that chemical signals play an important role in regulating phytoplankton community structure and trophic interactions (Legrand et al., 2003; Ianora et al., 2006, 2011; Pohnert et al., 2007; Van Donk et al., 2011). A better understanding of the ecological roles of potent allelochemicals and bioactive metabolites could help inform the development of new strategies to improve microalgal domestication and cultivation (Mendes and Vermelho, 2013). At this point we cannot meaningfully extrapolate these laboratory results to possible ecological consequences in a natural or engineered setting. While we have demonstrated the production of bioactive metabolites for two biofuel candidate strains of algae in response to iron limitation, the possibility that these metabolites function allelopathically or as infochemicals was not investigated here but should be considered in the future. The experimental treatments imposed here are relevant to the large scale production of algae because nutrient depletion will be inherent to dense algal cultures, or used as an operational strategy to cut cost or stimulate oil production for biofuels. Our results suggest that iron might be useful to help boost the production of neutral lipids (specifically TAG) in *Chlorella* and *Scenedesmus* if the timing of these events can be coordinated, as well as trigger the induction of a chemical defense against a particularly devastating bacterial predator, *V. chlorellavorus*. Further work is needed to evaluate the complex interactions between key environmental parameters, the expression and stability of bioactive metabolites *in vivo*, and to examine the possible ecological interactions mediated by these chemicals within planktonic communities. Inducible chemical defenses could help facilitate the development of new crop protection strategies for algal cultivation and production facilities.

AUTHOR CONTRIBUTIONS

CB, AA, RB, CM, PN, TD, KB, and PM contributed intellectual input and assistance to this study and manuscript preparation. CB developed the original framework. TD, KB, and PM contributed reagents and data analysis; CB, PN, and TD performed statistical analysis and data integration and CB wrote the paper.

FUNDING

This research was jointly supported by the SRNL's Laboratory Directed Research and Development Program and the U.S.

Department of Energy, Office of Energy Efficiency and Renewable Energy, Biomass Program (Award # DE-NL0022905).

ACKNOWLEDGMENTS

The authors would like to thank the handling editor and the reviewers whose input greatly improved the quality and impact of the manuscript. We also express gratitude to Judith Brown at the University of Arizona for kindly providing access to *Vampirovibrio chlorellavorus*.

SUPPLEMENTARY MATERIAL

The Supplementary Material for this article can be found online at: http://journal.frontiersin.org/article/10.3389/fmicb.2016.00516

REFERENCES

Adolf, J. E., Krupatkina, D., Bachvaroff, T., and Place, A. R. (2007). Karlotoxin mediates grazing by *Oxyrrhis marina* on strains of *Karlodinium veneficum*. *Harmful Algae* 6, 400–412. doi: 10.1016/j.hal.2006.12.003

Anderson, D. M., Glibert, P. M., and Burkholder, J. M. (2002). Harmful algal blooms and eutrophication: nutrient sources, composition, and consequences. *Estuaries* 25, 704–726. doi: 10.1007/BF02804901

Bagwell, C. E., Milliken, C. E., Ghoshroy, S., and Blom, D. A. (2008). Intracellular copper accumulation enhances the growth of *Kineococcus radiotolerans* during chronic irradiation. *Appl. Environ. Microbiol.* 74, 1376–1384. doi: 10.1128/AEM.02175-07

Bagwell, C. E., Piskorska, M., Soule, T., Petelos, A., and Yeager, C. M. (2014). A diverse assemblage of indole-3-acetic acid producing bacteria associated with unicellular green algae. *Appl. Biochem. Biotechnol.* 173, 1977–1984. doi: 10.1007/s12010-014-0980-5

Bazilian, M., Davis, R., Pienkos, P. T., and Arent, D. (2013). The energy-water-food nexus through the lens of algal systems. *Ind. Biotechnol.* 9, 158–162. doi: 10.1089/ind.2013.1579

Berry, J. P., Gantar, M., Perez, M. H., Berry, G., and Noriega, F. G. (2008). Cyanobacterial toxins and allelochemicals with potential applications as algaecides, herbicides, and insecticides. *Mar. Drugs* 6, 117–146. doi: 10.3390/md20080007

Bertin, M. J., Zimba, P. V., Beauchesne, K. R., Huncik, K. M., and Moeller, P. D. R. (2012a). Identification of toxic fatty acid amides isolated from the harmful alga *Prymnesium parvum* Carter. *Harmful Algae* 20, 111–116. doi: 10.1016/j.hal.2012.08.004

Bertin, M. J., Zimba, P. V., Beauchesne, K. R., Huncik, K. M., and Moeller, P. D. R. (2012b). The contribution of fatty acid amides to *Prymnesium parvum* Carter toxicity. *Harmful Algae* 20, 117–125. doi: 10.1016/j.hal.2012.08.004

Boyd, P. W., Jickells, T., Law, C. S., Blain, S., Boyle, E. A., Buesseler, K. O., et al. (2007). Mesoscale iron enrichment experiments 1993-2005: synthesis and future directions. *Science* 315, 612–617. doi: 10.1126/science.1131669

Brennan, L., and Owende, P. (2010). Biofuels from microalgae – A review of technologies for production, processing, and extraction of biofuels and co-products. *Renew. Sust. Energy Rev.* 14, 557–577. doi: 10.1016/j.rser.2009.10.009

Buysens, S., Heungens, K., Poppe, J., and Hofte, M. (1996). Involvement of pyochelin and pyoverdin in suppression of pythium-induced damping-off of tomato by *Pseudomonas aeruginosa* 7NSK2. *Appl. Envion. Microbiol.* 62, 865–871.

Carney, L. T., and Lane, T. W. (2014). Parasites in algae mass culture. *Front. Microbiol.* 5:278. doi: 10.3389/fmicb.2014.00278

Coder, D., and Starr, M. (1978). Antagonistic association of the chlorellavorus bacterium ('*Bdellovibrio chlorellavorus*') with *Chlorella vulgaris*. *Curr. Microbiol.* 1, 59–64. doi: 10.1007/BF02601710

Coder, D. M., and Goff, L. J. (1986). The host range of the Chlorellavorous bacterium ("*Vampirovibrio chlorellavorus*"). *J. Phycol.* 22, 543–546. doi: 10.1111/j.1529-8817.1986.tb02499.x

de-Bashan, L. E., Hernandez, J. P., Morey, T., and Bashan, Y. (2004). Microalgae growth-promoting bacteria as 'helpers' for microalgae: a novel approach for removing ammonium and phosphorous from municipal wastewater. *Water Res.* 38, 466–474. doi: 10.1016/j.watres.2003.09.022

de Morais, M. G., da Silva Vaz, B., de Morais, E. G., and Costa, J. A. V. (2015). Biological active metabolites synthesized by microalgae. *Biomed Res. Int.* 2015, 835761. doi: 10.1155/2015/835761

Ding, C., Festa, R. A., Sun, T. S., and Wang, Z. Y. (2014). Iron and copper as virulence modulators in human fungal pathogens. *Mol. Microbiol.* 93, 10–23. doi: 10.1111/mmi.12653

Fields, M. W., Hise, A., Lohman, E. J., Bell, T., Gardner, R. D., Corredor, L., et al. (2014). Sources and resources: importance of nutrients, resource allocation, and ecology in cultivation for lipid accumulation. *Appl. Microbiol. Biotechnol.* 98, 4805–4816. doi: 10.1007/s00253-014-5694-7

Gademann, K., and Portmann, C. (2008). Secondary metabolites from cyanobacteria: complex structrures and powerful bioactives. *Curr. Org. Chem.* 12, 326–341. doi: 10.2174/138527208783743750

Gao, Y., Chapin, G., Liang, Y., Tang, D., and Tweed, C. (2012). Algae biodiesel – a feasibility report. *Chem. Cent. J.* 6(Suppl. 1), S1. doi: 10.1186/1752-153X-6-S1-S1

Gong, Y., Patterson, D. J., Li, Y., Hu, Z., Sommerfeld, M., Chen, Y., et al. (2015). *Vernalophrys algivore* gen. nov., sp. nov. (Rhizaria: Cercozoa: Vampyrellida), a new algal predator isolated from outdoor mass culture of *Scenedesmus dimorphus*. *Appl. Environ. Microbiol.* 81, 3900–3913. doi: 10.1128/AEM.00160-15

Granéli, E., Weberg, M., and Salomon, P. S. (2008). Harmful algal blooms of allelopathic microalgal species: the role of eutrophication. *Harmful Algae* 8, 94–102. doi: 10.1016/j.hal.2008.08.011

Hamed, S., and Klöck, G. (2014). Improvements of medium composition and utilization of mixotrophic cultivation for green and blue green microalgae towards biodiesel production. *Adv. Microbiol.* 4, 167–174. doi: 10.4236/aim.2014.43022

Hannon, M., Gimpel, J., Tran, M., Rasala, B., and Mayfield, S. (2010). Biofuels from algae: challenges and potential. *Biofuels* 1, 763–784. doi: 10.4155/bfs.10.44

Hardison, D. R., Sunda, W. G., Shea, D., and Litaker, R. W. (2013). Increased toxicity of *Karenia brevis* during phosphate limited growth: ecological and evolutionary implications. *PLoS ONE* 8:e58545. doi: 10.1371/journal.pone.0058545

Hecky, R. E., and Kilham, P. (1988). Nutrient limitation of phytoplankton in freshwater and marine environments: a review of recent evidence on the effects of enrichment. *Limnol. Oceanogr.* 33, 796–822. doi: 10.4319/lo.1988.33.4_part_2.0796

Henley, W. J., Litaker, R. W., Novoveská, L., Duke, C. S., Quemada, H. D., and Sayre, R. T. (2013). Initial risk assessment of genetically modified (GM) microalgae for commodity-scale biofuel cultivation. *Algal Res.* 1, 66–77. doi: 10.1016/j.algal.2012.11.001

Ianora, A., Bentley, M. G., Caldwell, G. S., Casotti, R., Cembella, A. D., Engström-Öst, J., et al. (2011). The relevance of marine chemical ecology to plankton and ecosystem function: an emerging field. *Mar. Drugs* 9, 1625–1648. doi: 10.3390/md9091625

Ianora, A., Boersma, M., Casotti, R., Fontana, A., Harder, J., Hoffmann, F., et al. (2006). The H.T. Odum synthesis essay. New trends in marine chemical ecology. *Estuaries Coasts* 29, 531–551. doi: 10.1007/BF02784281

Kazamia, E., Riseley, A. S., Howe, C. J., and Smith, A. G. (2014). An engineered community approach for industrial cultivation of microalgae. *Ind. Biotechnol.* 10, 184–190. doi: 10.1089/ind.2013.0041

Kellam, S. J., Cannell, R. J. P., Owsianka, A. M., and Walker, J. M. (1988). Results of a large-scale screening programme to detect antifungal activity from marine and freshwater microalgae in laboratory culture. *Br. Phycol. J.* 23, 45–47. doi: 10.1080/00071618800650061

Kuffner, I. B., and Paul, V. J. (2001). Effects of nitrate, phosphate, and iron on the growth of macroalgae and benthic cyanobacteria from Cocos Lagoon. *Guam. Mar. Ecol. Prog. Ser.* 222, 63–72. doi: 10.3354/meps222063

Larsen, A., and Bryant, S. (1998). Growth rate and toxicity of *Prymnesium parvum* and *Prymnesium patelliferum* (Haptophyte) in response to changes in salinity, light and temperature. *Sarsia* 83, 409–418. doi: 10.1080/00364827.1998.10413700

Leão, P. N., Pereire, A. R., Liu, W.-T., Ng, J., Pevzner, P. A., Dorrestein, P. C., et al. (2010). Synergistic allelochemicals from a freshwater cyanobacterium. *Proc. Natl. Acad. Sci. U.S.A.* 25, 11183–11188. doi: 10.1073/pnas.0914343107

Leflaive, J., and Ten-Hage, L. (2007). Algal and cyanobacterial secondary metabolites in freshwaters: a comparison of allelopathic compounds and toxins. *Freshw. Biol.* 52, 199–214. doi: 10.1111/j.1365-2427.2006.01689.x

Legrand, C., Rengefors, K., Fistarol, G. O., and Granéli, E. (2003). Allelopathy in phytoplankton – biochemical, ecological, and evolutionary aspects. *Phycologia* 42, 406–419. doi: 10.2216/i0031-8884-42-4-406.1

Letcher, P. M., Lopez, S., Schmieder, R., Lee, P. A., Behnke, C., Powell, M. J., et al. (2013). Characterization of *Amoeboaphelidium protococcarum*, an algal parasite new to the cryptomycota isolated from an outdoor algal pond used for the production of biofuel. *PLoS ONE* 8:e56232. doi: 10.1371/journal.pone.0056232

Lis, H., Shaked, Y., Kranzler, C., Keren, N., and Morel, F. M. M. (2015). Iron bioavailability to phytoplankton: an empirical approach. *ISME J.* 9, 1003–1013. doi: 10.1038/ismej.2014.199

Loper, J. E., and Buyer, J. S. (1991). Siderophores in microbial interactions on plant surfaces. *Mol. Plant Microbe Int.* 4, 5–13. doi: 10.1094/MPMI-4-005

Lukač, M., and Aegerter, R. (1993). Influence of trace metals on growth and toxin production of *Microcystis aeruginosa*. *Toxicon* 31, 293–305. doi: 10.1016/0041-0101(93)90147-B

Macías, F. A., Galindo, J. L. G., García-Díaz, M. D., and Galindo, J. C. G. (2008). Allelopathic agents from aquatic ecosystems: potential biopesticides models. *Phytochem. Rev.* 7, 155–178. doi: 10.1007/s11101-007-9065-1

Mandalam, R. K., and Palsson, B. Ø. (1998). Elemental balancing of biomass and medium composition enhances growth capacity in high-density *Chlorella vulgaris* cultures. *Biotechnol. Bioeng.* 59, 605–611. doi: 10.1002/(SICI)1097-0290(19980905)59:5<605::AID-BIT11>3.0.CO;2-8

Martin, J. H., Coale, K. H., Johnson, K. S., Fitzwater, S. E., Gordon, R. M., Tanner, S. J., et al. (1994). Testing the iron hypothesis in ecosystems of the equatorial Pacific Ocean. *Nature* 371, 123–129. doi: 10.1038/371123a0

Matz, C. J., Christensen, M. R., Bone, A. D., Gress, C. D., Widenmaier, S. B., and Weger, H. G. (2004). Only iron-limited cells of the cyanobacterium *Anabaena flos-aquae* inhibit growth of the green alga *Chlamydomonas reinhardtii*. *Can. J. Bot.* 82, 436–442. doi: 10.1139/b04-022

McBride, R. C., Lopez, S., Meenach, C., Burnett, M., Lee, P. A., Nohilly, F., et al. (2014). Contamination management in low cost open algae ponds for biofuels production. *Ind. Biotechnol.* 10, 221–227. doi: 10.1089/ind.2013.1614

Mendes, L. B. B., and Vermelho, A. B. (2013). Allelopathy as a potential strategy to improve microalgae cultivation. *Biotechnol. Biofuels* 6, 152. doi: 10.1186/1754-6834-6-152

Mey, A. R., Wyckoff, E. E., Kanukurthy, V., Fisher, C. R., and Payne, S. M. (2005). Iron and Fur regulation in *Vibrio cholerae* and the role for Fur in virulence. *Infect. Immun.* 73, 8167–8178. doi: 10.1128/IAI.73.12.8167-8178.2005

Moeller, P. D., Beauchesne, K. R., Huncik, K. M., Davis, W. C., Christopher, S. J., Riggs-Gelasco, P., et al. (2007). Metal complexes and free radical toxins produced by *Pfiesteria piscicida*. *Environ. Sci. Technol.* 41, 1166–1172. doi: 10.1021/es0617993

Mos, L. (2001). Domoic acid: a fascinating marine toxin. *Environ. Toxicol. Pharmacol.* 9, 79–85. doi: 10.1016/S1382-6689(00)00065-X

Mosmann, T. (1983). Rapid colorimetric assay for cellular growth and survival: application to proliferation and cytotoxicity assays. *J. Immunol. Methods* 65, 55–63. doi: 10.1016/0022-1759(83)90303-4

Oppenheimer, N. J., Rodriguez, L. O., and Hecht, S. M. (1979). Structural studies of 'active complex' of bleomycin: assignment of ligands to the ferrous ion in a ferrous-bleomycin-carbon monoxide complex. *Proc. Natl. Acad. Sci. U.S.A.* 76, 5616–5620. doi: 10.1073/pnas.76.11.5616

Pate, R., Klise, G., and Wu, B. (2011). Resource demand implications for US algae biofuels production scale-up. *Appl. Energy* 88, 3377–3388. doi: 10.1016/j.apenergy.2011.04.023

Paulsen, I. T., Press, C. M., Ravel, J., Kobayashi, D. Y., Myers, G. S., Mavrodi, D. V., et al. (2005). Complete genome sequence of the plant commensal *Pseudomonas fluorescens* Pf-5. *Nat. Biotechnol.* 23, 873–878. doi: 10.1038/nbt1110

Plumley, F. G. (1997). Marine algal toxins: biochemistry, genetics, and molecular biology. *Limnol. Oceanogr.* 42, 1252–1264. doi: 10.1111/j.1574-6976.2012.12000.x

Pohnert, G., Steinke, M., and Tollrian, R. (2007). Chemical cues, defence metabolites and the shaping of pelagic interspecific interactions. *Trends Ecol. Evol.* 22, 198–204. doi: 10.1016/j.tree.2007.01.005

Rasala, B. A., Choa, S.-S., Pier, M., Barrera, D. J., and Mayfield, S. P. (2014). Enhanced genetic tools for engineering multigene traits into green algae. *PLoS ONE* 9:e94028. doi: 10.1371/journal.pone.0094028

Sander, K., and Murthy, G. S. (2010). Life cycle analysis of algae biodiesel. *Int. J. Life Cycle Assess.* 15, 704–714. doi: 10.1007/s11367-010-0194-1

Silva, E. S. (1990). Intracellular bacteria: the origin of dinoflagellate toxicity. *J. Environ. Pathol. Toxicol. Oncol.* 10, 124–128.

Smith, V. H., and Crews, T. (2014). Applying ecological principles of crop cultivation in large-scale algal biomass production. *Algal Res.* 4, 23–34. doi: 10.1016/j.algal.2013.11.005

Soo, R. M., Woodcroft, B. J., Parks, D. H., Tyson, G. W., and Hugenholtz, P. (2015). Back from the dead; the curious tale of the predatory cyanobacterium *Vampirovibrio chlorellavorus*. *PeerJ* 3:e968. doi: 10.7717/peerj.968

Tanaka, K., Koga, T., Konishi, F., Nakamura, M., Mitsuyama, M., Himeno, K., et al. (1986). Augmentation of host defenses by a unicellular green alga, *Chlorella vulgaris*, to *Escherichia coli* infection. *Infect. Immun.* 53, 267–271.

Tillmann, U. (2003). Kill and eat your predator: a winning strategy of the planktonic flagellate *Prymnesium parvum*. *Aquat. Microb. Ecol.* 32, 73–84. doi: 10.3354/ame032073

Tillmann, U. (2004). Interactions between planktonic microalgae and protozoan grazers. *J. Eukaryot. Microbiol.* 51, 156–168. doi: 10.1111/j.1550-7408.2004.tb00540.x

U.S. Department of Energy [USDOE] (2010). *National Algal Biofuels Technology Roadmap, Rep. DOE/EE-0332, Biomass Program, Off. of Energy Efficiency and Renewable Energy*. Washington, DC: U.S. Department of Energy.

Ugwu, C. U., Aoyagi, H., and Uchiyama, H. (2008). Photobioreactors for mass cultivation of algae. *Bioresour. Technol.* 99, 4021–4028. doi: 10.1016/j.biortech.2007.01.046

Van Donk, E., Ianora, A., and Vos, M. (2011). Induced defences in marine and freshwater phytoplankton: a review. *Hydrobiologia* 668, 3–19. doi: 10.1007/s10750-010-0395-4

Van Ginkel, S. W., Igou, T., Hu, Z., Narode, A., Cheruvu, S., Doi, S., et al. (2015). Taking advantage of rotifer sensitivity to rotenone to prevent pond crashes for algal-biofuel production. *Algal Res.* 10, 100–103. doi: 10.1016/j.algal.2015.03.013

Venteris, E. R., McBride, R. C., Coleman, A. M., Skaggs, R. L., and Wigmosta, M. S. (2014). Siting algae cultivation facilities for biofuel production in the United States: trade-offs between growth rate, site constructability, water availability, and infrastructure. *Environ. Sci. Technol.* 48, 3559–3566. doi: 10.1021/es4045488

Wigmosta, M. S., Coleman, A. M., Skaggs, R. J., Huesemann, M. H., and Lane, L. J. (2011). National microalgae biofuel production potential and resource demand. *Water Resour. Res.* 47:W00H04. doi: 10.1029/2010WR009966

Wilhelm, S. W. (1995). Ecology of iron-limited cyanobacteria: a review of physiological responses and implications for aquatic systems. *Aquat. Microb. Ecol.* 9, 295–303. doi: 10.3354/ame009295

Wolfe, G. V. (2000). The chemical defense ecology of marine unicellular plankton: constraints, mechanisms, and impacts. *Biol. Bull.* 198, 225–244. doi: 10.2307/1542526

Xu, C., Wu, K., Van Ginkel, S. W., Igou, T., Lee, H. J., Bhargava, A., et al. (2015). The use of schizonticidal agent quinine sulfate to prevent pond crashes for algal-biofuel production. *Int. J. Mol. Sci.* 16, 27450–27456. doi: 10.3390/ijms161126035

Xu, H., Zhu, G., Qin, B., and Paerl, H. W. (2013). Growth response of *Microcystis* spp. to iron enrichment in different regions of Lake Taihu, China. *Hydrobiologia* 700, 187–202. doi: 10.1007/s10750-012-1229-3

Yasumoto, K., Nishigami, A., Aoi, H., Tsuchihashi, C., Kasai, F., Kusumi, T., et al. (2008). Isolation and absolute configuration determination of aliphatic sulfates as the *Daphnia* kairomones inducing morphological defense of a phytoplankton – Part 2. *Chem. Pharm. Bull.* 56, 129–132. doi: 10.1248/cpb.56.129

Zhu, X., Wang, J., Lu, Y., Chen, Q., and Yang, Z. (2015). Grazer-induced morphological defense in *Scenedesmus obliquus* is affected by competition against *Microcystis aeruginosa*. *Sci. Rep.* 5, 12743. doi: 10.1038/srep12743

Conflict of Interest Statement: The authors declare that the research was conducted in the absence of any commercial or financial relationships that could be construed as a potential conflict of interest.

frontiers in Microbiology

ORIGINAL RESEARCH
published: 13 June 2016
doi: 10.3389/fmicb.2016.00892

A Bacterial Pathogen Displaying Temperature-Enhanced Virulence of the Microalga *Emiliania huxleyi*

*Teaghan J. Mayers, Anna R. Bramucci, Kurt M. Yakimovich and Rebecca J. Case**

Department of Biological Sciences, University of Alberta, Edmonton, AB, Canada

Emiliania huxleyi is a globally abundant microalga that plays a significant role in biogeochemical cycles. Over the next century, sea surface temperatures are predicted to increase drastically, which will likely have significant effects on the survival and ecology of *E. huxleyi*. In a warming ocean, this microalga may become increasingly vulnerable to pathogens, particularly those with temperature-dependent virulence. *Ruegeria* is a genus of Rhodobacteraceae whose population size tracks that of *E. huxleyi* throughout the alga's bloom–bust lifecycle. A representative of this genus, *Ruegeria* sp. R11, is known to cause bleaching disease in a red macroalga at elevated temperatures. To investigate if the pathogenicity of R11 extends to microalgae, it was co-cultured with several cell types of *E. huxleyi* near the alga's optimum (18°C), and at an elevated temperature (25°C) known to induce virulence in R11. The algal populations were monitored using flow cytometry and pulse-amplitude modulated fluorometry. Cultures of algae without bacteria remained healthy at 18°C, but lower cell counts in control cultures at 25°C indicated some stress at the elevated temperature. Both the C (coccolith-bearing) and S (scale-bearing swarming) cell types of *E. huxleyi* experienced a rapid decline resulting in apparent death when co-cultured with R11 at 25°C, but had no effect on N (naked) cell type at either temperature. R11 had no initial negative impact on C and S type *E. huxleyi* population size or health at 18°C, but caused death in older co-cultures. This differential effect of R11 on its host at 18 and 25°C suggest it is a temperature-enhanced opportunistic pathogen of *E. huxleyi.* We also detected caspase-like activity in dying C type cells co-cultured with R11, which suggests that programmed cell death plays a role in the death of *E. huxleyi* triggered by R11 – a mechanism induced by viruses (EhVs) and implicated in *E. huxleyi* bloom collapse. Given that *E. huxleyi* has recently been shown to have acquired resistance against EhVs at elevated temperature, bacterial pathogens with temperature-dependent virulence, such as R11, may become much more important in the ecology of *E. huxleyi* in a warming climate.

Keywords: *Emiliania huxleyi*, *Ruegeria*, roseobacter, ocean warming, marine pathogen, temperature-enhanced virulence, climate change, phytoplankton

OPEN ACCESS

Edited by:
Xavier Mayali, Lawrence Livermore National Laboratory, USA

Reviewed by:
Torsten Thomas, The University of New South Wales, Australia
Kim Thamatrakoln, Rutgers University, USA

****Correspondence:***
Rebecca J. Case
rcase@ualberta.ca

Specialty section:
This article was submitted to Aquatic Microbiology, a section of the journal Frontiers in Microbiology

Received: *18 January 2016*
Accepted: *26 May 2016*
Published: *13 June 2016*

Citation:
Mayers TJ, Bramucci AR, Yakimovich KM and Case RJ (2016) A Bacterial Pathogen Displaying Temperature-Enhanced Virulence of the Microalga Emiliania huxleyi. Front. Microbiol. 7:892. doi: 10.3389/fmicb.2016.00892

INTRODUCTION

Ocean warming is one of the largest contemporary threats to the stability of the marine ecosystem. Since the 1990s, the average global sea surface temperature (SST) has been reported to be rising – an increase as dramatic as 4°C in some regions – and the rate of increase continues to climb (Smith et al., 2008). In the last century, there has been a global decline in phytoplankton which

is strongly correlated to increasing SST (Boyce et al., 2010). This trend is disturbing, given the fact that phytoplankton form the base of the marine food web, and account for over half of the earth's primary productivity annually (Behrenfeld et al., 2001).

Emiliania huxleyi (Prymnesiophyta) is a ubiquitous marine phytoplankton and is the most common representative of the extant coccolithophores (Paasche, 2002). The life cycle of *E. huxleyi* alternates between diploid C type cells (non-motile coccolith bearing) and haploid S type cells (flagellated with organic scales), both of which are capable of propagating indefinitely via mitosis (Paasche, 2002). There is indirect evidence that S cells are generated through meiosis of C cells, and conversely, C cells are regenerated through syngamy of S cells; however, neither of these processes has been directly observed (Green et al., 1996; Paasche, 2002; von Dassow et al., 2009). A third, less common cell type, also exists – diploid non-motile N (naked) cells. These are thought to be naturally occurring mutants of C cells lacking the ability to produce coccoliths (Paasche, 2002; Frada et al., 2012).

Emiliania huxleyi is a model organism and has been studied extensively due to its significant role in global biogeochemical cycles (Simó, 2004). As a major producer of dimethylsulfoniopropionate (DMSP), the most abundant source of organic sulfur in the ocean, *E. huxleyi* is hypothesized to play a role in regulating earth's climate (Charlson et al., 1987; Ayers and Cainey, 2007). Under conditions that promote increased growth in *E. huxleyi* (increased temperature, increased availability of carbon for photosynthesis, etc.), DMSP production is increased (Ayers and Cainey, 2007). DMSP is degraded to dimethyl sulfide (DMS) by bacteria and phytoplankton, and this serves as the main contributor of cloud condensation nuclei (CCN) in marine environments (Charlson et al., 1987; Ayers and Cainey, 2007; Reisch et al., 2011). An increase in CCN production may lead to increased cloud cover and a subsequent increase in albedo, which has a cooling effect on atmospheric temperature (Charlson et al., 1987; Ayers and Cainey, 2007). However, this feedback hypothesis is highly debated (Quinn and Bates, 2011). Recent work has shown that the production of DMS by *E. huxleyi* cultures decreases at high CO_2 concentrations in mesocosm experiments (Webb et al., 2016). This indicates that one of the marine environments temperature regulation mechanisms may be hindered by anthropogenic CO_2 emissions.

Emiliania huxleyi also plays a unique role in carbon cycling. In addition to organic photosynthate production, *E. huxleyi* produces elaborate calcium carbonate disks (coccoliths) that cover its cells. Although the function of these coccoliths remains unclear, they may aid in UV protection (Gao et al., 2009). During the natural senescence (Voss et al., 1998; Chow et al., 2015) and virally induced (Wilson et al., 2002) death of an *E. huxleyi* cell, its coccoliths are shed. These calcite coccoliths are denser than the surrounding seawater, so they sink and are eventually deposited in the deep ocean where they are essentially removed from the carbon cycle (Schmidt et al., 2013). Since *E. huxleyi* displays a lifestyle in which expansive blooms – sometimes hundreds of thousands of square kilometers in size – appear suddenly and unpredictably, then collapse rapidly (Brown and Yoder, 1994), the influence of this phytoplankton on the sulfur and carbon cycles, as well as the proximate biological ecosystem, is maximized during these bloom events. Because of these major roles in global processes, it is essential to understand the ecology of such an influential organism.

Emiliania huxleyi lives in close association with a diverse assemblage of microbes (Green et al., 2015). This microbial community is defined by complex and intimate metabolic exchange and communication (Sapp et al., 2007). Some members of this microbial consortium are mutualistic. For example, *E. huxleyi* lacks the ability to synthesize vitamin B12 – a nutrient essential to its growth – however, it has been shown that it is able to survive in culture due to the exogenous production of vitamin B12 by a closely associated bacterium (Helliwell et al., 2011).

Conversely, several microbes associated with *E. huxleyi* are pathogenic. Bloom collapse has been attributed to outbreaks of EhVs – members of the *Phycodnaviridae*, a group of viruses known to infect microalgae (Wilson et al., 2009). The EhVs elicit death in *E. huxleyi* by up-regulating metacaspase activity and causing the associated caspase-like programmed cell death (PCD) of the alga (Bidle et al., 2007). The role of metacaspases and PCD in the defense of land plants to microbial pathogens has been repeatedly characterized (Lam et al., 2001). The same type of response has been suggested for *E. huxleyi* to prevent outbreaks of disease in large clonal populations (Bidle et al., 2007).

The roseobacter clade (α-Proteobacteria) is one of the most abundant bacterial groups present during *E. huxleyi* blooms (second only to SAR lineages; Gonzalez et al., 2000), and contains several pathogenic representatives. One such representative has been demonstrated to be the causative agent in the formation of gall-like tumors on *Prionitis lanceolata* (Rhodophyta; Ashen and Goff, 1998). Additionally, the roseobacter clade also contains the only known bacterial pathogen of *E. huxleyi* – *Phaeobacter gallaeciensis* – that produces potent algaecides in response to *p*-coumaric acid, a senescent signal in plants (Seyedsayamdost et al., 2011).

Another example of an algaecidal roseobacter is *Ruegeria* sp. R11 (syn. *Nautella* sp. R11; Fernandes et al., 2011), which causes bleaching disease in the habitat forming *Delisea pulchra* – a red macroalgae native to the waters surrounding southern Australia (Case et al., 2011). The ability of R11 to cause bleaching events in *D. pulchra* has been demonstrated in both field and laboratory experiments to be temperature-dependent, with the disease only presenting at elevated temperature (Case et al., 2011). R11 was originally isolated from *D. pulchra* in the Tasman Sea (Case et al., 2011), one of the global hot spots for *E. huxleyi* blooms (Brown and Yoder, 1994). The present study aims to test the pathogenicity of R11 on *E. huxleyi*, a ubiquitous microalgae, which blooms in regions overlapping with *D. pulchra*'s geographical distribution (western and southern Australia, and New Zealand; Huisman, 2000), and to assess the role a warming ocean might play in this interaction. Bacterial–macroalgal symbioses have been studied in detail, however, very few bacterial–microalgal interactions have been described (Egan et al., 2013).

It has been predicted that ocean warming will increase the frequency and severity of pathogenic attacks (Harvell et al., 2002). Consequently, it is essential to study the effects of shifting

temperature on the biotic interactions of ecologically important organisms, like *E. huxleyi*. In the present study, we demonstrate that R11 is a temperature-enhanced pathogen of both the C and S cell types of *E. huxleyi*, but not N cell type, and that a caspase-like response is induced by R11 in the C cells at elevated temperature, which results in precipitous algal death.

MATERIALS AND METHODS

Growth and Maintenance of Algal and Bacterial Strains

Three axenic strains of *Emiliania huxleyi* were obtained from the Provasoli-Guillard National Centre for Marine Algae and Microbiota (NCMA): a C type diploid coccolith-bearing strain – CCMP3266; an S type haploid sexual strain – CCMP3268; and an N type diploid bald strain – CCMP2090. All strains were maintained in L1-Si media (Guillard and Hargraves, 1993) at 18°C in a diurnal incubator (8:16 h dark–light cycle). Algal cultures and media were checked for bacterial contamination prior to use in experiments by microscopic observations and by inoculation onto ½ marine agar (18.7 g Difco Marine Broth 2216 supplemented 9 g NaCl and 15 g Difco agar in 1 L). All strains were grown statically for 5 days in the 18°C incubator under the same light–dark regimen under which they were maintained. These incubation periods allowed the cultures to reach early-log phase prior to the start of an experiment.

The bacterium, *Ruegeria* sp. R11, was maintained on ½ marine agar at 30°C. It was grown to stationary phase in 5 mL ½ marine broth (18.7 g Difco Marine Broth 2216 supplemented 9 g NaCl) in a shaking incubator (160 rpm) at 21.5°C for 24 h prior to experiments.

Control Cultures and Co-cultures

For each algal strain tested, control cultures of the algae alone and *Ruegeria* sp. R11 alone, as well as a co-culture of R11 and algae, were prepared as previously described by Bramucci et al. (2015). Briefly, a stationary phase culture of R11 was grown, washed twice by centrifugation and re- in L1-Si media before undergoing a serial dilution in L1-Si to the 10^2 cfu/mL (cells are diluted to the correct order of magnitude and the exact initial cell concentration is calculated from cfu counts). To prepare the co-culture, an early log-phase culture (5-day-old, 10^4– 0^5 cells/mL) was mixed volumetrically 1:1 with the 10^2 cfu/mL R11. Control cultures of both R11 and the algae were prepared by mixing the respective culture volumetrically 1:1 with sterile L1-Si medium, to account for the ½ dilution of the co-culture. The controls and co-culture were then aliquoted in 1 mL volumes into 48-well microtiter plates (Becton, Dickinson and Company, Franklin Lakes, NJ, USA). Aliquots were dispensed in such a way that three independent replicates of each culture type could be sampled and sacrificed for each time point. This method allowed a time course experiment to be conducted using sacrificial sampling, eliminating the need for re-sampling and reducing the error involved in an experiment with diminishing culture volume (Bramucci et al., 2015).

Half of the microtiter plates were incubated at 18°C, while the other half were incubated at 25°C. The microtiter plates were then incubated statically (8:16 h dark–light cycle) at the respective temperatures for 24 days. This protocol was carried out for each of the three algal strains tested.

Fluorescence Measurements

A pulse-amplitude-modulation (PAM) fluorometer (WATER-PAM, Waltz, Effeltrich, Germany) was used to measure photosynthetic yield (F_v/F_m) of cultures containing algae (Schreiber et al., 1986). On sampling days, all samples were taken at the mid-point of the dark cycle (at 4 h) and diluted in L1-Si media to within the detection range of the PAM fluorometer. Samples were kept in the dark and at the appropriate temperature (18 or 25°C) throughout sampling. For each sample, an initial dark adaption period of 3 min was administered, after which a saturating pulse was applied and the fluorescence readings were taken twice at intervals of 1 min 30 s to calculate the photosystem II (PSII) potential quantum yield (F_v/F_m) – which indicates the efficiency of PSII (van Kooten and Snel, 1990). Duplicate readings of each sample were averaged and this average was used to determine the F_v/F_m of each sample (in triplicate). After culture death occurred, artificial yield values were detected for some samples. Severe damage to the chloroplasts and calvin cycle has been shown to result in an artificially high yield (1998), and for this reason yield data were reported as not detectable for samples where both chlorophyll content and cell number indicated that the culture was dead. Data were analyzed using SigmaPlot 12.

Enumerating Algal and Bacterial Population Density

Algal samples were prepared for flow cytometry from control cultures and co-cultures. Cells were fixed for flow cytometry by incubating in the dark for 10 min with 0.6% glutaraldehyde. Cells were then flash-frozen in liquid nitrogen and stored at −80°C until flow cytometry was performed using a FACSCalibur (Becton Dickinson, San Jose, CA, USA). A single replicate was randomly chosen and analyzed for each experimental day, as experimental variability was low. A 488 nm laser was used for excitation and a 670 nm laser was used for detection of chlorophyll. Chlorophyll autofluorescence was used for cellular enumeration. Cells were subsequently stained with SYBRgreen-I (Life Technologies, Carlsbad, CA, USA) for DNA detection (520 nm). Data were processed using FlowJo 9.2.

The R11 population density from co-culture experiments was enumerated by counting colony forming units (cfu) to enumerate planktonic R11 cells and those attached to *E. huxleyi* cells. Samples were first vortexed vigorously to remove R11 cells from *E. huxleyi* and reduce bacterial cell clumping. Then a dilution series was prepared in L1-Si media, plated on ½ marine agar and incubated for 2 days at 30°C.

Caspase-Like Activity Measurement

In vitro caspase-like IETDase (Ile-Glu-Thr-Asp) activity in *E. huxleyi* was measured as previously described by Bidle et al. (2007) with a few amendments. A single replicate was randomly

chosen and analyzed for each experimental day. Briefly, aliquots of 850 μL of control cultures and co-cultures were pelleted by centrifugation for 10 min at 14,000 × *g* at 4°C. The supernatant was removed, discarded and replaced with 0.1 mL sterile PBS. The tube containing the pellet and PBS was immediately flash-frozen in liquid nitrogen, and stored at −80°C until processed. Pellets were resuspended and a subsample was analyzed for protein content using standard protein extraction (BCA protein assay, Pierce). The remaining sample was centrifuged and pellets were resuspended in caspase activity buffer according to manufacturer specifications (Caspase Activity Kit, EMB Millipore) and sonicated on ice. Cellular debris was pelleted (16,000 × *g*, room temp, 2 min) and cell lysates were incubated with IETD-AFC (Ile-Glu-Thr-Asp-7-amino-4-trifluoromethylcoumarin) according to the manufacturer's instructions. Extracts were then incubated for 4 h at 25°C as IETDase activity from the cell lysate produces a fluorescent product from cleavage of ETD-AFC. Fluorescence was measured every 10 min using a Spectra Max Gemini XS plate reader (excitation 400 nm, emission 505 nm). Caspase activity was successfully abolished (>90%) with the irreversible caspase inhibitor z-VAD-FMK (z-Val-Ala-Asp-fluoromethyl-ketone; Calbiochem).

In vivo detection of active caspase-like proteases was accomplished using a cell permeable fluorescently labeled active site inhibitor (Millipore: FITC-VAD-FMK). Labeled algal proteases were visualized with epifluorescence microscopy after *in vivo* cell staining. After staining, cells were pelleted by centrifugation for 5 min at 5,000 × *g*, gently suspended in sterile PBS according to manufactures instructions; cells were imaged within 5 h of staining. Epifluorescence microscopy was used to assess algal chlorophyll autofluorescence. Cells were also stained with DAPI (4′,6-Diamidino-2-Phenylindole; Dihydrochloride; Life Technologies, Carlsbad, CA, USA) according to manufacturer's instructions. DAPI was used instead of SYBRgreen-I, as the emission spectrum of the latter overlaps with that of the caspase inhibitor.

RESULTS

Population Dynamics of *Emiliania huxleyi* and *Ruegeria* sp. R11 in Co-culture

Three cell types of *E. huxleyi* were tested for their interaction with R11 at 18 and at 25°C. For each algal strain tested, control cultures of the algae alone and *Ruegeria* sp. R11 alone, as well as a co-culture of R11 and algae, were prepared as previously described by Bramucci et al. (2015).

Coccolith-Bearing C Type *E. huxleyi*

At 18°C, C type *E. huxleyi* (CCMP3266) in co-culture with R11 remained healthy until 14 days, when death of CCMP3266 was observed (**Figures 1A,C**). The PSII potential quantum yield (F_v/F_m) – a measure of photosynthetic efficiency hereafter referred to as yield (Schreiber, 1998) – of CCMP3266 in co-culture began to drop from 12 to 14 days, and continued dropping until the damage to PSII resulted in an undetectable yield at 20 days, and did not recover at any subsequent time in the experiment (**Figure 1A**). Algal cell numbers followed a similar pattern, with a small decrease occurring from 12 to 14 days, and a greater decrease to near zero values between 16 and 20 days (**Figure 1C**). In contrast, control cultures of CCMP3266 at 18°C retained a consistently high yield and cell density throughout the experiment (**Figures 1A,C**).

Death was observed much earlier in the co-culture of CCMP3266 with R11 grown at 25°C compared to 18°C (**Figures 1B,D**). At 25°C, the yield (**Figure 1B**) and algal cell density (**Figure 1D**) began to decline by 2 days and reached an undetectable level by 4 days (compared to 14 and 20 days at 18°C). A small resurgence in cell density with high yield values was observed on 8 days, which was again undetectable by 12 days and remained so through the experiment (**Figures 1B,D**). Like those grown at 18°C, control cultures of CCMP3266 at 25°C retained a consistently high yield throughout the experiment (**Figure 1B**). CCMP3266 cell density in control culture at 25°C was initially similar to the control culture at 18°C (1.4×10^6 cells/mL and 1.5×10^6 cells/mL, respectively, on 4 days), but later decreased on 6 and 8 days to approximately half of it's peak cell density and then experienced large oscillations around this number from 10 to 24 days (**Figure 1D**).

The R11 population density in co-culture with CCMP3266 at 18 and 25°C both increased from 10^2 cfu/mL to 10^7 cfu/mL (**Figures 1E,F**). However, the 25°C co-cultures reached this cell density faster (on 2 days) than the co-culture at 18°C (on 4 days; **Figures 1E,F**). At both temperatures, the R11 populations benefited from the presence of CCMP3266. At 18°C, control R11 (bacteria alone) population density crashed by 2 days (**Figure 1E**), while at 25°C, the R11 population remained present, but experienced large oscillations from 10^3 to 10^6 cfu/mL for the remainder of the experiment (**Figure 1F**). The R11 control population remained present at a significant level throughout the experiment at 25°C but not 18°C, a temperature it grows well at in ½ marine broth, suggests that R11 does not thrive in L1-Si media at 18°C due to the additive effects of a low nutrient medium and low temperature.

Scale-Bearing Swarming S Type *E. huxleyi*

Similar to the C cell type (CCMP3266), the co-culture of the S cell type (CCMP3268) with R11 at 18°C remained healthy until 10 days, after which death was observed (**Figures 2A,C**). The yield began to decline on 10 days, becoming negligible by 14 days and no recovery was observed by 24 days (**Figure 2A**). Both control (CCMP3268 alone) and co-culture S cell density experienced a rapid increase from 0 to 4 days, but declined after 6 days (**Figure 2C**). The CCMP3268 control culture cell density remained steady at this lower level for the remainder of the experiment (**Figure 2C**). However, the algal cell density of the co-culture kept declining, approaching zero by 12 days, where it remained until the end of the experiment (**Figure 2C**).

Death was observed much earlier in the co-culture of CCMP3268 with R11 at 25°C in comparison to 18°C (**Figures 2B,D**). At this higher temperature, the yield (**Figure 2B**) and cell count (**Figure 2D**) of the co-culture were similar to control values (no R11) on 2 days, but had crashed by 4 days. Algal cell density remained near zero for the remainder of the

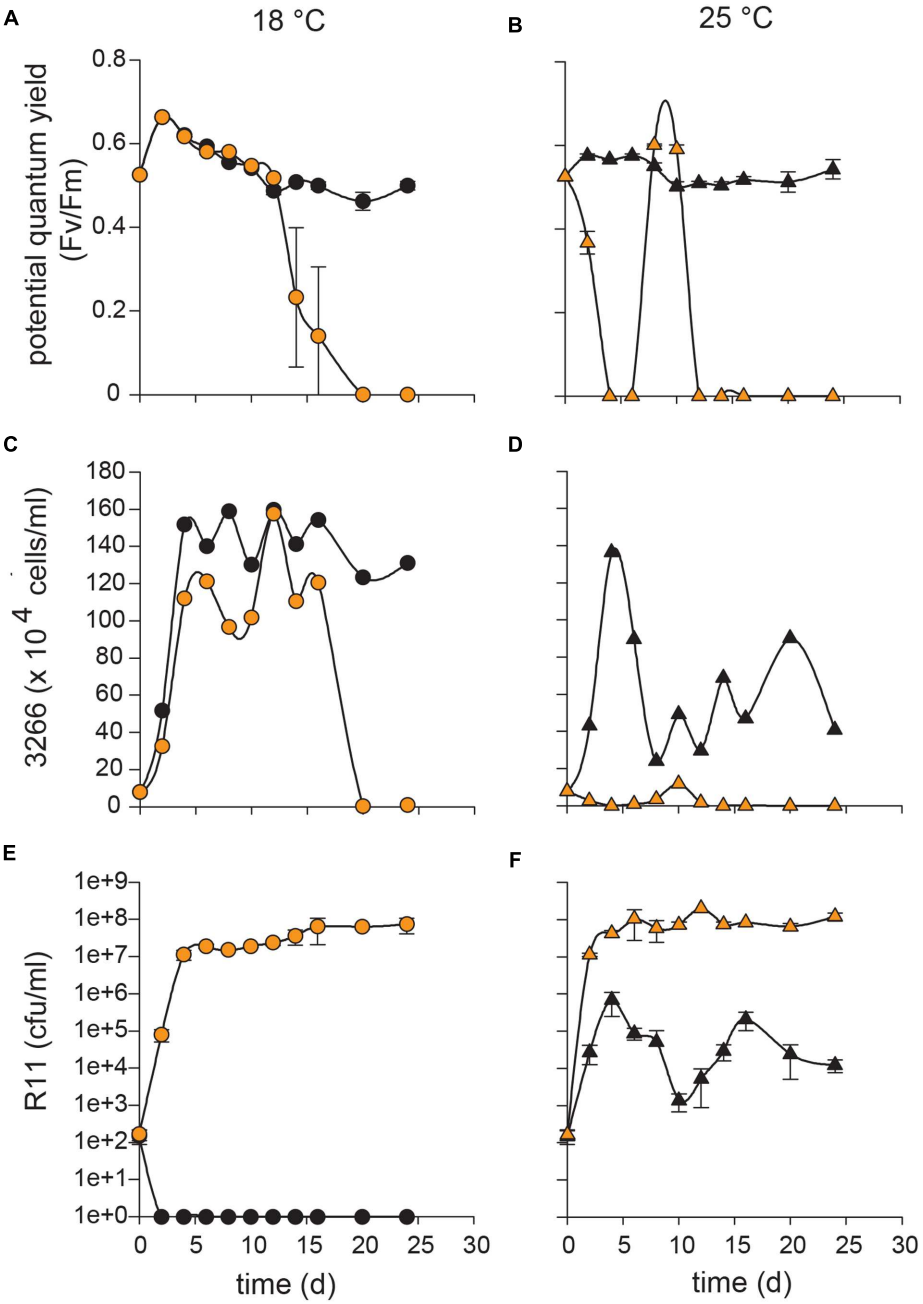

FIGURE 1 | Influence of temperature on co-cultures of *Ruegeria* sp. R11 with C type *Emiliania huxleyi* (CCMP3266). R11 (10^2 cells/ml) was co-cultured with CCMP3266 (10^5 cells/ml) at 18 and 25°C and monitored over 24 days to determine the influence of temperature on co-cultures. For co-cultures and CCMP3266 grown alone, the potential quantum yield (F_v/F_m) was measured at 18°C **(A)** and 25°C **(B)**. Algal cell counts (cells/ml) were measured using flow cytometry for co-cultures and CCMP3266 alone at 18°C **(C)** and 25°C **(D)**. Bacterial enumeration (cfu/ml) was performed for R11 alone and in co-culture with CCMP3266 in L1-Si medium at 18°C **(E)** and 25°C **(F)**. Data for R11-CCMP3266 co-cultures are indicated with orange data points and control cultures (R11 or CCMP3266 grown alone) with black data points. All control cultures and co-cultures were performed in triplicate. Error bars: ±SE.

experiment (**Figure 2D**). Co-culture yield values also remained undetectable, except for an anomaly on 16 days where a single replicate gave a detectable reading (**Figure 2B**). This type of outlier is due to the nature of the sacrificial sampling method and was observed in replicate experiments (results not shown). On a given sampling day, three replicates of the 1 mL wells are sacrificed and sampled for each culture type (algal control, bacterial control, and co-culture). At 25°C, control cultures of CCMP3268 retained a high yield for 10 days after the death of the co-culture, falling significantly only on 16 days (**Figure 2B**).

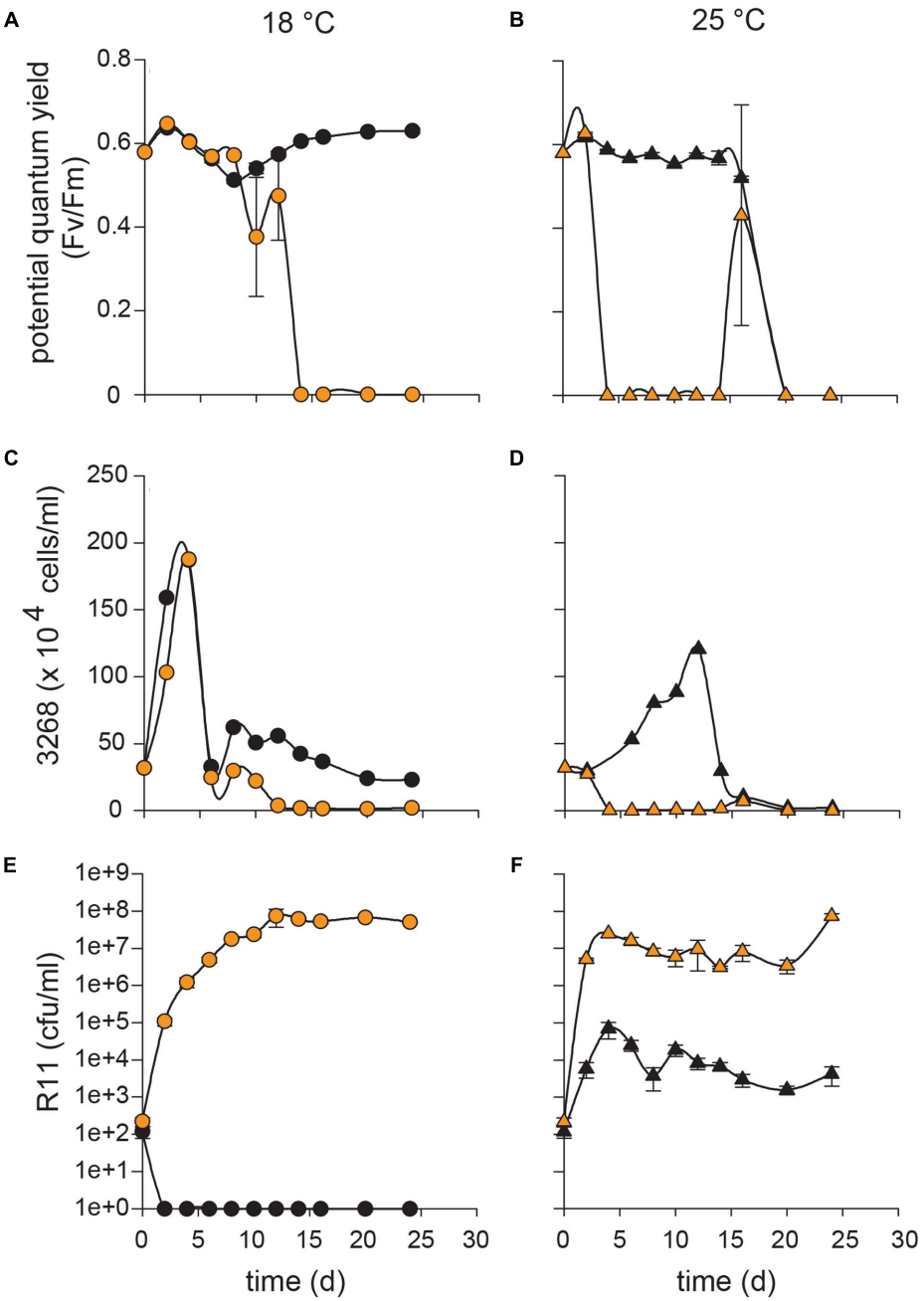

FIGURE 2 | Influence of temperature on co-cultures of *Ruegeria* sp. R11 with S type *Emiliania huxleyi* (CCMP3268). R11 (10^2 cells/ml) was co-cultured with CCMP3268 (10^5 cells/ml) at 18 and 25°C and monitored over 24 days to determine the influence of temperature on co-cultures. For co-cultures and CCMP3268 grown alone, the potential quantum yield (F_v/F_m) was measured at 18°C **(A)** and 25°C **(B)**. Algal cell counts (cells/ml) were measured using flow cytometry for co-cultures and CCMP3268 alone at 18°C **(C)** and 25°C **(D)**. Bacterial enumeration (cfu/ml) was performed for R11 alone and in co-culture with CCMP3268 in L1-Si medium at 18°C **(E)** and 25°C **(F)**. Data for R11-CCMP3268 co-cultures are indicated with orange data points and control cultures (R11 or CCMP3268 grown alone) with black data points. All control cultures and co-cultures were performed in triplicate. Error bars: ±SE.

Compared to the control culture at 18°C, which grew to ~1.5 × 10^6 cells/mL by 4 days and maintained this cell density throughout the experiment, the cell density of the CCMP3268 control culture at 25°C increased slowly, peaking at ~1.3 × 10^6 cells/mL on 12 days, after which it followed the same pattern as the yield (**Figure 2D**). Neither the yield, nor the cell count recovered by the end of the experiment.

R11 populations attained equally high density (10^7 cfu/mL) in co-culture with CCMP3268 at both 18 and 25°C (**Figures 2E,F**). Similar to the co-culture with CCMP3266, this level was

achieved twice as quickly at 25 as at 18°C (**Figures 2E,F**). Control populations of R11 reached the same density as control bacterial populations from the CCMP3266 co-culture experiment, crashing rapidly at 18°C (on 2 days) and maintaining their population at 25°C at a lower level than in the co-culture (**Figures 2E,F**).

Bald N Type *E. huxleyi*

At 18 and 25°C, both the co-culture and control culture of the N type *E. huxleyi* cells (CCMP2090) retained a high yield through 24 days (**Figures 3A,B**). Death was never observed in these co-cultures. Co-cultures were established with the same density of R11 (10^2 cfu/mL) and reached the same population density (10^7 cfu/mL) as it did in co-culture with CCMP3266 and CCMP3268. Absolute numbers of R11 were not quantified at every time point within the experiment, but its presence was confirmed with drop plating of the co-culture on ½ marine agar at every sampling point. Flow cytometry was not run for this cell type, as no effect of co-culturing on yield or minimum fluorescence (a proxy for chlorophyll fluorescence) was observed.

Observation of Algal Bleaching in *E. huxleyi* and *Ruegeria* sp. R11 Co-Cultures

Since R11 is known to cause bleaching in the macroalga *D. pulchra* (Case et al., 2011), the bleaching effect of R11 on *E. huxleyi* was assessed using flow cytometry. R11 pathogenesis of *E. huxleyi* caused the loss of chlorophyll autofluorescence, or bleaching, of CCMP3266 (**Figure 4**) and CCMP3268 (**Figure 5**). At 18°C, co-culture populations of CCMP3266 and CCMP3268 with R11 are indistinguishable from control populations (algae alone) at 12 and 8 days respectively, when the chlorophyll autofluorescence (670 nm) of cells was plotted against the forward scatter for both populations (**Figures 4A** and **5A**). On 14 and 10 days, when yield and cell density indicated the start of algal decline (**Figures 1A,C** and **2A,C**), CCMP3266 and CCMP3268 cells lost chlorophyll autofluorescence, but retained forward scatter values (**Figures 4B** and **5B**). This shows that the algae lose chlorophyll autofluorescence before cell size (i.e., lysis). This decrease in chlorophyll autofluorescence happened relatively gradually (compared to 25°C), resulting in a 'smear' of cells in the process of losing chlorophyll on the scatter plot. On days where yield and cell density were near zero, a population of cells was present with the same forward scatter as control cultures, but almost all fluorescence (chlorophyll) was gone (**Figures 4C** and **5C**).

At 25°C, the decrease in chlorophyll content occurred more rapidly, and the gradual loss observed at 18°C is not present (**Figures 4** and **5**). Instead, the co-cultures appear to experience a rapid loss of fluorescence (chlorophyll) from populations similar to control cultures with no bacteria (same forward scatter and chlorophyll values), to populations of cells with the same forward scatter as control cultures, but a low level of fluorescence (chlorophyll) by the next time point (**Figures 4** and **5**).

As a secondary measure of cell death, cells were stained cells with SYBRgreen-I that stains DNA. The DNA content of cells decreased in both CCMP3266 (Supplementary Figure S1) and CCMP 3268 following the same general pattern as the chlorophyll bleaching. However, this process of DNA loss was slower and cells were observed microscopically to have DNA throughout the cytoplasm when co-cultured with R11, while control cells had a clear nucleus (Supplementary Figure S1).

Measurement of Caspase-Like Activity in C Type *E. huxleyi* Co-Cultures with *Ruegeria* sp. R11

The major known pathogens of *E. huxleyi* are viruses, which are collectively called *E. huxleyi* viruses (EhVs). Infection by these viruses triggers caspase-like activity (likely mediated by algal metacaspase activity), which coincides with death and production of viral particles in various diploid N type *E. huxleyi* strains (Bidle et al., 2007). Caspase-like activity has been observed in cells after the loss of their chlorophyll and therefore of the corresponding autofluorescence (Bidle et al., 2007). To determine if a bacterial pathogen of *E. huxleyi* would also trigger caspase-like activity, CCMP3266 was assayed for caspase-like IETDase (Ile-Glu-Thr-Asp) using the Caspase-8 Activity Kit (EMB Millipore). In the control cultures (*E. huxleyi* only) at 18 and 25°C, a background level of caspase-like activity was present throughout the experiment (∼50–200 RFU/h/μg; **Figures 6A,B**). For CCMP3266 in co-culture with R11 at 18°C, there was a slight (0.25- to 0.5-fold) increase in caspase-like activity on 16, 20, and 24 days (time points at which the co-culture was dead or dying), compared to the control (**Figure 6A**). However, the caspase-like activity was a much greater in the co-culture at 25°C – a 3.5-fold increase was observed at 2 and 4 days, and a twofold increase on 6 and 8 days (all days on which the co-culture was dead or dying; **Figure 6B**).

Caspase-like activity was directly visualized using microscopy of cells stained with a fluorescently labeled caspase-marker (FITC-VAD-FMK). Cells showing clear VAD labeling - an indicator of active caspase-like proteases - in both the 18 and 25°C R11-CCMP3266 co-cultures were characterized as having less or no chlorophyll and compromised cell integrity. The image in **Figures 6C,D** is a representative cell taken from an 18°C R11-CCMP3266 co-culture at 14 days. This cell bears coccoliths, shows minimal autofluorescence (indicating a small amount of chlorophyll; **Figure 6C**) and displays caspase-like activity (**Figure 6D**). On the other hand, chlorophyll-containing cells (showing strong autofluorescence) were rare in declining R11-CCMP3266 co-cultures. These were typical in young control cultures, however, some could be found even within the 25°C co-culture using microscopy (Supplementary Figure S2). In addition to significant chlorophyll autofluorescence, these cells were characterized by the presence of structural integrity and lack of visible FITC-VAD-FMK labeling. The image in **Figures 6E,F** was taken from 4 days R11-CCMP3266 co-culture at 25°C and displays a chlorophyll-containing cell (smaller and showing chlorophyll autofluorescence in red but lacking FITC-VAD-FMK labeling) and a cell displaying strong caspase activity (larger and staining green from FITC-VAD-FMK labeling but lacking autofluorescence from loss of chlorophyll). In this image, both

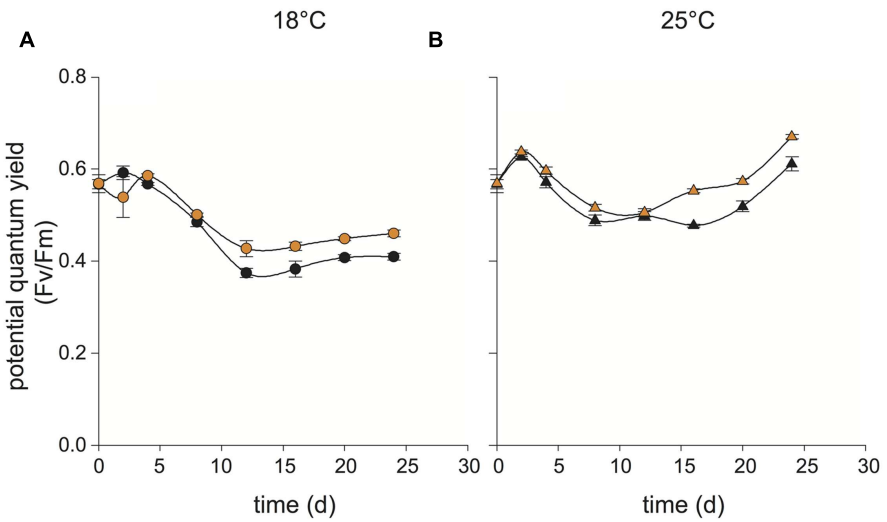

FIGURE 3 | Influence of temperature on co-cultures of *Ruegeria* sp. R11 with N type *Emiliania huxleyi* (CCMP2090). R11 (10^2 cells/ml) was co-cultured with CCMP2090 at 18 and 25°C and monitored over 24 days to determine the influence of temperature on co-cultures. For co-cultures and CCM2090 grown alone, the potential quantum yield (F_v/F_m) was measured at 18°C **(A)** and 25°C **(B)**. Data for R11-CCMP2090 co-cultures are indicated with orange data points and control cultures (CCMP2090 grown alone) with black data points. All control cultures and co-cultures were performed in triplicate. Error bars: ±SE.

cells have lost their coccoliths, a normal result of senescence (Chow et al., 2015). In many cases, R11 cells were observed attached to *E. huxleyi* cells (**Figures 6G,H**).

DISCUSSION

Ruegeria sp. R11 Pathogenicity Varies between Cell Types of *Emiliania huxleyi*

The present study demonstrates that *Ruegeria* sp. R11 is a pathogen of *E. huxleyi*, but that this pathogenicity, or host resistance, is strain dependent. Both *E. huxleyi* CCMP3266 and CCMP3268 are killed when in co-culture with R11 (**Figures 1** and **2,** respectively). CCMP3268, an S type haploid flagellated cell, was originally isolated from cultures of CCMP3266, a C type diploid coccolith bearing cell isolated from the Tasman Sea, after part of the original culture of CCMP3266 was observed to undergo a shift to this haploid cell type (Frada et al., 2008; von Dassow et al., 2009). It is hypothesized that CCMP3268 is the sexual cell of CCMP3266. However, since neither meiosis nor syngamy has ever been directly observed, this cannot be confirmed. Given this relationship between CCMP3266 and CCMP3268, it follows that they should be similar in their sensitivity to pathogens unless the cell type conveyed resistance. Transcriptomic analyses have shown that these strains display ∼50% transcript similarity, with the major functional differences relating to motility and biogenic $CaCO_3$ production – the haploid CCMP3268 cells are flagellated while the diploid CCMP3266 cells are coccolith bearing (von Dassow et al., 2009). However, it has been shown that while CCMP3266 is sensitive to the bloom-collapse causing EhVs, CCMP3268 is resistant due to a lack of host recognition by the virus (Frada et al., 2008). As opposed to the C or S type strains, bald N type *E. huxleyi* CCMP2090 is seemingly resistant to infection by R11 (**Figure 3**), although interestingly, CCMP2090 is susceptible to two of the major strains of EhV (EhV1 and EhV86; Fulton et al., 2014). Since the bacteria infects different cell types than the previously described EhVs, the complex interplay between these two algal pathogens will be important to understand as the ecology of *E. huxleyi* blooms.

It is unclear from the present study what is the key difference between the *E. huxleyi* strains that causes the observed variability in susceptibility to R11 infection, but there are several possibilities. CCMP2090 is the diploid axenic non-coccolith bearing (bald) isolate of the diploid coccolith bearing CCMP1516, which was collected off the coast of Ecuador, making it geographically distant from both CCMP3266 and R11, which were both isolated from the Tasman Sea. The ability of phylogenetically closely related strains of the Roseobacter clade to induce gall formation on species of *Prionitis* has been shown to be geographically specific – strains of gall-forming roseobacter isolated from infected *Prionitis* in one geographical area were unable to induce gall formation in closely related *Prionitis* from a distant geographical location (Ashen and Goff, 2000). Similarly, it has been demonstrated in land plants that geographically distant subpopulations of a single species can differ in their resistance/susceptibility to pathogens, likely due to decreased interbreeding (Thrall et al., 2001). Diploid cells of *E. huxleyi* have been shown to have a more complex transcriptome than haploid cells, suggesting that there may be greater phenotypic diversity between diploid strains (von Dassow et al., 2009) and thus greater diversity in their resistance to pathogens (i.e., CCMP3266 and CCMP2090 are both diploid strains). Additionally, the nature of the CCMP2090 cell – naked, lacking both coccoliths and organic scales – may contribute to the differences in sensitivity between strains. It may be that R11 has different levels of attachment

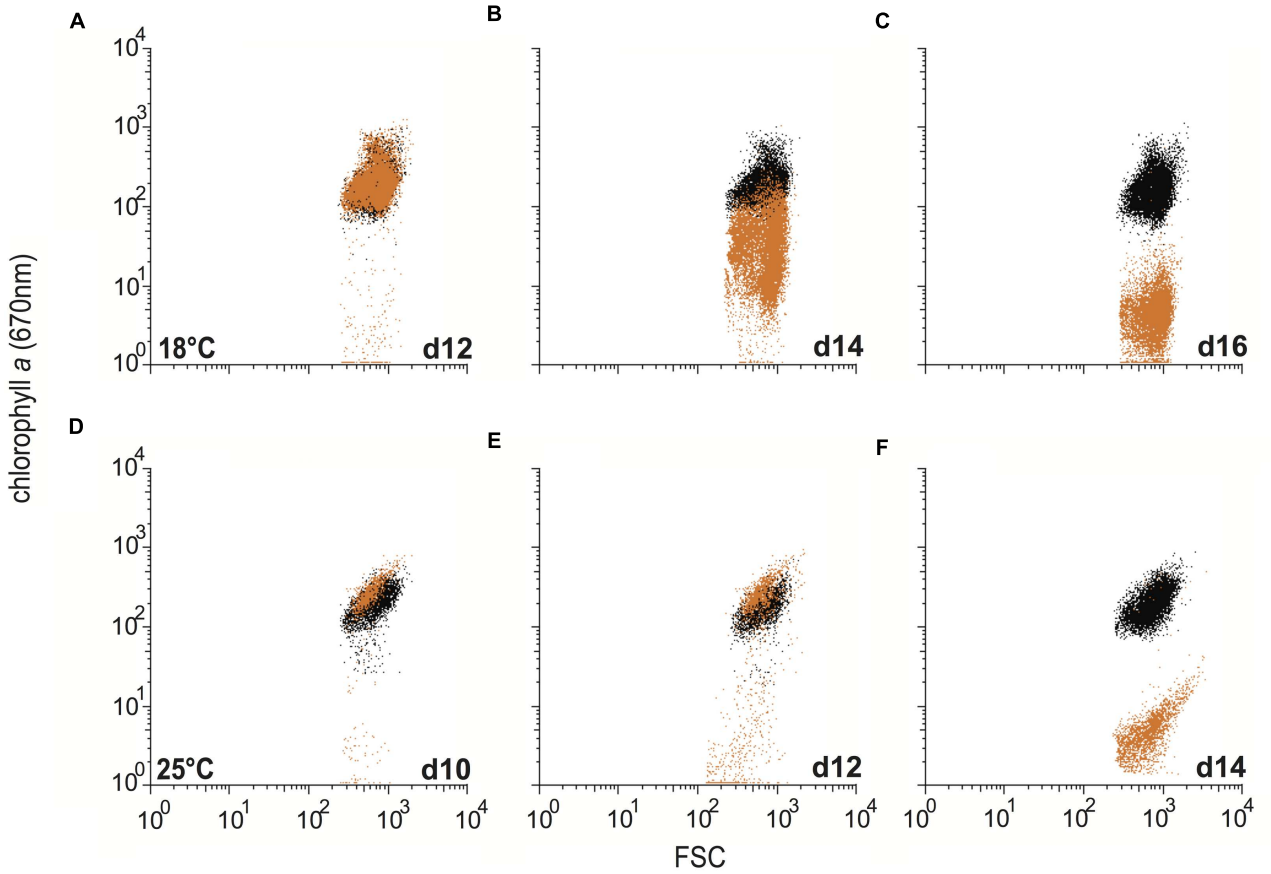

FIGURE 4 | Bleaching in C type *Emiliania huxleyi* (CCMP3266) in co-culture with *Ruegeria* sp. R11. Control cultures of CCMP3266 and co-cultures of CCMP3266 with R11 were assessed for chlorophyll content using flow cytometry at 18°C on 12 days **(A)**, 14 days **(B)**, and 16 days **(C)**; and at 25°C on 10 days **(D)**, day 12 **(E)**, and day 14 **(F).** Data for R11-CCMP3266 co-cultures are indicated with orange data points and control cultures (CCMP3266 grown alone) with black data points.

and/or colonization of the naked, organic or calcite liths covering *E. huxleyi's* cell surface.

N type cells, like CCMP2090, are thought to be a rare natural variant of C type cells, such as CCMP3266 (Paasche, 2002). However, if the mutation that causes the non-calcifying N cell type to occur provides an escape strategy from pathogens, the abundance and distribution patterns of this cell type may change in the future, and this would have consequences for the carbon sequestration role of *E. huxleyi*.

Although the mode of R11's pathogenesis is not currently known, several virulence factors have been identified, including the production of ammonia (inhibits photosynthesis), cytolytic toxins (lyses cells; Fernandes et al., 2011), and glutathione peroxidase (resists oxidative bursts from the host; Gardiner et al., 2015). It has also been hypothesized that the virulence of R11 may be related to its production of indole-3-acetic acid (IAA) – a phytohormone with various roles in the growth and development of land plants known to be produced by R11 (Fernandes et al., 2011). An extracellular excess of IAA causes hypertrophy and may increase the amount of algal exudates available to R11 (Fernandes et al., 2011). Interestingly, it has recently been shown that the exogenous addition of IAA causes increased cell permeability and cell size in CCMP2090, but not in CCMP3266 (Labeeuw et al., 2016). However, a difference in R11 virulence toward CCMP3266 is observed when tryptophan is added to stimulate IAA production, R11 killing CCMP3266 twice as fast (1 day compared to 2 days without the addition of tryptophan; Labeeuw et al., 2016). This is suggestive that IAA influences the virulence of R11 toward *E. huxleyi*. However, this effect is likely influenced by host factors, given that unlike CCMP3266, CCMP2090 cell size and permeability are responsive to IAA, but is not susceptible to the virulence of R11.

The Virulence of R11 toward *E. huxleyi* Is Temperature-Enhanced

The decrease in CCMP3266 and CCMP3268 health observed when grown in co-culture with R11 at 25°C compared to 18°C indicates that the pathogenicity of this bacterium toward them is temperature-enhanced. While R11 ultimately causes the death of CCMP3266 and CCMP3268 at both 18 and 25°C, the course of the infection is accelerated at elevated temperature (**Figures 1A–D** and **2A–D**). This increase in the

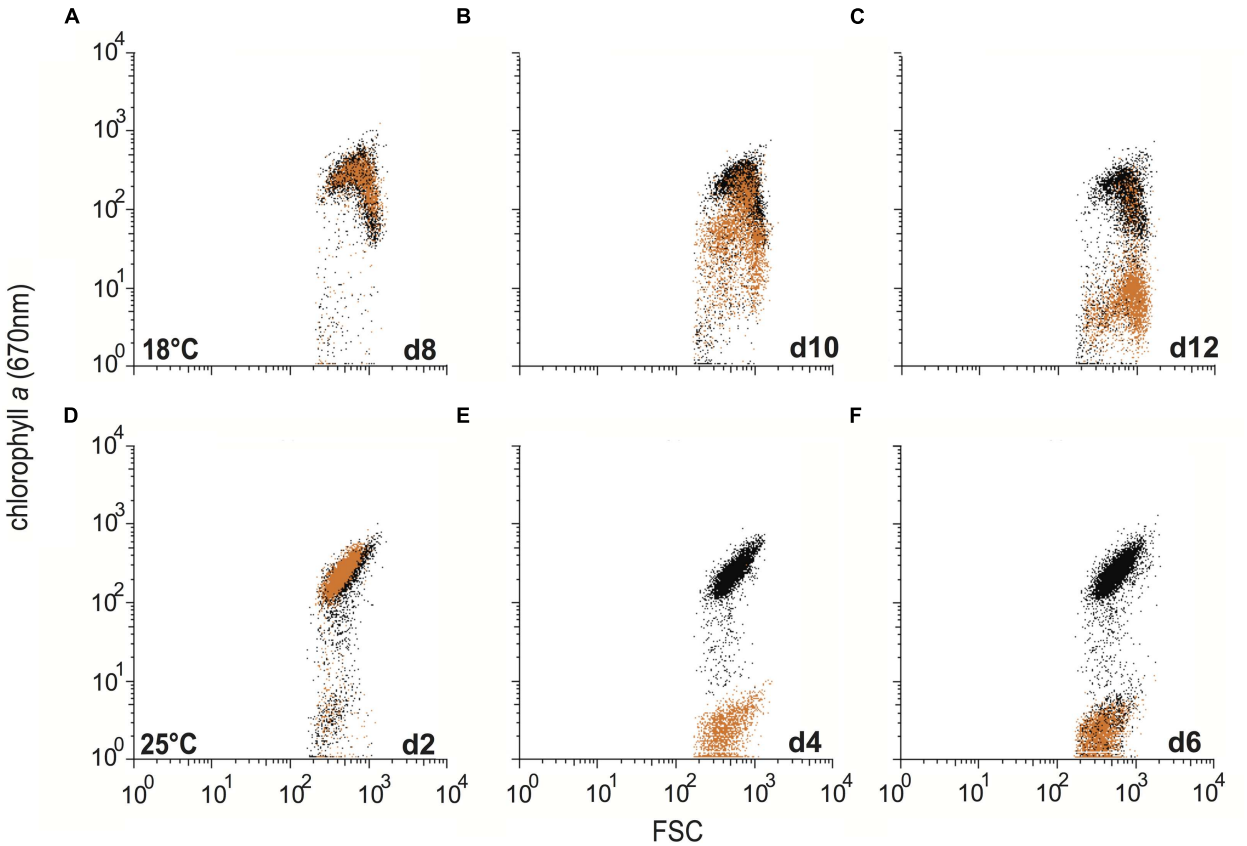

FIGURE 5 | Bleaching in S type *Emiliania huxleyi* (CCMP3268) in co-culture with *Ruegeria* sp. R11. Control cultures of CCMP3268 and co-cultures of CCMP3268 with R11 were assessed for chlorophyll content using flow cytometry at 18°C on 8 days **(A)**, 10 days **(B)**, and 12 days **(C)**; and at 25°C on 2 days **(D)**, 4 days **(E)**, and 6 days **(F)**. Data for R11-CCMP3268 co-cultures are indicated with orange data points and control cultures (CCMP3268 grown alone) with black data points.

pathogenicity of R11 at elevated temperature cannot be explained by differential bacterial loads, as the R11 populations reached the same order of magnitude (10^7 cfu/mL) in co-culture with both algal strains at both temperatures (**Figures 1E,F** and **2E,F**). Although R11 attains this carrying capacity 2–4 days earlier at 25°C than at 18°C, this is also insufficient to explain the differences (**Figures 1E,F** and **2E,F**). With CCMP3266, the initial drop in algal yield at 25°C occurs on the same day that R11 cell density reach their carrying capacity, while at 18°C, algal death in co-culture does not begin until 10 days after the carrying capacity of R11 is reached (**Figure 1**). With CCMP3268, the timelines are slightly closer together, with the death of the 25°C co-culture beginning 2 days after R11 cell density reached carrying capacity and the death of the 18°C co-culture beginning 4 days after R11 carrying capacity had been reached (**Figure 2**).

The differences in timeline leading to death also cannot be explained by differences in the photosynthetic health of the algae at the two temperatures. CCMP3266 control cultures displayed equal yield values at both temperatures for the duration of the experiment (**Figures 1A,B**). CCMP3268 control cultures also maintained equivalent yield values at both 18 and 25°C, until the control culture experienced death starting on 16 days (**Figures 2A,B**).

Taken together, these results support the hypothesis that the virulence of R11 on *E. huxleyi* is temperature-enhanced. This is in keeping with the original *Delisea pulchra*-R11 model of virulence in which R11 was pathogenic to *D. pulchra* at 24°C, but not pathogenic at 19°C (Case et al., 2011). Temperature-enhanced bacterial pathogens have been linked to several other algal diseases including 'white tip disease' in *Gracilaria conferta* – in which a bacterial isolate was found to be the causative agent and that increasing temperature above 20°C increased the rate of infection (Weinberger et al., 1994). Another example of temperature-enhanced virulence in the marine environment can be found in the bleaching of the coral *Pocillopora damicornis* by the bacterium *Vibrio coralliilyticus*, triggered by elevated temperature (Kushmaro et al., 1996; Ben-Haim et al., 2003; Rosenberg et al., 2009). In fact, this temperature-induced bleaching results from an attack by *V. coralliilyticus* on the zooxanthellae algal symbionts living within the coral tissue (Ben-Haim et al., 2003). It appears that the increased pathogenicity in this case was due to both the increased expression of virulence factors and a possible increase in sensitivity of the algae to

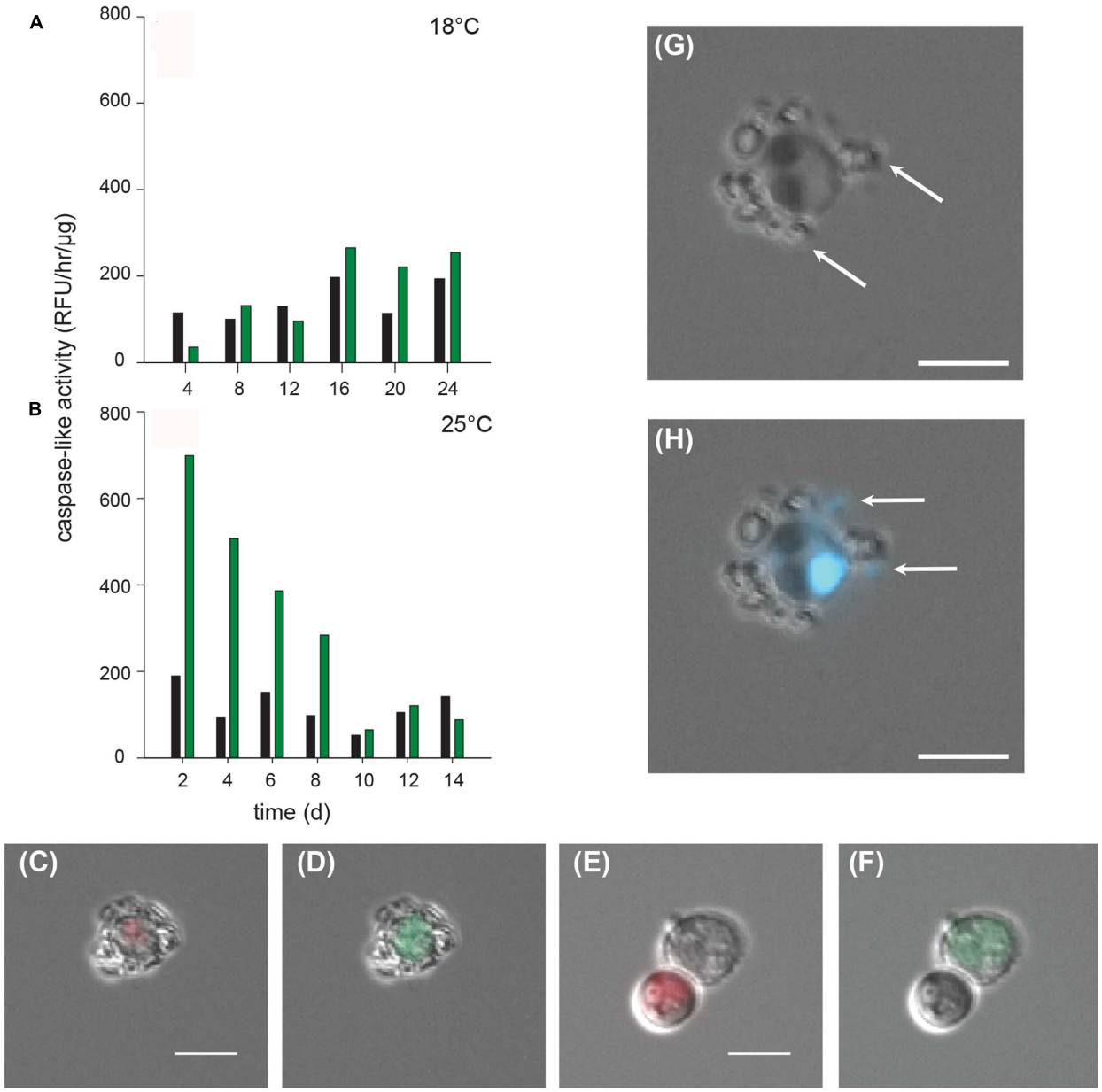

FIGURE 6 | Detection of caspase-like activity in C type *Emiliania huxleyi* (CCMP3266) in co-culture with *Ruegeria* sp. R11. R11 (10^2 cells/ml) was co-cultured with CCMP3266 (10^5 cells/ml) at 18 and 25°C to determine the influence of temperature on the degree of IETDase activity detected in CCMP3266 throughout the co-culture with R11. *In vitro* IETDase activity was measured (Caspase Activity Kit, EMB Millipore) at 18°C for CCMP3266 grown alone and in co-culture with R11 **(A)**; and at 25°C for CCMP3266 grown alone and in co-culture with R11 **(B)**. Data for R11-CCMP3266 co-cultures are indicated with green bars and control cultures (CCMP3266 grown alone) with black bars. Chlorophyll autofluorescence (red) was monitored microscopically in CCMP3266 cells at 18°C **(C)** and 25°C **(E)**. *In vivo* detection of active capsase-like molecules (green) was monitored microscopically in cells stained with CaspACE (*in situ* VAD-marker: FITC-VAD-FMK) at 18°C **(D)** and at 25°C **(F)**. DIC imaging shows cells bearing coccoliths (individual coccoliths indicated with 'Co') and DNA within algal and bacterial cells is stained with DAPI **(G)** and attached R11 cells are distinguished from coccoliths as bacteria contain DAPI stained DNA (bacteria indicated with 'R11') **(H)**. The scale bar is 5 μm.

pathogen attack due to temperature stress (Kushmaro et al., 1996; Ben-Haim et al., 2003; Rosenberg et al., 2009).

In the present study, there is evidence of temperature stress in CCMP3266 and CCMP3268 at 25°C, as there were marked differences in the algal population size and dynamics at 18 and 25°C. For CCMP3266 at 25°C, the population size initially followed the same trajectory as the culture at 18°C, reaching nearly the same peak cell density, but subsequently dropping to around half the density of the 18°C culture, where it stabilized for the remainder of the experiment (**Figures 1C,D**). For

CCMP3268, the control culture at 25°C followed a completely different trajectory to the 18°C control culture, slowly increasing to a peak only two thirds the density of the maximum at 18°C, 8 days later (**Figures 2C,D**). After this peak, cell density dropped sharply and remained near zero for the remainder of the experiment.

The fact that the cell densities were lower at 25°C for both CCMP3266 and CCMP3268 likely indicates temperature stress. The reported temperature range of *E. huxleyi* is highly variable (spanning 6–26°C; Rhodes et al., 1995; Paasche, 2002; Daniels et al., 2014), with marked differences in temperature optima reported even between strain clones (Paasche, 2002). In the present study, while cultures of both CCMP3266 and 3268 grow normally at 18°C (with a rapid log phase and a stable stationary phase), they both display altered dynamics at 25°C (slow initial growth rate and low or un-sustained stationary phase), which is near the upper limit of the species' temperature range. However, 25°C is an ecologically relevant temperature for these strains, as current SST in the Tasman Sea, where both CCMP3266/3268 and R11 originate, regularly reaches 25°C in the austral summer. This area – sometimes referred to as the 'Tasman Hot Spot' – is predicted to have a rate of SST warming 3–4 times the global average (Oliver et al., 2014). Additionally, a metagenomic study has shown that EhVs are absent from populations of *E. huxleyi* in warm equatorial waters (von Dassow et al., 2015). This raises the possibility that regions likely to be even warmer in the future, such as the Tasman Sea, which currently host populations of *E. huxleyi* infected with EhVs, may soon represent a niche open to new pathogens such as R11.

It is unclear from the data presented whether the cause of the increase in pathogenicity of R11 at 25°C was the result of increased susceptibility of *E. huxleyi*, or was due to an increase in the production of virulence factors by R11 at elevated temperature, or a combination of the two factors. Plant pathogens are known to be triggered by temperatures outside the optimal range for host growth – in other words, by temperatures at which the defenses of the host may be compromised (Smirnova et al., 2001). For example, the blight pathogen *Pseudomonas syringae* significantly increases production of a phytotoxin at 18°C (7–10°C below the growth optimum of its host; Budde and Ullrich, 2000).

It is possible that R11 is an opportunistic pathogen, as its host range appears to be broad – including a red macroalga (Case et al., 2011) and a haptophyte (present study). For a pathogen with diverse hosts, a versatile strategy of triggering virulence might be to sense the stress of a host directly, instead of sensing the conditions that would cause a host's defenses to be compromised. This is a mechanism known to exist in *Phaeobacter gallaeciensis* BS107, another member of the Roseobacter clade. *P. gallaeciensis* produces algaecides in response to *p*-coumaric acid (*p*CA) – produced by *E. huxleyi* and thought to be a product of senescence (Seyedsayamdost et al., 2011). However, R11 is unlikely to use this particular molecule as a cue, since the addition of *p*CA did not stimulate a change in its production of small molecules (Seyedsayamdost et al., 2011). The evidence from the present study – the fact that R11 displays a broad host range and increased virulence under conditions at which the host displays evidence of temperature stress – supports the hypothesis that R11 is an opportunistic pathogen.

Ruegeria sp. R11 Causes Bleaching in *E. huxleyi*

Bleaching – the loss of pigmentation – is a common phenomenon in marine corals and macroalgae (Jenkins et al., 1999; Douglas, 2003; Egan et al., 2013). In corals, this color loss refers to the death or loss of the symbiotic algae that live within the coral's tissue – a temperature-dependent effect often linked to bacterial infection – that ultimately leads to the death of coral host (Kushmaro et al., 1996; Ben-Haim et al., 2003; Rosenberg et al., 2009). In macroalgae, the bleaching effect is due to the degradation of photosynthetic pigment that, depending of the extent of the bleaching, may lead to the death of the whole organism. In the present study, a color change was clearly visible in dead or dying cultures of *E. huxleyi*. R11-*E. huxleyi* co-culture wells changed from green to white. This bleaching was also evident from the flow cytometry results (**Figures 4** and **5**). In the case of both CCMP3266 (**Figure 4**) and CCMP3268 (**Figure 5**), during culture death, cells maintained their size (forward scatter) but lost their chlorophyll α content over 2 days at 25°C (**Figures 4D–F** and **5D–F**) or 4 days at 18°C (**Figures 4A–C** and **5A–C**).

Algal bleaching has been mostly attributed to temperature or UV stress alone (Jenkins et al., 1999), except in the case of *D. pulchra*, in which R11 is the temperature-dependent causative agent of the bleaching disease – *D. pulchra* grown without R11 at high temperature does not exhibit bleaching (Case et al., 2011). With the mentioned exception of *D. pulchra*, these studies do not assess the microbial community component of the system, and as such, bacterially mediated temperature induced bleaching in marine algae could be far more common than the literature reports. Here we demonstrate that it occurs in a microscopic unicellular haptophyte, distantly related, both phylogenetically and physiologically, to the red macroalgae in which it was previously found.

Increased Caspase-Like Activity in Co-cultures of *E. huxleyi* and *Ruegeria* sp. R11

While PCD was historically considered a phenomenon linked to multicellularity, it has recently been identified in several unicellular lineages, including coccolithophores (Bidle et al., 2007; Bidle and Kwityn, 2012). PCD is the genetically programmed deconstruction of cellular components by highly specific proteases. Caspases are cysteine proteases that cleave target substrate proteins containing the corresponding cleavage motif (4–5 amino acid motifs), resulting in apoptotic-PCD. While metacaspases differ from true caspases in both activity and specificity, there are reports of target substrates being similar between these enzymes (Sundström et al., 2009), as well as some reports of metacaspases exhibiting a biochemical activity (e.g., cleavage motifs) that is similar to that of true caspases (Madeo et al., 2002; Wilkinson and Ramsdale, 2011). Caspase-like activity was observed both *in vivo* and *in vitro* in the co-culture of CCMP3266 and R11. The method used in this study to quantify

caspase-like activity *in vitro* detects the activity of IETDase caspases and structurally similar caspase-like proteases, some of which have been linked to increased metacaspase gene expression in the model EhV system (Bidle et al., 2007). Since the genome of *E. huxleyi* does not contain the genes encoding for caspases, but does contain 13 genes encoding for metacaspases (Choi and Berges, 2013), the activity detected here is likely due to the latter. Some background level of caspase-like activity was found in control cultures of CCMP3266 alone at both temperatures (**Figures 6A,D**), which has been previously reported in the viral experiments (Bidle et al., 2007; Bidle and Kwityn, 2012). A slight increase in activity from that background level was detected in co-cultures on days during which CCMP3266 was dead or dying at 18°C, and a large increase on days during which CCMP3266 was dead or dying at 25°C. This spike in caspase-like activity at 25°C might explain why death happened much earlier and more rapidly at elevated temperature. Bacterial pathogens of several land plant genera, including *Solanum* and *Arabidopsis*, have been shown to trigger the expression of metacaspases during the course of infection (Coll et al., 2011), but to our knowledge, caspase-like activity has not previously been shown to be induced in marine algae by a bacterial pathogen.

CONCLUSION

Natural blooms of *E. huxleyi* often experience a rapid collapse that has been attributed to lytic EhV infections causing PCD in the blooming algae (Vardi et al., 2009). However, it has recently been demonstrated that EhV strains become avirulent at increased temperature due to a change in the structure of the glycosphingolipid required for viral recognition (Kendrick et al., 2014). This algal resistance is gained with only a 3°C increase in temperature – from 18 to 21°C (Kendrick et al., 2014).

In the context of a rapidly warming ocean, the emergence of temperature-induced resistance in *E. huxleyi* to its major pathogen may present an ecological gap. Our findings indicate that opportunistic bacterial pathogens like R11 with temperature-enhanced virulence have the ability to fill this gap and a transition between viral and bacterial disease outbreaks in *E. huxleyi* may be observed as SST continues to rise.

AUTHOR CONTRIBUTIONS

TM and RC conceived the research. AB, TM, and RC conducted the flow cytometry, TM, AB, and KY conducted the growth experiments. TM, AB, and RC drafted the manuscript. All authors have read and approved the manuscript.

FUNDING

This work was supported by Natural Sciences and Engineering Research Council of Canada (grant 402105) to RC.

SUPPLEMENTARY MATERIAL

The Supplementary Material for this article can be found online at: http://journal.frontiersin.org/article/10.3389/fmicb.2016.00892

REFERENCES

Ashen, J. B., and Goff, L. J. (1998). Galls on the marine red alga *Prionitis laceolata* (Halymeniaceae): specific induction and subsequent development of an algal-bacterial symbiosis. *Am. J. Bot.* 85, 1710–1721. doi: 10.2307/2446505

Ashen, J. B., and Goff, L. J. (2000). Molecular and ecological evidence for species specificity and coevolution in a group of marine algal-bacterial symbioses. *Appl. Environ. Microbiol.* 66, 3024–3030. doi: 10.1128/AEM.66.7.3024-3030.2000

Ayers, G. P., and Cainey, J. M. (2007). The CLAW hypothesis: a review of the major developments. *Environ. Chem.* 4, 366–374. doi: 10.1071/EN07080

Behrenfeld, M. J., Randerson, J. T., McClain, C. R., Feldman, G. C., Los, S. O., Tucker, C. J., et al. (2001). Biospheric primary production during an ENSO transition. *Science* 291, 2594–2597. doi: 10.1126/science.1055071

Ben-Haim, Y., Zicherman-Keren, M., and Rosenberg, E. (2003). Temperature-regulated bleaching and lysis of the coral *Pocillopora damicornis* by the novel pathogen *Vibrio coralliilyticus*. *Appl. Environ. Microbiol.* 69, 4236–4242. doi: 10.1128/AEM.69.7.4236-4242.2003

Bidle, K. D., Haramaty, L., Barcelos, E., Ramos, J., and Falkowski, P. (2007). Viral activation and recruitment of metacaspases in the unicellular coccolithophore, *Emiliania huxleyi*. *Proc. Natl. Acad. Sci. U.S.A.* 104, 6049–6054. doi: 10.1073/pnas.0701240104

Bidle, K. D., and Kwityn, C. J. (2012). Assessing the role of caspase activity and metacaspase expression on viral susceptibility of the coccolithophore, *Emiliania huxleyi* (*Haptophyta*). *J. Phycol.* 48, 1079–1089. doi: 10.1111/j.1529-8817.2012.01209.x

Boyce, D. G., Lewis, M. R., and Worm, B. (2010). Global phytoplankton decline over the past century. *Nature* 466, 591–596. doi: 10.1038/nature09268

Bramucci, A. R., Labeeuw, L., Mayers, T. J., Saby, J. A., and Case, R. J. (2015). A small volume bioassay to assess bacterial/phytoplankton co-culture using WATER-Pulse-Amplitude-Modulated (WATER-PAM) fluorometry. *J. Vis. Exp.* 97:e52455. doi: 10.3791/52455

Brown, C. W., and Yoder, J. A. (1994). Coccolithophorid blooms in the global ocean. *J. Geophys. Res.* 99, 7467–7482. doi: 10.1029/93JC02156

Budde, I. P., and Ullrich, M. S. (2000). Interactions of *Pseudomonas syringae* pv. glycinea with host and nonhost plants in relation to temperature and phytotoxin synthesis. *Mol. Plant Microbe Interact* 13, 951–961. doi: 10.1094/MPMI.2000.13.9.951

Case, R. J., Longford, S. R., Campbell, A. H., Low, A., Tujula, N., Steinberg, P. D., et al. (2011). Temperature induced bacterial virulence and bleaching disease in a chemically defended marine macroalga. *Environ. Microbiol.* 13, 529–537. doi: 10.1111/j.1462-2920.2010.02356.x

Charlson, R. J., Lovelock, J. E., Andreae, M. O., and Warren, S. G. (1987). Oceanic phytoplankton, atmospheric sulphur, cloud albedo and climate. *Nature* 326, 655–661. doi: 10.1038/326655a0

Choi, C. J., and Berges, J. A. (2013). New types of metacaspases in phytoplankton reveal diverse origins of cell death proteases. *Cell Death Dis.* 4, 1–7. doi: 10.1038/cddis.2013.21

Chow, J. S., Lee, C., and Engel, A. (2015). The influence of extracellular polysaccharides, growth rate, and free coccoliths on the coagulation efficiency of *Emiliania huxleyi*. *Mar. Chem.* 175, 5–17. doi: 10.1016/j.marchem.2015.04.010

Coll, N. S., Epple, P., and Dangl, J. L. (2011). Programmed cell death in the plant immune system. *Cell Death Differ.* 18, 1247–1256. doi: 10.1038/cdd.2011.37

Daniels, C. J., Sheward, R. M., and Poulton, A. J. (2014). Biogeochemical implications of comparative growth rates of *Emiliania huxleyi* and *Coccolithus species*. *Biogeosciences* 11, 6915–6925. doi: 10.5194/bg-11-6915-2014

Douglas, A. E. (2003). Coral bleaching—how and why? *Ma. Pollut. Bull.* 46, 385–392. doi: 10.1016/S0025-326X(03)00037-7

Egan, S., Harder, T., Burke, C., Steinberg, P., Kjelleberg, S., and Thomas, T. (2013). The seaweed holobiont: understanding seaweed-bacteria interactions. *FEMS Microbiol. Rev.* 37, 462–476. doi: 10.1111/1574-6976.12011

Fernandes, N., Case, R. J., Longford, S. R., Seyedsayamdost, M. R., Steinberg, P. D., Kjelleberg, S., et al. (2011). Genomes and virulence factors of novel bacterial pathogens causing bleaching disease in the marine red alga *Delisea pulchra*. *PLoS ONE* 6:e27387. doi: 10.1371/journal.pone.0027387

Frada, M., Probert, I., Allen, M. J., Wilson, W. H., and de Vargas, C. (2008). The "Cheshire Cat" escape strategy of the coccolithophore *Emiliania huxleyi* in response to viral infection. *Proc. Natl. Acad. Sci. U.S.A.* 105, 15944–15949. doi: 10.1073/pnas.0807707105

Frada, M. J., Bidle, K. D., Probert, I., and de Vargas, C. (2012). In situ survey of life cycle phases of the coccolithophore *Emiliania huxleyi* (Haptophyta). *Environ. Microbiol.* 14, 1558–1569. doi: 10.1111/j.1462-2920.2012.02745.x

Fulton, J. M., Fredricks, H. F., Bidle, K. D., Vardi, A., Kendrick, B. J., DiTullio, G. R., et al. (2014). Novel molecular determinants of viral susceptibility and resistance in the lipidome of *Emiliania huxleyi*. *Environ. Microbiol.* 16, 1137–1149. doi: 10.1111/1462-2920.12358

Gao, K., Ruan, Z., Villafane, V. E., Gattuso, J., and Helbling, E. W. (2009). Ocean acidification exacerbates the effect of UV radiation on the calcifying phytoplankter *Emiliania huxleyi*. *Limnol. Oceanogr.* 54, 1855–1862. doi: 10.4319/lo.2009.54.6.1855

Gardiner, M., Thomas, T., and Egan, S. (2015). A glutathione peroxidase (GpoA) plays a role in the pathogenicity of Nautella italica strain R11 towards the red alga *Delisea pulchra*. *FEMS Microbiol. Ecol.* 91:fiv021. doi: 10.1093/femsec/fiv021

Gonzalez, J. M., Simo, R., Massana, R., Covert, J. S., Casamayor, E. O., Pedros-Alio, C., et al. (2000). Bacterial community structure associated with a dimethylsulfoniopropionate-producing North Atlantic algal bloom. *Appl. Environ. Microbiol.* 66, 4237–4246. doi: 10.1128/AEM.66.10.4237-4246.2000

Green, D. H., Echavarri-Bravo, V., Brennan, D., and Hart, M. C. (2015). Bacterial diversity associated with the coccolithophorid algae *Emiliania huxleyi* and *Coccolithus pelagicus* f. braarudii. *Biomed. Res. Int.* 2015, 1–15. doi: 10.1155/2015/194540

Green, J. C., Course, P. A., and Tarran, G. A. (1996). The life-cycle of *Emiliania huxleyi*: a brief review and a study of ploidy levels analysed by flow cytometry. *J. Mar. Syst.* 9, 33–44. doi: 10.1016/0924-7963(96)00014-0

Guillard, R. R. L., and Hargraves, P. E. (1993). Stichochrysis immobilis is a diatom, not a chrysophyte. *Phycologia* 32, 234–236. doi: 10.2216/i0031-8884-32-3-234.1

Harvell, C. D., Mitchell, C. E., Ward, J. R., Altizer, S., Dobson, A. P., Ostfeld, R. S., et al. (2002). Climate warming and disease risks for terrestrial and marine biota. *Science* 296, 2158–2162. doi: 10.1126/science.1063699

Helliwell, K. E., Wheeler, G. L., Leptos, K. C., Goldstein, R. E., and Smith, A. G. (2011). Insights into the evolution of vitamin B12 auxotrophy from sequenced algal genomes. *Mol. Biol. Evol.* 28, 1–13. doi: 10.1093/molbev/msr124

Huisman, J. (2000). *Marine Plants of Australia*. Nedlands, WA: University of Western Australia Press.

Jenkins, S. R., Hawkins, S. J., and Norton, T. A. (1999). Direct and indirect effects of a macroalgal canopy and limpet grazing in structuring a sheltered inter-tidal community. *Mar. Ecol. Prog. Ser.* 188, 81–92. doi: 10.3354/meps188081

Kendrick, B. J., DiTullio, G. R., Cyronak, T. J., Fulton, J. M., Van Mooy, B. A., and Bidle, K. D. (2014). Temperature-induced viral resistance in *Emiliania huxleyi* (*Prymnesiophyceae*). *PLoS ONE* 9:e112134. doi: 10.1371/journal.pone.0112134

Kushmaro, A., Loya, Y., Fine, M., and Rosenberg, E. (1996). Bacterial infection and coral bleaching. *Nature* 380:396. doi: 10.1038/380396a0

Labeeuw, L., Khey, J., Bramucci, A. R., Atwal, H., de la Mata, P., Haryunk, J., et al. (2016). Indole-3-acetic acid is produced by *Emiliania huxleyi* cocolith-bearing cells and triggers a physiological response in bald cells. *Front. Microbiol.* 7:828. doi: 10.3389/fmicb.2016.00828

Lam, E., Kato, N., and Lawton, M. (2001). Programmed cell death, mitochondria and the plant hypersensitive response. *Nature* 411, 848–853. doi: 10.1038/35081184

Madeo, F., Herker, E., Maldener, C., Klissing, S., Lachelt, S., Herlan, M., et al. (2002). A caspase-related protease regulated apoptosis in yeast. *Mol. Cell.* 9, 911–917.

Oliver, E. C. J., Wotherspoon, S. J., Chamberlain, M. A., and Holbrook, N. J. (2014). Projected Tasman Sea extremes in sea surface temperature through the twenty-first century. *J. Climate* 27, 1980–1998. doi: 10.1175/JCLI-D-13-00259.1

Paasche, E. (2002). A review of the coccolithophorid *Emiliania huxleyi* (Prymnesiophyceae), with particular reference to growth, coccolith formation, and calcification-photosynthesis interactions. *Phycologia* 40, 503–529. doi: 10.2216/i0031-8884-40-6-503.1

Quinn, P. K., and Bates, T. S. (2011). The case against climate regulation via oceanic phytoplankton sulphur emissions. *Nature* 480, 51–56. doi: 10.1038/nature10580

Reisch, C. R., Moran, M. A., and Whitman, W. B. (2011). Bacterial catabolism of dimethylsulfoniopropionate (DMSP). *Front. Microbiol.* 2:172. doi: 10.3389/fmicb.2011.00172

Rhodes, L. L., Peake, B. M., MacKenzie, A. L., and Marwick, S. (1995). Coccolithophores *Gephyrocapsa oceanica* and *Emiliania huxleyi* (Prymnesiophyceae=Haptophyceae) in New Zealand's coastal waters: characteristics of blooms and growth in laboratory culture. *N. Z. J. Mar. Freshw. Res.* 29, 345–357. doi: 10.1080/00288330.1995.9516669

Rosenberg, E., Kushmaro, A., Kramarsky-Winter, E., Banin, E., and Yossi, L. (2009). The role of microorganisms in coral bleaching. *ISME J.* 3, 139–146. doi: 10.1038/ismej.2008.104

Sapp, M., Schwaderer, A. S., Wiltshire, K. H., Hoppe, H. G., Gerdts, G., and Wichels, A. (2007). Species-specific bacterial communities in the phycosphere of microalgae? *Microb Ecol.* 53, 1–17. doi: 10.1007/s00248-006-9162-5

Schmidt, S., Harlay, J., Borges, A. V., Groome, S., Delilled, B., Roevros, N., et al. (2013). Particle export during a bloom of *Emiliania huxleyi* in the North-West European continental margin. *J. Mar. Syst.* 109–110, 182–190. doi: 10.1016/j.jmarsys.2011.12.005

Schreiber, U. (1998). Chlorophyll fluorescence: new instruments for special applications. *Photosynthesis Mech. Effects* 5, 4253–4258.

Schreiber, U., Schliwa, U., and Bilger, W. (1986). Continuous recording of photochemical and non-photochemical chlorophyll fluorescence quenching with a new type of modulation fluorometer. *Photosynthesis Res.* 10, 51–62. doi: 10.1007/BF00024185

Seyedsayamdost, M. R., Case, R. J., Kolter, R., and Clardy, J. (2011). The Jekyll-and-Hyde chemistry of *Phaeobacter gallaeciensis*. *Nat. Chem.* 3, 331–335. doi: 10.1038/nchem.1002

Simó, R. (2004). From cells to globe: approaching the dynamics of DMS(P) in the ocean at multiple scales. *Can. J. Fisheries Aquat. Sci.* 61, 673–684. doi: 10.1139/f04-030

Smirnova, A., Li, H., Weingart, H., Aufhammer, S., Burse, A., Finis, K., et al. (2001). Thermoregulated expression of virulence factors in plant-associated bacteria. *Arch. Microbiol.* 176, 393–399. doi: 10.1007/s002030100344

Smith, T. M., Reynolds, R. W., Peterson, T. C., and Lawrimore, J. (2008). Improvements to NOAA's Historical Merged Land–Ocean Surface Temperature Analysis (1880–2006). *J. Climate* 21, 2283–2296. doi: 10.1175/2007JCLI2100.1

Sundström, J. F., Vaculova, A., Smertenko, A. P., Savenkov, E. I., Golovko, A., Minina, E., et al. (2009). Tudor staphylococcal nuclease is an evolutionarily conserved component of the programmed cell death degradome. *Nat. Cell Biol.* 11, 1347–1354. doi: 10.1038/ncb1979

Thrall, P. H., Burdon, J. J., and Young, A. (2001). Variation in resistance and virulence among demes of a plant host-pathogen metapopulation. *J. Ecol.* 86, 736–748. doi: 10.1111/j.1461-0248.2012.01749.x

van Kooten, O., and Snel, J. F. H. (1990). The use of chlorophyll fluorescence nomenclature in plant stress physiology. *Photosynthesis Res.* 25, 147–150. doi: 10.1007/BF00033156

Vardi, A., Van Mooy, B. A., Fredricks, H. F., Popendorf, K. J., Ossolinski, J. E., Haramaty, L., et al. (2009). Viral glycosphingolipids induce lytic infection and cell death in marine phytoplankton. *Science* 326, 861–865. doi: 10.1126/science.1177322

von Dassow P., John, U., Ogata, H., Probert, I., Bendif, M., Kegel, J. U., et al. (2015). Life-cycle modification in open oceans accounts for genome variability in a cosmopolitan phytoplankton. *ISME J.* 9, 1365–1377. doi: 10.1038/ismej.2014.221

von Dassow P., Ogata, H., Probert, I., Wincker, P., Da, Silva, C., Audic, S., et al. (2009). Transcriptome analysis of functional differentiation between haploid and diploid cells of *Emiliania huxleyi*, a globally significant photosynthetic calcifying cell. *Genome Biol.* 10, 1–33. doi: 10.1186/gb-2009-10-10-r114

Voss, K. J., Balch, W. M., and Kilpatrick, K. A. (1998). Scattering and attenuation properties of *Emiliania huxleyi* cells and their detached coccoliths. *Limnol. Oceanogr.* 43, 870–876. doi: 10.4319/lo.1998.43.5.0870

Webb, A. L., Malin, G., Hopkins, F. E., Ho, K. L., Riebesell, U., Schulz, K. G., et al. (2016). Ocean acidification has different effects on the production of dimethylsulfide and dimethylsulfoniopropionate measured in cultures of *Emiliania huxleyi* and a mesocosm study: a comparison of laboratory monocultures and community interactions. *Environ. Chem.* 13, 314–329. doi: 10.1071/EN14268

Weinberger, F., Freidlander, M., and Gunkel, W. (1994). A bacterial facultative parasite of *Gracilaria* conferta. *Dis. Aquat. Organ.* 18, 135–141. doi: 10.3354/dao018135

Wilkinson, D., and Ramsdale, M. (2011). Proteases and caspase-like activity in the yeast Saccharomyces cerevisiae. *Biochem. Soc. Trans.* 39, 1502–1508. doi: 10.1042/BST0391502

Wilson, W. H., Tarran, G. A., Schroeder, D., Cox, M., Oke, J., and Malin, G. (2002). Isolation of viruses responsible for the demise of an *Emiliania huxleyi* bloom in the English Channel. *J. Mar. Biol. Assoc.* 82, 369–377. doi: 10.1017/S002531540200560X

Wilson, W. H., Van Etten, J. L., and Allen, M. J. (2009). The phycodnaviridae: the story of how tiny giants rule the world. *Curr. Top. Microbiol. Immunol.* 328, 1–42.

Conflict of Interest Statement: The authors declare that the research was conducted in the absence of any commercial or financial relationships that could be construed as a potential conflict of interest.

frontiers in Microbiology

ORIGINAL RESEARCH
published: 12 September 2016
doi: 10.3389/fmicb.2016.01433

Phytoplankton-Associated Bacterial Community Composition and Succession during Toxic Diatom Bloom and Non-Bloom Events

Marilou P. Sison-Mangus[1], Sunny Jiang[2], Raphael M. Kudela[1] and Sanjin Mehic[1]*

[1] *Department of Ocean Sciences and Institute of Marine Sciences, University of California, Santa Cruz, Santa Cruz, CA, USA,*
[2] *Department of Civil and Environmental Engineering, University of California, Irvine, Irvine, CA, USA*

Pseudo-nitzschia blooms often occur in coastal and open ocean environments, sometimes leading to the production of the neurotoxin domoic acid that can cause severe negative impacts to higher trophic levels. Increasing evidence suggests a close relationship between phytoplankton bloom and bacterial assemblages, however, the microbial composition and succession during a bloom process is unknown. Here, we investigate the bacterial assemblages before, during and after toxic and non-toxic *Pseudo-nitzschia* blooms to determine the patterns of bacterial succession in a natural bloom setting. Opportunistic sampling of bacterial community profiles were determined weekly at Santa Cruz Municipal Wharf by 454 pyrosequencing and analyzed together with domoic acid levels, phytoplankton community and biomass, nutrients and temperature. We asked if the bacterial communities are similar between bloom and non-bloom events and if domoic acid or the presence of toxic algal species acts as a driving force that can significantly structure phytoplankton-associated bacterial communities. We found that bacterial diversity generally increases when *Pseudo-nitzschia* numbers decline. Furthermore, bacterial diversity is higher when the low-DA producing *P. fraudulenta* dominates the algal bloom while bacterial diversity is lower when high-DA producing *P. australis* dominates the algal bloom, suggesting that the presence of algal toxin can structure bacterial community. We also found bloom-related succession patterns among associated bacterial groups; Gamma-proteobacteria, were dominant during low toxic *P. fraudulenta* blooms comprising mostly of *Vibrio* spp., which increased in relative abundance (6–65%) as the bloom progresses. On the other hand, Firmicutes bacteria comprising mostly of *Planococcus* spp. (12–86%) dominate during high toxic *P. australis* blooms, with the bacterial assemblage showing the same bloom-related successional patterns in three independent bloom events. Other environmental variables such as nitrate and phosphate and temperature appear to influence some low abundant bacterial groups as well. Our results suggest that phytoplankton-associated bacterial communities are strongly affected not just by phytoplankton bloom in general, but also by the type of algal species that dominates in the natural bloom.

Keywords: algal bloom, *Pseudo-nitzschia*, diatom, bacteria, *Vibrio*, *Planococcus*, nutrients, domoic acid

OPEN ACCESS

Edited by:
Xavier Mayali, Lawrence Livermore National Laboratory, USA

Reviewed by:
Ingrid Obernosterer, Observatoire Océanologique de Banyuls-sur-Mer – Centre National de la Recherche Scientifique, France
Guang Gao, Nanjing Institute of Geography and Limnology (CAS), China

****Correspondence:***
Marilou P. Sison-Mangus
msisonma@ucsc.edu

Specialty section:
This article was submitted to Aquatic Microbiology, a section of the journal Frontiers in Microbiology

Received: *10 May 2016*
Accepted: *29 August 2016*
Published: *12 September 2016*

Citation:
Sison-Mangus MP, Jiang S, Kudela RM and Mehic S (2016) Phytoplankton-Associated Bacterial Community Composition and Succession during Toxic Diatom Bloom and Non-Bloom Events. Front. Microbiol. 7:1433. doi: 10.3389/fmicb.2016.01433

INTRODUCTION

Phytoplankton plays an important role in global carbon cycling by consuming carbon dioxide from the atmosphere for photosynthesis and sequestering the fixed carbon as cells sink down into the deep ocean. Phytoplankton bloom, happening either in the coast, upwelling regions or open ocean, not only provides organic materials to the higher trophic food web but also provides photosynthate-released dissolved organic matter (Larsson and Hagstrom, 1979) and organic suspended matter for bacterial attachment and subsequent degradation by heterotrophic bacterial communities (Smith et al., 1995). Azam et al. (1983) reported that bacterial biomass and production is tightly coupled with phytoplankton biomass. With the use of molecular tools, many workers discovered that bacterial communities change in composition as algal bloom peak and decline (Riemann et al., 2000; Teeling et al., 2012; Klindworth et al., 2014). Bacterial groups such as Alpha-proteobacteria, Gamma-proteobacteria and Flavobacteria are often reported as the dominant free-living bacterioplankton during algal bloom (reviewed in Buchan et al., 2014). It is still unclear, however, if phytoplankton-associated bacteria undergo the same pattern and if bacterial composition and succession is being influenced by the algal species in bloom or if the phytotoxins produced by harmful algae also play a role in structuring bacterial communities during algal bloom.

Many bacteria associate with phytoplankton (Schafer et al., 2002; Grossart et al., 2005; Sison-Mangus et al., 2014) and are often seen attached on healthy or dying cells (Kaczmarska et al., 2005; Gardes et al., 2011; Mayali et al., 2011; Smriga et al., 2016), as they feed off on the released dissolved organic matter, breaking down the dead algal cell (Bidle and Azam, 1999) or actively killing the phytoplankton (Mayali and Azam, 2004). Phytoplankton cultivates close associations with bacteria as imposed by their dependence on vitamins, recycled nutrients, photooxidation of assimilable iron or amino acids (Croft et al., 2005; Amin et al., 2009, 2015). On the other hand, phytoplankton varies in terms of biochemical composition, organic excretions (Reitan et al., 1994; Hellebust, 1980; Bjornsen, 1988) or phytotoxins (Doucette et al., 1998), which may act as selective agents for bacterial types with algal-attached lifestyle. It is therefore interesting to determine if bloom-forming phytoplankton species can also facilitate the dominance of different bacterial groups during bloom events.

In this study, we focus on the domoic acid producing *Pseudo-nitzschia* (Pn) and studied the phytoplankton-associated bacterial community from four independent natural bloom events. We asked what bacterial groups dominate in bloom events formed by different *Pseudo-nitzschia* species. We determined how bacterial composition changes before, during and after the decline of *Pseudo-nitzschia* bloom, as it was replaced or co-dominated by other phytoplankton species. Aside from phytoplankton biomass (as chlorophyll *a*), we also looked at environmental variables such as nutrients (nitrate, phosphate, silicate, urea, and ammonium), and temperature to determine if these physical factors also play a role in bacterial succession. Our results indicated that bacterial composition and structure are strongly influenced by the *Pseudo-nitzschia* species in bloom and domoic acid can play a role in limiting bacterial diversity.

MATERIALS AND METHODS

Plankton Tow, Bacteria Sampling and Environmental Data Collection and Processing

Sampling Site

The samples used in the study were subsamples from the weekly monitoring of harmful algal bloom adjacent to Santa Cruz Municipal Wharf (36.9633°N, 122.0172°W) in Monterey Bay, California, one of the ocean observing sites in Central and Northern California (CeNCOOS). The site was established to monitor the presence, abundance and population dynamics of red tide forming species, where weekly monitoring of nutrients, environmental parameters, phytoplankton abundance, chlorophyll *a* and fecal indicator bacteria are measured. Water condition in Monterey Bay is characterized by seasonal upwelling that brings low temperature, high salinity nutrient-rich water from approximately February to August, followed by an oceanic period characterized by upwelling relaxation in August to mid-November. In winter (mid November–mid February), the Davidson Current surfaces along the coast and brings in relatively warm, high salinity, nutrient-rich water (Skogsberg, 1936; Skogsberg and Phelps, 1946; Wyllie and Lynn, 1971; Pennington and Chavez, 2000). Upwelled water together with agricultural run-offs from numerous watersheds feed nutrients into the bay to support massive phytoplankton blooms (Kudela and Chavez, 2004; Kudela et al., 2008; Fischer et al., 2014). Different *Pseudo-nitzschia* species bloom in regular pattern in the bay since their initial discovery in 1991 (Buck et al., 1992; Scholin et al., 2000; Lane et al., 2009).

Water and Phytoplankton Sampling

Vertical phytoplankton tows are normally collected in the early morning at an integrated depth of 1–10 ft depth (5 × 10 ft vertical effort) using a 20 μm mesh with a cod end volume of 300 mL. A 2-L Niskin bottle was used to collect water samples at the same integrated depth and used for nutrients and chlorophyll analysis. Temperature was measured immediately after water collection. For this study, opportunistic sampling was carried out at different phases of the bloom, from the beginning and end of the bloom in November to December 2010 (Fall) and peak and demise in March (Spring), July and August 2011 (Summer). Bloom phases were categorized based on total number of *Pseudo-nitzschia* cells per liter and are as follows: No bloom – 0 to 10000; Low Bloom – 10, 001 to 30,000; Medium bloom – 30,001 – 100, 000; High Bloom – 100001 to 300000; Highest Bloom- >300, 000. Closure of shellfish harvesting commonly occurs when DA-producing *Pseudo-nitzschia* bloom is seen at 100, 000 cells L^1 (Bates et al., 1998).

Algal Counting, Domoic Acid, Chlorophyll and Nutrients Measurement

Algal counts were initially assessed microscopically based on relative percentage abundance followed by counting of total *Pseudo-nitzschia* cells by microscopy and counting of toxic *Pseudo-nitzschia* species using DNA fluorescent in-situ hybridization (FISH) (Miller and Scholin, 1998). Domoic acid in bloom samples were measured using LC/MS method as described in Lane et al. (2010). Briefly, water samples were filtered on GFF filters and stored in −80°C. Ice-thawed filters were submerged in 3 mL 10% MeOH and intermittently sonicated on ice for 30 sec at an output power of <8 Watts. The thick suspension was syringe filtered with 0.22 μm Millex PVDF membrane (EMD Millepore, USA), and stored in −80°C until further processing. DA samples were purified prior to LC/MS analysis. Steps are as follows: DA samples were first prepared by adding 0.5 mL of formic acid and MeOH diluted with Milli-Q water (2:5:93 ratio) and briefly vortexed. The solid phase extraction (SPE) columns (Agilent, USA) were first conditioned with 10-mL 100% MeOH followed by 10-mL Milli-Q water under gentle vacuum of 10Pka, and not letting the SPE columns to dry. After addition of DA samples to the conditioned columns, the sample tubes were rinsed with 4-mL 0.5% aqueous formic acid, and combined with the samples already in the columns. An additional step of adding 4-mL 0.15% formic acid was carried out. DA in the columns were recovered with 3 mL 50% MeOH and transferred to a pre-weighed glass vial for storage at 4°C until analysis of DA via LC/MS (described in Lane et al., 2010). Nutrient samples (nitrate + nitrite hereafter referred to here as nitrate, phosphate and silicate) pre-filtered in GF/F filters (nominal size of 0.7 μm) were analyzed using a Lachat QuikChem 8500 Flow Injection Analyst System and Omnion 3.0 software (Lachat Instruments; Hach Company, Loveland, CO, USA) following the method described in Smith and Bogren (2001) and Knepel and Bogren (2002). Ammonium and urea were analyzed with the method of Holmes et al. (1999) and Price and Harrison (1987), respectively. Chlorophyll *a* analysis was carried out following the non-acidification method described in Welschmeyer (1994).

Bacteria Sampling

Phytoplankton tow samples were first pre-filtered with 300-μm mesh net (bleached and UV-exposed) to remove debris and zooplankton. Three of 30-mL tow samples were filtered with sterile 5 μm Durapore filters (EMD Millipore, USA) and washed with sterile seawater to filter out unassociated bacteria. Algae were collected by resuspending filters in 10 ml of PCR water. Samples were then pelleted via centrifugation at 3000 × *g* for 10 min. Algal pellets were finally resuspended in 500 μL of sterile TE buffer and stored at −80°C. For sequencing, raw samples were sent to Research and Testing Laboratory (Lubbock, TX, USA) for 454 pyrosequencing using the universal primers Yellow939F and Yellow1492R. Sample preparation for sequencing and sequencing methods are described in Sison-Mangus et al. (2014).

Pseudo-nitzschia Isolation and Genotyping

Single cells of *Pseudo-nitzschia* were manually isolated from bloom samples with a microcapillary tip from a sterile glass Pasteur pipette. Prior to cell isolation, an aliquot of the pre-filtered tow sample was filtered with 100 μm nylon mesh (bleached and UV-sterilized) and washed two times with autoclaved-sterilized 0.2 μm filtered seawater (FSW) to remove unassociated bacteria. Algal suspension was diluted with FSW. Isolated cells were washed 10 times with FSW, inoculated in F/10-Se medium and incubated under growth conditions of 12:12 photoperiod, 15°C and 80 μE m^{-2} in an algal incubator. Successful isolates were transferred in F/2-SE medium for maintenance. The *Pseudo-nitzschia* cultures were identified by morphology using light microscopy and genotyped by sequencing the 18S rRNA gene.

Pseudo-nitzschia genomic DNA was extracted with PowerSoil DNA Isolation Kit (MoBio Laboratories Inc., Solana Beach, CA, USA). *P. pungens* and *P. fraudelenta* were amplified with primer pairs 1360F (5′-GCGTTGAT/ATACGTCCCTGCC- 3′) and ITS055R (5′-CTCCTTGGTCCGTGTTTCAAGACGGG-3′), while *P. australis* and *P. multiseries* was amplified with primer pairs 18S-F (5′-CTGCGGAAGGATCATTACCACA-3′) and ITS055R using EconoTaq DNA Polymerase (Lucigen, Middleton, WI, USA) under the following PCR conditions: 94°C for 2 min, 30 cycles of 94°C for 1 min, 55°C for 1 min, and 72°C for 1.5 min and 72°C for 10 min extension. The products were sent to a service facility (Laragen Inc, Culver, CA, USA) for direct sequencing after labeling with the Big Dye Terminator with AmpliTaq FS Sequencing Kit (Applied Biosystems, Foster City, CA, USA) using the PCR primers as sequencing primers.

454 Sequence Data Processing

Short sequence reads (length <150 bp), low quality sequences (score <25; Huse et al., 2007) and any non-bacterial ribosome sequences and chimeras (Gontcharova et al., 2010) were removed prior to sequence analysis using Quantitative Insights Into Microbial Ecology (QIIME 1.8) pipeline (Caporaso et al., 2010b). Uclust (Edgar, 2010) was used in picking operational taxonomic units (OTUs) based on clustering sequences at 97% similarity. Representative sequences were aligned using Pynast (Caporaso et al., 2010a) using Greengenes core alignment as a reference (DeSantis et al., 2006). OTUs were assigned based on RDP classifier 2.2 (Wang et al., 2007), while the assignment of abundant bacterial taxon at the genus level was performed using BLAST [Altschul et al., 1990, *E*-value 10_20 (megablast only); minimum coverage 97%; minimum pairwise identity 90–97%]. Singletons and chloroplast sequences were filtered from the OTU table prior to bacterial diversity analyses. A phylogenetic tree of the OTUs was generated and viewed with Fast Tree 2.1.3 (Price et al., 2010).

The raw sequencing reads have been deposited at the NCBI Short Read Archive under BioProject ID PRJNA329303 with the following BioSample accession numbers: SAMN05410841 (Tow_

11.17.10), SAMN05410842 (Tow_12.01.10), SAMN0541084 (Tow_12.08.10), SAMN05410844 (Tow_12.15.10), SAMN054 10845 (Tow_12.22.10), SAMN05410846 (Tow_03.16.11), SAMN 05410847 (Tow_03.23.11), SAMN05410848 (Tow_07.06.11), SAMN05410849 (Tow_07.13.11), SAMN05410850 (Tow_ 08.24.11), SAMN05410851 (Tow_08.31.11).

Statistical Analysis

Correlation tests using multivariate non-parametric Spearman rank's correlation coefficient and Student's *t*-test were carried out using the software JMP 12.0.

RESULTS

Phytoplankton Community at Different Phases of *Pseudo-nitzschia* Bloom

Opportunistic sampling was done in Santa Cruz Municipal Wharf during the occurrence of *Pseudo-nitzschia* bloom. In mid-November 2010, phytoplankton diversity was high with the community being co-dominated by *Pseudo-nitzschia*, *Prorocentrum* and *Ceratium* (**Figure 1**). The assemblage changed into mostly *Pseudo-nitzschia* as the massive bloom progressed for 4 weeks. At the end of the bloom at week 5, there was an equal presence between *Pseudo-nitzschia* and dinoflagellates. Single algal cell isolations followed by genotyping indicated that *P. fraudulenta* dominated the *Pseudo-nitzschia* community and FISH probing and counting indicated that *P. australis* were also present in small number (**Figure 2C**).

In 2011, an early spring bloom of *P. australis* occurred in mid-March, but this bloom did not last as the population of the dinoflagellate *Ceratium* co-dominated the following weeks. In July 2011, a small bloom of *P. australis* was seen together with *Chaetoceros* and *Eucampia,* but noticeably decreased the following weeks and was replaced by higher diversity of phytoplankton with the co-dominance of *Guinardia*, *Chaetoceros* and *Eucampia*. In August 2011, a massive *P. australis* bloom occurred that lasted for 3 weeks. The algal community shifted and co-dominated both by the dinoflagellates *Protoperidinium* and *P. australis* during the fourth week, but phytoplankton biomass has decreased. *P. australis* were the dominant *Pseudo-nitzschia* species in 2011 (**Figure 2C**), with a small number of *P. multiseries* (3450 cells/ L) seen on March 23, 2011. Chlorophyll levels for the data gathered during opportunistic sampling showed that overall phytoplankton biomass range from 2.8 to 11.7 mg m^{-3}, with the highest chlorophyll level observed in 2010 during the bloom dominated by *P. fraudulenta*, where positive correlation existed (Spearman rho $= 0.76$, $p < 0.006$). Temperature range during late Fall 2010 sampling was between 11–14°C, while it was 12°C during Spring 2011 and 14–15°C in the Summer 2011. There was no correlation seen between temperature and chlorophyll level, or between temperature and total *Pseudo-nitzschia* cells, *Pseudo-nitzschia* species or DA. Additionally, a negative correlation of temperature with nitrate was seen (Spearman rho $= -0.84$, $p < 0.001$).

Nutrients, *Pseudo-nitzschia* Number and DA Level Are De-coupled during *Pseudo-nitzschia* Algal Bloom

We looked at the correlation between nutrients and total *Pseudo-nitzschia* cell number and the presence of toxic *Pseudo-nitzschia* species (**Figure 2**). Interestingly, none of the nutrients (urea, ammonium, nitrate, phosphate, and silicate) were correlated with cell abundance of *Pseudo-nitzschia* in a natural bloom and the five nutrients did not show any correlation with *P. fraudulenta*, *P. australis*, *P. multiseries* cell numbers (data not shown). Notably, DA level was positively correlated only with *P. australis* cell numbers (Spearman rho $= 0.69$, $p < 0.02$) but not with total *Pseudo-nitzschia* number or with *P. fraudulenta* cell number, even though this low-toxin producing species was present in very high numbers in 2010 bloom (**Figures 2B,C**). Likewise, temperature did not show any correlation with total *Pseudo-nitzschia* cell numbers, *P. fraudulenta* or *P. australis* cell numbers or with any of the aforementioned parameters, except for nitrate, to which it showed negative correlation (Spearman rho $= -0.84$, $p < 0.001$).

High DA-Producing *P. australis* Negatively Affects Bacterial Diversity in Natural Bloom

A total of 83,284 clean 16S rDNA sequences was obtained from 11 samples belonging to four *Pseudo-nitzschia* bloom events captured at different bloom phases (before, during and at the decline phases in 2010 and during and at decline phases in 2011). These sequences were assigned into 4732 OTUs (>97% ID), but reduced to 2621 OTUs after removing singletons and chloroplast sequences. The remaining OTUs were analyzed for bacterial diversity in every sample. Statistical analysis indicated that there was no significant correlation between phytoplankton biomass (i.e., chlorophyll *a*) and bacterial diversity (measured as Observed number of OTUs, Phylogenetic diversity, Shannon and Chao indices) suggesting that total phytoplankton biomass did not influence bacterial diversity (**Table 1**).

We determined if bacterial diversity was specifically affected by the presence of *Pseudo-nitzschia* bloom. Although bacterial diversity was lower during *Pseudo-nitzschia* bloom (**Figure 3A**), comparison of four bacterial indices (calculated at 2000 sequences depth) between *Pseudo-nitzschia* bloom and no-bloom suggested that bacterial diversity was not significantly different between the two events (Student's *t*-test, $p > 0.05$). However, the correlation analysis at the *Pseudo-nitzschia* species level indicated that the presence of high DA-producing *P. australis* negatively affected bacterial diversity (**Table 1**). Bacterial diversity was generally lower when the *Pseudo-nitzschia* bloom was dominated by *P. australis* versus *P. fraudulenta* (**Figure 3B**). Because low DA-producing *P. fraudulenta* were only present in 2010, correlation analysis for *P. fraudulenta* number versus bacterial diversity was carried out on this small data set. We found that as *P. fraudulenta* increased in number, bacterial diversity also declined (**Table 1**). Also, closer inspection indicated that bacterial diversity was lower as DA accumulated, due to increasing number of *P. fraudulenta* and the combined presence of *P. australis*

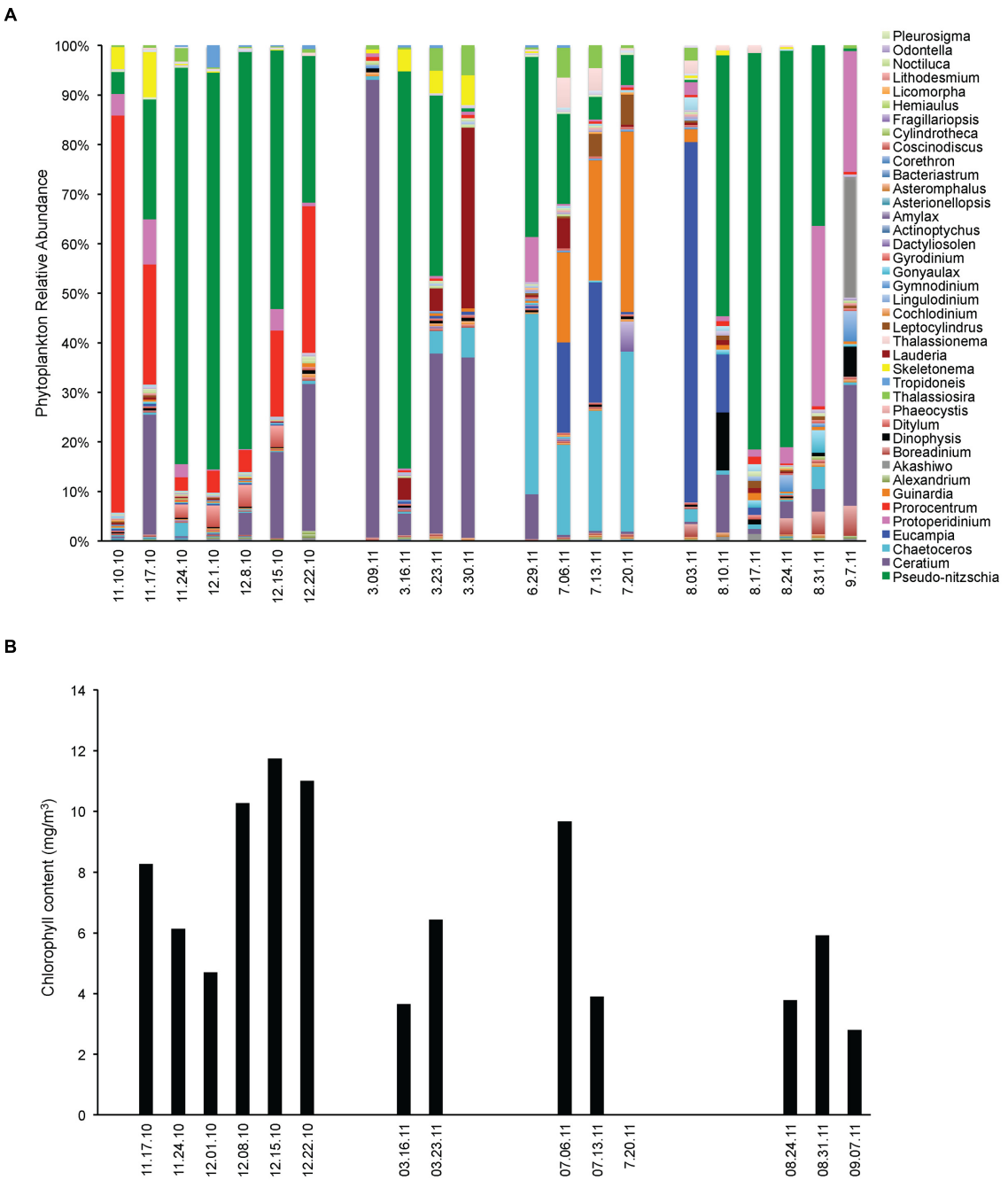

FIGURE 1 | Phytoplankton community assemblage before, during and after *Pseudo-nitzschia* bloom events in 2010 and 2011. (A) Phytoplankton relative abundance for each algal group assessed by microscopy. **(B)** Phytoplankton biomass expressed as total chlorophyll content.

(**Figures 3B** and **2C**). Bacterial diversity also negatively correlated with temperature while it positively correlated with phosphate and nitrate concentrations (**Table 1**).

Dominant Bacterial Groups Vary with Different *Pseudo-nitzschia* Bloom Events

We asked which bacterial groups dominate before, during or at the decline phase of *Pseudo-nitzschia* bloom and looked at other environmental variables that may facilitate their dominance. At least ten bacterial phyla (or class) were frequently found associating with phytoplankton during non-bloom events (**Figure 4**). However, during *Pseudo-nitzschia* bloom events, only a few bacterial phyla dominated the bacterial assemblages (**Figure 4A**) and these bacterial assemblages changed depending on the dominant *Pseudo-nitzschia* species that comprised the bloom. In 2010, Gamma-proteobacteria (65–85%) were prevalent

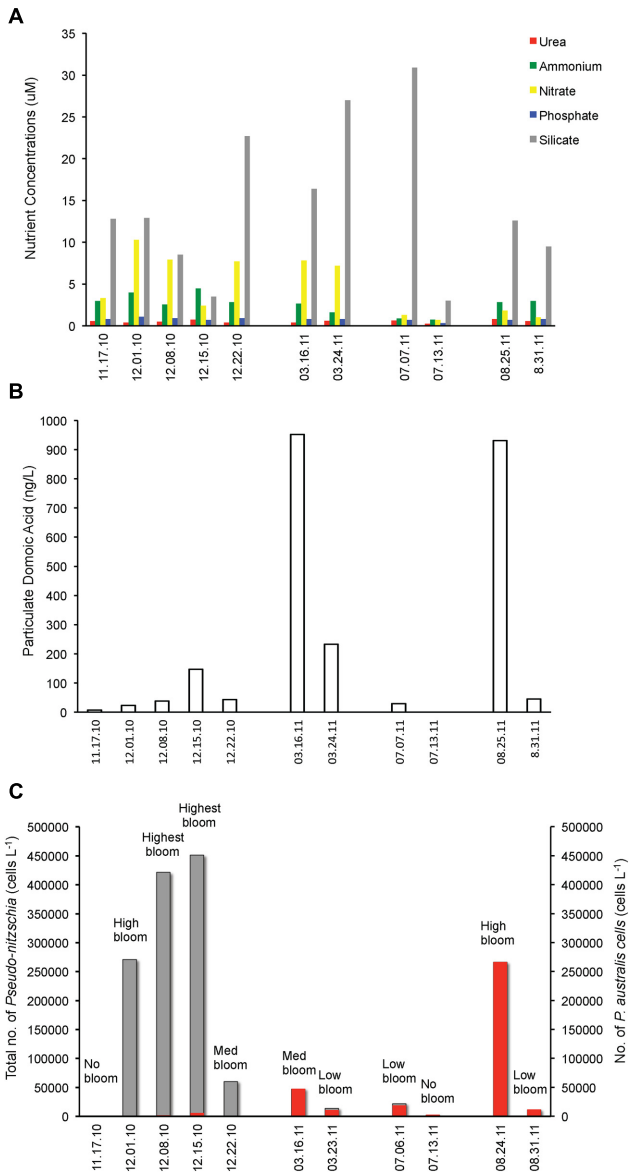

FIGURE 2 | *Pseudo-nitzschia* cell numbers, domoic acid (DA) and nutrient concentrations before, during and after *Pseudo-nitzschia* bloom events in 2010 and 2011. (A) Urea, ammonium, nitrate, phosphate, and silicate concentrations. **(B)** Particulate domoic acid content. **(C)** Total number of *Pseudo-nitzschia* cells (gray) superimposed with the *P. australis* cell numbers (red).

when a low-toxic species, *P. fraudulenta*, dominated the *Pseudo-nitzschia* populations (Spearman rho $= -0.79$, $p < 0.004$) and decreased in relative abundance during *P. australis* bloom (0–38%). These bacterial groups were also correlated with nitrate concentrations (Spearman rho $= -0.64$, $p < 0.035$). The Firmicutes phyla (20–95%) dominated in 2011 during high toxin blooms and were highly correlated with *P. australis* cell number (Spearman rho $= -0.72$, $p < 0.013$). Bacteroidetes (0–32%) and Epsilonbacteria (0–19%) groups were mostly present in the background but were not significantly correlated with the environmental conditions studied; Bacteroidetes, however, had higher relative abundance during non-Pn bloom events (14–32%) than during Pn bloom (0–9%; **Figure 4A**). Similarly, Alphaproteobacteria were also always present but their abundance was negatively correlated with the total number of *Pseudo-nitzschia* cells especially in the presence of high number of *P. fraudulenta* (1–3% vs. 15–20% during low or no Pn-bloom; Spearman rho $= -0.77$, $p < 0.006$). On the contrary, Fusobacteria (1–2%) were only present in 2010 bloom and positively correlated with *P. fraudulenta* abundance (Spearman rho $= -0.79$, $p < 0.004$). Bacterial groups that were present but in low relative abundance such as the Chloroflexi (0–3%), Acidobacteria (0–12%), and Betaproteobacteria (0–4%) groups were negatively correlated with temperature (Spearman rho $= -0.60$–0.79, $p < 0.05$). Actinobacteria (0–6%), another low abundant bacterial group,

TABLE 1 | Correlations between environmental variables and bacterial diversity as measured by four diversity indices.

	Spearman rho	*p*-level
Phyto biomass (chl *a*) vs. bacterial diversity		
No. of OTUs	0.40	0.223
Shannon index	0.08	0.811
Phylo. diversity index	0.40	0.223
Chao index	0.40	0.223
Total no. of Pn cells vs. bacterial diversity		
No. of OTUs	0.14	0.689
Shannon index	−0.13	0.709
Phylo. diversity index	0.15	0.670
Chao index	0.14	0.689
***P. australis* no. vs. bacterial diversity**		
No. of OTUs	−0.85	0.001
Shannon index	−0.62	0.043
Phylo. diversity index	−0.85	0.001
Chao index	−0.85	0.001
***P. fraudulenta* no. vs. bacterial diversity**		
No. of OTUs	−0.90	0.037
Shannon Index	−0.70	0.1881
Phylo. diversity index	−1.0	<0.0001
Chao index	−0.90	0.037
Temperature vs. bacterial diversity		
No. of OTUs	−0.65	0.032
Shannon index	−0.78	0.005
Phylo. diversity index	−0.55	0.077
Chao index	−0.65	0.032
Nitrate vs. bacterial diversity		
No. of OTUs	0.70	0.017
Shannon index	0.72	0.013
Phylo. diversity index	0.64	0.035
Chao index	0.70	0.017
Phosphate vs. bacterial diversity		
No. of OTUs	0.65	0.032
Shannon index	0.60	0.052
Phylo. diversity index	0.55	0.082
Chao index	0.65	0.032

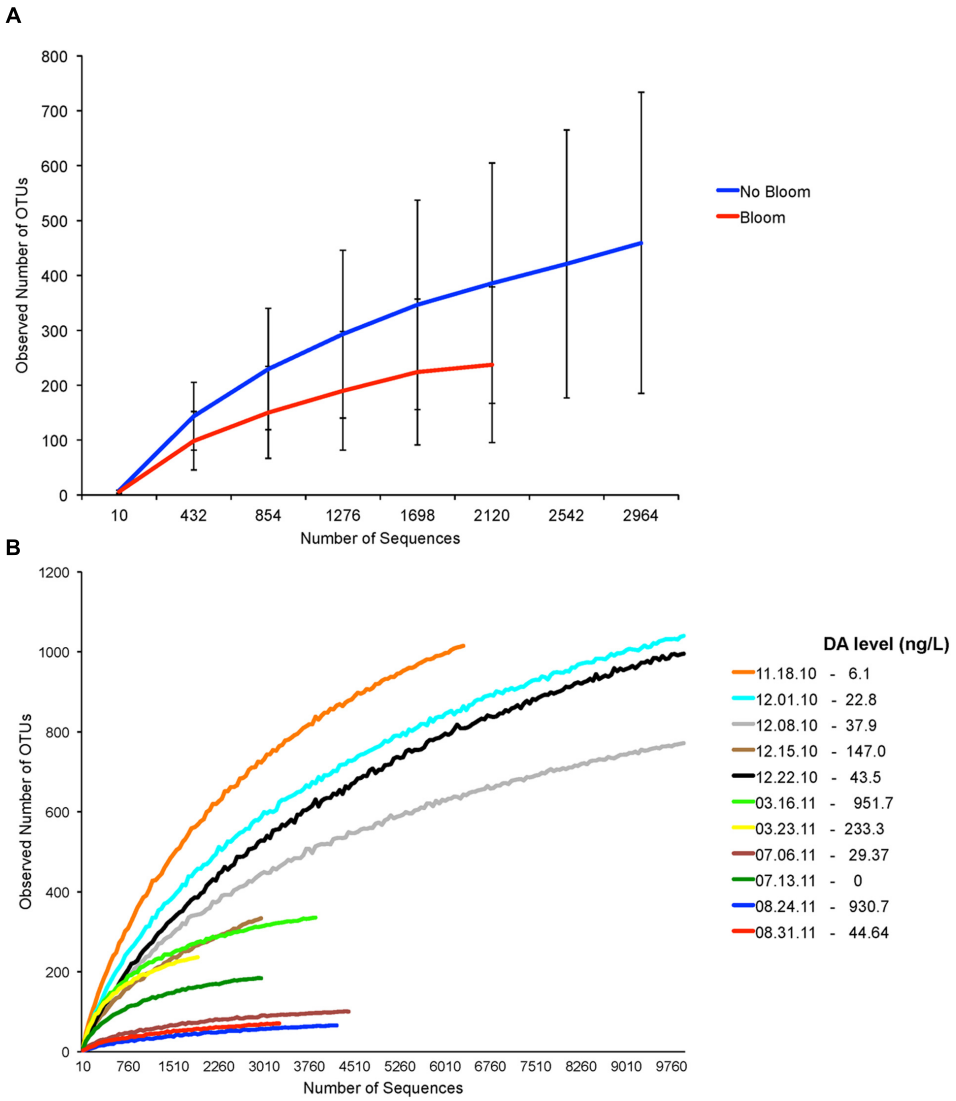

FIGURE 3 | Assessment of bacterial diversity based on number of Operational Taxonomic Units (OTUs) from samples before, during and after *Pseudo-nitzschia* bloom events in 2010 and 2011. (A) Rarefaction curves generated from samples with no *Pseudo-nitzschia* bloom and *Pseudo-nitzschia* bloom. **(B)** Individual rarefaction curves generated for each sample. Particulate domoic acid level is shown for each sample in the legend. Low-toxin producer *P. fraudulenta* dominated in 2010 bloom while the high-toxin producer *P. australis* dominated in 2011 blooms.

was only present when there was low number of *Pseudo-nitzschia* cells in the water (in 2011) (Spearman rho = 0.67, $p < 0.02$). The presence of the very low abundant group Verrucomicrobia (1–4%) and Planctomycetes (0–1%) were not correlated with any of the aforementioned environmental parameters.

At the genus level, *Vibrio* spp. was the Gamma-proteobacteria that dominated the *Pseudo-nitzschia* bloom in 2010 (**Figure 4B**). *Vibrio* increased in relative abundance (6–65%) as the bloom of *Pseudo-nitzschia* progressed into its peak, and positively correlated with the increase of *P. fraudulenta* cells, the abundant *Pseudo-nitzschia* species in 2010 bloom (Spearman rho = 0.8913, $p < 0.0002$). *Vibrio* was also positively influenced by phytoplankton biomass (chl) (Spearman rho = 0.78, $p < 0.004$) but it did not dominate in *P. australis* bloom in 2011. *Planococcus* spp. (12–93%), bacteria from the Firmicutes group, was positively correlated with the bloom of *P. australis* in 2011 (Spearman rho = 0.60, $p < 0.05$), where it dominated in three independent *P. australis* blooms. Temperature might have also significantly influenced its dominance (Spearman rho = 0.7426, $p < 0.009$).

Shewanella (1–27%), the third most abundant bacteria in the samples, is an Alpha-proteobacteria that was present in 2010 bloom and showed positive correlations with *P. fraudulenta* (Spearman rho = 0.90, $p < 0.0002$), together with nitrate and phosphate (Spearman rho = 0.84 and 0.71, $p < 0.01$). *Erythrobacter* (0–8%), another Alpha-proteobacteria, was present only in 2011 blooms and was negatively correlated with nitrate and ammonium (Spearman rho = −0.78 and −0.68, $p < 0.03$).

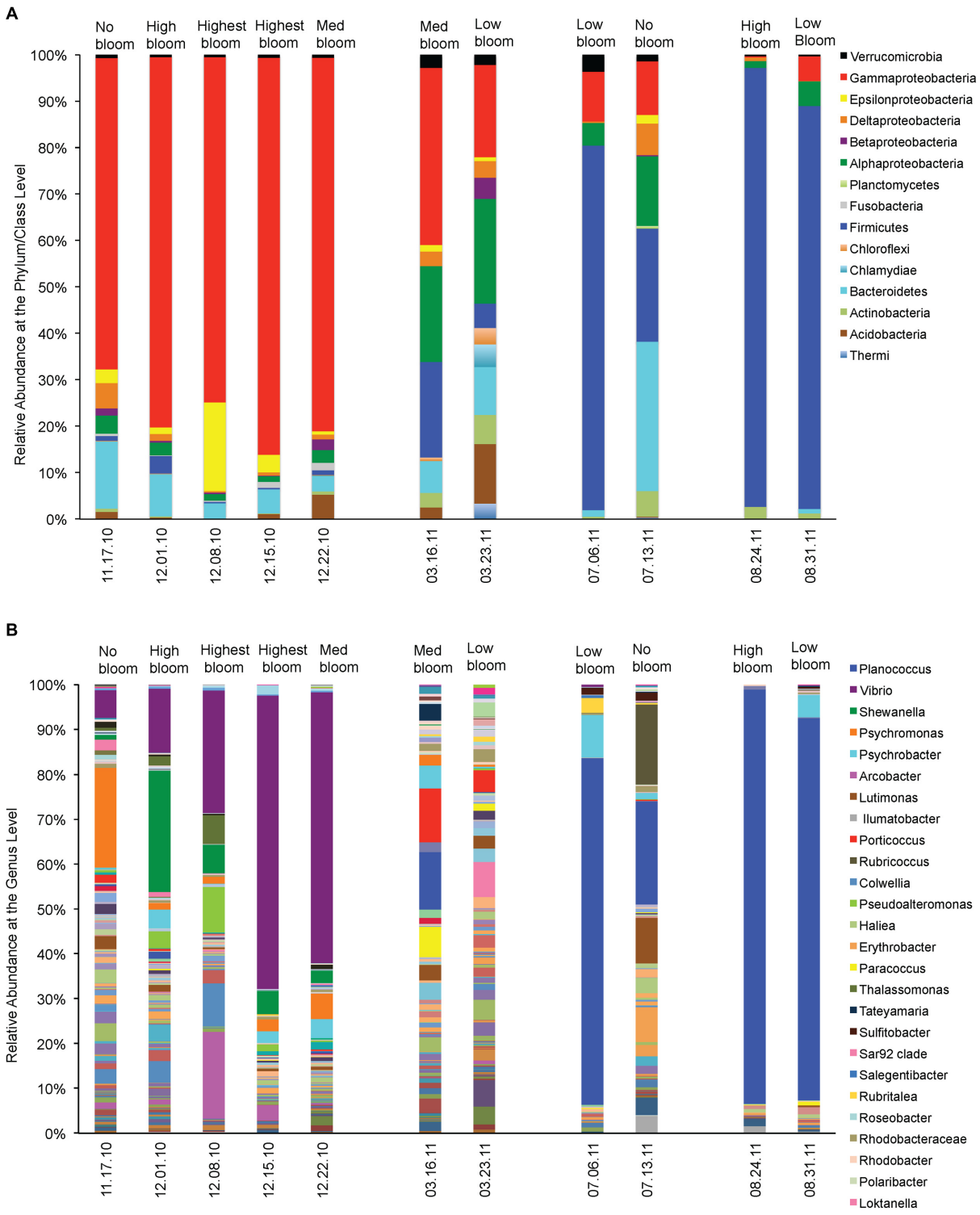

FIGURE 4 | Relative abundances of phytoplankton-associated bacteria before, during and after *Pseudo-nitzschia* bloom events in 2010 and 2011. **(A)** Relative abundance of bacteria at the phylum/ class level. **(B)** Relative abundance of bacteria at the Genus level.

The abundant Gamma-proteobacteria bacteria, *Psychromonas* (1–21%), was mostly seen in 2010 and its presence was not significantly influenced by any of the environmental variable studied other than *P. fraudulenta* cell number (Spearman rho = 0.65, $p < 0.03$). *Psychrobacter* (0–9%), another Gamma-proteobacteria, was ubiquitous in many samples but was not specifically influenced by any of the environmental variables. The *Lutimonas* bacteria and other Flavobacteriaceae (0–10%) also did not show any correlations with any of the environmental variables. *Rubricoccus* (0–18%), another Bacteroidetes, showed positive correlation with temperature (Spearman rho = 0.62, $p < 0.04$). The Epsilonbacteria, *Arcobacter* (0.4–19%), was abundant in 2010 blooms and was positively correlated with *P. fraudulenta* and nitrate (Spearman rho = 0.85 and 0.67, $p < 0.02$, respectively).

DISCUSSION

This study followed phytoplankton-associated bacterial community composition and succession from four natural *Pseudo-nitzschia* blooms in the same biogeographical location sampled before, during and after bloom and looked at how harmful algal bloom species and phytotoxin, domoic acid, influence phytoplankton-associated bacterial communities. Our study showed that the composition of the bacterial communities is driven by the phytoplankton species that comprised the bloom, while some less-abundant bacterial genera are also driven by phytoplankton biomass, temperature and nutrients (specifically nitrate and phosphate). Two species of *Pseudo-nitzschia* were found to dominate in the four bloom events, with the low-DA producing *P. fraudulenta* dominating in late Fall 2010 bloom (with a mix of small numbers of *P. australis*), and the high-DA producing *P. australis* dominating in three blooms in the spring, mid-summer and late summer of 2011. The dominant bacterial group changed with the dominant algal species that comprised the algal bloom. Moreover, with each bloom phase shift (increasing or decreasing of *Pseudo-nitzschia* cell numbers), these dominant bacterial groups also followed the same trend with the algal shift, that is high *P. fraudulenta* or *P. australis* cell number also increased the abundance of the respective dominant bacterial group. In this study, our approach did not allow us to study the composition of the bacterial community associated to a specific algal species but rather from a community of phytoplankton species that was dominated by *Pseudo-nitzschia* during bloom events. The Gamma-proteobacteria *Vibrio* spp., for instance, increased in relative abundance as *P. fraudulenta* cells increased in number, while the Firmicutes bacteria, *Planoccocus* spp. decreased in abundance as *P. australis* decreased in abundance. *Vibrio* spp. are known to associate with phytoplankton and zooplankton (Tamplin et al., 1990; Hsieh et al., 2007; Main et al., 2015) while *Planococcus* spp. are often isolated from *Pseudo-nitzschia* and are reported to be members of *Pseudo-nitzschia* microbiome (Sison-Mangus et al., 2014).

We also observed that when *P. australis* were replaced or co-dominated by other diatoms (*Chaetoceros*, *Eucampia*) or dinoflagellates (*Guinardia*, *Protoperidinium*), the bacteria *Planococcus* spp. was also replaced or co-dominated by the abundance of other bacterial groups from Bacteroidetes, Gamma- and Alpha-proteobacteria. This suggests that specific bacteria and phytoplankton groups can influence each other and their abundance does not only depend on phytoplankton biomass abundance during bloom but that the relationship can also be dictated by the diversity of algal species in the phytoplankton community. Rooney-Varga et al. (2005) have reported similar findings where the phytoplankton community is responsible for the significant amount of variability in the attached-bacterial community composition. Just like in their study, we did not see any correlation between bacterial diversity and phytoplankton biomass (i.e., chlorophyll *a*, **Table 1**), hence a closer look at the phytoplankton species composition during and after phytoplankton blooms is necessary if we want to understand the factors that facilitate the dominance of phytoplankton-associated bacterial groups and their role in the degradation of phytoplankton-derived organic matter.

Temperature, nitrate and phosphate seem to play a role in facilitating the abundance of some bacterial groups, but our data set is not enough to resolve if these abiotic factors can drive bacterial succession. Indeed, these physical factors affect the metabolism of phytoplankton and influences algal growth, which ultimately can influence phytoplankton-associated bacterial composition and diversity. In our study, we found no correlation between phytoplankton biomass, *Pseudo-nitzschia* cell number, nutrients (urea, ammonium, phosphate, silicate) and temperature, but nitrate and temperature did show negative correlation. Hence, a longer time series is suggested to give sufficient evidence to confirm the direct influence of these physical factors on bacterial community composition and succession.

Our current study showed that the neurotoxin domoic acid tend to limit bacterial diversity or bacterial OTU richness. For instance, the abundance of high-DA producing *P. australis* depressed bacterial diversity when it dominated the bloom in 2011. *P. fraudulenta*, a low-DA toxin producing *Pseudo-nitzschia*, also depressed bacterial diversity as DA increased when *P. fraudulenta* increased in cell number, but the bacteria diversity is not as low as that observed in *P. australis* bloom (**Figure 3B**). Interestingly, the presence of *P. australis* (albeit in small number), with *P. fraudulenta* in the December 15, 2010 bloom sample increased the DA level and drove the bacterial diversity further down (**Figure 3B**). These field-based results agreed with our past laboratory study, where we found a higher bacterial diversity harbored by cultured *P. fraudulenta* strains and a lower bacterial diversity in cultured *P. australis* strains (Sison-Mangus et al., 2014). This lends strong support to the idea that DA can structure *Pseudo-nitzschia*-associated bacterial communities. Domoic acid may act as a selective agent that can structure bacterial communities either by serving as a nutrient source for associated bacteria that can effectively assimilate DA or the toxin may act as deterrent to other associative bacteria. Previously, domoic acid has been hypothesized to be anti-bacterial (Bates et al., 1995) but concrete evidence is currently lacking to support this hypothesis.

Current efforts are now focused on understanding which bacterial groups can degrade various types of phytoplankton-derived organic matter. The pervading principle is that bacterial diversity and composition is largely driven by the availability of organic material from phytoplankton biomass, and the bacteria that can degrade this copious amount of algal-derived organic material will get selected and proliferate in the marine environment. Landa et al. (2016), for instance, reported that bacterial groups traditionally known for being algal bloom-associated, have dominated the pool of enriched bacterial groups observed from artificially iron-induced phytoplankton blooms in the Southern Ocean. Recent studies have also looked at the genome of free-living bacteria that are dominant during phytoplankton bloom, which comprises mostly of Flavobacteriaceae, *Roseobacters* and Gamma-proteobacteria to determine their genetic capability of degrading phytoplankton-derived material (Teeling et al., 2012, 2016; Klindworth et al., 2014). We can use the same argument on the selection process undergone by bacterial groups that develop an associative lifestyle with phytoplankton. Associated bacteria are proximally at an advantage to readily access phytoplankton exudates when the algal host secretes them and can access the algal organic material for consumption once the host cell is dead, a niche filled by copiotrophic bacteria that may have led to the observation that attached bacteria are distinct and showed little to high diversity than free-living bacteria (Delong et al., 1993; Acinas et al., 1999; Mohit et al., 2014). Association of bacteria with phytoplankton can evolve into mutualistic partnership such as that observed between *Sulfitobacter* and *P. multiseries* (Amin et al., 2015) or to commensal-parasitic relationship between *Phaeobacter* and *Emiliania huxleyi* (Seyedsayamdost et al., 2011), or host-specificity between *Pseudo-nitzschia* and its microbiome (Sison-Mangus et al., 2014). To understand the evolution of attached lifestyle among phytoplankton-associated bacteria, comparative genome analysis complemented with physiological and biochemical approaches are inviting if we want to gain a mechanistic insight of their evolutionary strategy. Similarly, field-based studies complemented with laboratory manipulations are required to understand the various influences of associated bacteria on phytoplankton physiology such as those related to toxin production, organic material production and recycling and algal bloom formation.

AUTHOR CONTRIBUTIONS

MSM and SJ conceived the project. MSM and RK executed the project, MSM and SM did the data analysis. MSM, SJ, and RK wrote the paper.

FUNDING

The National Science Foundation OCE 1131770 to SJ supported this work. MSM would like to thank UC-PPFP for fellowship support during her postdoc. STEM Diversity Program funded SM. Collection of environmental data from the Santa Cruz Municipal Wharf was supported by Cal-PReEMPT with funding from the NOAA-MERHAB program (Grant no. NA04NOS4780239, MERHAB #194).

ACKNOWLEDGMENT

We gratefully thank Kendra Negrey for providing plankton tow samples and Keah Ying Lim for assistance with sample processing.

REFERENCES

Acinas, S. G., Anton, J., and Rodriguez-Valera, F. (1999). Diversity of free-living and attached bacteria in offshore western Mediterranean waters as depicted by analysis of genes encoding 16S rRNA. *Appl. Environ. Microbiol.* 65, 514–522.

Altschul, S. F., Gish, W., Miller, W., Myers, E. W., and Lipman, D. J. (1990). Basic local alignment search tool. *J. Mol. Biol.* 215, 403–410. doi: 10.1016/S0022-2836(05)80360-2

Amin, S. A., Green, D. H., Hart, M. C., Kupper, F. C., Sunda, W. G., and Carrano, C. J. (2009). Photolysis of iron-siderophore chelates promotes bacterial-algal mutualism. *Proc. Nat. Acad. Sci. U.S.A.* 106, 17071–17076. doi: 10.1073/pnas.0905512106

Amin, S. A., Hmelo, L. R., van Tol, H. M., Durham, B. P., Carlson, L. T., Heal, K. R., et al. (2015). Interaction and signalling between a cosmopolitan phytoplankton and associated bacteria. *Nature* 522, 98–101. doi: 10.1038/nature14488

Azam, F., Fenchel, T., Field, J. G., Gray, J. S., Meyerreil, L. A., and Thingstad, F. (1983). The ecological role of water-column microbes in the sea. *Mar. Ecol. Progr. Ser.* 10, 257–263. doi: 10.3354/meps010257

Bates, S. S., Douglas, D. J., Doucette, G. J., and Leger, C. (1995). Enhancement of domoic acid production by reintroducing bacteria to axenic cultures of the diatom *Pseudo-nitzschia* multiseries. *Nat. Toxins* 3, 428–435. doi: 10.1002/nt.2620030605

Bates, S. S., Garrison, D. L., and Horner, R. A. (1998). "Bloom dynamics and physiology of domoic acid-producing *Pseudo-nitzschia* species," in *Physiological Ecology of Harmfull Algal Blooms*, eds D. M. Anderson, A. D. Cembella, and G. M. Hallegraeff (Heidelberg: Springer-Verlag), 267–292.

Bidle, K. D., and Azam, F. (1999). Accelerated dissolution of diatom silica by marine bacterial assemblages. *Nature* 397, 508–512. doi: 10.1038/17351

Bjornsen, P. K. (1988). Phytoplankton exudation of organic matter: why do healthy cells do it. *Limnol. Oceanogr.* 33, 151–154. doi: 10.4319/lo.1988.33.1.0151

Buchan, A., LeCleir, G. R., Gulvik, C. A., and Gonzalez, J. M. (2014). Master recyclers: features and functions of bacteria associated with phytoplankton blooms. *Nat. Rev. Microbiol.* 12, 686–698. doi: 10.1038/nrmicro3326

Buck, K. R., Uttalcooke, L., Pilskaln, C. H., Roelke, D. L., Villac, M. C., Fryxell, G. A., et al. (1992). Autecology of the Diatom Pseudonitzschia-Australis, a domoic acid producer, from monterey bay, California. *Mar. Ecol. Prog. Ser.* 84, 293–302. doi: 10.3354/meps084293

Caporaso, J. G., Bittinger, K., Bushman, F. D., DeSantis, T. Z., Andersen, G. L., and Knight, R. (2010a). PyNAST: a flexible tool for aligning sequences to a template alignment. *Bioinformatics* 26, 266–267. doi: 10.1093/bioinformatics/btp636

Caporaso, J. G., Kuczynski, J., Stombaugh, J., Bittinger, K., Bushman, F. D., Costello, E. K., et al. (2010b). QIIME allows analysis of high-throughput community sequencing data. *Nat. Methods* 7, 335–336. doi: 10.1038/nmeth.f.303

Croft, M. T., Lawrence, A. D., Raux-Deery, E., Warren, M. J., and Smith, A. G. (2005). Algae acquire vitamin B12 through a symbiotic relationship with bacteria. *Nature* 438, 90–93. doi: 10.1038/nature04056

Delong, E. F., Franks, D. G., and Alldredge, A. L. (1993). Phylogenetic diversity of aggregate-attached vs free-living marine bacterial assemblages. *Limnol. Oceanogr.* 38, 924–934. doi: 10.4319/lo.1993.38.5.0924

DeSantis, T. Z., Hugenholtz, P., Larsen, N., Rojas, M., Brodie, E. L., Keller, K., et al. (2006). Greengenes, a chimera-checked 16S rRNA gene database and workbench compatible with ARB. *Appl. Environ. Microbiol.* 72, 5069–5072. doi: 10.1128/AEM.03006-05

Doucette, G. J., Kodama, M., Franca, S., and Gallacher, S. (1998). "Bacterial interactions with harmful algal bloom species: bloom ecology, toxigenesis, and cytology," in *Physiological Ecology of Harmful Algal Blooms. NATO ASI Series 41*, eds D. M. Anderson, A. D. Cembella, and G. M. Hallegraeff (Berlin: Springer), 619–647.

Edgar, R. C. (2010). Search and clustering orders of magnitude faster than BLAST. *Bioinformatics* 26, 2460–2461. doi: 10.1093/bioinformatics/btq461

Fischer, A. M., Ryan, J. P., Levesque, C., and Welschmeyer, N. (2014). Characterizing estuarine plume discharge into the coastal ocean using fatty acid biomarkers and pigment analysis. *Mar. Environ. Res.* 99, 106–116. doi: 10.1016/j.marenvres.2014.04.006

Gardes, A., Iversen, M. H., Grossart, H. P., Passow, U., and Ullrich, M. S. (2011). Diatom-associated bacteria are required for aggregation of *Thalassiosira weissflogii*. *ISME J.* 5, 436–445. doi: 10.1038/ismej.2010.145

Gontcharova, V., Youn, E., Wolcott, R. D., Hollister, E. B., Gentry, T. J., and Dowd, S. E. (2010). Black box chimera check (B2C2): a windows-based software for batch depletion of chimeras from bacterial 16S rRNA gene datasets. *Open Microbiol. J.* 4, 47–52. doi: 10.2174/1874285801004010047

Grossart, H. P., Levold, F., Allgaier, M., Simon, M., and Brinkhoff, T. (2005). Marine diatom species harbour distinct bacterial communities. *Environ. Microbiol.* 7, 860–873. doi: 10.1111/j.1462-2920.2005.00759.x

Hellebust, J. A. (1980). Citation classic – Excretion of some organic-compounds by marine-phytoplankton. *Agric. Biol. Environ. Sci.* 47:16.

Holmes, R. M., Aminot, A., Kérouel, R., Hooker, B. A. and Peterson, B. J., (1999). A simple and precise method for measuring ammonium in marine and freshwater ecosystems. *Can. J. Fish. Aquat. Sci.* 56, 1801–1808. doi: 10.1139/f99-128

Hsieh, J. L., Fries, J. S., and Noble, R. T. (2007). Vibrio and phytoplankton dynamics during the summer of 2004 in a eutrophying estuary. *Ecol. Appl.* 17, S102–S109. doi: 10.1890/05-1274.1

Huse, S. M., Huber, J. A., Morrison, H. G., Sogin, M. L., and Mark Welch, D. (2007). Accuracy and quality of massively parallel DNA pyrosequencing. *Genome Biol.* 8:R143. doi: 10.1186/gb-2007-8-7-r143

Kaczmarska, I., Ehrman, J. M., Bates, S. S., Green, D. H., Leger, C., and Harris, J. (2005). Diversity and distribution of epibiotic bacteria on *Pseudo-nitzschia* multiseries (Bacillariophyceae) in culture, and comparison with those on diatoms in native seawater. *Harmful Algae* 4, 725–741. doi: 10.1016/j.hal.2004.10.001

Klindworth, A., Mann, A. J., Huang, S., Wichels, A., Quast, C., Waldmann, J., et al. (2014). Diversity and activity of marine bacterioplankton during a diatom bloom in the North Sea assessed by total RNA and pyrotag sequencing. *Mar. Genomics* 18 (Pt. B), 185–192. doi: 10.1016/j.margen.2014.08.007

Knepel, K., and Bogren, K. (2002). *Determination of Orthophosphate by Flow Injection Analysis: Quikchemr Method 31-115-01-1-H*. Milwaukee, WI: Lachat Instruments, 14.

Kudela, R. M., and Chavez, F. P. (2004). The impact of coastal runoff on ocean color during an El Niño year in central California. *Deep Sea Res. Part II Top. Stud. Oceanogr.* 51, 1173–1185. doi: 10.1016/S0967-0645(04)00106-7

Kudela, R. M., Lane, J. Q., and Cochlan, W. P. (2008). The potential role of anthropogenically derived nitrogen in the growth of harmful algae in California, USA. *Harmful Algae* 8, 103–110. doi: 10.1016/j.hal.2008.08.019

Landa, M., Blain, S., Christaki, U., Monchy, S., and Obernosterer, I. (2016). Shifts in bacterial community composition associated with increased carbon cycling in a mosaic of phytoplankton blooms. *ISME J.* 10, 39–50. doi: 10.1038/ismej.2015.105

Lane, J. Q., Raimondi, P. T., and Kudela, R. M. (2009). Development of a logistic regression model for the prediction of toxigenic *Pseudo-nitzschia* blooms in Monterey Bay, California. *Mar. Ecol. Prog. Ser.* 383, 37–51. doi: 10.3354/meps07999

Lane, J. Q., Roddam, C. M., Langlois, G. W., and Kudela, R. M. (2010). Application of solid phase adsorption toxin tracking (SPATT) for field detection of the hydrophilic phycotoxins domoic acid and saxitoxin in coastal California. *Limnol. Oceanogr. Methods* 8, 645–660. doi: 10.4319/lom.2010.8.0645

Larsson, U., and Hagstrom, A. (1979). Phytoplankton exudate release as an energy-source for the growth of pelagic bacteria. *Mar. Biol.* 52, 199–206. doi: 10.1007/BF00398133

Main, C. R., Salvitti, L. R., Whereat, E. B., and Coyne, K. J. (2015). Community-level and species-specific associations between phytoplankton and particle-associated *Vibrio* species in Delaware's Inland Bays. *Appl. Environ. Microbiol.* 81, 5703–5713. doi: 10.1128/AEM.00580-15

Mayali, X., and Azam, F. (2004). Algicidal bacteria in the sea and their impact on algal blooms. *J. Eukaryot. Microbiol.* 51, 139–144. doi: 10.1111/j.1550-7408.2004.tb00538.x

Mayali, X., Franks, P. J. S., and Burton, R. S. (2011). Temporal attachment dynamics by distinct bacterial taxa during a dinoflagellate bloom. *Aquat. Microb. Ecol.* 63, 111–122. doi: 10.3354/ame01483

Miller, P. E., and Scholin, C. A. (1998). Identification and enumeration of cultured and wild *Pseudo-nitzschia* (Bacillariophyceae) using species-specific LSU rRNA-targeted fluorescent probes and filter-based whole cell hybridization. *J. Phycol.* 34, 371–382. doi: 10.1046/j.1529-8817.1998.340371.x

Mohit, V., Archambault, P., Toupoint, N., and Lovejoy, C. (2014). Phylogenetic differences in attached and free-living bacterial communities in a temperate coastal lagoon during summer, revealed via high-throughput 16S rRNA gene sequencing. *Appl. Environ. Microbiol.* 80, 2071–2083. doi: 10.1128/AEM.02916-13

Pennington, J. T., and Chavez, F. P. (2000). Seasonal fluctuations of temperature, salinity and primary production at station H3/M1 over 1989-1996 in Monterey Bay, California. *Deep Sea Res. Part II Top. Stud. Oceanogr.* 47, 947–973. doi: 10.1016/S0967-0645(99)00132-0

Price, M. N., Dehal, P. S., and Arkin, A. P. (2010). FastTree 2-approximately maximum-likelihood trees for large alignments. *PLoS ONE* 5:e9490. doi: 10.1371/journal.pone.0009490

Price, N. M., and Harrison, P. J. (1987). Comparison of methods for the analysis of dissolved urea in seawater. *Mar. Biol.* 94, 307–317. doi: 10.1007/BF00392945

Reitan, K. I., Rainuzzo, J. R, and Olsen, Y. (1994). Effect of nutrient limitation on fatty acid and lipid content of marine microalgae. *J. Phycol.* 30, 972–979. doi: 10.1111/j.0022-3646.1994.00972.x

Riemann, L., Steward, G. F., and Azam, F. (2000). Dynamics of bacterial community composition and activity during a mesocosm diatom bloom. *Appl. Environ. Microbiol.* 66, 578–587. doi: 10.1128/AEM.66.2.578-587.2000

Rooney-Varga, J. N., Giewat, M. W., Savin, M. C., Sood, S., LeGresley, M., and Martin, J. L. (2005). Links between phytoplankton and bacterial community dynamics in a coastal marine environment. *Microb. Ecol.* 49, 163–175. doi: 10.1007/s00248-003-1057-0

Schafer, H., Abbas, B., Witte, H., and Muyzer, G. (2002). Genetic diversity of 'satellite' bacteria present in cultures of marine diatoms. *FEMS Microbiol. Ecol.* 42, 25–35. doi: 10.1111/j.1574-6941.2002.tb00992.x

Scholin, C. A., Gulland, F., Doucette, G. J., Benson, S., Busman, M., Chavez, F. P., et al. (2000). Mortality of sea lions along the central California coast linked to a toxic diatom bloom. *Nature* 403, 80–84. doi: 10.1038/47481

Seyedsayamdost, M. R., Case, R. J., Kolter, R., and Clardy, J. (2011). The Jekyll-and-Hyde chemistry of *Phaeobacter* gallaeciensis. *Nat. Chem.* 3, 331–335. doi: 10.1038/nchem.1002

Sison-Mangus, M. P., Jiang, S., Tran, K. N., and Kudela, R. M. (2014). Host-specific adaptation governs the interaction of the marine diatom, *Pseudo-nitzschia* and their microbiota. *ISME J.* 8, 63–76. doi: 10.1038/ismej.2013.138

Skogsberg, T. (1936). Hydrography of Monterey Bay, California. Thermal conditions, 1929-1933. *Trans. Am. Philos. Soc.* 29, 1–152. doi: 10.2307/1005510

Skogsberg, T., and Phelps, A. (1946). Hydrography of Monterey Bay, California. Thermal conditions, part II (1934-1937). *Proc. Amer. Philos. Soc.* 90, 350–386.

Smith, D. C., Steward, G. F., Long, R. A., and Azam, F. (1995). Bacterial mediation of carbon fluxes during a diatom bloom in a mesocosm. *Deep Sea Res. Part II Top. Stud. Oceanogr.* 42, 75–97. doi: 10.1016/0967-0645(95)00005-B

Smith, P., and Bogren, K. (2001). *Determination of Nitrate and/or Nitrite in Brackish or Seawater by Flow Injection Analysis Colorimeter: Quickchem Method 31-107-04-1-E*. Milwaukee, WI: Lachat Instruments, 12.

Smriga, S., Fernandez, V. I., Mitchell, J. G., and Stocker, R. (2016). Chemotaxis toward phytoplankton drives organic matter partitioning among marine bacteria. *Proc. Natl. Acad. Sci. U.S.A.* 113, 1576–1581. doi: 10.1073/pnas.1512307113

Tamplin, M. L., Gauzens, A. L., Huq, A., Sack, D. A., and Colwell, R. R. (1990). Attachment of Vibrio-cholerae eerogroup-O1 to zooplankton and phytoplankton of Bangladesh Waters. *Appl. Environ. Microbiol.* 56, 1977–1980.

Teeling, H., Fuchs, B. M., Becher, D., Klockow, C., Gardebrecht, A., Bennke, C. M., et al. (2012). Substrate-controlled succession of marine bacterioplankton populations induced by a phytoplankton bloom. *Science* 336, 608–611. doi: 10.1126/science.1218344

Teeling, H., Fuchs, B. M., Bennke, C. M., Kruger, K., Chafee, M., Kappelmann, L., et al. (2016). Recurring patterns in bacterioplankton dynamics during coastal spring algae blooms. *Elife* 5:e11888. doi: 10.7554/eLife.11888

Wang, Q., Garrity, G. M., Tiedje, J. M., and Cole, J. R. (2007). Naive bayesian classifier for rapid assignment of rRNA sequences into the new bacterial taxonomy. *Appl. Environ. Microbiol.* 73, 5261–5267. doi: 10.1128/AEM.00062-07

Welschmeyer, N. A. (1994). Fluorometric analysis of chlorophyll a in the presence of chlorophyll b and pheopigments. *Limnol. Oceanogr.* 39, 1985–1992. doi: 10.4319/lo.1994.39.8.1985

Wyllie, J. G., and Lynn, R. J. (1971). Distribution of temperature and salinity of 10 meters, 1960-69 and mean temperatures, salinity and oxygen at 150 meters, 1950-1968 in the California current. *Calif. Coop. Ocean. Fish. Invest. Atlas* 15, 1–188.

Conflict of Interest Statement: The authors declare that the research was conducted in the absence of any commercial or financial relationships that could be construed as a potential conflict of interest.

frontiers in Microbiology

ORIGINAL RESEARCH
published: 22 March 2016
doi: 10.3389/fmicb.2016.00339

Identification of Associations between Bacterioplankton and Photosynthetic Picoeukaryotes in Coastal Waters

Hanna M. Farnelid[1,2], Kendra A. Turk-Kubo[1] and Jonathan P. Zehr[1]*

[1] Ocean Sciences Department, University of California at Santa Cruz, Santa Cruz, CA, USA, [2] Centre for Ecology and Evolution in Microbial Model Systems, Linnaeus University, Kalmar, Sweden

Photosynthetic picoeukaryotes are significant contributors to marine primary productivity. Associations between marine bacterioplankton and picoeukaryotes frequently occur and can have large biogeochemical impacts. We used flow cytometry to sort cells from seawater to identify non-eukaryotic phylotypes that are associated with photosynthetic picoeukaryotes. Samples were collected at the Santa Cruz wharf on Monterey Bay, CA, USA during summer and fall, 2014. The phylogeny of associated microbes was assessed through 16S rRNA gene amplicon clone and Illumina MiSeq libraries. The most frequently detected bacterioplankton phyla within the photosynthetic picoeukaryote sorts were Proteobacteria (*Alphaproteobacteria* and *Gammaproteobacteria*) and Bacteroidetes. Intriguingly, the presence of free-living bacterial genera in the photosynthetic picoeukaryote sorts could suggest that some of the photosynthetic picoeukaryotes were mixotrophs. However, the occurrence of bacterial sequences, which were not prevalent in the corresponding bulk seawater samples, indicates that there was also a selection for specific OTUs in association with photosynthetic picoeukaryotes suggesting specific functional associations. The results show that diverse bacterial phylotypes are found in association with photosynthetic picoeukaryotes. Taxonomic identification of these associations is a prerequisite for further characterizing and to elucidate their metabolic pathways and ecological functions.

Keywords: microbial associations, bacterivory, flow cytometry, photosynthetic picoeukaryotes, symbiosis

OPEN ACCESS

Edited by:
Xavier Mayali, Lawrence Livermore National Laboratory, USA

Reviewed by:
Cécile Lepère, Blaise Pascal University, France
Manuela Hartmann, National Oceanography Centre, UK
Michael Morando, University of Southern California, USA

****Correspondence:***
Hanna M. Farnelid
hannafarnelid@gmail.com

Specialty section:
This article was submitted to Aquatic Microbiology, a section of the journal Frontiers in Microbiology

Received: *30 December 2015*
Accepted: *03 March 2016*
Published: *22 March 2016*

Citation:
Farnelid HM, Turk-Kubo KA and Zehr JP (2016) Identification of Associations between Bacterioplankton and Photosynthetic Picoeukaryotes in Coastal Waters. Front. Microbiol. 7:339. doi: 10.3389/fmicb.2016.00339

INTRODUCTION

Marine ecosystems are comprised of networks of interacting organisms and marine microbes that are frequently associated (Anderson, 2014; Cooper and Smith, 2015). Interestingly, associated bacteria are often distinct from species or strains in the surrounding seawater (Goecke et al., 2013) suggesting that there is niche speciation and co-evolution in habitat-specific cell consortia. Phytoplankton–bacteria associations can range from commensal to mutualistic or parasitic, and bacterial associations are known to directly influence phytoplankton growth, reproduction, and mortality (Grossart and Simon, 2007; Sher et al., 2011). Bacteria may also colonize dying or dead phytoplankton or protists which provide a source of organic matter (Azam and Malfatti, 2007). Thereby, associations between marine microorganisms play an important role in the food web and can have large impacts on phytoplankton dynamics and biogeochemical cycling.

In the marine environment, the majority of phytoplankton cells are microscopic and unicellular. Consequently bacteria–phytoplankton associations are methodologically challenging to study. The phycosphere is a region in close proximity to phytoplankton cells assumed to be rich in organic matter that attracts free-living bacteria (Stocker, 2012). Although species-specific bacteria–phytoplankton associations have been described it remains difficult to determine the metabolic functions and exchange between associated cells (Sapp et al., 2007; Worden et al., 2015). Recently, single cell sorting has been used to identify associations between bacteria and individual diatom cells and picoeukaryotes (Yoon et al., 2011; Martinez-Garcia et al., 2012a; Baker and Kemp, 2014), providing increasing evidence of close cell-to-cell associations in marine ecosystems. In addition, links between the phylogeny and metabolic function of an organism may be identified (e.g., Stepanauskas and Sieracki, 2007; Swan et al., 2011) which will be important for characterizing bacteria–phytoplankton interactions.

Photosynthetic picoeukaryotes are significant contributors to phytoplankton biomass and primary production (Worden et al., 2004; Jardillier et al., 2010). Interestingly, an increasing number of studies have demonstrated that photosynthetic picoeukaryotes can be mixotrophs (González et al., 1993; Zubkov and Tarran, 2008; Sanders and Gast, 2012; Hartmann et al., 2013; McKie-Krisberg and Sanders, 2014). With such trophic flexibility, photosynthetic picoeukaryotes have the potential to dominate both primary production and control bacterioplankton abundances in diverse marine ecosystems (Hartmann et al., 2012; McKie-Krisberg and Sanders, 2014). The recent discovery of a symbiosis between a photosynthetic picoeukaryote and the nitrogen-fixing cyanobacterium *Atelocyanobacterium thalassa* (UCYN-A; Thompson et al., 2012), contributing significantly to global nitrogen fixation (Montoya et al., 2004), suggests that associations with photosynthetic picoeukaryotes may also be important in key biogeochemical processes.

In this study, we aimed to determine if there were associations between bacterioplankton and photosynthetic picoeukaryotes. Seawater samples were collected from the Santa Cruz wharf on Monterey Bay, CA, USA, a coastal site with high photosynthetic picoeukaryote abundances. Using flow cytometry, populations of photosynthetic picoeukaryotes were sorted and analyzed. The associated bacterioplankton cells were characterized using 16S rRNA gene amplicon clone and Illumina MiSeq libraries. In addition, bacterial isolates from photosynthetic picoeukaryote populations were obtained, providing potential model systems and gene targets for future studies. The results describe the occurrence patterns and phylogenetic specificity of associated cells and provide knowledge of species associations forming the foundation of the marine ecosystem.

MATERIALS AND METHODS

Sampling

Surface seawater was collected in the morning from the Santa Cruz wharf (36.95 N, 122.02 W) in Monterey Bay, CA in summer and fall, 2014 using a 10 L bucket. Water was transferred into an acid washed sampling bottle, and transported immediately to University of California Santa Cruz (UCSC) for processing. As part of the Monterey Bay weekly phytoplankton sampling program, samples for phytoplankton community assessment and nutrient analyses were collected. Net plankton samples were collected with a 20 μm mesh net in the upper 3 m of the water column. The live net tow material was viewed under a dissecting microscope at 64× magnification. The Relative Abundance Index (RAI) of the most frequently observed genera of dinoflagellates and diatoms were recorded according to the system of the California Department of Public Health (CDPH) Phytoplankton Monitoring Program (Jester et al., 2009). For nutrient analyses, water was filtered onto 0.7 μm GF/F filters (Whatman, GE Healthcare, Little Chalfont, UK), placed into Falcon centrifuge tubes and stored at −20°C until processing. Nitrate, phosphate, and silicate were analyzed using a Lachat QuikChem 8500 Flow Injection Analyst System and Omnion 3.0 software (Lachat Instruments; Hach Company, Loveland, CO, USA). Ammonium and urea were analyzed fluorometrically as described by Gibble and Kudela (2014).

For DNA samples of bulk seawater, 300–500 ml seawater was pre-filtered through a 10 μm polycarbonate filter and subsequently though a 0.2 μm supor filter (Pall Corporation, New York, NY, USA) in 25 mm Swinnex filter holders (Millipore, Billerca, MA, USA) using a peristaltic pump. The filters were placed in sterile 1.5 ml cryovials containing 0.1 g autoclaved glass beads, flash frozen in liquid nitrogen and stored at −20°C until DNA extraction. Seawater samples to be sorted for catalyzed reporter deposition – fluorescence *in situ* hybridization (CARD-FISH) were collected, as described above, in fall 2015 (September 15 and October 27), but no complementary phytoplankton, nutrient or DNA samples were collected at this time.

DNA Extraction

Community DNA was extracted using the Qiagen Plant Minikit and QIAcube (Qiagen, Valencia, CA, USA). Briefly, 400 μl AP1 buffer (Qiagen Plant Minikit) was added to the sample tubes, followed by three freeze-thaw cycles using liquid nitrogen and a 65°C water bath (30 s and 2 min, respectively). The tubes were placed in a FastPrep-24 bead beater (MP Biomedicals, Irvine, CA, USA) and shaken at full speed for 2 min. The samples were Proteinase K treated for 1 h at 55°C with moderate shaking using 45 μl of Proteinase K (20 mg ml^{-1}; Qiagen) and treated with 4 μl RNase A and incubated for 10 min at 65°C. The filters were removed using sterile needles, 130 μl AP2 buffer (Qiagen Plant Minikit) was added to each tube, and samples were then vortexed and incubated on ice for 10 min. To pellet the precipitates and beads, the tubes were centrifuged for 5 min at 14 000 rpm at 4°C, and the supernatant was transferred to 2 ml sample tubes and placed in the QIAcube for further extraction steps according to the manufacturer's protocol. The samples were eluted using 100 μl AE buffer (Qiagen Plant Minikit) and concentrations were measured fluorometrically using Picogreen according to the manufacturer's protocol. Extracted DNA samples were stored at −20°C.

Flow Cytometry Sorting

Populations of photosynthetic picoeukaryotes were sorted using a BD Biosciences Influx Cell Sorter equipped with a small particle detector (BD Biosciences, San Jose, CA, USA) and a 488 nm Sapphire laser (Coherent, Santa Clara, CA, USA). The sorting was done using sterile filtered BioSure Sheath fluid diluted in ultrapure water to 1x concentration. Prior to flow cytometric sorting, the seawater samples were prefiltered using a 30 μm filter (Partec CellTrics, Swedesboro, NJ, USA) to prevent clogging of the 70 μm diameter nozzle. To minimize the risk of dislodging associations there was no concentration step and only fresh samples were processed. Data collection and sorting was triggered in the forward scatter (FSC) channel. The sorting gates were constructed in the BD FACS software using FSC as a proxy for cell size and red fluorescence (692–740 nm) as a proxy for chlorophyll *a* content. Photosynthetic picoeukaryotes were distinguished from *Synechococcus* populations using a NOT gate, deselecting cells with orange fluorescence (572–627 nm; i.e., phycoerythrin containing cells). For photosynthetic picoeukaryotes a smaller (P1, ∼ <3 μm beads) and a larger (P2, ∼ >3 μm beads) population was sorted (see **Figure 1** and Supplementary Figure 1). All sorts were collected in "1.0 Drop Purity" mode, and in combination with the small particle detection capabilities and triggering sorts on the FSC signal, this configuration is the optimal set-up for ensuring a low probability of co-sorting of unattached particles. Cell counts and cytograms were processed in FlowJo v10.0.7 (Tree Star). To minimize the risk of contamination, fluidic lines were regularly decontaminated with 1% bleach.

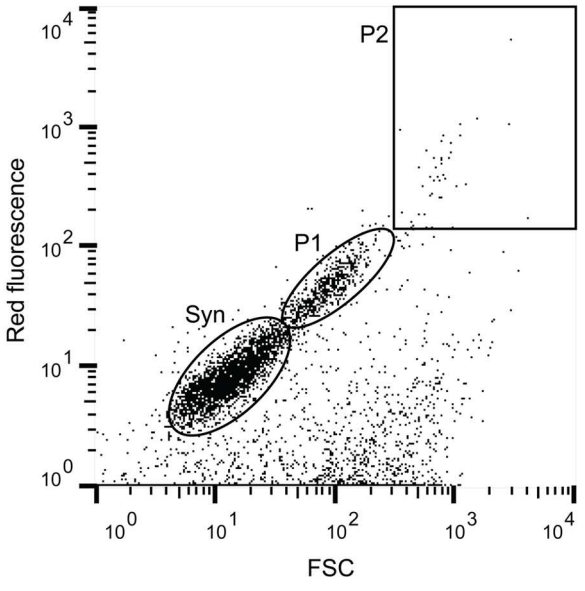

FIGURE 1 | Example of a flow cytogram with the cell populations that were targeted in this study. Red fluorescence was used as a proxy for chlorophyll *a* content and forward scatter (FSC) as a proxy for size. The indicated cell populations are Syn (*Synechococcus*) as defined by phycoerythrin content (Orange fluorescence), and two size fractions of photosynthetic picoeukaryotes, small (P1, ∼ <3 μm beads) and large (P2, ∼ >3 μm beads).

For sequencing, populations of 100–1,000 cells were sorted directly into sterile PCR tubes. To investigate if sheath fluid or the fluidic system of the cytometer was a source of contamination in the sort samples, sheath fluid was sampled using the test stream mode. For PCR applications, 2 μl aliquots of the sheath fluid, were collected on all but one sampling occasion, corresponding to the volume of approximately 2,000 sorted cells. Samples were stored at –80°C until further processing. To minimize cell loss, no additional DNA extraction step was added before PCR applications (Thompson et al., 2012). For CARD-FISH analyses, populations of 15,000 and 30,000 photosynthetic picoeukaryote cells (P1) were sorted into a PCR tube or onto a Poly-Prep slide (Sigma–Aldrich, St. Louis, MO, USA) and fixed in an equal volume of PBS-buffered 2% EM-grade paraformaldehyde (Electron Microscopy Sciences, Hatfield, PA, USA) for >1 h at room temperature in the dark. Poly-Prep slides were dried in a Bambino Hybridization Oven (Boekel Scientific, Feasterville-Trevose, PA, USA) at 28°C for ∼20 min and stored at –20°C until further processing. Samples in PCR tubes were frozen at –80°C until further processing.

16S rRNA Gene Clone Libraries

For all PCR applications extra precautions were taken to minimize contamination risks. Preparations took place in a UV hood in an amplicon free room using UV exposed tubes and 5 kD filtered ultrapure water. For clone libraries, a fragment of the 16S rRNA gene was amplified from sorted populations using the 27F (5′-AGA GTT TGA TCM TGG CTC AG-3′) or the 895F primer (5′-CRC CTG GGG AGT RCR G-3′) and 1492R (5′-GGT TAC CTT GTT ACG ACT T-3′). The 895F primer was previously designed to facilitate exploration of bacterial diversity in samples where DNA concentrations from cyanobacteria and plastids were high (Hodkinson and Lutzoni, 2010) and could thereby increase the proportion of non-Eukaryota sequences in the libraries. The composition of the 25 μl PCR mixture was 1x PCR buffer, 0.3 μl Invitrogen Platinum Taq (Invitrogen, Carlsbad, CA, USA), 2.5 mM $MgCl_2$, 200 μM dNTP mix, and 0.5 μM of the respective primers. The PCR conditions were as follows: 3 min initial denaturation at 95°C, followed by 30 cycles of 30 s denaturation at 95°C, annealing for 30 s at 55°C, and elongation for 60 s at 72°C, and ending with a final elongation for 7 min at 72°C. Samples with sheath fluid and negative controls with only ultrapure water added to the reactions were run together with the sorted samples. Neither the sheath fluid controls nor the negative controls produced amplicons that could be visualized using gel electrophoresis (1.2% agarose, 1 h, 86 V), whereas sorted populations produced strong amplification products.

The amplified PCR products were purified (QIAquick PCR purification; Qiagen) and cloned using the Invitrogen TOPO TA cloning kit for sequencing according to the manufacturer's protocol. Plasmid DNA was extracted in 96-well plates using the Montage Plasmid Miniprep Kit (EMD Millipore, Merck KGaA, Darmstadt, Germany) following manufacturer's instructions. Sanger sequencing was done at the UC Berkeley DNA Sequencing

Facility[1]. Low quality sequences were removed and the sequences were screened for chimeras using Decipher[2]. Sequences were deposited in GenBank under accession numbers KT906713–KT906977. For phylogenetic analyses of the sequences, clustering was done using CD-HIT-EST (Huang et al., 2010) with a 97% similarity level (Stackebrandt and Goebel, 1994). Sequences were taxonomically classified using the RDP classifier (Wang et al., 2007) and closest relatives were determined using NCBI Blastn. Neighbor-joining trees were constructed using MEGA6 using ClustalW for sequence alignment and neighbor-joining and maximum composite likelihood for distance estimation with 1,000 bootstrap replications (Tamura et al., 2013).

Isolates

To isolate bacteria from photosynthetic picoeukaryote sorts on agar plates, cells (P1) from the October 22 sample were sorted onto Zobell agar plates (5 g peptone, 1 g yeast extract, 15 g bacto agar in 800 ml 0.2 μm filtered Santa Cruz wharf seawater and 200 ml ultrapure water). To assess if live bacteria were present in the sheath fluid, plates were also inoculated with 20 puddles of sheath fluid that had passed through the cytometer (∼10 μl each, corresponding to the volume of ∼10,000 sorted cells). The plates were incubated at room temperature in the dark for a total of 4 weeks. As colonies grew, they were clean streaked onto fresh Zobell agar plates three times prior to inoculation into 5 ml Zobell medium (5 g peptone, 1 g yeast extract in 800 ml, 0.2 μm filtered, Santa Cruz wharf seawater and 200 ml ultrapure water). DNA from the isolates was extracted using the E.Z.N.A Tissue DNA kit (Omega Biotek, Norcross, GA, USA) according to manufacturer's protocol. 16S rRNA genes were amplified using the 27F and 1492R primers and the amplicons were bi-directionally sequenced. The sequence analyses were performed as described above and sequences were deposited in GenBank under accession numbers KT906978–KT907037.

High-Throughput 16S rRNA Gene Amplicon Sequence Libraries

The associated bacteria within the sorted photosynthetic picoeukaryote populations and the microbial composition of the bulk seawater that the populations were sorted from were further investigated using next generation sequencing (NGS). The dominance of chloroplast sequences in the libraries from the sorted samples was less of a concern due to the depth of total sequencing. The PCR was performed in 25 μl reaction volumes as described above but with 0.25 μM of each primer. The PCR conditions were as follows: 5 min initial denaturation at 95°C, followed by 30 cycles of 40 s, denaturation at 95°C, annealing for 40 s at 53°C and elongation for 60 s at 72°C, and ending with a final elongation for 7 min at 72°C. When working with samples with low cell abundances it is important to take extra precaution against background contamination as it could have a large impact on the signal from the sample itself. NGS amplicon sequencing is highly sensitive and consequently low detection of microbial contaminants is an unavoidable and a consistent feature (e.g., Laurence et al., 2014; Salter et al., 2014). Although the two negative (water only) PCR controls were not visible using agarose gel electrophoresis, these were included in the pool of amplicons with unique separate barcodes.

The widely used primer set 341F and 806R, targeting the V3–V4 variable region of the 16S rRNA gene of Bacteria (Caporaso et al., 2011; Herlemann et al., 2011), was used for amplification, with slight modifications. Briefly, genomic DNA extracted from sorted populations was used as template for PCR amplification using a targeted amplicon sequencing (TAS) approach, as described by Bybee et al. (2011) and Green et al. (2015). In the first of the two-stage amplification procedure, the template was amplified (25 cycles) using gene-specific primers containing previously described CS1 and CS2 linkers (Moonsamy et al., 2013). The amplicons were then submitted for sequencing to the DNA Services (DNAS) Facility at the University of Illinois at Chicago. At the DNAS Facility, a second PCR amplification (eight cycles) was performed to incorporate barcodes and sequencing adapters into the final PCR products. These amplifications were performed using the Fluidigm Access Array barcoding system (Fluidigm, South San Francisco, CA, USA). Primers synthesized by Fluidigm contained Illumina sequencing adapters, sample-specific barcodes (10 bases, with a minimum hamming distance of 3), and CS1 and CS2 linkers (see Green et al., 2015). The large hamming distance minimizes the risk of mis-assignment of reads to the wrong sample which can occur at low frequencies in NGS datasets (e.g., Kircher et al., 2012). Sequencing was performed on an Illumina MiSeq sequencer at the DNAS facility using standard V3 chemistry with paired-end, 300 base reads. Fluidigm sequencing primers, targeting the CS1 and CS2 linker regions, were used to initiate sequencing. Demultiplexing of reads was performed on instrument.

The resulting paired-end FASTQ files were merged using the software package PEAR (Zhang et al., 2014). The software package CLC genomics workbench (v7; CLC Bio, Qiagen, Boston, MA, USA) was used for primer, quality (Q20) and length trimming (sequences <390 bp were removed). A chimera check (USEARCH61; Edgar et al., 2011) was performed and putative chimeras were removed from the dataset. Subsequently, sequences were clustered and taxonomy was assigned with the Greengenes database (v13_8) as reference using the QIIME bioinformatics pipeline (Caporaso et al., 2010). For phylogenetic analyses, operational taxonomic units (OTUs) were defined based on 97% similarity clustering using CD-HIT-EST with >10 sequence reads and performed as described above. Mitochondrial sequences and sequences affiliated with species not associated with environmental studies as closest relatives were identified and removed manually from the dataset. A Bray-Curtis similarity matrix was calculated based on OTUs normalized to the total number of sequences for each sample using the software package Primer6 (Primer-E). The sequences have been submitted to NCBI Sequence Read Archive (SRA) with accession number SRP065334.

Microscopy

The presence of bacteria associated with picoeukaryotes was investigated visually using CARD-FISH as described by

[1]http://mcb.berkeley.edu/barker/dnaseq/

[2]www.decipher.cee.wisc.edu

Pernthaler et al. (2002) with modifications described below. The probes used in this study were the general bacteria probe, EUB338 (Amann et al., 1990) and GAM42a (Manz et al., 1992), targeting *Gammaproteobacteria*. Unspecific binding and/or background autofluorescence was examined using the non-sense probe non338 (Wallner et al., 1993) and no probe controls. Pre-sorted fixed samples were thawed and pipetted onto pre-coated poly-L-lysine slides (Poly-Prep slides, Sigma–Aldrich) and dried in a Bambino Hybridization Oven (Boekel Scientific) at 28°C for ∼20 min. As an initial test of the protocol, 15 μl culture of isolates 1, 2, 12 and 15 (**Table 2**) were fixed and mounted to slides as described above. The fixed cells were permeabilized in excess fresh lysozyme solution (10 mg ml^{-1}, 0.05 M EDTA, pH 8.0; 0.1 M Tris-HCl, pH 8.0) and the slides were incubated in a Thermo Brite™ Slide Hybridization System (StatSpin, Abbott Molecular, Des Plaines, IL, USA) at 37°C for 1 h. The cells were washed by pipetting cold ultrapure water to the slide followed by absolute ethanol at a ∼20° angle and air-dried. Endogenous peroxidase was inactivated using 0.01 M HCl and slides were incubated for 10 min at room temperature (Sekar et al., 2003). The cells were dehydrated in 96% ethanol and air-dried. For the hybridization (35°C, 3 h), horseradish peroxidase labeled probe working stocks (50 ng μl^{-1}; Biomers, Ulm, Germany) were diluted 1:100 in hybridization buffer (0.9 M NaCl, 20 mM Tris-HCl, 0.01% SDS, and 2% blocking reagent; Roche Diagnostic Boehringer, Basel, Switzerland) containing 55% formamide. The slides were washed (2 × 10 min) in pre-warmed washing buffer (13 mM NaCl, 20 mM Tris-HCl, 5 mM EDTA, and 0.01% SDS) in a Coplin jar placed in a 37°C water bath. After the washing, excess liquid was removed by dabbing the edge of the slide on Whatman paper and the slides were incubated in 1x PBS for 15 min at mild agitation and room temperature. Excess liquid was removed and 100 μl Cy3 TSA plus working solution (Perkin Elmer, Santa Clara, CA, USA) was pipetted onto the marked area of the slide. The slides were incubated for 3–10 min at room temperature in the dark. Slides were washed in 1x PBS and incubated again in 1x PBS for 15 min at mild agitation and room temperature followed by a rinse in cold ultrapure water and absolute ethanol as described above. The slides were air-dried, mounted with a drop of ProLong Diamond Antifade Mountant with DAPI (Molecular Probes, Eugene, OR, USA) and incubated at room temperature in the dark for 24 h.

Images were acquired on a Leica SP5 confocal microscope using a 63×/1.4 n.a. objective. The pixel size was set to 38.6 nm, oversampling Nyquist rates. A 405 nm laser was used to excite DAPI and light was collected between (415–485 nm). A 543 nm laser was used to excite Cy3 and light was collected between (555–625 nm). The scan rate was set between 10–100 Hz and eight line averaging was used. Gain was set for each channel to maximize dynamic range without saturating the signal. Cells were counted over an area of 32 mm^2, corresponding to the size of the sort puddle, on tiled images acquired on a Zeiss AxioImager Z2 using a 63×/1.4 n.a. objective. Images were analyzed in Imaris ×64 version 8.1.2 as follows. DAPI or Cy3 stained objects were segmented using the Surfaces tool with background subtraction thresholds set to 10.5 and 6.28 for DAPI and Cy3 respectively. Segmented objects that were above 6.00 μm^2 were included in the counts.

RESULTS

Environmental Data

The water temperature during both summer and fall ranged between ∼14–17°C, which is characteristic of each season in Monterey Bay (Pennington and Chavez, 2000). Nutrient availability was generally high but there was variability among the sampling days (**Table 1**). Diatoms, including *Proboscia*, *Chaetoceros,* and *Leptocylindrus* dominated the phytoplankton community during the summer sampling (Supplementary Figure 2). In contrast, during the fall sampling, dinoflagellates dominated the phytoplankton community. The potentially toxic *Pseudo-nitzschia*, *Alexandrium,* and *Dinophysis* were observed during both summer and fall but were not dominant on our sampling dates. Flow cytometry showed that cell abundances of *Synechococcus* (see **Figure 1** and Supplementary Figure 1) were the lowest on July 9, with 1.1×10^3 cells ml^{-1} and increased by one to two orders of magnitude in early October (**Table 1**). Compared to *Synechococcus*, the abundances of the photosynthetic picoeukaryote populations (P1 and P2; **Figure 1**) were less variable between the sampling dates and the abundances of the smaller population (P1) was generally one order of magnitude greater that the larger population (P2; **Table 1**).

TABLE 1 | Environmental data for each sampling date and cell abundances as determined by flow cytometry for Syn (*Synechococcus*), P1 (photosynthetic picoeukaryotes with size ∼ <3 μm beads) and P2 (photosynthetic picoeukaryotes with size ∼ >3 μm beads).

Date	Temp (°C)	NO_3 (μM)	PO_4 (μM)	SiO_3 (μM)	NH_4 (μM)	Urea (μM)	Syn cells ml^{-1}	P1 cells ml^{-1}	P2 cells ml^{-1}
June 18	14.9	1.04	0.24	4.31	0.89	0.31	na	na	na
July 2	14.1	0.05	0.06	1.64	0.82	0.20	na	na	na
July 9	15.6	1.78	0.89	23.07	5.37	0.63	1.1×10^3	2.8×10^4	3.2×10^3
October 8	17.1	0.04	0.17	7.42	1.16	0.36	1.7×10^5	2.3×10^4	1.1×10^4
October 15	16.0	2.68	0.95	9.11	5.58	2.14	5.9×10^4	1.1×10^4	1.6×10^3
October 22	14.9	2.46	0.56	8.43	5.00	1.62	4.9×10^4	1.3×10^4	1.5×10^3
October 29	15.3	1.93	1.42	14.39	4.04	0.85	4.2×10^4	6.6×10^3	6.1×10^2

na, data not available.

16S rRNA Gene Clone Libraries

To investigate the presence of associated cells within the sorted photosynthetic picoeukaryote populations, 16S rRNA gene clone libraries were analyzed. For amplicons of the 27F and 1492R primer pair, only 2.7% of the sequences were non-Eukaryota (not mitochondrial or chloroplast). However, using the 895F and 1492R primer pair, designed to not amplify cyanobacteria and plastids, 31% of the sequences were non-Eukaryota (Supplementary Table 1). For the P2 sorts, only one non-Eukaryota sequence, a gammaproteobacterium 99% identical to an isolate from marine seabed sediments (accession number HE803906), was recovered. Thus, for subsequent analysis we focused on the P1 population.

The most frequently detected phylum among the non-Eukaryota sequences was Proteobacteria including *Alphaproteobacteria* and *Gammaproteobacteria* (**Figure 2**). Several clusters were detected on multiple sampling dates (**Figure 2**). In the summer samples, sequences within the *Roseobacter* clade were found. Members of the *Roseobacter* clade are one of the most abundant groups of pelagic bacterioplankton

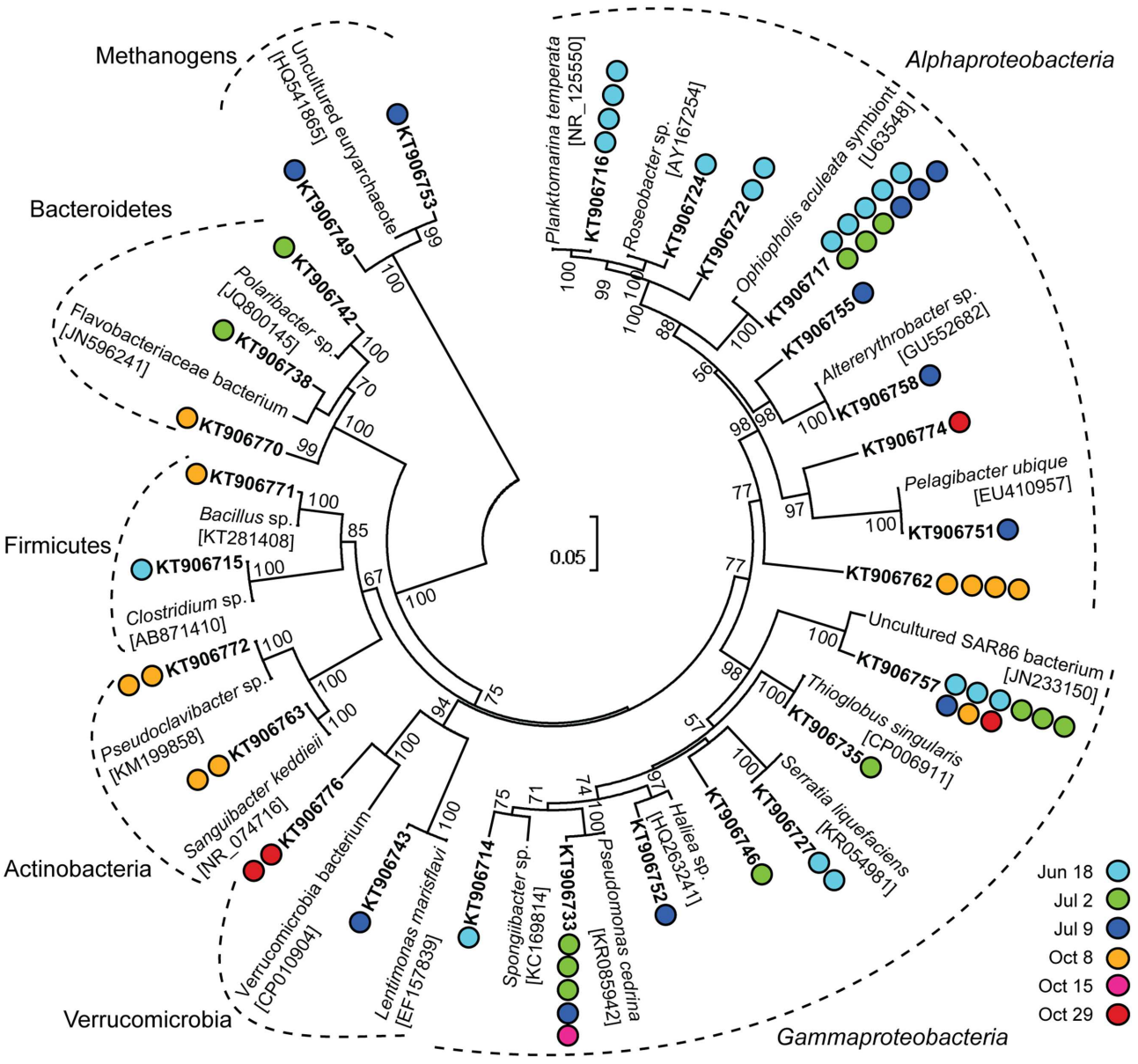

FIGURE 2 | Neighbor-joining phylogenetic tree of 97% similarity clustered non-Eukaryota sequences in 16S rRNA gene clone libraries from photosynthetic picoeukaryote cell sorts (P1, 1,000 cells) and their closest relatives. GenBank accession numbers are written in square brackets for the closest relatives and in bold for the representative clones. Colored circles indicate the number of sequences in each cluster and the corresponding date for each clone. Bootstrap values >50% (1,000 replicates) are indicated next to the node.

TABLE 2 | List of isolates from this study and their affiliations.

Isolate number	Sort population	Number of sorted cells or volume	Closest cultivated relative	% Identity	Accession number	Classification
1	P1	1 cell	*Pseudomonas* sp.	98	AB180241	*Gammaproteobacteria*
2	P1	50 cells	*Colwellia asteriadis*	98	NR_116385	*Gammaproteobacteria*
3	P1	50 cells	*Staphylococcus pasteuri*	99	KP267845	*Firmicutes*
4	P1	50 cells	*Alteromonas stellipolaris*	99	AJ295715	*Gammaproteobacteria*
5	P1	50 cells	*Colwellia psychrerythraea*	98	CP000083	*Gammaproteobacteria*
6	P1	50 cells	*Arthrobacter* sp.	99	FR667186	*Actinobacteria*
7	P1	50 cells	*Lentimonas marisflavi*	98	EF157839	*Verrucomicrobia*
8	P1	100 cells	*Arthrobacter oxydans*	99	KP235208	*Actinobacteria*
9	P1	100 cells	*Colwellia asteriadis*	98	NR_116385	*Gammaproteobacteria*
10	P1	100 cells	*Sulfitobacter* sp.	99	KC160637	*Alphaproteobacteria*
11	P1	100 cells	*Altererythrobacter* sp.	97	JN848799	*Alphaproteobacteria*
12	P1	100 cells	*Sulfitobacter* sp.	99	KC160637	*Alphaproteobacteria*
13	P1	100 cells	*Sulfitobacter* sp.	99	KC428714	*Alphaproteobacteria*
14	P1	100 cells	*Novosphingobium* sp.	96	AY690709	*Alphaproteobacteria*
15	P1	1,000 cells	*Pseudoalteromonas citrea*	99	NR_037073	*Gammaproteobacteria*
16	P1	1,000 cells	*Colwellia* sp.	98	JF825446	*Gammaproteobacteria*
17	Sheath fluid	~10 μl	*Ochrobactrum* sp.	99	KP410395	*Alphaproteobacteria*
18	Sheath fluid	~10 μl	*Achromobacter* sp.	99	KT321695	*Betaproteobacteria*
19	Sheath fluid	~10 μl	*Stenotrophomonas maltophilia*	99	GU254017	*Gammaproteobacteria*
20	Sheath fluid	~10 μl	*Stenotrophomonas maltophilia*	99	GU254017	*Gammaproteobacteria*
21	Sheath fluid	~10 μl	*Ochrobactrum* sp.	99	KP410395	*Alphaproteobacteria*
22	Sheath fluid	~10 μl	*Achromobacter* sp.	99	KT321695	*Betaproteobacteria*
23	Sheath fluid	~10 μl	*Achromobacter* sp.	99	KT321695	*Betaproteobacteria*

and have a central role in organic sulfur cycling (González et al., 1999). Within this clade, a cluster of sequences (KT906717; **Figure 2**) were 99% identical to a symbiont of the brittle star *Ophiopholis aculeata* (accession number U63548) and a Single Amplified Genome (SAG) from the Gulf of Maine (SAG ID MS024-1C; Stepanauskas and Sieracki, 2007). In the October 8 sample, an alphaproteobacterial cluster (KT906762; **Figure 2**) was 99% identical to a sequence from a photosynthetic picoeukaryote population sort from Station ALOHA in the Pacific Ocean (accession number EU187888; Zehr et al., 2008). The largest gammaproteobacterial cluster (KT906757; **Figure 2**) contained sequences from five sampling days and was related to SAR86, an abundant uncultivated marine bacterial clade that is metabolically streamlined (Dupont et al., 2012). In summary, the clone library results showed that sequences from associated bacterioplankton could be amplified from the sorted photosynthetic picoeukaryote populations.

Isolates

In total, 16 bacterial isolates representing 12 phylotypes (>97% similarity clustering) were obtained from photosynthetic picoeukaryote cell sorts (P1) onto agar plates (**Table 2**). Three alphaproteobacterial isolates were closely related (99% identical) to *Sulfitobacter* sp., a member of the *Roseobacter* clade (**Table 2**). Four gammaproteobacterial isolates were 98% identical to members of the genus *Colwellia* and clustered with isolates from the starfish *Asterias amurensis* (accession number NR_116385; Choi et al., 2010) and a symbiont of deep-sea *Adipicola pacifica* mussels living attached to whale falls (accession number AB539012; Fujiwara et al., 2010). Isolates affiliated with typical opportunistic (r-strategist) bacteria such as *Alteromonas* and *Pseudomonas* were also obtained. From the sheath fluid puddles, seven isolates were obtained. These included three phylotypes that belonged to genera that have previously been reported as contaminants (e.g., Salter et al., 2014).

High-Throughput 16S rRNA Gene Amplicon Sequence Libraries

16S rRNA gene amplicons from triplicate samples of 1,000 photosynthetic picoeukaryote cell sorts (P1) and the corresponding bulk seawater samples from five sampling occasions were sequenced (**Table 3**). The composition of OTUs among the triplicate sorts were more similar to each other compared to samples from a different day but the adjacent sampling dates October 15, October 22, and October 29 showed high Bray–Curtis similarity (>80%; **Figure 3A**). Most of the sequences in the photosynthetic picoeukaryote sort samples were plastid (**Figure 4**). A large cluster of OTUs were 96–100% identical to *Micromonas pusilla* and these sequences were most frequently detected in all sorted samples (accounting for between 75–96% of chloroplast sequences). *Micromonas*, a marine prasinophyte within the order Mamiellales, are known to be diverse and globally distributed (Guillou et al., 2004; Worden et al., 2009). *Bathycoccus prasinos* and *Ostreococcus*

TABLE 3 | Total number of sequences and OTUs (97% similarity) with >10 sequences obtained using Illumina MiSeq for each sample.

Date	Sample	Number of sequences	Number of OTUs	Number of non-Eukaryota sequences	Number of non-Eukaryota OTUs
July 9	P1, 1,000 cells	22,871	501	1,055	60
July 9	P1, 1,000 cells	36,107	558	1,577	67
July 9	P1, 1,000 cells	39,811	621	1,990	88
October 8	P1, 1,000 cells	60,253	735	17,485	171
October 8	P1, 1,000 cells	44,326	637	14,718	148
October 8	P1, 1,000 cells	49,950	676	21,439	195
October 15	P1, 1,000 cells	48,500	649	1,219	70
October 15	P1, 1,000 cells	46,421	671	1,279	82
October 15	P1, 1,000 cells	50,868	665	1,226	71
October 22	P1, 1,000 cells	51,827	644	618	44
October 22	P1, 1,000 cells	66,302	729	1,447	79
October 22	P1, 1,000 cells	81,184	761	2,202	103
October 29	P1, 1,000 cells	38,845	570	780	36
October 29	P1, 1,000 cells	54,227	647	773	37
October 29	P1, 1,000 cells	26,428	478	1,137	44
July 9	Seawater	70,141	923	63,683	812
October 8	Seawater	69,548	1,172	60,703	1,036
October 15	Seawater	56,095	1,156	51,657	1,035
October 22	Seawater	73,012	1,250	65,462	1,063
October 29	Seawater	63,590	1,120	60,092	1,041
–	Negative PCR control 1	42	5	9	4
–	Negative PCR control 2	49	14	25	12
Total		1,050,488	2,352	370,576	1,372

tauri OTUs were also detected in all samples. Notably, at lower relative abundances in the summer sample compared to the fall samples (**Figure 4**). In comparison to the sorted samples, the chloroplast sequences from bulk seawater were more diverse and not solely dominated by Chlorophyta. For example, in the bulk seawater samples, Haptophytes and Stramenopiles were present at high relative abundances (18–24%) while these phyla composed <10% in all of the sorted samples. The photosynthetic picoeukaryote populations were sorted based on chlorophyll *a* content and size. Thereby larger eukaryotes (∼ >3 μm beads) as well as heterotrophic picoeukaryotes would be excluded unless they had attached or ingested chlorophyll *a* containing cells. Thus, a difference in composition and a greater diversity of eukaryotic cells was expected in the bulk seawater samples compared to the sorted samples (**Figures 3A** and **4**).

The Illumina MiSeq sequencing confirmed the presence of non-Eukaryota cells among the sorted photosynthetic picoeukaryote cells. In total, 1,372 OTUs of non-Eukaryota origin were present in the dataset ranging from between 36 and 103 OTUs present in each sorted sample (**Table 3**). The most frequently detected phyla in the photosynthetic picoeukaryote sorts were Proteobacteria (*Alphaproteobacteria* and *Gammaproteobacteria*), Bacteroidetes, and Cyanobacteria, corresponding to the main phyla in the bulk seawater samples (**Figure 5**) but the OTU composition was different in the sorted samples compared to the bulk seawater samples (**Figure 3B**). In general, there was patchiness in the presence/abundance of non-Eukaryota OTUs between replicates even among the OTUs with highest relative abundances (**Figures 3B** and **6**). The patchiness between the biological replicates indicate that there is a large variation in the associated microbes and that larger population sorts will be required in order to reliably quantify the occurrences of specific taxa.

Among the cyanobacterial OTUs in photosynthetic picoeukaryote sorts, *Synechococcus*-like OTUs were most frequently detected (**Figure 6**). The *Synechococcus* OTU with the highest relative abundance was 98% identical to *Synechococcus* sp. WH 8020; a member of sub-cluster 5.1B clade I which has been described as a coastal and opportunist strain (Dufresne et al., 2008). In the October 8 sample, when the highest observed abundance of *Synechococcus* occurred in the bulk water samples (**Table 1**), there was a dominance of *Synechococcus* sequences in the sorted photosynthetic picoeukaryote populations (90.5% ± 0.3 of sequences; **Figure 5**). Thereby, they were more similar in OTU composition to the bulk seawater samples compared to the other sorted samples (**Figure 3B**). The separation of *Synechococcus* from the photosynthetic picoeukaryote population was done based on orange fluorescence. Depending on the definition of the sorting gates, some *Synechococcus* may have been co-sorted if the gate for the orange fluorescence was defined too stringently. However, if gates would be defined more broadly (i.e., excluding

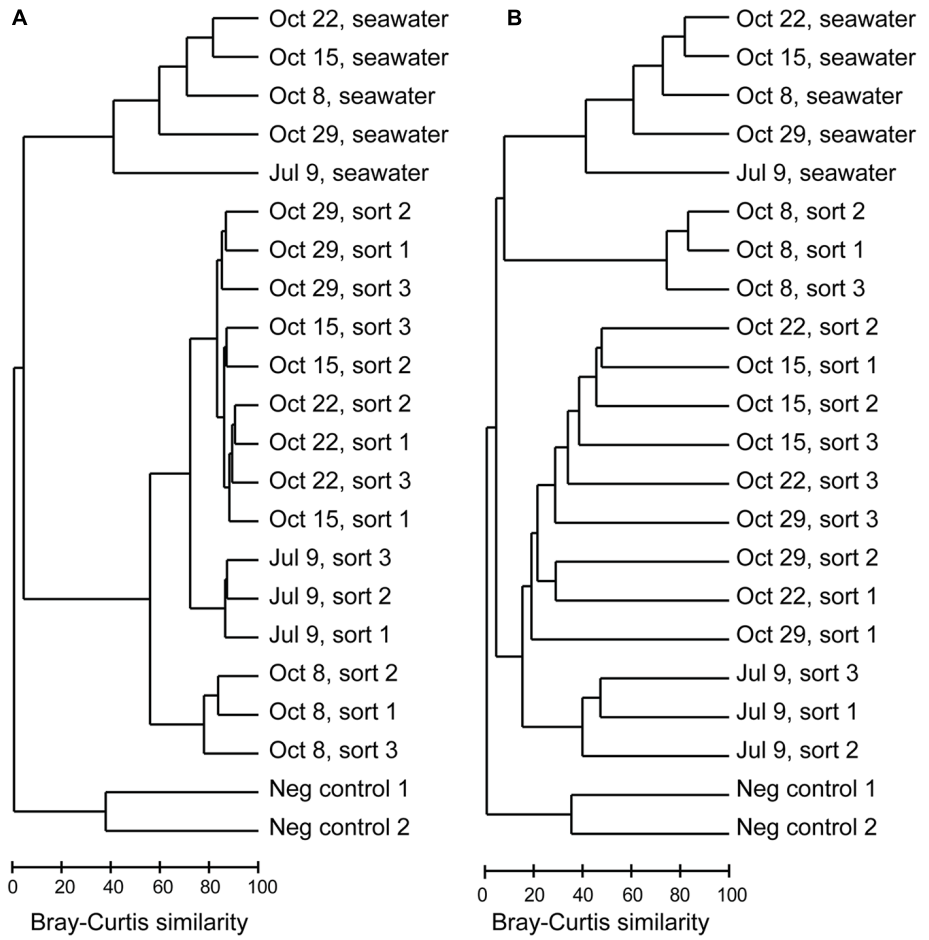

FIGURE 3 | Dendrograms based on Bray–Curtis similarity between Illumina MiSeq 16S rRNA gene libraries for (A) all OTUs, (B) non-Eukaryota OTUs.

all orange fluorescence cells) other phycoerythrin containing picoeukaryotic cells such as some Cryptophytes would also be excluded. Since the relative abundances of *Synechococcus* in the October 8 sorts were very high in comparison to other sampling dates, it cannot be dismissed that this may have resulted from not fully excluding the *Synechococcus* population from the photosynthetic picoeukaryote sorts using the NOT gate. The inclusion of these cells could potentially influence the composition of non-Eukaryota sequences in the October 8 sorts. However, because of the stringency used for the flow cytometry sorting we consider co-sorting events from other populations to be unlikely.

The *Pelagibacter*-like OTU (denovo6) was consistently present in all samples and was the second most frequently detected alphaproteobacterial OTU (**Figure 6**). The most frequently detected alphaproteobacterial OTU (denovo8658) was 98% identical to a symbiont of the brittle star *Ophiopholis aculeata* (accession number U63548), the same closest relative as for clone KT906717 which was detected in all summer samples (**Figure 2**). Notably, all isolates from photosynthetic picoeukaryote sorts in this study had closely related OTUs (94–99% identity) in the Illumina MiSeq dataset (Supplementary Table 2). For example, nine OTUs clustered within the *Roseobacter* clade and an OTU present in a sort from July 9 (denovo87, 34 sequences) was 96–98% identical to the *Sulfitobacter* sp. isolates (Supplementary Table 2) suggesting that this may be another interesting alphaproteobacterial target. Several gammaproteobacterial OTUs (e.g., denovo59) were consistently present in the triplicate sort samples from specific sampling dates even though the relative abundances in bulk seawater were low (**Figure 6**), making them interesting targets for future studies. The most frequently detected gammaproteobacterial OTU in the sorted samples (denovo10) was 100% identical to a group of 12 SAGs isolated from the Gulf of Maine (accession number JF488603; Martinez-Garcia et al., 2012b). In contrast to the clone libraries, OTUs within the SAR86-like cluster were present but showed no indication of being enriched in the sorted populations as they were not detected on several occasions, even when the relative abundance in bulk seawater was high (>1%; **Figure 6**).

The Bacteroidetes sequences were diverse and several OTUs were consistently present in July 9 sorts (**Figure 6**). The Bacteroidetes OTUs were dominated by *Flavobacteria* with

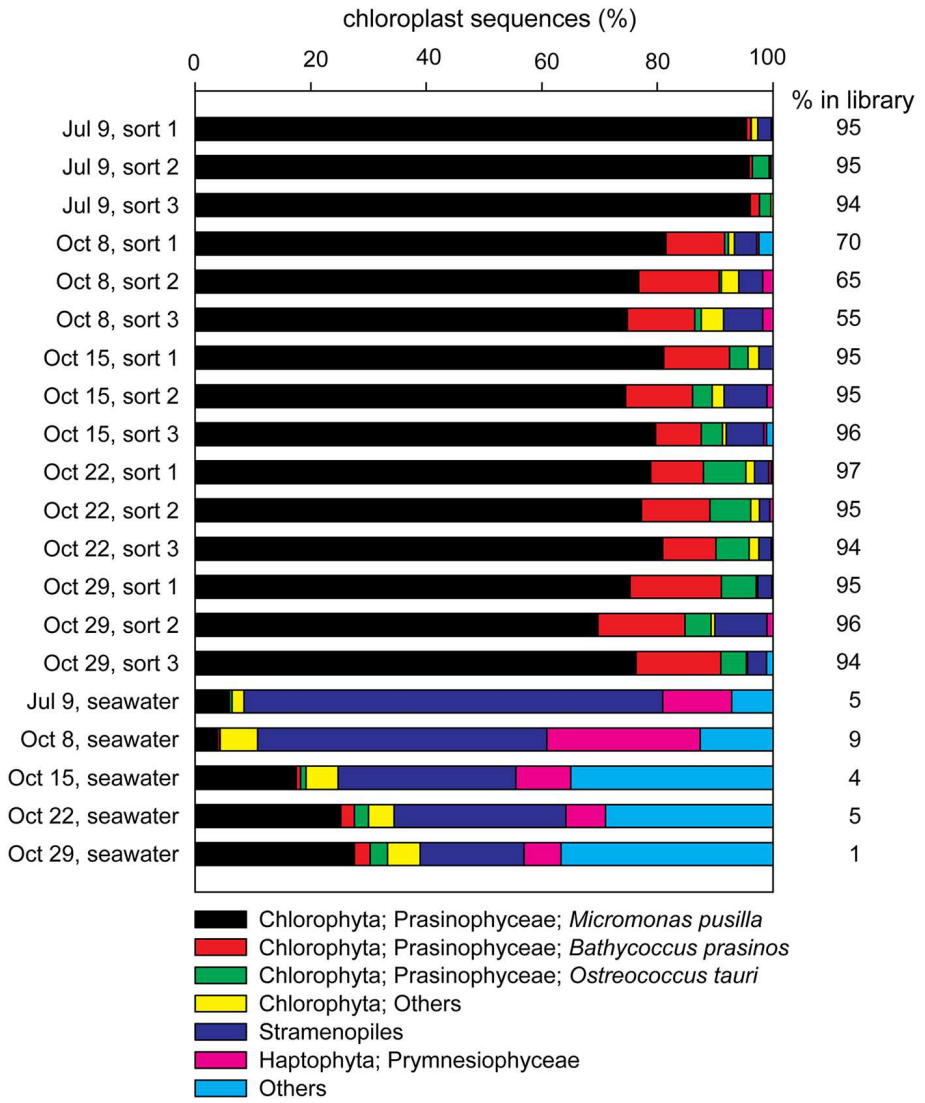

FIGURE 4 | Contributions of the most frequently occurring eukaryotic phyla among chloroplast sequences detected in each of the sorted photosynthetic picoeukaryote samples (1,000 P1 cells, triplicate samples) and the corresponding seawater samples (0.2–10 μm) for each sampling date. The percentage of chloroplast sequences within each library is indicated to the right of each bar.

the two most prominent OTUs (denovo9 and denovo15) 99% identical to SAGs isolated from the Gulf of Maine (accession numbers JF488529 and JF488568; Martinez-Garcia et al., 2012b). The only actinobacterial OTU with >100 sequences (denovo4) was 100% identical to a SAG from the same study (accession number JF488172; Martinez-Garcia et al., 2012b) and was detected in all of the October samples (**Figure 6**). Interestingly, the closest relatives of many of the other dominant OTUs also had high similarity to SAGs reported by Martinez-Garcia et al. (2012b; see closest relatives with accession numbers starting with JF488 in **Figure 6**).

Molecular analyses of samples with low DNA concentrations require extra precautions to rule out contamination. To investigate the possibility of reagent contamination two negative PCR controls were sequenced together with the samples on the Illumina MiSeq platform. The recovery of sequences from the negative PCR controls was poor (<100 sequences total, **Table 3**) and the overlap with the environmental samples was minimal (six OTUs; **Figure 3**). One sequence from the negative PCR control clustered with the most abundant *Synechococcus* sp. OTU (49,249 sequences total), which was likely the result of a technical mis-assignment associated with Illumina MiSeq sequencing. The other overlapping OTUs consisted of Proteobacteria and Actinobacteria and represented <0.05% of the total sequences. These OTUs were excluded from the taxonomic and phylogenetic analyses (**Figures 5** and **6**). Within the samples, eight clusters (corresponding to 0.1% of total sequences) were classified with sequences that were not similar

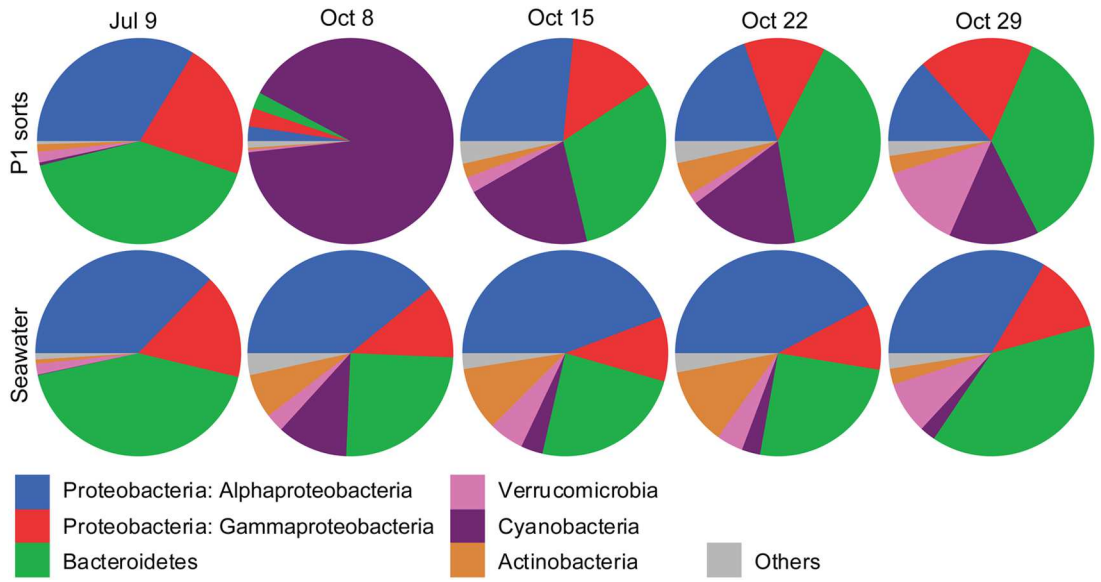

FIGURE 5 | Pie graphs showing the phylogenetic affiliations of non-Eukaryota 16S rRNA gene sequences in photosynthetic picoeukaryote sorts (P1, 1,000 cells), and bulk seawater (0.2–10 μm) from Illumina MiSeq libraries for each sampling date. The absolute numbers of sequences for the triplicate sort samples from each sampling date have been pooled. The colors for each phyla are indicated below the graphs.

to sequences found in environmental studies (e.g., *Mycoplasma* and *Staphylococcus*). The finding of such non-environmental sequences is not uncommon in studies using similar approaches (e.g., Baker and Kemp, 2014). Interestingly, the majority (94%) of these sequences were from one sample (October 22, sort 3) indicating that this was not a systematic problem. Notably, the isolates from sheath fluid did not cluster (<97% similarity) with any of the sequences in the Illumina MiSeq dataset suggesting that the sheath fluid and fluidic system were not a source of contamination in the sorted samples. Based on the limited overlap and few occurrences of negative control sequences, we conclude that putative contamination in our study was limited and the finding of diverse bacteria in association with photosynthetic picoeukaryote populations was not due to contamination.

Microscopy

For the CARD-FISH protocol, initial tests and protocol optimization was done using four isolates from this study. The EUB338 probe labeled cells from all cultures while the GAM42a probe only labeled the gammaproteobacterial cultures. The no probe and the non338 probe controls indicated that autofluorescence signal was low compared to the Cy3 signal and could easily be distinguished. The EUB338 probe labeled 43% of the sorted photosynthetic picoeukaryote cells (P1, 1,770 cells were counted in the Cy3 channel and 4,156 cells in the DAPI channel). The average cell diameter of the cells with both DAPI and Cy3 signal was 3.9 μm with a standard deviation of 2.6 μm and the median value of the cell diameter was 2.8 μm. Morphological cell differences were observed with a dominance of spherical, followed by crescent shaped cells. Since the EUB338 probe is known to hybridize with chloroplasts of several marine picoeukaryotes, e.g., *Micromonas*, *Bathycoccus*, and *Ostreococcus* (NCBI Blastn), it is likely that a large fraction of the observations were eukaryotic organelles (Supplementary Figure 3). In an attempt to visualize the associated bacteria, the GAM42a probe, a probe that is more specific and less likely to hybridize to picoeukaryotes (Biegala et al., 2005), was used. In total three slides were screened but no hybridization with the GAM42a probe was observed within the sorted photosynthetic picoeukaryote populations.

DISCUSSION

Associations between bacterioplankton and picoeukaryotes are thought to frequently occur in the marine environment, but are thus far poorly characterized. In this study, a combination of flow cytometry sorting and sequencing, as well as bacterial isolation on agar plates, was used to demonstrate that diverse bacterioplankton were present within photosynthetic picoeukaryote populations. Previous studies showed that the association between the nitrogen-fixing unicellular cyanobacterium UCYN-A and its prymnesiophyte host were easily dislodged if seawater samples were concentrated (Thompson et al., 2012). Therefore all sorts in this study were done using fresh, unpreserved seawater samples. In this study, extensive efforts were taken to minimize and identify methodological biases as well as putative contamination. The sequencing of negative PCR controls showed no indications of an external source of the detected non-Eukaryota sequences. Considering that the sorting was done in the 1.0 drop purity-mode, based on red fluorescence, a non-chlorophyll *a* cell can

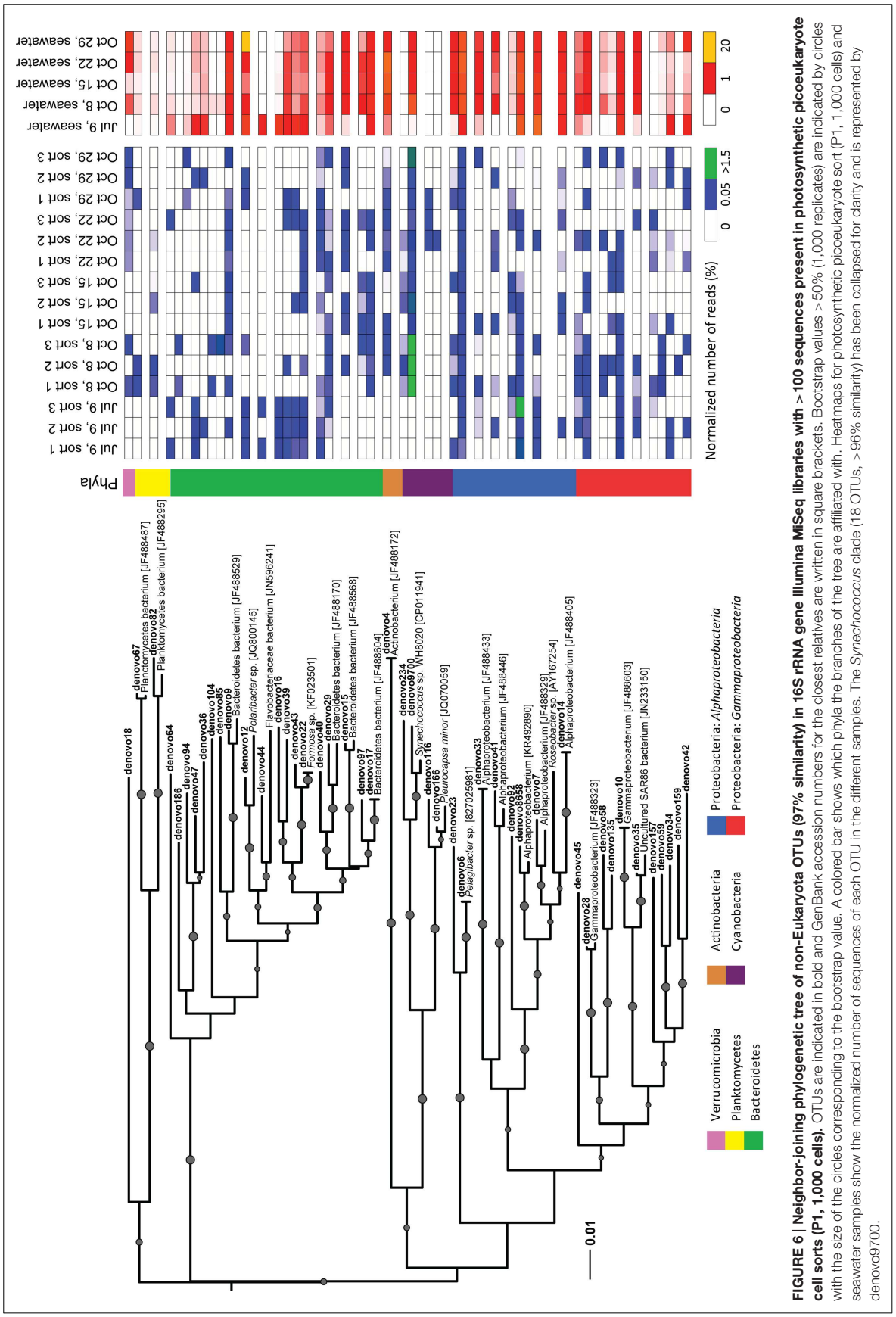

FIGURE 6 | Neighbor-joining phylogenetic tree of non-Eukaryota OTUs (97% similarity) in 16S rRNA gene Illumina MiSeq libraries with >100 sequences present in photosynthetic picoeukaryote cell sorts (P1, 1,000 cells). OTUs are indicated in bold and GenBank accession numbers for the closest relatives are written in square brackets. Bootstrap values >50% (1,000 replicates) are indicated by circles with the size of the circles corresponding to the bootstrap value. A colored bar shows which phyla the branches of the tree are affiliated with. Heatmaps for photosynthetic picoeukaryote sort (P1, 1,000 cells) and seawater samples show the normalized number of sequences of each OTU in the different samples. The *Synechococcus* clade (18 OTUs, >96% similarity) has been collapsed for clarity and is represented by denovo9700.

theoretically only be co-sorted if it is attached to or within a chlorophyll *a* containing cell. However, despite the strict sorting criteria used in this study, the complete absence of co-sorting of unattached bacteria cannot be certain.

As expected from a coastal site with high nitrate concentrations, the abundances of photosynthetic picoeukaryotes (P1) were high on all sampling occasions (**Table 1**). The most frequently occurring chloroplast sequences were affiliated with *Micromonas pusilla* but *Bathycoccus* and *Ostreococcus* were also detected (**Figure 4**), corresponding to the most significant picoeukaryotes in coastal areas (Massana, 2011). Interestingly, the bacterial OTUs with the highest relative abundances in the bulk seawater samples were also present in the photosynthetic picoeukaryote sort samples (**Figure 6**). Although we cannot rule out the possibility of these being a result of co-sorting, an intriguing possibility is that these dominating taxa in the free-living community could have been ingested through bacterivory. An increasing number of environmental studies suggest that mixotrophy may be widespread among photosynthetic picoeukaryotes (Zubkov and Tarran, 2008; Sanders and Gast, 2012; Hartmann et al., 2013). In a recent study, using a dual CARD-FISH protocol, Prymnesiophyceae, Chrysophyceae, and Pelagophyceae cells from the Atlantic Ocean showed internalization with *Prochlorococcus* and SAR11 cells (Hartmann et al., 2013). Hartmann et al. (2013) concluded that because *Prochlorococcus* or SAR11 are considered free-living genera, the presence of these cells inside the eukaryote cells indicated bacterivory. Bacterivory has also been demonstrated for a *Micromonas pusilla* culture (González et al., 1993) and a recent study suggests that *Micromonas* was selective for small size pray, represented by 0.5 μm microspheres, while larger microspheres (0.9 μm) were also ingested, albeit at a lower rate (McKie-Krisberg and Sanders, 2014). Thus, if bacterivory was widespread within these natural populations of photosynthetic picoeukaryotes it can be expected that grazing strategy and selectivity will affect the non-Eukaryota sequences present within the photosynthetic picoeukaryote sorts (Worden et al., 2015).

The composition of non-Eukaryota OTUs in the sorted samples was different from the bulk seawater samples (**Figure 3B**). With an exception of the October 8 sorts, which consisted of a dominating *Synechococcus* OTU (**Figure 5**, <20% Bray–Curtis similarity **Figure 3B**), the sorted samples had <10% Bray–Curtis similarity compared with the bulk seawater samples (**Figure 3B**) suggesting that specific phylotypes were enriched in the sorted populations and thereby may represent functional associations between bacteria and photosynthetic picoeukaryotes. Although the probability is low, the sequencing of several samples simultaneously may result in a mis-assignment of reads to the wrong sample (e.g., Kircher et al., 2012; Mitra et al., 2015). By limiting our phylogenetic analysis to OTUs with >100 sequences within the photosynthetic picoeukaryote sorts (**Figure 6**), we view such occurrences as unlikely to influence the findings of this study.

Similarly to what has been observed in a wide range of diatom–bacterial interactions (Amin et al., 2012), the most frequently detected bacterioplankton phyla within the sorted photosynthetic picoeukaryote populations were Proteobacteria (*Alpha-* and *Gammaproteobacteria*) and Bacteroidetes (**Figures 2** and **5**). *Gammaproteobacteria* and Bacteroidetes also predominated bacterial 16S rRNA gene sequences recovered from mixotrophic protist SAGs and *Gammaproteobacteria* were found to be more likely to be association with protists in comparison to the free bacterioplankton SAGs (Martinez-Garcia et al., 2012a). Although not directly comparable because of the different sequencing regions, the clone libraries in this study also suggest that Proteobacteria may be prevalent in association with photosynthetic picoeukaryotes. An interesting alphaproteobacterial cluster of clone sequences (KT906717) was observed in all summer samples (**Figure 2**) and the second most frequently detected alphaproteobacterial OTU (denovo8658; **Figure 6**) were both 98% identical to a bacterial symbiont of the brittle star *Ophiopholis aculeata* (accession number U63548). The re-occurrence of this phylotype and its high relative abundances in comparison to other non-Eukaryota OTUs within the sorted photosynthetic picoeukaryote populations suggests that it may be an interesting target for further characterization.

The composition of the non-Eukaryota phylotypes detected in the photosynthetic picoeukaryote populations was likely influenced by the design of this study. For example, by the definition of the sort gate, cells associated with larger photosynthetic picoeukaryotes were excluded since only the smaller size-fraction (∼ <3 μm beads) was examined. In addition, NGS sequencing of amplicons is associated with regular PCR biases which influence the observed community composition. In the Illumina MiSeq libraries, triplicate cell sorts from the same seawater samples were sequenced and the lack of replication between the samples was surprising (**Figure 6**). This is an indication that associated non-Eukaryota cells are likely of low abundance within the photosynthetic picoeukaryote populations and may be highly diverse. However, the re-occurrence of specific OTUs on different sampling days suggests that the associations with these phylotypes were prevalent. The different patterns of non-Eukaryota OTUs observed between bulk seawater and sorted photosynthetic picoeukaryote populations indicate that co-sorting plays a negligible role in this study. Furthermore, many of the OTUs detected in this study, distributed over different phyla, were most identical to sequences reported from SAGs from the Gulf of Maine (see accession numbers starting with JF488 in **Figure 6**; Martinez-Garcia et al., 2012a) rather than sequences reported from seawater studies which are numerically dominating in databases. This is an indication that flow-cytometry sorting and downstream molecular analysis more easily accesses parts of the microbial community which are not generally captured when bulk seawater samples are observed.

Some aquatic bacteria have complex lifestyles and may quickly alternate between free-living and associated stages, exploiting nutrient rich microenvironments in association with phytoplankton (Grossart, 2010). For example, dead phytoplankton cells may be quickly colonized and enzymatically degraded by bacteria (Azam and Malfatti, 2007). The high nutrient cultivation plates used in this study likely selected for bacteria that thrive under nutrient rich conditions. Interestingly, all of the isolates had closely related, but generally not numerically dominant, OTUs within the Illumina MiSeq libraries

(Supplementary Table 2). Thus indicating that bacteria present in association with photosynthetic picoeukaryotes were isolated using this method. Several of the isolates obtained in this study were close relatives to bacteria that are known to thrive on algal surfaces and/or on aggregates. An OTU 97% identical to the *Alteromonas* sp. isolate was observed in two photosynthetic picoeukaryote sorts (Supplementary Table 2). *Alteromonas* sp. is an *r*-strategist *Gammaproteobacteria* that is known to quickly exploit nutrient rich hot spots in the environment (Fontanez et al., 2015) and have frequently been reported in association with protists (Su et al., 2011). Four isolates in this study were closely related to *Colwellia* (**Table 2**). Although *Colwellia psychrerythraea* has been described as a facultative anaerobic psychrophile (Methé et al., 2005), a sequence similar to *Colwellia psychrerythraea* was detected in aggregates from the Santa Barbara Channel (DeLong et al., 1993), suggesting that there could be an adaptation for an associated lifestyle within *Colwellia*. In the Pacific Ocean, *Sulfitobacter* sp., a member of the alphaproteobacterial *Roseobacter* clade, was a rapid colonizer of sinking marine aggregates (LeCleir et al., 2014). In this study, three *Sulfitobacter* sp. isolates were obtained from 100 photosynthetic picoeukaryote cells (**Table 2**) and an OTU with 96–98% identity was detected in all seawater samples and in one sort sample (Supplementary Table 2). *Sulfitobacter* are known for diverse species-specific associations with marine eukaryotes (Jasti et al., 2005; Amin et al., 2012). Recently, four *Sulfitobacter* strains were shown to promote cell division in the coastal diatom *Pseudo-nitzschia multiseries* (Amin et al., 2015). The authors used transcriptomics and targeted metabolite analysis to characterize the association and suggested that a complex exchange of nutrients took place between the diatom–bacteria consortia. It is possible that the isolates obtained in this study were involved in similar interactions but further studies are needed to assess if these associations are purely opportunistic or if there was species-specific adaptation.

In addition to being ingested or surface attached to the phytoplankton cell, associated cells may be present intracellularly as endosymbionts. Endosymbionts have been described within the cultured heterotrophic picoeukaryote *Symbiomonas scintillans* (Guillou et al., 1999) but to what extent endosymbionts may be present within photosynthetic picoeukaryotes is not well known. To try to visualize bacteria associated with photosynthetic picoeukaryotes we developed an on-slide CARD-FISH protocol on flow cytometry sorted photosynthetic picoeukaryote cells. We used the EUB338 probe that has been widely used for enumerating bacteria in seawater and in association with algae (e.g., Tujula et al., 2006). However, similarly to the observations by Biegala et al. (2005), the hybridization of the EUB338 probe to a large fraction of the picoeukaryote cells caused difficulties in distinguishing associated cells from chloroplasts (Supplementary Figure 3). Biegala et al. (2005) found hybridization associated with picoeukaryotes using the more specific probe targeting *Gammaproteobacteria* (GAM42a), which is unlikely to hybridize to eukaryotic organelles. However, when using the GAM42a probe in this study, no hybridized cells were observed within the photosynthetic picoeukaryote sorts. Although the developed on-slide CARD-FISH protocol was successful in labeling cells from sorts, providing information about the cell size and morphology of the sorted population, it was a low-throughput method because of the low number of cells visible on the slides (<30% of the sorted cells). Difficulties associated with sorting raw seawater such as low abundances and the small cell size of the sorted populations also made identification and replication challenging. In the future, optimization of the protocol to prevent cell loss and the use of several more specific probes targeting for example *Synechococcus* will likely enable visualization of associated microbes.

In contrast to associations by opportunistic colonizers on dead or alive phytoplankton cells, some symbioses may have co-evolved for a long period of time and exhibit extreme genome reductions with metabolic pathways missing in one partner but present in the other (McCutcheon and Moran, 2012). However, to establish the metabolic processes and benefits gained by the associated organisms can be challenging, especially if the associated organism have not been cultured. In a recent study, the microbiome of non-axenic *Ostreococcus tauri* cultures was studied and specific genes involved in cell-to cell-interactions identified (Abby et al., 2014). In the future, similar studies may expand the microbial tool kit of putative targets that are much needed to study bacterioplankton–picoeukaryote associations *in situ*. In the light of recent discoveries, it is not unlikely that ecological associations between bacterioplankton and picoeukaryotes are diverse and frequently occurring. Consequently, identifying, characterizing and understanding the metabolic mechanisms underlying these interactions is a prerequisite in order to improve community modeling approaches. Here, we identify specific phylotypes found in association with photosynthetic picoeukaryotes which can be used as targets for further characterization and visualization of the associations.

AUTHOR CONTRIBUTIONS

HF, KT-K, and JZ designed the experiments. HF performed the experiments. HF, KT-K, and JZ wrote the paper.

FUNDING

This work was supported by the Swedish Research Council VR 637-2013-7502 to HF, the NSF C-MORE (#EF0424599) and the Simons Collaboration on Ocean Processes and Ecology (SCOPE).

ACKNOWLEDGMENTS

First, we would like to thank the reviewers for their valuable suggestions and comments which helped to improve the manuscript. We would also like to thank Raphael Kudela and his lab members for providing access to the Monterey Bay weekly phytoplankton monitoring data and the MEGAMER facility at UCSC for assistance with flow cytometry sorting. We thank Mary Hogan, María del Carmen Muñoz-Marín, and Britt Henke in the Zehr lab at UCSC for laboratory

assistance. We would also like to acknowledge Stefan Green and the DNAS Facility at the University of Illinois at Chicago for the Illumina MiSeq sequencing and Benjamin Adams and the UCSC Life Science Microscopy Center for microscopy assistance.

REFERENCES

Abby, S. S., Touchon, M., De Jode, A., Grimsley, N., and Piganeau, G. (2014). Bacteria in *Ostreococcus tauri* cultures - friends, foes or hitchhikers? *Front. Microbiol.* 5:505. doi: 10.3389/fmicb.2014.00505

Amann, R. I., Binder, B. J., Olson, R. J., Chisholm, S. W., Devereux, R., and Stahl, D. A. (1990). Combination of 16S rRNA-targeted oligonucleotide probes with flow cytometry for analyzing mixed microbial populations. *Appl. Environ. Microbiol.* 56, 1919–1925. doi: 10.1111/j.1469-8137.2004.01066.x

Amin, S. A., Hmelo, L. R., van Tol, H. M., Durham, B. P., Carlson, L. T., Heal, K. R., et al. (2015). Interaction and signalling between a cosmopolitan phytoplankton and associated bacteria. *Nature* 522, 98–101. doi: 10.1038/nature14488

Amin, S. A., Parker, M. S., and Armbrust, E. V. (2012). Interactions between diatoms and bacteria. *Microbiol. Mol. Biol. Rev.* 76, 667–684. doi: 10.1128/MMBR.00007-12

Anderson, O. R. (2014). Living together in the plankton: a survey of marine protist symbioses. *Acta Protozool.* 53, 29–38. doi: 10.4467/16890027AP.13.0019.1116

Azam, F., and Malfatti, F. (2007). Microbial structuring of marine ecosystems. *Nat. Rev. Microbiol.* 5, 782–791. doi: 10.1038/nrmicro1747

Baker, L., and Kemp, P. (2014). Exploring bacteria–diatom associations using single-cell whole genome amplification. *Aquat. Microb. Ecol.* 72, 73–88. doi: 10.3354/ame01686

Biegala, I. C., Cuttle, M., Mary, I., and Zubkov, M. (2005). Hybridisation of picoeukaryotes by eubacterial probes is widespread in the marine environment. *Aquat. Microb. Ecol.* 41, 293–297. doi: 10.3354/ame041293

Bybee, S. M., Bracken-Grissom, H., Haynes, B. D., Hermansen, R. A., Byers, R. L., Clement, M. J., et al. (2011). Targeted amplicon sequencing (TAS): a scalable next-gen approach to multilocus, multitaxa phylogenetics. *Genome Biol. Evol.* 3, 1312–1323. doi: 10.1093/gbe/evr106

Caporaso, J. G., Kuczynski, J., Stombaugh, J., Bittinger, K., Bushman, F. D., Costello, E. K., et al. (2010). QIIME allows analysis of high-throughput community sequencing data. *Nat. Methods* 7, 335–336. doi: 10.1038/nmeth0510-335

Caporaso, J. G., Lauber, C. L., Walters, W. A., Berg-Lyons, D., Lozupone, C. A., Turnbaugh, P. J., et al. (2011). Global patterns of 16S rRNA diversity at a depth of millions of sequences per sample. *Proc. Natl. Acad. Sci. U.S.A.* 108, 4516–4522. doi: 10.1073/pnas.1000080107

Choi, E. J., Kwon, H. C., Koh, H. Y., Kim, Y. S., and Yang, H. O. (2010). *Colwellia asteriadis* sp. nov., a marine bacterium isolated from the starfish *Asterias amurensis*. *Int. J. Syst. Evol. Microbiol.* 60, 1952–1957. doi: 10.1099/ijs.0.016055-0

Cooper, M. B., and Smith, A. G. (2015). Exploring mutualistic interactions between microalgae and bacteria in the omics age. *Curr. Opin. Plant Biol.* 26, 147–153. doi: 10.1016/j.pbi.2015.07.003

DeLong, E. F., Franks, D. G., and Alldredge, A. L. (1993). Phylogenetic diversity of aggregate-attached vs. free-living marine bacterial assemblages. *Limnol. Oceanogr.* 38, 924–934. doi: 10.4319/lo.1993.38.5.0924

Dufresne, A., Ostrowski, M., Scanlan, D. J., Garczarek, L., Mazard, S., Palenik, B., et al. (2008). Unraveling the genomic mosaic of a ubiquitous genus of marine cyanobacteria. *Genome Biol.* 9:R90. doi: 10.1186/gb-2008-9-5-r90

Dupont, C. L., Rusch, D. B., Yooseph, S., Lombardo, M.-J., Richter, R. A., Valas, R., et al. (2012). Genomic insights to SAR86, an abundant and uncultivated marine bacterial lineage. *ISME J.* 6, 1186–1199. doi: 10.1038/ismej.2011.189

Edgar, R. C., Haas, B. J., Clemente, J. C., Quince, C., and Knight, R. (2011). UCHIME improves sensitivity and speed of chimera detection. *Bioinformatics* 27, 2194–2200. doi: 10.1093/bioinformatics/btr381

Fontanez, K. M., Eppley, J. M., Samo, T. J., Karl, D. M., and DeLong, E. F. (2015). Microbial community structure and function on sinking particles in the North Pacific Subtropical Gyre. *Front. Microbiol.* 6:469. doi: 10.3389/fmicb.2015.00469

Fujiwara, Y., Kawato, M., Noda, C., Kinoshita, G., Yamanaka, T., Fujita, Y., et al. (2010). Extracellular and mixotrophic symbiosis in the whale-fall mussel *Adipicola pacifica*: a trend in evolution from extra- to intracellular symbiosis. *PLoS ONE* 5:e11808. doi: 10.1371/journal.pone.0011808

Gibble, C. M., and Kudela, R. M. (2014). Detection of persistent microcystin toxins at the land–sea interface in Monterey Bay, California. *Harmful Algae* 39, 146–153. doi: 10.1016/j.hal.2014.07.004

Goecke, F., Thiel, V., Wiese, J., Labes, A., and Imhoff, J. F. (2013). Algae as an important environment for bacteria - phylogenetic relationships among new bacterial species isolated from algae. *Phycologia* 52, 14–24. doi: 10.2216/12

González, J. M., Kiene, R. P., and Moran, M. A. (1999). Tranformation of sulfur compounds by an abundant lineage of marine bacteria in the α-subclass of the class *Proteobacteria*. *Appl. Environ. Microbiol.* 65, 3810–3819.

González, J. M., Sherr, B. F., and Sherr, E. B. (1993). Digestive enzyme activity as a quantitative measure of protistan grazing: the acid lysozyme assay for bacterivory. *Mar. Ecol. Prog. Ser.* 100, 197–206. doi: 10.3354/meps100197

Green, S. J., Venkatramanan, R., and Naqib, A. (2015). Deconstructing the polymerase chain reaction: understanding and correcting bias associated with primer degeneracies and primer-template mismatches. *PLoS ONE* 10:e0128122. doi: 10.1371/journal.pone.0128122

Grossart, H., and Simon, M. (2007). Interactions of planktonic algae and bacteria: effects on algal growth and organic matter dynamics. *Aquat. Microb. Ecol.* 47, 163–176. doi: 10.3354/ame047163

Grossart, H. P. (2010). Ecological consequences of bacterioplankton lifestyles: changes in concepts are needed. *Environ. Microbiol. Rep.* 2, 706–714. doi: 10.1111/j.1758-2229.2010.00179.x

Guillou, L., Chrétiennot-Dinet, M.-J., Boulben, S., Moon-van der Staay, S. J., and Vaulot, D. (1999). *Symbiomonas scintillans* gen. et sp. nov. and *Picophagus flagellatus* gen. et sp. nov. (Heterokonta): two new heterotrophic flagellates of picoplanktonic size. *Protist* 150, 383–398. doi: 10.1016/S1434-4610(99)70040-4

Guillou, L., Eikrem, W., Chrétiennot-Dinet, M.-J., Le Gall, F., Massana, R., Romari, K., et al. (2004). Diversity of picoplanktonic prasinophytes assessed by direct nuclear SSU rDNA sequencing of environmental samples and novel isolates retrieved from oceanic and coastal marine ecosystems. *Protist* 155, 193–214. doi: 10.1078/143446104774199592

Hartmann, M., Grob, C., Tarran, G. A., Martin, A. P., Burkill, P. H., and Scanlan, D. J. (2012). Mixotrophic basis of Atlantic oligotrophic ecosystems. *Proc. Natl. Acad. Sci. U.S.A.* 109, 5756–5760. doi: 10.1073/pnas.1118179109

Hartmann, M., Zubkov, M. V., Scanlan, D. J., and Lepère, C. (2013). In situ interactions between photosynthetic picoeukaryotes and bacterioplankton in the Atlantic Ocean: evidence for mixotrophy. *Environ. Microbiol. Rep.* 5, 835–840. doi: 10.1111/1758-2229.12084

Herlemann, D. P., Labrenz, M., Jürgens, K., Bertilsson, S., Waniek, J. J., and Andersson, A. F. (2011). Transitions in bacterial communities along the 2000 km salinity gradient of the Baltic Sea. *ISME J.* 5, 1571–1579. doi: 10.1038/ismej.2011.41

Hodkinson, B. P., and Lutzoni, F. (2010). A microbiotic survey of lichen-associated bacteria reveals a new lineage from the Rhizobiales. *Symbiosis* 49, 163–180. doi: 10.1007/s13199-009-0049-3

Huang, Y., Niu, B., Gao, Y., Fu, L., and Li, W. (2010). CD-HIT Suite: a web server for clustering and comparing biological sequences. *Bioinformatics* 26, 680–682. doi: 10.1093/bioinformatics/btq003

Jardillier, L., Zubkov, M. V., Pearman, J., and Scanlan, D. J. (2010). Significant CO_2 fixation by small prymnesiophytes in the subtropical and tropical northeast Atlantic Ocean. *ISME J.* 4, 1180–1192. doi: 10.1038/ismej.2010.36

Jasti, S., Sieracki, M. E., Poulton, N. J., Giewat, M. W., and Rooney-Varga, J. N. (2005). Phylogenetic diversity and specificity of bacteria closely associated with *Alexandrium* spp. and other phytoplankton. *Appl. Environ. Microbiol.* 71, 3483–3494. doi: 10.1128/AEM.71.7.3483-3494.2005

Jester, R., Lefebvre, K., Langlois, G., Vigilant, V., Baugh, K., and Silver, M. W. (2009). A shift in the dominant toxin-producing algal species in central California alters phycotoxins in food webs. *Harmful Algae* 8, 291–298. doi: 10.1016/j.hal.2008.07.001

SUPPLEMENTARY MATERIAL

The Supplementary Material for this article can be found online at: http://journal.frontiersin.org/article/10.3389/fmicb.2016.00339

Kircher, M., Sawyer, S., and Meyeret, M. (2012). Double indexing overcomes inaccuracies in multiplex sequencing on the Illumina platform. *Nucleic Acids Res*. 40:e3. doi: 10.1093/nar/gkr771

Laurence, M., Hatzis, C., and Brash, D. E. (2014). Common contaminants in next-generation sequencing that hinder discovery of low-abundance microbes. *PLoS ONE* 9:e97876. doi: 10.1371/journal.pone.0097876

LeCleir, G. R., Debruyn, J. M., Maas, E. W., Boyd, P. W., and Wilhelm, S. W. (2014). Temporal changes in particle-associated microbial communities after interception by nonlethal sediment traps. *FEMS Microbiol. Ecol.* 87, 153–163. doi: 10.1111/1574-6941.12213

Manz, W., Amann, R., Ludwig, W., Wagner, M., and Schleifer, K. H. (1992). Phylogenetic oligodeoxynucleotide probes for the major subclasses of *Proteobacteria*: problems and solutions. *Syst. Appl. Microbiol.* 15, 593–600. doi: 10.1016/S0723-2020(11)80121-9

Martinez-Garcia, M., Brazel, D., Poulton, N. J., Swan, B. K., Gomez, M. L., Masland, D., et al. (2012a). Unveiling in situ interactions between marine protists and bacteria through single cell sequencing. *ISME J.* 6, 703–707. doi: 10.1038/ismej.2011.126

Martinez-Garcia, M., Brazel, D. M., Swan, B. K., Arnosti, C., Chain, P. S. G., Reitenga, K. G., et al. (2012b). Capturing single cell genomes of active polysaccharide degraders: an unexpected contribution of Verrucomicrobia. *PLoS ONE* 7:e35314. doi: 10.1371/journal.pone.0035314

Massana, R. (2011). Eukaryotic picoplankton in surface oceans. *Annu. Rev. Microbiol.* 65, 91–110. doi: 10.1146/annurev-micro-090110-102903

McCutcheon, J. P., and Moran, N. A. (2012). Extreme genome reduction in symbiotic bacteria. *Nat. Rev. Microbiol.* 10, 13–26. doi: 10.1038/nrmicro2670

McKie-Krisberg, Z. M., and Sanders, R. W. (2014). Phagotrophy by the picoeukaryotic green alga *Micromonas*: implications for Arctic Oceans. *ISME J.* 8, 1953–1961. doi: 10.1038/ismej.2014.16

Methé, B. A., Nelson, K. E., Deming, J. W., Momen, B., Melamud, E., Zhang, X., et al. (2005). The psychrophilic lifestyle as revealed by the genome sequence of *Colwellia psychrerythraea* 34H through genomic and proteomic analyses. *Proc. Natl. Acad. Sci. U.S.A.* 102, 10913–10918. doi: 10.1073/pnas.0504766102

Mitra, A., Skrzypczak, M., Ginalski, K., and Rowicka, M. (2015). Strategies for achieving high sequencing accuracy for low diversity samples and avoiding sample bleeding using Illumina platform. *PLoS ONE* 10:e0120520. doi: 10.1371/journal.pone.0120520

Montoya, J. P., Holl, C. M., Zehr, J. P., Hansen, A., Villareal, T. A., and Capone, D. G. (2004). High rates of N_2 fixation by unicellular diazotrophs in the oligotrophic Pacific Ocean. *Nature* 430, 1027–1031. doi: 10.1038/nature02744.1

Moonsamy, P. V., Williams, T., Bonella, P., Holcomb, C. L., Höglund, B. N., Hillman, G., et al. (2013). High throughput HLA genotyping using 454 sequencing and the Fluidigm Access ArrayTM system for simplified amplicon library preparation. *Tissue Antigens* 81, 141–149. doi: 10.1111/tan.12071

Pennington, T. J., and Chavez, F. P. (2000). Seasonal fluctuations of temperature, salinity, nitrate, chlorophyll and primary production at station H3/M1 over 1989-1996 in Monterey Bay, California. *Deep. Res. Part II Top. Stud. Oceanogr.* 47, 947–973. doi: 10.1016/S0967-0645(99)00132-0

Pernthaler, A., Pernthaler, J., and Amann, R. (2002). Fluorescence in situ hybridization and catalyzed reporter deposition for the identification of marine bacteria. *Appl. Environ. Microbiol.* 68, 3094–3101. doi: 10.1128/AEM.68.6.3094

Salter, S. J., Cox, M. J., Turek, E. M., Calus, S. T., Cookson, W. O., Moffatt, M. F., et al. (2014). Reagent and laboratory contamination can critically impact sequence-based microbiome analyses. *BMC Biol.* 12:87. doi: 10.1186/s12915-014-0087-z

Sanders, R. W., and Gast, R. J. (2012). Bacterivory by phototrophic picoplankton and nanoplankton in Arctic waters. *FEMS Microbiol. Ecol.* 82, 242–253. doi: 10.1111/j.1574-6941.2011.01253.x

Sapp, M., Schwaderer, A., Wiltshire, K., Hoppe, H.-G., Gerdts, G., and Wichels, A. (2007). Species-specific bacterial communities in the phycosphere of microalgae? *Microb. Ecol.* 53, 683–699. doi: 10.1007/s00248-006-9162-5

Sekar, R., Pernthaler, A., Pernthaler, J., Posch, T., Amann, R., and Warnecke, F. (2003). An improved protocol for quantification of freshwater Actinobacteria by fluorescence in situ hybridization. *Appl. Environ. Microbiol.* 69, 2928–2935. doi: 10.1128/AEM.69.5.2928

Sher, D., Thompson, J. W., Kashtan, N., Croal, L., and Chisholm, S. W. (2011). Response of *Prochlorococcus* ecotypes to co-culture with diverse marine bacteria. *ISME J.* 5, 1125–1132. doi: 10.1038/ismej.2011.1

Stackebrandt, E., and Goebel, B. M. (1994). Taxonomic note: a place for DNA-DNA reassociation and 16S rRNA sequence analysis in the present species definition in bacteriology. *Int. J. Syst. Bacteriol.* 44, 846–849. doi: 10.1099/00207713-44-4-846

Stepanauskas, R., and Sieracki, M. E. (2007). Matching phylogeny and metabolism in the uncultured marine bacteria, one cell at a time. *Proc. Natl. Acad. Sci. U.S.A.* 104, 9052–9057. doi: 10.1073/pnas.0700496104

Stocker, R. (2012). Marine microbes see a sea of gradients. *Science* 338, 628–633. doi: 10.1126/science.1208929

Su, J., Yang, X., Zhou, Y., and Zheng, T. (2011). Marine bacteria antagonistic to the harmful algal bloom species *Alexandrium tamarense* (Dinophyceae). *Biol. Control* 56, 132–138. doi: 10.1016/j.biocontrol.2010.10.004

Swan, B. K., Martinez-Garcia, M., Preston, C. M., Sczyrba, A., Woyke, T., Lamy, D., et al. (2011). Potential for chemolithoautotrophy among ubiquitous bacteria lineages in the dark ocean. *Science* 333, 1296–1300. doi: 10.1126/science.1203690

Tamura, K., Stecher, G., Peterson, D., Filipski, A., and Kumar, S. (2013). MEGA6: molecular evolutionary genetics analysis version 6.0. *Mol. Biol. Evol.* 30, 2725–2729. doi: 10.1093/molbev/mst197

Thompson, A. W., Foster, R., Krupke, A., Carter, B. J., Musat, N., Vaulot, D., et al. (2012). Unicellular cyanobacterium symbiotic with a single-celled eukaryotic alga. *Science* 337, 1546–1550. doi: 10.1126/science.1222700

Tujula, N. A., Holmström, C., Mußmann, M., Amann, R., Kjelleberg, S., and Crocetti, G. R. (2006). A CARD-FISH protocol for the identification and enumeration of epiphytic bacteria on marine algae. *J. Microbiol. Methods* 65, 604–607. doi: 10.1016/j.mimet.2005.09.006

Wallner, G., Amann, R., and Beisker, W. (1993). Optimizing fluorescent in situ hybridization with rRNA-targeted oligonucleotide probes for flow cytometric identification of microorganisms. *Cytometry* 14, 136–143. doi: 10.1002/cyto.990140205

Wang, Q., Garrity, G. M., Tiedje, J. M., and Cole, J. R. (2007). Naive bayesian classifier for rapid assignment of rRNA sequences into the new bacterial taxonomy. *Appl. Environ. Microbiol.* 73, 5261–5267. doi: 10.1128/AEM.00062-07

Worden, A. Z., Follows, M. J., Giovannoni, S. J., Wilken, S., Zimmerman, A. E., and Keeling, P. J. (2015). Rethinking the marine carbon cycle: factoring in the multifarious lifestyles of microbes. *Science* 347:1257594. doi: 10.1126/science.1257594

Worden, A. Z., Lee, J.-H., Mock, T., Rouzé, P., Simmons, M. P., Aerts, A. L., et al. (2009). Green evolution and dynamic adaptations revealed by genomes of the marine picoeukaryotes *Micromonas*. *Science* 324, 268–272. doi: 10.1126/science.1167222

Worden, A. Z., Nolan, J. K., and Palenik, B. (2004). Assessing the dynamics and ecology of marine picophytoplankton: the importance of the eukaryotic component. *Limnol. Ocean.* 49, 168–179. doi: 10.4319/lo.2004.49.1.0168

Yoon, H. S., Price, D. C., Stepanauskas, R., Rajah, V. D., Sieracki, M. E., Wilson, W. H., et al. (2011). Single-cell genomics reveals organismal interactions in uncultivated marine protists. *Science* 332, 714–717. doi: 10.1126/science.1203163

Zehr, J. P., Bench, S. R., Carter, B. J., Hewson, I., Niazi, F., Shi, T., et al. (2008). Globally distributed uncultivated oceanic N_2-fixing cyanobacteria lack oxygenic photosystem II. *Science* 322, 1110–1112. doi: 10.1126/science.1165340

Zhang, J., Kobert, K., Flouri, T., and Stamatakis, A. (2014). PEAR: a fast and accurate Illumina Paired-End reAd mergeR. *Bioinformatics* 30, 614–620. doi: 10.1093/bioinformatics/btt593

Zubkov, M. V., and Tarran, G. A. (2008). High bacterivory by the smallest phytoplankton in the North Atlantic Ocean. *Nature* 455, 224–226. doi: 10.1038/nature07236

Conflict of Interest Statement: The authors declare that the research was conducted in the absence of any commercial or financial relationships that could be construed as a potential conflict of interest.

frontiers in Microbiology

ORIGINAL RESEARCH
published: 21 April 2016
doi: 10.3389/fmicb.2016.00517

Spatio-Temporal Interdependence of Bacteria and Phytoplankton during a Baltic Sea Spring Bloom

*Carina Bunse[1], Mireia Bertos-Fortis[1], Ingrid Sassenhagen[2], Sirje Sildever[3], Conny Sjöqvist[4,5], Anna Godhe[6], Susanna Gross[6], Anke Kremp[4], Inga Lips[3], Nina Lundholm[7], Karin Rengefors[2], Josefin Sefbom[6], Jarone Pinhassi[1] and Catherine Legrand[1]**

[1] Centre for Ecology and Evolution in Microbial Model Systems - EEMiS, Linnaeus University, Kalmar, Sweden, [2] Aquatic Ecology, Lund University, Lund, Sweden, [3] Marine Systems Institute, Tallinn University of Technology, Tallinn, Estonia, [4] Finnish Environmental Institute/Marine Research Centre, Helsinki, Finland, [5] Environmental and Marine Biology, Åbo Akademi University, Åbo, Finland, [6] Department of Marine Sciences, University of Gothenburg, Gothenburg, Sweden, [7] Natural History Museum of Denmark, University of Copenhagen, Copenhagen, Denmark

In temperate systems, phytoplankton spring blooms deplete inorganic nutrients and are major sources of organic matter for the microbial loop. In response to phytoplankton exudates and environmental factors, heterotrophic microbial communities are highly dynamic and change their abundance and composition both on spatial and temporal scales. Yet, most of our understanding about these processes comes from laboratory model organism studies, mesocosm experiments or single temporal transects. Spatial-temporal studies examining interactions of phytoplankton blooms and bacterioplankton community composition and function, though being highly informative, are scarce. In this study, pelagic microbial community dynamics (bacteria and phytoplankton) and environmental variables were monitored during a spring bloom across the Baltic Proper (two cruises between North Germany to Gulf of Finland). To test to what extent bacterioplankton community composition relates to the spring bloom, we used next generation amplicon sequencing of the 16S rRNA gene, phytoplankton diversity analysis based on microscopy counts and population genotyping of the dominating diatom *Skeletonema marinoi*. Several phytoplankton bloom related and environmental variables were identified to influence bacterial community composition. Members of *Bacteroidetes* and *Alphaproteobacteria* dominated the bacterial community composition but the bacterial groups showed no apparent correlation with direct bloom related variables. The less abundant bacterial phyla *Actinobacteria, Planctomycetes,* and *Verrucomicrobia,* on the other hand, were strongly associated with phytoplankton biomass, diatom:dinoflagellate ratio, and colored dissolved organic matter (cDOM). Many bacterial operational taxonomic units (OTUs) showed high niche specificities. For example, particular *Bacteroidetes* OTUs were associated with two distinct genetic clusters of *S. marinoi*. Our study revealed the complexity of interactions of bacterial taxa with inter- and intraspecific genetic variation in phytoplankton. Overall, our findings imply that biotic and abiotic factors during spring bloom influence bacterial community dynamics in a hierarchical manner.

Keywords: 16S rRNA, marine bacteria, bacterioplankton, phytoplankton, *Skeletonema marinoi*, spring bloom, Baltic Sea, spatio-temporal

OPEN ACCESS

Edited by:
Xavier Mayali, Lawrence Livermore National Laboratory, USA

Reviewed by:
James T. Hollibaugh, University of Georgia, USA
Jeffrey A. Kimbrel, Lawrence Livermore National Laboratory, USA

****Correspondence:***
Catherine Legrand
catherine.legrand@lnu.se

Specialty section:
This article was submitted to Aquatic Microbiology, a section of the journal Frontiers in Microbiology

Received: *15 January 2016*
Accepted: *29 March 2016*
Published: *21 April 2016*

Citation:
Bunse C, Bertos-Fortis M, Sassenhagen I, Sildever S, Sjöqvist C, Godhe A, Gross S, Kremp A, Lips I, Lundholm N, Rengefors K, Sefbom J, Pinhassi J and Legrand C (2016) Spatio-Temporal Interdependence of Bacteria and Phytoplankton during a Baltic Sea Spring Bloom. Front. Microbiol. 7:517. doi: 10.3389/fmicb.2016.00517

INTRODUCTION

In the brackish Baltic Sea, the phytoplankton spring bloom generally begins in coastal areas and propagates toward the central parts of the basins. The timing of the onset is slightly lagged in the northern parts compared to the southern Baltic (Godhe et al., 2016). Dinoflagellates and diatoms dominate the spring bloom (Wasmund et al., 1998) and the model diatom species *Skeletonema marinoi* accounts for up to 10^4 cells per ml in the Kattegat during spring (Saravanan and Godhe, 2010). *Skeletonema marinoi* forms two distinct genetic populations in the Baltic Sea, one mainly dominating in the southern Baltic and the other being predominant in the middle and northern Baltic Proper (Sjöqvist et al., 2015; Godhe et al., 2016). The genetic population structure of *S. marinoi* is influenced by oceanographic dispersal barriers and the salinity regime, similar to population structures of other marine organisms (Jørgensen et al., 2005; Johannesson and Andre, 2006). The Baltic Sea salinity gradient also influences the bacterioplankton community composition during summer (Herlemann et al., 2011; Dupont et al., 2014). However, the bacterioplankton community composition during the spring bloom has to our knowledge not been assessed in a spatial-temporal survey covering the entire Baltic Proper. In addition, knowledge about how spring phytoplankton populations structure co-occurring bacteria in the Baltic Sea is still limited.

The primary production of the spring bloom in the Baltic Sea exceeds production estimates of the summer cyanobacterial bloom (Legrand et al., 2015) and the organic matter produced during the spring bloom is a main source for bacterial production (Lindh et al., 2014). Bacterial taxa differ in their capabilities to degrade organic carbon compounds (Gómez-Consarnau et al., 2012) and especially *Flavobacteria* are reported to utilize high molecular organic matter released from phytoplankton blooms (Buchan et al., 2014). Therefore, the bacterial community composition during spring, commonly dominated by *Bacteroidetes*, *Alphaproteobacteria,* and *Actinobacteria* (Andersson et al., 2010; Lindh et al., 2014), might also indirectly be influenced by environmental variables that structure the phytoplankton spring bloom. So far, studies focusing on bacterial communities accompanying and interacting with phytoplankton blooms have been mostly carried out in limnic systems or laboratory mesocosm experiments (Bell and Lang, 1974; Cole, 1982; Riemann et al., 2000; Pinhassi et al., 2004; Fandino et al., 2005; Teeling et al., 2012; Buchan et al., 2014).

This study aimed to assess the bacterioplankton community composition during the Baltic Sea spring bloom. We studied how bacterial groups interacted with phytoplankton phyla and which bacteria co-occurred with specific populations of the diatom *S. marinoi*. Further, we identified the correlations of marine bacteria to environmental and bloom related variables, such as phytoplankton biomass.

MATERIALS AND METHODS

Sampling and Environmental Variables

To analyze the phytoplankton spring bloom succession and its consequences, surface water samples (8 m depth) were collected during four research cruises [Cruise A (4th–7th March), B (19th–22nd March), C (4th–7th April), and D (16th–19th April)] during spring 2013. We used the Alg@line facilities on board the ship of opportunity MS *Finnmaid*, organized by SYKE (Finnish Environment Institute) and PRODIVERSA (Population genetics and intraspecific diversity of aquatic protists across habitats and eucaryotic clades, NordForsk Researcher Network). Ten stations were sampled along a northeast to southwest transect across the Baltic Proper from the Gulf of Finland to the southern Baltic Proper. Environmental variables and chlorophyll *a* (measured by relative chl*a* fluorescence, as a proxy for phytoplankton biomass) were measured using a ferrybox measurement system connected to a flow through system onboard. More specifically, the ferrybox is an automated system that measures chlorophyll fluorescence, temperature, salinity, and cDOM fluorescence while the ship is moving (Rantajärvi, 2003). Nutrients (nitrate, phosphate, silicate) were automatically collected on board utilizing an automated sample carousel containing 24 bottles, and were analyzed at SYKE using methods as described in Grasshoff et al. (1983) and Godhe et al. (2016). The map of the Baltic Sea and chl*a* values (**Figure 1**) were drawn with Ocean Data View 4 (Schlitzer, 2014).

Phytoplankton Counts and *S. marinoi* Genotypying

Phytoplankton samples were fixed with acidic Lugol onboard and were counted using a light microscope (LEICA DM IL Bio, GF10/18M Ocular, 200x or 400x magnification). Water samples from each station (25 ml sample water) were sedimented for 24 h in a sedimentation chamber (26 mm diameter), HELCOM biovolume guidelines (Olenina et al., 2006) were followed and carbon concentrations were estimated, and are presented in **Figure 1C**.

S. marinoi strains were genotyped using eight microsatellite loci (Almany et al., 2009), and assigned to populations using a Bayesian structure analysis using the software STRUCTURE [cluster membership ($K = 2$); Pritchard et al., 2000], based on the microsatellite data as previously reported (Figure S1 in Godhe et al., 2016).

Bacterial Analyses

Samples for bacterial abundance were fixed in duplicates with formalin (3% final concentration, Sigma-Aldrich) and stored at −20°C until processing. Subsamples were stained with SYTO®-13, a green fluorescence nucleic acid stain (Life technologies™), normalized with truecount beads and counted with a flow cytometer (FACScalibur). Bacterial abundance data were averaged for technical duplicates, bacterial counts and standard deviations are provided in Supplementary Table 1.

Samples for bacterial biomass were obtained during cruises C (five stations) and D (nine stations) in April 2013. Water samples for DNA extraction (1 L) were filtered on 0.2 μm supor® membrane filters (PALL Life Sciences) and preserved in TE-buffer (Tris-EDTA Buffer, Sigma® Life Science) at −20°C. DNA was extracted using a phenol/chloroform protocol adapted from Boström et al. (2004). In brief, lysozyme was added to the samples (1.1 mg ml^{-1} final concentration in TE buffer) and incubated at 37°C for 30 min. SDS and proteinase K were added to the

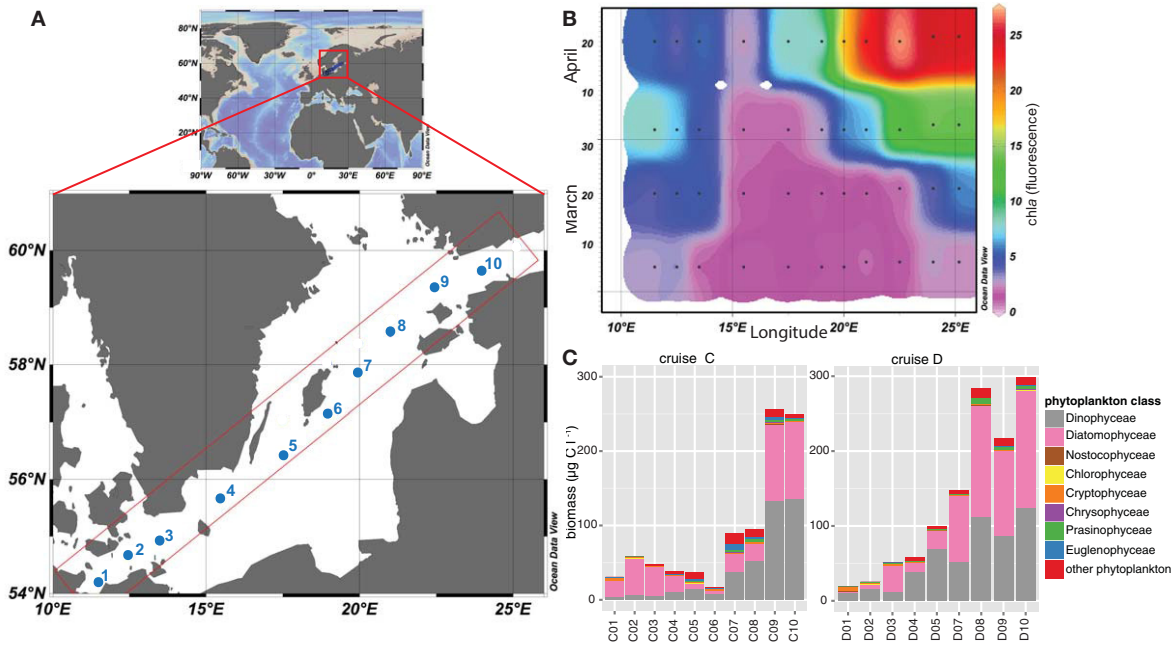

FIGURE 1 | Map of the Baltic Sea illustrating the sampling stations included in this study. (A) The map demonstrates the Baltic Sea, within Europe, and the sampling transect over the Baltic Proper. Sampling stations during the four cruises (A–D) are labeled from 1 to 10, ranging from stations 1-3 in the southern and stations 8–10 in the northern coastal part of the Baltic Proper. Stations 4-7 were located in the open Baltic Proper. **(B)** Relative chla fluorescence [measured with the flow through system on board and modified from Godhe et al. (2016)] across the transects over the Baltic Proper from March to April 2013 (cruise A–D). Black dots describe sampling occasions, values were extrapolated using Ocean Data View. **(C)** Phytoplankton biomass in µg C l^{-1} during cruise C (early April) and D (late April) along the transect, based on microscopy counts.

samples (final concentration 1%, and 0.1 mg ml^{-1}, respectively) and incubated at 55°C overnight. Phenol/chloroform/isoamyl alcohol (25:24:1) was added in equal volumes prior to transfer of the water phase, before the samples were washed with chloroform/isoamyl alcohol (24:1). This phenol extraction step was repeated twice before sodium acetate was added (1/10 volume) and DNA was precipitated with 100% ethanol (equal amounts) before centrifugation to receive a DNA pellet. The DNA pellet was air dried and dissolved in 1x TE buffer.

The V3–V5 region of the 16S rRNA gene was amplified using the primers 341F and 805R by Herlemann et al. (2011), as previously described (Lindh et al., 2015). Briefly, two PCRs were conducted per sample. The first PCR amplified the 16S rRNA gene and added Illumina adapters [per reaction: 1.25 µl F/R primer-Illumina adapter at 10 pM, 0.5 µl DNA template, 12.5 µl Phusion Mastermix (ThermoScientific) and 9.5 µl H_2O] in 20 PCR cycles [98°C 30 s, (98°C 10 s/58°C 30 s/72°C 15 s) × 20 cycles, 72°C 2 min]. After cleaning the PCR1 product using AmpPureXP following the manufacturer's instructions, the second PCR served to attach standard Illumina handles and Illumina index primers. PCR conditions [per reaction 11.5 µl cleaned PCR1 product, 12.5 µl Phusion Mastermix (ThermoScientific) and 0.5 µl F/R primer] included 12 cycles [98°C 30 s, (98°C 10 s/62°C 30 s/72°C 5 s) × 12 cycles, 72°C 2 min]. DNA concentrations of PCR products were measured using a Qubit 2.0 fluorometer (Invitrogen) and quality controlled for appropriate fragment length on an agarose gel. Samples were pooled and sequenced on a Miseq Illumina platform (2 × 300 bp) at Scilife (SciLifeLab, Stockholm). DNA sequences have been deposited at the NCBI Sequence Read Archive under project number PRJNA308537.

Bioinformatics and Statistical Analyses

To analyze factors that structure the bacterial community composition, stations C1:C3, C9:C10, D1:D5, and D7:D10 were sampled simultaneously with the phytoplankton bloom and environmental variables. Illumina 16S rRNA gene sequences were analyzed according to the Uparse pipeline (Edgar, 2013). In short, sequences were stripped, merged, and quality filtered according to default settings (Edgar, 2013). The total number of sequences obtained from the Illumina platform was 1.6 million sequences. After merging the sequences (0.9 million r1-sequences) 82% passed quality control, resulting in 700,474 total sequences with an average read length of 453 bp. Sequences that passed quality control were sorted and clustered using a radius of 1.5%, resulting in 97% sequence identity, 586,308 sequences were obtained after quality control. Reads were annotated using a basic local alignment tool (BLAST) against the SILVA database SSURef99 release 119 (downloaded 14th June 2014), using the SINA aligner (Altschul et al., 1990; Pruesse et al., 2012). Clustering and annotation of the sequences resulted in 45.6% chloroplast reads. On average, 25,127 sequences were obtained per sample after excluding chloroplast sequences. Three bacterial OTUs of the 50 most abundant OTUs in the dataset were annotated as "bacteria" in the SILVA database (OTU_0016, OTU_0031, OTU_0040). An additional search in the NCBI

database (NCBI Resource Coordinators, 2013; 29th February 2016) resulted in ≤92% sequence similarity to actinobacterial sequences, thus the OTUs are referred to as "other bacteria."

Bacterial community analyses and statistical analysis were conducted in RStudio Version 0.98.1103 using the packages vegan, ggplot2, dplyr, ComplexHeatmap, pls, gridExtra, and RColorBrewer (Gentleman et al., 2004; Oksanen et al., 2007; Wickham, 2009; Neuwirth, 2014; Auguie, 2015; Gu, 2015; Mevik et al., 2015; Wickham and Francois, 2015). The bacterioplankton community is hereafter referred to as annotated OTUs excluding chloroplast reads. To obtain relative OTU abundances, the OTU reads were normalized using a total-sum normalization and are presented as % of total abundance per sample.

Circos graphs for bacterial community compositions were drawn using the online circos software (Krzywinski et al., 2009). Betadiversity measurements were based on Bray-Curtis dissimilarity matrices (Bray and Curtis, 1957). Partial least squares (PLS) regressions was performed by using the PLS package in R (Mevik et al., 2015). Correlations between bacterial families and chemical and biological variables, as well as between the top 50 OTUs and chemical and biological variables were generated using Pearson correlations.

RESULTS

Environmental Variables and Phytoplankton Bloom Dynamics

On the route between Finland and Germany (**Figure 1A**), salinity ranged from 5.5 PSU in the northernmost part of the transect to 10.2 PSU in the South (Supplementary Table 1). Temperature ranged from 2.8°C in the southernmost station (station C1) to 1.4°C and ice cover in the northernmost station (station C10) in early April (4th–7th April), and 5.8 to 2.3°C in late April (16th–19th April, Supplementary Table 1). The spring bloom successively depleted the inorganic nutrients along the entire transects. Concentrations of nitrate and nitrite were low in late April, on average 0.03 μM. Silica was high at the northernmost station (station D10; 16.7 μM) during the first sampling, and still measured 11.6 μM in the second half of April at the Gotland Deep (station D5) and up to 10.1 μM in the north (station D10). At the southernmost station (station D1), the silica level had dropped to 0.1 μM. Phosphate concentrations in late April ranged between values below detection limit and 0.3 μM (Supplementary Table 1). Chl*a* fluorescence followed the spring bloom progression and increased constantly from March until late April, and ranged from 1.7 at the Gotland Deep (station C5) up to 27.0 at the northern stations (station D9; **Figure 1B**). Station 4, close to Bornholm Deep, exhibited the lowest chl*a* values, but increased from 1.9 to 2.7 during April.

Phytoplankton biomass (based on microscopy counts excluding ciliates) was significantly lower in the sea area south of the Gotland Deep (station 1–4) compared with values obtained for the Northern Baltic Proper and Gulf of Finland during both cruises in April (station 9–10; **Figure 1C**). Phytoplankton biomass ranged from 30.8 μg C l^{-1} at the southern stations to 16.9 μg C l^{-1} at station C6 in the Baltic Proper, and up to 297 μg C l^{-1} at station in the north (station D10). Diatoms and dinoflagellates dominated the spring bloom with on-average 43 and 41% of the total phytoplankton biomass, respectively (**Figure 1C**). Dinoflagellates displayed a pronounced bloom at stations 9 and 10 during both cruises with biomass up to 133.6 μg C l^{-1}. Among the southern stations, diatom biomass peaked at 49 μg C l^{-1} at station C2, while among the northern stations, diatom biomass peaked at 156 μg C l^{-1} at station D10. The ratio between diatom and dinoflagellate biomass, as a proxy for phytoplankton community composition, was higher in the southern stations, emphasizing the dominance of diatoms in these areas. Other phytoplankton classes, e.g., *Euglenophyceae*, *Cryptophyceae,* and *Nostocophyceae* were identified, but biomass of these phyla did not exceed 10 μg C l^{-1}.

The diatom *S. marinoi* accounted for on average 5.88% ($sd = 7.39\%$) of total phytoplankton biomass (data not shown) and exhibited two genetic clusters (cluster 1 and cluster 2), as defined in a related study (Godhe et al., 2016) and reprinted in Supplementary Table 1. Cluster 1 dominated stations C1–C3, C9–C10, and D1–D4, whereas cluster 2 dominated stations D5–D10.

Bacterial Abundance and Community Composition

Bacterial abundance ranged between 9×10^5 cells ml^{-1} at stations 9 and 10 to 1.7×10^6 cells ml^{-1} at stations 1–3 during cruise C and reached a maximum of 2.8×10^6 cells ml^{-1} during cruise D.

Analysis of bacterioplankton community composition (excluding chloroplasts) showed that *Actinobacteria* (13.5%), *Alphaproteobacteria* (15.4%), and *Bacteroidetes* (42.4%) dominated the bacterial community during the spring bloom (**Figure 2A**). Beta-diversity analysis of all normalized sequences grouped the bacterial communities into three clusters (**Figure 2B**). The first cluster comprised the southern stations 1, 2 and 3. The second cluster grouped the middle stations 4, 5, 7, and 8 while the third cluster grouped stations 9 and 10 in the Gulf of Finland together.

The most abundant bacterial OTUs (top 50 OTUs) displayed pronounced differences in spatial-temporal distribution patterns (**Figure 2C**). Some OTUs showed enhanced relative abundances in the middle of the Baltic Proper; for example OTU_0002 (*Flavobacteriaceae*) accounted for on average 5.9% of the relative bacterial abundance per station and peaked at station D07 (**Figure 2C**). Other OTUs increased in relative abundance with time, OTU_0022 (*Polaribacter*) showed the highest relative abundance right after the chl*a* peak in the northernmost stations. Some OTUs bloomed in the southernmost stations (e.g., OTU_0017, *Rhodobacteriaceae*), while OTU_0016 (other bacteria) showed higher relative abundances in early April compared to late April.

Bacterial Community Linked to Environmental Variables and Phytoplankton Groups

Partial least squares regression analysis (PLSr analysis) identified the cluster of environmental variables shaping bacterial community composition depending on the sampling location

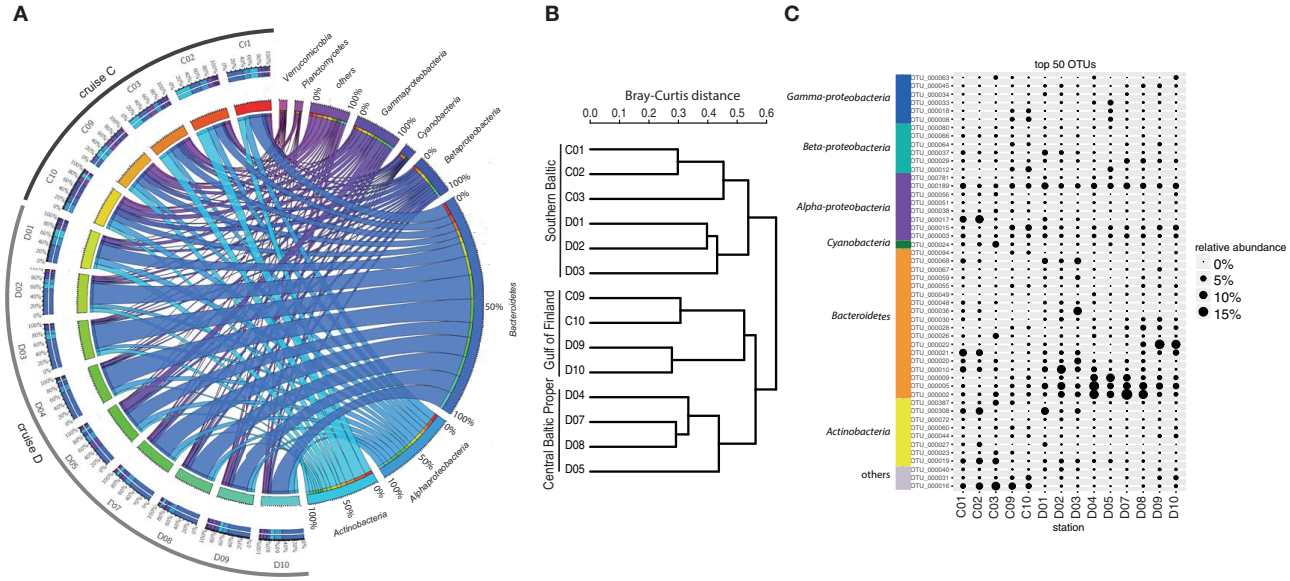

FIGURE 2 | Bacterial community composition and most abundant OTUs. (A) The figure displays relative OTU abundances grouped by bacteria phyla/classes in a circus graph. The right side of the graph visualizes relative OTU abundances of major bacteria phyla/classes summed over cruises C and D, as indicated by the size of the cells for each taxon (note color coding of ribbons connecting taxa with stations). Also shown are axes/cells for the taxon-normalized abundances at each station, as color-coded by station in the left side of the graph. Ribbons connect the relative abundances of the taxa with the color-coded stations on the left side of the graph, and width of ribbons is proportional to relative abundance. The left side of the graph indicates the relative abundances of the major taxa (color-coded according to taxa on right side of graph) at each sampled station during cruises C and D. Color-coding of stations (from red to blue-green) identifies proportions in inner circle/cells on right side of graph. **(B)** Beta-diversity analysis (beta-dendrogram, based on Bray–Curtis distance matrix), and **(C)** relative abundance patterns of the 50 most abundant OTUs across all stations. The group "others" in panel C comprises OTUs that have ≤92% sequence similarities to known sequences in NCBI (NCBI Resource Coordinators, 2013). Relative abundance is calculated as % of total sequences obtained per sample (excluding sequences annotated as chloroplasts).

(**Figure 3A**). In the PLSr, the first and second component explained 77.6% of the bacterioplankton community structure variability. No clear pattern of community structure could be detected with salinity and latitude gradients. While higher levels of nutrients, turbidity and ratio of diatoms:dinoflagellates were linked to communities sampled in cruise C, high temperatures were associated to bacterioplankton during cruise D. Northern stations assemblages were related to high cDOM, phytoplankton biomass, chl*a*, and *S. marinoi* cluster 1. On the other hand, *S. marinoi* cluster 2 was tightened to southern station communities. To further disentangle the relationship between environmental variables and bacteria families and individual OTUs, we conducted correlation analysis.

Pearson correlations of bacterial families to biotic and abiotic factors revealed that *Bacteroidetes* were positively correlated to temperature and negatively correlated to nutrient concentrations [nitrate ($p = 0.001$), phosphate ($p = 0.003$), silicate ($p = 0.005$), temperature ($p = 0.040$); **Figure 3B**]. *Planctomycetes* were most prevalent in the Gulf of Finland (stations 9 and 10) and were positively correlated with phytoplankton biomass ($p = 0.009$), cDOM ($p = 0.016$), and nutrients [nitrate ($p = 0.000$), phosphate ($p = 0.000$), silicate ($p = 0.002$)]. Diatom:dinoflagellate ratios positively influenced *Cyanobacteria* ($p = 0.001$), *Actinobacteria* ($p = 0.000$), and *Verrucomicrobia* ($p = 0.015$). Furthermore, *Actinobacteria* ($p = 0.045$) and *Verrucomicrobia* ($p = 0.014$) correlated significantly with the genetic population structure of *S. marinoi*. *Betaproteobacteria* linked to nutrient concentrations [(nitrate ($p = 0.003$), phosphate ($p = 0.020$), silicate ($p = 0.075$)], while relative abundances of *Alphaproteobacteria* could not be explained by any measured environmental variables.

The relative abundance patterns of the 50 most abundant OTUs (top 50 OTUs) correlated differently to the measured environmental variables (Pearson correlation, **Figure 3C**). The environmental and bloom related variables could be separated into three clusters according to how they correlated to the top 50 OTUs: (i) nutrients (nitrate, phosphate, and silicate); (ii) salinity, turbidity, diatoms/dinoflagellates, temperature, *S. marinoi* cluster 1; and (iii) chl*a*, cDOM, phytoplankton biomass, *S. marinoi* cluster 2. The first group of the most abundant OTUs was positively associated to cluster i and iii, and negatively correlated to cluster ii and consisted of a variety of taxa. The second group consisted of mostly *Bacteroidetes* and *Alphaproteobacteria*, but excluded *Actinobacteria* and was only positively correlated to cluster iii. The third group mainly consisted of *Flavobacteria* and *Actinobacteria* that were only positively linked to cluster ii while negatively correlated to cluster i and iii. Lastly, the fourth group included three OTUs of the *Actinobacteria*, three *Alphaproteobacteria* OTUs, two *Flavobacteria* and one *Betaproteobacteria* OTU and was largely positively correlated to cluster i, and the variables in cluster ii, and negatively to the variables in cluster iii. Furthermore, four *Bacteroidetes* populations (OTU_0056, OTU_0024, and OTU_0026) were only positively correlated to diatom:dinoflagellate ratio, whereas several OTUs of groups 1

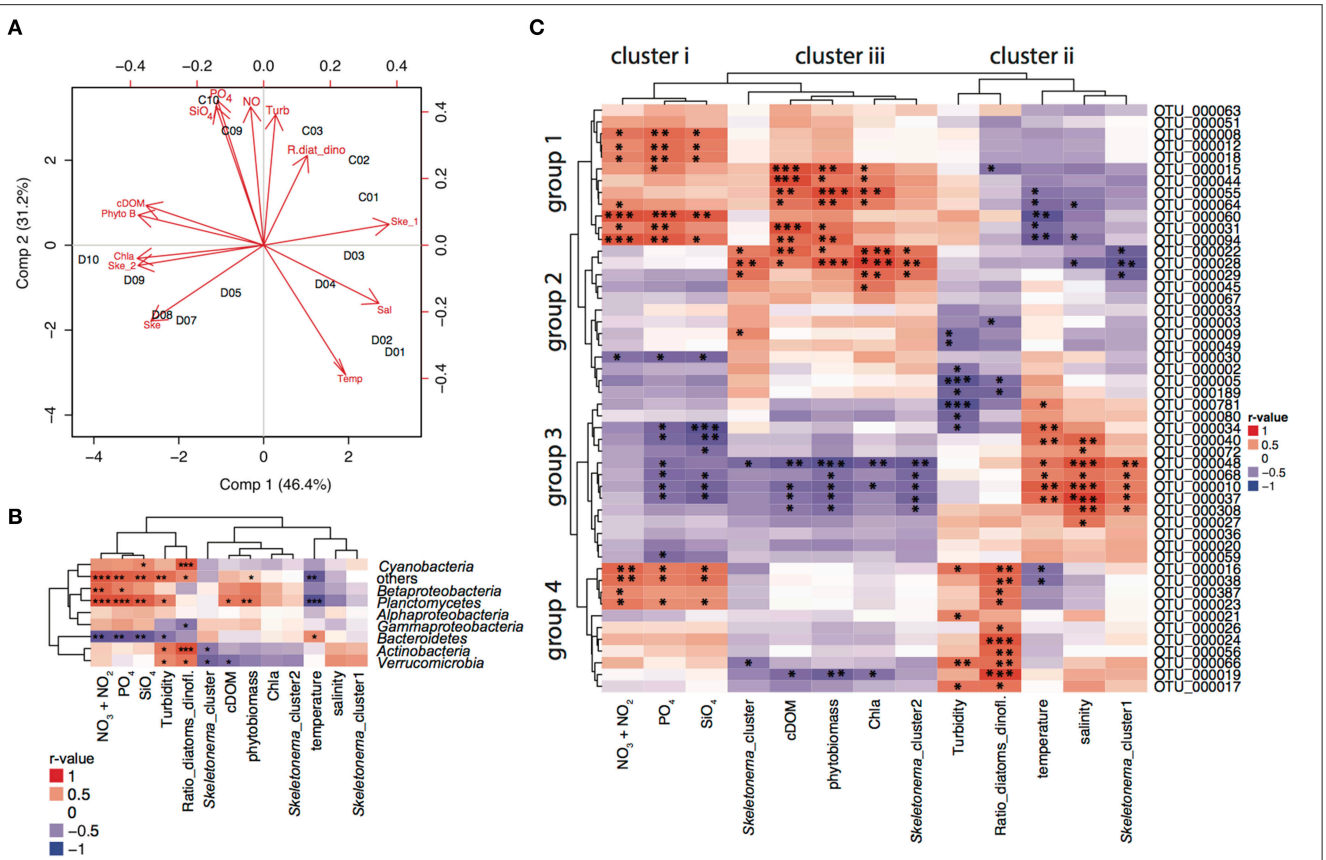

FIGURE 3 | PLSr and correlations to environmental variables. (A) Partial least squares regression analysis (PLSr) linking bacterial community composition (including all OTUs) with environmental variables and biotic factors in stations 1–3, 9–10 during cruise C, and 1–10 during cruise D. Red short labels describe the environmental variables (PO_4; phosphate, NO; nitrate and nitrite, SiO_4; silicate, Turb; turbidity, R.diat_dino; diatom/dinoflagelate ratio, cDOM; colored fluorescent DOM, Phyto B; phytoplankton biomass, Chla; chlorophyll a fluorescence, Ske_2; S. marinoi cluster 2, Ske; S. marinoi cluster, Temp; temperature, Sal; salinity, Ske_1; S. marinoi cluster 1) whereas black labels describe the sampling stations. **(B)** Correlation analysis between relative abundances of bacterial families and environmental variables based on Pearson correlations for relative abundances of bacterial families and environmental variables. Correlation values depict *r*-values of Pearson correlations and the dendograms are based on Pearson correlations. Statistical significance levels: $^{*}p < 0.05$, $^{**}p < 0.01$, $^{***}p < 0.001$. **(C)** Correlation analysis between relative abundances of 50 most abundant OTUs and environmental variables based on Pearson correlations. Correlation values depict *r*-values of Pearson correlations. Statistical significance levels: $^{*}p < 0.05$, $^{**}p < 0.01$, $^{***}p < 0.001$.

and 2 showed strong correlations with phytoplankton biomass. OTU_0022 (*Polaribacter*) was strongly correlated to chl*a*, *S. marinoi* cluster 2 and phytoplankton biomass (**Figure 3C**). OTU_0189 (*Pseudorhodobacter*) was ubiquitously found at all stations but was still negatively correlated to turbidity and diatom:dinoflagellate ratio. *S. marinoi* cluster 1 impacted strongly on several co-occuring *flavobacteria* (OTU_0048, OTU_0068, OTU_0010), *Comamonadaceae* BAL58, and one OTU annotated as *Candidatus aquiluna*.

OTUs Uniquely Associated to *S. marinoi* Populations

Within the *Alphaproteobacteria*, *Gammaproteobacteria,* and the *Flavobacteriia* family, numerous OTUs were commonly found at several stations during April, comprising >0.1% of relative abundances (**Figure 4**). To investigate if these showed unique abundance patterns correlating with the different genetic populations of *S. marinoi*, the sampling stations were grouped according to the dominant *S. marinoi* genetic cluster at each station. Twenty-five *Alphaproteobacteria* OTUs were shared among the two diatom populations, while 18 OTUs were uniquely found at stations where *S. marinoi* cluster 1 dominated. Three of these OTUs reached relative abundances >5% of the bacterial community. Of these, *Rhodobacteriaceae* (OTU_0017) and a member of the SAR11 clade annotated as Chesapeake-Delaware Bay (OTU_0015) co-occurred with *S.marinoi* cluster 1. *Pseudorhodobacter* (OTU_0189) on the other hand exhibited high abundances (>5%) during the second half of April at stations D1, D7, and D10, and was not uniquely associated with any *S. marinoi* cluster. Among *Gammaproteobacteria*, 25 OTUs occurred with both *S. marinoi* populations, nine OTUs were associated with station where *S. marinoi* cluster 1 dominated, and six OTUs were exclusive to the dominating *S. marinoi* cluster 2 found in the northern Baltic during cruise

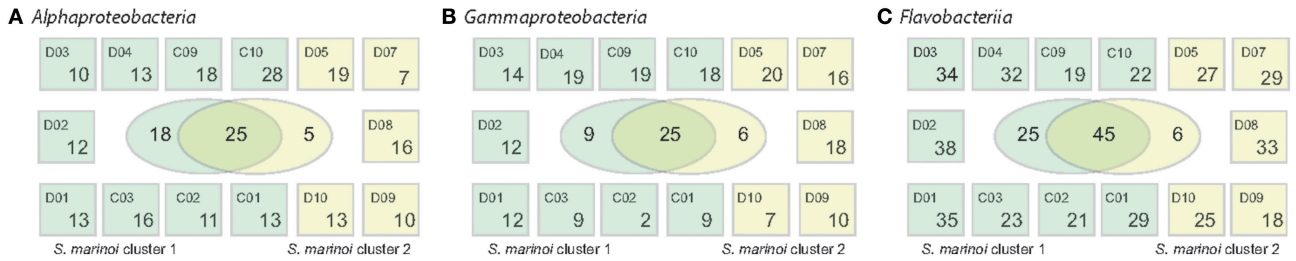

FIGURE 4 | Spatial distribution of OTUs across the Baltic Sea. (A) *Alphaproteobacteria*, **(B)** *Gammaproteobacteria*, and **(C)** *Flavobacteriia*. The Venn diagrams in the center of each panel depict the number of OTUs unique or shared between the stations where *S. marinoi* cluster 1 (dark green) or *S. marinoi* cluster 2 (light green) dominated. Small boxes depict how many OTUs of each major taxon that were detected at each station (numbers include OTUs that occur at single or multiple stations). Only OTUs with relative abundances >0.1% are included.

D. None of the gammaproteobacterial OTUs accounted for relative abundances >5%. Interestingly, *Flavobacteriia* showed an even stronger trend compared to the *Proteobacteria*, and 45 OTUs were shared between stations dominated by ether genetic clusters while 25 flavobacteriial OTUs were uniquely found at stations with a dominance of *S. marinoi* cluster 1. Four of the OTUs unique to *S. marinoi* cluster 1 accounted for >5% of the bacterial abundance (OTU_0036, OTU_0010, OTU_0068, OTU_0026). Three of the highly abundant OTUs were shared while *Polaribacter* (OTU_0022) was uniquely found at stations dominated by *S. marinoi* cluster 2.

DISCUSSION

In the present study we assessed the microbial community composition and co-occurrences on a spatio-temporal gradient during a Baltic Sea phytoplankton spring bloom. This analysis uncovered that bacterial community composition in the surface waters, both at the level of major families and at the level of individual populations (OTUs), was strongly correlated to various environmental variables. Most notably, bacterial community structure was associated with a number of variables directly related to phytoplankton, i.e., measures of chl*a*, phytoplankton biomass, diatom:dinoflagellate ratio, and *S. marinoi* population clusters. Secondly, the distribution of bacteria was also correlated with variables indirectly influenced by phytoplankton, including nutrient concentrations and DOM. Physicochemical variables, such as temperature and salinity also had additional but minor effects on bacterioplankton dynamics. We thus suggest that biotic and abiotic factors during spring bloom influence spatio-temporal bacterioplankton dynamics in a hierarchical manner.

The southern areas of the Baltic Sea are influenced by saline water inflows from the North Sea, and salinity decreases northwards. This strongly controls the distribution of phytoplankton in the Baltic Sea. For the diatom *S. marinoi*, which is typically a dominant component of Baltic Sea spring blooms, oceanographic connectivity and salinity are key determinants of population dynamics in space and time (Sjöqvist et al., 2015; Godhe et al., 2016). Salinity is a recognized overall driver also affecting the spatial distribution of bacterial populations in surface waters in the Baltic Sea, as shown for 16S rRNA gene amplicon and metagenome studies (Herlemann et al., 2011; Dupont et al., 2014). These spatial studies were undertaken during summer when environmental conditions are relatively stable in stratified surface waters. Laboratory experiments have shown a similar trend, in that salinity can act as a selective force for bacterial community compositions (Langenheder et al., 2003; Kaartokallio et al., 2005). During our spring study on the other hand, salinity and oceanic connectivity varied minimally over time, although the salinity gradient affected bacteria at the spatial scale (Gulf of Finland and southern Baltic). Therefore, the observed changes in bacterioplankton community composition over time indicated that salinity (or temperature) were minor determinants shaping bacterial temporal dynamics. This substantiated that phytoplankton played a major role for structuring bacterioplankton composition.

Various seasonal studies and laboratory mesocosm experiments have established that peaks in phytoplankton blooms are followed by elevated bacterial production and abundance (see for example: Cole, 1982; Brussaard et al., 1996; Riemann et al., 2000; Pinhassi et al., 2004; Lindh et al., 2014). In our study, bacterial community composition was linked to phytoplankton biomass and chl*a*, whereas bacterial abundance was not. Though phytoplankton biomass was higher in the Gulf of Finland, bacteria did not show as high abundance as in the south, possibly due to lower temperature. Diatom:dinoflagellate ratio is a measure for phytoplankton community composition and succession of the bloom and correlated to the bacterioplankton community composition. Different phytoplankton groups are commonly accompanied by specific bacterial taxa (Pinhassi et al., 2004; Amin et al., 2012; Buchan et al., 2014). Diatoms are often associated with *Alphaproteobacteria* and *Bacteroidetes* (Amin et al., 2012), while mainly *Flavobacteria* (*Bacteroidetes*) have been shown to co-occur with the particle fraction of a dinoflagellate bloom (Fandino et al., 2001). At the family level of resolution, *Bacteroidetes* did not show significant correlations to phytoplankton biomass or the diatom:dinoflagellate ratio. Still, among the most abundant specific bacterial populations, such associations were observed. For example, three bacterial

populations (*Bacteroidetes*, *Alphaproteobacteria*, *Cyanobacteria*) showed preferences for only high diatom:dinoflagellate ratios, whereas two *Bacteroidetes* OTUs were associated with more even ratios. Notably, those bacteria were not correlated to phytoplankton biomass or chl*a*, but mainly to phytoplankton groups. These findings emphasize the importance of phytoplankton species composition, not solely phytoplankton biomass, for determining bacterioplankton community composition.

During the spring bloom, the contrasting influence of oceanic and coastal factors is recognized to determine the distribution of the two genotypically distinct populations of the diatom *S. marinoi* population (denoted cluster 1 and 2; Godhe et al., 2016). The bloom in the southern Baltic was dominated by *S. marinoi* cluster 1, influenced by mainly oceanic features like higher salinity and temperature and lower chl*a*. Accompanying this diatom cluster was a higher richness of *Alphaproteobacteria*, *Gammaproteobacteria,* and *Flavobacteriia*. This might result in a high diversification of metabolic strategies of bacterioplankton feeding on the wide spectrum of DOM compounds so as not to waste valuable, good quality DOM and their associated bacterioplankton communities.

Skeletonema marinoi cluster 2 was accompanied by coastal features such as cDOM from land runoff, exceeding 50% of marine DOM in the Baltic Sea (Deutsch et al., 2012), low temperatures due to late ice melt, and relatively high nutrients and chl*a.* Bacteria associated with *S. marinoi* cluster 2 therefore likely benefit from both phytoplankton DOM and terrestrial DOM. *Flavobacteriia*, *Alphaproteobacteria,* and *Gammaproteobacteria* showed a lower richness at stations where *S. marinoi* cluster 2 dominated the diatom population. This lower richness could be due to a slight delay of the bacteria responding to the bloom and diatom cluster 2 and low temperatures, but since *S. marinoi* strains co-occur in all stations, this does not seem likely. A delayed response in bacterial richness, commonly observed during phytoplankton blooms (Buchan et al., 2014), seems instead to be linked to gene cluster dominance and not to the succession of gene clusters.

Our study revealed a potential influence of phytoplankton genotypes on bacterial populations. Accordingly, several bacterial OTUs showed distinct distributions associated to *S. marinoi* genotypes. A number of papers indicate direct interactions between phytoplankton and bacteria (Delucca and McCracken, 1977; Amin et al., 2015; Durham et al., 2015) and point to molecular mechanisms as possible explanations for the tight correlations observed in this study. Overall correlations of major phytoplankton and bacterial groups, and additionally more taxonomically restricted relations support the hypothesis that such interactions are important in structuring microbial communities in the sea.

Phytoplankton indirectly affects DOM concentrations by using up available nutrients and producing organic molecules during photosynthesis. Commonly, phytoplankton blooms release up to 20% of their daily primary production as dissolved organic matter (DOM) into the water (Baines and Pace, 1991; Wear et al., 2015), and create an environment with niches that are exploited by numerous, opportunistic bacteria (Bell and Lang, 1974; Gilbert et al., 2012; Martin, 2012; Teeling et al., 2012; Needham et al., 2013). Marine bacteria utilize various DOM compounds, leading to complex community dynamics (composition, taxa abundance and richness) during the duration of phytoplankton blooms (Riemann et al., 2000; Pinhassi et al., 2004; Buchan et al., 2014). In our study, high abundance of opportunistic *Flavobacteriia* and an increase in *Alphaproteobacteria* were observed during late April, coinciding with a detected depletion of inorganic nutrients. Thus, it appears that inorganic nutrient concentrations, together with an increase of DOM, fuelled bacterial growth and affected bacterial community composition. Increases in DOM lead to remineralization of nutrients and possibly prolong the growth phase of both phytoplankton and bacterioplankton, which in turn can increase the activity of the microbial loop.

In offshore waters of the central Baltic Sea, the bacterial community composition was distinct in comparison to the ones from the coastal basins (Gulf of Finland and southern Baltic Proper, **Figure 2B**). The presence of three highly abundant *Bacteroidetes* populations (OTU_0009, OTU_0002, OTU_0005) associated with low turbidity, but not phytoplankton biomass. This suggests that this community dominated by *Bacteroidetes* could be a relict from overwintering, or characteristic of a bacterial community composition during early spring bloom initiation. Unfortunately, our data timeline (March–April) did not include these bloom stages in the coastal areas, hence limiting the comparison. However, the coastal to offshore gradient in the Baltic Sea, although small compared to oceanic province, still is relevant to explain the succession of microbial populations, including phytoplankton and bacterioplankton.

The contribution of *Actinobacteria* to the total bacterial community in the Gulf of Finland, as compared to *Flavobacteria*, was lower than expected. *Actinobacteria* commonly display high abundances in low salinity habitats of the Baltic Sea (Herlemann et al., 2011; Dupont et al., 2014). This can partly be explained by the increased contribution of *Flavobacteria* to the bacterial community composition following the bloom. *Flavobacteria* and other bacterial groups may be better or faster at using phytoplankton exudates. In fact, a recent study reported that *Actinobacteria* from the Baltic Sea seem to use lipids, rather than carbohydrates as a carbon source and are found more abundantly during the second half of the year and not during spring (Hugerth et al., 2015). The Luna bacteria, a subgroup of *Actinobacteria*, coincided with phytoplankton blooms, though these were different populations with distinctive metabolic features compared to the summer group (Hugerth et al., 2015). Moreover, one *Polaribacter* population reoccurs at high abundance during spring in the Gulf of Finland (Laas et al., 2015), indicating that this taxon is highly linked to coastal conditions. However, the relative abundance of this taxon is lower during other times of the year (Laas et al., 2015). In our study, a *Polaribacter* population was highly abundant in the Gulf of Finland and correlated to several coastal features, especially chl*a*, illustrating a tight coupling to spring phytoplankton biomass and possibly dinoflagellates. Consequently, synergistic effects of multiple direct and indirect bloom related factors, likely influence

actinobacterial and overall bacterioplankton dynamics during spring.

CONCLUSIONS

Our study revealed a complex array of interactions and interdependence of bacterial populations with intra-specific diversity of phytoplankton groups. Variables related to the spring bloom progression were of principal importance for determining bacterioplankton composition. In the Baltic Sea, oceanographic connectivity and salinity shape two different *S. marinoi* populations co-occurring with distinct bacterial communities. In large spring blooms, interactions between bacteria with distinct niches and specific phytoplankton populations may have implications for biomass production and cycling of energy to higher trophic levels. Altogether, our novel findings imply that biotic and abiotic factors during spring bloom influence overall bacterial community dynamics in a hierarchical manner.

AUTHOR CONTRIBUTIONS

AG, KR, AK, CL, and NL conceived the study, CB and CL designed research, CB, MB-F, CL, CS, JS, NL, and SG performed sampling, CB and MB-F performed molecular analysis, SS and IL counted phytoplankton samples, CB, MB-F, IS, CS, JP, and CL analyzed data, CB, MB-F, JP, and CL wrote the paper. All authors discussed the results and commented on the manuscript.

FUNDING

The study was funded by grants from the Nordforsk research network (PRODIVERSA), the Swedish Research Council Formas through the Strong Research Environment ECOCHANGE to CL and JP, institutional research funding (IUT 19-6) of the Estonian Ministry of Education and Research, and the Centre for Ecology and Evolution in Microbial Model Systems (EEMiS) at Linnaeus University. AK and CS received funding from the Academy of Finland grants 283061 and 251564.

ACKNOWLEDGMENTS

We would like to thank Finnlines, especially the crew of MS Finnmaid for the opportunities to use the boat facilities, and the Algaline monitoring service for support. We acknowledge Sara Harðardóttir, Petri Manula, Pia Varmanen, and Matthias Fast for sampling and technical support onboard, nutrient analysis and sample processing. We greatly thank Daniel Lundin for bioinformatical discussions and Caroline Littlefield Karlsson for language editing. We thank two anonymous reviewers for constructive comments improving the manuscript.

SUPPLEMENTARY MATERIAL

The Supplementary Material for this article can be found online at: http://journal.frontiersin.org/article/10.3389/fmicb.2016.00517

REFERENCES

Almany, G. R., De Arruda, M. P., Arthofer, W., Atallah, Z., Beissinger, S. R., Berumen, M. L., et al. (2009). Permanent genetic resources added to molecular ecology resources database 1 May 2009–31 July 2009. *Mol. Ecol. Resour.* 9, 1460–1466. doi: 10.1111/j.1755-0998.2009.02759.x

Altschul, S. F., Gish, W., Miller, W., Myers, E. W., and Lipman, D. J. (1990). Basic local alignment search tool. *J. Mol. Biol.* 215, 403–410. doi: 10.1016/S0022-2836(05)80360-2

Amin, S. A., Hmelo, L. R., van Tol, H. M., Durham, B. P., Carlson, L. T., Heal, K. R., et al. (2015). Interactions and signalling between a cosmopolitan phytoplankton and associated bacteria. *Nature* 522, 98–101. doi: 10.1038/nature14488

Amin, S. A., Parker, M. S., and Armbrust, E. V. (2012). Interactions between diatoms and bacteria. *Microbiol. Mol. Biol. Rev.* 76, 667–684. doi: 10.1128/MMBR.00007-12

Andersson, A. F., Riemann, L., and Bertilsson, S. (2010). Pyrosequencing reveals contrasting seasonal dynamics of taxa within Baltic Sea bacterioplankton communities. *ISME J.* 4, 171–181. doi: 10.1038/ismej.2009.108

Auguie, B. (2015). *Gridextra: Miscellaneous Functions for "Grid" Graphics. R Package Version 200.* Available online at: http://CRAN.R-project.org/package=gridExtra

Baines, S. B., and Pace, M. L. (1991). The production of dissolved organic matter by phytoplankton and its importance to bacteria: patterns across marine and freshwater systems. *Limnol. Oceanogr.* 36, 1078–1090. doi: 10.4319/lo.1991.36.6.1078

Bell, W. H., and Lang, J. M. (1974). Selective stimulation of marine bacteria by algal extracellular products. *Limnol. Oceanogr.* 19, 833–839. doi: 10.4319/lo.1974.19.5.0833

Boström, K. H., Simu, K., Hagström, Å., and Riemann, L. (2004). Optimization of DNA extraction for quantitative marine bacterioplankton community analysis. *Limnol. Oceanogr. Methods* 2, 365–373. doi: 10.4319/lom.2004.2.365

Bray, J. R., and Curtis, J. T. (1957). An ordination of the upland forest communities of southern Wisconsin. *Ecol. Monographs* 27, 325–349. doi: 10.2307/1942268

Brussaard, C. P. D., Gast, G. J., van Duyl, F. C., and Riegman, R. (1996). Impact of phytoplankton bloom magnitude on a pelagic microbial food web. *Mar. Ecol. Prog. Ser.* 144, 211–221. doi: 10.3354/meps144211

Buchan, A., LeCleir, G. R., Gulvik, C. A., and González, J. M. (2014). Master recyclers: features and functions of bacteria associated with phytoplankton blooms. *Nat. Rev. Microbiol.* 12, 686–698. doi: 10.1038/nrmicro3326

Cole, J. J. (1982). Interactions between bacteeria and algae in aquatic ecosystems. *Annu. Rev. Ecol. Syst.* 13, 291–314. doi: 10.1146/annurev.es.13.110182.001451

Delucca, R., and McCracken, M. D. (1977). Observations on interactions between naturally-collected bacteria and several species of algae. *Hydrobiologia* 55, 71–75. doi: 10.1007/BF00034807

Deutsch, B., Alling, V., Humborg, C., Korth, F., and Mörth, C. (2012). Tracing inputs of terrestrial high molecular weight dissolved organic matter within the Baltic Sea ecosystem. *Biogeosciences* 9, 4465–4475. doi: 10.5194/bg-9-4465-2012

Dupont, C. L., Larsson, J., Yooseph, S., Ininbergs, K., Goll, J., Asplund-Samuelsson, J., et al. (2014). Functional tradeoffs underpin salinity-driven divergence in microbial community composition. *PLoS ONE* 9:e89549. doi: 10.1371/journal.pone.0089549

Durham, B. P., Sharma, S., Luo, H., Smith, C. B., Amin, S. A., Bender, S. J., et al. (2015). Cryptic carbon and sulfur cycling between surface ocean plankton. *Proc. Natl. Acad. Sci. U.S.A.* 112, 453–457. doi: 10.1073/pnas.1413137112

Edgar, R. C. (2013). Uparse: highly accurate OTU sequences from microbial amplicon reads. *Nat. Methods* 10, 996–998. doi: 10.1038/nmeth.2604

Fandino, L. B., Riemann, L., Steward, G. F., and Azam, F. (2005). Population dynamics of cytophaga-flavobacteria during marine phytoplankton blooms analyzed by real-time quantitative PCR. *Aquat. Microb. Ecol.* 40, 251–257. doi: 10.3354/ame040251

Fandino, L. B., Riemann, L., Steward, G. F., Long, R. A., and Azam, F. (2001). Variations in bacterial community structure during a dinoflagellate bloom

analyzed by DGGE and 16s rDNA sequencing. *Aquat. Microb. Ecol.* 23, 119. doi: 10.3354/ame023119

Gentleman, R. C., Carey, V. J., Bates, D. M., Bolstad, B., Dettling, M., Dudoit, S., et al. (2004). Bioconductor: open software development for computational biology and bioinformatics. *Genome Biol.* 5:R80. doi: 10.1186/gb-2004-5-10-r80

Gilbert, J. A., Steele, J. A., Caporaso, J. G., Steinbrück, L., Reeder, J., Temperton, B., et al. (2012). Defining seasonal marine microbial community dynamics. *ISME J.* 6, 298–308. doi: 10.1038/ismej.2011.107

Godhe, A., Sjöqvist, C., Sildever, S., Sefbom, J., Harðardóttir, S., Bertos-Fortis, M., et al. (2016). Physical barriers and environmental gradients cause spatial and temporal genetic differentiation of an extensive algal bloom. *J. Biogeogr.* doi: 10.1111/jbi.12722. [Epub ahead of print].

Gómez-Consarnau, L., Lindh, M. V., Gasol, J. M., and Pinhassi, J. (2012). Structuring of bacterioplankton communities by specific organic carbon compounds. *Environ. Microbiol.* 14, 2361–2378. doi: 10.1111/j.1462-2920.2012.02804.x

Grasshoff, K., Erhardt, M., and Kremling, K. (1983). *Methods of Seawater Analyses*. Weinheim: Verlag Chemie.

Gu, Z. (2015). *Complexheatmap: Making Complex Heatmaps. R package version 100.* Available online at: https://github.com/jokergoo/ComplexHeatmap

Herlemann, D. P., Labrenz, M., Jürgens, K., Bertilsson, S., Waniek, J. J., and Andersson, A. F. (2011). Transitions in bacterial communities along the 2000 km salinity gradient of the Baltic Sea. *ISME J.* 5, 1571–1579. doi: 10.1038/ismej.2011.41

Hugerth, L. W., Larsson, J., Alneberg, J., Lindh, M. V., Legrand, C., Pinhassi, J., et al. (2015). Metagenome-assembled genomes uncover a global brackish microbiome. *Genome Biol.* 16, 279. doi: 10.1186/s13059-015-0834-7

Johannesson, K., and Andre, C. (2006). Life on the margin: genetic isolation and diversity loss in a peripheral marine ecosystem, the Baltic Sea. *Mol. Ecol.* 15, 2013–2029. doi: 10.1111/j.1365-294X.2006.02919.x

Jørgensen, H. B., Hansen, M. M., Bekkevold, D., Ruzzante, D. E., and Loeschcke, V. (2005). Marine landscapes and population genetic structure of herring (*Clupea harengus* l.) in the Baltic Sea. *Mol. Ecol.* 14, 3219–3234. doi: 10.1111/j.1365-294X.2005.02658.x

Kaartokallio, H., Laamanen, M., and Sivonen, K. (2005). Responses of Baltic Sea ice and open-water natural bacterial communities to salinity change. *Appl. Environ. Microbiol.* 71, 4364–4371. doi: 10.1128/AEM.71.8.4364-4371.2005

Krzywinski, M. I., Schein, J. E., Birol, I., Connors, J., Gascoyne, R., Horsman, D., et al. (2009). An information aesthetic for comparative genomics. *Genome Res.* 19, 1639–1645. doi: 10.1101/gr.092759.109

Laas, P., Simm, J., Lips, I., Lips, U., Kisand, V., and Metsis, M. (2015). Redox-specialized bacterioplankton metacommunity in a temperate estuary. *PLoS ONE* 10:e0122304. doi: 10.1371/journal.pone.0122304

Langenheder, S., Kisand, V., Wikner, J., and Tranvik, L. J. (2003). Salinity as a structuring factor for the composition and performance of bacterioplankton degrading riverine DOC. *FEMS Microbiol. Ecol.* 45, 189–202. doi: 10.1016/S0168-6496(03)00149-1

Legrand, C., Fridolfsson, E., Bertos-Fortis, M., Lindehoff, E., Larsson, P., Pinhassi, J., et al. (2015). Interannual variability of phyto-bacterioplankton biomass and production in coastal and offshore waters of the Baltic Sea. *Ambio* 44, 427–438. doi: 10.1007/s13280-015-0662-8

Lindh, M. V., Figueroa, D., Sjöstedt, J., Baltar, F., Lundin, D., Andersson, A., et al. (2015). Transplant experiments uncover Baltic Sea basin specific responses in bacterioplankton community composition and metabolic activities. *Front. Microbiol.* 6:223. doi: 10.3389/fmicb.2015.00223

Lindh, M. V., Sjöstedt, J., Andersson, A. F., Baltar, F., Hugerth, L. W., Lundin, D., et al. (2014). Disentangling seasonal bacterioplankton population dynamics by high frequency sampling. *Env. Microbiol.* 17, 2459–2476. doi: 10.1111/1462-2920.12720

Martin, A. (2012). The seasonal smorgasbord of the seas. *Science* 337, 46–47. doi: 10.1126/science.1223881

Mevik, B., Wehrens, R., and Hovde Liland, K. (2015). *Pls: Partial Least Squares and Principal Component Regression. R package version 25-0.* Available online at: http://CRAN.R-project.org/package=pls

NCBI Resource Coordinators (2013). Database resources of the national center for biotechnology information. *Nucleic Acids Res.* 41, D8–D20. doi: 10.1093/nar/gks1189

Needham, D. M., Chow, C.-E. T., Cram, J. A., Sachdeva, R., Parada, A., and Fuhrman, J. A. (2013). Short-term observations of marine bacterial and viral communities: patterns, connections and resilience. *ISME J.* 7, 1274–1285. doi: 10.1038/ismej.2013.19

Neuwirth, E. (2014). *Rcolorbrewer: Colorbrewer Palettes. R Package Version 11-2.* Available online at: http://CRAN.R-project.org/package=RColorBrewer

Oksanen, J., Kindt, R., Legendre, P., O'Hara, B., Stevens, M. H. H., Oksanen, M. J., et al. (2007). *The Vegan Package: Community Ecology Package. R Package Version 117-5.* Available online at: http://vegan.r-forge.r-project.org/

Olenina, I., Hajdu, S., Edler, L., Andersson, A., Wasmund, N., Busch, S., et al. (2006). Biovolumes and size-classes of phytoplankton in the Baltic Sea. *HELCOM Balt. Sea Environ. Proc.* 106:144.

Pinhassi, J., Sala, M. M., Havskum, H., Peters, F., Guadayol, O., Malits, A., et al. (2004). Changes in bacterioplankton composition under different phytoplankton regimens. *Appl. Environ. Microbiol.* 70, 6753–6766. doi: 10.1128/AEM.70.11.6753-6766.2004

Pritchard, J. K., Stephens, M., and Donnelly, P. (2000). Inference of population structure using multilocus genotype data. *Genetics* 155, 945–959. Available online at: http://www.genetics.org/content/155/2/945.article-info

Pruesse, E., Peplies, J., and Glöckner, F. O. (2012). Sina: accurate high-throughput multiple sequence alignment of ribosomal rna genes. *Bioinformatics* 28, 1823–1829. doi: 10.1093/bioinformatics/bts252

Rantajärvi, E. (2003). *Alg@line in 2003: 10 Years of Innovative Plankton Monitoring and Research and Operational Information Service in the Baltic Sea.* Finish Institute of Marine Research, Helsinki.

Riemann, L., Steward, G. F., and Azam, F. (2000). Dynamics of bacterial community composition and activity during a mesocosm diatom bloom. *Appl. Env. Microbiol.* 66, 578–587. doi: 10.1128/AEM.66.2.578-587.2000

Saravanan, V., and Godhe, A. (2010). Genetic heterogeneity and physiological variation among seasonally separated clones of *Skeletonema marinoi* (bacillariophyceae) in the Gullmar Fjord, Sweden. *Eur. J. Phycol.* 45, 177–190. doi: 10.1080/09670260903445146

Schlitzer, R. (2014). *Ocean Data View*. Available online at: http://odvawide

Sjöqvist, C., Godhe, A., Jonsson, P. R., Sundqvist, L., and Kremp, A. (2015). Local adaptation and oceanographic connectivity patterns explain genetic differentiation of a marine diatom across the North Sea–Baltic Sea salinity gradient. *Mol. Ecol.* 24, 2871–2885. doi: 10.1111/mec.13208

Teeling, H., Fuchs, B. M., Becher, D., Klockow, C., Gardebrecht, A., Bennke, C. M., et al. (2012). Substrate-controlled succession of marine bacterioplankton populations induced by a phytoplankton bloom. *Science* 336, 608–611. doi: 10.1126/science.1218344

Wasmund, N., Nausch, G., and Matthäus, W. (1998). Phytoplankton spring blooms in the Southern Baltic Sea spatio-temporal development and long-term trends. *J. Plankton Res.* 20, 1099–1117. doi: 10.1093/plankt/20.6.1099

Wear, E. K., Carlson, C. A., James, A. K., Brzezinski, M. A., Windecker, L. A., and Nelson, C. E. (2015). Synchronous shifts in dissolved organic carbon bioavailability and bacterial community responses over the course of an upwelling-driven phytoplankton bloom. *Limnol. Oceanogr.* 60, 657–677. doi: 10.1002/lno.10042

Wickham, H. (2009). *Ggplot2: Elegant Graphics For Data Analysis.* New York, NY: Springer. Available online at: https://cran.r-project.org/web/packages/ggplot2/index.html

Wickham, H., and Francois, R. (2015). *Dplyr: A Grammar of Data Manipulation. R Package Version 043.* Available online at: http://CRAN.R-project.org/package=dplyr

Conflict of Interest Statement: The authors declare that the research was conducted in the absence of any commercial or financial relationships that could be construed as a potential conflict of interest.

frontiers in Microbiology

ORIGINAL RESEARCH
published: 08 June 2016
doi: 10.3389/fmicb.2016.00828

Indole-3-Acetic Acid Is Produced by *Emiliania huxleyi* Coccolith-Bearing Cells and Triggers a Physiological Response in Bald Cells

*Leen Labeeuw[1], Joleen Khey[1], Anna R. Bramucci[1], Harjot Atwal[1], A. Paulina de la Mata[2], James Harynuk[2] and Rebecca J. Case[1]**

[1] Department of Biological Sciences, University of Alberta, Edmonton, AB, Canada, [2] Department of Chemistry, University of Alberta, Edmonton, AB, Canada

OPEN ACCESS

Edited by:
Xavier Mayali, Lawrence Livermore National Laboratory, USA

Reviewed by:
Shady A. Amin, New York University Abu Dhabi, UAE
Ludovic Delage, Centre National de la Recherche Scientifique, France

***Correspondence:**
Rebecca J. Case
rcase@ualberta.ca

Specialty section:
This article was submitted to Aquatic Microbiology, a section of the journal Frontiers in Microbiology

Received: *13 January 2016*
Accepted: *17 May 2016*
Published: *08 June 2016*

Citation:
Labeeuw L, Khey J, Bramucci AR, Atwal H, de la Mata AP, Harynuk J and Case RJ (2016) Indole-3-Acetic Acid Is Produced by Emiliania huxleyi Coccolith-Bearing Cells and Triggers a Physiological Response in Bald Cells. Front. Microbiol. 7:828. doi: 10.3389/fmicb.2016.00828

Indole-3-acetic acid (IAA) is an auxin produced by terrestrial plants which influences development through a variety of cellular mechanisms, such as altering cell orientation, organ development, fertility, and cell elongation. IAA is also produced by bacterial pathogens and symbionts of plants and algae, allowing them to manipulate growth and development of their host. They do so by either producing excess exogenous IAA or hijacking the IAA biosynthesis pathway of their host. The endogenous production of IAA by algae remains contentious. Using *Emiliania huxleyi*, a globally abundant marine haptophyte, we investigated the presence and potential role of IAA in algae. Homologs of genes involved in several tryptophan-dependent IAA biosynthesis pathways were identified in *E. huxleyi.* This suggests that this haptophyte can synthesize IAA using various precursors derived from tryptophan. Addition of L-tryptophan to *E. huxleyi* stimulated IAA production, which could be detected using Salkowski's reagent and GC×GC-TOFMS in the C cell type (coccolith bearing), but not in the N cell type (bald). Various concentrations of IAA were exogenously added to these two cell types to identify a physiological response in *E. huxleyi*. The N cell type, which did not produce IAA, was more sensitive to it, showing an increased variation in cell size, membrane permeability, and a corresponding increase in the photosynthetic potential quantum yield of Photosystem II (PSII). A roseobacter (bacteria commonly associated with *E. huxleyi*) *Ruegeria* sp. R11, previously shown to produce IAA, was co-cultured with *E. huxleyi* C and N cells. IAA could not be detected from these co-cultures, and even when stimulated by addition of L-tryptophan, they produced less IAA than axenic C type culture similarly induced. This suggests that IAA plays a novel role signaling between different *E. huxleyi* cell types, rather than between a bacteria and its algal host.

Keywords: algae, auxin, cell type, coccolith, *Emiliania huxleyi*, haptophyte, indole-3-acetic acid (IAA), phytohormone

INTRODUCTION

Small signaling molecules are important components of inter-species interactions, and have been shown to play a role in multicellularity, settlement, and pathogenesis (Joint et al., 2002; Manefield et al., 2002; Matsuo et al., 2005; Schaefer et al., 2008). While these interactions occur at the cell-to-cell interface, they can have large-scale effects at the community and ecosystem levels (Charlson et al., 1987; Vardi et al., 2009; Cooper and Smith, 2015). Many of these small molecules are specific in their mode of action, and can be restricted to a specific sub-population of cells in an organism. Current research indicates that signaling molecules are important components of inter-kingdom communication in bacterial-host systems (Hughes and Sperandio, 2008). One such group of small molecules, which is well-studied in plants, is the phytohormone indole-3-acetic acid (IAA). IAA is one of the most abundant and important plant auxins, and also among the first plant hormones to be discovered (Went, 1926; Teale et al., 2006). Auxins are responsible for growth and development, such as in tissue differentiation, fertility, cell division, orientation, and enlargement in terrestrial plants (Lau et al., 2009; Zhao, 2010; Finet and Jaillais, 2012). Although auxins were originally thought to exist only in plants, their biosynthetic pathway has since been characterized in bacteria and fungi (Spaepen et al., 2007). However, much of what is known about IAA's physiological roles comes from studies of plants' responses to exogenous IAA (Sakata et al., 2010). Indeed, IAA has commercial use and is frequently sprayed over agricultural fields to increase crop yields (Sudha et al., 2012).

At elevated levels, IAA can cause physiological damage. For instance, IAA stimulates the production of ethylene, which inhibits plant growth (Xie et al., 1996). It has also been implicated in pathogenesis of plants, as bacterial symbionts have the potential to take over the plant biosynthetic pathway (Yamada et al., 1985; Yamada, 1993) and produce it in plant hosts (Patten and Glick, 2002; Gravel et al., 2007). The diverse effects on the host (ranging from stimulation to pathogenesis) depends on the amount of free IAA produced, as well as the host's sensitivity to this compound (Spaepen et al., 2007). Pathogenic bacteria can alter host metabolic processes for their own benefit, such as by up-regulating the production of IAA, which produces uncontrolled cellular division leading to gall disease in plants (Escobar and Dandekar, 2003). A well-studied example of this pathogenic strategy is the crown gall disease caused by *Agrobacterium tumefaciens,* which involves the formation of galls on the lower stem and roots of infected plants (Zhu et al., 2000; Escobar and Dandekar, 2003). *A. tumefaciens* hijacks the infected plant cells to promote unregulated growth, resulting in the formation of galls, which act as nutrient factories producing amino acids and sugar derivatives that the pathogen uses for energy (Zhu et al., 2000).

In algae, bacterially-produced auxins have been implicated in bud induction in the macroalgal rhodophyte *Gracilaria dura* (Singh et al., 2011). Roseobacters, a clade of marine α-proteobacteria, have been shown to produce IAA or alter its production by a host. Bacterial cells identified as roseobacters using FISH have been localized to the intercellular spaces within galls, in the red macroalga *Prionitis lanceolata* (Ashen and Goff, 2000). These galls have elevated levels of IAA; however it is not known if the bacterium or algal host produce the IAA as neither has been isolated as an axenic culture (Ashen et al., 1999). Both micro- and macroalgal chlorophytes have shown sensitivity and increased growth when exposed to exogenous IAA (Jin et al., 2008; Salama et al., 2014). Amin et al. (2015) recently demonstrated the role IAA plays between the unicellular diatom *Pseudo-nitzschia multiseries* and its associated bacterial community, specifically looking at the roseobacter, *Sulfitobacter* sp. SA11. They showed an up-regulation of tryptophan synthesis in the alga led to a corresponding increase in IAA production by the bacterium, which in turn acted as an inter-kingdom signaling molecule that increased growth of *Pseudo-nitzschia* (Amin et al., 2015). It's perhaps serendipitous that roseobacters were first coined marine *Agrobacterium* as the similarity of the roseobacter—algae interaction to the *A. tumefaciens*—plant host system is striking (Ahrens and Rheinheimer, 1967). Another roseobacter, *Ruegeria* sp. R11, is a known algal pathogen and produces IAA (Case et al., 2011; Fernandes et al., 2011; Mayers et al., 2016), although the role IAA plays in this interaction (if any) is unknown.

The question of whether eukaryotic algae produce IAA remains largely unresolved (Cooke et al., 2002; Lau et al., 2009; Ross and Reid, 2010). Commercially, addition of algal extracts has been claimed to induce growth responses in plants characteristic of auxins (Crouch and Van Staden, 1993). A vast body of studies spanning from the 1940s to the present have reported IAA in various unicellular and multicellular forms of brown, green, and red algae (Van Overbeek, 1940; Jacobs et al., 1985; Sanderson et al., 1987; Tarakhovskaya et al., 2007; Lau et al., 2009). The different lifestyles and forms of multicellular macroalgae compared to unicellular microalgae suggest that IAA would play a different signaling role in these organisms, as cell growth, fertility, and development occur within a macroorganism and between microorganisms within a population. The differences of IAA signaling at the intra-and inter-organismal level will be key to understanding its role in micro- and macroalgae.

In macroalgae, IAA was detected in the brown algae *Fucus distichus* and *Ectocarpus siliculosus* (Basu et al., 2002; Le Bail et al., 2010), as well as in the red algae *Pyropia yezoensis* and *Bangia fuscopurpurea* (Mikami et al., 2015). *Nitella*, which is part of Charophyta, the algal phylum most closely related to land plants has also been suggested to produce IAA. This suggests that primitive auxin metabolism was present at least as early as the ancestor of land plants and charophytes (Sztein et al., 2000). De Smet et al. (2011) found putative auxin biosynthesis and auxin transporter orthologs encoded in unicellular chlorophyte genomes. IAA has also been detected in various microalgal chlorophytes, including *Chlorella pyrenoidosa* and *Scenedesmus* spp. (Mazur et al., 2001; Prieto et al., 2011). These studies have found evidence corroborating the hypothesis that evolution of auxin biosynthesis predates the divergence of land plants and some algal taxa. However, many of these studies used non-axenic algal cultures, and as some algae-associated bacteria produce auxins (Evans and Trewavas, 1991; Fernandes et al., 2011; Bagwell et al., 2014; Dittami et al., 2014; Amin et al., 2015), it remains

unknown if these studies are reporting auxin concentrations from the alga itself or its bacterial epiphytes. Furthermore, the concentration of IAA observed in some studies may not be high enough to play a role in algal development (Lau et al., 2009). It is possible that multi-step IAA extractions underestimates the auxin concentration due to degradation of IAA during the procedure (Mazur et al., 2001). Auxins could also be concentrated within specific algal structures or cells, making whole plant extractions an underestimation of local concentrations within the alga. Nonetheless, Lau et al. (2009) and Ross and Reid (2010) expressed reservations regarding evidence for IAA biosynthesis by algae described in literature, especially microalgae, which they reported to lack auxin signaling pathways homologous to those present in land plants.

Using bioinformatics and empirical experimentation, this study aims to elucidate the presence and function of IAA in a unicellular algal species, *Emiliania huxleyi*. This microalga is a small (5 μm), globally abundant haptophyte, part of a different eukaryotic supergroup than all other algae so far investigated for the presence of IAA (Archibald, 2009). It is also a major primary producer in oceans and plays a substantial role in the carbon and sulfur cycles (Holligan et al., 1993). It has three distinct cell types: the non-motile diploid bald cells (type N), the coccolith producing cells (type C), and the haploid motile type cells (type S) (Klaveness and Paasche, 1971; Laguna et al., 2001).

We identified homologs for the genes of several complete tryptophan dependant IAA biosynthesis pathways in the genome of *E. huxleyi*. To confirm this genotype, axenic cultures of C and N type *E. huxleyi* cell types were screened for the production of IAA after stimulation with L-tryptophan. These cell types were also exposed to exogenous IAA to look at their phenotypic response. Interestingly, only C type cells were able to produce IAA and only N type cells had a phenotypic response to it. To verify if the known IAA producer, the roseobacter *Ruegeria* sp. R11, could also influence its host through this signaling molecule, the two organisms were co-cultured. R11 and *E. huxleyi* grown together produce less IAA than *E. huxleyi* grown alone (with stimulation by tryptophan addition in both cases). The lack of response to the bacterium able to produce IAA, combined with the differential production and response to this signal according to cell type, is unlike what has been previously observed in any other algae.

MATERIALS AND METHODS

Genomic Survey of Tryptophan Dependant IAA Biosynthesis Pathways

Sequences for enzymes in the tryptophan dependant IAA biosynthesis pathways of *Arabidopsis thaliana*, which were used to query algal databases for homologs, were obtained from Le Bail et al. (2010). Query sequences to search for the bacterial IAA biosynthesis genes were obtained from Spaepen et al. (2007). BLASTp searches for algal homologs were performed and up to three representative completed genomes were searched for each major algal group (chlorophytes, rhodophytes, glaucophyte, diatoms, pelagophyte, brown algae, eustigmatophyte, chrysophyte, dinoflagellate, haptophyte, and cryptophyte) (**Table 1**). Additionally, the *E. huxleyi* genome was specifically surveyed for homologs of plant signaling and transport proteins, using sequences from Le Bail et al. (2010) as queries. Available complete roseobacter genomes (as listed on http://www.roseobase.org) and the genome of *Ruegeria* sp. R11 (from which IAA production has been identified) (Fernandes et al., 2011) were surveyed. For all homolog searches, a bi-directional best hit (BBH) BLASTp search of the resulting hits was performed against the organism(s) from which the query sequenced was obtained. An *e*-value of 10^{-10} or less for the BLASTp and the BBH BLASTp search was used as a cut-off for homology (Le Bail et al., 2010; Kiseleva et al., 2012; Mikami et al., 2015).

The sequences were assigned to orthologous groups using OrthoMCL (Li et al., 2003), where the hits grouping with the query sequence were considered positive. Functional prediction using the ESG package (Chitale et al., 2009) was concurrently performed and only homologs which had confidence scores similar to or higher than the predicted function of the query sequences, were considered positive.

Algae and Bacteria Strains

Axenic *Emiliania huxleyi* strains CCMP2090 (bald N cell type), and CCMP3266 (coccolith producing C cell type) were obtained from the Provasoli-Guillard National Centre for Marine Algae and Microbiota (NCMA). The *E. huxleyi* strains were maintained in L1-Si medium made using natural filtered seawater (Bamfield Marine Science Centre, BC, Canada) (Guillard and Hargraves, 1993) at 18°C in a diurnal incubator (12:12 h dark-light cycle). The algal cultures and L1-Si medium were checked for bacterial contamination by microscopy and by inoculation onto ½ marine agar (18.7 g Difco Marine Broth 2216 supplemented 9 g NaCl and 15 g Difco agar in 1 L) followed by incubation at 30°C for 2 d. However, this screening can't exclude the possibility of contaminating unculturable bacteria that are not readily visualized with microscopy. The algae were grown statically for 5 d to 10^4 cells/mL (early-log) for experiments.

The bacterium *Ruegeria* sp. R11 was maintained at 30°C on ½ marine agar plates then grown on a rotating drum to stationary phase in 5 mL ½ marine broth (18.7 g Difco Marine Broth 2216 supplemented 9 g NaCl in 1 L) for 24 h before experiments.

Algal Growth Experiments with Tryptophan, IAA, and *Ruegeria* sp. R11

L- and D-tryptophan (Sigma-Aldrich, St. Louis, MO, USA) were freshly prepared for each experiment in L1-Si medium and filter sterilized. *E. huxleyi* was grown in 0.02 mM NaOH, 1 and 2% ethanol solutions in L1-Si medium as these were the final concentrations in experiments where they are used as the solvent for IAA. The 1% ethanol solution had no observable effect on algal cells while the 2% ethanol and 0.02 mM NaOH resulted in a decreased chlorophyll concentration and potential quantum yield. Subsequently, IAA was prepared in 50% ethanol-water solution and all IAA additions were made to a final 1% ethanol concentration in L1-Si medium. The compound screening and co-cultivation experiments were performed as

TABLE 1 | Distribution of IAA biosynthesis genes in algal genomes.

	YUCCA	AMI1	TAA1	CYP79B2	CYP79B3	AAO1	CYP71A13	TDC	MYR1	SUR1	SUR2	NIT1
LAND PLANTS												
Arabidopsis thaliana	AEE86075	Q9FR37	Q9S7N2	NP_195705	NP_179820	Q7G193	O49342	Q8RY79	P37702	O65782	Q9SIV0	AEE77887
GREEN ALGAE												
Ostreococcus sp RCC809[a]	−	−/+	−	−/+	−/+	−	−	−	−/+	−/+	+	−
Coccomyxa subellipsoidea[a]	−	+	−	−/+	−/+	+	−	+	−/+	−/+	−/+	+
Chlamydomonas reinhardtii[a]	−	+	−	−/+	−/+	+	−	+	−/+	−/+	−	−
RED ALGAE												
Cyanidioschyzon merolae[b]	−	−/+	−	−	−	−	−	−	−	−	+	−
Porphyridium purpureum[c]	−	−	−	−	−	−	−	−	−	−	−	−
Chondrus crispus[d]	−	−/+	−	−/+	−/+	+	−	−	−/+	−/+	+	−
GLAUCOPHYTES												
Cyanophora paradoxa[d]	−	−	−	−	−	−	−	−	−	−	−	−
DIATOMS												
Fragilariopsis cylindrus[a]	−	−	−	−	−	−	−	−	−	−	−	−
Phaeodactylum tricornutum[a]	−	−/+	−	−/+	−/+	+	−	−	−/+	−/+	+	−/+
Pseudo-nitzschia multiseries CLN-47[a]	+/−	−/+	−	−	−/+	+	−	−	−/+	−/+	+	−
PELAGOPHYTE												
Aureococcus anophagefferens[a]	−	−/+	−	−/+	−/+	+	−	−	−	−	+	−
BROWN ALGAE												
Ectocarpus siliculosus[d]	−	+	−	+	+	+	−	+	+	+	+	−
EUSTIGMATOPHYTES												
Nannochloropsis oculata[d]	−	−	−	−	−	−	−	−	−	−	−	−
CHRYSOPHYTES												
Ochromonas danica[d]	−	−	−	−	−	−	−	−	−	−	−	−
DINOFLAGELLATES												
Symbiodinium minutum[e]	−	−	−	−	−	−	−	−	−	−	−	−
CRYPTOPHYTES												
Guillardia theta[a]	+/−	−/+	−/+	−/+	−/+	+	−	−	−	−/+	−/+	−
Hemiselmis andersenii[d]	−	−	−	−	−	−	−	−	−	−	−	−
HAPTOPHYTES												
E. huxleyi CCMP1516[d]	+/-	−/+	−/+	−/+	−/+	+	−	+	−/+	−/+	+	+

Presence is determined initially by a bi-directional best hit (BBH) BLASTP hit with an E-value $< 1 \times 10^{-10}$ or less using the characterized land plant A. thaliana gene as a query, as well as correct functional prediction using ESG and orthology with the plant enzyme as determined by OrthoMCL. (+) indicates that it matches all three criteria, (−/+) indicates it is confirmed by ESG but not OrthoMCL, while (+/−) indicates confirmation by OrthoMCL but not ESG. The following databases were searched: JGI ([a]), http://merolae.biol.s.u-tokyo.ac.jp/blast/blast.html ([b]), Bhattacharya et al. (2013) ([c]), NCBI ([d]), and OIST Marine Genomics Unit (http://marinegenomics.oist.jp/genomes/gallery/) ([e]). The abbreviations used for the enzyme can be described as follows: YUCCA, Tryptamine monooxygenase; AMI1, Indole-3-acetamide hydrolase; TAA1, Tryptophan amino transferase; CYP79B2 and CYP79B3, Cytochrome P450s; AAO1, Indole-3-acetaldehyde oxidase; CYP71A13, Indole-acetaldoxime dehydratase; TDC, Tryptophan decarboxylase; MYR1, Myrosinase; SUR1, C-S lyase; SUR2, CYP83B1; and NIT1, Nitralase.

previously described (Bramucci et al., 2015). Briefly, *E. huxleyi* strains (CCMP2090 and CCMP3266) were supplemented with 1, 0.1, and 0.01 mM L-tryptophan and 0.1 mM D-tryptophan in L1-Si medium. IAA was added to CCMP2090 and CCMP3266 at a concentration of 0.1, 0.01, and 0.001 mM in L1-Si medium and controls of 0 and 1% ethanol. There was no significant difference between the 0 and 1% ethanol controls, so data analysis uses the 1% ethanol as the control as treated samples include 1% ethanol (from the IAA stock solution). Wells were randomly assigned in 48-well plates (Becton, Dickinson and Company, Franklin Lakes, NJ, USA) with triplicate samples for each condition such that each plate contained all the samples for a single time point. *E. huxleyi* had an initial concentration of 10^4 cells/mL for all treatments.

For the bacterial-algal co-cultures, bacterial cells were washed twice by centrifugation and re-suspended in L1-Si medium,

before being diluted to the initial concentration of 10^4 CFU/mL. Co-cultures were performed with and without 0.1 mM L-tryptophan. All microtiter plates were incubated in a diurnal incubator (12:12 h dark-light cycle) at 18°C for all experiments.

Microscopy

Algal cells were visualized throughout the experiment using an Axio Imager M2 microscope (Zeiss, Oberkochen, Germany) and processed using Zen 2012 (Zeiss).

Fluorescence Measurements

To measure the chlorophyll fluorescence and photosynthetic yield, samples were taken at the mid-point of their dark cycle (5–7 h into the dark cycle) and diluted in L1-Si medium to within the detection range using a pulse-amplitude-modulation (PAM) fluorometer (WATER-PAM, Waltz, Effeltrich, Germany). A dark adaption period of 3 min was determined, after which a saturating pulse was applied and the fluorescence readings were taken to calculate the minimal dark fluorescence (F_0) that is directly correlated to the chlorophyll content, the maximum dark fluorescence (F_m) and the Photosystem II (PSII) potential quantum yield (F_v/F_m) ($F_v/F_m = (F_m - F_0)/F_m$) (Schreiber et al., 1986; Kooten et al., 1990). Three-microtiter wells were sampled (and not re-sampled) as replicates at each time point to determine the yield. Data were processed using SigmaPlot 12. Statistical significance was determined using a one-way ANOVA and Student-Newman-Keuls (SNK) test.

Biomass and IAA Measurements

Samples were taken from sampled well at each time point and biomass measured (OD at 680 nm) using a Synergy H1 microplate reader (BioTek, Winooski, VT, USA). A colorimetric test was used to determine if IAA, indole-3-pyruvic acid, or indole-3-acetamide is produced as previously described (Glickmann and Dessaux, 1995). In brief, samples were taken and centrifuged (10 min at 5000 rpm for algae and 2 min at 14,000 rpm for bacteria) then the supernatant was mixed in a 1:1 volume ratio with fresh Salkowski reagent [12 g $FeCl_3$ (EMB Millipore, Billerica, MA, USA) in 1 L of 7.9 M H_2S0_4 (Sigma-Aldrich)]. Samples were then incubated in the dark for 30 min at room temperature. The OD (530 nm) and emission spectra for peak wavelength were measured. The IAA concentration of L1-Si medium was measured using the Salkowski reagent and sterile molecular water as the blank to determine if the seawater in L1-Si medium was a potential source of IAA; L1-Si medium did not contain a detectable IAA concentration. Subsequently L1-Si medium was used to blank all readings. IAA concentrations were prepared in L1-Si medium to construct a standard curve to determine the IAA concentration from samples. Statistical significance was determined using a one-way ANOVA and SNK test.

Flow Cytometry

Algal samples were fixed with 0.15% glutaraldehyde (Sigma-Aldrich) for flow cytometry by incubating cells in the dark for 10 min, then flash-frozen in liquid nitrogen and stored at −80°C until flow cytometry was performed using a FACSCalibur (Becton, Dickinson and Company). A 488 nm laser was used for excitation. Samples were first run using chlorophyll fluorescence (670 nm) for detection. Membrane integrity was evaluated using Celltox Green (Promega, Madison, WI, USA) (520 nm). Data were processed using FlowJo 9.2.

GC×GC-TOFMS

Replicate 100 mL cultures of CCMP2090 and CCMP3266 were grown in 250 mL Erlenmeyer flasks. Flasks were inoculated with 10^4 cells/mL *E. huxleyi* in 0.1 mM L- or D-tryptophan and no tryptophan addition for the control. Cells were harvested at 16 d by centrifuging at 5000 rpm for 10 min.

IAA standards were created by adding 2.8 mM (∼500 ppm) IAA to control algal samples. All samples were then extracted using an equal volume of methanol, ultrasonicated, and vacuum filtered on 1.6 μm Whatman 1820-047 GF/A, 47 mm diameter filters (Sigma-Aldrich) three times. This was then passed through a column of sodium sulfate (Sigma-Aldrich). Derivatization was done according to previous literature (Birkemeyer et al., 2003), whereby 5 μL of the extracted algal sample was added to 100 μL of *N*-methyl-*N*-(trimethylsilyl) trifluoroacetamide (MSTFA) (Sigma-Aldrich), then incubated at 90°C for 30 min. To determine if L1-Si medium contained IAA at a concentration below detection of the Salkowski reagent, 10 mL of L1-Si medium was tested. Additional treatment was needed as this extraction was performed on liquid (L1-Si medium) rather than biomass. First, the pH of the sample was lowered to ∼1.5 using hydrochloric acid (Sigma-Aldrich), then the liquid sample was extracted by adding 1 mL methylene chloride (Sigma-Aldrich), vortexing vigorously, and removing the methylene chloride layer. This was repeated three times. The methylene chloride was then evaporated and 10 mL methanol was added. The algal extraction procedure was then followed following biomass concentration (i.e., filtration). To confirm the extraction worked, a sample of L1-Si medium was first spiked with IAA at ∼6 mM, and the expected IAA peak was detected.

The samples were analyzed on a Leco Pegasus 4D GC×GC-TOFMS (Leco Instruments, St. Joseph, MI, USA). The columns used for the first- and second- dimensions were a 30 m × 0.25 μm, 1 μm film thickness Rtx-5MS (Chromatographic Specialties, Brockville, ON, Canada) and a 1.6 m × 0.25 mm, 0.25 μm film thickness Rtx-200MS (Chromatographic Specialties) respectively. Helium (5.0 grade; Praxair, Edmonton, AB, Canada) was used as the carrier gas with flow controlled at 1.5 mL/min. The analytes were desorbed in the split/splitless injection port of the GC×GC-TOFMS using an inlet temperature set at 230°C, operating in splitless mode. The 47 min GC method began with an initial oven temperature of 70°C for 1 min, followed by a ramp of 6°C/min up to 320°C, and ending with a 5 min hold in the first oven. Relative to the primary oven, the secondary oven was programmed to have a constant offset of +5°C and the modulator a constant offset of +15°C. The modulation period was 2.0 s. The TOFMS had an acquisition rate of 100 Hz and acquired over a mass range of m/z 10–700. The detector voltage was −1350 V, the ion source temperature was 200°C, and the MS transfer line temperature was 250°C.

GC×GC-TOFMS data were processed using ChromaTOF® (v.4.43; Leco). For processing, the baseline offset was set at the middle of the noise (0.5), the minimum S/N for the base peak and the sub-peaks were set at 10, and the data were auto smoothed by the software. The first dimension peak width was set at 14 s while the second dimension peak width was set at 0.15 s. Identifications of the compounds were made based on library matches with the NISTMS 2008 Library mass spectral database and relative retention index. In this case, a minimum match factor of 75% of the library was required before a name was assigned to a compound.

RESULTS AND DISCUSSION

Presence of Tryptophan Dependent IAA Biosynthesis Pathways in Algae and Roseobacters

IAA biosynthesis consists of a complex set of tryptophan dependent and independent pathways that is not yet fully understood (Zhao, 2010; Tivendale et al., 2014). The tryptophan independent pathway remains genetically undefined (Normanly, 2010; Nonhebel, 2015). In contrast, the tryptophan dependent pathways have been well studied in *A. thaliana* (Sztein et al., 2000; Zhao, 2010), with many of the genes encoding for its enzymes functionally described. Biosynthesis of IAA by bacteria has also been studied, but members of this domain are thought to use pathways and enzymes different than those found in plants (Spaepen et al., 2007). To investigate the presence of tryptophan dependent pathways outside of plants, public databases were searched using *A. thaliana* and known bacterial IAA biosynthesis genes as queries against algal and roseobacter genomes. Homologs of several of these genes were found in a wide array of algae (**Table 1**) and roseobacters (Supplementary Table 1). However, it should be noted that the presence of homologs does not necessarily translate to the presence of the bona-fide functional enzyme involved in this pathway, especially for those that fall under a functionally broad protein family (such as CYP79B2 and CYP79B3 that are cytochrome P450s). To determine which homologs were likely to have a conserved function with plant enzymes, functional prediction was performed with the ESG package (Chitale et al., 2009) and homologs were categorized in orthologous groups using OrthoMCL (Li et al., 2003). Only homologs part of the same orthologous groups as the plant enzymes and/or with identical functions predicted with ESG were included (**Table 1** and Supplementary Tables 1, 2). Patterns of co-occurring genes suggesting the presence of complete tryptophan dependent pathways were found in some algae, and genes encoding partial pathways in others (**Table 1**). In algae in which only partial pathways were found, IAA could potentially be produced as a result of the completion of essential biochemical steps by their proximal bacterial symbionts (Dittami et al., 2014). We also found homologs of some bacterial IAA biosynthesis genes in algae (Supplementary Table 2), suggesting that alternate pathways for IAA biosynthesis to those found in plants might be present.

As shown in previous studies (Kobayashi et al., 1993; Amin et al., 2015), the roseobacter genomes encode for the genes known in bacteria to be involved in the synthesis of IAA through the indole-3-acetamide (IAM) pathway (**Figure 1**). There is a possibility that roseobacters are capable of synthesizing IAA through another pathway, as they contain a putative tryptophan decarboxylase that produces the IAA precursor tryptamine, a putative indole-3-pyruvate decarboxylase, as well as indole-3-acetaldehyde (IAAd) dehydrogenase, which converts the tryptamine derivative IAAd to IAA (Supplementary Table 1). However, Amin et al. (2015) highlighted the difficulty in determining whether the IAAd dehydrogenase found in roseobacters is specific to IAA biosynthesis or used in other pathways. Nitrile hydratase and IAM hydrolase, which can together convert indole-3-acetonitrile (IAN) to IAA, have also been identified in roseobacters ((Fernandes et al., 2011); **Figure 1** and Supplementary Table 1). However, there is currently no known pathway in bacteria that can produce the IAN this enzyme pair uses as an initial substrate. Interestingly, the genes to produce IAN from tryptophan (the indole-3-acetaldoximine, or IAOx, pathway) are widely distributed in algae (**Figure 1**). This complementarity could form the basis of a symbiosis between algae and roseobacters enabling the production of IAA. This symbiosis has been suggested as the basis for the presence of IAA in the brown algae *E. siliculosus*, as the bacterial symbiont *Candidatus* Phaeomarinobacter ectocarpi contains the genes necessary to complete the synthesis of IAA in complementarity with the genes found in the alga (Dittami et al., 2014).

The survey of public sequence databases also revealed that the principal tryptophan dependent IAA biosynthesis pathway in plants, the indole-3-pyruvic acid (IPyA) pathway, using tryptophan amino transferase (TAA) and YUCCA (Mashiguchi et al., 2011), is not widely distributed in algae, if at all. It has been previously noted in genomic surveys that some chlorophytes have the genetic potential for IAA biosynthesis, but that the tryptamine (TAM) and IAOx pathways are the most likely candidates for the synthesis of this compound (De Smet et al., 2011; Kiseleva et al., 2012). More distantly related algae (outside the supergroup Archaeplastida, which contains plants, chlorophytes, and rhodophytes) have not been thoroughly investigated, except for the brown alga *E. siliculosus*, in which the IAOx and TAM pathways had the most supporting evidence for being at least partially present (Le Bail et al., 2010), although it should be noted that combining known bacterial and plant genes, at least one complete putative pathway is present (**Figure 1**). Surprisingly, phylogenetically diverse microalgae such as diatoms, haptophytes, and cryptophytes, have a wide distribution of putative enzymes enabling the production of IAA from tryptophan (**Figure 1** and **Table 1**). The haptophyte *E. huxleyi,* for example has a complete putative pathway to yield IAA from tryptophan, combining plant and bacterial enzymes (using tryptophan decarboxylase, bacterial amine oxidase, and indole-3-acetaldehyde oxidase; **Figure 1** and Supplementary Table 2). However, some of these enzymes, such as indole-3-acetamide hydrolase, may not be specific to the IAA biosynthesis pathway. Therefore, the identification of homologs does not necessarily mean that algae can produce IAA from tryptophan.

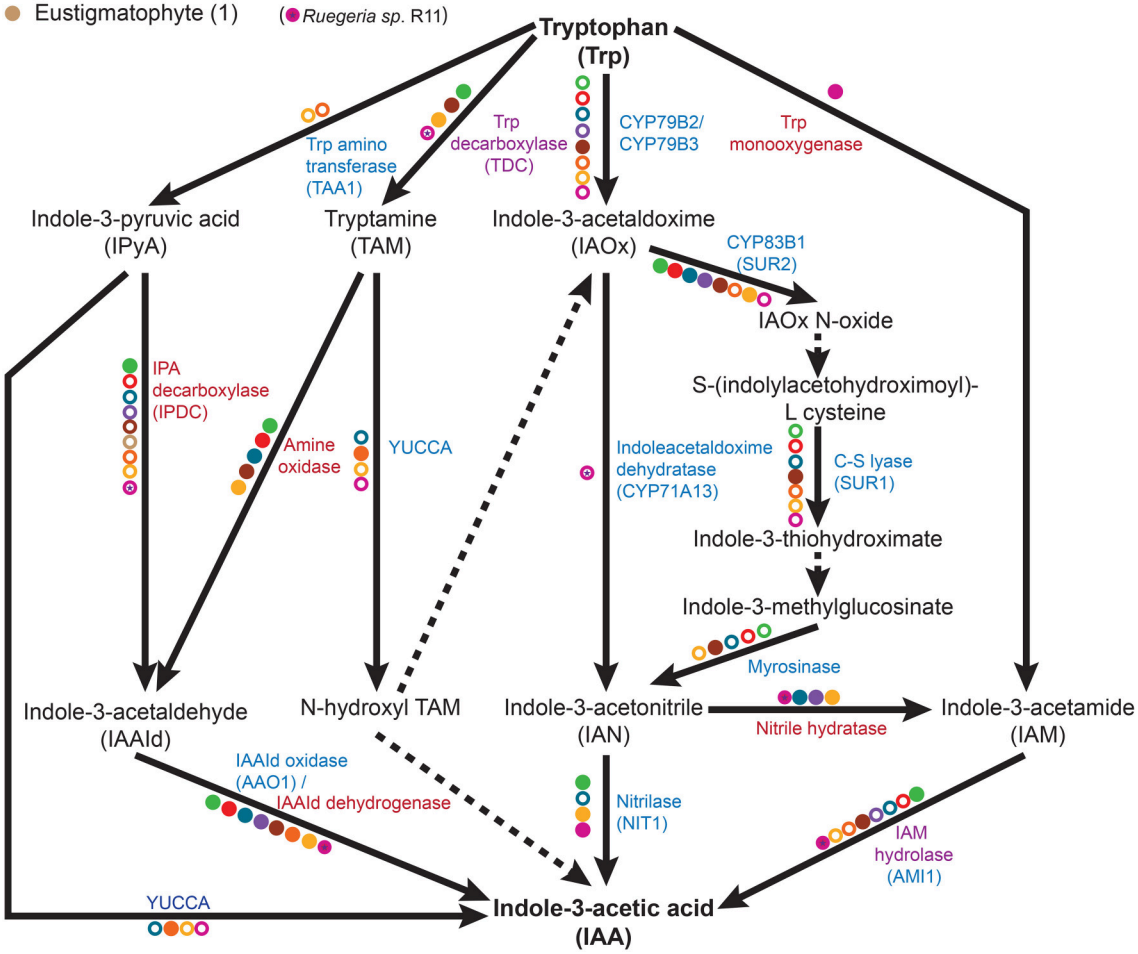

FIGURE 1 | The tryptophan dependent indole-3-acetic acid (IAA) biosynthesis pathways. Metabolic reactions catalyzed by known enzymes are indicated with solid lines while dashed lines indicate a currently unknown enzyme. Listed in blue are the enzymes with a plant seed sequence, while in red are the enzymes with a bacterial seed sequence. Listed in purple are the enzymes that are found in plants, algae, and bacteria. Colored dots represent the presence of the given enzyme in at least one member of a specific taxonomic group, as indicated by bi-directional best hit (BBH) BLAST search (minimum *e*-value of 10^{-10}) followed by Ortho MCL and ESG functional prediction.

The fact that this haptophyte contains homologs of all the genes for a complete putative pathway, as well as homologs of some genes involved in nearly every other tryptophan dependent pathway, makes it a good candidate for further investigation.

Putative homologs of genes belonging to the IAOx pathway seem to be the most widely distributed in algae, which in plants is limited to the Brassicaceae family (Mano and Nemoto, 2012). When putative IAA biosynthesis genes are found in an alga, they are not always present in every member of the group to which it belongs. For example, Mikami et al. (2015) did not find any homologs for IAA biosynthesis genes in bangiophycean red algae (not included in this study), while this study found homologs in cyanidiophyceaen and florideaphycean red algae (**Table 1**). Such a patchy distribution of the genes that could be involved in IAA biosynthesis within each algal group and between algal groups can be interpreted in two main ways. It could suggest that the basic mechanisms for IAA biosynthesis were present in the ancestor of terrestrial plants and archaeplastid algae, with multiple loss events occurring, or alternatively that the pathway was distributed by lateral gene transfer (LGT). These hypotheses have been greatly debated for the IPyA pathway, which is composed of the tryptophan aminotransferase and flavin-containing monooxygenase (YUCCA) enzymes, converting tryptophan in IAA via indole-3-pyruvic acid. LGT

from bacteria to an ancestor of land plants was argued to be the most parsimonious explanation for the origin of IPyA pathway (Yue et al., 2014; Turnaev et al., 2015). Another view is that the pathway evolved earlier in the ancestor of land plants and charophytes (Wang et al., 2014, 2016). Interestingly, IAA biosynthesis genes found in bacteria but not plants were also found widely in algae, giving additional evidence for LGT events contributing to its evolution in eukaryotes (Supplementary Tables 1, 2). Further research would be needed to determine where the different tryptophan dependent IAA biosynthesis pathways originated and what role bacteria played in their evolution.

Although many algae may possess one or more tryptophan dependent IAA biosynthesis pathways (or parts of it), there has been little to no evidence to suggest that they contain the necessary receptor proteins known to facilitate IAA signaling and the polar auxin transport that is crucial in determining cell directionality in plants (Køeèek et al., 2009; Lau et al., 2009; De Smet et al., 2011). There have been recent studies suggesting a few possible homologs in the transcriptome and genome of brown and red algae (Le Bail et al., 2010; Wang et al., 2015). A survey of *E. huxleyi* did not identify any homologs of known response proteins, including: ARF (auxin response factors); PIN proteins (transmembrane proteins that actively regulate the transport and efflux of auxins); or the Aux/IAA transcriptional repressors. Only one hypothetical protein homologous to TIR1/AFB (transport inhibitor response/auxin signaling f-box) was found (XP_005761773, with an *e*-value of $3e^{-18}$). However, if IAA serves as a growth-promoting hormone in algal systems, it has been suggested that the AUX/IAA/ARF signaling pathway may not be required, and other signaling mechanisms may exist (Lau et al., 2009; Zhang and Van Duijn, 2014).

E. huxleyi Coccolith Bearing (C) Cells Produce IAA When Stimulated by Tryptophan

Since genes encoding enzymes of tryptophan dependent IAA biosynthetic pathways are present in the *E. huxleyi* genome, L-tryptophan was added to axenic cultures of coccolith bearing C type (CCMP3266) and bald N type (CCMP2090) cells at various concentrations to determine if these strains would convert it to IAA. IAA was detected using the Salkowski reagent, a rapid colorimetric assay which recognizes indolic compounds, with IAA having an optimal peak of 530 nm (Glickmann and Dessaux, 1995). The lower limit of detection of the Salkowski reagent in this experimental set-up is 0.001 mM. While 1 mM L-tryptophan was inhibitory to the growth of CCMP3266 (Supplementary Figure 1), the Salkowski reagent indicated that the alga was converting the L-tryptophan into IAA at concentrations of L-tryptophan as low as 0.1 mM, with the characteristic color and optimal wavelength observed (**Figure 2**). IAA was detected soon after the addition of L-tryptophan, and its concentration stayed constant, reaching 0.1 mM when 1 mM of L-tryptophan was added, and 0.07 mM with 0.1 mM L-tryptophan. The addition of D-tryptophan, which should not stimulate IAA production (Baldi et al., 1991), yielded no detectable IAA (**Figure 2**).

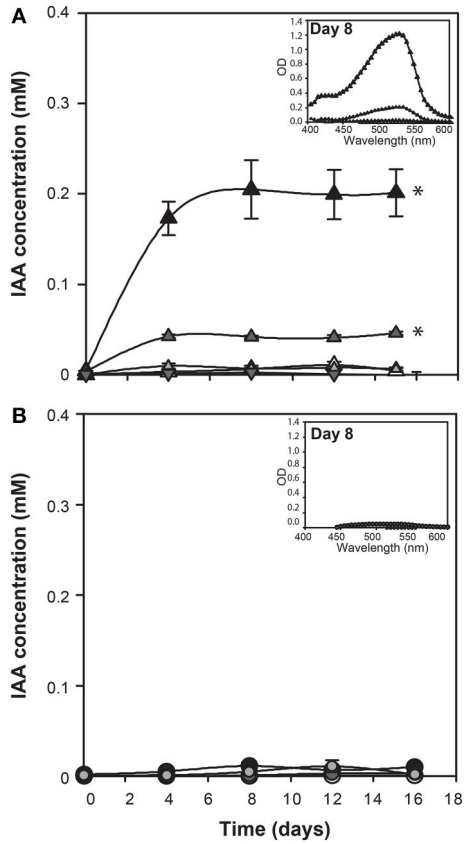

FIGURE 2 | *E. huxleyi* production of indole-3-acetic acid (IAA) in the presence of various concentrations of tryptophan. IAA concentration was derived from OD measurements of culture supernatants after addition of Salkowski reagent. The experiment was performed with coccolith bearing CCMP3266 **(A)** and bald CCMP2090 **(B)** *E. huxleyi* strains. Triangles represent CCMP3266 with various concentrations of L-tryptophan (black for 1 mM, dark gray for 0.1 mM, light gray for 0.01 mM, and white for the control with no L-tryptophan added). Inverted triangles represent CCMP3266 grown with 0.1 mM D-tryptophan. Using the same color scheme, circles represent CCMP2090 grown with various concentrations of L-tryptophan. Inset is the emission spectrum taken on 8 d to indicate the peak wavelength. Error bars represent ±1 SE. An asterisk (*) at a time point indicates that it is significantly different to the control and an asterisk at the end of the line indicates that the treatment is significantly different to the control.

Unlike CCMP3266, growth of CCMP2090 was not inhibited at 1 mM of L-tryptophan, although it did cause a slight decrease in PSII health (Supplementary Figure 1). However, when CCMP2090 was supplemented with tryptophan, IAA was not produced (**Figure 2**).

The Salkowski reagent is a rapid assay demonstrating the conversion of L-tryptophan to IAA, but use of the reagent in algal samples has been criticized due to its lack of specificity for IAA, as its absorption spectra can overlap with indole-3-pyruvic acid (Buggeln and Craigie, 1971; Glickmann and Dessaux, 1995). Consequently, we performed GC×GC-TOFMS analysis on the samples to determine whether the main auxin produced was indeed IAA, and/or to identify other auxins or intermediates if they were present. GC×GC-TOFMS was run

on the harvested 16 d samples of CCMP3266 and CCMP2090 grown with 0.1 mM L- and D-tryptophan. Co-culture samples of *E. huxleyi* with R11 were not analyzed with GC×GC-TOFMS as the presence of R11 lowered the IAA concentration, as detected by the Salkowski reagent, when co-cultured with CCMP3266 compared to when it was grown alone. GC×GC-TOFMS is an analysis that facilitates detection of unknown compounds using the retention times in two dimensions and uses a library search for the resulting hits. It has several distinct advantages, including better separation of components, simplified sample preparation, increased peak capacity, and high selectivity and sensitivity (Dallüge et al., 2002; Adahchour et al., 2008). An IAA standard was added to algal samples and compared to the algal controls as well as samples with the addition of 0.1 mM of L- or D-tryptophan. Identification was based on the first and second retention time matching the standard, as well as the similarity (how well the peak matches the library) and reverse match (how well the library matches the peak) factors. The peak retention times and peak identification based on NISTMS 2008 Library mass spectral

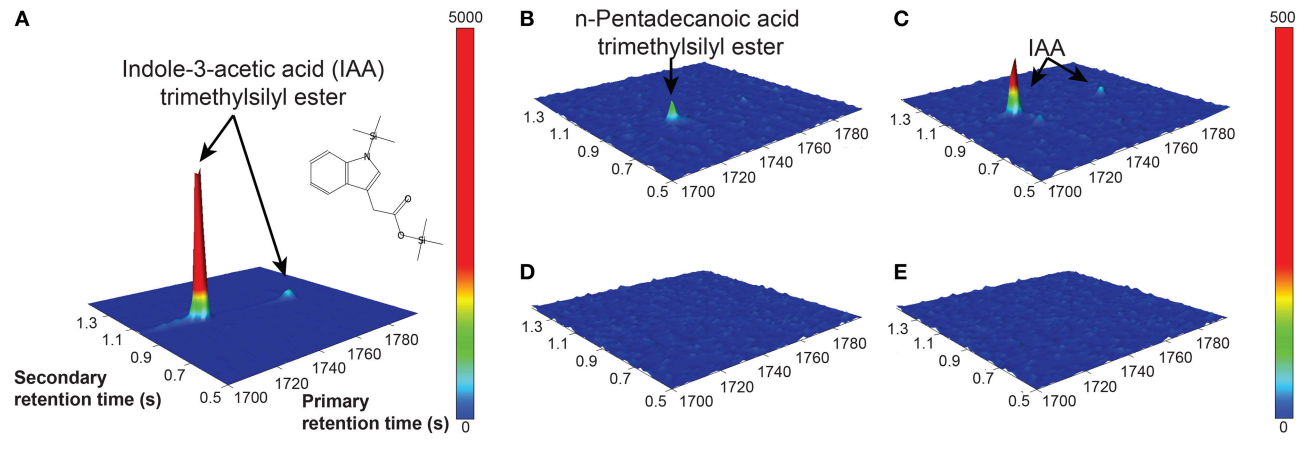

FIGURE 3 | GC×GC–TOFMS surface plots of selected mass channel (*m/z*) of 130. A standard of 2.8 mM IAA is shown **(A)**, along with *E. huxleyi* C type culture (CCMP3266) control (no tryptophan added) **(B)**, CCMP3266 grown with 0.1 mM L-tryptophan **(C)**, *E. huxleyi* N type culture (CCMP2090) control (no tryptophan added) **(D),** and CCMP2090 growth with 0.1 mM L-tryptophan **(E)**. Cells were harvested from cultures on 16 d. Identifiable peaks are labeled with the compound to which they correspond.

TABLE 2 | GC×GC-TOFMS peak table.

Sample ID	Name	R.T. (s) (1D*, 2D**)	Peak area	Quant masses	Similarity	Reverse	Signal to noise (S/N) ratio
IAA standard	3-Indoleacetic acid, trimethylsilyl ester	(1728, 1.020)	23810	73	816	846	812.56
2.8 mM	3-Indoleacetic acid, trimethylsilyl ester	(1774, 1.000)	218651	73	862	862	2760.90
CCMP3266	3-Indoleacetic acid, trimethylsilyl ester	(1728, 1.020)	1299	73	416	796	34.08
0.1 mM L-tryptophan	3-Indoleacetic acid, trimethylsilyl ester	(1772, 0.990)	17418	73	765	793	639.58
CCMP3266 0.1 mM D-tryptophan	No peak found						
CCMP3266 Control	No peak found						
CCMP2090 0.1 mM L-tryptophan	No peak found						
CCMP2090 0.1 mM D-tryptophan	No peak found						
CCMP2090 Control	No peak found						
L1-Si Medium (seawater)	Unknown	(1772, 0.990)	290	73	NS#	NS	10.80

**1D, 1st Dimension; **2D, 2nd Dimension; #NS, Not searchable.*

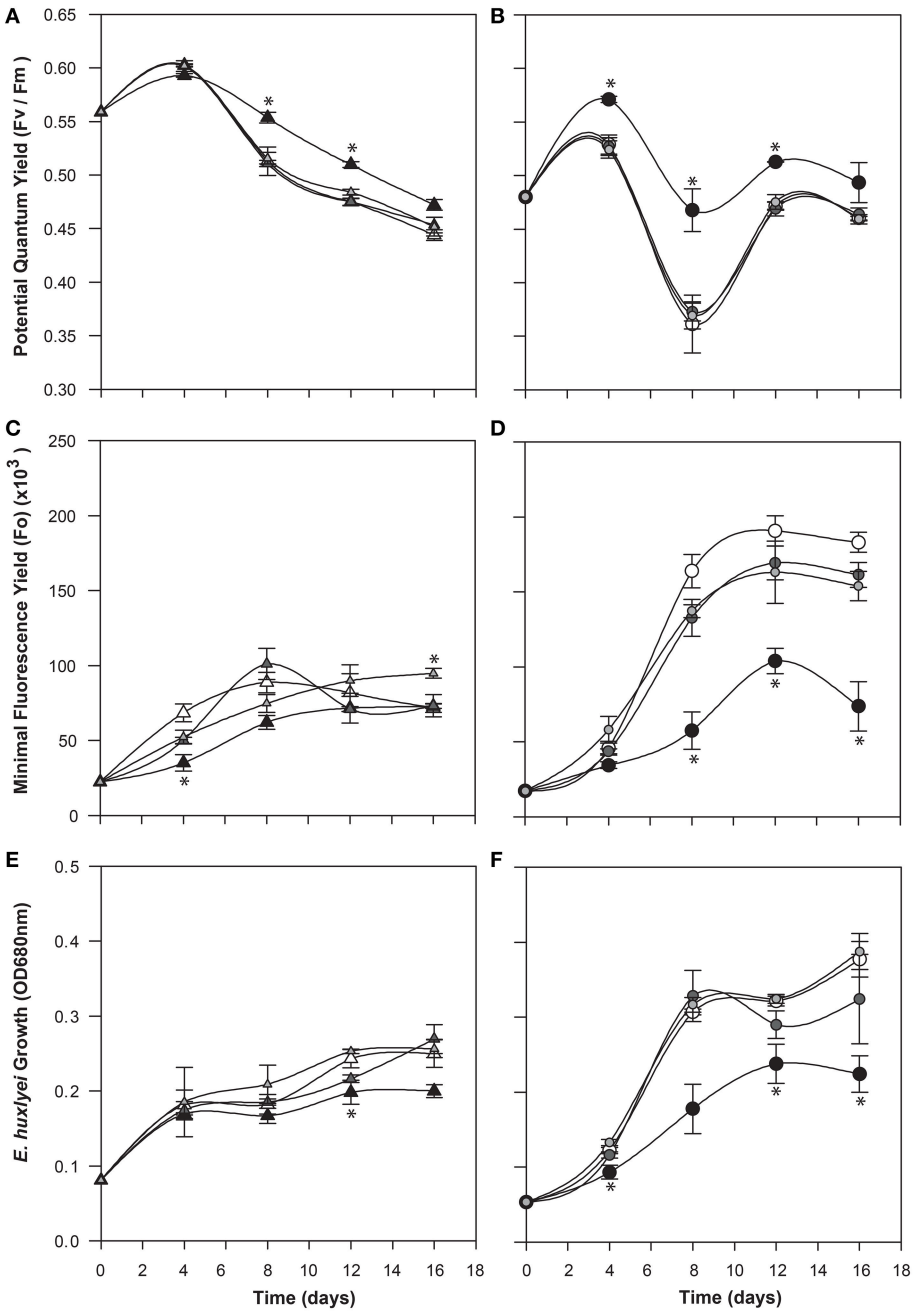

FIGURE 4 | Effect of exogenous indole-3-acetic acid (IAA) on the bald (CCMP2090) and coccolith bearing (CCMP3266) *E. huxleyi* strains. The algae were co-cultured with concentrations of 0.1–0.001 mM of IAA [black for 0.1 mM, dark gray for 0.01 mM, and light gray for 0.001 mM, and white for the control (L1-Si medium with 1% ethanol)]. Triangles represent CCMP3266 while circles represent CCMP2090. The potential quantum yield of CCMP3266 **(A)** and CCMP2090 **(B)** with various concentrations of IAA is shown, as well as the minimal fluorescence for the two strains, CCMP3266 **(C)** and CCMP2090 **(D)**. Growth is displayed as the OD measurement at 680 nm for CCMP3266 **(E)** and CCMP2090 **(F)**. Error bars represent ±1 SE. An asterisk (*) at a time point indicates that it is significantly different to the control and an asterisk at the end of the line indicates that the treatment is significantly different to the control.

database determined the presence of IAA in the CCMP3266 sample containing L-tryptophan (**Figure 3**), and the absence of hits in the control, D-tryptophan supplemented sample, or any of the CCMP2090 samples (**Table 2** and **Figure 3**). L1-Si medium did however contain a barely detectable peak with the same retention times as IAA (**Table 2**). However, peak area and the signal to noise ratio was very low (**Table 2**). Additionally, the volume of liquid medium used for the control extraction (10 mL) was much larger than that of the biomass subsample (0.1 mL), from which IAA was detected at a ∼10,000 fold

lower IAA signal per unit volume compared to CCMP3266 biomass. This provides strong evidence that the *E. huxleyi* C cells produces IAA when stimulated with L-tryptophan, but that N cells are unable to produce this compound when grown with or without L-tryptophan under the conditions tested.

Differential Effect of Exogenous IAA Added to Bald (N) and Coccolith Bearing (C) *E. huxleyi* Cell Types

To determine a potential role for IAA produced by C cells of *E. huxleyi*, various concentrations of exogenous IAA were added to axenic cultures of both the C and N type strains in early log phase and then monitored for biomass (OD), cell morphology (microscopy and flow cytometry), chlorophyll and PSII health (PAM fluorometry), and membrane integrity (cell staining and flow cytometry; **Figures 4–6**). The C strain (CCMP3266) showed a small increase in potential quantum yield (F_v/F_m) with the addition of 0.1 mM exogenous IAA, while the N strain (CCMP2090) showed a greater increase in potential quantum yield with 0.1 mM of IAA (**Figure 4**). Lower concentrations of IAA did not affect the potential quantum yield (**Figures 4A,B**). An effect on potential quantum yield, which is an indicator of PSII health and overall photosynthetic performance, is consistent with the suggestion that IAA stimulates photosynthetic reactions in the chloroplast of plants (Tamás et al., 1972). Such a stimulating effect on photosynthesis has also been demonstrated in diatoms, which harbor bacterial symbionts producing IAA (Amin et al., 2015).

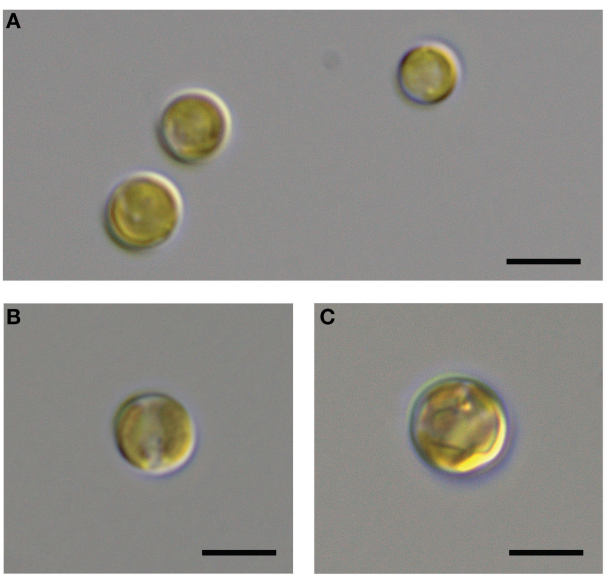

FIGURE 5 | DIC microscopic observation of the bald *E. huxleyi* strain (CCMP2090) exposed to indole-3-acetic acid (IAA). The CCMP2090 control is grown in L1-Si medium with 1% ethanol at 8 d **(A)**, the alga with 0.01 mM IAA at 8 d **(B)**, and the alga with 0.1 mM IAA at 12 d **(C)**. The scale bar represents 5 μm.

CCMP3266 was relatively unaffected physiologically even by high concentrations of IAA, showing a minor decrease in growth, with F_o (chlorophyll fluorescence) unaffected (**Figure 4**). However, IAA had a notable effect on the chlorophyll content and biomass of CCMP2090 from 8 to 16 d of the experiment (**Figure 4**). The more noticeable effect of IAA was at the transition from log to stationary phase, which is consistent with IAA having been shown to be most effective on aged plants samples, such as old samples of maize, rather than freshly cut samples (Evans and Cleland, 1985). Auxins are important regulators of the cell cycle (De Veylder et al., 2007), and have been shown to influence cell division in algae (Vance, 1987). The addition of IAA to diatoms, as well as the addition of IAA and IAA-like compounds (from kelp extracts) to unicellular green algae has been shown to increase biomass (Mazur et al., 2001; Li et al., 2007; Amin et al., 2015). However, elevated IAA can be toxic, with the concentration range for growth promotion being quite narrow (Fässler et al., 2010), which is consistent with its effect on *E. huxleyi* (**Figure 4**).

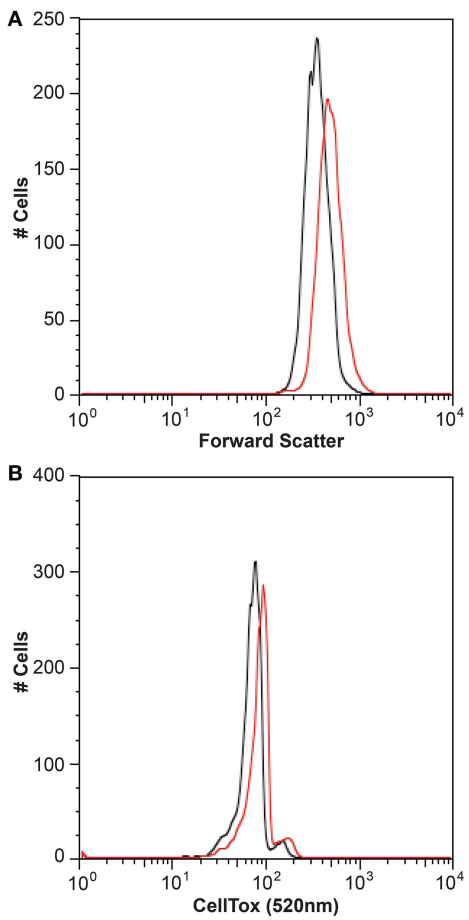

FIGURE 6 | Flow cytometry analysis of the bald *E. huxleyi* strain (CCMP2090) treated with indole-3-acetic acid (IAA). Histograms of the algal cell population with and without 0.01 mM IAA addition are shown with the forward scatter **(A)** and Celltox green stain **(B)** after 8 d. The control in L1-Si medium with 1% ethanol is in black while the culture with IAA added is in red.

It is generally thought that auxin function in algae would most likely parallel its function in land plants (Bradley, 1991; Tarakhovskaya et al., 2007), and therefore macro-algae were more likely to be responsive to auxin addition due to its role in cell differentiation (Mazur et al., 2001). It has also been suggested that auxins would have no signaling role in microalgae, and that they are merely side-products of other metabolic functions in these organisms (Stirk et al., 2014). While there was no visual difference between CCMP3266 cultures with or without the addition of IAA, CCMP2090 showed a morphological switch when grown in the presence of IAA. Cells were noticeably larger when grown with IAA compared to the 1% EtOH solvent control (**Figure 5**), or with the addition of the IAA precursor L-tryptophan. This morphological change was confirmed by an increase in the forward scatter of the algal population taken at 8 d (**Figure 6A**). Cells were also stained with Celltox Green cytotoxicity assay, which binds to the DNA of cells with impaired membrane integrity, resulting in a fluorescent signal. Under this treatment, there was an increase in the fluorescence of cells treated with IAA, indicating an increase in membrane permeability and as such, an overall loss of cell membrane integrity (**Figure 6B**).

While auxins do not act directly on cell walls, stimulation of cell elongation and cell wall synthesis is one of its functions in plants (Evans and Cleland, 1985; Cleland, 2010), although high concentrations (∼0.2 mM) of IAA can cause inhibition of cell wall synthesis (Baker and Ray, 1965). Auxins can induce acidification in cell walls and an increase in the cell membrane potential. This can be through the transport of the lipophilic form of IAA (IAAH) into the cell which affects the membrane potential as it then dissociates into the anionic form (IAA^-) (Nelles, 1977; Cleland, 2010; Zhang and Van Duijn, 2014), which leads to the activation of plasma membrane H^+-ATPases and potassium channels, inducing modifications to the cell wall and hyperpolarizing the membrane (Osakabe et al., 2013; Ng et al., 2015; Velasquez et al., 2016). This change in a cell membrane's pH gradient, and the subsequent modifications on the cell wall by the released enzymes, leads to the cleavage of load-bearing cell-wall crosslinks promoting the turgor pressure needed for cell expansion (Cleland, 2010; Velasquez et al., 2016). The hyperpolarization of the membrane potential has also been demonstrated in the macroalgae *Chara corallina* (Zhang et al., 2016). These changes in cell membrane structure may explain why the N cell type is more affected by IAA than the C cell type in terms of morphological differences, as coccoliths and acidic extracellular polysaccharide coat C type cells and perhaps provide protection from these effects of IAA. Although the coccoliths would not prevent the IAA from entering the cell, and the role of coccoliths has not been fully established, they have been suggested to provide additional strength due to their interweaving structure and may protect the integrity of the cell (Paasche, 2002). Alternatively, it is possible that the lack of a visual morphological effect in C cells as a result of exposure to exogenous IAA is a consequence of the capability of these cells to produce it endogenously.

Role of IAA in Bacterial-Algal Interactions

IAA has been shown to be an important bioactive molecule mediating bacterial-algal interactions between a diatom *Pseudo-nitzschia* and its bacterial community (Amin et al., 2015). In that system, the diatom up-regulated its tryptophan biosynthesis, resulting in its symbiotic bacterium *Sulfitobacter* sp. SA11 up-regulating its IAA biosynthesis genes. This relationship, where the alga produces tryptophan for the bacterium to convert into IAA, which in turn promotes algal growth, demonstrates a cross-kingdom relationship in which there is a metabolic and signaling exchange (Amin et al., 2015). The roseobacter *Ruegeria* sp. R11 has been shown to produce IAA (Fernandes et al., 2011), and its genome encodes the biosynthetic pathway (**Figure 1** and Supplementary Table 1). Therefore, we postulated a role of IAA in the relationship between R11 and *E. huxleyi,* as R11 has recently been shown to be pathogenic to *E. huxleyi* CCMP3266, but not CCMP2090 (Mayers et al., 2016). However, the Salkowski reagent did not detect indolic compounds from R11 cultures grown in L1-Si medium or when co-cultured with *E. huxleyi*. Furthermore, the addition of L-tryptophan at a concentration that is not inhibitory to the growth of CCMP3266 did not stimulate the production of IAA in the bacterium (**Figure 7**). As R11 is known to make IAA, it may be that our methods are not sensitive enough to detect IAA production by R11, or that R11's biomass is not great enough to detect its IAA (since IAA was identified from 10 d cultures in ½YTSS medium which is much more nutrient rich than L1-Si medium and supports R11 cell density 1000 times higher) or that the host, *E. huxleyi*, drives IAA production in this partnership.

There was also little difference in *E. huxleyi's* potential quantum yield when co-cultured with R11 with or without the addition of L-tryptophan for CCMP2090 or CCMP3266. The only difference is that CCMP3266 died twice as fast from R11 infection when L-tryptophan was added to the co-culture (**Figure 7**). This could implicate tryptophan or IAA produced from tryptophan in R11 virulence or CCMP3266 host susceptibility, however further experiments are needed to decipher how tryptophan addition accelerates CCMP3266 death in co-culture with R11.

IAA concentration was expected to be elevated in the R11 co-cultures. However, less IAA was present compared to the alga grown alone for CCMP3266 supplemented with L-tryptophan and no IAA was detected from the R11-CCMP2090 co-culture. The source of the IAA produced in the R11-CCMP3266 co-culture supplemented with L-tryptophan is not known but this result is suggestive that R11 may divert L-tryptophan into alternate pathways. This is unlike the symbiotic relationship found by Amin et al. (2015) in *Pseudo-nitzschia*, where IAA plays a crucial role in the bacterial-host interaction. While R11 has been found in the same geographic area as *E. huxleyi*, they may not have a shared natural history. Their interaction is also different, pathogenic not symbiotic, and so IAA may play differing roles in symbiotic and pathogenic marine bacteria as it does with their terrestrial counterparts (Escobar and Dandekar, 2003; Vessey, 2003).

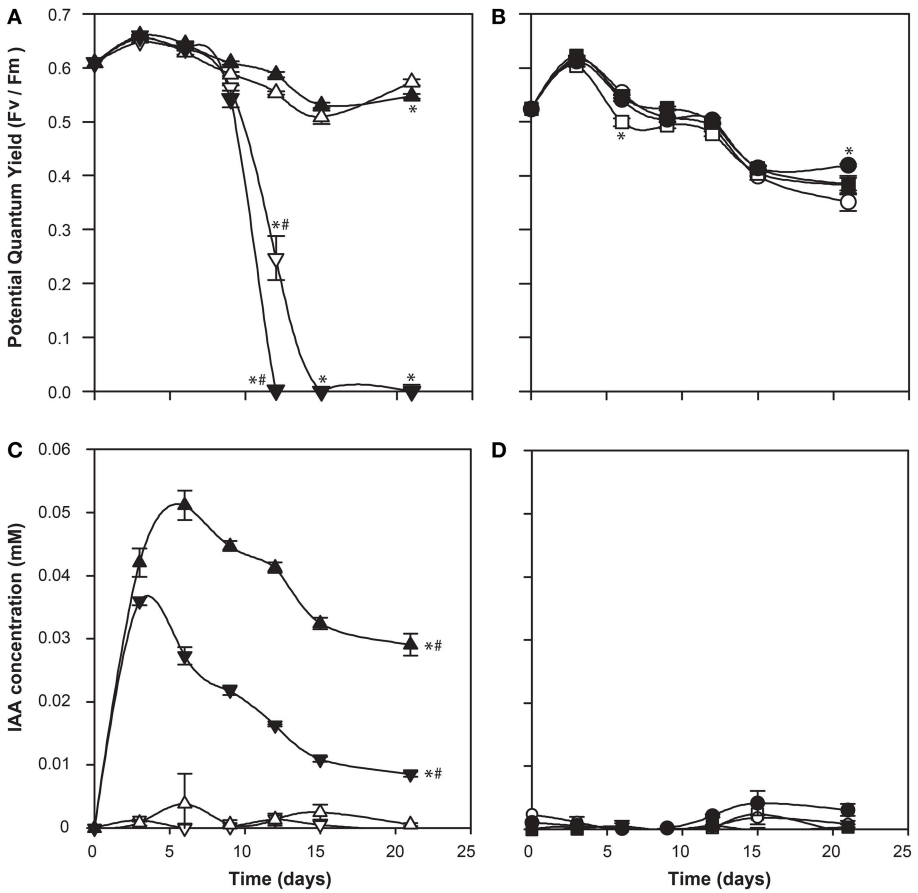

FIGURE 7 | Co-culture of *Ruegeria* sp. R11 with bald (CCMP2090) and coccolith bearing (CCMP3266) *E. huxleyi* strains. The potential quantum yield of CCMP3266 **(A)** and CCMP2090 **(B)**, while IAA production (measured using the Salkowski reagent) for CCMP3266 **(C)**, and CCMP2090 **(D)** is shown. Triangles represent CCMP3266 alone, inverted triangles represent CCMP3266 co-cultured with R11, circles represent CCMP2090 alone and squares represent CCMP2090 co-cultured with R11. White shapes represent the control grown in L1-Si medium, while black indicates the addition of 0.1 mM tryptophan. Error bars represent ±1 SE. An asterisk (*) at a time point indicates that it is significantly different to the control and an asterisk at the end of the line indicates that the treatment is significantly different to the control. A hashtag (#) indicates the treatments are significantly different to the other treatment with a hashtag.

Regardless of its origin, we propose that IAA has evolved different signaling functions in haptophytes and diatoms. The data presented here suggest that IAA plays a role in cell-cell signaling between different cell types within an *E. huxleyi* population. In terrestrial plants and the red alga *G. dura,* IAA influences cell membrane permeability so as to direct cell maturation and differentiation. Therefore, IAA could be involved in similar processes in a unicellular alga, which while not having a multicellular form, has differentiated cell types within its population.

Conclusion

IAA has been identified from a variety of photosynthetic organisms, including cyanobacteria (Sergeeva et al., 2002; Ahmed et al., 2010; Hussain et al., 2010), chlorophytes (Sztein et al., 2000; Mazur et al., 2001; Jirásková et al., 2009; Stirk et al., 2013), as well as some rhodophytes and brown algae (Le Bail et al., 2010; Mikami et al., 2015), but to our knowledge, this is the first time auxins have been identified from an axenic haptophyte culture. This raises further questions about the evolution of auxins, and their possible early role in cell-cell signaling between differentiated cell types within populations of unicellular organisms. Several lines of evidence suggest that the coccolith bearing (C) strain of *E. huxleyi* produces IAA, including: the putative presence of the pathway in the genome; the positive result of the Salkowski reagent when grown with L-tryptophan as well as the correct peak when analyzed with GC×GC-TOFMS; and the lack of this peak or Salkowski result when grown with D-tryptophan. The bald (N) strain did not test positive for IAA, but did show morphological changes in response to IAA. This suggests that not only does IAA play a role in the interaction between algae and their consortia of bacteria (Amin et al., 2015), but could play a role in the signaling between different cell types of algae themselves. These two cell types of *E. huxleyi* co-occur in *E. huxleyi* blooms, but have their highest population density at different times, with the N cell type increasing in proportion at the end of a bloom (Frada et al., 2012). It is therefore

possible that IAA could play a role in cell-cell signaling in blooms, acting as a molecular signal throughout the bloom-bust cycle.

AUTHOR CONTRIBUTIONS

LL and RC conceived the research. LL and JK carried out the bioinformatics analyses, AB, LL, and RC conducted the flow cytometry, LL, PM, and JH performed IAA analysis and LL conducted the growth experiments. LL, JK, HA, and RC drafted the manuscript. All authors have read and approved the manuscript.

FUNDING

This work was supported by Natural Sciences and Engineering Research Council of Canada (grant 402105) to RC. JH and PM acknowledge the support of Genome Canada and Genome Alberta through grants to the Metabolomics Innovation Centre (TMIC).

SUPPLEMENTARY MATERIAL

The Supplementary Material for this article can be found online at: http://journal.frontiersin.org/article/10.3389/fmicb.2016.00828

REFERENCES

Adahchour, M., Beens, J., and Brinkman, U. A. T. (2008). Recent developments in the application of comprehensive two-dimensional gas chromatography. *J. Chromatogr.* 1186, 67–108. doi: 10.1016/j.chroma.2008.01.002

Ahmed, M., Stal, L. J., and Hasnain, S. (2010). Production of indole-3-acetic acid by the cyanobacterium *Arthrospira platensis* strain MMG-9. *J. Microbiol. Biotechnol.* 20, 1259–1265. doi: 10.4014/jmb.1004.04033

Ahrens, R., and Rheinheimer, G. (1967). Über einige sternbildende Bakterien aus der Ostsee. *Kieler Meeresforsch* 23, 127–136.

Amin, S. A., Hmelo, L. R., Van Tol, H. M., Durham, B. P., Carlson, L. T., Heal, K. R., et al. (2015). Interaction and signalling between a cosmopolitan phytoplankton and associated bacteria. *Nature* 522, 98–101. doi: 10.1038/nature14488

Archibald, J. M. (2009). The puzzle of plastid evolution. *Curr. Biol.* 19, R81–R88. doi: 10.1016/j.cub.2008.11.067

Ashen, J. B., Cohen, J. D., and Goff, L. J. (1999). GC-SIM-MS detection and quantification of free indole-3-acetic acid in bacterial galls on the marine alga *Prionitis lanceolata* (Rhodophyta). *J. Phycol.* 35, 493–500. doi: 10.1046/j.1529-8817.1999.3530493.x

Ashen, J. B., and Goff, L. J. (2000). Molecular and ecological evidence for species specificity and coevolution in a group of marine algal-bacterial symbioses. *Appl. Environ. Microbiol.* 66, 3024–3030. doi: 10.1128/AEM.66.7.3024-3030.2000

Bagwell, C. E., Piskorska, M., Soule, T., Petelos, A., and Yeager, C. M. (2014). A diverse assemblage of indole-3-acetic acid producing bacteria associate with unicellular green algae. *Appl. Biochem. Biotechnol.* 173, 1977–1984. doi: 10.1007/s12010-014-0980-5

Baker, D. B., and Ray, P. M. (1965). Relation between effects of auxin on cell wall synthesis and cell elongation. *Plant Physiol.* 40, 360–368. doi: 10.1104/pp.40.2.360

Baldi, B. G., Maher, B. R., Slovin, J. P., and Cohen, J. D. (1991). Stable isotope labeling, *in vivo*, of D- and L-Tryptophan pools in *Lemna gibba* and the low incorporation of label into indole-3-acetic acid. *Plant Physiol.* 95, 1203–1208. doi: 10.1104/pp.95.4.1203

Basu, S., Sun, H., Brian, L., Quatrano, R. L., and Muday, G. K. (2002). Early embryo development in *Fucus distichus* is auxin sensitive. *Plant Physiol.* 130, 292–302. doi: 10.1104/pp.004747

Bhattacharya, D., Price, D. C., Chan, C. X., Qiu, H., Rose, N., Ball, S., et al. (2013). Genome of the red alga *Porphyridium purpureum*. *Nat. Commun.* 4:1941. doi: 10.1038/ncomms2931

Birkemeyer, C., Kolasa, A., and Kopka, J. (2003). Comprehensive chemical derivatization for gas chromatography-mass spectrometry-based multi-targeted profiling of the major phytohormones. *J. Chromatogr.* 993, 89–102. doi: 10.1016/S0021-9673(03)00356-X

Bradley, P. M. (1991). Plant hormones do have a role in controlling growth and development of algae. *J. Phycol.* 27, 317–321. doi: 10.1111/j.0022-3646.1991.00317.x

Bramucci, A. R., Labeeuw, L., Mayers, T. J., Saby, J. A., and Case, R. J. (2015). A small volume bioassay to assess bacterial/phytoplankton co-culture using WATER-pulse-amplitude-modulated (WATER-PAM) fluorometry. *J. Vis. Exp.* 97:e52455. doi: 10.3791/52455

Buggeln, R. G., and Craigie, J. S. (1971). Evaluation of evidence for the presence of indole-3-acetic acid in marine algae. *Planta* 97, 173–178. doi: 10.1007/BF00386764

Case, R. J., Longford, S. R., Campbell, A. H., Low, A., Tujula, N., Steinberg, P. D., et al. (2011). Temperature induced bacterial virulence and bleaching disease in a chemically defended marine macroalga. *Environ. Microbiol.* 13, 529–537. doi: 10.1111/j.1462-2920.2010.02356.x

Charlson, R. J., Lovelock, J. E., Andreae, M. O., and Warren, S. G. (1987). Oceanic phytoplankton, atmospheric sulphur, cloud albedo, and climate. *Nature* 326, 655–661. doi: 10.1038/326655a0

Chitale, M., Hawkins, T., Park, C., and Kihara, D. (2009). ESG: Extended similarity group method for automated protein function prediction. *Bioinformatics* 25, 1739–1745. doi: 10.1093/bioinformatics/btp309

Cleland, R. E. (2010). "Auxin and cell elongation," in *Plant Hormones: Biosynthesis, Signal Transduction, Action!*, ed P. J. Davies (Dordrecht: Springer), 204–220.

Cooke, T. J., Poli, D., Sztein, A. E., and Cohen, J. D. (2002). Evolutionary patterns in auxin action. *Plant Mol. Biol.* 49, 319–338. doi: 10.1023/A:1015242627321

Cooper, M. B., and Smith, A. G. (2015). Exploring mutualistic interactions between microalgae and bacteria in the omics age. *Curr. Opin. Plant Biol.* 26, 147–153. doi: 10.1016/j.pbi.2015.07.003

Crouch, I. J., and Van Staden, J. (1993). Evidence for the presence of plant growth regulators in commercial seaweed products. *Plant Growth Regul.* 13, 21–29. doi: 10.1007/BF00207588

Dallüge, J., Vreuls, R. J. J., Beens, J., and Brinkman, U. A. T. (2002). Optimization and characterization of comprehensive two-dimensional gas chromatography with time-of-flight mass spectrometric detection (GC x GC – TOF MS). *J. Sep. Sci.* 25, 201–214. doi: 10.1002/1615-9314(20020301)25:4<201::AID-JSSC201>3.0.CO;2-B

De Smet, I., Voß, U., Lau, S., Wilson, M., Shao, N., Timme, R. E., et al. (2011). Unraveling the evolution of auxin signaling. *Plant Physiol.* 155, 209–221. doi: 10.1104/pp.110.168161

De Veylder, L., Beeckman, T., and Inzé, D. (2007). The ins and outs of the plant cell cycle. *Nat. Rev. Mol. Cell Biol.* 8, 655–665. doi: 10.1038/nrm2227

Dittami, S. M., Barbeyron, T., Boyen, C., Cambefort, J., Collet, G., Delage, L., et al. (2014). Genome and metabolic network of "*Candidatus* Phaeomarinobacter ectocarpi" Ec32, a new candidate genus of Alphaproteobacteria frequently associated with brown algae. *Front. Genet.* 5:241. doi: 10.3389/fgene.2014.00241

Escobar, M. A., and Dandekar, A. M. (2003). *Agrobacterium tumefaciens* as an agent of disease. *Trends Plant Sci.* 8, 380–386. doi: 10.1016/S1360-1385(03)00162-6

Evans, L., and Trewavas, A. (1991). Is algal development controlled by plant growth substances? *J. Phycol.* 27, 322–326. doi: 10.1111/j.0022-3646.1991.00322.x

Evans, M. L., and Cleland, R. E. (1985). The action of auxin on plant cell elongation. *Crit. Rev. Plant Sci.* 2, 317–365. doi: 10.1080/07352688509382200

Fässler, E., Evangelou, M. W., Robinson, B. H., and Schulin, R. (2010). Effects of indole-3-acetic acid (IAA) on sunflower growth and heavy metal uptake in

combination with ethylene diamine disuccinic acid (EDDS). *Chemosphere* 80, 901–907. doi: 10.1016/j.chemosphere.2010.04.077

Fernandes, N., Case, R. J., Longford, S. R., Seyedsayamdost, M. R., Steinberg, P. D., Kjelleberg, S., et al. (2011). Genomes and virulence factors of novel bacterial pathogens causing bleaching disease in the marine red alga *Delisea pulchra*. *PLoS ONE* 6:e27387. doi: 10.1371/journal.pone.0027387

Finet, C., and Jaillais, Y. (2012). Auxology: when auxin meets plant evo-devo. *Dev. Biol.* 369, 19–31. doi: 10.1016/j.ydbio.2012.05.039

Frada, M. J., Bidle, K. D., Probert, I., and De Vargas, C. (2012). *In situ* survey of life cycle phases of the coccolithophore *Emiliania huxleyi* (Haptophyta). *Environ. Microbiol.* 14, 1558–1569. doi: 10.1111/j.1462-2920.2012.02745.x

Glickmann, E., and Dessaux, Y. (1995). A critical examination of the specificity of the salkowski reagent for indolic compounds produced by phytopathogenic bacteria. *Appl. Environ. Microbiol.* 61, 793–796.

Gravel, V., Antoun, H., and Tweddell, R. J. (2007). Growth stimulation and fruit yield improvement of greenhouse tomato plants by inoculation with *Pseudomonas putida* or *Trichoderma atroviride*: possible role of indole acetic acid (IAA). *Soil Biol. Biochem.* 39, 1968–1977. doi: 10.1016/j.soilbio.2007.02.015

Guillard, R. R. L., and Hargraves, P. E. (1993). *Stichochrysis immobilis* is a diatom, not a chrysophyte. *Phycologia* 32, 234–236. doi: 10.2216/i0031-8884-32-3-234.1

Holligan, P. M., Fernández, E., Aiken, J., Balch, W. M., Boyd, P., Burkill, P. H., et al. (1993). A biogeochemical study of the coccolithophore, *Emiliania huxleyi*, in the North Atlantic. *Global Biogeochem. Cycles* 7, 879–900. doi: 10.1029/93GB01731

Hughes, D. T., and Sperandio, V. (2008). Inter-kingdom signalling: communication between bacteria and their hosts. *Nat. Rev. Microbiol.* 6, 111–120. doi: 10.1038/nrmicro1836

Hussain, A., Krischke, M., Roitsch, T., and Hasnain, S. (2010). Rapid determination of cytokinins and auxin in cyanobacteria. *Curr. Microbiol.* 61, 361–369. doi: 10.1007/s00284-010-9620-7

Jacobs, W. P. J., Falkenstein, K., and Hamilton, R. H. (1985). Nature and amount of auxin in algae. *Plant Physiol.* 78, 844–848. doi: 10.1104/pp.78.4.844

Jin, Q., Scherp, P., Heimann, K., and Hasenstein, K. H. (2008). Auxin and cytoskeletal organization in algae. *Cell Biol. Int.* 32, 542–545. doi: 10.1016/j.cellbi.2007.11.005

Jirásková, D., Poulíèková, A., Novák, O., Sedláková, K., Hradecká, V., and Strnad, M. (2009). High-throughput screening technology for monitoring phytohormone production in microalgae. *J. Phycol.* 45, 108–118. doi: 10.1111/j.1529-8817.2008.00615.x

Joint, I., Tait, K., Callow, M. E., Callow, J. A., Milton, D., Williams, P., et al. (2002). Cell-to-cell communication across the prokaryote-eukaryote boundary. *Science* 298, 1207. doi: 10.1126/science.1077075

Kiseleva, A. A., Tarachovskaya, E. R., and Shishova, M. F. (2012). Biosynthesis of phytohormones in algae. *Russ. J. Plant Physiol.* 59, 595–610. doi: 10.1134/S1021443712050081

Klaveness, D., and Paasche, E. (1971). Two different *Coccolithus huxleyi* cell types incapable of coccolith formation. *Archiv. Microbiol.* 385, 382–385. doi: 10.1007/bf00407700

Kobayashi, M., Izui, H., Nagasawa, T., and Yamada, H. (1993). Nitrilase in biosynthesis of the plant hormone indole-3-acetic acid from indole-3-acetonitrile: cloning of the *Alcaligenes* gene and site-directed mutagenesis of cysteine residues. *Proc. Natl. Acad. Sci. U.S.A.* 90, 247–251. doi: 10.1073/pnas.90.1.247

Kooten, O., Snel, J. F. H., Van Kooten, O., Snel, J. F. H., Kooten, O., and Snel, J. F. H. (1990). The use of chlorophyll fluorescence nomenclature in plant stress physiology. *Photosynthesis Res.* 25, 147–150. doi: 10.1007/BF00033156

Køeèek, P., Skùpa, P., Libus, J., Naramoto, S., Tejos, R., Friml, J., et al. (2009). The PIN-FORMED (PIN) protein family of auxin transporters. *Genome Biol.* 10:249. doi: 10.1186/gb-2009-10-12-249

Laguna, R., Romo, J., Read, B. A., Wahlund, M., and Wahlund, T. M. (2001). Induction of phase variation events in the life cycle of the marine coccolithophorid *Emiliania huxleyi*. *Appl. Environ. Microbiol.* 67, 3824–3831. doi: 10.1128/AEM.67.9.3824-3831.2001

Lau, S., Shao, N., Bock, R., Jürgens, G., and De Smet, I. (2009). Auxin signaling in algal lineages: fact or myth? *Trends Plant Sci.* 14, 182–188. doi: 10.1016/j.tplants.2009.01.004

Le Bail, A., Billoud, B., Kowalczyk, N., Kowalczyk, M., Gicquel, M., Le Panse, S., et al. (2010). Auxin metabolism and function in the multicellular brown alga *Ectocarpus siliculosus*. *Plant Physiol.* 153, 128–144. doi: 10.1104/pp.109.149708

Li, L., Stoeckert, C. J., and Roos, D. S. (2003). OrthoMCL: identification of ortholog groups for Eukaryotic genomes. *Genome Res.* 13, 2178–2189. doi: 10.1101/gr.1224503

Li, T., Wang, C., and Miao, J. (2007). Identification and quantification of indole-3-acetic acid in the kelp *Laminaria japonica* Areschoug and its effect on growth of marine microalgae. *J. Appl. Phycol.* 19, 479–484. doi: 10.1007/s10811-007-9159-6

Manefield, M., Rasmussen, T. B., Henzter, M., Andersen, J. B., Steinberg, P., Kjelleberg, S., et al. (2002). Halogenated furanones inhibit quorum sensing through accelerated LuxR turnover. *Microbiology* 148, 1119–1127. doi: 10.1099/00221287-148-4-1119

Mano, Y., and Nemoto, K. (2012). The pathway of auxin biosynthesis in plants. *J. Exp. Bot.* 63, 2853–2872. doi: 10.1093/jxb/ers091

Mashiguchi, K., Tanaka, K., Sakai, T., Sugawara, S., Kawaide, H., Natsume, M., et al. (2011). The main auxin biosynthesis pathway in *Arabidopsis*. *Proc. Natl. Acad. Sci. U.S.A.* 108, 18512–18517. doi: 10.1073/pnas.1108434108

Matsuo, Y., Imagawa, H., Nishizawa, M., and Shizuri, Y. (2005). Isolation of an algal morphogenesis inducer from a marine bacterium. *Science* 307, 1598. doi: 10.1126/science.1105486

Mayers, T., Bramucci, A. R., Yakimovich, K., and Case, R. (2016). A bacterial pathogen displaying temperature-enhanced virulence of the microalga *Emiliania huxleyi*. *Front. Microbiol.* 7:892. doi: 10.3389/fmicb.2016.00892

Mazur, H., Konop, A., and Synak, R. (2001). Indole-3-acetic acid in the culture medium of two axenic green microalgae. *J. Appl. Phycol.* 13, 35–42. doi: 10.1023/A:1008199409953

Mikami, K., Mori, I. C., Matsuura, T., Ikeda, Y., Kojima, M., Sakakibara, H., et al. (2015). Comprehensive quantification and genome survey reveal the presence of novel phytohormone action modes in red seaweeds. *J. Appl. Phycol.* doi: 10.1007/s10811-015-0759-2. [Epub ahead of print].

Nelles, A. (1977). Short-term effects of plant hormones on membrane potential and membrane permeability of dwarf maize coleoptile cells (*Zea mays* L. dl) in comparison with growth responses. *Planta* 137, 293–298. doi: 10.1007/BF00388165

Ng, J., Perrine-Walker, F., Wasson, A., and Mathesius, U. (2015). The control of auxin transport in parasitic and symbiotic root–microbe interactions. *Plants* 4, 606–643. doi: 10.3390/plants4030606

Nonhebel, H. M. (2015). Tryptophan-independent IAA synthesis: critical evaluation of the evidence. *Plant Physiol.* 169, 1001–1005. doi: 10.1104/pp.15.01091

Normanly, J. (2010). Approaching cellular and molecular resolution of auxin biosynthesis and metabolism. *Cold Spring Harb. Perspect. Biol.* 2:a001594. doi: 10.1101/cshperspect.a001594

Osakabe, Y., Arinaga, N., Umezawa, T., Katsura, S., Nagamachi, K., Tanaka, H., et al. (2013). Osmotic stress responses and plant growth controlled by potassium transporters in *Arabidopsis*. *Plant Cell* 25, 609–624. doi: 10.1105/tpc.112.105700

Paasche, E. (2002). A review of the coccolithophorid *Emiliania huxleyi* (Prymnesiophyceae), with particular reference to growth, coccolith formation, and calcification-photosynthesis interactions. *Phycologia* 40, 503–529. doi: 10.2216/i0031-8884-40-6-503.1

Patten, C. L., and Glick, B. R. (2002). Role of *Pseudomonas putida* indoleacetic acid in development of the host plant root system. *Appl. Environ. Microbiol.* 68, 3795–3801. doi: 10.1128/AEM.68.8.3795-3801.2002

Prieto, C. R. E. Cordoba, C., N. M., Montenegro, J. A. M., and González-Mariño, G. E. (2011). Production of indole-3-acetic acid in the culture medium of microalga *Scenedesmus obliquus* (UTEX 393). *J. Braz. Chem. Soc.* 22, 2355–2361. doi: 10.1590/S0103-50532011001200017

Ross, J. J., and Reid, J. B. (2010). Evolution of growth-promoting plant hormones. *Funct. Plant Biol.* 37, 795–805. doi: 10.1071/FP10063

Sakata, T., Oshino, T., Miura, S., Tomabechi, M., Tsunaga, Y., Higashitani, N., et al. (2010). Auxins reverse plant male sterility caused by high temperatures. *Proc. Natl. Acad. Sci. U.S.A.* 107, 8569–8574. doi: 10.1073/pnas.1000869107

Salama, E.-S., Kabra, A. N., Ji, M.-K., Kim, J. R., Min, B., and Jeon, B.-H. (2014). Enhancement of microalgae growth and fatty acid content under the influence of phytohormones. *Bioresour. Technol.* 172C, 97–103. doi: 10.1016/j.biortech.2014.09.002

Sanderson, K. J., Jameson, P. E., and Zabkiewicz, J. A. (1987). Auxin in a seaweed extract: identification and quantitation of indole-3-acetic acid by Gas Chromatography-Mass Spectrometry. *J. Plant Physiol.* 129, 363–367. doi: 10.1016/S0176-1617(87)80093-7

Schaefer, A. L., Greenberg, E. P., Oliver, C. M., Oda, Y., Huang, J. J., Bittan-Banin, G., et al. (2008). A new class of homoserine lactone quorum-sensing signals. *Nature* 454, 595–599. doi: 10.1038/nature07088

Schreiber, U., Schliwa, U., and Bilger, W. (1986). Continuous recording of photochemical and non-photochemical chlorophyll fluorescence quenching with a new type of modulation fluorometer. *Photosynthesis Res.* 10, 51–62. doi: 10.1007/BF00024185

Sergeeva, E., Liaimer, A., and Bergman, B. (2002). Evidence for production of the phytohormone indole-3-acetic acid by cyanobacteria. *Planta* 215, 229–238. doi: 10.1007/s00425-002-0749-x

Singh, R. P., Bijo, A. J., Baghel, R. S., Reddy, C. R. K., and Jha, B. (2011). Role of bacterial isolates in enhancing the bud induction in the industrially important red alga *Gracilaria dura*. *FEMS Microbiol. Ecol.* 76, 381–392. doi: 10.1111/j.1574-6941.2011.01057.x

Spaepen, S., Vanderleyden, J., and Remans, R. (2007). Indole-3-acetic acid in microbial and microorganism-plant signaling. *FEMS Microbiol. Rev.* 31, 425–448. doi: 10.1111/j.1574-6976.2007.00072.x

Stirk, W. A., Bálint, P., Tarkowská, D., Novák, O., Maróti, G., Ljung, K., et al. (2014). Effect of light on growth and endogenous hormones in *Chlorella minutissima* (Trebouxiophyceae). *Plant Physiol. Biochem.* 79, 66–76. doi: 10.1016/j.plaphy.2014.03.005

Stirk, W. A., Ördög, V., Novák, O., Rolèík, J., Strnad, M., Bálint, P., et al. (2013). Auxin and cytokinin relationships in 24 microalgal strains. *J. Phycol.* 49, 459–467. doi: 10.1111/jpy.12061

Sudha, M., Shyamala Gowri, R., Prabhavathi, P., Astapriya, P., Yamuna Devi, S., and Saranya, A. (2012). Production and optimization of indole acetic acid by indegenous micro flora using agro waste as substrate. *Pak. J. Biol. Sci.* 15, 39–43. doi: 10.3923/pjbs.2012.39.43

Sztein, A. E., Cohen, J. D., and Cooke, T. J. (2000). Evolutionary patterns in the auxin metabolism of green plants. *Int. J. Plant Sci.* 161, 849–859. doi: 10.1086/317566

Tamás, I. A., Atkins, B. D., Ware, S. M., and Bidwell, R. G. S. (1972). Indoleacetic acid stimulation of phosphorylation and bicarbonate fixation by chloroplast preparations in light. *Can. J. Bot.* 50, 1523–1527. doi: 10.1139/b72-189

Tarakhovskaya, E. R., Maslov, Y. I., and Shishova, M. F. (2007). Phytohormones in algae. *Russ. J. Plant Physiol.* 54, 163–170. doi: 10.1134/S1021443707020021

Teale, W. D., Paponov, I. A., and Palme, K. (2006). Auxin in action: signalling, transport and the control of plant growth and development. *Nat. Rev. Mol. Cell Biol.* 7, 847–859. doi: 10.1038/nrm2020

Tivendale, N. D., Ross, J. J., and Cohen, J. D. (2014). The shifting paradigms of auxin biosynthesis. *Trends Plant Sci.* 19, 44–51. doi: 10.1016/j.tplants.2013.09.012

Turnaev, I. I., Gunbin, K. V., and Afonnikov, D. A. (2015). Plant auxin biosynthesis did not originate in charophytes. *Trends Plant Sci.* 20, 463–465. doi: 10.1016/j.tplants.2015.06.004

Vance, B. D. (1987). Phytohormone effects on cell division in *Chlorella pyrenoidosa* chick (TX-7-11-05) (chlorellaceae). *J. Plant Growth Regul.* 5, 169–173. doi: 10.1007/BF02087185

Van Overbeek, J. (1940). Auxin in marine algae. *Plant Physiol.* 15, 291–299. doi: 10.1104/pp.15.2.291

Vardi, A., Van Mooy, B. A. S., Fredricks, H. F., Popendorf, K. J., Ossolinski, J. E., Haramaty, L. et al. (2009). Viral glycosphingolipids induce lytic infection and cell death in marine phytoplankton. *Science* 326, 861–865. doi: 10.1126/science.1177322

Velasquez, S. M., Barbez, E., Kleine-Vehn, J., and Estevez, J. (2016). Auxin and cellular elongation. *Plant Physiol.* 170, 1206–1215. doi: 10.1104/pp.15.01863

Vessey, J. K. (2003). Plant growth promoting rhizobacteria as biofertilizers. *Plant Soil* 255, 571–586. doi: 10.1023/A:1026037216893

Wang, C., Li, S.-S., and Han, G.-Z. (2016). Commentary: Plant auxin biosynthesis did not originate in charophytes. *Front. Plant. Sci.* 7:158. doi: 10.3389/fpls.2016.00158

Wang, C., Liu, Y., Li, S.-S., and Han, G.-Z. (2014). Origin of plant auxin biosynthesis in charophyte algae. *Trends Plant Sci.* 19, 741–743. doi: 10.1016/j.tplants.2014.10.004

Wang, W., Li, H., Lin, X., Yang, S., Wang, Z., and Fang, B. (2015). Transcriptome analysis identifies genes involved in adventitious branches formation of *Gracilaria lichenoides in vitro*. *Sci. Rep.* 5, 17099. doi: 10.1038/srep17099

Went, F. W. (1926). On growth accelerating substances in the coleoptile of *Avena sativa*. *Koninklijke Akademie Wetenschappen Amsterdam* 30, 10–19.

Xie, H., Pasternak, J. J., and Glick, B. R. (1996). Isolation and characterization of mutants of the plant growth promoting rhizobacterium *Pseudomonas putida* GR12-2 that overproduce indoleacetic-acid. *Curr. Microbiol.* 32, 67–71. doi: 10.1007/s002849900012

Yamada, T. (1993). The role of auxin in plant-disease development. *Annu. Rev. Phytopathol.* 31, 253–273. doi: 10.1146/annurev.py.31.090193.001345

Yamada, T., Palm, C. J., Brooks, B., and Kosuge, T. (1985). Nucleotide sequences of the *Pseudomonas savastanoi* indoleacetic acid genes show homology with *Agrobacterium tumefaciens* T-DNA. *Proc. Natl. Acad. Sci. U.S.A.* 82, 6522–6526. doi: 10.1073/pnas.82.19.6522

Yue, J., Hu, X., and Huang, J. (2014). Origin of plant auxin biosynthesis. *Trends Plant Sci.* 19, 764–770. doi: 10.1016/j.tplants.2014.07.004

Zhang, S., De Boer, A. H., and Van Duijn, B. (2016). Auxin effects on ion transport in *Chara corallina*. *J. Plant Physiol.* 193, 37–44. doi: 10.1016/j.jplph.2016.02.009

Zhang, S., and Van Duijn, B. (2014). Cellular auxin transport in algae. *Plants* 3, 58–69. doi: 10.3390/plants3010058

Zhao, Y. (2010). Auxin biosynthesis and its role in plant development. *Annu. Rev. Plant Biol.* 61, 49–64. doi: 10.1146/annurev-arplant-042809-112308

Zhu, J., Oger, P. M., Schrammeijer, B., Hooykaas, P. J., Farrand, S. K., and Winans, S. C. (2000). The bases of crown gall tumorigenesis. *J. Bacteriol.* 182, 3885–3895. doi: 10.1128/JB.182.14.3885-3895.2000

Conflict of Interest Statement: The authors declare that the research was conducted in the absence of any commercial or financial relationships that could be construed as a potential conflict of interest.

frontiers in Microbiology

ORIGINAL RESEARCH
published: 03 February 2016
doi: 10.3389/fmicb.2016.00059

A Bacterial Quorum-Sensing Precursor Induces Mortality in the Marine Coccolithophore, *Emiliania huxleyi*

Elizabeth L. Harvey[1†], Robert W. Deering[2], David C. Rowley[2], Abrahim El Gamal[3], Michelle Schorn[3], Bradley S. Moore[3], Matthew D. Johnson[4], Tracy J. Mincer[5] and Kristen E. Whalen[5*†]*

[1] Department of Marine Sciences, Skidaway Institute of Oceanography, University of Georgia, Savannah, GA, USA, [2] Department of Biomedical and Pharmaceutical Sciences, University of Rhode Island, Kingston, RI, USA, [3] Scripps Institution of Oceanography, University of California at San Diego, La Jolla, CA, USA, [4] Biology Department, Woods Hole Oceanographic Institution, Woods Hole, MA, USA, [5] Marine Chemistry and Geochemistry Department, Woods Hole Oceanographic Institution, Woods Hole, MA, USA

OPEN ACCESS

Edited by:
Xavier Mayali, Lawrence Livermore National Laboratory, USA

Reviewed by:
Assaf Vardi, Weizmann Institute of Science, Israel
Travis Blake Meador, University of Bremen, Germany

***Correspondence:**
Elizabeth L. Harvey
elizabeth.harvey@skio.uga.edu;
Kristen E. Whalen
kwhalen@whoi.edu

†These authors have contributed equally to this work.

Specialty section:
This article was submitted to Aquatic Microbiology, a section of the journal Frontiers in Microbiology

Received: *23 October 2015*
Accepted: *13 January 2016*
Published: *03 February 2016*

Citation:
Harvey EL, Deering RW, Rowley DC, El Gamal A, Schorn M, Moore BS, Johnson MD, Mincer TJ and Whalen KE (2016) A Bacterial Quorum-Sensing Precursor Induces Mortality in the Marine Coccolithophore, Emiliania huxleyi. Front. Microbiol. 7:59. doi: 10.3389/fmicb.2016.00059

Interactions between phytoplankton and bacteria play a central role in mediating biogeochemical cycling and food web structure in the ocean. However, deciphering the chemical drivers of these interspecies interactions remains challenging. Here, we report the isolation of 2-heptyl-4-quinolone (HHQ), released by *Pseudoalteromonas piscicida*, a marine gamma-proteobacteria previously reported to induce phytoplankton mortality through a hitherto unknown algicidal mechanism. HHQ functions as both an antibiotic and a bacterial signaling molecule in cell–cell communication in clinical infection models. Co-culture of the bloom-forming coccolithophore, *Emiliania huxleyi* with both live *P. piscicida* and cell-free filtrates caused a significant decrease in algal growth. Investigations of the *P. piscicida* exometabolome revealed HHQ, at nanomolar concentrations, induced mortality in three strains of *E. huxleyi*. Mortality of *E. huxleyi* in response to HHQ occurred slowly, implying static growth rather than a singular loss event (e.g., rapid cell lysis). In contrast, the marine chlorophyte, *Dunaliella tertiolecta* and diatom, *Phaeodactylum tricornutum* were unaffected by HHQ exposures. These results suggest that HHQ mediates the type of inter-domain interactions that cause shifts in phytoplankton population dynamics. These chemically mediated interactions, and other like it, ultimately influence large-scale oceanographic processes.

Keywords: infochemicals, algicidal compound, bacteria–phytoplankton interaction, HHQ, *Pseudoalteromonas*, *Emiliania huxleyi*, IC50, mortality

INTRODUCTION

In the marine environment, interactions between bacteria and eukaryotic phytoplankton are pervasive and drive oceanic biogeochemical cycles (Legendre and Rassoulzadegan, 1995), and can have consequences for both microbial communities (Bratbak and Thingstad, 1985) and structuring of marine food webs (Azam et al., 1983). Bacteria–phytoplankton interactions are complex, being both temporally variable (Danger et al., 2007) and species-specific (Fukami et al., 1997), and remain largely enigmatic. These interactions can be beneficiary, as bacteria and phytoplankton can support the growth of one another via the exchange or recycling

of nutrients (Azam et al., 1983); however, the interaction can also be detrimental, resulting in phytoplankton morbidity or mortality (Mayali and Azam, 2004). The intricate relationships between these two kingdoms are often mediated via excreted compounds that can direct communication between the two organisms. Identifying these released compounds, and their influence on the population dynamics of both phytoplankton and bacteria, will enhance our understanding of the role of "infochemicals" on large-scale biogeochemical processes.

The marine genus *Pseudoalteromonas* constitutes 0.5–6.0% of bacterial species globally (Wietz et al., 2010), and has been found in seawater, marine sediments, and associated with marine eukaryotes (Bowman, 2007; Skovhus et al., 2007; Sneed et al., 2014). Secondary metabolites secreted by members of this genus fulfill a variety of ecological roles, including involvement in chemical protection, settlement, induction of metamorphosis in marine invertebrates, and commercially, as antifouling, antifungal agents (Bowman, 2007; Ross et al., 2014; Sneed et al., 2014). Moreover, *Pseudoalteromonas* species have been implicated in producing algal-lytic compounds that cause mortality in dinoflagellates (Skerratt et al., 2002; Kim et al., 2009), diatoms (Mitsutani et al., 2001), and raphidophytes (Lovejoy et al., 1998); however, in each of these cases the causative chemical compound is yet unidentified.

In order to gain a more mechanistic understanding of this chemically mediated phytoplankton mortality, we exposed the globally important coccolithophore, *Emiliania huxleyi* to cultures of *Pseudoalteromonas piscicida*. *E. huxleyi* plays a predominant role in oceanic carbon (Balch et al., 1992; Iglesias-Rodriguez et al., 2008) and sulfur (Simo, 2001) cycling; therefore, understanding the factors that mediate the population abundance and distribution of this algal species is important for predicting its role in marine nutrient cycling and global climate. Further, *E. huxleyi* has been shown to form complex relationships with bacteria. For example, it has been observed that the Roseobacter, *Phaeobacter gallaeciensis* maintains a mutualistic-turned-to-parasitic relationship with *E. huxleyi* dependent on the metabolic stage of the algae (Seyedsayamdost et al., 2011). While no direct relationship between a *Pseudoalteromonas* species and *E. huxleyi* has been established, Seymour et al. (2010) found that *Pseudoalteromonas haloplanktis* exhibited strong chemoattraction to dimethlysulfoniopropionate (DMSP), a sulfur compound abundantly produced by *E. huxleyi*. Additionally, bacterial OTUs, including *Pseudoalteromonas*, were positively correlated with coccolithophores and *E. huxleyi* abundance in samples from a temperate marine coastal site off Plymouth, UK (Gilbert et al., 2012). Thus, these two taxa do co-occur in the water column, and have opportunity to interact with one another.

Here, we report the isolation and identification of a potent algicidal compound excreted by *P. piscicida* with specificity for *E. huxleyi*. We found that the presence of *P. piscicida* resulted in mortality of *E. huxleyi*, and used bioassay-guided fractionation to identify the responsible chemical mediator(s) of this interaction. This research further reveals the importance of the bacterial exometabolome in inter-domain interactions, especially those that can have significant biogeochemical implications.

MATERIALS AND METHODS

Culture Conditions and Crude Extract Preparation

A pure culture of *P. piscicida* was isolated from open ocean plastic debris in the North Atlantic (Mincer culture ID; A757; Whalen et al., 2015), cryopreserved in 10% sterile DMSO, and stored at −85°C prior to experiments. From these stocks, multiple 'starter' cultures were prepared by inoculating 8 mL of TSW media (1 g tryptone in 1 L of 75:25 seawater/MilliQ water) with 100 μL of cryopreserved culture, and then incubated at 23°C while shaking at 100 rpm for 3 days. After 3 days, 2 mL of 'starter' culture was used to inoculate seven, 1.5 L Fernbach flasks of TSY media (1 g tryptone, 1 g yeast extract, 75% seawater), the newly inoculated cultures were then grown at 100 rpm for 8 days at 23°C. On day 7, 20 mL (approximately weight = 7.8 g) of 1:1 mixture of sterile Amberlite® XAD-7 and XAD-16 resin that had been extensively washed in organic solvent, dried, and autoclaved was added to each 1.5 L culture. Twenty-four hours later (day 8), the resin was filtered from the bacterial culture through combusted stainless steel mesh under gentle vacuum (<5 in Hg), desalted by rinsing with MilliQ water, pooled, and allowed to dry overnight at room temperature. Bacterial metabolites were eluted from the resin first in 800 mL of (1:1) methanol (MeOH):dichloromethane (DCM), followed by 800 mL of methanol. This crude extract was dried under vacuum centrifugation and stored at −85°C until testing in phytoplankton growth assays.

Emiliania huxleyi (Plymouth Algal Culture Collection: DHB624 and National Center for Marine Algae: CCMP374, CCMP379), *Dunaliella tertiolecta* (CCMP1320), and *Phaeodactylum tricornutum* (CCMP2561) were used in these experiments. All phytoplankton cultures were grown in 0.2 μm sterile-filtered, autoclaved seawater (FSW), enriched with f/2 (*P. tricornutum*) or f/2 -Si (all other species) media (Guillard, 1975). All cultures were maintained on a 12:12 h light:dark at 18°C, salinity of approximately 20 psu, and light intensity of 85–100 μmol photon m^{-2} s^{-1}. Hereafter, these conditions will be referred to as general culturing conditions. Phytoplankton cultures were transferred every 7–10 days to maintain exponential growth. Unless specified, cultures were not axenic. Axenic cultures of *E. huxleyi* 624 were prepared by adding 1 mL of a dense *E. huxleyi* culture into 4 mL of f/2 -Si containing an antibiotic cocktail of penicillin G (3 mM), dihydrostreptomycin sulfate (0.2 mM), and gentamicin (0.5 mM). The culture was incubated under the general culturing conditions described above for 48 h, after which a 500 μL aliquot of the culture was transferred to fresh, antibiotic-free f/2 -Si media. This culture was maintained in exponential growth, similar to the other phytoplankton cultures. The culture was tested with DAPI (4′, 6-diamidino-2-phenylindole) to ensure it remained axenic throughout the course of the experiments, and this culture was used for all experiments that called for axenic *E. huxleyi*. For all phytoplankton counts, a 200 μL aliquot of culture was run on a flow cytometer (Guava, Millipore). Cell abundance was determined by using species-specific settings

determined based on chlorophyll a (692 nm) and side scatter (SSC) for each species examined.

Phytoplankton Growth Inhibition Assay

The growth rate of *E. huxleyi* (strain 624) was measured in response to both live *P. piscicida* cells (10^3 and 10^6 cell mL^{-1}) and filtrate from *P. piscicida* cells equivalent to 10^3 and 10^6 cell mL^{-1} in TSY media (between <1 and 40 μL of filtrate per 1 mL of algal culture). Cells from strain 624 in their exponential growth phase were plated in 24- well plates at a final concentration of 10^5 cell mL^{-1}, and exposed to either live *P. piscicida* cells or filtrate. These experiments were conducted with both xenic and axenic cultures of *E. huxleyi*. Each treatment was replicated in triplicate. Prior to inoculation into 24-well plates, the bacteria were enumerated on a flow cytometer and diluted appropriately. Filtrate from the *P. piscicida* culture was obtained by filtering 5 mL of live culture through a 0.2 μm sterile syringe tip filter. Prior to sampling for phytoplankton cell abundance, triplicate wells were gently mixed via pipet and 50–200 μL aliquots were taken from each replicate, pipetted into a 96-well plate, and run on the flow cytometer. Growth rate was calculated by using the exponential growth equation,

$$\text{Growth rate} = \ln(A_f/A_i)/T_f - T_i$$

where A is the abundance and T is the time, over the first 72 h of the experiment. Significant differences in growth rates of *E. huxleyi* in response to chemical additions were determined by using a one-way analysis of variance (ANOVA) and Tukey's HSD *post hoc* analysis. All statistical analyses were performed using MatLAB (v. 8.3). Those treatments where the growth rate was significantly different from the algae only control ($p < 0.05$) were considered to have activity.

Bioassay-Guided Fractionation of Exudates from *P. piscicida*

Assessment of semi-purified fractions via the growth inhibition assay was carried out using axenic *E. huxleyi* strain 624 to determine those algicidal compounds exuded by *P. piscicida* (**Supplementary Figure S1**). *E. huxleyi* (624) cells in exponential growth phase were plated at 10^5 cell mL^{-1} in to 24-well plates in triplicate and exposed to crude and semi-purified fractions dissolved in DMSO, with DMSO concentrations not exceeding 0.2% v/v. Appropriate controls were run with each growth inhibition assay, i.e., f/2 media only, DMSO without compounds, were performed in triplicate. Well plates were incubated under general culturing conditions, and enumerated on the flow cytometer, as described above. At each step of the chemical fractionation process described below, semi-purified fractions were tested in the growth inhibition assay using axenic *E. huxleyi* strain 624 and included the addition of paired controls (TSY media only, f/2, and DMSO). Statistical comparison of growth rates resulting from semi-purified fractions were compared to controls as described in Section "Phytoplankton Growth Inhibition Assay."

The entire crude extract (1260 mg; described above) was applied to a silica gel column and eluted with a step-gradient of isooctane, (4:1) isooctane/ethylacetate (EtOAc), (3:2) isooctane/EtOAc, (2:3) isooctane/EtOAc, (1:4) isooctane/EtOAc, EtOAc, (1:1) EtOAc/MeOH, and 100% MeOH, yielding eight fractions. A total of 458 mg of material eluting with (1:1) EtOAc/MeOH from the silica column was separated further by solid-phase extraction (Supelclean ENVI-18) eluting with a step-gradient of (20:1) water/acetonitrile, (4:1) water/acetonitrile, (3:2) water/acetonitrile, (2:3) water/acetonitrile, (1:20) water/acetonitrile, and acetone. All solvents, except acetone, were acidified with 0.1% formic acid. The active fraction, totaling 9.73 mg, eluted with (2:3) water/acetonitrile, and was separated further by semipreparative HPLC using an Agilent 1200 series HPLC and a Phenomenex Kinetex 5 μm C_{18} 100 Å (150 mm × 10 mm) column, heated to 30°C, and a gradient of 42–95% acetonitrile in water with a flow rate of 4 mL min^{-1}. All solvents were acidified with 0.1% formic acid. Fractions were pooled according to UV adsorption characteristics at 276 nm. A single active fraction eluted in the 58% water/42% acetonitrile fraction. A total of 1 mg of the active compound, determined to be 2-heptyl-4-quinolone, was recovered from 10.5 L of culture after 8 days of growth, yielding a final concentration of 0.39 μM.

Structure Determination of Bacterial Compounds

NMR experiments were conducted using an Agilent NMR 500 MHz (Agilent Technologies, Santa Clara, CA, USA) with DMSO-d_6 as the solvent (referenced to residual DMSO at δ_H 2.50 and δ_C 39.5) at 25°C. HHQ standard was acquired from Sigma Aldrich (St. Louis, MO, USA).

Accurate mass spectra for 2-heptyl-4-quinolone was acquired on an Agilent Technologies 6230 TOF with a Dual Agilent Jet Stream Electrospray Ionization source, equipped with an Agilent 1260 Infinity series HPLC with a Phenomenex Kinetex 2.6 μm, C_{18}, 100 Å, LC column (150 mm × 2.1 mm) as the stationary phase with a flow rate of 0.2 mL min^{-1}. The ion source was operated at 350°C and 3500 V with a nitrogen gas flow of 8 L min^{-1}, nebulizer pressure of 40 psi and fragmentor voltage of 135 V. The chromatrography method was as follows: 0–10 min at (1:1) water/acetonitrile; then ramped to (1:20) water/acetonitrile over the next 7 min; held at (1:20) water/acetonitrile for 3 min; then returned to (1:1) water/acetonitrile and held for 3 min. All solvents were acidified with 0.1% formic acid. The instrument was equipped with an Agilent Mass Hunter Workstation version B0.4.00 software.

Bioinformatic Analysis of *P. piscicida* Genome

High purity *P. piscicida* genomic DNA was extracted, purified, and sequenced using the Ion PGM™ Hi-Q Sequencing Kit according to the methods of Agarwal et al. (2014). Genomic DNA sequences were assembled into contigs using the SPAdes Genome Assembler (v 3.6.0; Bankevich et al., 2012), and the draft genome was annotated using RAST (Aziz et al., 2008). Following RAST annotation, a homology search was conducted for *P. piscicida* homologs matching the *Pseudomonas aeruginosa pqsABCDE* operon, *pqsR*, and *pqsH* genes, previously determined

to be involved in alkylquinoline synthesis (Dulcey et al., 2013; Drees and Fetzner, 2015) using SEED Viewer (Version 2.0; Overbeek et al., 2005).

Dose-Response Experiments

The dose-response relationship of 2-heptyl-4-quinolone was measured in *E. huxleyi* (strains 624, 374, 379), *D. tertiolecta,* and *P. tricornutum* in growth inhibition assays with pure compounds tested at various concentrations in triplicate. All the *E. huxleyi* strains were axenic, where as the strains of *D. tertiolecta* and *P. tricornutum* were xenic. Dose-response experiments were conducted similarly to the growth inhibition assays. Cells from exponentially growing cultures were grown in triplicate 24-well plates. Initial cell abundance was determined by carbon concentration (Menden-Deuer and Lessard, 2000), where each well had an initial carbon concentration of 1.2×10^6 pg C mL^{-1}. Well plates were kept under general culturing conditions, and cell abundance was monitored daily using a flow cytometer (Guava, Millipore) as described above.

Phytoplankton growth rate (μ d^{-1}) was plotted against the concentration of each pure compound in order to determine the concentration of compound resulting in 50% growth inhibition (IC_{50}). Pure compound IC_{50} values were calculated and 95% confidence intervals were estimated using Prism 6.0 software (GraphPad) by fitting the log transformation of the response variable (I; inhibitor concentration) by non-linear regression to the equation (1); where the slope factor (Hill Slope) is equal to −1.0 and the "Top" and "Bottom" numerals are equal the plateaus of curve in units of growth rate.

$$(1)\ Y = \text{Bottom} + (\text{Top} - \text{Bottom})/(1 + 10^{((\text{LogIC}_{50} - I) * \text{Hill Slope})})$$

Chemical Profiling and Phylogenetic Analysis of *Pseudoalteromonas* sp.

DNA sequencing and phylogenetic analysis of marine isolate B030a (GenBank No. KT804650) was performed as described in Whalen et al. (2015). Evolutionary history of *Pseudoalteromonas* isolates were inferred using the neighbor-joining methods and the optimal tree is shown for topology. Exuded metabolites from 37 *Pseudoalteromonas* isolates in our chemical library underwent untargeted metabolomic fingerprint analysis as described in Whalen et al. (2015). A list of chemical features [*m/z* – retention time (RT) pairs] was filtered to include only those features that had concentrations that were at least one order of magnitude higher in the *Pseudoalteromonas* sample than in the media blank. This filtered list of features was then searched for the corresponding ion and RT in (-)-HRESI mode matching the standard 2-heptyl-4-quinolone. Phylogenetic analysis was performed as described in Whalen et al. (2015) and a heat map was generated showing the relative abundances of 2-heptyl-4-quinolone in each *Pseudoalteromonas* isolate.

RESULTS

Phytoplankton Response to Live Bacterial Cells and Crude Extract

The presence of live *P. piscicida* cells caused significant mortality in *E. huxleyi*. When cultures of *E. huxleyi* (strain 624) were exposed to "high" concentrations of *P. piscicida* cells (10^6 cells mL^{-1}), the growth rate of both axenic and xenic *E. huxleyi* cultures decreased 14 ± 5 and 28 ± 9%, respectively (**Figure 1A**; axenic, $p = 0.015$; xenic, $p = 0.001$). When exposed to "low" concentrations of *P. piscicida* cells at 10^3 cells mL^{-1}, only xenic *E. huxleyi* had a significantly depressed (6 ± 1%) growth rate ($p = 0.0048$); whereas, axenic *E. huxleyi* were unaffected compared to f/2 controls. Additionally, filtrate from *P. piscicida* cells at 10^6 cells mL^{-1} significantly reduced the growth of xenic *E. huxleyi* by 32 ± 6% ($p < 0.001$).

Axenic *E. huxleyi* was exposed to crude extracts of exuded compounds produced by *P. piscicida* at a final concentration of 50.7 and 0.05 $\mu g\ mL^{-1}$, concentrations approximately equivalent to the material exuded by 10^6 and 10^3 cells mL^{-1}, respectively. Exposure to crude extracts resulted in significant mortality for *E. huxleyi* (**Figure 1B**; $p < 0.001$), with negative growth rates for *E. huxleyi* when exposed to either concentration of crude extract. Conversely, when exposed to crude extracts of TSY media, no significant difference in growth rate was observed relative to the DMSO and media only controls, indicating the causative agent of mortality was the result of a compound excreted by *P. piscicida*.

Compound Identification and Metabolomic Fingerprinting

The secreted algicidal compound produced by *P. piscicida,* was isolated using bioassay-guided fractionation. The purified active fraction was investigated with 1D-NMR and ESIMS experiments. ^1H and ^{13}C NMR showed the presence of a seven carbon straight alkyl chain (δ_H 0.85, 1.26, 1.32, 1.67, and 2.58 and δ_C 13.9, 22.0, 28.3, 28.4, 28.5, 31.1, and 33.2) and a 1,2 substituted benzene ring [δ_H 7.26 (d), 7.52 (t), 7.60 (t), and 8.03 (d); **Figure 2A** and **Supplementary Figure S2**]. These data along with a robust negative ESIMS ion at 242.155 *m/z* (**Figure 2B**) strongly suggested the known bacterial metabolite 2-heptyl-4-quinolone (HHQ, $C_{16}H_{21}NO$; Bredenbruch et al., 2005). Comparison of ^1H and ^{13}C NMR spectra of the active compound to an HHQ standard confirmed that the chemical structures were identical. Untargeted metabolomic profiling of *Pseudoalteromonas* crude extracts as detailed in Whalen et al. (2015), indicated HHQ was present in isolates A757, A754, A746, and B030a (**Figures 2C,D**). The production of HHQ is the most pronounced in a clade containing A757, A754, and A746 representing a distinct chemotype characterized by halogenation of the exometabolome (Whalen et al., 2015). 16S rDNA sequencing indicates A757, A754, and A756 are all *P. piscicida* and were isolated from plastic debris in the North Atlantic (Whalen et al., 2015). The HHQ-producing marine isolate B030a was isolated from macroalgae along the coast of Woods Hole, MA, USA, but is not in the same clade as A757, A754, and A746, rather this B030a falls within a

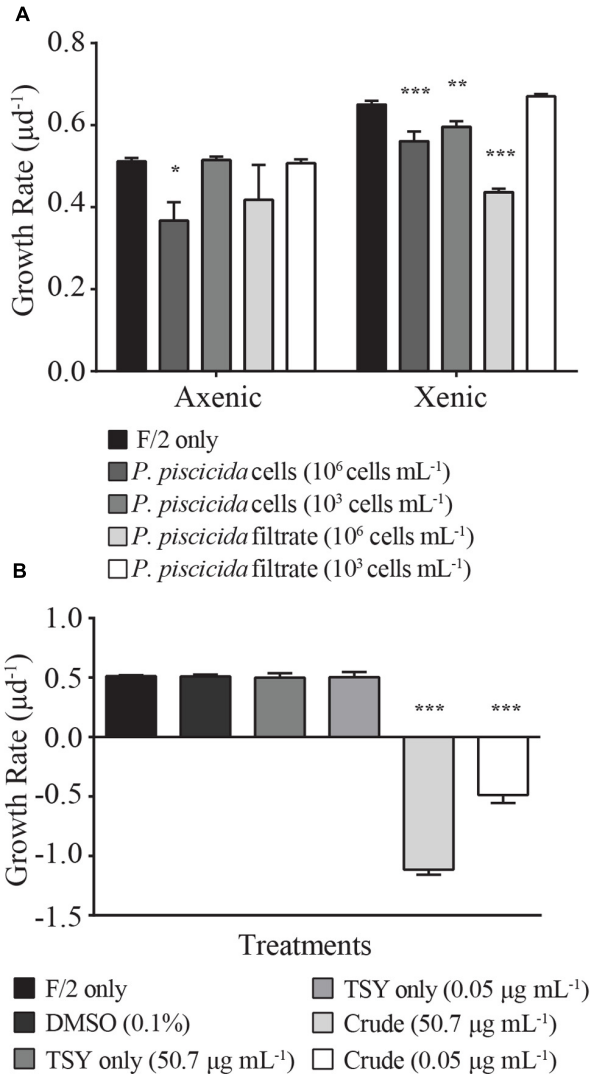

FIGURE 1 | Growth rates (μ d^{-1}) of *Emiliania huxleyi* (strain 624, either xenic or axenic) were measured in response to (A) live *Pseudoalteromonas piscicida* cells and filtrate. Growth rates (μ d^{-1}) of axenic *E. huxleyi* (strain 624) were measured in response to **(B)** crude extracts of *P. piscicida* secreted metabolites and appropriate media (F/2 and TSY) and solvent (DMSO) controls. Compared to the control, the growth rate of *E. huxleyi* significantly decreased in response to high concentrations (10^6 cells mL^{-1}) of *P. piscicida* and the crude extracts. Additionally, high concentrations of culture filtrate and low concentrations (10^3 cells mL^{-1}) of *P. piscicida* resulted in a significant decrease in *E. huxleyi* growth but only in the xenic subculture. Significance is denoted as being less than 0.05 (*), less than 0.01 (**), or less than 0.001 (***). For all treatments, $n = 3$. All error bars are one standard deviation of the mean.

large clade represented by diverse group of *Pseudoalteromonas* sp. (**Figure 2C**).

Identification of HHQ Biosynthetic Machinery in *P. piscicida*

The draft genome sequence of *P. piscicida* was determined to be 5.1 Mbp in size with an estimated 4543 coding sequences. The *P. piscicida* genome was mined using SEED Viewer for the identification of genes involved alkylquinoline synthesis (GenBank Accession numbers, KT879191–KT879199). In *P. aeruginosa*, quorum sensing is controlled by the transcriptional regulators LasR, RhIR, and MvfR (PqsR). The former two are controlled by homoserine lactones, while the signaling molecules that activate MvfR, a LysR-type transcriptional regulator, belong to a family of 4-hydroxy-2-alkylquinolines (HAQs), including 3,4-dihydroxy-2-heptylquinoline (PQS, 258.149 *m/z* [M-H]), its direct precursor 2-heptyl-4-quinolone (HHQ), and 4-hydroxy-2-heptylquinoline-*N*-oxide (HQNO; Dulcey et al., 2013). The presence of a single homolog to each of the *P. aeruginosa pqsA, pqsC, pqsD,* and *pqsE* genes were identified in the *P. piscicida* genome, with amino acid identities of 37.9, 28.5, 47.2, and 30.1%, respectively. However, *in silico* analysis indicated the operon arrangement was different to that of *P. aeruginosa* (**Figure 2E**). The coding sequence with the highest similarity to *P. aeruginosa pqsB* was positioned immediately upstream of the homolog *pqsC* in the *P. piscicida* genome with 20.3% amino acid identity. The position of this hypothetical protein within the operon containing other *pqsABCDE* homologs would suggest it is a possible homolog to *pqsB*. The genome of *P. aeruginosa* also encodes two anthranilate synthases, PhnA and PhnB, immediately downstream of the *pqsABCDE* operon, which supply anthranilic acid. The genome of *P. piscicida* contains two homologs of PhnA and PhnB (**Figure 2E**) with amino acid identities of 29.8 and 40.5%, respectively; however, their position is shifted in comparison to *P. aeruginosa* and downstream of the homolog to *pqsA*.

After finding the *pqsABCDE* homologs in our *P. piscicida* (A757) isolate, we were interested in determining if this operon exists in other *Pseudoalteromonas* sp. whose genome has been made publically available. Using the Department of Energy – Joint Genome Institute's Integrated Microbial Genome (IMG) system, we searched 67 *Pseudoalteromonas* sp. available genomes that were categorized as finished, in permanent draft, or draft stage against two *P. aeruginosa* PAO1 genomes (637000218 and 2623620964) for *pqsABCDE* operon homologs. Using a minimum identity cutoff of 10% and e-value of 0.01, we were able to find representatives of many of the genes in the pqs operon (**Supplementary Figure S3A**). However, upon closer manual inspection of these genomes, only *Pseudoalteromonas citrea* NCIMB 1889 maintained the synteny of the pqs operon as seen in *P. piscicida* (A757; **Supplementary Figure S3B**).

Dose-Response Experiments with Various Phytoplankton Species

Dose-response experiments with axenic *E. huxleyi* (strain 624) determined the IC_{50} concentration for the isolated pure compound to be 88.3 ng mL^{-1}, which was not significantly different ($p = 0.92$) from the IC_{50} obtained when exposed to the purchased HHQ standard (**Figure 3A**, **Table 1**; Sigma-Aldrich). For all three *E. huxleyi* strains, IC_{50} concentrations for the isolated pure compound ranged from 44.51 to 115.4 ng mL^{-1} (**Figure 3B**; **Table 2**). IC_{50} values were found to differ significantly ($p = 0.003$) when all three strains of *E. huxleyi* were compared.

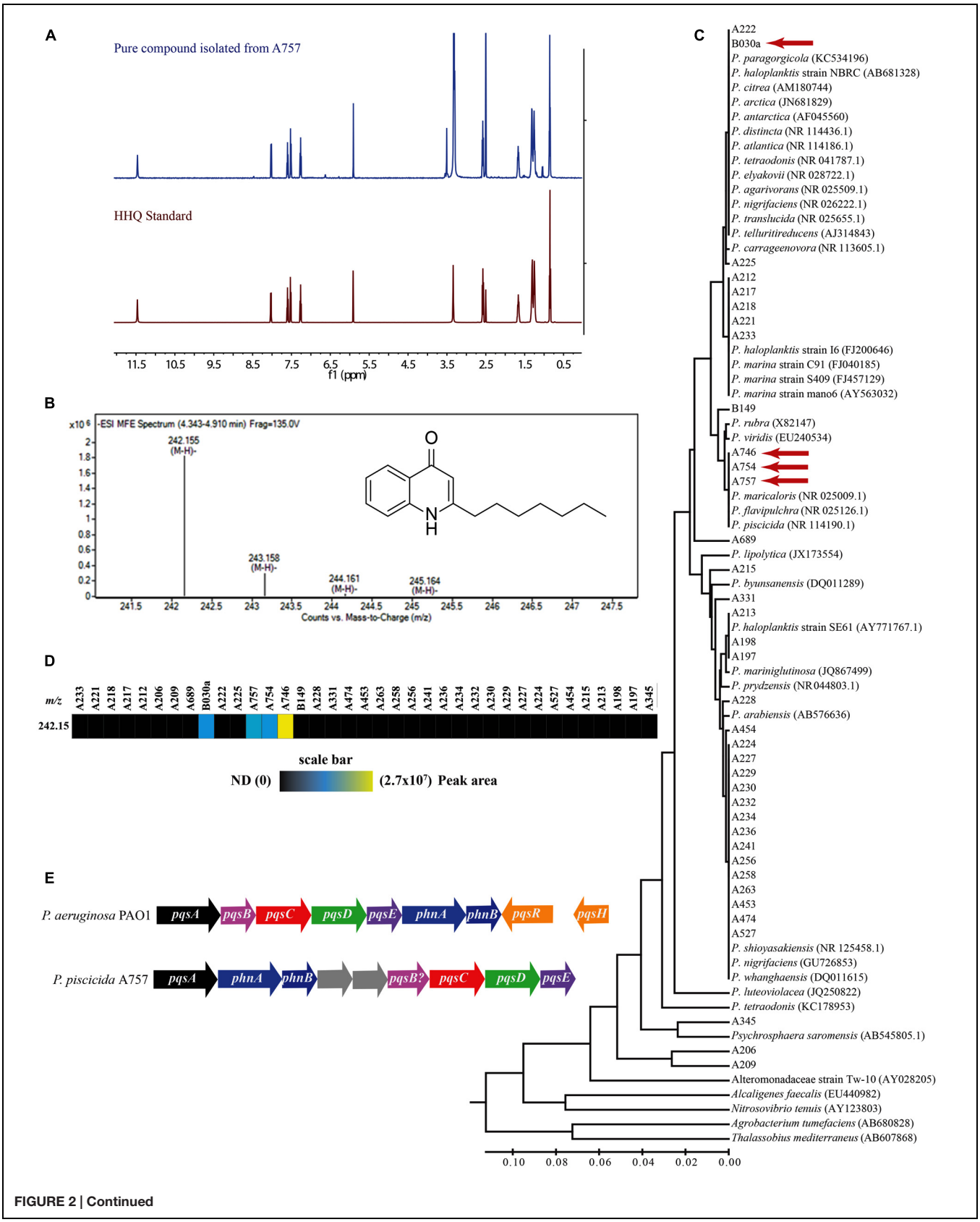

FIGURE 2 | Continued

FIGURE 2 | Continued

Composite figure showing HHQ structural elucidation from isolate A757, chemophylogenetic analysis of HHQ producing *Pseudoalteromonas* sp., and HHQ biosynthetic machinery in *P. piscicida* (A757). (A) Structural identification of 2-heptyl-4-quinolone (HHQ) from *P. piscicida*. ^{1}H-NMR spectrum 500 MHz, DMSO-*d6* of the pure compound isolated from *P. piscicida* (blue) and the authentic standard HHQ (red). **(B)** Mass spectrum [(-)-HRESI] of the active constituent from *P. piscicida* (A757; structure of HHQ in inset). **(C)** Phylogenetic tree and comparison of HHQ production in 37 isolates of *Pseudoalteromonas* sp. The evolutionary history was inferred using the UPGMA method (Sneath and Sokal, 1973). The optimal tree with the sum of branch length = 0.83629248 is shown. The tree is drawn to scale, with branch lengths in the same units as those of the evolutionary distances used to infer the phylogenetic tree. The evolutionary distances were computed using the Maximum Composite Likelihood method (Tamura et al., 2004) and are in the units of the number of base substitutions per site. The analysis involved 77 nucleotide sequences. All positions containing gaps and missing data were eliminated. There were a total of 394 positions in the final dataset. Evolutionary analyses were conducted in MEGA6 (Tamura et al., 2013). Isolates identified to produce HHQ are indicated with a red arrow. **(D)** Heat map showing the relative abundance of HHQ produced by *Pseudoalteromonas* sp. profiled in Whalen et al. (2015). Colored bars indicate the peak area of HHQ for each marine isolate indicated by the column headings. **(E)** A comparison of the alkylquinoline biosynthetic pathway in *Pseudomonas aeruginosa* PAO1 and *Pseudoalteromonas piscicida* (A757; GenBank Accession numbers, KT879191–KT879199).

The naked strain, 374 was found to be the most sensitive to HHQ, having the lowest IC_{50} value, while the haploid strain, 379 was the least sensitive. A comparison of IC_{50} values obtained for all three strains of *E. huxleyi* with other phytoplankton species, *D. tertiolecta* and *P. tricornutum*, indicated *E. huxleyi* was significantly more susceptible to HHQ, despite both *D. tertiolecta* and *P. tricornutum* being vulnerable to the crude *P. piscicida* extract (**Supplementary Figure S4**).

In order to decipher when HHQ-induced mortality of *E. huxleyi* (strain 624) occurred, growth rates of the alga were examined across 24 h time increments (**Figure 4**). While the growth rate of *E. huxleyi* when exposed to HHQ concentrations was dose-dependent, daily growth rate in many of the concentrations remained relatively stable over time. For example, daily growth rate when exposed to 132 ng mL^{-1} of HHQ ranged from -0.19 to -0.32 d^{-1}, over the experimental time period. This indicates that the total loss of *E. huxleyi* when exposed to high concentrations of HHQ occurs over time, rather than a singular loss event.

DISCUSSION

Bacterially Mediated Mortality of Marine Phytoplankton

Quorum sensing molecules mediate bacterial cell–cell communication allowing cells to respond collectively to changes in their environment. This study is the first to identify a quorum sensing precursor molecule that induces mortality in marine phytoplankton. Initial culturing experiments with high *P. piscicida* cell densities (10^6 cells mL^{-1}) resulted in significant mortality in *E. huxleyi* cultures. This finding is concurrent with previous observations demonstrating high concentrations of *Pseudoalteromonas* sp. induced mortality in a wide range of phytoplankton species including raphidophytes, gymnodinoids, and diatoms (Lovejoy et al., 1998; Mitsutani et al., 2001). While the concentration of bacteria used in these experiments is high compared to natural abundances, bacterial behavior (e.g., swarming, biofilm formation) can create localized concentrations of bacteria on or around phytoplankton cells. Furthermore, in some instances, it is only when bacteria are attached to surfaces that they produce active metabolites, thereby generating microenvironments of high metabolite concentrations (Long et al., 2003).

Algicidal activity can be mediated either directly (bacterial cell – phytoplankton contact) or indirectly via chemical interactions (**Figure 1**). Filtrate from *P. piscicida* cells resulted in *E. huxleyi* mortality, indicating a possible chemical basis for the algicidal activity observed. Bio-assay guided fractionation revealed that HHQ, a compound released by *P. piscicida*, caused inhibition of *E. huxleyi* growth. This study is the first observation of HHQ production by a marine *Pseudoalteromonas* species. Previous work describes PQS and HHQ production as occurring during the stationary phase of growth, and both can function as antibiotics and signaling molecules in cell–cell communication, with roles in virulence, apoptosis, and viability of fungal and mammalian cells (Bredenbruch et al., 2005; Calfee et al., 2005; Reen et al., 2011). Unlike PQS, which has poor solubility in water; HHQ can passively diffuse into the external aqueous environment (Deziel et al., 2004). These diffusible signaling molecules, termed autoinducers, are a form of intercellular communication released by bacteria in a cell density-dependent manner, designed to engage cells in cooperative and coordinated behavior beneficial to the entire bacterial population. Once these autoinducers reach critical threshold, they cause the transcriptional activation of quorum-sensing-controlled genes that are key in biofilm formation, virulence factor production (Bredenbruch et al., 2005), secondary metabolite production, motility (Reen et al., 2011), and pathogenesis (Zaborin et al., 2009).

Exposure to HHQ resulted in a significant decrease in growth rate and eventual mortality of *E. huxleyi* (**Figures 3** and **4**). While this is the first observation of HHQ-induced mortality in a phytoplankton species, responses to other alkyl-quinolones have been documented in phytoplankton. For example, Long et al. (2003) found that exposure to 2-*n*-pentyl-4-quinolinol (PQ), also produced in the PQS pathway, resulted in mortality of several phytoplankton species. These results imply that HHQ and other compounds produced in the PQS pathway may have functions beyond quorum sensing and anti-microbial activity, and function as inter-domain cues that initiate eukaryotic cell death. While the concentration of HHQ in the marine environment has not been measured, acyl-homoserine lactones (AHLs), another class of autoinducers, have been measured at nanomolar concentrations in the aqueous phase or higher in biofilms (Wheeler et al.,

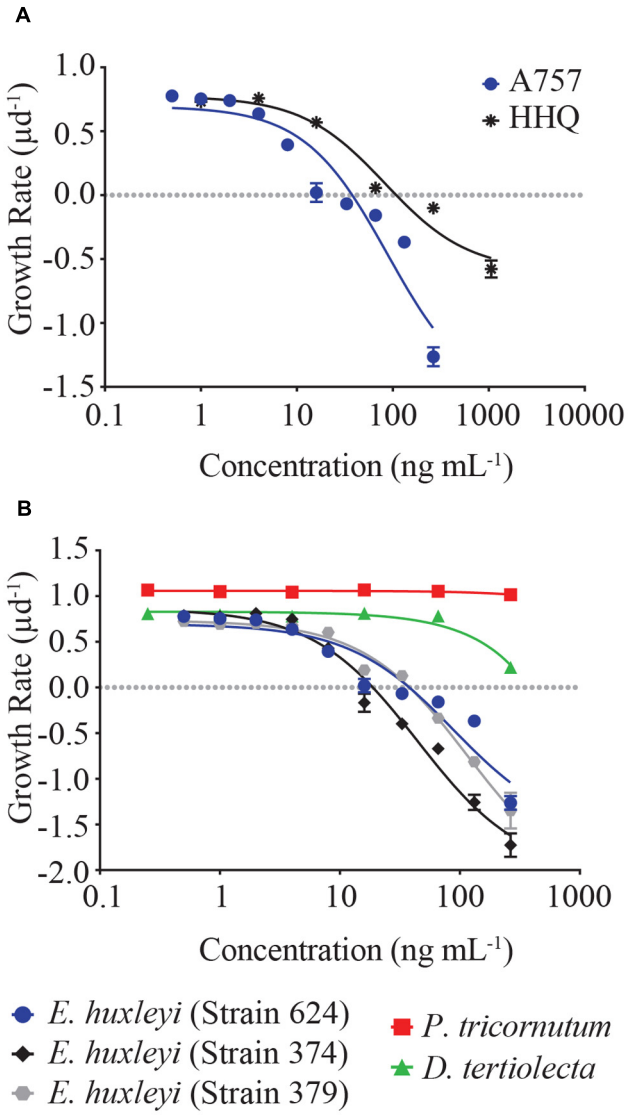

FIGURE 3 | (A) Dose-response comparison of *E. huxleyi* (strain 624, axenic) growth rate in response to a gradient of extracted (labeled A757) and reference HHQ. **(B)** Dose-response curves of five different strains of phytoplankton in response to HHQ extracted from *P. piscicida*. Each symbol represents the mean of three independent replicates ± the standard deviation. IC50 values were calculated for each curve (see **Table 1**).

2006) and have been implicated in the control of degradation of sinking detritus (Hmelo et al., 2011) and involved in phosphorus acquisition by epibonts of *Trichodesmium* sp. (Van Mooy et al., 2012). The IC_{50} observed for *E. huxleyi* in response to HHQ is within the nanomolar range (**Tables 1** and **2**), implying that if the concentration of HHQ parallels other quorum sensing molecules in the marine environment, especially within the context of a biofilm, *E. huxleyi* would be highly susceptible to this autoinducer.

It is worth noting that HHQ was not toxic to all phytoplankton. When *D. tertiolecta* and *P. tricornutum* were exposed to HHQ, no significant change in growth rate was observed, even at high concentrations (**Figure 3**). This specificity in phytoplankton susceptibility to bacterial cells has been observed previously in response to the presence of live *Pseudoalteromonas* sp. cells (Lovejoy et al., 1998), indicating differential species sensitivity resulting from variability in chemical resistance mechanisms or target-site insensitivity. Interestingly, when *D. tertiolecta* and *P. tricornutum* were exposed to extracts of *P. piscicida* exudate, both phytoplankton species exhibited significant mortality in comparison to controls, suggesting this bacterium may produce a cocktail of algicidal compounds specific to different phytoplankton species.

Phylogenetic Evaluation of HHQ Biosynthetic Pathways

Our survey of HHQ production in the *Pseudoalteromonas* sp. within our chemical library indicated that two clades contained representatives capable of producing HHQ at measureable levels in culture. Isolates A757, A754, A746, and B030a fall out by 16S rDNA into two clades that contain 19 different *Pseudoalteromonas* sp. HHQ-producing clades represent both open ocean and coastal species isolated from both abiotic and biotic surfaces, indicating HHQ-producing species can inhabit diverse marine environments. With the recent re-evaluation of the alkylquinoline biosynthetic pathway described from the pathogen *P. aeruginosa* in Dulcey et al. (2013) and Drees and Fetzner (2015), we identified homologs of the *pqsABCDE* operon responsible for HHQ synthesis in *P. piscicida* A757. PQS and HHQ are able to bind MvfR (PqsR) and induce the expression of the *pqsABCDE* operon, which controls biosynthesis of HAQs (Deziel et al., 2004; Dubern and Diggle, 2008). The presence of PqsA, anthranilate-CoA ligase, activates anthranilic acid into anthraniloyl-CoA which reacts with PqsD, a 3-oxoacyl synthase, to produce the intermediate, anthraniloyl-PqsD that is further modified by the synthases, PqsB, PqsC (Dulcey et al., 2013). The product of the gene *pqsE* is thought to be a thioesterase, hydrolyzing the biosynthetic intermediate 2-aminobenzoylacetyl-coenzyme A to

TABLE 1 | Statistical comparison of the dose-response curves and IC_{50} values generated for *Emiliania huxleyi* (Strain 624) exposed to pure compound from A757 and the HHQ standard.

Compound	IC_{50} (ng mL^{-1})	nM	R^2	95% CI	*p*-value
A757	88.31	362	0.91	45.7–170.4	0.9218
HHQ standard	83.07	341	0.96	50.0–138.0	

TABLE 2 | Inhibitory concentration (IC_{50}) of HHQ isolated from *Pseudoalteromonas piscicida* in five different strains of phytoplankton.

Species	IC_{50} (ng mL^{-1})	nM	R^2	95% CI
Emiliania huxleyi (624)	88.31	362	0.91	45.7–170.4
E. huxleyi (374)	44.51	182	0.98	33.3–59.4
E. huxleyi (379)	115.4	474	0.98	87.2–152.8
Dunaliella tertiolecta	>100000	–	–	–
Phaeodactylum tricornutum	>100000	–	0.93	–

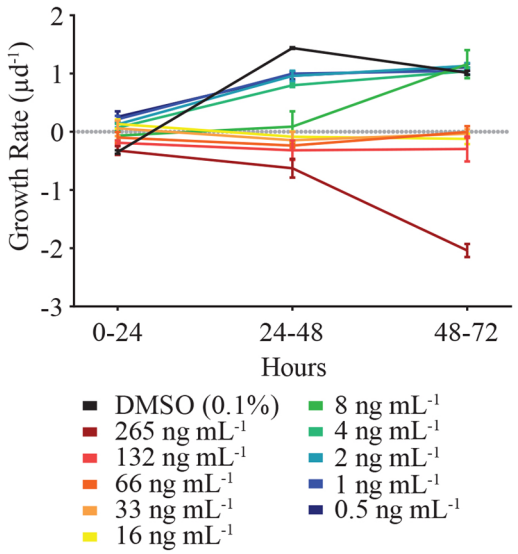

FIGURE 4 | The incremental growth rate (μ d^{-1}) of *E. huxleyi* (strain 624) over the experimental time period. At toxic concentrations (between 8 ng mL^{-1} and above), *E. huxleyi* growth rate remained relatively consistent among the time periods examined. Thus, the presence of HHQ results in static *E. huxleyi* growth rather than cell lysis. Error bars are one standard deviation of the mean.

form 2-aminobenzoylacetate, the precursor of HHQ (Drees and Fetzner, 2015).

We did not find PQS in our metabolomic analysis of *Pseudoalteromonas* sp. excretome, which is supported by the lack of a conclusive *P. piscicida* homolog to *pqsH*, the monooxygenase responsible for converting HHQ to PQS. The loss of the *pqsH* has been observed in two *Burkholderia* sp., which lacked PQS production, but produced HHQ (Diggle et al., 2006). The lack of an ion corresponding to PQS in *P. piscicida* A757 was confirmed by our untargeted metabolomic fingerprint analysis (Whalen et al., 2015). In *P. aeruginosa*, the LysR transcriptional regulator MvfR (PqsR) binds to the promoter of the *pqsABCDE* and is induced by HAQs. *P. piscicida* does contain a putative *pqsR* homolog identified as a LysR family transcriptional regulator with 23.2% similarity and located 2.1 Kbp away from *psqE*.

An analysis of the presence of this pathway in the publically available genomes of marine Pseudoalteromonads indicated that other species in this genus, including *P. citrea*, would have the biosynthetic capacity to produce HHQ. Interestingly, the mining of two additional *P. piscicida* publically available genomes (JGI: 2519899641 and 2541047159) indicated the lack of the pqs operon, suggesting the loss or reshuffling of these genes in subspecies. A recent study also indicated that the lack of PqsE homologs might not prohibit the synthesis of HHQ, rather the thioesterase function could be taken over to an extent by broad-specificity thioesterases, like TesB (Drees and Fetzner, 2015). This finding is significant to our study, as we generally lacked identifying homologs to *pqsE* in our genomic analysis.

In addition, other marine members of the gamma-proteobacteria have also been described to produce HHQ (Wratten et al., 1977; Debitus et al., 1998), including *P. aeruginosa*. Indeed, we confirmed the production of HHQ by comparison to the authentic standard via LC–MS from a marine isolate of *P. aeruginosa* (B323) in the Mincer Culture Collection isolated from water samples 430 km north of the British Virgin Islands (data not shown). These data indicate a more phylogenetically diverse grouping of marine members of the gamma-proteobacteria have the ability to produce algicidal compounds, including HHQ, consistent with earlier predictions of algicidal clades (Mayali and Azam, 2004); however, molecules responsible for the bioactivity have yet to be described. Additionally, Machan et al. (1992) reported HHQ inhibited the growth of *Staphylococcus aureus* and other gram-positive bacteria. While this finding was reported in clinical isolates of *P. aeruginosa*, an additional role of HHQ other than mediating cell–cell communication and phytoplankton abundance could include mediating Gram-positive bacterial populations, possibly associated with phytoplankton surfaces.

Mode of Mortality and Biogeochemical Implications

Exposure to HHQ resulted in static growth of *E. huxleyi,* which eventually led to mortality of the alga, rather than an immediate cell lysis event upon exposure (**Figure 4**). Static growth upon exposure to HHQ has been observed in bacteria, with growth inhibition observed in several *Vibrio* species and a marine sponge bacterial isolate (Reen et al., 2011). In contrast, other studies have observed phytoplankton that were exposed to *Pseudoalteromonas* sp. and lysed within several hours of exposure (Lovejoy et al., 1998), indicating multiple compounds are acting through different mechanisms of action. We did identify a second compound from A757 exudate whose activity results in immediate cell lysis; however, attempts to identify this compound are still ongoing. Cell lysis verses static growth is an important distinction, as it ultimately impacts the fate of algal cells and carbon cycling. With static growth, *E. huxleyi* cells would remain in the water column, which could increase aggregation and export. Conversely, cell lysis is a final fate for the alga, fueling the microbial loop and decreasing carbon flow to higher trophic levels.

These results suggest that pelagic bacteria are not passive receivers of dissolved organic material. For example, it has been observed that when co-cultured under low iron conditions, *P. aeruginosa* cells lysed *Staphylococcus aureus* for its useable iron. Similar relationships have been proposed for bacteria–phytoplankton interactions, with bacteria having the potential to control algal blooms (Doucette et al., 1998). When the concentration of bacteria is high enough to induce quorum sensing (and the production of HHQ) the bacterial population could use the nutrients regenerated from static and dead phytoplankton cells to maintain growth. Algal substrates can provide ecological niches for species-specific bacterial

populations to thrive (Teeling et al., 2012). These surface-associated bacteria may be relatively impervious to changes in seawater chemistry (pCO_2); however, their population dynamics are tightly coupled to phytoplankton bloom development (Allgaier et al., 2008). Even a small increase in the exponential growth rate of a bacterial population can have large consequences for overall population abundance. Our results, while preliminary, provide novel hypotheses for further inquiry into the role of antagonistic phytoplankton-bacterial interactions. Furthermore, identification of the chemical compounds responsible for phytoplankton mortality will provide an enhanced ability to project shifts in population dynamics of both organisms.

The ability of HHQ to modulate interspecies interactions and cross-kingdom behavior (i.e., fungi and animals) as seen here and other studies (Reen et al., 2011), implicates alkylquinolone-signaling molecules as having important ecological roles in regulating primary production and affecting phytoplankton successions. HHQ could potentially alter both bacterial and phytoplankton composition, and physiologic parameters. Elucidating the impacts of this pathway will enable us to better parameterize phytoplankton population dynamics, and ultimately, provide better understanding of planktonic food web structure and biogeochemical cycling.

AUTHOR CONTRIBUTIONS

EH and KW designed experiments; KW performed the chemical isolation; EH performed phytoplankton growth assays; RD and DR solved the chemical structure; AE, MS, BM performed genome sequencing and assembly; EH and KW analyzed data; all authors participated in writing and editing manuscript.

FUNDING

This research was support through funding from the Gordon and Betty Moore Foundation through Grant GBMF3301 to MJ and TM; NIH grant from the National Institute of Allergy and Infectious Disease (NIAID – 1R21Al119311-01) to TM and KW; the National Science Foundation (OCE – 1313747) and US National Institute of Environmental Health Science (P01-ES021921) through the Oceans and Human Health Program to BM. Additional financial support was provided to TM from the Flatley Discovery Lab. Instruments used for the various chemical analyses were supported by an Institutional Development Award (IDeA) from the National Institute of General Medical Sciences of the National Institutes of Health (grant number 2 P20 GM103430). NMR data was acquired at a research facility supported in part by the National Science Foundation EPSCoR Cooperative Agreement #EPS-1004057.

ACKNOWLEDGMENT

We thank K. Bidle for provision of the *E. huxleyi* strains.

SUPPLEMENTARY MATERIAL

The Supplementary Material for this article can be found online at: http://journal.frontiersin.org/article/10.3389/fmicb.2016.00059

FIGURE S1 | Flow chart detailing the bioassay guided fractionation process that was used to eventually identify HHQ as a causative compound influencing growth of *E. huxleyi*.

FIGURE S2 | Structural identification of 2-heptyl-4-quinolone (HHQ) from *P. piscicida*. ^{13}C-NMR spectrum (75 MHz, DMSO-d_6) of the pure compound isolated from *P. piscicida* (blue) and the authentic standard HHQ (red).

FIGURE S3 | Genome mining of pqs operon in *Pseudoalteromonas* sp. (A) The *pqs* operon from two species of *Pseudomonas aeruginosa* PAO1 were used to query 67 publically available *Pseudoalteromonas* sp. genomes. Joint Genome Institute (JGI) genome accession numbers are listed for each isolate in parentheses. Red boxes indicate the presence of a homolog and black boxes indicate no homolog identified with BLAST cutoffs set at ≥10% identity and a maximum e-value of 0.01. White asterisks indicate two homologs (*pqsB* and *pqsE*) from *P. citrea* that were initially identified as absent in the genome using the Integrated Microbial Genome (IMG) gene-genome comparison analysis, but upon manual inspection, were found to be present. **(B)** A comparison of the alkylquinoline biosynthetic pathway in *Pseudoalteromonas piscicida* (A757; GenBank Accession no., KT879191–KT879199) and *P. citrea* (NCIMB 1889). Shading of homologs in *P. citrea* indicates percent amino acid identity to *P. piscicida* (A757) genes.

FIGURE S4 | Growth rate (μ d^{-1}) for three species of phytoplankton exposed to the crude extract of the secreted metabolites of *P. piscicida*. Despite HHQ having little effect on *D. tertiolecta* and *P. tricornutum*, toxicity to the crude extract of *P. piscicida* is observed in all species, indicating that *P. piscicida* likely produces additional compounds that result in algal mortality. Error bars are one standard deviation from the mean.

REFERENCES

Agarwal, V., El Gamal, A. A., Yamanaka, K., Poth, D., Kersten, R. D., Schorn, M., et al. (2014). Biosynthesis of polybrominated aromatic organic compounds by marine bacteria. *Nat. Chem. Biol.* 10, 640–647. doi: 10.1038/nchembio.1564

Allgaier, M., Riebesell, U., Vogt, M., Thyrhaug, R., and Grossart, H.-P. (2008). Coupling of heterotrophic bacteria to phytoplankton bloom development at different pCO_2 levels: a mesocosm study. *Biogeosciences* 5, 1007–1022. doi: 10.5194/bg-5-1007-2008

Azam, F., Fenchel, T., Field, J. G., Meyer-Reil, L. A., and Thingstad, F. (1983). The ecological role of water-column microbes in the sea. *Mar. Ecol. Prog. Ser.* 10, 257–263. doi: 10.3354/meps010257

Aziz, R. K., Bartels, D., Best, A. A., DeJongh, M., Disz, T., Edwards, R. A., et al. (2008). The RAST Server: rapid annotations using subsystems technology. *BMC Genomics* 9:75. doi: 10.1186/1471-2164-9-75

Balch, W. M., Holligan, P. M., and Kilpatrick, K. A. (1992). Calcification, photosynthesis and growth of the bloom-forming coccolithophore, *Emiliania huxleyi*. *Cont. Shelf Res.* 12, 1353–1374. doi: 10.1016/0278-4343(92)90059-S

Bankevich, A., Nurk, S., Antipov, D., Gurevich, A. A., Dvorkin, M., Kulikov, A. S., et al. (2012). SPAdes: a new genome assembly algorithm and its applications to single-cell sequencing. *J. Comput. Biol.* 19, 455–477. doi: 10.1089/cmb.2012.0021

Bowman, J. P. (2007). Bioactive compound synthetic capacity and ecological signifcance of marine bacterial genus *Pseudoalteromonas*. *Mar. Drugs* 5, 220–241. doi: 10.3390/md504220

Bratbak, G., and Thingstad, T. F. (1985). Phytoplankton-bacteria interactions: an apparent paradox? Analysis of a model system with both competition and commensalism. *Mar. Ecol. Prog. Ser.* 25, 23–30.

Bredenbruch, F., Nimtz, M., Wray, V., Moor, M., Muller, R., and Haussler, S. (2005). Biosynthetic pathway of *Pseudomonas aeruginosa* 4-hydroxy-2-alkylquinolines. *J. Bacteriol.* 187, 3630–3635. doi: 10.1128/JB.187.11.3630-3635.2005

Calfee, M. W., Shelton, J. G., McCubrey, J. A., and Pesci, E. C. (2005). Solubility and bioactivity of the *Pseudomonas* quinolone signal are increased by a *Pseudomonas aeruginosa*-produced surfactant. *Infect. Immun.* 73, 878–882. doi: 10.1128/IAI.73.2.878-882.2005

Danger, M., Oumarou, C., Benest, D., and Lacroix, G. (2007). Bacteria can control stoichiometry and nutrient limitation of phytoplankton. *Funct. Ecol.* 21, 202–210. doi: 10.1111/j.1365-2435.2006.01222.x

Debitus, C., Guella, G., Mancini, I. I., Waikedre, J., Guemas, J. P., Nicolas, J. L., et al. (1998). Quinolones from a bacterium and tyrosine metabolites from its host sponge, *Suberea creba* from the Coral Sea. *J. Mar. Biotechnol.* 6, 136–141.

Deziel, E., Lepine, F., Milot, S., He, J. X., Mindrinos, M. N., Tompkins, R. G., et al. (2004). Analysis of *Pseudomonas aeruginosa* 4-hydroxy-2-alkylquinolines (HAQs) reveals a role for 4-hydroxy-2-heptylquinoline in cell-to-cell communication. *Proc. Natl. Acad. Sci. U.S.A.* 101, 1339–1344. doi: 10.1073/pnas.0307694100

Diggle, S. P., Lumjiaktase, P., Dipilato, F., Winzer, K., Kunakorn, M., Barrett, D. A., et al. (2006). Functional genetic analysis reveals a 2-alkyl-4-quinolone signalling system in the human pathogen *Burkholderia pseudomallei* and related bacteria. *Chem. Biol.* 13, 701–710. doi: 10.1016/j.chembiol.2006.05.006

Doucette, G. J., Kodama, M., Franca, S., and Gallacher, S. (1998). "Bacterial interactions with harmful algal bloom species: bloom ecology, toxigenesis, and cytology," in *The Physiological Ecology of Harmful Algal Blooms*, eds D. M. Anderson, A. D. Cembella, and G. M. Hallegraeff (Berlin: Springer Verlag), 619–647.

Drees, S. L., and Fetzner, S. (2015). PqsE of *Pseudomonas aeruginosa* acts as pathway-specific thioesterase in the biosynthesis of alkylquinolone signaling molecules. *Chem. Biol.* 22, 611–618. doi: 10.1016/j.chembiol.2015.04.012

Dubern, J. F., and Diggle, S. P. (2008). Quorum sensing by a 2-alkyl-4-quinolones in *Pseudomonas aeruginosa* and other bacterial species. *Mol. Biosyst.* 4, 882–888. doi: 10.1039/b803796p

Dulcey, C. E., Dekimpe, V., Fauvelle, D. A., Milot, S., Groleau, M. C., Doucet, N., et al. (2013). The end of an old hypothesis: the *Pseudomonas* signalling molecules 4-hydroxy-2-alkylquinolines derive from fatty acids, not 3-ketofatty acids. *Chem. Biol.* 20, 1481–1491. doi: 10.1016/j.chembiol.2013.09.021

Fukami, K., Nishijima, T., and Ishida, Y. (1997). Stimulative and inhibitory effects of bacteria on the growth of microalgae. *Hydrobiologia* 358, 185–191. doi: 10.1023/A:1003141104693

Gilbert, J. A., Steele, J. A., Caporaso, J. G., Steinbrück, L., Reeder, J., Temperton, B., et al. (2012). Defining seasonal marine microbial community dynamics. *ISME J.* 6, 298–308. doi: 10.1038/ismej.2011.107

Guillard, R. R. L. (1975). "Culture of phytoplankton for feeding marine invertebrates," in *Culture of Marine Invertebrate Animals*, eds W. L. Smith and M. H. Chaney (New York, NY: Plenum Press), 29–60.

Hmelo, L. R., Mincer, T. J., and Van Mooy, B. A. S. (2011). Possible influences of bacterial quorum sensing on the hydrolysis of sinking particulate organic carbon in marine environments. *Environ. Microbiol. Rep.* 3, 682–688. doi: 10.1111/j.1758-2229.2011.00281.x

Iglesias-Rodriguez, M. D., Halloran, P. R., Rickaby, R. E. M., Hall, I. R., Colmenero-Hidalgo, E., Gittins, J. R., et al. (2008). Phytoplankton calcification in a high-CO_2 world. *Science* 320, 336–340. doi: 10.1126/science.1154122

Kim, J.-D., Kim, J.-Y., Park, J.-K., and Lee, C.-G. (2009). Selective control of the *Prorocentrum* minimum harmful algal blooms by a novel algal-lytic bacterium *Pseudoalteromonas haloplanktis* AFMB-008041. *Mar. Biotech.* 11, 463–472. doi: 10.1007/s10126-008-9167-9

Legendre, L., and Rassoulzadegan, F. (1995). Plankton and nutrient dynamics in marine waters. *Ophelia* 41, 153–172. doi: 10.1080/00785236.1995.10422042

Long, R. A., Qureshi, A., Faulkner, D. J., and Azam, F. (2003). 2-n-Pentyl-4-quinolinol produced by a marine *Alteromonas* sp. and its potential ecological and biogeochemical roles. *Appl. Environ. Microbiol.* 69, 568–576. doi: 10.1128/AEM.69.1.568-576.2003

Lovejoy, C., Bowman, J. P., and Hallegraeff, G. M. (1998). Algicidal effects of a novel marine *Pseudoalteromonas* isolate (class *Proteobacteria*, gamma subdivision) on harmful algal bloom species of the genera *Chattonella*, *Gymnodinium*, and *Heterosigma*. *Appl. Environ. Microbiol.* 64, 2806–2813.

Machan, Z. A., Taylor, G. W., Pitt, T. L., Cole, P. J., and Wilson, P. (1992). 2-heptyl-4-hydroxyquinoline n-oxide, an antistaphylococcal agent produced by *Pseudomonas aeruginosa*. *J. Antimicrob. Chemother.* 30, 615–623. doi: 10.1093/jac/30.5.615

Mayali, X., and Azam, F. (2004). Algicidal bacteria in the sea and their impact on algal blooms. *J. Eukaryot. Microbiol.* 51, 139–144. doi: 10.1111/j.1550-7408.2004.tb00538.x

Menden-Deuer, S., and Lessard, E. J. (2000). Carbon to volume relationships for dinoflagellates, diatoms, and other protist plankton. *Limnol. Oceanogr.* 45, 569–579. doi: 10.4319/lo.2000.45.3.0569

Mitsutani, A., Yamasaki, I., Kitaguchi, H., Kato, J., Ueno, S., and Ishida, Y. (2001). Analysis of algicidal proteins of a diatom-lytic marine bacterium *Pseudoalteromonas* sp. strain A25 by two-dimensional electrophoresis. *Phycologia* 40, 286–291. doi: 10.2216/i0031-8884-40-3-286.1

Overbeek, R., Begley, T., Butler, R. M., Choudhuri, J. V., Chuang, H. Y., Cohoon, M., et al. (2005). The subsystems approach to genome annotation and its use in the project to annotate 1000 genomes. *Nucleic Acids Res.* 33, 5691–5702. doi: 10.1093/nar/gki866

Reen, F. J., Mooij, M. J., Holcombe, L. J., McSweeney, C. M., McGlacken, G. P., Morrissey, J. P., et al. (2011). The *Pseudomonas* quinolone signal (PQS), and its precursor HHQ, modulate interspecies and interkingdom behaviour. *FEMS Microbiol. Ecol.* 77, 413–428. doi: 10.1111/j.1574-6941.2011.01121.x

Ross, A. C., Gulland, L. E., Dorrestein, P. C., and Moore, B. S. (2014). Targeted capture and heterologous expression of the *Pseudoalteromonas* alterchormide gene cluster in *Escherichia coli* represents a promising natural products exploratory platform. *ACS Synth. Biol.* 4, 414–420. doi: 10.1021/sb500280q

Seyedsayamdost, M. R., Carr, G., Kolter, R., and Clardy, J. (2011). Roseobacticides: small molecule modulators of an algal-bacterial symbiosis. *J. Am. Chem. Soc.* 133, 18343–18349. doi: 10.1021/ja207172s

Seymour, J. R., Simo, R., Ahmed, T., and Stocker, R. (2010). Chemoattraction to dimethyl-sulfoniopropionate throughout the marine microbial food web. *Science* 329, 342–345. doi: 10.1126/science.1188418

Simo, R. (2001). Production of atmospheric sulfur by oceanic plankton: biogeochemical, ecological, and evolutionary links. *Trends Ecol. Evol.* 16, 287–294. doi: 10.1016/S0169-5347(01)02152-8

Skerratt, J. H., Bowman, J. P., Hallegraeff, G., James, S., and Nichols, P. D. (2002). Algicidal bacteria associated with blooms of a toxic dinoflagellate in a temperate Australian estuary. *Mar. Ecol. Prog. Ser.* 244, 1–15. doi: 10.3354/meps244001

Skovhus, T. L., Holmstrom, C., Kjelleberg, S., and Dahllof, I. (2007). Molecular investigation of the distribution, abundance, and diversity of the genus *Pseudoalteromonas* in marine samples. *FEMS Microbiol. Ecol.* 61, 348–361. doi: 10.1111/j.1574-6941.2007.00339.x

Sneath, P. H. A., and Sokal, R. R. (1973). *Numerical Taxonomy: The Principles and Practice of Numerical Classification.* San Francisco, CA: W. H. Freeman.

Sneed, J. M., Sharp, K. H., Ritchie, K. B., and Paul, V. J. (2014). The chemical cue tetrabromopyrrole from a biofilm bacterium induces settlement of multiple Caribbean corals. *Proc. Biol. Sci.* 281:pii20133086. doi: 10.1098/rspb.2013.3086

Tamura, K., Nei, M., and Kumar, S. (2004). Prospects for inferring very large phylogenies by using the neighbor-joining method. *Proc. Nat. Acad. Sci. U.S.A.* 101, 11030–11035. doi: 10.1073/pnas.0404206101

Tamura, K., Stecher, G., Peterson, D., Filipski, A., and Kumar, S. (2013). MEGA6: molecular evolutionary genetics analysis version 6.0. *Mol. Biol. Evol.* 30, 2725–2729. doi: 10.1093/molbev/mst197

Teeling, H., Fuchs, B. M., Becher, D., Klockow, C., Kabisch, A., and Bennke, C. M. (2012). Substrate-controlled succession of marine bacterioplankton populations induced by a phytoplankton bloom. *Science* 336, 608–611. doi: 10.1126/science.1218344

Van Mooy, B. A. S., Hmelo, L. R., Sofen, L. E., Campagna, S. R., May, A. L., Dyhrman, S. T., et al. (2012). Quorum sensing control of phosphorus acquisition in *Trichodesmium* consortia. *ISME J.* 6, 422–429. doi: 10.1038/ismej.2011.115

Whalen, K. E., Poulson-Ellestad, K. L., Deering, R. W., Rowely, D. C., and Mincer, T. J. (2015). Enhancement of antibiotic activity against multidrug-resistant bacteria by the efflux pump inhibitor 3,4-dibromopyrrole-2,5-dione isolated from a *Pseudoalteromonas* sp. *J. Nat. Prod.* 78, 402–412. doi: 10.1021/np500775e

Wheeler, G. L., Tait, K., Taylor, A., Brownlee, C., and Joint, I. (2006). Acyl-homoserine lactones modulate the settlement rate of zoospores of the marine alga *Ulva intestinalis* via a novel chemokinetic mechanism. *Plant Cell Environ.* 29, 608–618. doi: 10.1111/j.1365-3040.2005.01440.x

Wietz, M., Schramm, A., Jorgensen, B., and Gram, L. (2010). Latitudinal patterns in the abundance of major marine bacterioplankton groups. *Aquat. Microb. Ecol.* 61, 179–189. doi: 10.3354/ame01443

Wratten, S. J., Wolfe, M. S., Andersen, R. J., and Faulkner, D. J. (1977). Antibiotic metabolites from a marine pseudomonad. *Antimicrob. Agents Chemother.* 11, 411–414. doi: 10.1128/AAC.11.3.411

Zaborin, A., Romanowski, K., Gerdes, S., Holbrook, C., Lepine, F., Long, J., et al. (2009). Red death in *Caenorhabditis elegans* caused by *Pseudomonas aeruginosa* PAO1. *Proc. Natl. Acad. Sci. U.S.A.* 106, 6327–6332. doi: 10.1073/pnas.0813199106

Conflict of Interest Statement: The authors declare that the research was conducted in the absence of any commercial or financial relationships that could be construed as a potential conflict of interest.

frontiers in Marine Science

ORIGINAL RESEARCH
published: 08 July 2016
doi: 10.3389/fmars.2016.00123

Effects of Nitrogen Limitation on *Dunaliella* sp.–*Alteromonas* sp. Interactions: From Mutualistic to Competitive Relationships

Myriam Le Chevanton, Matthieu Garnier, Ewa Lukomska, Nathalie Schreiber, Jean-Paul Cadoret, Bruno Saint-Jean and Gaël Bougaran*

Laboratoire de Physiologie et de Biotechnologie des Algues, Institut Français de Recherche pour l'Exploitation de la Mer (IFREMER), Nantes, France

Interactions between photosynthetic and non-photosynthetic microorganisms play an essential role in natural aquatic environments and the contribution of bacteria and microalgae to the nitrogen cycle can lead to both competitive and mutualistic relationships. Nitrogen is considered to be, with phosphorus and iron, one of the main limiting nutrients for primary production in the oceans and its availability experiences large temporal and geographical variations. For these reasons, it is important to understand how competitive and mutualistic interactions between photosynthetic and heterotrophic microorganisms are impacted by nitrogen limitation. In a previous study performed in batch cultures, the addition of a selected bacterial strain of *Alteromonas* sp. resulted in a final biomass increase in the green alga *Dunaliella* sp. as a result of higher nitrogen incorporation into the algal cells. The present work focuses on testing the potential of the same microalgae–bacteria association and nitrogen interactions in chemostats limited by nitrogen. Axenic and mixed cultures were compared at two dilution rates to evaluate the impact of nitrogen limitation on interactions. The addition of bacteria resulted in increased cell size in the microalgae, as well as decreased carbon incorporation, which was exacerbated by high nitrogen limitation. Biochemical analyses for the different components including microalgae, bacteria, non-living particulate matter, and dissolved organic matter, suggested that bacteria uptake carbon from carbon-rich particulate matter released by microalgae. Dissolved organic nitrogen released by microalgae was apparently not taken up by bacteria, which casts doubt on the remineralization of dissolved organic nitrogen by *Alteromonas* sp. in chemostats. *Dunaliella* sp. obtained ammonium-nitrogen more efficiently under lower nitrogen limitation. Overall, we revealed competition between microalgae and bacteria for ammonium when this was in continuous but limited supply. Competition for mineral nitrogen increased with nitrogen limitation. From our study we suggest that competitive or mutualistic relationships between microalgae and bacteria largely depend on the ecophysiological status of the two microorganisms. The outcome of microalgae–bacteria interactions in natural and artificial ecosystems largely depends on environmental factors. Our results indicate the need to improve understanding of the interaction/s between these microbial players.

Keywords: ***Dunaliella***, ***Alteromonas***, **microalgae, bacteria, interactions, chemostat, nitrogen, DON**

OPEN ACCESS

Edited by:
Xavier Mayali, Lawrence Livermore National Laboratory, USA

Reviewed by:
Dedmer Bareld Van De Waal, Netherlands Institute of Ecology, Netherlands
Sophie Rabouille, Centre National de la Recherche Scientifique, France

****Correspondence:***
Matthieu Garnier
matthieu.garnier@ifremer.fr

Specialty section:
This article was submitted to Aquatic Microbiology, a section of the journal Frontiers in Marine Science

Received: *12 January 2016*
Accepted: *27 June 2016*
Published: *08 July 2016*

Citation:
Le Chevanton M, Garnier M, Lukomska E, Schreiber N, Cadoret J-P, Saint-Jean B and Bougaran G (2016) Effects of Nitrogen Limitation on Dunaliella sp.–Alteromonas sp. Interactions: From Mutualistic to Competitive Relationships. Front. Mar. Sci. 3:123. doi: 10.3389/fmars.2016.00123

INTRODUCTION

Phytoplankton primary production at the ocean surface contributes strongly to biochemical cycles of the Earth and especially to sequestration of atmospheric carbon dioxide (Falkowski et al., 1998). Nitrogen is considered to be the most limiting nutrient of oceanic productivity, especially in low-latitude oceans, even though other nutrients such as phosphorus, iron, and vitamins can also co-limit oceanic productivity (Moore et al., 2013). Because the N cycle involves physical processes, biological activities of the different levels of the aquatic food chain, oceanic transport, and human activities, there are large temporal and geographical variations in the sources and fluxes of nitrogen in the oceans (Capone, 2000). It is acknowledged that nitrogen availability for primary production in marine systems is controlled by the N cycle and drives carbon sequestration by phytoplankton (Falkowski et al., 2008).

Autotrophic and heterotrophic microorganisms in photic zones live and interact within communities whose structure is mainly driven by trophic relationships (Strom, 2008). For example, heterotrophic bacteria can produce growth-promoting compounds for algae such as vitamins (Cole, 1982; Croft et al., 2005; Park et al., 2008) or can improve nutrient supply (Tai et al., 2009; Vasseur et al., 2012). Nitrogen and phosphorus are the main macro-elements required by phytoplankton. It is generally assumed that phytoplankton mainly uptake nitrogen in its mineral forms, including nitrate (NO_3^-), nitrite (NO_2^-), and ammonium (NH_4^+) (Lipschultz, 1995), by a set of high-affinity transporters that compensate for the low concentration of these forms in the oceans (Charrier et al., 2015). On the other hand, several published works have made it clear that microalgae can also use organic forms of nitrogen via cell-surface and extracellular enzymatic processes (Palenik and Morel, 1990, 1991; Mulholland et al., 2002; Stoecker and Gustafson, 2003). The primary role of heterotrophic bacteria in the nitrogen cycle was presumed to be the release of inorganic nutrients during the decomposition of organic matter, thereby recycling nutrients to phytoplankton (Azam et al., 1983; Capblancq, 1990). In this picture, heterotrophic bacteria play the role of microbial decomposers helping primary productivity. However, more recent studies revealed a more complex picture, with bacteria using both inorganic and organic nitrogen and possibly even competing with microalgae for inorganic nitrogen (Kirchman, 1994; Kirchman and Wheeler, 1998; Zehr and Ward, 2002). Such competition for mineral nitrogen is, however, overlooked by most studies. One remaining issue is the impact of nitrogen limitation on the structure of planktonic communities driven by competitive and mutualistic interactions, especially on the abundance and activity of photosynthetic species.

Faced with the increasing potential of microalgae for diverse applications such as healthcare, cosmetics, food, animal feed, energy and phycoremediation (Spolaore et al., 2006; Barzegari et al., 2009; Mata et al., 2010; Park et al., 2010), there is growing interest in studies on bacteria–microalgae interactions for nutrient supply. Additionally, the cost of nitrogen for microalgal cultures is driven by fossil energy costs and can impair the economics of microalgae production. Therefore, such interaction studies are of particular interest for algae species cultivated on a large scale, such as microalgae of the genus *Dunaliella* (Hosseini Tafreshi and Shariati, 2009). Indeed, the maintenance of axenic cultures in large-scale production systems such as open ponds is unrealistic and most industrial cultures are therefore grown together with uncontrolled bacterial populations that may either improve or impair microalgae growth (see Natrah et al., 2014 for a review).

The present paper addresses the impact of nitrogen limitation on the interactions between heterotrophic bacteria and phytoplankton species. We studied the influence of the bacterium *Alteromonas* sp. on the physiology of the microalga *Dunaliella* sp. and on nitrogen repartition between the different fractions. In an earlier study, we had found that the addition of the bacteria *Alteromonas* sp. to batch cultures of *Dunaliella* sp. resulted in higher final biomass and nitrogen incorporation in microalgae (Le Chevanton et al., 2013). We suggested that the underlying mechanisms could be related to a better use of nitrogen, resulting from bacterial remineralization of dissolved organic nitrogen released by the algae. Benefits for *Dunaliella* sp. growth in mixed culture with *Alteromonas* sp. were observed in batch mode when nitrogen was tapering off and producing a final starvation effect, but it remained to be seen how such a mixed system would behave under a continuous but limiting supply of nitrogen and how culture conditions could affect the outcome of the interactions. Indeed, several previous studies (Currie and Kalff, 1984; Bratbak and Thingstad, 1985; Mindl et al., 2005) on microalgae–bacteria interactions in continuous culture under phosphorus-limited conditions revealed competitive relationships for phosphorus. In the present study, we therefore focused on testing mixed *Dunaliella* sp.–*Alteromonas* sp. cultures in terms of growth and nitrogen incorporation in ammonium-limited chemostat. Replicated mixed cultures were thus compared to axenic cultures at two different dilution rates. Carbon and nitrogen were monitored in microalgal and bacterial populations and in non-living particulate matter. Dissolved organic and inorganic nitrogen were monitored in the medium. This made it possible to assess the influence of *Alteromonas* sp. on biomass and nitrogen incorporation by *Dunaliella* sp. cultivated in chemostat for the two dilution rates and to compare our results with those previously obtained in batch culture (Le Chevanton et al., 2013).

MATERIALS AND METHODS

Mixed and Axenic Strains

The axenic culture of *Dunaliella* sp. strain SAG19.3 and the mixed *Dunaliella* sp.–*Alteromonas* sp. SY007 culture were set up as previously described in Le Chevanton et al. (2013). Both strains were maintained at 20°C under continuous light with daylight fluorescent tubes (100 μmolphotons.m^{-}2.s^{-1}) on artificial seawater (ASW, salinity 35) enriched with modified Walne's medium (Walne, 1970), with ammonium used as the nitrogen source instead of nitrate.

Experimental Design for Axenic Cultures in Chemostat

Starter cultures of axenic and mixed strains were grown by batch. Cells were harvested by centrifugation, suspended in ASW then

transferred into the 5 L flasks at 0.1×10^6 C/ml with modified Walne's medium. Bubbling with 0.22 μm filtered air (Midisart, Sartorius) allowed the homogenization of cultures and slightly positive pressure to protect against biological contamination. Temperature was set at 20°C and irradiance at 250 μmol photons.m^{-2}.s^{-1} with six fluorescent tubes (Osram, 54W965). pH was regulated at 7.7 with a PID controller device by automatic CO_2 supply. Chemostats were maintained by the continuous input of modified Walne's medium with 250 μM ammonium to ensure nitrogen limitation. The N:P ratio of medium is =1.

Axenic *Dunaliella* sp. and the *Dunaliella* sp.–*Alteromonas* sp. mixture were cultured in duplicate for 85 days in chemostat where they were subjected to two successive dilution rates (D): low dilution rate at 0.05 d^{-1} from day 1 to 35 and high dilution rate at 0.3 d^{-1}, from day 35 to 79. These D correspond to conditions that allow 15 and 90% of the experimental maximal growth rate of *Dunaliella* sp. SAG19.3, measured in a previous study (Le Chevanton et al., 2013). D was checked daily by weighing the output of the system (see Supplementary Material). At day 80, a batch phase was started by stopping the pumps and adding 150 μM ammonium in order to ensure that the cultures are limited by nitrogen.

Analyses

Populations

Bacterial and algae populations were monitored daily during the entire duration of the experiment. *Dunaliella* sp. cell density and cell size were measured using a cell counter (HIAC, Hach Ultra, USA). Cell biovolume was computed from mean cell diameter by assuming spherical shape. Bacterial concentration was estimated by cytometric analysis (BD Accuri Cytometer, USA) after fixation with 2% formaldehyde and SYBR-green staining (Lonza, Switzerland). Microscopic observations were made weekly on an Olympus BH2-RFCA microscope equipped with an Olympus light source for excitation. Images were acquired using a CCD camera (Qimaging RETIGA 2000R). At the end of the experiment, bacteria from the mixed culture were isolated on Marine Agar (BD Difco^{TM}212185 USA, 10 days of incubation at 20°C) and characterized by random amplification of polymorphic DNA (RAPD) to verify the absence of contamination. Extraction PCR and RAPD reactions were performed as described in Le Chevanton et al. (2013).

Particulate Organic Carbon and Nitrogen

Culture samples were filtered daily on precombusted 25 mm GF/D (2.7 μm, Whatman) and GF/F (0.7 μm, Whatman) filters, producing filtrates corresponding to the 2.7 μm size fraction (2.7 SF) and 0.7 μm (0.7 SF) size fractions, respectively. Particulate organic carbon and nitrogen of both SF were analyzed on a CN elemental analyzer (Flash 2000 NC Soil Thermo Fisher scientific, Waltham, MA, USA). The difference between 2.7 SF and 0.7 SF will be referred to hereafter as 0.7–2.7 SF. Preliminary experiments on filtration of *Alteromonas* sp. showed that 71% of the cells were recovered in 0.7–2.7 SF and 29% in 2.7 SF. Consequently, 2.7 SF results were considered as estimators of algae cells alone, and 0.7–2.7 SF results as estimators of bacteria and non-living particulate matter.

Dissolved Organic and Inorganic Nitrogen

Dissolved organic and inorganic nitrogen (DON and DIN, respectively) were estimated daily in the cultures, with a quantification limit of 0.1 μM. Organic particulate matter (algae and bacteria) was excluded by filtration on GF/F filters (0.7 μm, Whatman). The recovered filtrate was then divided into two samples to estimate total dissolved nitrogen and DIN. Dissolved organic nitrogen (DON) was calculated as the difference.

Total dissolved nitrogen was estimated by the wet-oxidation method (Pujo-Pay and Raimbault, 1994), which oxidizes nitrogen of organic compounds into nitrate. DIN and oxidized total dissolved nitrogen samples were stored at −20°C until mineral nitrogen analysis. Ammonium, nitrite, and nitrate in all samples were measured with an autoanalyzer (Autoanalyzer II, Seal Analytical) according to the colorimetric methods of Koroleff (1983) and Solorzano (1969) for ammonium, and Bendschneider and Robinson (1952) for nitrate and nitrite.

Calculations

Calculations were made at each steady state for the different cultures and for the two dilution rates tested in the experiment. Cell Carbon quota (Algae Q_C) was calculated as the carbon recovered on GF/D filters divided by the *Dunaliella* sp. cell concentration. Microalgal C: N (mol C: mol N) ratio was computed as the ratio of particulate carbon to particulate nitrogen on the GF/D filters. Nitrogen partitioning was calculated as the percentage of N recovered in the different size fractions relative to the N input with the medium. The rate of DON release was calculated as DON/Algal carbon × dilution rate in molN.molC^{-1}.day^{-1}. At steady state, N uptake rate (ρ in molN.molC^{-1}.day^{-1}) in axenic cultures and N excretion rate (ε in molN.molC^{-1}.day^{-1}) are given by equations 1 and 2, respectively:

$$\rho = \frac{D * (Ni - N)}{X} \quad (1)$$

$$\varepsilon = \frac{D * DON}{X} \quad (2)$$

where X is the carbon algae biomass (molC.L^{-1}), D is the dilution rate (day^{-1}), N_i is ammonium concentration in the input medium (molN.L^{-1}), and N is ammonium concentration in the culture (Burmaster, 1979). At steady state, we consider that N is negligible since it was undetectable.

Nitrogen efficiency can be calculated from Equations (1) and (2), as shown in Equation (3):

$$E = \frac{\rho - \varepsilon}{\varepsilon} = \frac{Ni - DON}{Ni} \quad (3)$$

Where E varies between 0 and 1.

RESULTS

Chemostat

On the basis of the stability of algal carbon and dilution rate, two steady states of 12 days were defined in the four cultures

(**Figure 1A**). The first steady state (SS1) for low dilution rate was reached at day 22 and lasted until day 34. The increase in dilution rate at day 35 resulted in a decrease in algal carbon (**Figure 1A**) and algae C: N ratio (**Figure 1D**). The second steady state (SS2) was reached at day 41 and lasted until day 53. After day 53, we measured a lower stability of the dilution rate, which was likely due to aging of the tubing of the peristaltic pumps (data not shown). For this reason, measures after day 53 were not taken into account for further analysis. Calculated relative standard deviation of carbon biomass was <5% within each steady state for all cultures. As soon as nitrogen was added to the cultures at day 77, a great increase in algal carbon was observed. These results confirmed prior nitrogen limitation in the chemostat.

For each culture, the increase in dilution rate resulted in a decrease in algal carbon concentration in the culture without any significant change in algal nitrogen concentration (**Figures 1B,C**). Consequently, a decrease in the C: N (mol C: mol N) ratio of algae was observed. Conversely, the increase in dilution rate resulted in a decrease in algal cell biovolume and algal carbon quota per cell (pmolC.cell^{-1}).

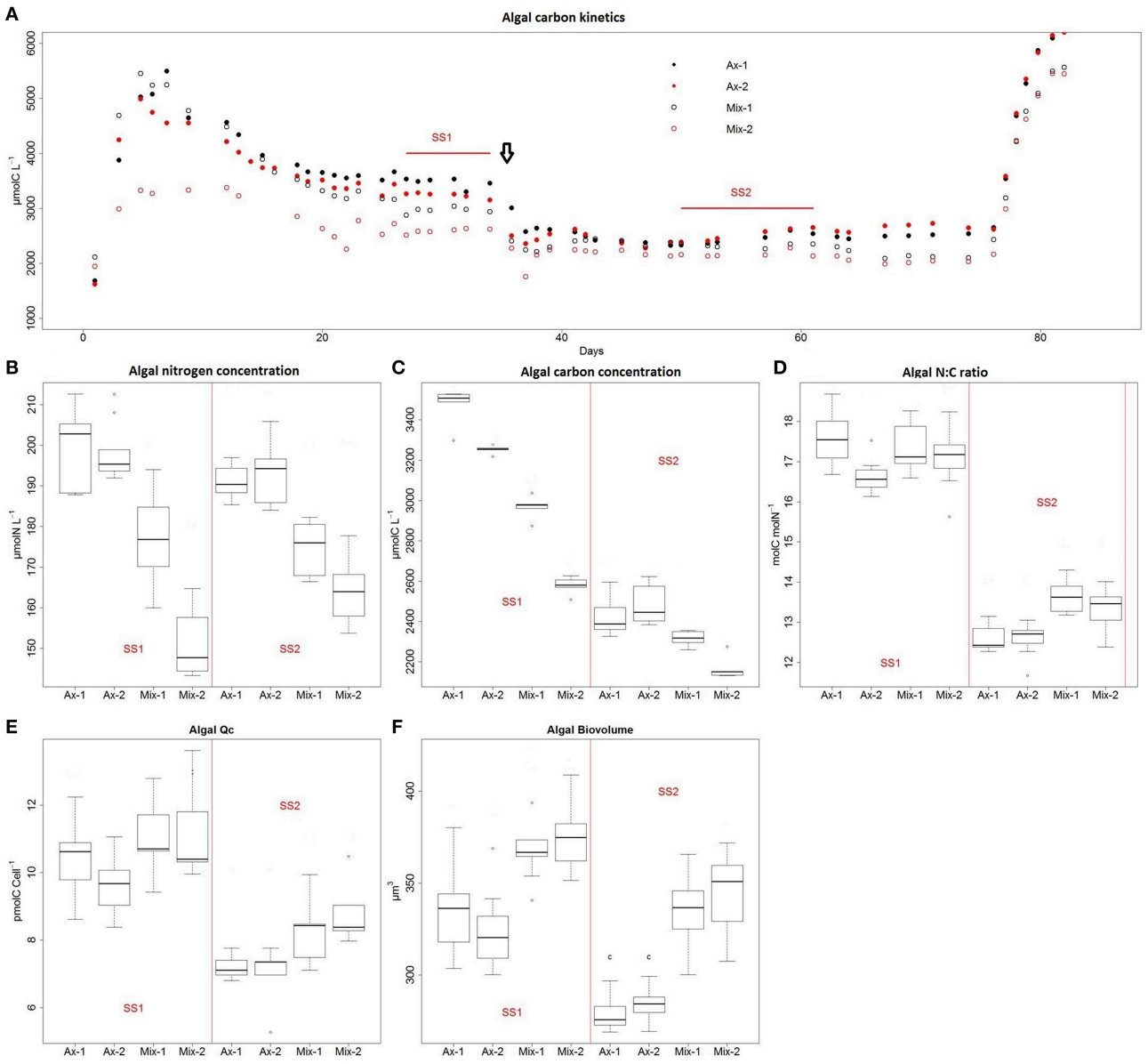

FIGURE 1 | Chemostat cultures of *Dunaliella* sp. under axenic (Ax) and mixed (Mix) conditions with *Alteromonas* sp. Dilution rate (D) were 0.05 d^{-1} from day 0 to 35, and 0.3 d^{-1} from day 35 to 65. The vertical arrow indicates the change of D. SS1 was obtained for the first D and SS2 for the second D. A batch phase was applied from day 65. Cultures were made in duplicate. Kinetics of algal carbon concentration were monitored throughout the experiment **(A)**. Distribution analysis by box plot with $n = 10$ of algal nitrogen concentration **(B)**, algal carbon concentration **(C)**, algal C: N ratio **(D)**, carbon cell quota for algae **(E)**, and algae biovolume **(F)** are shown for each culture and steady state (SS).

Impact of Bacteria on Algal Physiology

In SS1, addition of *Alteromonas* sp. resulted in a 8–26% decrease in algal carbon concentration and a 9–27% decrease in algal nitrogen concentration according to the cultures considered (**Figures 1B,C**). In SS2, an 8–15% decrease of algal nitrogen concentration was recorded. The impact of the addition of bacteria on algal carbon in SS2 was much lower than in SS1 and was only significant in Mix-2 culture. During the two steady states, *Alteromonas* sp. addition resulted in a 10–30% increase in algae biovolume and a 12–20% increase in algal carbon cell quota (**Figures 1E,F**).

Bacteria and Extracellular Non-living Particulate Matter

Axenic algae and bacteria-algae mixtures were cultured for 3 months in chemostats without any external contamination being detected by flow cytometric analysis or microscopic observations. No physical interaction by cell contact between algae and bacteria was observed by microscopy. RAPD analyses of strains isolated in mixed cultures showed 100% similarity with *Alteromonas* sp. strain SY007 regardless of which of the two primers was used (RAPD1 or RAPD4), again demonstrating the absence of contamination (data not shown). Flow cytometry analysis recorded 1.2–2.2 $\times$ 10^6 bacteria ml^{-1} at SS1 and 1.9–4 $\times$ 10^6 bacteria ml^{-1} at SS2 (**Figures 2A,E**). This corresponded to 6–10 bacteria per alga at SS1 and 10–20 at SS2.

In axenic cultures, carbon-rich, nitrogen-free particulate matter was detected in the 0.7–2.7 SF (**Figures 2B,C**). We made the assumption that this organic fraction could be related to non-living particulate matter released by microalgae during growth. Because nitrogen is absent from this fraction, it is unlikely that its origin was cell death. The particulate organic carbon measured in the 0.7–2.7 SF of axenic cultures decreased significantly with the increase of dilution rate (**Figure 4C**).

Biochemical analysis of the 0.7–2.7 SF of mixed cultures revealed a C: N ratio of 6 mol C/mol N, similar to that of bacteria (**Figure 2D**). No significant differences in carbon quota between mixed and axenic cultures were recorded in the 0.7–2.7 SF. Therefore, we hypothesized that the 0.7–2.7 SF of axenic cultures contained mainly non-living particulate, and that the 0.7–2.7 SF of mixed cultures contained mainly bacteria. In mixed culture, the increase in dilution rate induced a decrease in carbon and nitrogen content in the 0.7–2.7 SF, together with an increase in bacterial concentration. This suggested a decrease in the size of bacterial cells when dilution rate increased.

Nitrogen Partitioning

Because the cultures were grown in nitrogen-limited conditions and because algal nitrogen was decreased by the addition of *Alteromonas* sp., the partitioning of nitrogen between microalgae, bacteria, dissolved organic matter and dissolved inorganic matter was analyzed in the four chemostats and in both steady states. Under all conditions, dissolved inorganic nitrogen (DIN) remained undetectable. Accordingly, most of the continuously-supplied ammonium was immediately taken up and used in the growth and metabolism of the organisms present, as expected in nitrogen-limited culture. **Figure 3** shows how dissolved organic nitrogen (DON) was the second largest nitrogen compartment after the microalgae compartment in axenic and mixed cultures, and the amount of DON was not impacted by the presence of bacteria.

Increasing dilution rate resulted in: (1) an increase in the proportion of microalgal nitrogen in all cultures with 58–75% of total nitrogen under SS1 and 74–81% under SS2; (2) a decrease in the proportion of bacterial nitrogen in mixed cultures with 9–13% of total nitrogen at SS1 and 4–6% at SS2; (3) a decrease in the proportion of DON in all cultures with 25–29% of total nitrogen at SS1 and 18–21% at SS2 (**Figure 3**). Calculated data given in **Table 1** indicate that the N limitation imposed resulted in an increase in microalgal N efficiency.

Furthermore, the addition of bacteria resulted in a decrease in the proportion of microalgal nitrogen from 74–75 to 58–64% at SS1 and from 80–81 to 74–75% at SS2 (**Figure 3**). Interestingly, the loss of nitrogen in the algae roughly corresponded to the nitrogen fixed in the bacterial compartment. Our analyses of nitrogen in the different compartments resulted in an almost balanced nitrogen budget.

DISCUSSION

Relationship between plankton communities are driven by a combination of competition and facilitation that may involve relationships for nitrogen between the different components of bacterioplankton and phytoplankton. On the one hand, during nitrate and ammonium limitation, diazotroph cyanobacteria can fix dinitrogen and consequently may promote the growth of non diazotroph cyanobacteria (Agawin et al., 2007), bacterial communities (Brauer et al., 2015), diatoms and dinoflagellates (Lenes et al., 2001; Mulholland et al., 2006). These interactions may be temperature dependent, and involve facilitation and competition between N2-fixing and non-fixing communities (Brauer et al., 2013, 2015). On the other hand, the relationships for nitrogen include complex promoting and competing interactions for nitrate ammonium and organic nitrogen. These interactions have been of interest for decade (Hutchinson, 1961; Tilman et al., 1982; Bratbak and Thingstad, 1985; Doucette, 1995; Thingstad et al., 1997; Grossart, 1999; Zehr and Ward, 2002) and diatoms-bacteria interactions are subjected to new insights by the use of molecular technical advances (Amin et al., 2015; Bertrand et al., 2015; Diner et al., 2016). The present paper examines the impact of nitrogen limitation on the interactions between heterotrophic bacteria and phytoplankton species by comparing cultures in chemostats and previous batch cultures (Le Chevanton et al., 2013). It underlines interactions for nitrogen and carbon and the role of nutrient limitation on the switch from competition to mutualistic relationships.

Cultures in N-limited chemostat resulted in established equilibrium between bacteria and algae, similar to the observations reported in previous studies under phosphorus limitation (Currie and Kalff, 1984; Bratbak and Thingstad, 1985). At both dilution rates, we obtained steady states that lasted 12 days, offering the possibility to confidently analyze the interactions between bacteria and microalgae in different

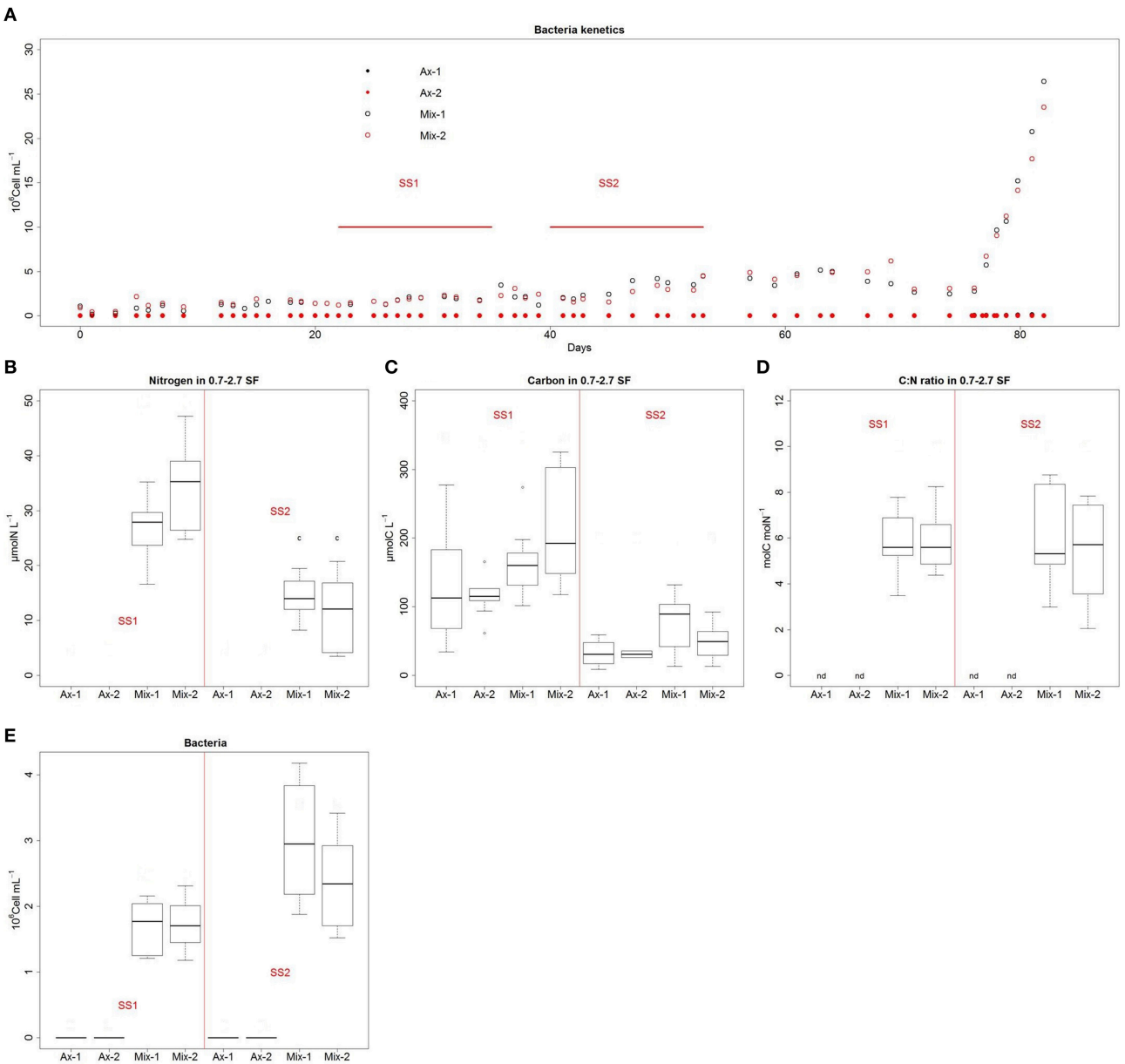

FIGURE 2 | Bacterial concentration and biochemical analysis of the 0.7–2.7 µM size fraction. Bacterial concentration kinetics were monitored throughout the experiment **(A)**. Distribution analysis by box plot with $n = 10$ of nitrogen **(B)**, carbon **(C)**, C: N ratio **(D)**, and bacterial concentration **(E)**.

conditions of nitrogen limitation. On the whole, replicates of cultures gave very similar results except for algal nitrogen and carbon in Mix-1 and Mix-2. By checking the total concentration of nitrogen in cultures at steady states (DON + DIN + algal nitrogen + nitrogen in the 0.7–2.7 SF), it was obvious that total nitrogen in Mix-2 was 20 µM lower than in Mix-1. The lower nitrogen input explains the lower steady-state algal carbon and nitrogen in Mix-2, when compared to Mix-1. Nevertheless the two cultures responded similarly to dilution rate variations.

The addition of *Alteromonas* sp. SY007 strongly increased microalgal cell size– in chemostats, as had been recorded in batch cultures (Le Chevanton et al., 2013). Conversely, a decrease in N limitation resulted in a reduced cell size for microalgae. While similar effects of nitrogen limitation on cell size of unicellular photosynthetic and non-photosynthetic microorganisms have been described in the past (Shuter, 1978), the effect of bacteria on microalgal cell size is less often described. de-Bashan et al. (2002) showed that the addition of the microalgae-growth-promoting bacterium *Azospirillum brasilense* increased cell size for a strain of the freshwater alga *Chlorella vulgaris*, but not for another strain of same species or for *Chlorella sorokiniana* (de-Bashan et al., 2002). Hence, the impact of bacteria on algal cell size

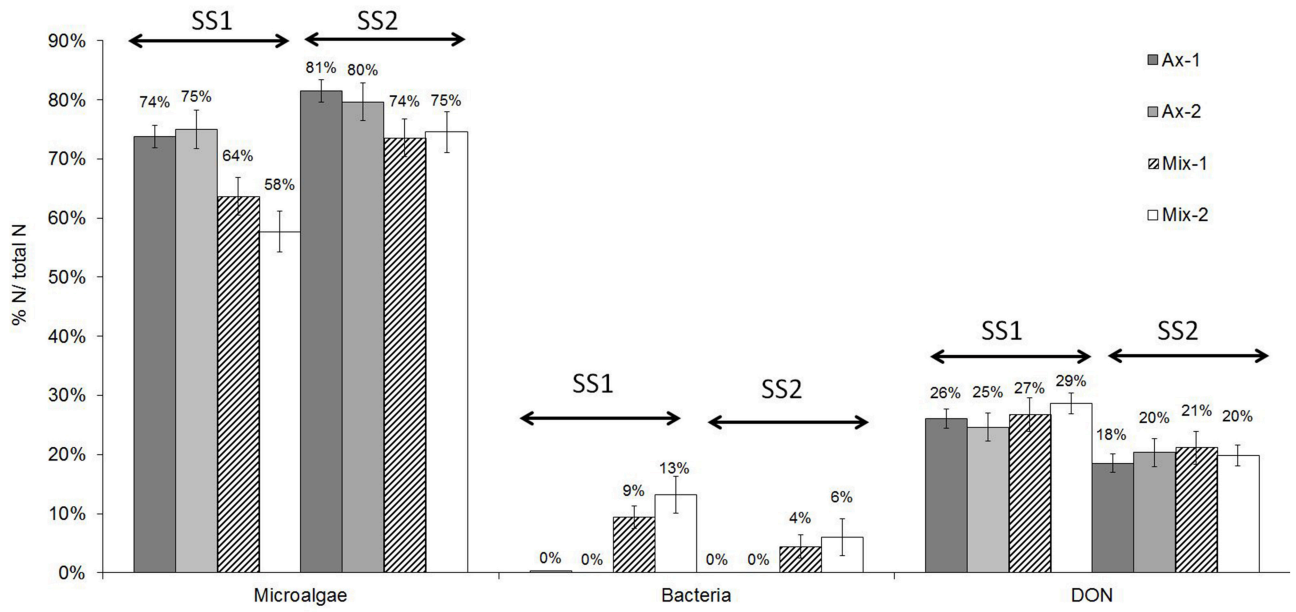

FIGURE 3 | Nitrogen fractioning in axenic and mixed cultures expressed as percentage of the total nitrogen input. Values presented are medians and error bars show standard deviation with $n = 5$. DIN remained undetectable.

TABLE 1 | N efficiency (E) in axenic cultures (standard deviation numbers in brackets, $n = 8$).

	SS1		SS2	
	Ax1	**Ax2**	**Ax1**	**Ax2**
E (molN: molN)	0.72 (0.02)	0.75 (0.02)	0.82 (0.05)	0.83 (0.06)

seems to depend on species and strain. The reasons for such morphological adaptation to bacteria remain unclear. It has been suggested that larger surface to volume ratio would increase the competitive advantage by increasing the nutrient input capacity (Kuenen et al., 1977; Smith and Kalff, 1982). The observed decrease in cell size concomitant with the increase in nitrogen limitation is in accordance with this hypothesis. However, the increase in microalgal cell size as a result of bacteria addition seems to be somewhat paradoxical, resulting in less competitive cell physiology when competition for nitrogen increases.

Dissolved organic nitrogen (DON) in chemostats represented 18–30% of total nitrogen. These amounts are in accordance with previous analysis of DON excretion by phytoplankton species in general (Bronk and Flynn, 2006) and by batch-cultivated *Dunaliella tertiolecta* in particular (Hulatt and Thomas, 2010). Traditionally, DON has been ignored as a source of nitrogen for phytoplankton, despite evidence that they can use urea directly and free amino-acid via cell-surface and extracellular enzymatic processes (Palenik and Morel, 1990, 1991; Mulholland et al., 2002; Stoecker and Gustafson, 2003). Despite the nitrogen-limited conditions in the chemostats, our results suggest that DON was poorly taken up by *Dunaliella* sp. Therefore, we hypothesize that ammonium was the major, if not the sole, source of nitrogen for microalgae in this experiment. Moreover, several studies showed that DON excretion and uptake are affected by nitrogen limitation (Tamminen and Irmisch, 1996; Nagao and Miyazaki, 2002). In batch cultures of the green algae *Scenedesmus quadricauda* and the cyanobacteria *Microcystis novacekii* and *Synechococcus* sp., DON was released more readily by nitrogen-replete algae than by nitrogen-limited algae (Bronk, 1999; Nagao and Miyazaki, 2002). Conversely, Newell et al. observed that the production of DON was not affected by nitrogen limitation in chemostats (Newell et al., 1972). In our experiments, DON release was not detected in batch cultures of *Dunaliella* sp. Focusing on the effect of nitrogen limitation in axenic chemostats on the nitrogen efficiency (**Table 1**), it becomes obvious that *Dunaliella* sp. used ammonium-nitrogen more effectively under lower nitrogen limitation.

From mutualism to competition. Batch (Le Chevanton et al., 2013) and continuous cultures (this study) of *Dunaliella* sp. mixed with *Alteromonas* sp. SY007 produced apparently contradictory results, i.e., mutualism for nitrogen in batch and competition in chemostat. Since similar growth conditions were applied in the two experiments, we suggest that microbial interactions are mainly driven by nitrogen limitation and initial bacteria: algae ratio. Given that (1) nitrogen resources limit the growth of microalgae, and (2) growth of heterotrophic bacteria depends on organic carbon secretion by microalgae, we propose a schematic picture of the interactions depending on nitrogen input and initial bacteria: algae ratio (**Figure 4**).

Bacteria use organic carbon excreted by algae. *Alteromonas* are marine gram-negative heterotrophic proteobacteria (Baumann et al., 1972). Therefore, in continuous and batch cultures without any organic supply, *Alteromonas* sp. SY007 should have used pre-formed organic matter as a source of energy and

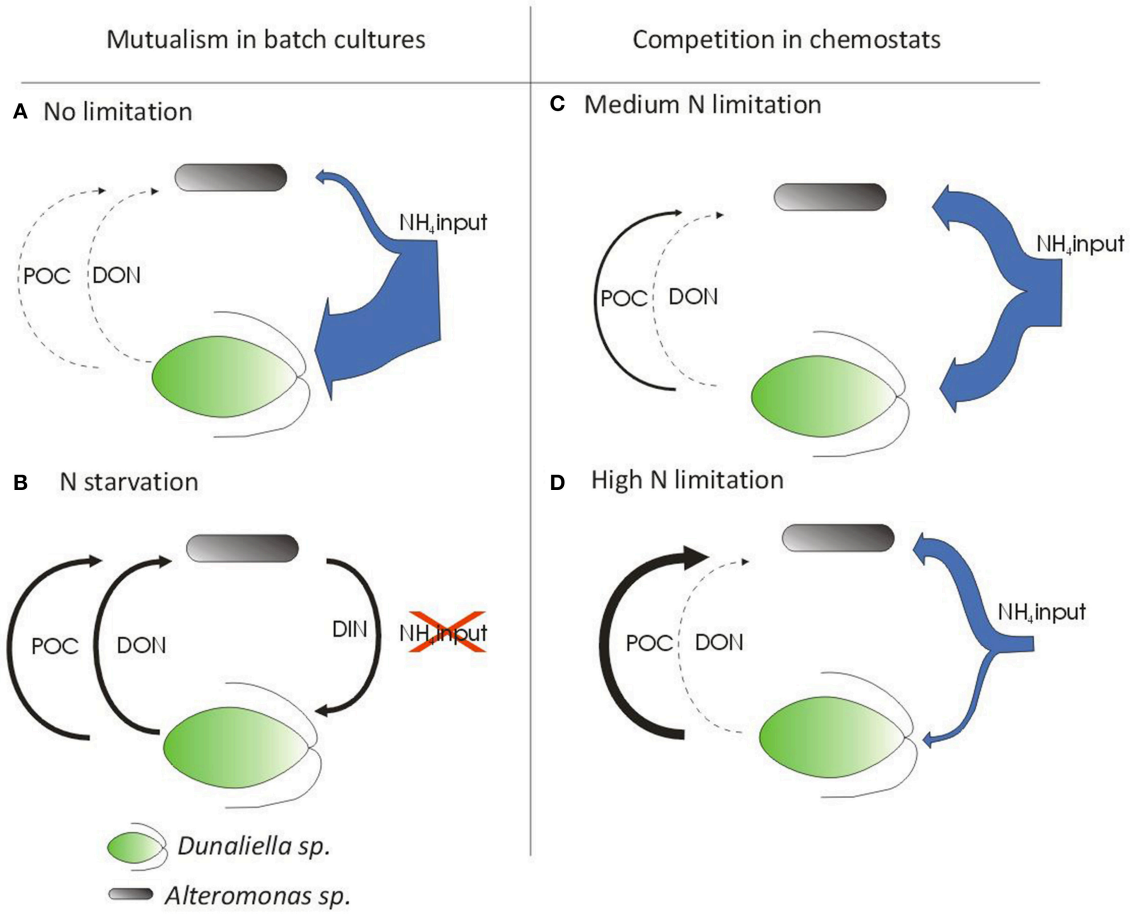

FIGURE 4 | Schematic presentation of relationships between bacteria and microalgae in batch cultures and chemostat. (A) Start of batch cultures where NH_4 provided by the media is high. **(B)** Nitrogen limitation in batch cultures when NH_4 provided by growth media was totally depleted. **(C)** Chemostat limited in nitrogen at high dilution rate (SS2). Continuous NH4 input is high and nitrogen limitation of algae considered as low. **(D)** Chemostat limited in nitrogen at low dilution rate (SS1). Continuous NH4 input is lower and nitrogen limitation of algae is high. Arrow size indicates the presumed magnitude of fluxes.

metabolic precursors. Biochemical analyses of the 0.7–2.7 SF suggest that the bacteria consumed organic carbon from non-living particulate matter. This non-living particulate matter was observed by microscope in the axenic batch and chemostat, and is likely released by microalgae. Unsurprisingly, this confirms that primary production of phytoplankton is a source of carbon and energy for heterotrophic bacterioplankton.

Bacteria use DON and DIN for growth. In our previous study (Le Chevanton et al., 2013), there was strong evidence that NH_4 depletion at the end of batch cultures forces bacteria to use DON released by microalgae for their development. Therefore, we suggested that DON was remineralized by bacteria, leading to the observed increase of microalgal nitrogen at the stationary phase in batch culture (**Figure 4**). In chemostat, ammonium was continuously supplied to both bacteria and algae. Given the absence of direct measurements of bacterial DON uptake and release, it is unclear to what extent this organic substrate supported bacterial growth. However, nitrogen was not observed in the non-living particulate matter of axenic cultures (0.7–2.7 SF). Moreover, DON was not affected by the presence of Alteromonas sp. As a consequence, the use of organic nitrogen released by algae for bacterial growth in chemostats should be questioned. Indeed, our results strongly suggest that bacteria use NH_4 rather than DON when NH_4 is available. The competitive behavior of bacteria in this study therefore strongly contrasts with the mutualism observed in Le Chevanton et al. (2013). In the chemostat, the decrease of microalgal nitrogen resulting from *Alteromonas* sp. addition was similar to the amount of nitrogen sequestered in bacteria. Indeed, Baumann et al. (1972) showed that *Alteromonas* species can use ammonium as their sole nitrogen source. We therefore interpreted our observations as bacteria taking up part of the NH_4 in the mixed continuous cultures, leading to competition between bacteria and microalgae for NH_4 (**Figure 4**). Such competition has been previously reported in mesocosms and in cultures of the marine prasinophyte *Tetraselmis chui* with a bacterial community (Joint et al., 2002; Meseck et al., 2006). Although it is well documented that bacteria collect elements in mineral forms when their needs

are not fully met by organic matter, (Bratbak and Thingstad, 1985; Joint et al., 2002; Mindl et al., 2005), the reason for the lack of DON consumption by *Alteromonas* remains unclear. In oceans, bacterioplankton participates in DON consumption by using multiple membrane transporters and extracellular and intracellular hydrolases (Hoppe, 1983; Howarth et al., 1988). On the one hand, it is acknowledged that not all organic matter can be readily metabolized by bacteria, as part of it is refractory. On the other hand, (Barofsky et al., 2009) recorded that diatoms exude different metabolites through the period of bloom development. These authors suggested that most of the compounds exuded are under the control of the physiological state of the algae or the environmental conditions. The apparent paradox observed between batch and chemostat cultures in the present study could therefore have arisen from different DON compounds exuded by microalgae being differentially refractory to bacterial metabolization. Another hypothesis is based on the possibility that enzymatic mechanisms for DON assimilation by bacteria are more energy consuming than direct NH_4 assimilation.

One of the outstanding issues in ecology and biodiversity is known as the "paradox of the plankton" (Hutchinson, 1961): How can many species coexist in a seemingly environment limited by a limited number of nutrients when the species compete for these nutrient? Several studies have proposed non-exclusive competition, as reviewed by Wilson (2011). Here, we address a shift between competitive and mutualistic interactions within a simplified community with only two microorganisms. Below we detail two mechanisms that are supported by our results.

Under nitrogen sufficiency, nitrogen competition is driven by the bacteria/algae ratio. In batch cultures, competition for mineral nitrogen only occurred at the beginning of the culture when mineral nitrogen was still available. The batch cultures were inoculated with nitrogen-starved microalgae and an initially low bacteria: algae cell ratio (B: A = 0.3). It is well-known that nitrogen-starved microalgae, with low nitrogen quotas, take up mineral nitrogen rapidly by increasing their cell nitrogen quotas (Droop, 1968). Consequently, in batch cultures, most of the available ammonium was quickly taken up mainly by microalgae. The bacterial population could, therefore, only develop based on DON released by microalgae. The effect of competition from bacteria for DIN would depend on the bacteria: algae ratio and on the absorption rates of algae driven by their physiological nitrogen status. A recent study on interactions in coastal plankton communities showed the role of signaling molecules on the complex exchanges of nitrogen between diatoms and bacteria (Amin et al., 2015) and similar infochemicals could play a role in the *Alteromonas* sp. – *Dunaliella* sp. nitrogen interactions.

The results of the present paper indicate that bacteria compete with algae for mineral nitrogen, but nitrogen-limited algae release extracellular particulate organic carbon (POC) that stimulate the growth of the bacterial competitors. The release of POC results from an unbalance between photosynthesis (carbon fixation) and N uptake (Granum and Myklestad, 2001; Baklouti et al., 2006) and we showed that the release of POC was higher under more severe nitrogen limitation conditions. Paradoxically, microalgae stimulate their competitors for DIN, particularly when they are themselves limited by DIN. Our results are in line with previous studies on interactions between diatoms and marine bacteria under phosphorus limitation (Bratbak and Thingstad, 1985; Mindl et al., 2005). The authors suggested that "algae stressed by lack of mineral nutrients respond in a manner whereby they stimulate their competitors for the lacking nutrients" (Bratbak and Thingstad, 1985). Our study gives insight on the underlying mechanisms in nitrogen limitation. Recent studies on interactions between phytoplankton communities dominated by diatoms and bacterial populations at the costal Antartic sea ice edge have underlined a variety of interactions such as mutualistic relationships for organic carbon, competition for iron and mutualistic or competition for cobalamin that is produced by only certain groups of bacteria (Bertrand et al., 2015). Our studies are in line with these observations of complex relationships and give insight on the importance of nutrient limitation on nature of interactions.

As a conclusion, we have shown that microalgae and heterotrophic bacteria coexist in cultures at a stable equilibrium thanks to complex win-win relationships. These interactions are the results of (1) the need of bacteria to take up carbon released by microalgae and (2) a complex relationship for nitrogen that can shift from competitive to mutualistic relationship, this driven by mineral nitrogen availability. These results participate to the growing field of research on the relationships inside planktonic communities that drive marine primary productivity.

AUTHOR CONTRIBUTIONS

ML, MG, JC, and GB participated to the conception of the work in the whole. ML, MG, EL, NS, and GB contributed to the experiments and analysis of data. ML, MG, BS, and GB contributed to the interpretation of the data and to the redaction of the paper.

ACKNOWLEDGMENTS

This publication presents results supported by the ANR BIOE 2008 Symbiose project. Thanks to the IFREMER LER/MPL laboratory for technical support for elemental CN and ion-chromatography analysis. We also thank the anonymous reviewers for their critical comments that greatly improves the manuscript and Helen McCombie for editing the English of the manuscript.

SUPPLEMENTARY MATERIAL

The Supplementary Material for this article can be found online at: http://journal.frontiersin.org/article/10.3389/fmars.2016.00123

REFERENCES

Agawin, N. S. R., Rabouille, S., Veldhuis, M. J. W., Servatius, L., Hol, S., van Overzee, H. M. J., et al. (2007). Competition and facilitation between unicellular nitrogen-fixing cyanobacteria and non-nitrogen-fixing phytoplankton species. *Limnol. Oceanogr.* 52, 2233–2248. doi: 10.4319/lo.2007.52.5.2233

Amin, S. A., Hmelo, L. R., van Tol, H. M., Durham, B. P., Carlson, L. T., Heal, K. R., et al. (2015). Interaction and signalling between a cosmopolitan phytoplankton and associated bacteria. *Nature* 522, 98–101. doi: 10.1038/nature14488

Azam, F., Fenchel, T., Field, J., Gray, J., Meyer-Reil, L., and Thingstad, F. (1983). The ecological role of water-column microbes in the sea. *Mar. Ecol. Prog. Ser.* 10, 257–263. doi: 10.3354/meps010257

Baklouti, M., Diaz, F., Pinazo, C., Faure, V., and Quéguiner, B. (2006). Investigation of mechanistic formulations depicting phytoplankton dynamics for models of marine pelagic ecosystems and description of a new model. *Prog. Oceanogr.* 71, 1–33. doi: 10.1016/j.pocean.2006.05.002

Barofsky, A., Vidoudez, C., and Pohnert, G. (2009). Metabolic profiling reveals growth stage variability in diatom exudates. *Limnol. Oceanogr. Methods* 7, 382–390. doi: 10.4319/lom.2009.7.382

Barzegari, A., Hejazi, M. A., Hosseinzadeh, N., Eslami, S., Aghdam, E. M., and Hejazi, M. S. (2009). Dunaliella as an attractive candidate for molecular farming. *Mol. Biol. Rep.* 37, 3427–3430. doi: 10.1007/s11033-009-9933-4

Baumann, L., Baumann, P., Mandel, M., and Allen, R. D. (1972). Taxonomy of aerobic marine Eubacteria. *J. Bacteriol.* 110, 402 –429.

Bendschneider, K., and Robinson, R. J. (1952). A new spectrophotometric determination of nitrite in sea water. *J. Mar. Res.* 11, 87–96.

Bertrand, E. M., McCrow, J. P., Moustafa, A., Zheng, H., McQuaid, J. B., Delmont, T. O., et al. (2015). Phytoplankton–bacterial interactions mediate micronutrient colimitation at the coastal Antarctic sea ice edge. *Proc. Natl. Acad. Sci. U.S.A.* 112, 9938–9943. doi: 10.1073/pnas.1501615112

Bratbak, G., and Thingstad, T. (1985). Phytoplankton-bacteria interactions - an apparent paradox - analysis of a model system with both competition and commensalism. *Mar. Ecol. Prog. Ser.* 25, 23–30. doi: 10.3354/meps025023

Brauer, V. S., Stomp, M., Bouvier, T., Fouilland, E., Leboulanger, C., Confurius-Guns, V., et al. (2015). Competition and facilitation between the marine nitrogen-fixing cyanobacterium Cyanothece and its associated bacterial community. *Front. Microbiol.* 5:795. doi: 10.3389/fmicb.2014.00795

Brauer, V. S., Stomp, M., Rosso, C., van Beusekom, S. A., Emmerich, B., Stal, L. J., et al. (2013). Low temperature delays timing and enhances the cost of nitrogen fixation in the unicellular cyanobacterium Cyanothece. *ISME J.* 7, 2105–2115. doi: 10.1038/ismej.2013.103

Bronk, D. (1999). Rates of NH4+ uptake, intracellular transformation and dissolved organic nitrogen release in two clones of marine Synechococcus spp. *J. Plankton Res.* 21, 1337–1353. doi: 10.1093/plankt/21.7.1337

Bronk, D. A., and Flynn, K. J. (2006). "Algal cultures as a tool to study the cycling of dissolved organic *Nitrogen*," in *Algal Cultures, Analogues of Blooms and Applications*, ed S. R. V. Durvasula (New Delhi: Oxford & IBH Publishing), 301–341.

Burmaster, D. E. (1979). The continuous culture of phytoplankton: mathematical equivalence among three steady-state models. *Am. Nat.* 113, 123–134. doi: 10.1086/283368

Capblancq, J. (1990). Nutrient dynamics and pelagic food web interactions in oligotrophic and eutrophic environments - an overview. *Hydrobiologia* 207, 1–14. doi: 10.1007/BF00041435

Capone, D. G. (2000). "The marine nitrogen cycle," in *Microbial Ecology of the Oceans*, ed D. L. Kirchman (New York, NY: Wiley), 455–494.

Charrier, A., Bérard, J.-B., Bougaran, G., Carrier, G., Lukomska, E., Schreiber, N., et al. (2015). High-affinity nitrate/nitrite transporter genes (Nrt2) in *Tisochrysis lutea*: identification and expression analyses reveal some interesting specificities of Haptophyta microalgae. *Physiol. Plant.* 154, 572–590. doi:10.1111/ppl.12330

Cole, J. J. (1982). Interactions between bacteria and algae in aquatic ecosystem. *Annu. Rev. Ecol. Syst.* 13, 291–314. doi: 10.1146/annurev.es.13.110182.001451

Croft, M. T., Lawrence, A. D., Raux-Deery, E., Warren, M. J., and Smith, A. G. (2005). Algae acquire vitamin B12 through a symbiotic relationship with bacteria. *Nature* 438, 90–93. doi: 10.1038/nature04056

Currie, D. J., and Kalff, J. (1984). Can bacteria outcompete phytoplankton for phosphorus? A chemostat test. *Microb. Ecol.* 10, 205–216. doi: 10.1007/BF02010935

de-Bashan, L. E., Bashan, Y., Moreno, M., Lebsky, V. K., and Bustillos, J. J. (2002). Increased pigment and lipid content, lipid variety, and cell and population size of the microalgae Chlorella spp. when co-immobilized in alginate beads with the microalgae-growth-promoting bacterium *Azospirillum brasilense*. *Can. J. Microbiol.* 48, 514–521. doi: 10.1139/w02-051

Diner, R. E., Schwenck, S. M., McCrow, J. P., Zheng, H., and Allen, A. E. (2016). Genetic manipulation of competition for nitrate between heterotrophic bacteria and diatoms. *Aquat. Microbiol.* 7:880. doi: 10.3389/fmicb.2016.00880

Doucette, G. J. (1995). Interactions between bacteria and harmful algae: a review. *Nat. Toxins* 3, 65–74. doi: 10.1002/nt.2620030202

Droop (1968). Vitamin B12 and marine ecology IV. The kinetics of uptake, growth and inhibition in monochrysis lutheri. *J. Marine Biol. Assoc. U.K.* 48, 689–733. doi: 10.1017/S0025315400019238

Falkowski, P. G., Barber, R. T., and Smetacek, V. (1998). Biogeochemical controls and feedbacks on ocean primary production. *Science* 281, 200–206. doi: 10.1126/science.281.5374.200

Falkowski, P. G., Fenchel, T., and Delong, E. F. (2008). The microbial engines that drive Earth's biogeochemical cycles. *Science* 320, 1034–1039. doi: 10.1126/science.1153213

Granum, E., and Myklestad, S. M. (2001). Mobilization of β-1,3-glucan and biosynthesis of amino acids induced by NH4+ addition to N-limited cells of the marine diatom *Skeletonema costatum* (Bacillariophyceae). *J. Phycol.* 37, 772–782. doi: 10.1046/j.1529-8817.2001.01005.x

Grossart, H. (1999). Interactions between marine bacteria and axenic diatoms (*Cylindrotheca fusiformis*, *Nitzschia laevis*, and *Thalassiosira weissflogii*) incubated under various conditions in the lab. *Aquat. Microb. Ecol.* 19, 1–11. doi: 10.3354/ame019001

Hoppe, H.-G. (1983). Significance of exoenzymatic activities in the ecology of brackish water: measurements by means of methylumbelliferyl-substrates. *Mar. Ecol. Prog. Ser.* 11, 299–308. doi: 10.3354/meps011299

Hosseini Tafreshi, A., and Shariati, M. (2009). Dunaliella biotechnology: methods and applications. *J. Appl. Microbiol.* 107, 14–35. doi: 10.1111/j.1365-2672.2009.04153.x

Howarth, R. W., Marino, R., and Cole, J. J. (1988). Nitrogen fixation in freshwater, estuarine, and marine ecosystems. 2. Biogeochemical controls. *Limnol. Oceanogr.* 33, 688–701. doi: 10.4319/lo.1988.33.4part2.0688

Hulatt, C. J., and Thomas, D. N. (2010). Dissolved organic matter (DOM) in microalgal photobioreactors: a potential loss in solar energy conversion? *Bioresour. Technol.* 101, 8690–8697. doi: 10.1016/j.biortech.2010.06.086

Hutchinson, G. E. (1961). The paradox of the plankton. *Am. Nat.* 95, 137–145. doi: 10.1086/282171

Joint, I., Henriksen, P., Fonnes, G. A., Bourne, D., Thingstad, T. F., and Riemann, B. (2002). Competition for inorganic nutrients between phytoplankton and bacterioplankton in nutrient manipulated mesocosms. *Aquat. Microb. Ecol.* 29, 145–159. doi: 10.3354/ame029145

Kirchman, D. L. (1994). The uptake of inorganic nutrients by heterotrophic bacteria. *Microb. Ecol.* 28, 255–271. doi: 10.1007/BF00166816

Kirchman, D. L., and Wheeler, P. A. (1998). Uptake of ammonium and nitrate by heterotrophic bacteria and phytoplankton in the sub-Arctic Pacific. *Deep Sea Res. Part Oceanogr. Res. Pap.* 45, 347–365. doi: 10.1016/S0967-0637(97)00075-7

Koroleff, F. (1983). "Determination of ammonia," in *Methods of Seawater Analysis*, eds K. Grasshoff, M. Ehrhardt, and K. Kremllng (Weinheim: Verlag Chemie), 150–157.

Kuenen, J. G., Boonstra, J., Schröder, H. G., and Veldkamp, H. (1977). Competition for inorganic substrates among chemoorganotrophic and chemolithotrophic bacteria. *Microb. Ecol.* 3, 119–130. doi: 10.1007/BF02010401

Le Chevanton, M., Garnier, M., Bougaran, G., Schreiber, N., Lukomska, E., Bérard, J.-B., et al. (2013). Screening and selection of growth-promoting bacteria for Dunaliella cultures. *Algal Res.* 2, 212–222. doi: 10.1016/j.algal.2013.05.003

Lenes, J. M., Darrow, B. P., Cattrall, C., Heil, C. A., Callahan, M., Vargo, G. A., et al. (2001). Iron fertilization and the Trichodesmium response on the West Florida shelf. *Limnol. Oceanogr.* 46, 1261–1277. doi: 10.4319/lo.2001.46.6.1261

Lipschultz, F. (1995). Nitrogen-specific uptake rates of marine-phytoplankton isolated from natural-populations of particles by flow-cytometry. *Mar. Ecol. Prog. Ser.* 123, 245–258. doi: 10.3354/meps123245

Mata, T. M., Martins, A. A., and Caetano, N. S. (2010). Microalgae for biodiesel production and other applications: a review. *Renew. Sustain. Energy Rev.* 14, 217–232. doi: 10.1016/j.rser.2009.07.020

Meseck, S. L., Smith, B. C., Wikfors, G. H., Alix, J. H., and Kapareiko, D. (2006). Nutrient interactions between phytoplankton and bacterioplankton under different carbon dioxide regimes. *J. Appl. Phycol.* 19, 229–237. doi: 10.1007/s10811-006-9128-5

Mindl, B., Sonntag, B., Pernthaler, J., Vrba, J., and Posch, R. P. (2005). Effects of phosphorus loading on interactions of algae and bacteria: reinvestigation of the "phytoplankton– bacteria paradox" in a continuous cultivation system. *Aquat. Microb. Ecol.* 38, 203–213. doi: 10.3354/ame038203

Moore, C. M., Mills, M. M., Arrigo, K. R., Berman-Frank, I., Bopp, L., Boyd, P. W., et al. (2013). Processes and patterns of oceanic nutrient limitation. *Nat. Geosci.* 6, 701–710. doi: 10.1038/ngeo1765

Mulholland, M. R., Bernhardt, P. W., Heil, C. A., Bronk, D. A., and O'Neil, J. M. (2006). Nitrogen fixation and release of fixed nitrogen by Trichodesmium spp. in the Gulf of Mexico. *Limnol. Oceanogr.* 51, 1762–1776. doi: 10.4319/lo.2006.51.4.1762

Mulholland, M. R., Gobler, C. J., and Lee, C. (2002). Peptide hydrolysis, amino acid oxidation, and nitrogen uptake in communities seasonally dominated by *Aureococcus anophagefferens*. *Limnol. Oceanogr.* 47, 1094–1108. doi: 10.4319/lo.2002.47.4.1094

Nagao, F., and Miyazaki, T. (2002). Release of dissolved organic nitrogen from *Scenedesmus quadricauda* (Chlorophyta) and *Microcystis novacekii* (Cyanobacteria). *Aquat. Microb. Ecol.* 27, 275–284. doi: 10.3354/ame027275

Natrah, F. M. I., Bossier, P., Sorgeloos, P., Yusoff, F. M., and Defoirdt, T. (2014). Significance of microalgal–bacterial interactions for aquaculture. *Rev. Aquac.* 6, 48–61. doi: 10.1111/raq.12024

Newell, B. S., Dalpont, G., and Grant, B. R. (1972). The excretion of organic nitrogen by marine algae in batch and continuous culture. *Can. J. Bot.* 50, 2605–2611. doi: 10.1139/b72-334

Palenik, B., and Morel, F. (1990). Comparison of cell-surface l-amino-acid oxidases from several marine-phytoplankton. *Mar. Ecol. Prog. Ser.* 59, 195–201. doi: 10.3354/meps059195

Palenik, B., and Morel, F. (1991). Amine oxidases of marine-phytoplankton. *Appl. Environ. Microbiol.* 57, 2440–2443.

Park, J., Jin, H.-F., Lim, B.-R., Park, K.-Y., and Lee, K. (2010). Ammonia removal from anaerobic digestion effluent of livestock waste using green alga Scenedesmus sp. *Bioresour. Technol.* 101, 8649–8657. doi: 10.1016/j.biortech.2010.06.142

Park, Y., Je, K.-W., Lee, K., Jung, S.-E., and Choi, T.-J. (2008). Growth promotion of Chlorella ellipsoidea by co-inoculation with Brevundimonas sp. isolated from the microalga. *Hydrobiologia* 598, 219–228. doi: 10.1007/s10750-007-9152-8

Pujo-Pay, M., and Raimbault, P. (1994). Improvement of the wet-oxidation procedure for simultaneous determination of particulate organic nitrogen and phosphorus collected on filters. *Mar. Ecol. Prog. Ser.* 105, 203–207. doi: 10.3354/meps105203

Shuter, B. J. (1978). Size dependence of phosphorus and nitrogen subsistence quotas in unicellular microorganisms. *Limnol. Oceanogr.* 23, 1248–1255. doi: 10.4319/lo.1978.23.6.1248

Smith, R. E. H., and Kalff, J. (1982). Size-dependent phosphorus uptake kinetics and cell quota in phytoplankton1. *J. Phycol.* 18, 275–284. doi: 10.1111/j.1529-8817.1982.tb03184.x

Solorzano, L. (1969). Determination of ammonia in natural sea waters by the phenol-hypochlorite method. *Am. Soc. Limnol. Oceanogr.* 14, 799–801. doi: 10.4319/lo.1969.14.5.0799

Spolaore, P., Joannis-Cassan, C., Duran, E., and Isambert, A. (2006). Commercial applications of microalgae. *J. Biosci. Bioeng.* 101, 87–96. doi: 10.1263/jbb.101.87

Stoecker, D., and Gustafson, D. (2003). Cell-surface proteolytic activity of photosynthetic dinoflagellates. *Aquat. Microb. Ecol.* 30, 175–183. doi: 10.3354/ame030175

Strom, S. L. (2008). Microbial ecology of ocean biogeochemistry: a community perspective. *Science* 320, 1043–1045. doi: 10.1126/science.1153527

Tai, V., Paulsen, I. T., Phillippy, K., Johnson, D. A., and Palenik, B. (2009). Whole-genome microarray analyses of *Synechococcus–Vibrio* interactions. *Environ. Microbiol.* 11, 2698–2709. doi: 10.1111/j.1462-2920.2009.01997.x

Tamminen, T., and Irmisch, A. (1996). Urea uptake kinetics of a midsummer planktonic community on the SW coast of Finland. *Mar. Ecol. Prog. Ser.* 130, 201–211. doi: 10.3354/meps130201

Tilman, D, Kilham, S S, and Kilham, P. (1982). Phytoplankton community ecology: the role of limiting nutrients. *Annu. Rev. Ecol. Syst.* 13, 349–372. doi: 10.1146/annurev.es.13.110182.002025

Thingstad, T. F., Hagstrom, A., and Rassoulzadegan, F. (1997). Accumulation of degradable DOC in surface waters: is it caused by a malfunctioning microbial loop? *Limnol. Oceanogr.* 42, 398–404. doi: 10.4319/lo.1997.42.2.0398

Vasseur, C., Bougaran, G., Garnier, M., Hamelin, J., Leboulanger, C., Le Chevanton, M., et al. (2012). Carbon conversion efficiency and population dynamics of a marine algae–bacteria consortium growing on simplified synthetic digestate: first step in a bioprocess coupling algal production and anaerobic digestion. *Bioresour. Technol.* 119, 79–87. doi: 10.1016/j.biortech.2012.05.128

Walne, P. R. (1970). *Studies On The Food Value of Nineteen Genera Of Algae To Juvenile Bivalves of The Genera Ostrea, Crassostrea, Mercenaria and Mytilus*. Fishery investigations Series II, Vol. 26. London: Ministry of Agriculture.

Wilson, J. B. (2011). The twelve theories of co-existence in plant communities: the doubtful, the important and the unexplored. *J. Veg. Sci.* 22, 184–195. doi: 10.1111/j.1654-1103.2010.01226.x

Zehr, J. P., and Ward, B. B. (2002). Nitrogen cycling in the ocean: new perspectives on processes and paradigms. *Appl. Environ. Microbiol.* 68, 1015–1024. doi: 10.1128/AEM.68.3.1015-1024.2002

Conflict of Interest Statement: The authors declare that the research was conducted in the absence of any commercial or financial relationships that could be construed as a potential conflict of interest.

frontiers in Microbiology

ORIGINAL RESEARCH
published: 09 June 2016
doi: 10.3389/fmicb.2016.00880

Genetic Manipulation of Competition for Nitrate between Heterotrophic Bacteria and Diatoms

*Rachel E. Diner[1,2], Sarah M. Schwenck[1,2], John P. McCrow[2], Hong Zheng[2] and Andrew E. Allen[1,2]**

[1] Integrative Oceanography Division, Scripps Institution of Oceanography, University of California San Diego, La Jolla, CA, USA, [2] Microbial and Environmental Genomics Group, J. Craig Venter Institute, La Jolla, CA, USA

Diatoms are a dominant group of eukaryotic phytoplankton that contribute substantially to global primary production and the cycling of important elements such as carbon and nitrogen. Heterotrophic bacteria, including members of the gammaproteobacteria, are commonly associated with diatom populations and may rely on them for organic carbon while potentially competing with them for other essential nutrients. Considering that bacterioplankton drive oceanic release of CO_2 (i.e., bacterial respiration) while diatoms drive ocean carbon sequestration vial the biological pump, the outcome of such competition could influence the direction and magnitude of carbon flux in the upper ocean. Nitrate availability is commonly a determining factor for the growth of diatom populations, particularly in coastal and upwelling regions. Diatoms as well as many bacterial species can utilize nitrate, however the ability of bacteria to compete for nitrate may be hindered by carbon limitation. Here we have developed a genetically tractable model system using the pennate diatom *Phaeodactylum tricornutum* and the widespread heterotrophic bacteria *Alteromonas macleodii* to examine carbon-nitrogen dynamics. While subsisting solely on *P. tricornutum* derived carbon, *A. macleodii* does not appear to be an effective competitor for nitrate, and may in fact benefit the diatom; particularly in stationary phase. However, allochthonous dissolved organic carbon addition in the form of pyruvate triggers *A. macleodii* proliferation and nitrate uptake, leading to reduced *P. tricornutum* growth. Nitrate reductase deficient mutants of *A. macleodii* (Δ*nasA*) do not exhibit such explosive growth and associated competitive ability in response to allochthonous carbon when nitrate is the sole nitrogen source, but could survive by utilizing solely *P. tricornutum*-derived nitrogen. Furthermore, allocthonous carbon addition enables wild-type *A. macleodii* to rescue nitrate reductase deficient *P. tricornutum* populations from nitrogen starvation, and RNA-seq transcriptomic evidence supports nitrogen-based interactions between diatoms and bacteria at the molecular level. This study provides key insights into the roles of carbon and nitrogen in phytoplankton-bacteria dynamics and lays the foundation for developing a mechanistic understanding of these interactions using co-culturing and genetic manipulation.

Keywords: diatoms, bacteria, nitrate, competition, genetic manipulation, transcriptomics, *Phaeodactylum*, *Alteromonas*

OPEN ACCESS

Edited by:
Xavier Mayali, Lawrence Livermore National Laboratory, USA

Reviewed by:
Song Xue, Dalian University of Technology, China
Daniel Jonathan Sher, University of Haifa, Israel

***Correspondence:**
Andrew E. Allen
aallen@ucsd.edu

Specialty section:
This article was submitted to Aquatic Microbiology, a section of the journal Frontiers in Microbiology

Received: *01 April 2016*
Accepted: *25 May 2016*
Published: *09 June 2016*

Citation:
Diner RE, Schwenck SM, McCrow JP, Zheng H and Allen AE (2016) Genetic Manipulation of Competition for Nitrate between Heterotrophic Bacteria and Diatoms. Front. Microbiol. 7:880. doi: 10.3389/fmicb.2016.00880

INTRODUCTION

Diatoms as well as bacteria are important drivers of oceanic biogeochemical cycling, and frequently occupy overlapping ecological niches. Diatoms are often the dominant primary producers in nutrient rich ecosystems, such as coastal upwelling regions, and can form dense and extensive blooms. Marine bacteria constitute the majority of oceanic biomass (Pomeroy, 1974; Fuhrman, 1989; Whitman et al., 1998), and heterotrophic bacteria utilize and rely on phytoplankton-derived organic matter for survival and growth (Azam and Malfatti, 2007; Sarmento and Gasol, 2012; Buchan et al., 2014). Diatoms and bacteria are subject to frequent environmental fluctuations in availability of essential nutrients such as nitrogen (N) and carbon (C). Nitrate (NO_3^-) in particular often reaches limiting concentrations during phytoplankton blooms (Falkowski and Oliver, 2007). Certain classes of heterotrophic bacteria, such as gammaproteobacteria, are consistently found in phytoplankton-associated microbial communities, and may potentially compete with diatoms for scarce nutrients while simultaneously relying on them for organic C (Buchan et al., 2014). While population dynamics of phytoplankton and bacteria under different environmental conditions have been extensively examined, outside of a few recent studies (e.g., Durham et al., 2014; Amin et al., 2015; Smriga et al., 2016) relatively little is known regarding the cellular, metabolic, or genetic basis for different types of interactions (Bell and Mitchell, 1972; Amin et al., 2012). This is particularly true for competitive interactions (Amin et al., 2012). Laboratory model systems and new experimental approaches can enable hypothesis-testing and lead to new discoveries regarding interactions between diatoms and heterotrophic bacteria in productive microbial ecosystems and the associated influence on C and nutrient cycling.

A common regulator of primary productivity in marine ecosystems is availability of NO_3^-. When estimating primary productivity and characterizing the magnitude of the biological pump it is assumed that inorganic N is converted into particulate organic matter entirely by phytoplankton (Dugdale and Goering, 1967; Bronk et al., 1994). Diatoms are excellent competitors for NO_3^-, and have evolved efficient assimilation, storage and associated recycling systems (Serra et al., 1978; Dortch, 1990; Lomas and Gilbert, 2000; Allen et al., 2006, 2011). The emerging laboratory model diatom *Phaeodactylum tricornutum* has been used in many studies to investigate diatom N utilization, as well as responses to many other environmental variables such as iron (Fe) and phosphorus (P) (Yongmanitchai and Ward, 1991; Geider et al., 1993; Allen et al., 2008; Jiao et al., 2011; Matthijs et al., 2015; Morrissey et al., 2015). These studies have been facilitated by development of a variety of tools for genetic manipulation in *P. tricornutum* (Siaut et al., 2007; Karas et al., 2015; Weyman et al., 2015; Nymark et al., 2016). Notably, mutant strains of *P. tricornutum* that are deficient in ability to utilize NO_3^- have been crucial for understanding N uptake and storage, and impacts on cellular physiology (Levitan et al., 2014). The sequencing of the *P. tricornutum* genome (Bowler et al., 2008) revealed that about 6% of *P. tricornutum* genes appear to be bacterial in origin, including a NAD(P)H dependent assimilatory NO_2^-, reductase, and are possibly the result of horizontal gene transfer. This suggests a historically intimate relationship between diatoms and bacteria, which might also have significant evolutionary implications.

Heterotrophic bacteria also play a large role in N cycling and remineralization (Zehr and Ward, 2002; Azam and Malfatti, 2007). They are known to utilize a variety of sources for satisfying their N requirements, including ammonium (NH_4^+), NO_3^-, urea, free amino acids, and various other organic N compounds. In some studies, NH_4^+ and organic N sources such as amino acids have been shown to satisfy the bulk of heterotrophic bacterial N demand, while other organic N sources and inorganic N such as NO_3^- appeared to play a more minor role (Wheeler and Kirchman, 1986; Keil and Kirchman, 1991). However, a large number of heterotrophic bacteria possess pathways for utilizing NO_3^- and are able to grow using NO_3^- as a sole N source. Studies examining the molecular ecology of heterotrophic bacterial nitrate reductase genes (*nasA*) and their functionality have suggested that bacterial NO_3^- utilization is globally widespread and may play an important role in inorganic N cycling in several ecosystems (Allen et al., 2001; Jiang et al., 2015). Further, heterotrophic bacteria have been shown to satisfy between 10 and 50% of their total N demand with dissolved inorganic nitrogen (NH_4^+ and NO_3^-), and can account for between 10 and 40% of total water column NO_3^- uptake (Allen et al., 2005). Stable isotope probing (SIP) experiments with $^{15}NO_3^-$ have also shown that heterotrophic bacteria in natural assemblages, including members of the *Alteromonas* genera, can and do take up NO_3^- (Wawrik et al., 2012). Methods based on sorting heterotrophic and autotrophic cells with flow cytometry following $^{15}NO_3^-$ incubation have also documented significant levels of heterotrophic bacterial NO_3^- utilization (Bradley et al., 2010a,b,c; Lomas et al., 2011). However, the role that bacterial NO_3^- assimilation plays in shaping microbial communities and regulating NO_3^- flux in pelagic ecosystems remains poorly understood, though it may have important consequences for understanding the biological pump.

To gain a deeper understanding of N-related interactions between diatoms and bacteria, we developed a model co-culture system using the diatom *P. tricornutum* CCMP 632 and the marine heterotrophic bacteria *Alteromonas macleodii*. *A. macleodii* represents an excellent model for investigating these interactions because *Alteromonas* sp. are ecologically important members of the gammaproteobacteria class, and have been shown to be amenable to genetic manipulation (Kato et al., 1998; Weyman et al., 2011). They are relatively large (∼1-2 μm), rod-shaped motile bacteria that are capable of utilizing a variety of C and N sources (López-Pérez and Rodríguez-Valera, 2014; Pedler Sherwood et al., 2015). Ecologically, they are frequently associated with nutrient and particle-rich environments and are commonly found as active and dominant members of phytoplankton-associated bacterial assemblages (Buchan et al., 2014; López-Pérez and Rodríguez-Valera, 2014). *Alteromonas* bacteria have previously been shown to interact with individual eukaryotic and prokaryotic phytoplankton species. These interactions range from impairing algal growth, sometimes by algicidal means (Kato et al., 1998; Mayali and Azam, 2004;

Aharonovich and Sher, 2016) to effects that are either neutral or beneficial to algal growth in co-culture (Morris et al., 2008, 2011; Sher et al., 2011; Aharonovich and Sher, 2016). When concentrated organic matter is available, *Alteromonas* bacteria have been shown to be among the most rapidly dividing heterotrophic prokaryotes, and can reach high population densities (Shi et al., 2012; Pedler et al., 2014). *A. macleodii,* the designated type species for the *Alteromonas* genus, is distributed globally and is exceptionally diverse genetically (García-Martínez et al., 2002; Ivars-Martínez et al., 2008; López-Pérez et al., 2012). The strain selected for this study, *A. macleodii* ATCC27126, is capable of utilizing NO_3^- as a sole N source in minimal (Aquil) media supplemented with a dissolved organic carbon (DOC) source, solidifying this strain as an excellent candidate for the model system employed in this study.

Through the use of targeted genetic manipulation we have gained new insights into the mechanisms governing physiological processes related to nutrient exchange and competition between diatoms and bacteria, particularly interactions involving C and N. We examined model diatoms and bacteria that are both capable of NO_3^- utilization. Leveraging new and existing genetic tools available for each organism in the model system presented here, we created both diatom and bacterial mutants lacking the ability to utilize NO_3^-. We then examined the response of these strains in co-culture under varying C and N availability scenarios. Additionally, we conducted transcriptional profiling experiments in order to identify molecular responses of diatoms to the bacteria as well as to gain insights into the physiological status of each partner.

MATERIALS AND METHODS

Strains and Culturing Conditions

Axenic cultures of *P. tricornutum* strain CCMP 632 were obtained from the Provasoli-Guillard National Center for Culture of Marine Algae and Microbiota. Axenic cultures were confirmed via microscopy (light and DAPI staining), in addition to regular plating on marine bacterial growth media. *P. tricornutum* monocultures and *A. macleodii* co-cultures were grown in Aquil artificial seawater media (ASW), with modified concentrations of NO_3^- added as sodium nitrate (Fisher Bioreagents, Waltham MA, USA) or NH_4^+ added as ammonium chloride (Fisher Bioreagents, Waltham MA, USA). Media was microwaved to ∼95°C two times prior to cooling, addition of nutrients and filter sterilization (0.2 μm bottle-top filters, Thermo Fisher Scientific, Waltham MA, USA). Experiments were conducted at 18°C with a light intensity of 170 μmol photons m^{-2} s^{-1} and a 14/10 h light/dark cycle. In order to minimize variability resulting from diel effects, measurements and sampling for each experiment occurred at the same time each day, ∼6 h after light cycle onset.

A. macleodii strain ATCC27126 monocultures were grown routinely either on Zobell 2216 marine broth (MB) 1% agar plates, or in MB liquid medium at 28°C. *A. macleodii* growth was also supported in half-strength marine broth media, and in Aquil ASW supplemented with 5 mM pyruvate. Liquid cultures were grown shaking at 225 rpm. Prior to co-culturing experiments, overnight cultures of *A. macleodii* culture were centrifuged at 6000 x g for 3 min; the supernatant was discarded, and cells were subsequently gently washed 3 times in the experimental seawater media. *E. coli* used for cloning was cultured in LB broth (Amresco, Solon OH, USA) or on LB agar plates at 37°C. Antibiotic concentrations for selective bacterial growth were provided as 100 μg/ml Kanamycin and 100 μg/ml Ampicillin for *A. macleodii* and 50 μg/ml Kanamycin, 100 μg/ml Ampicillin, 10 μg/ml Chloramphenicol, 10 μg/ml Tetracycline, or 10 μg/ml Spectinomycin for *E. coli* as needed.

Genetic Manipulation of *A. macleodii* and *P. tricornutum*

Previous studies genetically manipulating *Alteromonas* bacteria focused on either undesignated species (Kato et al., 1998) or species other than *A. macleodii* (Weyman et al., 2011 focused on the "deep ecotype" which was reclassified as *A. mediterranea*), making this study the first to genetically manipulate this widespread species. The genome sequence of *A. macleodii* strain ATCC27126 was obtained from the JGI IMG data base and the DNA sequence of the single copy nasA gene was identified and used to design the knockout (KO) construct. The *A. macleodii* Δ*nasA* line was engineered using SacB-mediated homologous recombination, as in Weyman et al. (2011). Gibson assembly was used to construct the suicide plasmid pRED16 (Supplementary Figure 1A), which contains an origin of replication from source plasmid pBBR1-MCS5 (incapable of replication in *A. macleodii* ATCC27126), an origin of transfer, a SacB gene conferring toxicity to sucrose, and 2 1-kb regions homologous to the *A. macleodii nasA* gene flanking a kanamycin resistance cassette (Kovach et al., 1995; Gibson et al., 2009; Weyman et al., 2011). This plasmid was assembled and transformed into *E. coli*, which was mated overnight with the *A. macleodii* WT strain. Transconjugants were dilution-plated to obtain Kanamycin resistant single colonies, and then streaked onto 5% sucrose plates to select for double-crossover recombinants. These were again plated to single colonies, which were screened by PCR to amplify regions specific to *A. macleodii* strain ATCC27126 (to confirm sole presence of this strain as the primers do not amplify in *E. coli*), and regions spanning both junctions of the genome insert, as well as the entire insert (data not shown). All colonies screened were identified as *A. macleodii* strain ATCC27126 and were positive for the KO insert. The KO phenotype (inability to utilize NO_3^-) was confirmed by plating transconjugant colonies and the WT strain on seawater-agar plates containing pyruvate as a C source, either NO_3^- or NH_4^+ as a N source, and X-gal solution (Takara, Meadow View CA, USA) to better visualize the phenotypic effect. The WT strain was able to grow on either N source, while the knockout strain displayed growth on NH_4^+ but not on NO_3^- (Supplementary Figure 1B).

P. tricornutum nitrate reductase knockout (NRKO) lines were constructed using Transcription activator-like effector nuclease (TALEN) genetic manipulation, as in Weyman et al. (2015). Using the JGI *P. tricornutum* genome (http://genome.jgi.doe.gov/Phatr2/Phatr2.home.html), the sequence encoding nitrate reductase (NR) (Phatr2 ID: 54983, Phatr3 ID: J54983) was identified and activity was eliminated by interrupting the sequence with a phleomycin-resistance cassette

suitable for downstream selection. Transformation of the NRKO plasmids was accomplished by microparticle bombardment (BIO-RAD PDS-1000/He Biolistic Particle Delivery System).

Experimental Design

To address baseline physiological and transcriptional profiles of diatom and diatom-bacteria co-cultures, 1L batch cultures were grown in autoclaved 2L Erlenmeyer flasks. Three treatments with three biological replicates each were examined: *P. tricornutum* monocultures, *P. tricornutum–A. macleodii* WT co-cultures, and *P. tricornutum–A. macleodii* Δ*nasA* co-cultures. Prior to starting the experiments, both phytoplankton and bacteria were cultured together in the relevant experimental conditions for >7 *P. tricornutum* generations (∼1 week), and inoculated during *P. tricornutum* exponential phase. Sampling was conducted daily for spectrophotometric measurement of NO_3^-, and for cell counts via flow cytometry (see below). Samples for additional physiological parameters and RNA-seq transcriptomic analysis were also collected during *P. tricornutum* exponential and stationary phase (**Figure 1**). Physiological parameters included *in vivo* fluorescence, pH, Chl-a, Fv/Fm, and dissolved and particulate organic C and N. The initial NO_3^- concentration was 300 μM. Diatom specific growth rates (μ) were calculated using cell densities obtained via flow cytometry on day 2 and day 5 of the experiment. For comparison to flow cytometry results, *P. tricornutum* cells were also counted on a counting chamber and bacteria colony forming units (CFU) ml^{-1} were determined for the *A. macleodii* (see below). Every second day, the *P. tricornutum* monocultures were plated on MB and co-cultures were plated on MB with Kanamycin in order to confirm lack of culture cross-contamination.

Several small-scale experiments were performed to examine the effects of C and N concentration on co-culture population dynamics, interactions between bacteria and the *P. tricornutum* NRKO line, and *A. macleodii* growth on multiple media types. For these experiments, 20ml cultures and co-cultures were grown in sterile glass tubes in triplicate and 300 μL samples were collected regularly and preserved with paraformaldehyde (PFA) for subsequent processing via flow cytometry (see below). Four hundred microlitre samples were also collected in order to measure NO_3^- concentration in the DOC addition experiment (see below). *A. macleodii* growth on different media sources was evaluated by growing overnight cultures of *A. macleodii* WT, gently rinsing the cells two times in nutrient free Aquil ASW, and resuspending in 1 ml of the same media prior to inoculating media treatments with 1:1000 dilution of the bacteria. Cells were grown in the following media treatments: Aquil ASW with and without 300 μM NO_3^- (Aq and Aq-N, respectively), MB, and expired media from a *P. tricornutum* stationary culture filtered through a 0.2 μm filter (PtF).

In DOC addition experiments, co-cultures that had been maintained semi-continuously were used for inoculations. For both the *A. macleodii* WT and Δ*nasA*-*P. tricornutum* co-cultures, five different DOC-addition treatments were established (each in triplicate): DOC added either at the time of inoculation (Day 0) or on days 2, 4, 6, and 8 of the experiment. A no DOC-addition control was included for a total of 6 treatments. Allochthonous DOC was added as pyruvate at a concentration of 5 mM. Media contained 300 μM final concentration of NO_3^-. As a result of pyruvate interference with spectrophotometer measurement of NO_3^- samples were sent for autoanalyzer NO_3^- analysis (see below).

To address the impacts of varying C and NO_3^- concentrations on *P. tricornutum* and *A. macleodii* WT population dynamics, co-cultures maintained semi-continuously from the baseline experiment were used to inoculate experiments using nine different media types. NO_3^- concentrations of 50 μM, 300 μM, and 1 mM and DOC concentrations of 0 μM, 50 μM, and 1 mM were tested in a factorial design. Twenty milliliter co-cultures were grown in sterile glass tubes in triplicate and 500 μL samples were collected for flow cytometry analysis on days 2, 4, 6, and 31. Co-cultures containing 300 μM NO_3^- and no DOC addition were cultured semi-continuously for 5 subsequent transfers to determine steady-state growth rates of *P. tricornutum* in co-culture. To account for variability in cell concentration, μ was determined using the highest growth rate observed between any 2 subsequent sampling points in each transfer experiment.

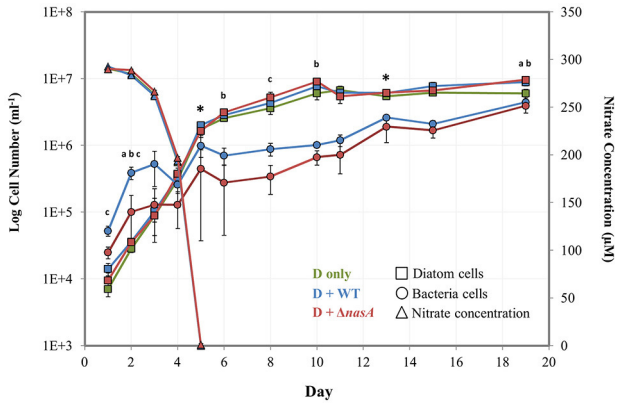

FIGURE 1 | Log number of bacteria and diatom cells (left vertical axis) determined by flow cytometry and nitrate concentrations (right vertical axis) determined by spectrophotometry during the baseline experiment. Squares = diatom cell numbers, circles = bacterial cell numbers, and triangles = nitrate concentrations (μM). Green markers = *P. tricornutum* monocultures (also noted as D only), blue markers = *P. tricornutum–A. macleodii* WT co-cultures (also noted as D + WT), and red markers = *P. tricornutum–A. macleodii* Δ*nasA* co-cultures (also noted as D + Δ*nasA*). Exponential growth stage was defined as days 1–6, and stationary growth phase as days 7–19. * indicates the two sampling points for physiology and transcriptomics. [a] indicates that diatom cell numbers were significantly different between *P. tricornutum* monocultures and *A. macleodii* WT co-cultures. [b] indicates that diatom cell numbers were significantly different between *P. tricornutum* monocultures and *A. macleodii* Δ*nasA* co-cultures. [c] indicates that bacteria cell numbers were significantly different between the WT and Δ*nasA* co-cultures. All data points represent the average of $n = 3$ replicates, and error bars are standard deviation. Some differences in cell numbers and nitrate concentrations (e.g., diatom monoculture nitrate concentrations, which are overlapped by the Δ*nasA* co-culture measurements) are difficult to discern, so average non-transformed cell numbers and nitrate concentrations have been listed in Supplementary Table 2.

For the *P. tricornutum* NRKO co-culturing experiments, three different co-cultures were grown in both NH_4^+ and NO_3^- amended Aquil ASW; *P. tricornutum* NRKO only, *P. tricornutum* NRKO + WT *A. macleodii*, and *P. tricornutum* NRKO + WT *A. macleodii* + DOC. The *P. tricornutum* NRKO with and without *A. macleodii* were acclimated in NH_4^+ amended media after which they were inoculated into both media types and pyruvate was added to the relevant treatments. N was added as 880 μM final concentration of the relevant source. Since some of the experiments included DOC amendments, we conducted an experiment to examine the impact of such DOC addition on *P. tricornutum* growth. *P. tricornutum* WT monocultures and *P. tricornutum* WT monocultures + 5 mM pyruvate cultures were established in 20 ml cultures as above, and run in triplicate, and media contained 880 μM final concentration of NO_3^-.

Sample Collection and Processing: Cell Numbers, Physiology, and NO_3^- Drawdown

Cell densities of diatoms and bacteria were determined by flow cytometry, and in the case of the baseline experiment, also by manual counting methods. *P. tricornutum* cells were counted manually on either a Sedgwick-Rafter hemocytometer (when cell densities were low) or an Improved-Neubauer hemocytometer (IN-Cyto, Chungnam-do, Korea). *A. macleodii* CFU were determined by dilution-plating onto MB agar plates. (Both WT and Δ*nasA* lines of *A. macleodii* were also plated on MB kanamycin plates to confirm the sole presence of Δ*nasA* lines. Samples for staining and cell counting via flow cytometry were preserved by adding PFA to a final concentration of 0.5%. Samples were incubated at 4°C prior to flash freezing and storage at −80°C until processing. Flow cytometry analysis was conducted on a BD FACS Aria II using the Bacteria Kit for flow cytometry (Thermo Fisher Scientific, Waltham MA, USA) for quantifying the number of diatom and bacteria cells in each sample. After the addition of beads to samples, SYBR green I DNA stain was added, effectively staining all three populations (diatoms, bacteria, and beads). Bacterial and diatom populations were quantified simultaneously, and typical flow cytometer settings were forward scatter (FSC) = 200, side scatter (SSC) = 250, FSC PMT = 550, SYBR Green (SYBR Grn) = 530, Yellow fluorescence (YFP) = 335, with the following thresholds: SSC = 200, FSC = 200.

Nitrate levels were measured either via spectrophotometer or autoanalyzer (in DOC addition experiments). For spectrophotometric measurement, samples were prepared by centrifuging whole sample in Eppendorf tubes at 8000g for 10 min. Supernatant was then recovered, and stored at −20°C until processing. NO_3^- values were determined by generating a standard curve using dilutions of 880 μM NO_3^- media, using only curves with >99% precision (Collos et al., 1999; Johnson and Coletti, 2002). Samples were then measured in triplicate. As allochthonous DOC addition interfered with the spectrophotometric readings, NO_3^- and NO_2^- analysis for DOC addition experiments was conducted using a Lachat QuikChem 8500 autoanalyzer as in Parsons et al. (1984).

Concentrations of total and dissolved organic C and N were determined using a Total Organic Carbon (TOCL) analyzer (Shimadzu) paired with an ASI-L autosampler (Shimadzu). Prior to sample collection, 24-ml glass vials were combusted at 450°C and vial caps were acid rinsed for >24 h. Five to ten milliliters samples were stored at −20°C prior to dilution with milliQ and processing. Standard curves for determining C and N concentrations were generated using automated dilution and sampling of 1000 ppm potassium hydrogen phthalate for C, and 1000 ppm potassium nitrate for N. Samples for determining C and N in the dissolved fraction were collected by gentle filtration through a 0.2 μm syringe filter. Particulate values were determined by subtracting dissolved values from total values. Chlorophyll A (Chl a) concentrations were measured by 90% acetone extraction. Ten milliliters of the sample was gently filtered onto GF/F filters, flash frozen in in liquid N_2, and stored at −20°C before overnight acetone extraction and measurement on a 10AU fluorometer (Turner). Culture Fv/Fm was measured using a pam-fluorometer (WALZ). pH was measured using an InLab Expert pH probe (Mettler Toledo), calibrated using 4, 7, and 10 pH standards (Orion Application Solutions).

Sample Collection and Processing: Transcriptomics

Transcriptomics samples were collected by gentle filtration onto 47 mm 0.2um polycarbonate filters (Whatmann), followed by flash freezing in liquid N_2 and storage at −80°C prior to processing. Total RNA was isolated using Trizol reagent (Thermo Fisher Scientific, Waltham MA, USA). The TURBO DNA-free Kit (Thermo Fisher Scientific, Waltham MA, USA) was used to digest genomic DNA. RNA was subsequently purified further using the Agencourt RNAClean XP kit (Beckman Coulter, Carlsbad CA, USA). The quality of RNA was evaluated using an Agilent 2100 Bioanalyzer (also used for subsequent quality analyses). Ribosomal RNA was removed using Ribo-Zero Magnetic kits (Epicentre, San Diego CA, USA) with a modification of the removal solution, using a mixture of the plant, bacterial, and human/mouse/rat Removal Solutions in a ratio of 2:1:1. Following mRNA enrichment via rRNA removal, RNA quality was further inspected via bioanalyzer. The Ovation RNA-Seq System V2 (NuGEN Technologies, Inc.) was used for first and second strand cDNA synthesis and amplification, followed by evaluation of cDNA quality via bioanalyzer. cDNA was sheared using the S2/E210 focused-ultrasonicator (Covaris) with a target size of 300 bp, confirmed by bioanalyzer. Libraries for sequencing were constructed using the Ovation® Ultralow System V2 (NuGEN Technologies, Inc.), and the quality of libraries verified by bioanalyzer prior to sequencing. Libraries were quantified using qPCR and a Library Quantification Kit (Kapa Biosystems), prior to sequencing on an Illumina NextSEQ500 DNA sequencer.

Paired Illumina reads were filtered for Illumina primer contamination and quality trimmed to Phred score 33 and a minimum length of 30 prior to read mapping. Reads were mapped to target genome contigs of *P. tricornutum* (http://genome.jgi.doe.gov/Phatr2/Phatr2.home.html) and

A. macleodii ATCC 27126 using BWA MEM alignment (Li, 2013). Raw read counts were calculated for each gene using featureCounts (Liao et al., 2014) based on gene models for *A. macleodii* (CP003841) and *P. tricornutum* (Phatr3, http://protists.ensembl.org/Phaeodactylum_tricornutum/Info/Index). Additional gene level *de novo* functional annotation was generated for *P. tricornutum* via KEGG, KO, KOG, Pfam, and TIGRfam assignments. RPKMs were computed using library mapped reads and lengths of CDS for each gene. Biological triplets were used to quantitatively estimate differential expression using edgeR (Robinson et al., 2010) to assign normalized fold-change and Benjamini-Hochberg adjusted *p*-values for each gene. Raw read counts for each gene were used in all edgeR analyses. Sequencing data generated as part of this study has been deposited at NCBI.

Statistical Analyses

In the baseline experiment, statistical analyses were conducted to examine potential differences in diatom cell numbers between the monoculture and co-culture treatments, bacteria cell numbers between co-culture treatments, and to explore whether any physiological parameters were different between treatments during the exponential or stationary phase. One-way ANOVAs were performed followed by Tukey HSD *post-hoc* tests. Statistical significance was assumed at $p \leq 0.05$. All statistical analyses were conducted using R (version 2.14.2), and were performed on raw data (i.e., not transformed).

RESULTS

Baseline Physiology and Transcriptomics in Diatom-Bacteria Co-Cultures

A baseline experiment was conducted initially to examine cell growth, culture physiology, N drawdown, and diatom gene expression in diatom-bacteria co-cultures. In this experiment, N was provided as NO_3^- and no DOC was added. Cell counts obtained via flow cytometry were used to examine population dynamics of *P. tricornutum* and the *A. macleodii* strains in co-culture, which were compared to manual cell counts. Diatom growth stages for this experiment were defined generally as exponential (Day 1–5) and stationary (Day 6–19). The presence of WT or Δ*nasA A. macleodii* in *P. tricornutum* cultures did not significantly affect growth rate (Supplementary Table 1). Maximum diatom cell densities were typically similar among treatments during diatom exponential phase, but were higher in bacteria-containing cultures during stationary phase (**Figure 1**, Supplementary Table 2). These differences were significant between *P. tricornutum* monocultures and the *A. macleodii* Δ*nasA* co-cultures on day 2 ($p < 0.01$), day 6 ($p < 0.05$), day 10 ($p < 0.05$), and day 19 ($p < 0.01$), and between *P. tricornutum* monocultures and the *A. macleodii* WT line on day 1 ($p < 0.05$), day 2 ($p < 0.005$), and day 19 ($p < 0.05$; **Figure 1**). Although the maximum *P. tricornutum* cell densities estimated with manual counts were slightly lower than those calculated via flow cytometry, cell counts obtained from the two methods were similar (Supplementary Figure 2).

Both *A. macleodii* strains were able to grow in co-culture with *P. tricornutum*, as indicated by a gradual increase in cell abundance following *P. tricornutum* exponential stage (**Figure 1**). This growth increase did not occur when *A. macleodii* was grown in Aquil ASW in the absence of *P. tricornutum* (Supplementary Figure 3). The *A. macleodii* WT strain maintained higher numbers than the Δ*nasA* line, though patterns of growth were similar for both strains (**Figure 1**). These differences were significant ($p < 0.05$) on days 1, 2, and 8 of the experiment. After an initial increase in bacterial cell number in both bacteria co-culture treatments, bacterial numbers either declined (WT) or plateaued (Δ*nasA*) during the *P. tricornutum* exponential phase (**Figure 1**). Subsequently, cell numbers of both strains increased during the diatom stationary phase beginning on day 5. Manual CFU counts of the bacteria showed generally the same pattern of growth, however the growth decrease during *P. tricornutum* exponential phase was more dramatic and overall CFU ml^{-1} were lower following this phase in the experiment (Supplementary Figure 2). This difference in cell counts due to methodology has been observed in prior studies (Singleton et al., 1982; Mouriño-Pérez et al., 2003), where CFU counts were lower than direct counts under low DOC conditions. Likely the CFU counts reflect only viable, culturable cells while flow cytometry counts represent all cells including dormant, active, and recently dead cells. Neither *A. macleodii* strain was observed to physically attach to *P. tricornutum* at any point of the *P. tricornutum* growth cycle (qualitative observation, data not shown).

Nitrate concentrations decreased rapidly as *P. tricornutum* cell concentrations increased, and were undetectable by day 5 in all treatments (**Figure 1**). *P. tricornutum* cell numbers continued to increase exponentially even after the complete depletion of NO_3^- in the media (**Figure 1**). NO_3^- drawdown was similar among treatments with and without bacteria. Samples for cell physiology that were collected during the diatom exponential (Day 5) and stationary phase (Day 13), including Chl-a, pH, and Fv/Fm, showed no significant differences between treatments (Supplementary Table 3). Organic C and N were also evaluated for both the dissolved and the particulate culture fractions, and no significant differences between the treatments were observed (Supplementary Table 3).

Baseline Transcriptomic Analysis

Whole-genome transcriptome analyses were conducted at exponential (Day 5) and stationary (Day 13) sampling points. In general, a very low percentage of sequenced and mapped reads were associated with the *A. macleodii* genome, with slightly more observed in the diatom stationary samples than in the exponential samples (**Table 1**). The large majority of sequenced reads (>98% in all co-culture treatments) mapped to the *P. tricornutum* genome (**Table 1**). As a result, analyses of *A. macleodii* gene expression are not included in this study. Genes were considered to be significantly differentially expressed (DE) when the adjusted $p < 0.05$, and only genes with differential expression of > 0.75 fold are discussed. All data reported in this paper are deposited in the NCBI sequence read archive (BioProject accession no. PRJNA319251; BioSample accession nos. SAMN04884450- SAMN04884467).

TABLE 1 | Sequencing data collected for transcriptomic sampling points, including the total number of raw reads, the total number of trimmed reads, the percentage of trimmed reads that mapped to either the a genome or a gene model belonging to *P. tricornutum* or *A. macleodii*, and the percentage of the total mapped reads that corresponded to the *A. macleodii* and *P. tricornutum* genomes.

	Raw Reads	Trimmed Reads	% Reads mapped to a genome	% Reads mapped to a gene model	% Mapped reads: *A. macleodii*	% Mapped reads: *P. tricornutum*
EXPONENTIAL SAMPLING POINT						
P. tricornutum Only	1.0E + 07	9.9E + 06	84.18	58.29	0.00	100.00
P. tricornutum + *A. macleodii* WT	7.7E + 06	7.6E + 06	80.74	35.78	0.21	99.79
P. tricornutum + *A. macleodii* Δ*nasA*	9.2E + 06	9.0E + 06	82.78	36.60	0.28	99.72
TOTAL	2.7E + 07	2.7E + 07				
STATIONARY SAMPLING POINT						
P. tricornutum Only	2.9E + 07	2.8E + 07	88.16	43.52	0.00	100.00
P. tricornutum + *A. macleodii* WT	3.7E + 07	3.6E + 07	88.61	43.96	1.70	98.30
P. tricornutum + *A. macleodii* Δ*nasA*	3.0E + 07	3.0E + 07	88.92	33.69	1.90	98.10
TOTAL	9.5E + 07	9.4E + 07				

No *P. tricornutum* genes were significantly differentially expressed (DE) between any of the treatment during the diatom exponential sampling point, however, during the stationary sampling point many genes were differentially expressed between the *P. tricornutum* monoculture and either or both of the *P. tricornutum*-bacteria co-cultures. A set of 34 genes were significantly DE between axenic cultures and both bacterial co-cultures (**Figure 2**). The gene most highly upregulated in *P. tricornutum* in response to the bacteria (>5.9 fold in both co-cultures) is a putative voltage-gated ion channel (Phatr2 ID: 49093, Phatr3 ID: 302957) that has been shown to be involved in NO_3^- sensing and transport (see discussion). Other upregulated genes include a putative ferredoxin-dependent bilin reductase (Phatr2 ID: 33770, Phatr3 ID: 303606), and a putative fatty acid desaturase (Phatr2 ID: 46830, Phatr3 ID: 306355). Several of the genes that were downregulated in *P. tricornutum* in response to bacteria were related to cellular information storage and processing such as transcriptional regulation and replication, including two different putative heat shock protein transcription factors. The two genes most highly downregulated in the presence of bacteria were a short chain dehydrogenase (Phatr2 ID: 13001, Phatr3 ID: 306282), which was downregulated 8.8 and 6.5-fold in the Δ*nasA* and WT co-cultures, respectively, and a fatty acid hydroxylase (Phatr2 ID: N/A, Phatr3 ID: 308140), which was downregulated 5.7 and 3.9-fold in the Δ*nasA* and WT co-cultures, respectively (**Figure 2**).

Several transcripts were either upregulated or downregulated in both co-cultures, but the difference was only significant for one of the co-cultures. An additional 9 genes were DE between *P. tricornutum* monocultures and the *P. tricornutum*–*A. macleodii* WT co-culture treatments (Supplementary Table 4). These include a putative NO_2^- transporter (Phatr2 ID: 13076, Phatr3 ID: 308281), and a putative membrane associated NO_3^- transporter (Phatr2 ID: 26029, Phatr3 ID: 307720), which exhibited a >2.5-fold difference. Both of these putative genes were upregulated in the *P. tricornutum* monoculture compared to the co-cultures, and had a larger expression change in the WT bacteria co-culture than the Δ*nasA* co-culture (Supplementary Table 4). There were 99 genes significantly DE in *P. tricornutum* monocultures compared to *P. tricornutum*-*A. macleodii* Δ*nasA* co-cultures (Supplementary Table 4), including upregulation of a putative glutamine synthetase gene (Phatr2 ID: 51092, Phatr3 ID: 306624), a putative tryptophan/tyrosine permease (Phatr2 ID: 45852, Phatr3 ID: 310088), and a putative ferredoxin nitrite reductase (Phatr2 ID: 12902, Phatr3 ID: 308097). A putative sugar transporter (Phatr3 ID: 49722, Phatr2 ID: 311238) was downregulated in diatom monocultures, as well as additional heat shock transcription factors, including one that was downregulated >19-fold (Phatr2 ID: 48554, Phatr3 ID: 304737).

We also identified and compared expression of genes related to NH_4^+ utilization and transport. 17 putative genes were identified (Supplementary Table 5), and none were significantly DE between any treatments at a given sampling point.

Growth Physiology of *A. macleodii* in Multiple Media Types

In all media types, *A. macleodii* WT showed a rapid increase in cell number between inoculation on day 1 and the next measured time-point on day 3 (Supplementary Figure 3). Following this initial increase, cell numbers either decreased in all aquil-based media (Aq, Aq-N, and PtF media), or experienced a modest decrease followed by little change (MB media) (Supplementary Figure 3). The highest cell density occurred when cells were grown in MB media, reaching $\sim 1 \times 10^8$ cells ml^{-1}. *A. macleodii* WT in PtF media reached a higher maximum cell density (2.2×10^6 cells ml^{-1}) than the Aq and Aq-N treatments (8.6×10^5 and 8.9×10^5 cells ml^{-1}, respectively).

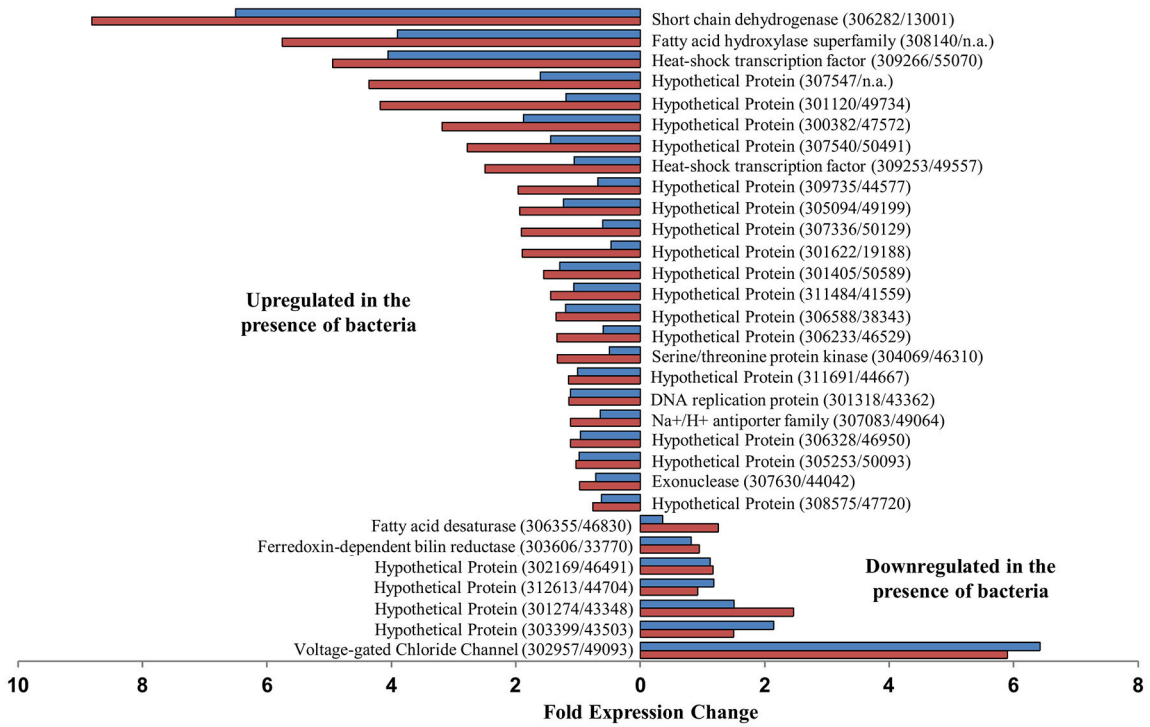

FIGURE 2 | Putative *P. tricornutum* genes that were significantly differentially expressed between *P. tricornutum* monocultures and both WT and Δ*nasA* bacterial co-cultures, and fold expression change. Blue bars = DE in WT co-cultures, red bars = DE in Δ*nasA* co-cultures. Gene descriptions are adjacent to relevant data bars, with gene IDs displayed as (Phatr3 ID/Phatr2 ID).

Competition between Diatoms and Bacteria for NO_3^-

We examined whether bacteria could impede diatom growth by competing for NO_3^- if sufficient DOC was present for bacterial growth. We hypothesized that the presence of DOC prior to NO_3^- depletion could enable bacterial competition for NO_3^-, but that competition would not occur if (1) DOC is not sufficient for bacterial growth, or (2) bacteria are unable to utilize the NO_3^- in the media. We tested this by culturing the diatoms with WT bacteria capable of utilizing NO_3^- and Δ*nasA* bacteria unable to utilize NO_3^- as a N source. We then added DOC at multiple time-points and included a no DOC addition control to better understand any competitive interactions observed, measuring diatom and bacteria growth and NO_3^- in the media (indicative of biological NO_3^- drawdown). In co-cultures containing Δ*nasA* bacteria, diatom growth and NO_3^- drawdown were similar in all treatments regardless of whether and when DOC was added (**Figures 3B,D,F**). Numbers of Δ*nasA* bacteria increased slightly when DOC was added prior to the depletion of NO_3^- from the media, but were not affected when DOC was added on days after NO_3^- depletion. In co-cultures containing diatoms and WT bacteria, when DOC was added early in the experiment (Day T_o or Day 2), bacteria cell numbers increased dramatically and diatom cell numbers reached lower maximum cell densities (**Figures 3A,C**). Diatom cell numbers with DOC added on Day $T_o$were > 6 times lower than in the no DOC addition control. Media NO_3^- was also depleted earlier in these cultures (**Figures 3E,F**), indicating a relationship between bacterial growth, NO_3^- drawdown, and diatom growth impairment. When DOC was added on later time points (Day 4, 6, and 8), diatom growth and NO_3^- drawdown were similar to the no DOC addition control. Bacteria growth increased slightly when DOC was added on Day 4, but DOC addition on subsequent days had no effect.

P. tricornutum cultures with and without the addition of pyruvate (final concentration 5 mM, as used in other DOC addition experiments) did not differ significantly in cell numbers as measured at 3 different time points (Supplementary Figure 4). Cell numbers were determined on days 4, 7, and 15 of the experiment.

Population Dynamics of NRKO Diatoms and WT Bacteria in Co-Culture

We explored whether bacteria can provide diatoms with a useable N source and potentially "rescue" N-starved diatoms. To do this, we cultured the NRKO diatom strain (lacking the ability to use NO_3^-) in media containing either NH_4^+ or NO_3^- as the sole N source, in the presence of absence WT *A. macleodii*, and with the bacteria and a DOC addition at T_o (**Figure 4**). The NRKO diatom was able to grow in all treatments with NH_4^+ as the provided N source, and in the absence of added DOC grew similarly with and without the addition of *A. macleodii* (**Figures 4A,B**). In NH_4^+ media amended with DOC, bacteria numbers were much higher, and NRKO diatom cell densities were lower (**Figures 4C,D**), an observation similar to the DOC addition experiment described

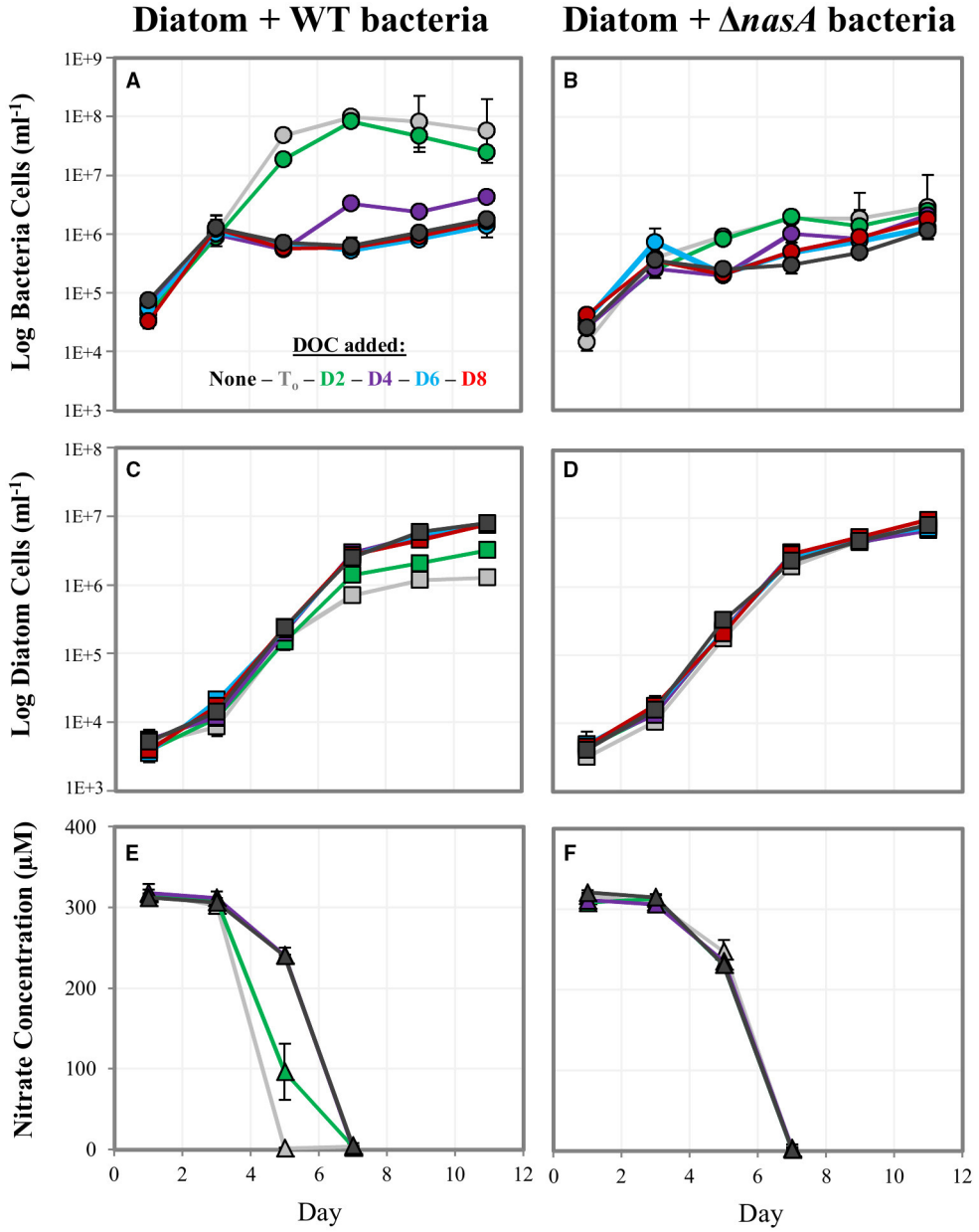

FIGURE 3 | Log cell numbers per ml and nitrate concentrations in DOC addition experiments. (A,C,E) are co-cultures containing the WT *A. macleodii* strain, and **(B,D,F)** contain the *A. macleodii* Δ*nasA* strain. Colors represent the day of the experiment on which DOC was added: black = control, no DOC added, gray = day of inoculation (T_0), green = day 2, purple = day 4, blue = day 6, red = day 8.

above. With NO_3^- as the sole N source and without DOC addition, the diatom NRKO strains displayed little detectable growth with and without *A. macleodii* addition. However, the NRKO diatom-WT bacteria co-culture to which DOC was added displayed a much different growth response; diatom density increased linearly ($R^2 = 0.96$) throughout the experiment, with a maximum cell density of 3.0×10^6 cells ml^{-1} measured on day 19 of the experiment (**Figures 4A,B**). Bacterial cell densities in this treatment peaked on day 9 of the experiment, and subsequently declined.

Effect of Various NO_3^- and DOC Concentrations on Diatom-Bacteria Population Dynamics

To better understand the influence of N and C concentration on diatom-bacteria growth dynamics, we conducted a factorial experiment in which diatom-WT bacteria co-cultures were grown in 9 different media types encompassing a range of NO_3^- and DOC levels. In general, higher NO_3^- levels resulted in higher numbers of both diatoms and bacteria. DOC concentrations

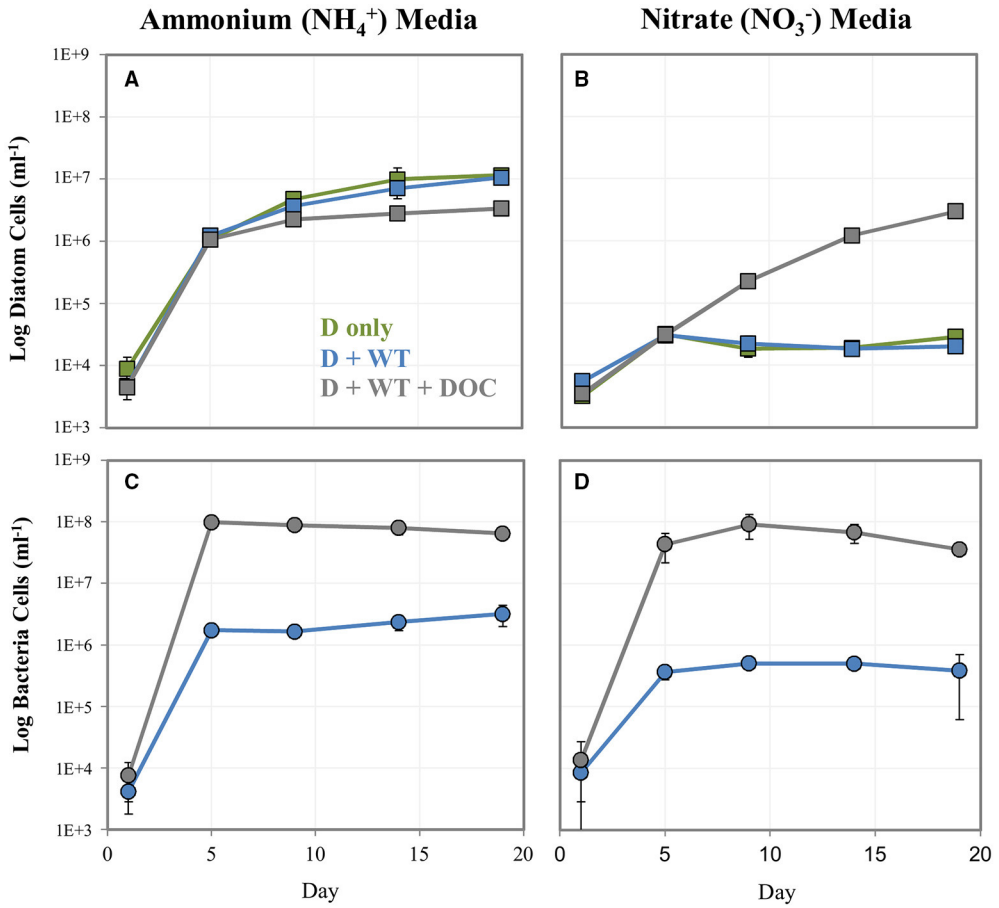

FIGURE 4 | Log cell numbers per ml of *P. tricornutum* NRKO (A,B) and *A. macleodii* WT bacteria (C,D) in co-culture, grown on NH_4^+ or NO_3^- and as the sole nitrogen source. Green markers = *P. tricornutum* NRKO monoculture (also noted as D only), blue = *P. tricornutum* NRKO + *A. macleodii* WT (also noted as D + WT), and gray = *P. tricornutum* NRKO + *A. macleodii* WT + DOC (also noted as D + WT + DOC).

had a strong effect on bacterial cell numbers, but less of an effect on diatom concentrations except for at low NO_3^-. At the lowest NO_3^- concentration tested (50 μM), diatom cell numbers decreased with increasing DOC concentration (**Figure 5A**) while bacterial cell numbers increased (**Figure 5D**). However, both diatom and bacteria concentrations were low at low NO_3^- level regardless of DOC concentration compared to the higher NO_3^- treatments. At the higher NO_3^- levels (300 μM and 1 mM), *P. tricornutum* concentrations were higher and similar to each other across DOC treatments (**Figures 5B,C**). In almost all treatments, *A. macleodii* concentrations were higher during the *P. tricornutum* exponential phase compared to the stationary sampling point on day 31 (**Figures 5D–F**). The reverse was true with the diatoms; cell numbers increased between day 6 and day 31 (**Figures 5A–C**). Final *A. macleodii* cell densities measured on day 31 were positively correlated with both DOC and NO_3^- concentration: lower concentrations were observed at the lower levels of both NO_3^- (50 and 300 μM) and DOC (0 and 50 μM), and highest concentrations were observed in the high NO_3^-, high DOC cultures and (**Figures 5D–F**).

In media containing 300 μM NO_3^- and no DOC addition (the same conditions as the baseline experiment), *P. tricornutum* maintained in semi-continuous cultures displayed consistent growth rates across 5 rounds of culture transfer, indicating steady-state growth. The average $\mu = 1.42$, with a range of $\mu = 1.25$ to 1.62 (Supplementary Table 6).

DISCUSSION

A Continuum: Diatom-Bacteria NO_3^- Utilization and the Role of Organic DOC Availability

Since phytoplankton and bacteria often co-occur in the same environments, the concept of competition for nutrients has been of interest for decades (Bratbak and Thingstad, 1985; Thingstad et al., 1993; Logan et al., 1995; Grossart and Simon, 2007; Amin et al., 2012). New relationships between phytoplankton and bacteria are being discovered and investigated with increasing frequency (Durham et al., 2014; Amin et al., 2015; Bertrand et al., 2015; Smriga et al., 2016), in part due to recent methodological

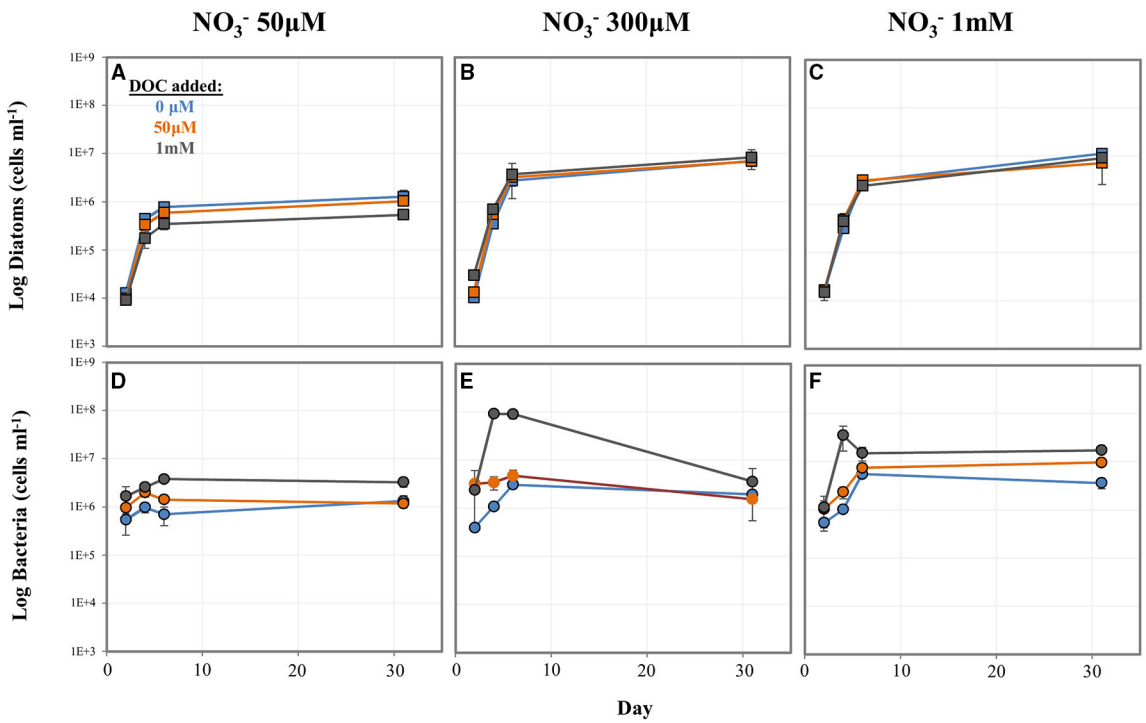

FIGURE 5 | Log cell numbers per ml of *P. tricornutum* and *A. macleodii* grown in co-culture under variable nitrate and dissolved organic carbon (DOC) concentrations. Diatom cell numbers are shown in **(A–C)** and bacterial numbers shown in **(D–F)**. Blue = 0 µM DOC added, orange = 50 µM DOC added, and gray = 1 mM DOC added.

advances. In particular, *Alteromonas* bacteria have been shown to have positive, negative, and seemingly neutral relationships with individual phytoplankton species. It is unclear, however, what role competition for nutrients may play in these observed interactions Understanding the heterogeneous landscape in which these interactions occur and the resulting impacts on global biogeochemical cycles, particularly carbon and nitrogen cycling, is an active area of research (Stocker, 2012; Worden et al., 2015; Smriga et al., 2016).

Many phytoplankton-bacteria interactions likely fall somewhere along a commensal-competitive continuum. Phytoplankton release increasing amounts of organic matter when nutrients become limited, stimulating the growth of bacteria which may compete with them for the same limiting nutrients, an apparent paradox (Bratbak and Thingstad, 1985; Bertrand et al., 2015). Studies examining acquisition of inorganic phosphate have found that bacteria can compete with phytoplankton, and that this potential competition can be nutrient concentration dependent (Bratbak and Thingstad, 1985; Thingstad et al., 1993), and bacteria-phytoplankton population dynamics may be dependent on what species are present as well as nutrient concentrations (Puddu et al., 2003; Grossart and Simon, 2007). Interestingly, while inorganic N availability is also a major driver in ocean productivity and biogeochemical cycling, and both phytoplankton and many bacteria can utilize it, few studies have examined these potentially important interactions (Dugdale and Goering, 1967; Allen et al., 2001; Amin et al., 2012; Jiang et al., 2015). This is despite findings that bacterial *nasA* genes are common, diverse, and highly expressed during phytoplankton blooms, especially for particular bacterial classes and genera (including *Alteromonas*) (Allen et al., 2012; Jiang et al., 2015). Recent advancements in microbiology, including genetic manipulation and the introduction of powerful next generation sequencing technology, call for an examination of these relationships with an aim to understand the underlying complex cellular mechanisms.

Utilizing both WT and Δ*nasA* bacteria in co-culture with diatoms presents the opportunity to explore how the bacteria and diatom in this model system impact one another and are impacted by NO_3^- availability and utilization. NO_3^- was drawn down quickly in the experiments, and the diatom population continued to increase in all co-cultures even after the complete depletion of NO_3^- from the media, which is consistent with reports of the ability of diatoms to rapidly accumulate and store N present in the environment (Cermeño et al., 2011). During exponential phase with no DOC added to the system, *P. tricornutum* growth rate, cell number, and other aspects of *P. tricornutum* physiology, including growth rate, Chl a concentration, Fv/Fm, and culture pH were not affected by the presence of either bacterial strain (**Figure 1**, Supplementary Figure 2, Supplementary Tables 1, 3). At this sampling point, bacterial numbers began to increase after an initial decrease in the experiment. One possible explanation for these observations is that during the exponential phase, the diatom and bacteria co-exist in a commensal relationship whereby the diatom is not affected by the presence of bacteria, but the bacteria are able to

benefit from diatom organic matter. However, it is also possible that low bacterial cell numbers and biomass obscure any positive or negative effect that the bacteria may be having on the diatoms on a smaller scale, and as a result differences are not observable based on the methods we used in this study. Later in the diatom's stationary phase, when nitrogen is limited, cultures containing bacteria reached higher cell densities than the *P. tricornutum* monocultures while bacterial numbers also continued to increase, suggesting a potential cooperative relationship. We hypothesize that the increase in diatom cell number is the result of bacteria providing diatoms with a viable nitrogen source in exchange for DOC (discussed further below).

Previous studies have examined growth effects of *Alteromonas* bacteria in co-culture with phytoplankton. *Alteromonas* bacteria species cultured with eukaryotic phytoplankton have been shown to exhibit algicidal (thought to be the result of secreted dissolved substances) and non-algicidal effects (reviewed in Mayali and Azam, 2004). When cultured with the prokaryotic cyanobacteria from the *Prochlorococcus* genus, the presence of *Alteromonas* sometimes provide the algae with benefits by protecting them from oxidative stress (Morris et al., 2008, 2011) while in other cases they can cause growth inhibition (Sher et al., 2011; Aharonovich and Sher, 2016). In prior non-*Alteromonas* co-culturing studies, dynamics between phytoplankton and bacteria have been shown to manifest late in the growth cycle (Grossart and Simon, 2007; Wang et al., 2014), though often the result is commensal bacteria turning algicidal, possibly to relieve nutrient stress. Immediate growth increases in diatom populations before and during exponential phase resulting from the presence of bacteria have also been observed (Grossart and Simon, 2007; Amin et al., 2015). These results are for the most part different from what we observed in our study, which may be due to the differences in the species of both phytoplankton and bacteria examined (even within the genus *Alteromonas*, species are quite diverse and were not always identified in these studies). Despite being observed in a prokaryote-prokaryote co-culturing system, the possibility that *Alteromonas* bacteria may protect phytoplankton from oxidative stress is interesting and could be examined in the future using the model system developed in this study.

While the presence of the bacteria alone did not hinder diatom growth, when DOC was added early in the diatom growth phase (prior to the depletion of NO_3^- from the media) the bacteria could acquire NO_3^- from the media, making it unavailable to the diatoms. Our data suggest that depending on the availability of allochthonous DOC, bacteria that have the ability to utilize NO_3^- in the environment are able to effectively compete for NO_3^-. This pattern was not observed in co-cultures containing Δ*nasA* bacteria, illustrating how bacteria that are unable to use NO_3^- cannot take advantage of surplus organic C in NO_3^- cultures, and in the case of Δ*nasA* appear to be limited by diatom C production. The WT bacteria generally maintained higher cell numbers than the Δ*nasA* bacteria, possibly suggesting that the WT bacteria were limited by C while the Δ*nasA* bacteria were limited by N. However, the addition of DOC to Δ*nasA* bacteria co-cultures did result in a slight bacterial growth increase (**Figure 3B**). Thus, it is possible that a co-limitation scenario may also arise in low concentrations of both bioavailable N and C.

When diatoms interact with bacteria that can utilize NO_3^-, the concentration of both NO_3^- and DOC present may impact their dynamics in complex ways. To explore this, we tested the effects of various NO_3^- and DOC levels on population dynamics of *P. tricornutum–A. macleodii* co-cultures. We observed that *P. tricornutum* cell densities were largely regulated by NO_3^- concentrations rather than DOC level or bacteria cell densities. An exception was at a low NO_3^- concentrations (50 μM), where bacterial accumulation of NO_3^- linked to increased bacteria cell numbers appeared to reduce diatom growth and final cell densities. This trend was not observed in the higher NO_3^- treatments, where diatom cell densities were similar between 50 μM and 1 mM DOC concentrations despite an increase in bacteria cell density. This suggests that at low NO_3^- levels, bacterial growth made possible by DOC availability can have a negative effect on diatom cell numbers. Based on a similar pattern observed in the DOC addition study discussed above, where NO_3^- drawdown was correlated with high bacterial and low diatom cell numbers in high DOC conditions, we hypothesize that in this experiment fast bacterial acquisition of NO_3^- in the media made NO_3^- limiting for diatom growth. At higher NO_3^- concentrations this effect was not observed, which could be explained by the diatoms having sufficient opportunity to acquire and store N since more was available. The diatoms may also be able to utilize nitrogen derived from dead or growth-arrested bacteria during stationary phase. This is supported by the observation that bacterial abundance peaked during the exponential phase of *P. tricornutum* regardless of NO_3^- level or DOC addition and subsequently declined, with the exception of the 1 mM NO_3^-/50 μM DOC treatment.

Bacterial cell numbers were strongly affected by DOC concentration. Without the addition of DOC, bacterial cell densities generally increased with increasing NO_3^- and corresponding increases in diatom cell density. This likely reflects the link between diatom population and DOC availability; higher diatom density as a result of higher N concentrations leads to higher total DOC available for bacteria utilization. It is also possible that changes in DOC composition may affect bacterial growth dynamics. At higher DOC concentrations, bacteria could utilize NO_3^- in the media to reach higher cell densities than with ambient DOC alone, a result consistent with other DOC addition experiments conducted in this study. By late stationary phase (Day 31), bacteria cell densities were variable. This may be the result of complex N and C recycling dynamics following initial uptake by bacteria and diatoms, and further studies may help to elucidate how cellular responses of diatoms and bacteria lead to the population changes we observed.

Exchange of Nitrogen Substrates between Diatoms and Bacteria

Our findings suggest that the diatoms and bacteria in our model system are able to exchange nitrogen substrates with each other. A large portion of N consumed by phytoplankton is ultimately released as dissolved organic nitrogen (DON) in oceanic, coastal, and estuarine environments (Wheeler and Kirchman, 1986; Bronk et al., 1994; Berman and Bronk, 2003), and is a valuable source of N for marine bacteria. Previous studies on *P. tricornutum* have shown that both organic C and N are

released by *P. tricornutum*, and that concentrations increase after the cells enter stationary phase (Chen and Wangersky, 1996; Pujo-Pay et al., 1997). The bacteria in the present study were able to survive and grow in co-culture with the diatom using diatom-derived organic C, and bacteria concentrations increased after the onset of diatom stationary phase, which is consistent with utilization of diatom derived organic matter. We further observed that the Δ*nasA* bacteria strain in co-culture grew despite the inability to use NO_3^-, which was the only N source provided in the ASW media. This leaves diatom-derived N as the most plausible source for bacterial growth.

While the paradigm for phytoplankton-bacteria relationships is typically that of bacteria utilizing phytoplankton-derived organic matter, and in some cases exchanging various substrates to facilitate this acquisition, few studies have examined if and how diatoms may use bacterial-derived N. Given the high rate of bacterial turnover in the ocean, this could potentially represent an important N source, especially under N limiting conditions. Diatoms are known to utilize a variety of organic and inorganic N substrates (Bronk et al., 1994, 2006; Waser et al., 1998). One recent study suggests that bacteria may use NH_4^+ as a diatom signaling molecule (Amin et al., 2015). Our results show that the NRKO diatom lines could survive and grow normally in NH_4^+ but not NO_3^-. The addition of *A. macleodii* to the diatom cultures without a coincident DOC media amendment resulted in low bacterial cell numbers and did not increase NRKO diatom cell numbers, suggesting that either the bacteria do not provide the diatom with useable N substrates in this physiological state, or that the amount supplied is not sufficient for diatom growth. Potentially, the bacteria could provide the diatoms with useable N, but the amount produced by the low cell numbers observed was not enough to detect diatom population recovery using our methods. Our study does not address other possible interactions at the cellular level (e.g., metabolic shifts perhaps observable using metabolomics or transcriptomics), which may clarify whether N is being provided by bacteria in this co-culture. When DOC was added to the NRKO co-cultures in NO_3^- media, both bacteria and diatom growth increased substantially. This strongly suggests that the bacteria supply the diatoms with a N substrate, perhaps made possible by the large bacterial numbers resulting from the DOC addition, followed by nitrogen release upon the onset of carbon-limited stationary phase. Alternatively or concurrently, after reaching maximum cell density early in the experiment the bacteria may subsequently die allowing *P. tricornutum* to recycle some of the organic N from the dead bacterial cells. Some bacteria were detected in the *P. tricornutum* NRKO cultures without the addition of *A. macleodii*. The addition of DOC to *A. macleodii* amended cultures resulted in high bacterial densities similar to what was observed in the *P. tricornutum* WT–*A. macleodii* co-cultures (**Figure 3**), thus we believe *A. macleodii* growth was responsible for the observed increase in *P. tricornutum* NRKO cell numbers. Even if this is not the case (i.e., the growth of other bacteria present contributed to the high bacterial cell numbers), our results strongly suggest that the high abundance of bacteria due to DOC addition was linked to diatom recovery, and our study presents a proof of concept that diatoms can utilize bacterial-derived N. Though the scope of this study does not directly address the specific bacterial N source, the transcriptomic analysis conducted during the baseline experiment elucidates N-related diatom cellular pathways that may be influenced by bacteria, such as those involved in NO_3^- and NH_4^+ acquisition and metabolism.

Further Insights into "Bacterial Responsive" Genes Revealed by RNA-seq

Using RNA-seq, we were able to identify several putative *P. tricornutum* genes that were responsive to the presence of bacteria, some of which suggest N-related interactions. A recent study examined the response of two *Prochlorococcus* strains in co-culture with *A. macleodii* bacteria, and they also found that several algal genes were bacterial-responsive (Aharonovich and Sher, 2016). The study examines prokaryotic rather than eukaryotic gene expression, and is thus difficult to compare. However, it demonstrates the value of transcriptome analyses in developing hypotheses about microbial interactions and, along with our study, lays the framework for a robust analysis of interactions involving *A. macleodii* bacteria with both prokaryotic and eukaryotic algae in a model laboratory system.

All differential gene expression in our study was observed in the stationary samples, long after NO_3^- had been depleted from the media (**Figure 1**), and cells were potentially N stressed. One discernable pattern is related to downregulation of multiple N transporters (NO_2^- and NO_3^-) in diatom cultures containing bacteria (**Figure 2**, Supplementary Table 4). One of these transporters (Phatr2ID: 49093, Phatr3 ID: 302957) was one of the mostly highly significantly DE putative genes identified in the data set. Orthologs of this ion transporter in *Arabidopsis* has been shown to bind to and sense NO_3^- (Huang et al., 1996; Liu et al., 1999), suggesting a possible role in diatom NO_3^- acquisition. Inorganic N transporters including those DE in our dataset are commonly upregulated during nitrogen stress conditions (Levitan et al., 2014; Alipanah et al., 2015; JGI genome annotation, Allen, 2006). Downregulation in cultures containing bacteria suggests that bacteria are contributing to alleviation of diatom N stress, which is further supported by the higher diatom cell numbers observed in co-cultures during stationary phase and also our finding that under certain N stress conditions (i.e., high DOC present) bacteria have the ability to provide diatoms with N in forms other than NO_3^-. In Levitan et al. (2014), expression of glutamine synthetase II (GSII) followed a similar expression pattern of downregulation under N-stress, and we also observed significant downregulation of this gene in bacteria-containing co-cultures. Another gene related to diatom N metabolism, ornithine cyclodeaminase (Phatr2: 54222, Phatr3: 305662), is involved in the diatom Urea cycle and was downregulated compared to *P. tricornutum* monocultures (Allen et al., 2011). While these two genes were only significantly DE between the *P. tricornutum* monoculture and the Δ*nasA* bacterial co-cultures (Supplementary Table 4), they were downregulated in both co-cultures indicating a common bacterial-responsive pattern.

Some NH_4^+ transporters have also been shown to be upregulated during N stress, while others are downregulated or unaffected (Levitan et al., 2014; Alipanah et al., 2015).

Examination of NH_4^+ acquisition and transport genes in our dataset did not reveal any significant DE between *P. tricornutum* monocultures and co-cultures (Supplementary Table 5). In Amin et al. (2015), it was suggested that bacteria provide NH_4^+ to diatoms as a signaling molecule, which was partially supported by the upregulation of NH_4^+ transport genes in bacteria, as well as an increase in NH_4^+ measured in co-cultures. However, NH_4^+ transport genes were not DE in the diatom they examined, which may suggest that the cellular impacts of this potential exchange are not apparent at the transcriptional level in diatoms.

Several other bacterial responsive genes, including the many unannotated hypothetical proteins in our dataset, may be interesting candidates for further investigation. Several heat shock transcription factors were upregulated in diatom-bacteria co-cultures compared to monocultures. These are transcriptional regulators of heat shock proteins involved in cellular stress responses (Sorger, 1991). High expression may indicate a stress response caused by the bacteria, however, little is known about the regulation of this complex pathway in diatoms, and many non-transcriptional steps are involved in heat shock protein expression and regulation (Sorger, 1991). Upregulation of other putative genes in co-cultures may play a role in exchange of important metabolites or intracellular signaling pathways. These include a putative sugar transporter (Phatr2 ID: 49722, Phatr3 ID: 311238) which was >2 fold upregulated in *P. tricornutum* in both co-cultures (Supplementary Table 4), and the two putative genes that were most highly upregulated and significantly DE in both co-cultures: a putative short chain dehydrogenase (Phatr2 ID: 13001, Phatr3 ID: 306282) and a putative fatty acid hydroxylase (Phatr3 ID: 308140). Short chain dehydrogenases in particular have been shown to serve as molecular links between nutrient signaling and plant hormone biosynthesis in *Arabidopsis* (Cheng, 2002). Further analysis using our model system may allow determination of the role of such genes in diatom-bacteria interactions.

Using the genetically tractable model system developed in this study, we have described mechanisms of interaction between diatoms and bacteria that may be of global biogeochemical significance. Our data strongly suggests bidirectional exchange of N substrates between diatoms and bacteria, and revealed putative diatom genes and pathways that may be impacted by the presence of bacteria and involved in N exchange. Furthermore, we have demonstrated that under certain environmental conditions (i.e., high DOC), marine bacteria are able to effectively compete with diatoms for NO_3^-, which may influence predictions of primary productivity and nutrient utilization by phytoplankton in the ocean and associated estimates of C export via the biological pump.

AUTHOR CONTRIBUTIONS

RD and AA designed research; RD, SS, and HZ performed research; RD, SS, and JM analyzed data; and RD and AA wrote the paper.

FUNDING

Funding was provided to AA by the Gordon and Betty Moore Foundation (GBMF3828 and GBMF5006), the US Department of Energy (DE-SC0008593) and the National Science Foundation (OCE-1136477). Funding was provided to RD by the UCSD/SIO Center for Marine Biodiversity and Conservation.

ACKNOWLEDGMENTS

We would like to acknowledge the following people for their contributions to this research project: Phillip Weyman for assistance with *A. macleodii* culturing and genetic engineering, Erin Bertrand for assistance with co-culturing techniques, Chris Dupont for assisting with organic carbon and nitrogen analysis, Mark Novotny for flow cytometry assistance, and Flip McCarthy for helping with data interpretation and engineering the *P. tricornutum* NRKO line. We would also like to thank Karen Beeri for sequencing assistance.

SUPPLEMENTARY MATERIAL

The Supplementary Material for this article can be found online at: http://journal.frontiersin.org/article/10.3389/fmicb.2016.00880

REFERENCES

Aharonovich, D., and Sher, D. (2016). Transcriptional response of *Prochlorococcus* to co-culture with a marine *Alteromonas*: differences between strains and the involvement of putative infochemicals. *ISME J.* doi: 10.1038/ismej.2016.70. [Epub ahead of print].

Alipanah, L., Rohloff, J., Winge, P., Bones, A. M., and Brembu, T. (2015). Whole-cell response to nitrogen deprivation in the diatom *Phaeodactylum tricornutum*. *J. Exp. Bot.* 66, 6281–6296. doi: 10.1093/jxb/erv340

Allen, A. E. (2006). Transcript annotation: JGI Genome Portal *Phaeodactylum tricornutum*. Available online at: http://genome.jgi.doe.gov/annotator/servlet/jgi.annotation.Annotation?pDb=Phatr2&pStateVar=View&pProteinId=26029&pViewType=protein&pDummy=699949276669001 (Accessed March 15, 2016).

Allen, A. E., Booth, M. G., Frischer, M. E., Verity, P. G., Zehr, J. P., and Zani, S. (2001). Diversity and detection of nitrate assimilation genes in marine bacteria. *Appl. Environ. Microbiol.* 67, 5343–5348. doi: 10.1128/AEM.67.11.5343-5348.2001

Allen, A. E., Booth, M. G., Verity, P. G., and Frischer, M. E. (2005). Influence of nitrate availability on the distribution and abundance of heterotrophic bacterial nitrate assimilation genes in the Barents Sea during summer. *Aquat. Microb. Ecol.* 39, 247–255. doi: 10.3354/ame039247

Allen, A. E., Dupont, C. L., Oborník, M., Horák, A., Nunes-Nesi, A., McCrow, J. P., et al. (2011). Evolution and metabolic significance of the urea cycle in photosynthetic diatoms. *Nature* 473, 203–207. doi: 10.1038/nature10074

Allen, A. E., Laroche, J., Maheswari, U., Lommer, M., Schauer, N., Lopez, P. J., et al. (2008). Whole-cell response of the pennate diatom *Phaeodactylum tricornutum* to iron starvation. *Proc. Natl. Acad. Sci. U.S.A.* 105, 10438–10443. doi: 10.1073/pnas.0711370105

Allen, A. E., Vardi, A., and Bowler, C. (2006). An ecological and evolutionary context for integrated nitrogen metabolism and related signaling pathways in marine diatoms. *Curr. Opin. Plant Biol.* 9, 264–273. doi: 10.1016/j.pbi.2006.03.013

Allen, L. Z., Allen, E. E., Badger, J. H., McCrow, J. P., Paulsen, I. T., Elbourne, L. D., et al. (2012). Influence of nutrients and currents on the genomic composition of microbes across an upwelling mosaic. *ISME J.* 6, 1403–1414. doi: 10.1038/ismej.2011.201

Amin, S. A., Hmelo, L. R., van Tol, H. M., Durham, B. P., Carlson, L. T., Heal, K. R., et al. (2015). Interaction and signalling between a cosmopolitan phytoplankton and associated bacteria. *Nature* 522, 98–101. doi: 10.1038/nature14488

Amin, S. A., Parker, M. S., and Armbrust, E. V. (2012). Interactions between diatoms and bacteria. *Microbiol. Mol. Biol. Rev.* 76, 667–684. doi: 10.1128/MMBR.00007-12

Azam, F., and Malfatti, F. (2007). Microbial structuring of marine ecosystems. *Nat. Rev. Microbiol.* 5, 782–791. doi: 10.1038/nrmicro1747

Bell, W., and Mitchell, R. (1972). Chemotactic and growth responses of marine bacteria to algal extracellular products. *Biol. Bull.* 143, 265–277. doi: 10.2307/1540052

Berman, T., and Bronk, D. a. (2003). Dissolved organic nitrogen: a dynamic participant in aquatic ecosystems. *Aquat. Microb. Ecol.* 31, 279–305. doi: 10.3354/ame031279

Bertrand, E. M., McCrow, J. P., Moustafa, A., Zheng, H., McQuaid, J. B., Delmont, T. O., et al. (2015). Phytoplankton–bacterial interactions mediate micronutrient colimitation at the coastal Antarctic sea ice edge. *Proc. Natl. Acad. Sci. U.S.A.* 112, 9938–9943. doi: 10.1073/pnas.1501615112

Bowler, C., Allen, A. E., Badger, J. H., Grimwood, J., Jabbari, K., Kuo, A., et al. (2008). The *Phaeodactylum* genome reveals the evolutionary history of diatom genomes. *Nature* 456, 239–244. doi: 10.1038/nature07410

Bradley, P. B., Lomas, M. W., and Bronk, D. A. (2010a). Inorganic and organic nitrogen use by phytoplankton along chesapeake bay, measured using a flow cytometric sorting approach. *Estuaries Coasts* 33, 971–984. doi: 10.1007/s12237-009-9252-y

Bradley, P. B., Sanderson, M. P., Frischer, M. E., Brofft, J., Booth, M. G., Kerkhof, L. J., et al. (2010b). Inorganic and organic nitrogen uptake by phytoplankton and heterotrophic bacteria in the stratified Mid-Atlantic Bight. *Estuar. Coast. Shelf Sci.* 88, 429–441. doi: 10.1016/j.ecss.2010.02.001

Bradley, P. B., Sanderson, M. P., Nejstgaard, J. C., Sazhin, A. F., Frischer, M. E., Killberg-Thoreson, L. M., et al. (2010c). Nitrogen uptake by phytoplankton and bacteria during an induced *Phaeocystis pouchetii* bloom, measured using size fractionation and flow cytometric sorting. *Aquat. Microb. Ecol.* 61, 89–104. doi: 10.3354/ame01414

Bratbak, G., and Thingstad, T. F. (1985). Phytoplankton-bacteria interactions: an apparant paradox? Analysis of a model system with both competition and commensalism. *Mar. Ecol. Prog. Ser.* 25, 23–30. doi: 10.3354/meps025023

Bronk, D. A., Glibert, P. M., and Ward, B. B. (1994). Nitrogen uptake, dissolved organic nitrogen release, and new production. *Science* 265, 1843–1846. doi: 10.1126/science.265.5180.1843

Bronk, D. A., See, J. H., Bradley, P., and Killberg, L. (2006). DON as a source of bioavailable nitrogen for phytoplankton. *Biogeosci. Discuss.* 3, 1247–1277. doi: 10.5194/bgd-3-1247-2006

Buchan, A., LeCleir, G. R., Gulvik, C. A., and González, J. M. (2014). Master recyclers: features and functions of bacteria associated with phytoplankton blooms. *Nat. Rev. Microbiol.* 12, 686–696. doi: 10.1038/nrmicro3326

Cermeño, P., Lee, J.-B., Wyman, K., Schofield, O., and Falkowski, P. G. (2011). Competitive dynamics in two species of marine phytoplankton under non-equilibrium conditions. *Mar. Ecol. Prog. Ser.* 429, 19–28. doi: 10.3354/meps09088

Chen, W., and Wangersky, P. J. (1996). Production of dissolved organic carbon in phytoplankton cultures as measured by high-temperature catalytic oxidation and ultraviolet photo- oxidation methods. *J. Plankton Res.* 18, 1201–1211. doi: 10.1093/plankt/18.7.1201

Cheng, W.-H. (2002). A unique short-chain dehydrogenase/reductase in *Arabidopsis* glucose signaling and abscisic acid biosynthesis and functions. *Plant Cell Online* 14, 2723–2743. doi: 10.1105/tpc.006494

Collos, Y., Mornet, F., Sciandra, A., Waser, N., Larson, A., and Harrison, P. J. (1999). An optical method for the rapid measurement of micromolar concentrations of nitrate in marine phytoplankton cultures. *J. Appl. Phycol.* 11, 179–184. doi: 10.1023/A:1008046023487

Dortch, Q. (1990). The interaction between ammonium and nitrate uptake in phytoplankton. *Mar. Ecol. Prog. Ser.* 61, 183–201. doi: 10.3354/meps061183

Dugdale, R. C., and Goering, J. J. (1967). Uptake of new and regenerated forms of nitrogen in primary productivity. *Limnol. Oceanogr.* 12, 196–206. doi: 10.4319/lo.1967.12.2.0196

Durham, B. P., Sharma, S., Luo, H., Smith, C. B., Amin, S. A., Bender, S. J., et al. (2014). Cryptic carbon and sulfur cycling between surface ocean plankton. *Proc. Natl. Acad. Sci. USA.* 112, 453–457. doi: 10.1073/pnas.1413137112

Falkowski, P. G., and Oliver, M. J. (2007). Mix and match: how climate selects phytoplankton. *Nat. Rev. Microbiol.* 5, 813–819. doi: 10.1038/nrmicro1751

Fuhrman, J. A. (1989). Dominance of bacterial biomass in the Sargasso Sea and its ecological implications. *Mar. Ecol. Prog. Ser.* 57, 207–217. doi: 10.3354/meps057207

García-Martínez, J., Acinas, S. G., Massana, R., and Rodríguez-Valera, F. (2002). Prevalence and microdiversity of *Alteromonas macleodii*-like microorganisms in different oceanic regions. *Environ. Microbiol.* 4, 42–50. doi: 10.1046/j.1462-2920.2002.00255.x

Geider, R. J., La Roche, J., Greene, R. M., and Olaizola, M. (1993). Response of the photosynthetic apparatus of *Phaeodactylum tricornutum* (*Bacillariophycea*) to nitrate, phosphate, or iron starvation. *J. Phycol.* 29, 755–766. doi: 10.1111/j.0022-3646.1993.00755.x

Gibson, D. G., Young, L., Chuang, R.-Y., Venter, J. C., Hutchison, C. A., and Smith, H. O. (2009). Enzymatic assembly of DNA molecules up to several hundred kilobases. *Nat. Methods* 6, 343–345. doi: 10.1038/nmeth.1318

Grossart, H., and Simon, M. (2007). Interactions of planktonic algae and bacteria: effects on algal growth and organic matter dynamics. *Aquat. Microb. Ecol.* 47, 163–176. doi: 10.3354/ame047163

Huang, N. C., Chiang, C. S., Crawford, N. M., and Tsay, Y. F. (1996). CHL1 encodes a component of the low-affinity nitrate uptake system in *Arabidopsis* and shows cell type-specific expression in roots. *Plant Cell* 8, 2183–2191. doi: 10.1105/tpc.8.12.2183

Ivars-Martínez, E., D'Auria, G., Rodríguez-Valera, F., Sánchez-Porro, C., Ventosa, A., Joint, I., et al. (2008). Biogeography of the ubiquitous marine bacterium *Alteromonas macleodii* determined by multilocus sequence analysis. *Mol. Ecol.* 17, 4092–4106. doi: 10.1111/j.1365-294X.2008.03883.x

Jiang, X., Dang, H., and Jiao, N. (2015). Ubiquity and diversity of heterotrophic bacterial nasA genes in diverse marine environments. *PLoS ONE* 10:e0117473. doi: 10.1371/journal.pone.0117473

Jiao, N., Herndl, G. J., Hansell, D. A., Benner, R., Kattner, G., Wilhelm, S. W., et al. (2011). The microbial carbon pump and the oceanic recalcitrant dissolved organic matter pool. *Nat. Rev. Microbiol.* 9, 555. doi: 10.1038/nrmicro2386-c5

Johnson, K. S., and Coletti, L. J. (2002). *In situ* ultraviolet spectrophotometry for high resolution and long-term monitoring of nitrate, bromide and bisulfide in the ocean. *Deep. Res. Part I Oceanogr. Res. Pap.* 49, 1291–1305. doi: 10.1016/S0967-0637(02)00020-1

Karas, B. J., Diner, R. E., Lefebvre, S. C., McQuaid, J., Phillips, A. P. R., Noddings, C. M., et al. (2015). Designer diatom episomes delivered by bacterial conjugation. *Nat. Commun.* 6:6925. doi: 10.1038/ncomms7925

Kato, J., Amie, J., Murata, Y., Kuroda, A., Mitsutani, A., and Ohtake, H. (1998). Development of a genetic transformation system for an Alga-Lysing Bacterium. *Appl. Environ. Microbiol.* 64, 2061–2064.

Keil, R., and Kirchman, D. (1991). Contribution of dissolved free amino acids and ammonium to the nitrogen requirements of heterotrophic bacterioplankton. *Mar. Ecol. Prog. Ser.* 73, 1–10. doi: 10.3354/meps073001

Kovach, M. E., Elzer, P. H., Hill, D. S., Robertson, G. T., Farris, M. A., Roop, R. M., et al. (1995). Four new derivatives of the broad-host-range cloning vector pBBR1MCS, carrying different antibiotic-resistance cassettes. *Gene* 166, 175–176. doi: 10.1016/0378-1119(95)00584-1

Levitan, O., Dinamarca, J., Zelzion, E., Lun, D. S., Guerra, L. T., Kim, M. K., et al. (2014). Remodeling of intermediate metabolism in the diatom *Phaeodactylum tricornutum* under nitrogen stress. *Proc. Natl. Acad. Sci. U.S.A.* 112, 412–417. doi: 10.1073/pnas.1419818112

Liao, Y., Smyth, G. K., and Shi, W. (2014). FeatureCounts: an efficient general purpose program for assigning sequence reads to genomic features. *Bioinformatics* 30, 923–930. doi: 10.1093/bioinformatics/btt656

Li, H. (2013). Aligning sequence reads, clone sequences and assembly contigs with BWA-MEM. arXiv: 1303.3997 [q-bio.GN].

Liu, K. H., Huang, C. Y., and Tsay, Y. F. (1999). CHL1 is a dual-affinity nitrate transporter of *Arabidopsis* involved in multiple phases of nitrate uptake. *Plant Cell* 11, 865–874. doi: 10.1105/tpc.11.5.865

Logan, B. E., Passow, U., Alldredge, A. L., Grossartt, H.-P., and Simont, M. (1995). Rapid formation and sedimentation of large aggregates is predictable from coagulation rates (half-lives) of transparent exopolymer particles (TEP). *Deep Sea Res. Part II Top. Stud. Oceanogr.* 42, 203–214. doi: 10.1016/0967-0645(95)00012-F

Lomas, M. W., Bronk, D. A., and van den Engh, G. (2011). Use of flow cytometry to measure biogeochemical rates and processes in the ocean. *Ann. Rev. Mar. Sci.* 3, 537–566. doi: 10.1146/annurev-marine-120709-142834

Lomas, M. W., and Gilbert, P. M. (2000). Comparisons of nitrate uptake, storage, and reduction in marine diatoms and flagellates. *J. Phycol.* 36, 903–913. doi: 10.1046/j.1529-8817.2000.99029.x

López-Pérez, M., Gonzaga, A., Martin-Cuadrado, A.-B., Onyshchenko, O., Ghavidel, A., Ghai, R., et al. (2012). Genomes of surface isolates of *Alteromonas macleodii*: the life of a widespread marine opportunistic copiotroph. *Sci. Rep.* 2:696. doi: 10.1038/srep00696

López-Pérez, M., and Rodriguez-Valera, F. (2014). "The family *Alteromonadaceae*." in *The Prokaryotes,* eds E. Rosenberg, E. F. DeLong, S. Lory, E. Stackebrandt, and F. Thompson (Berlin; Heidelberg: Springer), 69–92. doi: 10.1007/978-3-642-38922-1_233

Matthijs, M., Fabris, M., Broos, S., Vyverman, W., and Goossens, A. (2015). Profiling of the early nitrogen stress response in the diatom *Phaeodactylum tricornutum* reveals a novel family of RING-domain transcription factors. *Plant Physiol.* 170, 489–498. doi: 10.1104/pp.15.01300

Mayali, X., and Azam, F. (2004). Algicidal bacteria in the sea and their impact on algal blooms. *J. Eukaryot. Microbiol.* 51, 139–144. doi: 10.1111/j.1550-7408.2004.tb00538.x

Morris, J. J., Johnson, Z. I., Szul, M. J., Keller, M., and Zinser, E. R. (2011). Dependence of the cyanobacterium *Prochlorococcus* on hydrogen peroxide scavenging microbes for growth at the ocean's surface. *PLoS ONE* 6:e16805. doi: 10.1371/journal.pone.0016805

Morris, J. J., Kirkegaard, R., Szul, M. J., Johnson, Z. I., and Zinser, E. R. (2008). Facilitation of robust growth of Prochlorococcus colonies and dilute liquid cultures by "helper" heterotrophic bacteria. *Appl. Environ. Microbiol.* 74, 4530–4534. doi: 10.1128/AEM.02479-07

Morrissey, J., Sutak, R., Paz-Yepes, J., Tanaka, A., Moustafa, A., Veluchamy, A., et al. (2015). A novel protein, ubiquitous in marine phytoplankton, concentrates iron at the cell surface and facilitates uptake. *Curr. Biol.* 25, 364–371. doi: 10.1016/j.cub.2014.12.004

Mouriño-Pérez, R. R., Worden, A. Z., and Azam, F. (2003). Growth of *Vibrio cholerae* O1 in red tide waters off California. *Appl. Environ. Microbiol.* 69, 6923–6931. doi: 10.1128/AEM.69.11.6923-6931.2003

Nymark, M., Sharma, A. K., Sparstad, T., Bones, A. M., and Winge, P. (2016). A CRISPR/Cas9 system adapted for gene editing in marine algae. *Sci. Rep.* 6:24951. doi: 10.1038/srep24951

Parsons, T. R., Maita, Y., and Lalli, C. M. (1984). *A Manual of Chemical and Biological Methods for Seawater Analysis*. Oxford: Pergamon.

Pedler, B. E., Aluwihare, L. I., and Azam, F. (2014). Single bacterial strain capable of significant contribution to carbon cycling in the surface ocean. *Proc. Natl. Acad. Sci. U.S.A.* 111, 7202–7207. doi: 10.1073/pnas.1401887111

Pedler Sherwood, B., Shaffer, E. A., Reyes, K., Longnecker, K., Aluwihare, L. I., and Azam, F. (2015). Metabolic characterization of a model heterotrophic bacterium capable of significant chemical alteration of marine dissolved organic matter. *Mar. Chem.* 177, 357–365. doi: 10.1016/j.marchem.2015.06.027

Pomeroy (1974). The ocean's food web, a changing paradigm. *Bioscience* 24, 499–504. doi: 10.2307/1296885

Puddu, A., Zoppini, A., Fazi, S., Rosati, M., Amalfitano, S., and Magaletti, E. (2003). Bacterial uptake of DOM released from P-limited phytoplankton. *FEMS Microbiol. Ecol.* 46, 257–268. doi: 10.1016/S0168-6496(03)00197-1

Pujo-Pay, M., Conan, P., and Raimbault, P. (1997). Excretion of dissolved organic nitrogen by phytoplankton assessed by wet oxidation and 1 5 N tracer procedures. *Mar. Ecol. Prog. Ser.* 153, 99–111. doi: 10.3354/meps153099

Robinson, M. D., McCarthy, D. J., and Smyth, G. K. (2010). edgeR: a bioconductor package for differential expression analysis of digital gene expression data. *Bioinformatics* 26, 139–140. doi: 10.1093/bioinformatics/btp616

Sarmento, H., and Gasol, J. M. (2012). Use of phytoplankton-derived dissolved organic carbon by different types of bacterioplankton. *Environ. Microbiol.* 14, 2348–2360. doi: 10.1111/j.1462-2920.2012.02787.x

Serra, J. L., Llama, M. J., and Cadenas, E. (1978). Nitrate utilization by the diatom *Skeletonema costatum*: II. regulation of nitrate uptake. *Plant Physiol.* 62, 991–994. doi: 10.1104/pp.62.6.991

Sher, D., Thompson, J. W., Kashtan, N., Croal, L., and Chisholm, S. W. (2011). Response of *Prochlorococcus* ecotypes to co-culture with diverse marine bacteria. *ISME J.* 5, 1125– 1132. doi: 10.1038/ismej.2011.1

Shi, Y., McCarren, J., and Delong, E. F. (2012). Transcriptional responses of surface water marine microbial assemblages to deep-sea water amendment. *Environ. Microbiol.* 14, 191–206. doi: 10.1111/j.1462-2920.2011.02598.x

Siaut, M., Heijde, M., Mangogna, M., Montsant, A., Coesel, S., Allen, A., et al. (2007). Molecular toolbox for studying diatom biology in *Phaeodactylum tricornutum*. *Gene* 406, 23–35. doi: 10.1016/j.gene.2007.05.022

Singleton, F. L., Attwell, R., and Jangi, S. (1982). Effects of temperature and salinity on *Vibrio cholerae*. *Appl. Environ. Microbiol.* 44, 1047–1058.

Smriga, S., Fernandez, V. I., Mitchell, J. G., and Stocker, R. (2016). Chemotaxis toward phytoplankton drives organic matter partitioning among marine bacteria. *Proc. Natl. Acad. Sci. U.S.A.* 113, 1576–1581. doi: 10.1073/pnas.1512307113

Sorger, P. K. (1991). Heat shock factor and the heat shock response. *Cell* 65, 363–366. doi: 10.1016/0092-8674(91)90452-5

Stocker, R. (2012). Marine microbes see a sea of gradients. *Science* 338, 628–633. doi: 10.1126/science.1208929

Thingstad, T. F., Skjoldal, E. F., and Bohne, R., a (1993). Phosphorus cycling and algal bacterial competition in Sandsfjord, Western Norway. *Mar. Ecol. Prog. Ser.* 99, 239–259. doi: 10.3354/meps099239

Wang, H., Tomasch, J., Jarek, M., and Wagner-Dobler, I. (2014). A dual-species co-cultivation system to study the interactions between *Roseobacters* and dinoflagellates. *Front. Microbiol.* 5:311. doi: 10.3389/fmicb.2014.00311

Waser, N. A., Yu, Z., Tada, K., Paul, J., Turpin, D. H., and Calvertl, S. E. (1998). Nitrogen isotope fractionation during nitrate, ammonium and urea uptake by marine diatoms and coccolithophores under various conditions of N availability. *Mar. Ecol. Prog. Ser.* 169, 29–41. doi: 10.3354/meps169029

Wawrik, B., Boling, W. B., van Nostrand, J. D., Xie, J., Zhou, J., and Bronk, D. A. (2012). Assimilatory nitrate utilization by bacteria on the West Florida Shelf as determined by stable isotope probing and functional microarray analysis. *FEMS Microbiol. Ecol.* 79, 400–411. doi: 10.1111/j.1574-6941.2011.01226.x

Weyman, P. D., Beeri, K., Lefebvre, S. C., Rivera, J., McCarthy, J. K., Heuberger, A. L., et al. (2015). Inactivation of Phaeodactylum tricornutum urease gene using transcription activator-like effector nuclease-based targeted mutagenesis. *Plant Biotechnol. J.* 13, 460–470. doi: 10.1111/pbi.12254

Weyman, P. D., Smith, H. O., and Xu, Q. (2011). Genetic analysis of the *Alteromonas macleodii* [NiFe]-hydrogenase. *FEMS Microbiol. Lett.* 322, 180–187. doi: 10.1111/j.1574-6968.2011.02348.x

Wheeler, P. A., and Kirchman, D. L. (1986). Utilization of inorganic and organic nitrogen by bacteria in marine systems. *Limnol. Oceanogr.* 31, 998–1009. doi: 10.4319/lo.1986.31.5.0998

Whitman, W. B., Coleman, D. C., and Wiebe, W. J. (1998). Prokaryotes: the unseen majority. *Proc. Natl. Acad. Sci. U.S.A.* 95, 6578–6583. doi: 10.1073/pnas.95.12.6578

Worden, A. Z., Follows, M. J., Giovannoni, S. J., Wilken, S., Zimmerman, A. E., and Keeling, P. J. (2015). Rethinking the marine carbon cycle: factoring in the multifarious lifestyles of microbes. *Science* 347:1257594. doi: 10.1126/science.1257594

Yongmanitchai, W., and Ward, O. P. (1991). Growth of and Omega-3 fatty acid production by *Phaeodactylum tricornutum* under different culture conditions. *Appl. Environ. Microbiol.* 57, 419–425.

Zehr, J. P., and Ward, B. B. (2002). Nitrogen cycling in the ocean: new perspectives on processes and paradigms. *Appl. Environ. Microbiol.* 68, 1015–1024. doi: 10.1128/AEM.68.3.1015-1024.2002

Conflict of Interest Statement: The authors declare that the research was conducted in the absence of any commercial or financial relationships that could be construed as a potential conflict of interest.

frontiers in Microbiology

ORIGINAL RESEARCH
published: 03 August 2016
doi: 10.3389/fmicb.2016.01172

A Metaproteomic Analysis of the Response of a Freshwater Microbial Community under Nutrient Enrichment

*David A. Russo[1], Narciso Couto[1], Andrew P. Beckerman[2] and Jagroop Pandhal[1]**

[1] Department of Chemical and Biological Engineering, University of Sheffield, Sheffield, UK, [2] Department of Animal and Plant Sciences, University of Sheffield, Sheffield, UK

Eutrophication can lead to an uncontrollable increase in algal biomass, which has repercussions for the entire microbial and pelagic community. Studies have shown how nutrient enrichment affects microbial species succession, however details regarding the impact on community functionality are rare. Here, we applied a metaproteomic approach to investigate the functional changes to algal and bacterial communities, over time, in oligotrophic and eutrophic conditions, in freshwater microcosms. Samples were taken early during algal and cyanobacterial dominance and later under bacterial dominance. 1048 proteins, from the two treatments and two timepoints, were identified and quantified by their exponentially modified protein abundance index. In oligotrophic conditions, Bacteroidetes express extracellular hydrolases and Ton-B dependent receptors to degrade and transport high molecular weight compounds captured while attached to the phycosphere. Alpha- and Beta-proteobacteria were found to capture different substrates from algal exudate (carbohydrates and amino acids, respectively) suggesting resource partitioning to avoid direct competition. In eutrophic conditions, environmental adaptation proteins from cyanobacteria suggested better resilience compared to algae in a low carbon nutrient enriched environment. This study provides insight into differences in functional microbial processes between oligo- and eutrophic conditions at different timepoints and highlights how primary producers control bacterial resources in freshwater environments. The data have been deposited to the ProteomeXchange with identifier PXD004592.

Keywords: oligotrophic, eutrophic, metaproteomics, microbial loop, algae, freshwater

OPEN ACCESS

Edited by:
Xavier Mayali, Lawrence Livermore National Laboratory, USA

Reviewed by:
Carole Anne Llewellyn, Swansea University, UK
Zhou Li, Oak Ridge National Laboratory, USA

****Correspondence:***
Jagroop Pandhal
j.pandhal@sheffield.ac.uk

Specialty section:
This article was submitted to Aquatic Microbiology, a section of the journal Frontiers in Microbiology

Received: *27 January 2016*
Accepted: *14 July 2016*
Published: *03 August 2016*

Citation:
Russo DA, Couto N, Beckerman AP and Pandhal J (2016) A Metaproteomic Analysis of the Response of a Freshwater Microbial Community under Nutrient Enrichment. Front. Microbiol. 7:1172. doi: 10.3389/fmicb.2016.01172

INTRODUCTION

Freshwater ecosystems are subjected to nutrient enrichment on a local, regional, and global scale in a process known as eutrophication. Due to human activity, global aquatic fluxes of nitrogen and phosphorus have been amplified by 108 and 400%, respectively (Falkowski et al., 2000). These nutrient imbalances have led to a drastic increase in the occurrence of algal blooms, an event where photoautotrophic biomass may increase by several orders of magnitude (Elser et al., 2007). During a bloom, high amounts of organic carbon and nutrients are channeled through the bacterial community and made available for higher trophic levels in what is known as the microbial loop (Azam et al., 1983). The microbial loop plays a crucial role in the biogeochemical cycling of

elements, such as carbon, phosphorus and nitrogen, as well as organic matter. It is ultimately responsible for a substantial fraction of aquatic nutrient and energy fluxes (Azam and Malfatti, 2007). Thus, a better understanding of how the microbial loop and associated algae respond to nutrient enrichment, can reveal important features of how ecosystem processes are affected by eutrophication.

The development and application of "omics" technologies has allowed for an unprecedented view of microbial dynamics and their role in driving ecosystem function, including biogeochemical cycling of elements and decomposition and remineralization of organic matter. One approach is to obtain and sequence DNA from the microbial community in order to provide access to the genetic diversity of a microbial community (metagenomics). However, the genetic diversity gives us an incomplete view of what role these genes have in community processes. In contrast, metaproteomics can relate the intrinsic metabolic function by linking proteins to specific microbial activities and to specific organisms. Metaproteomics can thus address the long-standing objective in environmental microbiology of linking the identity of organisms comprising diversity in a community to ecosystem function (Hettich et al., 2013).

In the last few years metaproteomics has had a growing influence in aquatic environmental microbiology. It has been used to address questions about diversity, functional redundancy and provision of ecosystem services including nutrient recycling and energy transfer. For example, in one of the metaproteomic pioneering studies Giovannoni et al. (2005) demonstrated the ubiquity of proteorhodopsin-mediated light-driven proton pumps in bacteria (Giovannoni et al., 2005). Later, a study by Sowell et al. (2011) was the first of its kind to demonstrate the importance of high affinity transporters for substrate acquisition in marine bacteria (Sowell et al., 2011). Although, most of the notable metaproteomic aquatic studies have focused on marine environments, the tool has also been used in freshwater environments to examine, for example, the functional metaproteomes from the meromictic lake ecosystem in Antarctica (Ng et al., 2010; Lauro et al., 2011) or the microbes in Cayuga and Oneida Lake, New York (Hanson et al., 2014). The application of metaproteomics in such studies have successfully provided details regarding the importance of bacteriochlorophyll in the adaptation to low light (Ng et al., 2010), the metabolic traits that aid life in cold oligotrophic environments (Lauro et al., 2011) and nutrient cycling, photosynthesis and electron transport in freshwater lakes (Hanson et al., 2014).

In this paper we report a comprehensive discovery-driven (Aebersold et al., 2000) metaproteomic analysis of a freshwater microbial community under differing nutrient regimes to elucidate the predominant metabolic processes in each conditions. We expect that, overall, bacterial growth and abundance will be higher in the oligotrophic treatment but certain algal-bacterial processes (e.g., metabolite exchange) can benefit the microalgal community. In the eutrophic treatment, where algae have a growth advantage, proteins related to photosynthesis and energy generation should be highly expressed while it is expected that bacteria express proteins that aid adaptation to low dissolved organic matter (DOM) environments (e.g., switch from heterotrophy to autotrophy).

We inoculated microcosms with a microbial community subjected to two nutrient treatments to mimic oligotrophic and eutrophic conditions in freshwater lakes. Microcosms, as experimental systems, provide evidence for or against hypotheses that are difficult to test in nature (Drake and Kramer, 2011) and, here, allowed us to focus on the effects of nutrient enrichment on the microbial community. Bacterial, cyanobacteria and algal abundances were quantified throughout the experiment as were physicochemical measurements. The microbial metaproteome was extracted from two nutrient treatments (oligotrophic and eutrophic) at two time points. The time points were selected to represent phases of algal/cyanobacterial dominance and, later, heterotrophic bacterial dominance. For each treatment the extracted proteome was analyzed by nano-liquid chromatography–tandem mass spectrometry (LC-MS/MS). A meta-genetic community analysis of prokaryotic and eukaryotic diversity within the inoculum was used to generate a refined protein database for identifying proteins at the specified time-points. This approach reduced the spectral search space and led to reliable false discovery rate (FDR) statistics (Jagtap et al., 2013). The identified proteins at the two time points were then grouped into taxonomic and functional categories to link identity with function (Pandhal et al., 2008). We analyzed changes in protein expression in individual phylogenetic groups, over time and in both nutrient concentrations, to give an insight into the functional attributes of the major microbial players in the experimental microcosm community.

MATERIALS AND METHODS

Microcosm Setup

We constructed replicate experimental biological communities in 30 L white, opaque, polypropylene vessels, 42 cm high and with an internal diameter of 31 cm. The microcosms were housed in controlled environment facilities at the Arthur Willis Environmental Centre at the University of Sheffield, UK. These were filled with 15 L of oligotrophic artificial freshwater growth medium (for detailed composition see Supplementary Table S1). Over the course of the experiment the microcosms were kept at constant temperature, 23°C, under 100 μmol m^{-2} s^{-1}, provided by Hellelamp 400 watt IR Lamps HPS (Helle International, Ltd, UK), and 12:12 light dark cycle. A microbial community was introduced into each microcosm (detailed composition in Supplementary Tables S2 and S3). This inoculum was sourced from 100 L of water samples collected at Weston Park Lake, Sheffield, UK (53°22′56.849″ N, 1°29′21.235″ W). The inoculum was filtered with a fine mesh cloth (maximum pore size 200 μm) to exclude big particles, protists and grazer populations (Downing et al., 1999). The filtered sample was cultured for 5 days in the conditions described to allow acclimation to the controlled conditions. Subsequently, each 15 L microcosm was inoculated with 2.5 L of this sample.

The inoculated microcosms were subjected to two nutrient treatments to mimic oligotrophic and eutrophic conditions

in freshwater lakes. Our experimental elevation of initial nutrient levels followed United States Environmental Protection Agency guidelines for oligotrophic and eutrophic conditions in freshwater lakes and reservoirs (USEPA, 1986): (1) non-enriched growth medium to simulate oligotrophic conditions ($NO_3^- = 0.42$ mg L^{-1} and $PO_4^{3-} = 0.03$ mg L^{-1}) and (2) NO_3^- and PO_4^{3-} enriched growth medium ($NO_3^- = 4.20$ mg L^{-1} and $PO_4^{3-} = 0.31$ mg L^{-1}) to simulate eutrophic conditions. Each treatment was replicated 18 times, allowing for serial but replicated ($n = 3$ biological replicate microcosms) destructive sampling during the experiment. The experiment was run for 18 days to allow the added NO_3^- and PO_4^{3-} to deplete and generate batch microbial growth curves (see **Figure 1**). We also followed three control microcosms comprised of non-enriched growth medium, with no biological inoculum, allowing us to follow physicochemical variation in the absence of introduced biological activity (see Supplementary Figure S1).

Sampling of Abiotic Variables

Over the course of the experiment dissolved oxygen (DO), pH, temperature, nitrate (NO_3^-) and phosphate (PO_4^{3-}) were monitored in order to link the abiotic variation to the changes observed in the biological variables. DO, pH, and temperature were measured at 12:00 and 18:00 daily with a Professional Plus Quatro (YSI, USA). 15 mL aliquots were collected and filtered (0.45 μm), daily, for the estimation of NO_3^- and PO_4^{3-} concentrations. NO_3^- was estimated with a Dionex ICS-3000 ion chromatograph (Thermo Fisher Scientific, USA) using an AG18 2 mm × 250 mm column with a 0.25 mL min^{-1} flow rate and 31.04 mM potassium hydroxide as eluent. PO_4^{3-} concentrations were measured according to protocols defined by British standards (BS EN ISO 6878:2004; BSI, 2004).

Sampling of Biotic Variables

To estimate microalgae and cyanobacterial abundance, fluorescence was measured daily, at 12:00, with the AlgaeTorch (bbe Moldaenke GmbH, Germany). By measuring fluorescence, at 470, 525, and 610 nm for chlorophyll *a* and phycocyanin, the two spectral groups of microalgae and cyanobacteria, can be differentiated *in situ*. The relative amount of each group, expressed in terms of the equivalent amount of biomass per liter of water, was calculated according to Beutler et al. (2002).

Culturable heterotrophic bacteria were enumerated as an estimation of total bacteria (Lehman et al., 2001; Eaton and Franson, 2005; CSLC, 2009; Perkins et al., 2014) every 3 days by sampling 100 μL aliquots, in triplicate, plating on R2A agar (Oxoid, UK), incubating for 24 h at 37°C and counting colony forming units (CFU per mL). CFU were calculated with

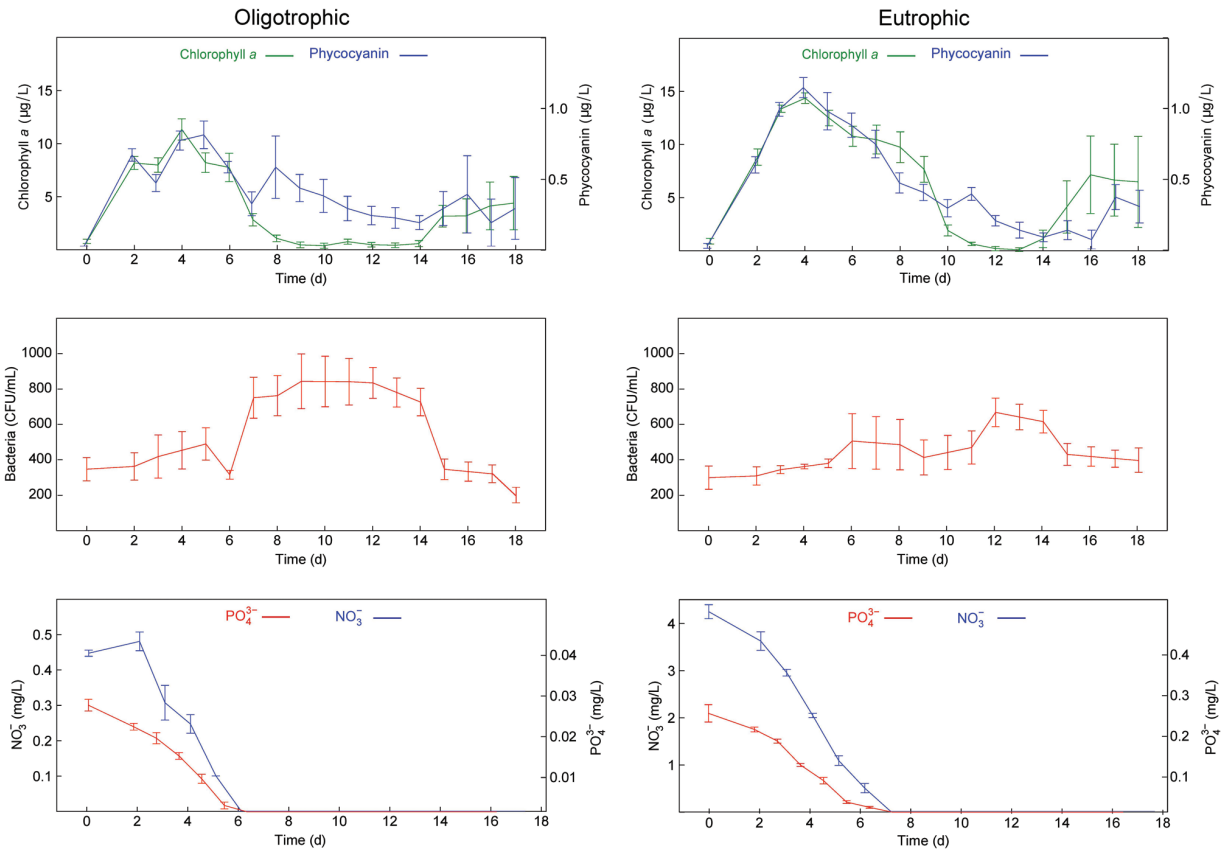

FIGURE 1 | Time series of the measured variables in the oligotrophic and eutrophic treatments. (Top) Chlorophyll *a* and phycocyanin fluorescence. **(Middle)** Culturable heterotrophic bacteria. **(Bottom)** NO_3^- and PO_4^{3-}. Error bars show standard errors ($n = 3$).

OpenCFU software (Geissmann, 2013). Because bacteria were only enumerated every 3 days, we used linear interpolation to generate a daily time series to obtain a uniform sample size across all variables. Interpolated values were calculated using the formula:

$$y = y_1 + (y_2 - y_1)\frac{x - x_1}{x_2 - x_1}$$

where y is the missing value, x is the missing time point, y_1, y_2 are the two closest measured bacterial counts and x_1, x_2 are the respective time points.

Protein Preparation

Microcosm samples were concentrated, in triplicate, at days 3 and 12 of the time course using a Centramate tangential flow filtration (TFF) system fitted with three 0.1 μm pore size Supor TFF membranes (Pall Corporation, USA). After every use, the filter system was sanitized with a 0.5 M sodium hydroxide solution and flushed with deionized water. The permeate was then filtered with a 3 μm pore size polycarbonate isopore membrane (EMD Millipore, USA) in order to obtain fractions dominated by free-living bacteria (<3 μm in size) and algae/particle-associated bacteria (>3 μm in size; Teeling et al., 2012). These fractions were harvested at 10, 000 × *g* for 15 min at 4°C. The resulting cell pellets were further washed in 0.5 M triethylammonium bicarbonate buffer (TEAB) prior to storage at −20°C. Cells were defrosted and resuspended in extraction buffer [250 μL of 0.5 M TEAB, 0.1% sodium dodecyl sulfate (SDS)] and 1 μL of halt protease inhibitor cocktail (Fisher Scientific, USA) incorporating a sonication bath step for 5 min with ice. The resulting suspension was submitted to five freeze-thaw cycles (each cycle corresponds to 2 min in liquid nitrogen and 5 min in a 37°C water bath; Ogunseitan, 1993). The lysed sample was centrifuged at 15,000 × *g* for 10 min at 4°C and the supernatant was transferred to a LoBind microcentrifuge tube (Eppendorf, Germany). The remaining cell pellet was resuspended in extraction buffer (125 μL) and homogenized with glass beads (425–600 μm) for 10 cycles (each cycle corresponds to 2 min homogenization and 2 min on ice). The lysed sample was centrifuged at 15,000 × *g* for 10 min at 4°C and the supernatants from both extraction methods were combined. 1 μL of benzonase nuclease (Sigma-Aldrich, USA) was added to the collected supernatants. Extracted proteins were precipitated overnight, at −20°C, using four volumes of acetone. The dried protein pellet was resuspended in 100 μL of 0.5 M TEAB and quantified using the 230/260 spectrophotometric assay described by Kalb and Bernlohr (1977). Biological replicates were pooled before reduction, alkylation, and digestion. This approach has been shown to be potentially valuable for proteomics studies where low amount of protein does not allow replication (Diz et al., 2009) whilst enhancing the opportunity to identify lower abundance proteins. Moreover, the small variances observed between replicate microcosms in terms of all biological and physiochemical measurements conducted (**Figure 1**; Supplementary Figure S1) gave further confidence to this approach. Protein samples (200 μg) were reduced with 20 mM tris-(2-carboxyethyl)-phosphine, at 60°C for 30 min, followed by alkylation with 10 mM iodoacetamide for 30 min in the dark. Samples were digested overnight, at 37°C, using trypsin (Promega, UK) 1:40 (trypsin to protein ratio) resuspended in 1 mM HCl. The samples were dried using a vacuum concentrator and stored at −20°C prior to fractionation.

Chromatography and Mass Spectrometry

The first dimensional chromatographic separation, off-line, was performed on a Hypercarb porous graphitic column (particle size: 3 μm, length: 50 mm, diameter: 2.1 mm, pore size: 5 μm; Thermo-Dionex, USA) on an Ultimate 3000 UHPLC (Thermo-Dionex, USA). Peptides were resuspended in 200 μL of Buffer A [0.1% (v/v) trifluoroacetic acid (TFA) and 3% (v/v) HPLC-grade acetonitrile (ACN) in HPLC-grade water] and eluted using a linear gradient of Buffer B [0.1% (v/v) TFA and 97% (v/v) ACN in HPLC-grade water] ranging from 5 to 60% over 120 min with a flow rate of 0.2 mL min^{-1}. Peptide elution was monitored at a wavelength of 214 nm and with Chromeleon software, version 6.8 (Thermo-Dionex, USA). Fractions were collected every 2 min, between 10 and 120 min, using a Foxy Junior (Teledyne Isco, USA) fraction collector and dried using a vacuum concentrator. Dried fractions were stored at −20°C prior to mass spectrometry analysis. The second dimensional chromatographic separation of each peptide fraction was performed on a nano-LC-CSI-MS/MS system. In this system a U3000 RSLCnano LC (Thermo-Dionex, USA), containing a trap column (300 μm × 5 mm packed with PepMap C18, 5 μm, 100 Å wide pore, Dionex) followed by a reverse phase nano-column (75 μm × 150 mm packed with PepMap C18, 2 μm, 100 Å wide pore, Dionex), was coupled to an ultra-high resolution quadrupole time-of-flight (UHR maXis Q-ToF 3G) mass spectrometer (Bruker, Germany) equipped with an Advance CaptiveSpray ion source. Peptide fractions were resuspended in loading buffer [0.1% (v/v) TFA and 3% (v/v) ACN in HPLC-grade water] and two injections were made. A 90 min linear gradient elution was performed using buffer A [0.1% (v/v) formic acid (FA) and 3% (v/v) ACN in HPLC-grade water] and buffer B [0.1% (v/v) FA and 97% (v/v) ACN in HPLC-grade water], during which buffer B increased from 4 to 40% at a flow rate of 0.3 μL min^{-1}. On the mass spectrometer, the following settings were specified: endplate Offset −500 V, capillary voltage 1000 V, nebulizer gas 0.4 bar, dry gas 6.0 L min^{-1}, and dry temperature 150°C. Mass range: 50–2200 *m/z*, at 4 Hz. Lock mass was used for enabling mass acquisition correction in real time, therefore high mass accuracy data were obtained. Data were acquired for positive ions in a dependent acquisition mode with the three most intense double, triple or quadruple charges species selected for further analysis by tandem mass spectrometry (MS/MS) under collision induced dissociation (CID) conditions where nitrogen was used as collision gas.

16 and 18S rDNA Gene Sequencing of Inoculum

DNA Extraction

Inoculum samples were lysed in 50 mM Tris-HCl (pH 8.0), 10 mM EDTA and 10% (w/v) SDS by vortexing with glass beads. DNA was extracted with a standard phenol-chloroform extraction protocol (Sambrook and Russel, 2001). The DNA

was precipitated using sodium acetate (50 μL of 3 M stock solution, pH 4.8–5.2) and ice-cold ethanol. PCR amplification, product pooling, purification sequencing and bioinformatics and statistical analysis were performed by Research and Testing Laboratory (Lubbock, TX, USA).

PCR Amplification

Markers were amplified from DNA extractions using adapted Illumina tagged primers. Forward primers were constructed with Illumina adapter i5 (AATGATACGGCGACCACCGAGATC TACAC) an 8–10 bp barcode, a primer pad and either primer 28F (GAGTTTGATCNTGGCTCAG) or TAReukF (CCAGCASC YGCGGTAATTCC). Reverse primers were constructed with Illumina adapter i7 (CAAGCAGAAGACGGCATACGAGAT) an 8–10 bp barcode, a primer pad and either primer 519R (GTNTTACNGCGGCKGCTG) or TAReukR (ACTTTCGTTC TTGATYRA). Primer pads were used to ensure a primer melting temperature of 63–66°C, as per the Schloss method (Schloss et al., 2009). Reactions were performed using corresponding primer pairs (i.e., 28F × 519R and TAReukF × TAReukR) using the Qiagen HotStar Taq master mix (Qiagen, Inc., Valencia, CA, USA) adding 1 uL of each 5 uM primer, and 1 uL of template to make a final 25 μL reaction volume, with a thermal cycling profile of 95°C for 5 min., then 35 cycles of 94°C for 30 s, 54°C for 40 s, 72°C for 1 min, followed by one cycle of 72°C for 10 min. Amplified products were visualized with eGels (Life Technologies, Grand Island, NY, USA) and pooled. Pools were purified (size selected) through two rounds of 0.7x Agencourt AMPure XP (BeckmanCoulter, Indianapolis, IN, USA) as per manufacturer's instructions, before quantification with a Quibit 2.0 fluorometer (Life Technologies). Finally pools were loaded and sequenced on an Illumina MiSeq (Illumina, Inc., San Diego, CA, USA) 2 × 300 flow cell at 10 pM. The sequence data are available from the European Nucleotide Archive under Study Accession Number PRJEB12443, and Sample Accession Numbers ERS1037123 (16S DNA) and ERS1037124 (18S DNA).

Bioinformatic and Statistical Analysis

Initially the forward and reverse reads were taken and merged together using the PEAR Illumina paired-end read merger (Zhang et al., 2014). Reads were then filtered for quality by trimming them once average quality dropped below 25 and prefix dereplication was performed using the USEARCH algorithm (Edgar, 2010). Sequences below 100 bp were not written to the output file and no minimum cluster size restriction was applied. Clustering was performed at a 4% divergence using the USEARCH clustering algorithm (Edgar, 2010). Clusters containing less than two members were removed. OTU selection was performed using the UPARSE OTU selection algorithm (Edgar, 2013). Chimeras were then checked for and removed from the selected OTUs using the UCHIME chimera detection software executed in *de novo* mode (Edgar et al., 2011). Reads were then mapped to their corresponding non-chimeric cluster using the USEARCH global alignment algorithm (Edgar, 2010). The denoised sequences were demultiplexed and the primer sequences removed. These sequences were then clustered into OTUs using the UPARSE algorithm (Edgar, 2013) which assigns each of the original reads back to their OTUs and writes the mapping data to an OTU table file. The centroid sequence from each OTU cluster was then run against the USEARCH global alignment algorithm and the taxonomic identification was done using a NCBI database as described in Bokulich et al. (2015). Finally, the OTU table output from sequence clustering was collated with the output generated during taxonomic identification and a new OTU table with the taxonomic information tied to each cluster was created (Bokulich et al., 2015).

Protein Identification and Quantification

All MS and MS/MS raw spectra were processed using Data Analysis 4.1 software (Bruker, Germany) and the spectra from each Bruker analysis file were output as a mascot generic file (MGF) for subsequent database searches using Mascot Daemon (version 2.5.1, Matrix Science, USA). The peptide spectra were searched against a eukaryotic and a prokaryotic database created by collating all Uniprot entries (retrieved on 24 February 2015) from organisms with an abundance of >1% in the 16 and 18S rDNA survey of our inoculum (**Table 1**, full list in Supplementary Tables S2 and S3). This search was undertaken utilizing the two-step approach described in Jagtap et al. (2013). Briefly, the initial database search was done without any FDR limitation and then was followed by a second search with a 1% FDR threshold against a refined database created by extracting the protein identifications derived from the first search. FDRs for assigning a peptide match were determined from the ratio of the number of peptides that matched to the reversed sequence eukaryotic and prokaryotic

TABLE 1 | List of the eukaryotic and prokaryotic organisms in the experimental freshwater microbial community inoculum, with an abundance higher than 1%, as determined by 16 and 18S rDNA sequencing.

Eukaryotic organisms	%	Prokaryotic organisms	%
Chloromonas pseudoplatyrhyncha	26.93	*Rhodoferax* sp.	21.94
Stephanodiscus sp.	18.17	Unsequenced organisms	17.84
Unsequenced organisms	17.87	*Flavobacterium* sp.	9.43
Chromulinaceae sp.	8.48	*Anabaena* sp.	8.85
Synedra angustissima	4.99	*Brevundimonas diminuta*	4.20
Ochromonadales sp.	3.01	*Hydrogenophaga* sp.	3.41
Chlamydomonas sp.	2.98	*Runella limosa*	2.47
Micractinium pusillum	1.62	*Haliscomenobacter* sp.	2.43
Chlorella sp.	1.08	*Rhodobacter* sp.	2.34
Pythiaceae sp.	1.07	*Planktophila limnetica*	2.13
		Agrobacterium tumefaciens	2.11
		Sphingobacterium sp.	2.03
		Ochrobactrum tritici	1.98
		Brevundimonas variabilis	1.83
		Sphingomonas sp.	1.73
		Curvibacter sp.	1.48
		Phenylobacterium falsum	1.42
		Roseomonas stagni	1.24
		Oceanicaulis sp.	1.03

These organisms were used to guide creation of a protein database.

databases to the number of peptides matched to the same databases in the forward sequence direction. The following search parameters were applied to both searches: up to one missed cleavage with trypsin, fixed modification of cysteine residues by carbamidomethylation, variable modification of methionine by oxidation, instrument specification ESI Q-ToF, peptide charge: 2+, 3+ and 4+, precursor mass tolerance of ±0.2 Da and fragment-ion mass tolerance of ±0.02 Da. For the second search only matches above a 95% confidence homology threshold, with significant scores defined by Mascot probability analysis, and a 1% FDR cut-off were considered confidently matched peptides. 'Show sub-sets' and 'require bold red' were applied on initial Mascot results to eliminate redundancy. The highest score for a given peptide mass (best match to that predicted in the database) was used to identify proteins, which in turn were assigned a most probable host. Furthermore, only when two or more unique peptides, per protein, were matched did we consider a protein identified. Protein abundance was relatively estimated through the exponentially modified protein abundance index (emPAI; Ishihama et al., 2005). emPAI is an approximate, label-free, relative quantitation of the proteins. This method is based on the protein abundance index (PAI) that calculates the number of different observed peptides divided by the number of observable peptides as a measure of abundance. This PAI value is then exponentially modified to derive the emPAI score. A protein abundance is then finally calculated after normalizing the emPAI score for a protein by dividing it by the sum of the emPAI scores for all identified proteins (Ishihama et al., 2005). The mass spectrometry proteomics data have been deposited to the ProteomeXchange Consortium[1] via the PRIDE partner repository (Vizcaíno et al., 2013) with the dataset identifier PXD004592 and DOI 10.6019/PXD004592.

Functional Classification of Proteins

Proteins were semi-automatically attributed a functional classification. Briefly, a list of UniProt accession numbers was collated from each sample and queried utilizing the UniProt Retrieve/ID mapping tool[2]. Column options 'Keywords' and 'Gene ontology (biological process)' were selected. Incomplete or ambiguous annotations were then manually completed by searching for the individual UniProt accession numbers on Pfam[3] and EggNOG[4].

RESULTS AND DISCUSSION

Biological and Physicochemical Measurements

The time points chosen for metaproteomic analysis of our samples were based on biological and physicochemical variables measured in our microcosms. Algal and cyanobacterial abundance peaked at day 3, and was maintained until nitrate and phosphate concentrations were no longer in detectable range, but declined after their depletion between days 6 and 8 (**Figure 1**). The decline in abundance of algae and cyanobacteria was followed by a peak of bacterial abundance at day 12 (**Figure 1**). Heterotrophic bacterial growth is known to be stimulated by an accumulation of DOM derived from senescent algae and cyanobacteria. Hence, in a given body of water the peak of heterotrophic bacterial activity tends to follow the peak of primary production.

Based on these patterns the samples selected for metaproteomic analyses were harvested at day 3, the peak of algal and cyanobacterial concentrations (early oligo- and eutrophic) and day 12, the peak of bacterial concentrations (late oligo- and eutrophic). The comparative analysis of these biologically distinct time points can provide information regarding the activity of the microbial community during algal/cyanobacterial dominance and bacterial dominance under low and high nutrient conditions.

Similar patterns were observed in DO, pH, and temperature measurements in both nutrient treatments (Supplementary Figure S1) and together with the low level of variation observed in biological measurements (**Figure 1**), provided additional confidence in the sample pooling approach for metaproteomics analyses.

Metaproteomic Database Creation and Search Results

The 18S rDNA sequencing of the microcosm inoculum indicated that, at day 0, the eukaryotic community was predominantly composed of Chlorophyceae (e.g., Chloromonas), Bacillariophyceae (e.g., Stephanodiscus), and Chrysophyceae (e.g., Chromulinaceae). These are typical unicellular freshwater microalgal species that are normally found in freshwater oligotrophic environments (Bailey-Watts, 1992).

The 16S rDNA sequencing of the microcosm inoculum showed that, at day 0, the prokaryotic community was predominantly composed of Alpha-proteobacteria (e.g., Brevundimonas), Beta-proteobacteria (e.g., Rhodoferax), Flaviobacteria (e.g., Flaviobacterium), and Cyanophyceae (e.g., *Anabaena*). Proteobacteria and Flaviobacteria are ubiquitous in freshwater environments with the latter being known to dominate eutrophic environments where phytoplankton population numbers are high (Eiler and Bertilsson, 2007; Newton et al., 2011). *Anabaena* is a well-researched freshwater cyanobacterium that is known to occasionally be responsible for harmful algal blooms (Elser et al., 2007).

This list of organisms was utilized to create a eukaryotic and a prokaryotic protein database by collating all Uniprot entries from organisms with an abundance of >1% in the 16 and 18S rDNA survey of the inoculum (**Table 1**; full list in Supplementary Tables S2 and S3). This approach was applied to limit the size of the resulting protein databases, which can lead to high false positive rates, and also in accordance with the nature of mass spectrometry based proteomics, where only the most abundant proteins are identified. As a result the eukaryotic and prokaryotic databases contained 86336 and

[1]http://proteomecentral.proteomexchange.org

[2]http://www.uniprot.org/uploadlists/

[3]http://pfam.xfam.org/

[4]http://eggnogdb.embl.de/

350356 sequence entries, respectively. These databases were utilized to identify proteins from peptide fragments in a two-step approach (Jagtap et al., 2013). This approach is valuable when dealing with large metaproteomic database searches where the target and decoy identifications may overlap significantly and valuable identifications are missed out (Muth et al., 2015). Proteins of eight samples, representing the two time points selected under different nutrient concentrations (early and late oligo- and eutrophic) and two size separated fractions, [free-living bacteria (<3 μm in size) and algae/particle-associated bacteria (>3 μm in size)] were identified and an average of 131 ± 28 proteins, above a 95% confidence homology threshold, a 1% FDR cut-off and with two unique peptides, were identified per sample. Values were pooled by broad protein annotation and taxonomic categories to evaluate differences between early and late oligotrophic and eutrophic conditions. The average coefficient of variation (CV) of emPAI across three biological replicates in non-fractionated protein samples, was 0.15. The average relative variance (RV) was also determined logarithmically and was 0.82 indicating a 18% discrepancy for relative quantitation. This provided us with confidence of a 1.5 fold cut off to minimize the identification of false positive differentially regulated proteins.

Phylogenetic Diversity According to the Metaproteomic Spectra

Identifying discrepancies between the phylogenetic classification of the identified proteins and the 16 and 18S rDNA sequencing used to create the metaproteomic database can indicate if any specific phylogenetic group is inadequately represented. rDNA sequencing was performed on the inoculum (i.e., at day 0 of the experiment) and therefore a direct comparison with the metaproteomes is not possible. Nevertheless, the 16 and 18S rDNA sequencing information provided a template to which the metaproteome could be compared. Of the total number of identified proteins in the >3 μm fraction, across all four samples, 48–55% were identified in Chlorophyta, 9–27% in Heterokontophyta and, finally, 12–33% in Cyanobacteria.

A more detailed look at the genus level of the phylogenetic distribution showed that *Chlamydomonas* sp. proteins are most abundant in the early part of the time series [oligotrophic (50%) and eutrophic (43%)], *Chlorella* sp. in late oligotrophic (39%) and *Anabaena* sp. in late eutrophic (37%) conditions. The 18S rDNA sequencing indicated that the abundance of the *Chlorella* genus was only 1.08% of the initial inoculum. However, proteins belonging to the *Chlorella* genus represented up to 39% of total protein. This is most likely due to an over representation of *Chlorella* sp. in the metaproteomic database due to it being a model genus with a large number of sequences available in Uniprot.

The phylogenetic distribution, based on proteins identified across the samples, mostly fitted with the biological measurements. Microalgae concentrations were always higher than cyanobacteria concentrations over the course of the experiment (**Figure 1**). Cyanobacteria had the highest number of proteins identified in late eutrophic (37%) mostly due to the expression of highly abundant proteins related to carbon concentration mechanisms (CCMs). It has been suggested that this is a mechanism of survival under adverse conditions that could, in the long term, favor cyanobacterial populations (Yeates et al., 2008).

Of the total number of identified proteins in the <3 μm fraction, across all four samples, 60–73% were identified in Proteobacteria and 27–40% in Bacteroidetes. Bacteroidetes proteins were more abundant in early oligotrophic conditions whereas Proteobacteria were more abundant in late oligotrophic and early eutrophic conditions. A more detailed look at the class level of the phylogenetic distribution showed that Bacteroidetes proteins were more abundant in the early phase [oligotrophic (29%) and eutrophic (30%)] while Alpha-proteobacteria proteins were abundant in late oligotrophic (30%) and Beta-proteobacteria proteins in late eutrophic (30%) conditions.

Again, the taxonomic community composition found by 16S rDNA sequencing and the metaproteome were in agreement and the phylogenetic distribution across the samples supports previous observations of these organisms. Bacteroidetes typically establish mutualistic relationships with algae on the cell surface and are more abundant when algal concentrations are high such as earlier in the time series (**Figure 1**). Alpha-proteobacteria and Beta-proteobacteria, as opportunistic heterotrophs, therefore thrive in the presence of DOM derived from algal and cyanobacterial decay which was abundant later in the time series (**Figure 1**; Teeling et al., 2012).

Functional Classification of Proteins

The distribution of identified proteins by their functional classification resulted in 20 distinct functional categories. The grouping of proteins identified in each fraction and nutrient condition can give an overview of how the community function differed over time and nutrient enrichment.

Of the total number of identified proteins, 25% were involved in photosynthesis, thus, dominating the >3 μm fraction (**Figure 2**). 9% of the total protein library were classified with unknown function. Proteins with assigned functions in each individual samples were dominated by photosynthesis (early oligotrophic, 21%; late oligotrophic, 25%; early eutrophic, 26%; late eutrophic, 30%). On the individual protein level, photosystem II (PSII) CP43 reaction center proteins were the most abundant in early oligotrophic (8%), histone H2 proteins in late oligotrophic (14%), PSII CP43 reaction center proteins and histone H4 proteins (8% each) in early eutrophic and microcompartment proteins (16%) in late eutrophic conditions.

In agreement with our findings, Hanson et al. (2014) observed that in both freshwater and marine surface samples (i.e., rich in primary production) there was widespread evidence of photosynthesis (e.g., PSII) and carbon fixation [e.g., ribulose-1,5-bisphosphate carboxylase oxygenase (RuBisCO; EC 4.1.1.39)]. Although our samples were not rich in RuBisCO, the presence of microcompartment proteins are evidence of carbon fixation.

Of the total number of identified proteins, transport (12%) and translation (12%) proteins were predominant in the <3 μm fraction (**Figure 3**). A more detailed view showed early

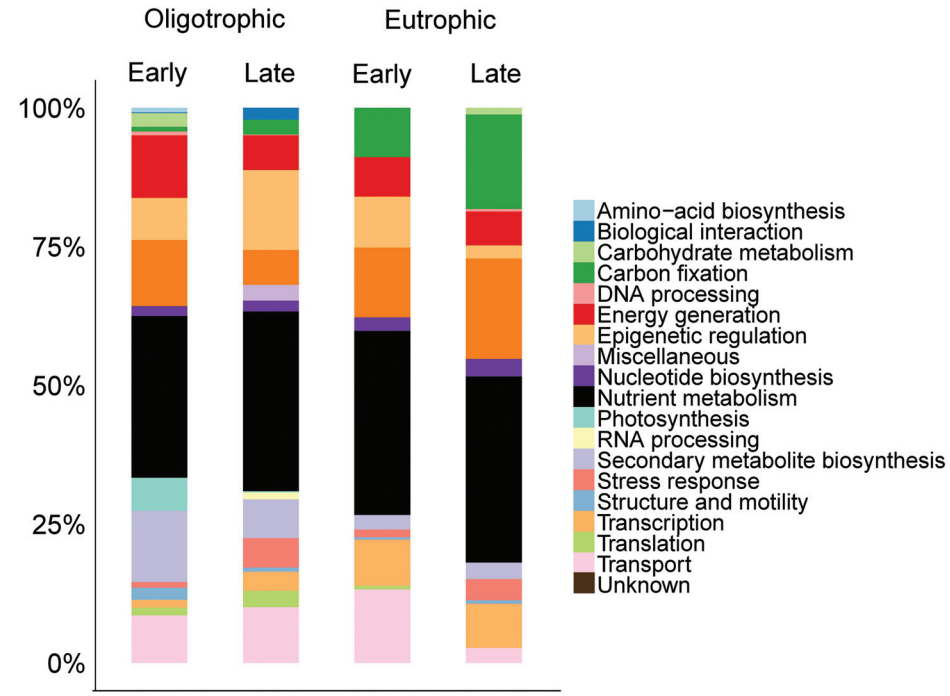

FIGURE 2 | Comparison across samples of the distribution of identified proteins by their functional classification in the >3 μm fraction.

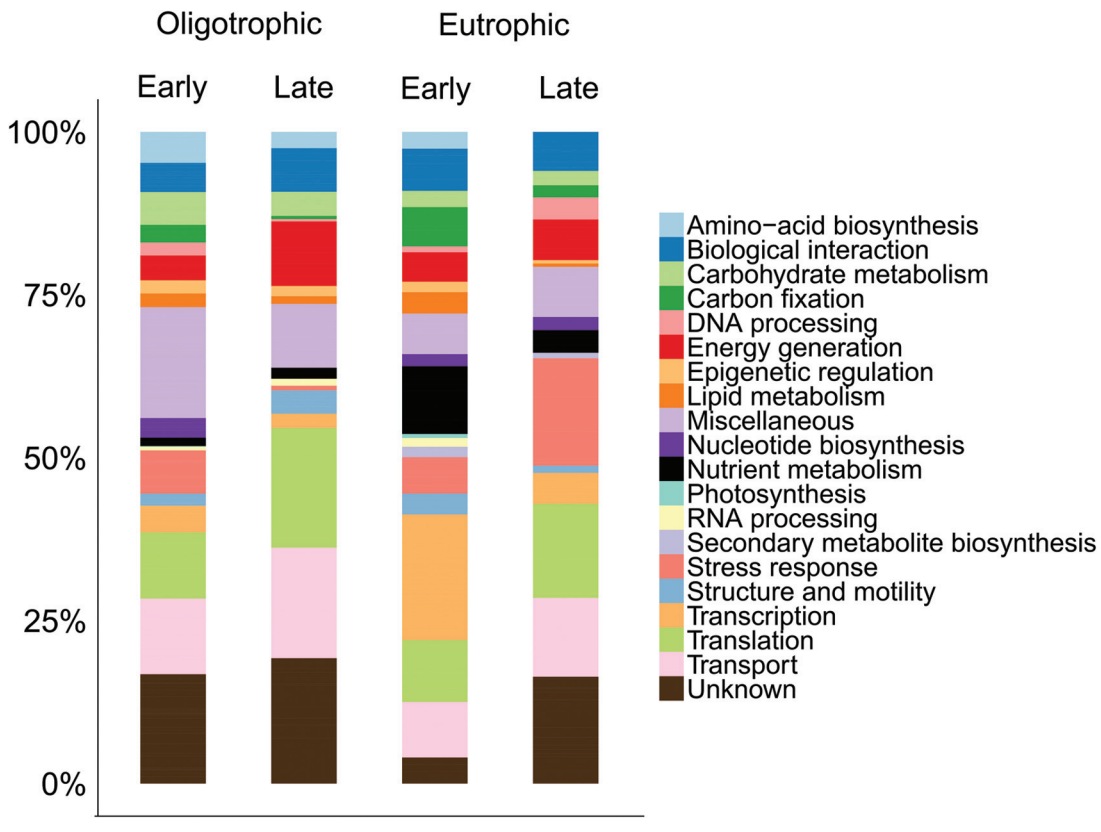

FIGURE 3 | Comparison across samples of the distribution of identified proteins by their functional classification in the <3 μm fraction.

oligotrophic conditions dominated by transport proteins (12%), late oligotrophic by translation proteins (18%), early eutrophic by transcription proteins (19%) and late eutrophic by stress response proteins (16%). On the individual protein level the ATP-binding cassette (ABC) transporter proteins were the most abundant in early oligotrophic (5%), elongation factor proteins in late oligotrophic (16%), DNA-directed RNA polymerase subunit beta (EC 2.7.7.6) in early eutrophic (19%) and ABC transporter proteins (7%) in late eutrophic conditions. Proteins involved in transport (e.g., ABC transporters), translation (e.g., elongation factors) and transcription (DNA-directed RNA polymerase subunit beta) are amongst the most commonly identified proteins in environmental samples (Ng et al., 2010; Sowell et al., 2011; Hanson et al., 2014).

Metaproteomic Analysis of Microcosm Microbial Activity

Having identified protein functional groups in eukaryotic and prokaryotic organisms throughout our samples, we can now assess functional differences between oligotrophic and eutrophic conditions, early and late in the time series. We found several patterns previously documented and several unexpected differences between time points and between oligotrophic and eutrophic conditions within each time point. **Figure 4** captures a summary of the functional differences among the times and treatments, and we now refer to this figure, and **Figures 2** and **3**, to provide detail.

First, virtually all the photosynthesis and carbon fixation proteins were identified in *Anabaena* sp., *Chlamydomonas* sp., and *Chlorella* sp. This is similar to previous metaproteomic studies where the freshwater surface is typically rich in photosynthetic organisms (Hanson et al., 2014). The most abundant of the two categories was photosynthesis (emPAI = 11.89) and it represented 40% of all proteins expressed by photoautotrophic organisms. The majority of the proteins were components of PSII (e.g., reaction center components). This was expected because PSII proteins are 40–90% more abundant than PSI proteins and are the most abundant membrane proteins in algae and cyanobacteria (Nobel, 2005). Photosynthetic proteins were abundant in both timepoints (early, emPAI = 5.27 and late, emPAI = 5.61) and in both nutrient treatments (oligotrophic, emPAI = 5.31 and eutrophic, emPAI = 5.57), suggesting that the phototrophs are demanding a constant energy supply, even outside of the exponential growth phase.

Second, amongst the photosynthetic microbes, there is interest in identifying mechanisms that could potentially favor cyanobacteria in eutrophic conditions. The increase in the

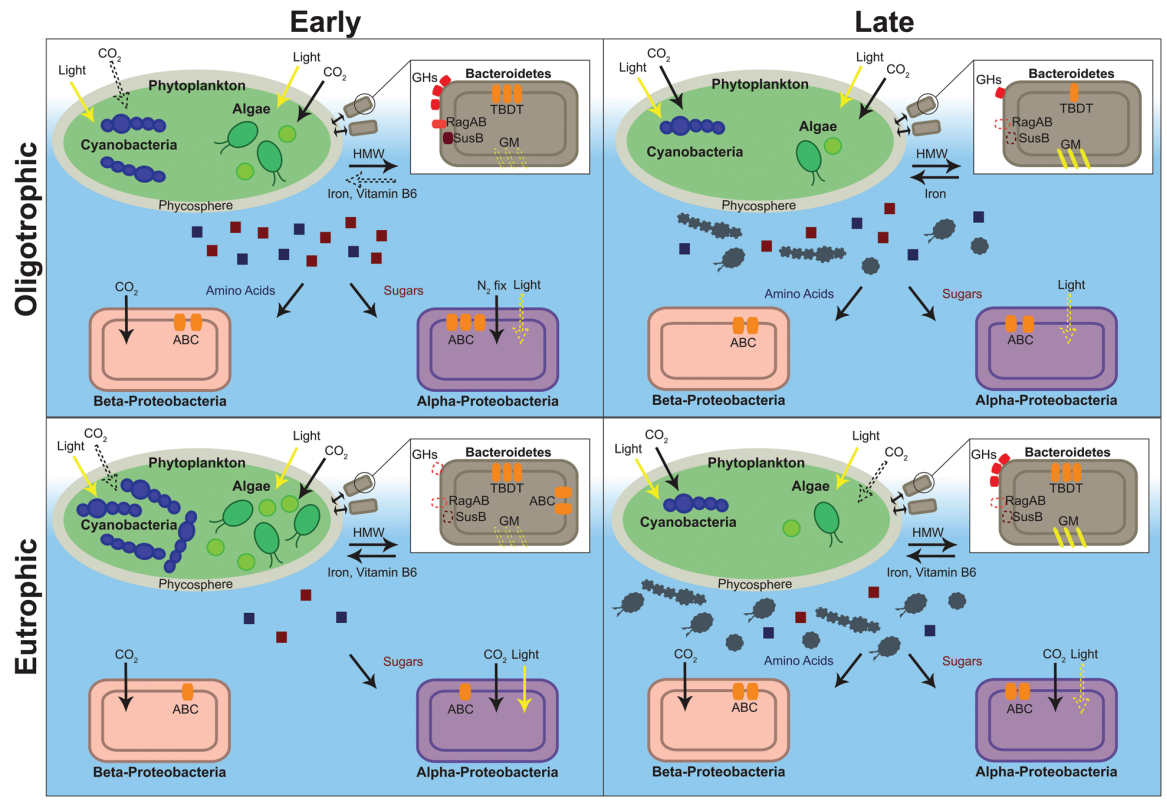

FIGURE 4 | Depiction of the metabolic characteristics of oligotrophic and eutrophic communities inferred from the metaproteome. Red and blue squares depict algal and cyanobacterial exudate (red, sugars; blue, amino acids). Gray algae and cyanobacteria depict senescent cells. Structures and processes that are hypothesized to be present, albeit with no direct evidence from our dataset, are depicted with a dashed line. ABC, ATP-binding cassette transporter; GHs, glycoside hydrolases; GM, gliding motility; HMW, high molecular weight compounds; N_2 fix, nitrogen fixation; TBDT, Ton-B-dependent transporter.

number of nutrient enriched water bodies has led to issues with freshwater quality and the proliferation of harmful cyanobacteria (O'Neil et al., 2012). There have been numerous proteomics studies of toxic bloom causing cyanobacteria that have focused on the molecular mechanisms of pure cultures. For example, a study of the proteomes of six toxic and non-toxic strains of *Microcystis aeruginosa* linked nitrogen regulation to toxicity (Alexova et al., 2011) and another study, of *Anabaena* sp. Strain 90, linked phosphorus starvation to the down regulation of the Calvin cycle and amino-acid biosynthesis (Teikari et al., 2015). Studies such as these provide valuable information regarding species in isolation, however, metaproteomics can go a step further and contextualize these findings within the microbial community structure and dynamics.

Our microcosm data showed that pigment proteins in *Anabaena* sp. were less abundant in oligotrophic than in eutrophic conditions (oligotrophic, emPAI = 0.42; eutrophic, emPAI = 0.96). A similar pattern was found for cyanobacterial proteins with roles in carbon fixation (oligotrophic, emPAI = 0.14; eutrophic, emPAI = 2.03). Cyanobacteria have the ability to adapt to different environments by adjusting their light harvesting abilities (i.e., increase in pigments) and carbon fixation mechanisms. However, these adaptation processes can be hampered by insufficient nutrient supply (Tilzer, 1987). Grossman et al. (1993) showed that during nutrient starvation, there is a rapid degradation of the phycobilisome. Phycobilisome degradation can provide nutrient-starved cells with amino acids used for the synthesis of proteins important for their metabolism (Grossman et al., 1993). This suggests that nutrient enrichment would allow cyanobacteria to increase pigment numbers, thus increasing light harvesting ability, and outcompete algal species in eutrophic conditions (Tilzer, 1987).

Regarding carbon fixation, microcompartment proteins were identified in *Anabaena* sp. and were only found in in late eutrophic conditions (eutrophic, emPAI = 1.52). Microcompartments sequester specific proteins in prokaryotic cells and are involved in CCMs in low CO_2 conditions. The carboxysome, a bacterial microcompartment that is found in cyanobacteria and some chemoautotrophs, encapsulates RuBisCO and carbonic anhydrase (EC 4.2.1.1) The carbonic anhydrase reversibly catalyzes the conversion of bicarbonate into carbon dioxide within the carboxysome therefore acting both as a intracellular equilibrator and a CO_2 concentrating mechanism (Yeates et al., 2008). However, no carbonic anhydrases were identified in our dataset. A higher abundance of carbon fixation proteins in *Anabaena* sp., in eutrophic conditions, indicates that carbon requirement was higher, likely matching higher photosynthesis rates compared to the oligotrophic conditions, where low nitrogen and phosphorus concentrations are likely limiting factors and therefore, not allowing the population to reach a point of carbon limitation.

Finally, carbon fixation proteins in *Chlamydomonas* sp. were also more abundant in eutrophic conditions (oligotrophic, emPAI = 0.17; eutrophic, emPAI = 0.40). The proteins identified were mainly involved in the Calvin cycle (i.e., RuBisCO), however, unexpectedly, a low-CO_2 inducible protein (LCIB) was identified. The LCIB is located around the pyrenoid and traps CO_2, either from escaping from the pyrenoid or entering from outside the cell, into the stromal bicarbonate pool thus, functioning as a CCM (Wang and Spalding, 2014). Wang and Spalding hypothesized that this system may reflect a versatile regulatory mechanism present in eukaryotic algae for acclimating quickly to changes in CO_2 availability that frequently occur in their natural environments. The possibility of switching between an energy-intensive bicarbonate transport system (low CO_2) and diffusion based CO_2 uptake system (high CO_2) that may be energetically less costly, would enable faster growth at a lower energy cost.

These observations suggest that algae and cyanobacteria both adapt to carbon limitation through an increase in carbon fixation proteins and the deployment of CCMs (e.g., carboxysomes). In a low-carbon lake, the microbial population may thus fix atmospheric CO_2 to correct the carbon deficiency and grow in proportion to existing nitrogen and phosphorus levels. This maps onto the hypothesis that carbon limitation may not be adequate for algal or cyanobacterial bloom mitigation (Schindler et al., 2008).

Bacterial Photosynthesis and Carbon Fixation

Heterotrophic bacteria are known to be responsible for the bulk of sequestration and remineralization of organic matter in phytoplankton associated bacterial assemblages (Buchan et al., 2014). However, the role of photoheterotrophic and chemoautotrophic bacteria in these assemblages, and how they vary along environmental gradients, remains under-studied (Yutin et al., 2007; Ng et al., 2010). The observations to date suggest that these bacteria are ubiquitous but have a preference for carbon limiting environments such as the DOM poor conditions found early in the time series, during algal and cyanobacterial dominance, in this study (**Figure 4**).

In support of this hypothesis, bacterial photosynthesis [i.e., magnesium chelatase (EC 6.6.1.1)] and carbon fixation proteins (i.e., RuBisCO, carbonic anhydrase) were identified in both treatments (**Figure 4**) with predominance early in the time series (early, emPAI = 1.28; late, emPAI = 0.11) and eutrophic conditions (oligotrophic, emPAI = 0.57; eutrophic, emPAI = 0.82). Specifically, in Alpha- and Beta-proteobacteria, magnesium chelatase (emPAI = 0.03), which is involved in bacteriochlorophyll biosynthesis, was identified in early oligotrophic (emPAI = 0.03) and RuBisCO was present in both nutrient treatments. Alpha- and Beta-proteobacteria include several mixotrophic species that are known to perform aerobic and anaerobic respiration and use combinations of photo-, chemo-, auto- and heterotrophic metabolism to adapt to different environmental conditions. Some of these bacterial species perform anoxygenic photosynthesis, where light energy is captured and converted to ATP without the production of oxygen, and are described as photo(chemo)heterotrophs due to their requirement of organic carbon. It has been suggested that these bacteria grow chemoheterotrophically but utilize light as an additional energy source (Eiler, 2006).

The low levels of DOM in early oligotrophic conditions (i.e., algal and cyanobacterial dominance) provided a niche for

phototrophy and autotrophy. Later, in the presence of DOM derived from algal and cyanobacterial cell lysis, the bacterial groups changed to a heterotrophic metabolism. This suggests that an increase in Proteobacterial metabolism depends more on the concentrations of organic matter than on nitrogen and phosphorus, and that bacterial mixotrophy is ubiquitous in low DOM freshwater environments. This has consequences for biogeochemical models such as the microbial loop. The classic separation of primary and secondary producers into photoautotrophs and organoheterotrophs, respectively, is no longer valid and may lead to the underestimation of bacterial biomass production and their importance to higher trophic levels (Eiler, 2006).

Finally, other bacterial groups found in our study, such as the Bacteroidetes, can also use non-photosynthetic routes of light-dependent energy generation. Previous metaproteomic studies have shown that proteorhodopsin, a light driven proton pump, is ubiquitous in marine and freshwater environments (Atamna-Ismaeel et al., 2008; Williams et al., 2013). Its expression has been linked to survival in situations where sources of energy are limiting and cells have to resort to alternative means of generating energy (González et al., 2008). However, proteorhodopsin was not detected either because of non-expression in the conditions tested, low abundance or low solubility of the protein; proteorhodopsin contains seven transmembrane helices and is imbedded in the plasma membrane thus making it difficult to solubilize and detect (Sowell et al., 2009).

Bacteroidetes: An Algal Associated Bacterial Group

The Bacteroidetes phylum has been hypothesized to specialize in degrading high molecular weight (HMW) compounds and growing whilst attached to particles, surfaces, and algal cells (Teeling et al., 2012; Fernandez-Gomez et al., 2013; Williams et al., 2013). Teeling et al. (2012) also observed that the bacterial response to a coastal algal bloom was characterized by an initial surge in Bacteroidetes abundance. Thus, it was hypothesized that this group colonizes the phytoplankton surface and acts as "first responders" to algal blooms (Williams et al., 2013). Therefore, the identification of proteins that suggest a tight algae – bacteria relationship were expected to be found early in the time series. Also, the higher algal concentrations in eutrophic conditions (**Figure 1**) would presumably provide a richer environment for the Bacteroidetes population.

As predicted, in both oligotrophic and eutrophic treatments, Bacteroidetes proteins were considerably more abundant in the early phase of the experiment (early, emPAI = 14.84, late, emPAI = 5.85) with several of the identified proteins suggesting a close association with algae (**Figure 4**). First, several proteins attributed to the TonB-dependent transporter (TBDT) system were identified. TBDTs are involved in proton motive force-dependent outer membrane transport and once thought to be restricted to iron-chelating compounds (i.e., siderophores) and vitamin B12 uptake. Recently TBDTs have been found to specialize in the uptake of HMW compounds that are too large to diffuse via porins (e.g., polysaccharides, proteins; Blanvillain et al., 2007). In Bacteroidetes, the genes for the TBDT system are located in the same gene cluster as several of the polymer capture (e.g., starch utilization system) and degradation genes [e.g., glycoside hydrolases (GHs), peptidases] suggesting an integrated regulation of capture, degradation, and transport of complex substrates (Fernandez-Gomez et al., 2013). The proteins identified in our Bacteroidetes dataset support this suggestion.

Second, three starch utilization system proteins (SusD/RagB) in Bacteroidetes were identified early in the time series (**Figure 4**). SusD proteins are present at the surface of the cell and they mediate starch-binding before transport into the periplasm for degradation. RagAB is involved in binding exogenous proteins (Gilbert, 2008; Dong et al., 2014). GHs from several families (GH3, GH29, GH30, and GH92), together with three peptidases [methionine aminopeptidase (EC 3.4.11.18), peptidase M16, peptidyl-dipeptidase (EC 3.4.15.1)] were also identified. As mentioned previously GHs are carbohydrate-active enzymes (CAZymes) specialized in the uptake and breakdown of complex carbohydrates, especially algal polysaccharides (Teeling et al., 2012; Mann et al., 2013). Together with peptidases these enzymes are responsible for extracellular breakdown of organic matter in order to be transported into the cytoplasm by the TBDT system.

Finally, the identification of proteins with cell adhesion functions (intimin, thrombospondin 1, gliding motility protein and YD repeat) provides further evidence that this bacterial phylum specializes in surface attachment. Intimin, thrombospondin and YD repeat protein are adhesive proteins that mediate cell-to-cell interactions and gliding mobility proteins allow exploration of solid surfaces (McBride, 2001). Other bacterial species utilize gliding motility for essential life cycle processes (e.g., swarming, predation) usually in coordinated groups but also as isolated adventurous individuals (Nan and Zusman, 2011). In a similar way Bacteroidetes species may use gliding motility to follow algal exudate trails and to move to advantageous positions within the phycosphere, the microscale mucus region rich in organic matter that surrounds algal and cyanobacterial cells. This could confer a competitive advantage over free-floating bacterial species.

When contrasting oligo- and eutrophic treatments, Bacteroidetes associated proteins were, unexpectedly, more abundant in oligotrophic rather than eutrophic conditions (oligotrophic, emPAI = 14.02; eutrophic, emPAI = 6.67). In eutrophic conditions proteins attributed to transport, macromolecule degradation, outer membrane capture and chemotaxis were virtually non-existent (**Figure 4**). The fact that very little capture and degradation was occurring in eutrophic conditions suggests algal exudation was substantially lower. In the past, it has been hypothesized that nutrient limitation is a requirement for algal and cyanobacterial exudation (Wood and Van Valen, 1990; Guenet et al., 2010). Van den Meersche et al. (2004) determined that contribution of algal derived DOM to the experimental ecosystem carbon pool varied from ∼2% (nutrient-replete early bloom) to 65% (nutrient-deplete mid-late bloom). Thus, the stimulation of DOM release, by nutrient limiting conditions, paradoxically provides carbon substrates for bacterial growth which then compete with the algae for

nutrients (Van den Meersche et al., 2004). Therefore, the survival of Bacteroidetes populations seems to be linked to environmental conditions and the physiological state of neighboring algae.

ABC Transporters Reveal Ecological Niches

In Alpha- and Beta-proteobacteria ATP-binding cassette (ABC) transporters were the most prevalent transport proteins identified (**Figure 4**). This is in agreement with previous freshwater and marine metaproteomic studies (Ng et al., 2010; Teeling et al., 2012; Georges et al., 2014). The majority of the ABC transporters were periplasmic-binding proteins (PBPs). The high representations of PBPs is commonly observed in aquatic metaproteomic studies. These subunits are far more abundant than the ATPase or permease components of ABC transporters in order to increase the frequency of substrate capture. Membrane proteins (e.g., permeases) are also inherently difficult to extract and solubilize therefore reducing the frequency of their detection (Williams and Cavicchioli, 2014).

In a metaproteomic comparison of Atlantic Ocean winter and spring microbial plankton, Georges et al. (2014) found ABC transporters were more abundant in low nutrient surface waters in mid-bloom and were mostly specific for organic substrates. Therefore, these type of transporters may be expected to more prevalent in the early oligotrophic conditions of our study where bacterial levels were higher (**Figure 1**) and the environment was rich in algal and cyanobacterial exudate (discussed in previous section). As expected, transporter proteins in Alpha- and Beta-proteobacteria were more abundant in oligotrophic than eutrophic conditions (emPAI = 3.32 and emPAI = 1.73, respectively). They were predominant in early phase in oligotrophic (early, emPAI = 1.42 and late, emPAI = 0.9) and late phase in eutrophic conditions (early, emPAI = 0.42 and late, emPAI = 0.88). Furthermore, in both treatments and timepoints the majority of ABC transporters were specific for organic substances (i.e., carbohydrates and amino acids). This suggests that both proteobacterial phyla are specialized in obtaining nutrients from DOM therefore investing more resources in the acquisition of organic rather than inorganic substrates and were favored in early oligotrophic when the rate of algal exudation was potentially higher (Teeling et al., 2012).

Finally, another particularity of ABC transporters is that the expression of these transporters comes at an additional metabolic cost and therefore they are mainly synthesized to target substrates that are limiting in the environment. Thus, determining which transporters are being expressed can provide clues to which substrate is limiting. There was a clear difference in substrate preference between the two (**Figure 4**); *Rhodobacter* sp. (Alpha-proteobacteria) carbohydrate transporter expression was more than twofold higher than amino acid transporter expression (carbohydrate, emPAI = 0.57; amino acid, emPAI = 0.21) whereas in the bacterial group *Hydrogenophaga* sp. (Beta-proteobacteria) only amino acid transporter expression was observed (carbohydrate, emPAI = 0.00; amino acid, emPAI = 0.81). This has been previously observed (Schweitzer et al., 2001; Pérez et al., 2015) and is a case of resource partitioning, a mechanism through which two phylogenetic groups can co-exist in the same environment without leading to competitive exclusion (Morin, 2011).

CONCLUSION

A label-free comparative metaproteomics approach was applied on an experimental microcosm community under differing trophic states. The identification of proteins in early and late oligo- and eutrophic conditions allowed us to link function to phylogenetic diversity and reveal individual transitional niches. The results from this study also compared favorably with many *in situ* aquatic metaproteomic studies.

Algae and cyanobacteria predominantly expressed, as would be expected, proteins related to photosynthesis and carbon fixation. Interestingly, proteins involved in mechanisms of carbon concentration were abundant in virtually all samples, which indicated that carbon could be a limiting factor throughout the experiment. The fact that cyanobacteria, in eutrophic conditions, expressed several proteins related to environmental adaptation (e.g., microcompartment proteins) suggests that they may be better equipped than algal species to dominate nutrient enriched environments.

Proteins identified in all bacterial species suggested an alignment with oligotrophic environments. In early oligotrophic, Bacteroidetes showed characteristics that suggest a role as a fast-growing population that is specialized in cell and particle attachment and are the first to respond to algal growth. This ecosystem role can coexist with bacterial heterotrophs that live suspended in the water column and depend on algal exudate and decaying organic matter. ABC transporters were amongst the most abundant proteins identified. In a case of resource partitioning it was found that Alpha- and Beta-proteobacteria co-exist and metabolize algal/cyanobacterial exudate, but the former will preferentially uptake carbohydrates whereas the latter will prefer amino acid uptake thus avoiding direct competition. There is the evidence that bacterial metabolism controls primary production through the remineralization of nutrients, however, here it is shown that primary producers can also be a driver of bacterial community composition and function.

This study successfully showed that microcosms can be used to observe microbial mechanisms that are typical of the natural environment. While these microcosm systems are simplified, and may not completely represent global biogeochemical cycles, they can accurately provide a snapshot of a microbial community in controlled conditions, and offer the potential to employ more manipulative experimentation to uncover functions and processes in oligo- and eutrophic conditions. The study also demonstrated that a community metagenetic analysis can provide a usable database for high mass accuracy metaproteomics studies. Ultimately, these data suggest that nutrient enrichment affected the dynamics of individual microbes and how they interact with others in their vicinity. Further manipulative experiments and associated 'omics' methodology will significantly contribute to our understanding of how microbial communities adapt to local environmental conditions.

AUTHOR CONTRIBUTIONS

This study was designed and coordinated by DR, AB, and JP. JP, as principal investigator, and AB provided technical and conceptual guidance for all aspects of the project. DR planned and undertook all the practical aspects of the manuscript. NC contributed to performing and analyzing all aspects of protein extraction and analysis. The manuscript was written by DR and commented on by all authors.

FUNDING

Natural Environment Research Council and Technology Strategy Board [NE/J024767/1].

ACKNOWLEDGMENTS

DR thanks Benjamin Strutton, Thomas Minshull, Mark Jones and the Groundwater Protection and Restoration group who assisted with sample collection and analyses, Joseph Longworth for assistance with database creation and search, Julie Zedler for valuable comments to the manuscript and Phillip Warren for constructive discussions on microcosm design.

SUPPLEMENTARY MATERIAL

The Supplementary Material for this article can be found online at: http://journal.frontiersin.org/article/10.3389/fmicb.2016.01172

REFERENCES

Aebersold, R., Hood, L. E., and Watts, J. D. (2000). Equipping scientists for the new biology. *Nat. Biotechnol.* 18, 359. doi: 10.1038/74325

Alexova, R., Haynes, P. A., Ferrari, B. C., and Neilan, B. A. (2011). Comparative protein expression in different strains of the bloom-forming cyanobacterium *Microcystis aeruginosa*. *Mol. Cell. Proteomics* 10, M110003749. doi: 10.1074/mcp.M110.003749

Atamna-Ismaeel, N., Sabehi, G., Sharon, I., Witzel, K.-P., Labrenz, M., Jurgens, K., et al. (2008). Widespread distribution of proteorhodopsins in freshwater and brackish ecosystems. *ISME J.* 2, 656–662. doi: 10.1038/ismej.2008.27

Azam, F., Fenchel, T., Field, J. G., Gray, J. S., Meyer-Reil, L. A., and Thingstad, F. (1983). The ecological role of water-column microbes in the sea. *Mar. Ecol. Prog. Ser.* 10, 257–263. doi: 10.3354/meps010257

Azam, F., and Malfatti, F. (2007). Microbial structuring of marine ecosystems. *Nat. Rev. Microbiol.* 5, 782–791. doi: 10.1038/nrmicro1747

Bailey-Watts, A. E. (1992). Growth and reproductive strategies of freshwater phytoplankton. *Trends Ecol. Evol.* 4, 359. doi: 10.1016/0169-5347(89)90095-5

Beutler, M., Wiltshire, K. H., Meyer, B., Moldaenke, C., Luring, C., Meyerhofer, M., et al. (2002). A fluorometric method for the differentiation of algal populations in vivo and in situ. *Photosynth. Res.* 72, 39–53. doi: 10.1023/A:1016026607048

Blanvillain, S., Meyer, D., Boulanger, A., Lautier, M., Guynet, C., Denance, N., et al. (2007). Plant carbohydrate scavenging through tonB-dependent receptors: a feature shared by phytopathogenic and aquatic bacteria. *PLoS ONE* 2:e224. doi: 10.1371/journal.pone.0000224

Bokulich, N., Rideout, J., Kopylova, E., Bolyen, E., Patnode, J., Ellett, Z., et al. (2015). A standardized, extensible framework for optimizing classification improves marker-gene taxonomic assignments. *PeerJ PrePrints* 3, e1156. doi: 10.7287/peerj.preprints.934v2

BSI (2004). *BS EN ISO 6878:2004: Water Quality. Determination of phosphorus. Ammonium molybdate spectrometric method*. London: British Standards Institution.

Buchan, A., LeCleir, G. R., Gulvik, C. A., and Gonzalez, J. M. (2014). Master recyclers: features and functions of bacteria associated with phytoplankton blooms. *Nat. Rev. Micro.* 12, 686–698. doi: 10.1038/nrmicro3326

CSLC (2009). *Assessment of the Efficacy, Availability and Environmental Impacts of Ballast Water Treatment Systems for Use in California Waters*. Sacramento, CA: California State Lands Commission.

Diz, A. P., Truebano, M., and Skibinski, D. O. (2009). The consequences of sample pooling in proteomics: an empirical study. *Electrophoresis* 30, 2967–2975. doi: 10.1002/elps.200900210

Dong, H.-P., Hong, Y.-G., Lu, S., and Xie, L.-Y. (2014). Metaproteomics reveals the major microbial players and their biogeochemical functions in a productive coastal system in the northern South China Sea. *Environ. Microbiol. Rep.* 6, 683–695. doi: 10.1111/1758-2229.12188

Downing, J. A., Osenberg, C. W., and Sarnelle, O. (1999). Meta-analysis of marine nutrient-enrichment experiments: variation in the magnitude of nutrient limitation. *Ecology* 80, 1157–1167. doi: 10.1890/0012-9658(1999)080[1157:MAOMNE]2.0.CO;2

Drake, J. M., and Kramer, A. M. (2011). Mechanistic analogy: how microcosms explain nature. *Theor. Ecol.* 5, 433–444. doi: 10.1007/s12080-011-0134-0

Eaton, A. D., and Franson, M. A. H. (2005). *Standard Methods for the Examination of Water and Wastewater*. Washington, DC: American Public Health Association.

Edgar, R. C. (2010). Search and clustering orders of magnitude faster than BLAST. *Bioinformatics* 26, 2460–2461. doi: 10.1093/bioinformatics/btq461

Edgar, R. C. (2013). UPARSE: highly accurate OTU sequences from microbial amplicon reads. *Nat. Methods* 10, 996–998. doi: 10.1038/nmeth.2604

Edgar, R. C., Haas, B. J., Clemente, J. C., Quince, C., and Knight, R. (2011). UCHIME improves sensitivity and speed of chimera detection. *Bioinformatics* 27, 2194–2200. doi: 10.1093/bioinformatics/btr381

Eiler, A. (2006). Evidence for the ubiquity of mixotrophic bacteria in the upper ocean: implications and consequences. *Appl. Environ. Microbiol.* 72, 7431–7437. doi: 10.1128/AEM.01559-06

Eiler, A., and Bertilsson, S. (2007). Flavobacteria blooms in four eutrophic lakes: linking population dynamics of freshwater bacterioplankton to resource availability. *Appl. Environ. Microbiol.* 73, 3511–3518. doi: 10.1128/AEM.02534-06

Elser, J. J., Bracken, M. E., Cleland, E. E., Gruner, D. S., Harpole, W. S., Hillebrand, H., et al. (2007). Global analysis of nitrogen and phosphorus limitation of primary producers in freshwater, marine and terrestrial ecosystems. *Ecol. Lett.* 10, 1135–1142. doi: 10.1111/j.1461-0248.2007.01113.x

Falkowski, P., Scholes, R. J., Boyle, E., Canadell, J., Canfield, D., Elser, J., et al. (2000). The global carbon cycle: a test of our knowledge of earth as a system. *Science* 290, 291–296. doi: 10.1126/science.290.5490.291

Fernandez-Gomez, B., Richter, M., Schuler, M., Pinhassi, J., Acinas, S. G., Gonzalez, J. M., et al. (2013). Ecology of marine Bacteroidetes: a comparative genomics approach. *ISME J.* 7, 1026–1037. doi: 10.1038/ismej.2012.169

Geissmann, Q. (2013). OpenCFU, a new free and open-source software to count cell colonies and other circular objects. *PLoS ONE* 8:e54072. doi: 10.1371/journal.pone.0054072

Georges, A. A., El-Swais, H., Craig, S. E., Li, W. K., and Walsh, D. A. (2014). Metaproteomic analysis of a winter to spring succession in coastal northwest Atlantic Ocean microbial plankton. *ISME J.* 8, 1301–1313. doi: 10.1038/ismej.2013.234

Gilbert, H. J. (2008). Sus out sugars in. *Structure* 16, 987–989. doi: 10.1016/j.str.2008.06.002

Giovannoni, S. J., Bibbs, L., Cho, J.-C., Stapels, M. D., Desiderio, R., Vergin, K. L., et al. (2005). Proteorhodopsin in the ubiquitous marine bacterium SAR11. *Nature* 438, 82–85. doi: 10.1038/nature04032

González, J. M., Fernández-Gómez, B., Fernàndez-Guerra, A., Gómez-Consarnau, L., Sánchez, O., Coll-Lladó, M., et al. (2008). Genome analysis of the proteorhodopsin-containing marine bacterium Polaribacter sp. MED152 (Flavobacteria). *Proc. Natl. Acad. Sci.* 105, 8724–8729. doi: 10.1073/pnas.0712027105

Grossman, A. R., Schaefer, M. R., Chiang, G. G., and Collier, J. L. (1993). Environmental effects on the light-harvesting complex of cyanobacteria. *J. Bacteriol.* 175, 575–582.

Guenet, B., Danger, M., Abbadie, L., and Lacroix, G. (2010). Priming effect: bridging the gap between terrestrial and aquatic ecology. *Ecology* 91, 2850–2861. doi: 10.1890/09-1968.1

Hanson, B. T., Hewson, I., and Madsen, E. L. (2014). Metaproteomic survey of six aquatic habitats: discovering the identities of microbial populations active in biogeochemical cycling. *Microb. Ecol.* 67, 520–539. doi: 10.1007/s00248-013-0346-5

Hettich, R. L., Pan, C., Chourey, K., and Giannone, R. J. (2013). Metaproteomics: harnessing the power of high performance mass spectrometry to identify the suite of proteins that control metabolic activities in microbial communities. *Anal. Chem.* 85, 4203–4214. doi: 10.1021/ac303053e

Ishihama, Y., Oda, Y., Tabata, T., Sato, T., Nagasu, T., Rappsilber, J., et al. (2005). Exponentially modified protein abundance index (emPAI) for estimation of absolute protein amount in proteomics by the number of sequenced peptides per protein. *Mol. Cell. Proteomics* 4, 1265–1272. doi: 10.1074/mcp.M500061-MCP200

Jagtap, P., Goslinga, J., Kooren, J. A., McGowan, T., Wroblewski, M. S., Seymour, S. L., et al. (2013). A two-step database search method improves sensitivity in peptide sequence matches for metaproteomics and proteogenomics studies. *Proteomics* 13, 1352–1357. doi: 10.1002/pmic.201200352

Kalb, V. F. Jr., and Bernlohr, R. W. (1977). A new spectrophotometric assay for protein in cell extracts. *Anal. Biochem.* 82, 362–371. doi: 10.1016/0003-2697(77)90173-7

Lauro, F. M., DeMaere, M. Z., Yau, S., Brown, M. V., Ng, C., Wilkins, D., et al. (2011). An integrative study of a meromictic lake ecosystem in Antarctica. *ISME J.* 5, 879–895. doi: 10.1038/ismej.2010.185

Lehman, R. M., Colwell, F. S., and Bala, G. A. (2001). Attached and unattached microbial communities in a simulated basalt aquifer under fracture- and porous-flow conditions. *Appl. Environ. Microbiol.* 67, 2799–2809. doi: 10.1128/aem.67.6.2799-2809.2001

Mann, A. J., Hahnke, R. L., Huang, S., Werner, J., Xing, P., Barbeyron, T., et al. (2013). The genome of the alga-associated marine flavobacterium Formosa *Agariphila* KMM 3901T reveals a broad potential for degradation of algal polysaccharides. *Appl. Environ. Microbiol.* 79, 6813–6822. doi: 10.1128/AEM.01937-13

McBride, M. J. (2001). Bacterial gliding motility: multiple mechanisms for cell movement over surfaces. *Annu. Rev. Microbiol.* 55, 49–75. doi: 10.1146/annurev.micro.55.1.49

Morin, P. J. (2011). *Community Ecology*, 2nd Edn. Oxford: Wiley-Blackwell, 407.

Muth, T., Kolmeder, C. A., Salojärvi, J., Keskitalo, S., Varjosalo, M., Verdam, F. J., et al. (2015). Navigating through metaproteomics data: a logbook of database searching. *Proteomics* 15, 3439–3453. doi: 10.1002/pmic.201400560

Nan, B., and Zusman, D. R. (2011). Uncovering the mystery of gliding motility in the myxobacteria. *Annu. Rev. Genet.* 45, 21–39. doi: 10.1146/annurev-genet-110410-132547

Newton, R. J., Jones, S. E., Eiler, A., McMahon, K. D., and Bertilsson, S. (2011). A guide to the natural history of freshwater lake bacteria. *Microbiol. Mol. Biol. Rev.* 75, 14–49. doi: 10.1128/MMBR.00028-10

Ng, C., DeMaere, M. Z., Williams, T. J., Lauro, F. M., Raftery, M., Gibson, J. A., et al. (2010). Metaproteogenomic analysis of a dominant green sulfur bacterium from Ace Lake, Antarctica. *ISME J.* 4, 1002–1019. doi: 10.1038/ismej.2010.28

Nobel, P. S. (2005). "5 - Photochemistry of Photosynthesis," in *Physicochemical and Environmental Plant Physiology,* 3rd Edn, ed. P. S. Nobel (Burlington, MA: Academic Press), 219–266.

Ogunseitan, O. A. (1993). Direct extraction of proteins from environmental samples. *J. Microbiol. Methods* 17, 273–281. doi: 10.1016/0167-7012(93)90056-N

O'Neil, J. M., Davis, T. W., Burford, M. A., and Gobler, C. J. (2012). The rise of harmful cyanobacteria blooms: the potential roles of eutrophication and climate change. *Harmful Algae* 14, 313–334. doi: 10.1016/j.hal.2011.10.027

Pandhal, J., Snijders, A. P., Wright, P. C., and Biggs, C. A. (2008). A cross-species quantitative proteomic study of salt adaptation in a halotolerant environmental isolate using 15N metabolic labelling. *Proteomics* 8, 2266–2284. doi: 10.1002/pmic.200700398

Pérez, M. T., Rofner, C., and Sommaruga, R. (2015). Dissolved organic monomer partitioning among bacterial groups in two oligotrophic lakes. *Environ. Microbiol. Rep.* 7, 265–272. doi: 10.1111/1758-2229.12240

Perkins, T. L., Clements, K., Baas, J. H., Jago, C. F., Jones, D. L., Malham, S. K., et al. (2014). Sediment composition influences spatial variation in the abundance of human pathogen indicator bacteria within an estuarine environment. *PLoS ONE* 9:e112951. doi: 10.1371/journal.pone.0112951

Sambrook, J., and Russel, D. W. (2001). *Molecular Cloning*. Cold Spring Harbor, NY: Cold Spring Harbor Laboratory Press.

Schindler, D. W., Hecky, R. E., Findlay, D. L., Stainton, M. P., Parker, B. R., Paterson, M. J., et al. (2008). Eutrophication of lakes cannot be controlled by reducing nitrogen input: results of a 37-year whole-ecosystem experiment. *Proc. Natl. Acad. Sci. U.S.A.* 105, 11254–11258. doi: 10.1073/pnas.0805108105

Schloss, P. D., Westcott, S. L., Ryabin, T., Hall, J. R., Hartmann, M., Hollister, E. B., et al. (2009). Introducing mothur: open-source, platform-independent, community-supported software for describing and comparing microbial communities. *Appl. Environ. Microbiol.* 75, 7537–7541. doi: 10.1128/aem.01541-09

Schweitzer, B., Huber, I., Amann, R., Ludwig, W., and Simon, M. (2001). Alpha- and beta-Proteobacteria control the consumption and release of amino acids on lake snow aggregates. *Appl. Environ. Microbiol.* 67, 632–645. doi: 10.1128/AEM.67.2.632-645.2001

Sowell, S. M., Abraham, P. E., Shah, M., Verberkmoes, N. C., Smith, D. P., Barofsky, D. F., et al. (2011). Environmental proteomics of microbial plankton in a highly productive coastal upwelling system. *ISME J.* 5, 856–865. doi: 10.1038/ismej.2010.168

Sowell, S. M., Wilhelm, L. J., Norbeck, A. D., Lipton, M. S., Nicora, C. D., Barofsky, D. F., et al. (2009). Transport functions dominate the SAR11 metaproteome at low-nutrient extremes in the Sargasso Sea. *ISME J.* 3, 93–105. doi: 10.1038/ismej.2008.83

Teeling, H., Fuchs, B. M., Becher, D., Klockow, C., Gardebrecht, A., Bennke, C. M., et al. (2012). Substrate-controlled succession of marine bacterioplankton populations induced by a phytoplankton bloom. *Science* 336, 608–611. doi: 10.1126/science.1218344

Teikari, J., Österholm, J., Kopf, M., Battchikova, N., Wahlsten, M., Aro, E.-M., et al. (2015). Transcriptomics and proteomics profiling of *Anabaena* sp. Strain 90 under inorganic phosphorus stress. *Appl. Environ. Microbiol.* 81, 5212–5222. doi: 10.1128/aem.01062-15

Tilzer, M. M. (1987). Light-dependence of photosynthesis and growth in cyanobacteria: implications for their dominance in eutrophic lakes. *N. Z. J. Mar. Freshwater Res.* 21, 401–412. doi: 10.1080/00288330.1987.9516236

USEPA (1986). *Quality Criteria for Water*. Washington, DC: United States Environmental Protection Agency.

Van den Meersche, K., Middelburg, J. J., Soetaert, K., van Rijswijk, P., Boschker, H. T. S., and Heip, C. H. R. (2004). Carbon-nitrogen coupling and algal-bacterial interactions during an experimental bloom: Modeling a 13C tracer experiment. *Limnol. Oceanogr.* 49, 862–878. doi: 10.4319/lo.2004.49.3.0862

Vizcaíno, J. A., Côté, R. G., Csordas, A., Dianes, J. A., Fabregat, A., Foster, J. M., et al. (2013). The Proteomics Identifications (PRIDE) database and associated tools: status in 2013. *Nucleic Acids Res.* 41, D1063–D1069. doi: 10.1093/nar/gks1262

Wang, Y., and Spalding, M. H. (2014). Acclimation to very low CO2: contribution of limiting CO2 inducible proteins, LCIB and LCIA, to inorganic carbon uptake in *Chlamydomonas reinhardtii*. *Plant Physiol.* 166, 2040–2050. doi: 10.1104/pp.114.248294

Williams, T. J., and Cavicchioli, R. (2014). Marine metaproteomics: deciphering the microbial metabolic food web. *Trends Microbiol.* 22, 248–260. doi: 10.1016/j.tim.2014.03.004

Williams, T. J., Wilkins, D., Long, E., Evans, F., DeMaere, M. Z., Raftery, M. J., et al. (2013). The role of planktonic *Flavobacteria* in processing algal organic matter in coastal East Antarctica revealed using metagenomics and metaproteomics. *Environ. Microbiol.* 15, 1302–1317. doi: 10.1111/1462-2920.12017

Wood, A. M., and Van Valen, L. M. (1990). Paradox lost? On the release of energy-rich compounds by phytoplankton. *Mar. Microb. Food Web* 4, 103–116.

Yeates, T. O., Kerfeld, C. A., Heinhorst, S., Cannon, G. C., and Shively, J. M. (2008). Protein-based organelles in bacteria: carboxysomes and related microcompartments. *Nat. Rev. Microbiol.* 6, 681–691. doi: 10.1038/nrmicro1913

Yutin, N., Suzuki, M. T., Teeling, H., Weber, M., Venter, J. C., Rusch, D. B., et al. (2007). Assessing diversity and biogeography of aerobic anoxygenic phototrophic bacteria in surface waters of the Atlantic and Pacific Oceans using the Global Ocean Sampling expedition metagenomes. *Environ. Microbiol.* 9, 1464–1475. doi: 10.1111/j.1462-2920.2007.01265.x

Zhang, J., Kobert, K., Flouri, T., and Stamatakis, A. (2014). PEAR: a fast and accurate Illumina Paired-End reAd mergeR. *Bioinformatics* 30, 614–620. doi: 10.1093/bioinformatics/btt593

Conflict of Interest Statement: The authors declare that the research was conducted in the absence of any commercial or financial relationships that could be construed as a potential conflict of interest.

frontiers in Microbiology

ORIGINAL RESEARCH
published: 26 July 2016
doi: 10.3389/fmicb.2016.01155

Changes in the Structure of the Microbial Community Associated with *Nannochloropsis salina* following Treatments with Antibiotics and Bioactive Compounds

Haifeng Geng[1], *Mary B. Tran-Gyamfi*[2], *Todd W. Lane*[1], *Kenneth L. Sale*[2]* and *Eizadora T. Yu*[1,3]

[1] Department of Systems Biology, Sandia National Laboratories, Livermore, CA, USA, [2] Department of Biomass Science and Conversion Technology, Sandia National Laboratories, Livermore, CA, USA, [3] Institute of Chemistry, University of the Philippines Diliman, Quezon City, Philippines

OPEN ACCESS

Edited by:
Xavier Mayali, Lawrence Livermore National Laboratory, USA

Reviewed by:
Russell T. Hill, University of Maryland Center for Environmental Science, USA
Christopher S. Ward, Duke University, USA

***Correspondence:**
Kenneth L. Sale
klsale@sandia.gov

Specialty section:
This article was submitted to Aquatic Microbiology, a section of the journal Frontiers in Microbiology

Received: *24 December 2015*
Accepted: *11 July 2016*
Published: *26 July 2016*

Citation:
Geng H, Tran-Gyamfi MB, Lane TW, Sale KL and Yu ET (2016) Changes in the Structure of the Microbial Community Associated with Nannochloropsis salina following Treatments with Antibiotics and Bioactive Compounds. Front. Microbiol. 7:1155. doi: 10.3389/fmicb.2016.01155

Open microalgae cultures host a myriad of bacteria, creating a complex system of interacting species that influence algal growth and health. Many algal microbiota studies have been conducted to determine the relative importance of bacterial taxa to algal culture health and physiological states, but these studies have not characterized the interspecies relationships in the microbial communities. We subjected *Nanochroloropsis salina* cultures to multiple chemical treatments (antibiotics and quorum sensing compounds) and obtained dense time-series data on changes to the microbial community using 16S gene amplicon metagenomic sequencing (21,029,577 reads for 23 samples) to measure microbial taxa-taxa abundance correlations. Short-term treatment with antibiotics resulted in substantially larger shifts in the microbiota structure compared to changes observed following treatment with signaling compounds and glucose. We also calculated operational taxonomic unit (OTU) associations and generated OTU correlation networks to provide an overview of possible bacterial OTU interactions. This analysis identified five major cohesive modules of microbiota with similar co-abundance profiles across different chemical treatments. The Eigengenes of OTU modules were examined for correlation with different external treatment factors. This correlation-based analysis revealed that culture age (time) and treatment types have primary effects on forming network modules and shaping the community structure. Additional network analysis detected *Alteromonadeles* and *Alphaproteobacteria* as having the highest centrality, suggesting these species are "keystone" OTUs in the microbial community. Furthermore, we illustrated that the chemical tropodithietic acid, which is secreted by several species in the *Alphaproteobacteria* taxon, is able to drastically change the structure of the microbiota within 3 h. Taken together, these results provide valuable insights into the structure of the microbiota associated with *N. salina* cultures and how these structures change in response to chemical perturbations.

Keywords: correlation network, microbiota, algae

INTRODUCTION

Open algal cultures are complex dynamic ecosystems inhabited by diverse microbial communities (Carney et al., 2014). In many cases, microbes in microalgae ecosystems have effects on algal physiology and nutrition as well as play critical roles on stability and homeostasis of algal ecosystems in both lab cultures and field studies (Kayser, 1979; Lee et al., 2000; Geng and Belas, 2010b). These types of algal-microbial interactions have been shown to either promote algal growth (Hold et al., 2001) and protect algae from invading pathogens (Geng and Belas, 2010b), or to inhibit algal growth and destabilize the algal ecosystem (Cole, 1982; Carney et al., 2014). Thus, knowledge of the composition and structure of algal-associated microbiota is important for understanding homeostasis in robust algal cultures, as aberrant microbiota have been reportedly linked with precipitous crashes of algal cultures (Cole, 1982; Carney et al., 2014). These observations argue for finding important relevant factors that contribute to the appropriate composition and proper structuring of this complex biological community (Carney et al., 2014; Sison-Mangus et al., 2014).

Given that microbial communities are enormously diverse, we are only able to characterize their diversity with the recent use of next-generation sequencing technologies (Gonzalez et al., 2012). In the past, algal microbiota researchers have focused on understanding the relationship between collective population diversity and environmental conditions in algal cultures (Alavi et al., 2001; Carney et al., 2014) and on linking individual membership composition to ecosystem descriptors (Costello et al., 2009). However, the overarching property of a microbial consortium may stem from the requisite biological functions of collective groups consisting of multiple interacting bacterial species (known as modules) found in the community. For example, biofilm formation and metabolic complementation are modules in which the collective bacteria species deliver the required functions (Raes and Bork, 2008; Geng and Belas, 2010b). However, limited information is available on the substructure of the microbial communities (e.g., formation of bacterial groups or modularities recapitulated from interacting bacterial species) associated with microalgae. This not only hinders the interpretation of topological structures that oversee the proper function of the microbial community but also reduces the reliability of prediction of the community structure and its effects on the long-term stability of microalgae cultures.

One way of exploring substructures in biological systems is to look for pairs of entity relationships and subsequently using this information to build a correlation network of potentially interacting entities. Correlation networks have been successfully used in studies of cancer (Choi et al., 2005), yeast genetics (Ge et al., 2001), and microbial ecology (Lovejoy et al., 1998; Duran-Pinedo et al., 2011; Gilbert et al., 2012), which focused on searching for groups of lineages that occur together more often than expected by chance. Once networks have been built, several measures and metrics such as node centrality and betweenness can be evaluated to assess and identify the most important and influential nodes in the network (Jeong et al., 2001). Centrality measures the importance of a node based on the number of connections it makes with other nodes (degree centrality) in the network and may include measures of the importance of the neighbors to which it is connected (eigenvalue centrality, Katz centrality, page rank). Nodes with high number of connections to other nodes are perceived as having greater influence over the entire network (Jeong et al., 2001). Betweenness centrality measures the extent to which a node lies on paths between other nodes and is an indicator of the influence a node exerts over other nodes in the network. Nodes with higher betweenness are perceived to have greater influence within a network by virtue of their control over information passing among the other nodes in the network (Yoon et al., 2006). In other microbial ecological systems, network analyses based on Weighted Correlation Network Analysis (WGCNA) were used to identify hub OTUs with influential roles in maintaining a mature biofilm (Duran-Pinedo et al., 2011).

Recently, we found a microbial community associated with *Nannochloropsis salina* (CCMP, 1776) that displayed community stability and resilience to environmental perturbations at a global level (Geng et al., 2016). To obtain clues about the substructuring of the microbial community associated with *N. salina*, we subjected *N. salina* containing communities to various chemicals (e.g., antibiotics, metabolites) and examined changes in the connectivities among taxa in the microbial community. We used longitudinal 16S gene amplicon sequencing of 23 samples descended from a single ancestral microbiota and built correlation networks to reflect the dynamics of the inter-taxa associations and to investigate variations in taxa organization in response to different chemical treatments. As a result, we identified five cohesive modules representing various chemical treatment responses. Subsequently, through network centrality analysis, our data showed that key nodes in the modeled network were primarily from the bacterial species belonging to *Alteromonadeles* and *Alphaproteobacteria*, suggesting species from these groups are of particular significance and serve as "keystone" OTUs in the microbial community associate with *N. salina*.

Species of the *Roseobacter* clade of *Alphaproteobacteria* are important symbionts of microalgae (Gonzalez and Moran, 1997; Treangen et al., 2013). One of the key aspects of the *Roseobacter*–microalgae symbiosis is founded on *Roseobacter*'s ability to produce a distinct set of infochemicals or signaling compounds with specialized functions (Mayali and Azam, 2004; Geng and Belas, 2010b; Seyedsayamdost et al., 2011; Treangen et al., 2013). For example, the antibiotic tropodithietic acid (TDA) produced by *Roseobacter* played a pivotal role in the bacterial-algal symbiosis by regulating TDA gene expression across various species (Geng and Belas, 2010a; Porsby et al., 2011) and preventing bacterial infection during prosperous algal blooms (Brinkhoff et al., 2004; Bruhn et al., 2007). Inspired by insights from network analysis, we treated the microbiota with various concentrations of TDA, simulating TDA secretion from some *Alphaproteobacteria*. The introduction of TDA drastically impacted community structure at a global level. Taken together, this experimental metagenomics study, while not fully characterizing OTU interactions in the microbial community associated with *N. salina*, provides a valuable

framework to aid modeling of interactions among the algal microbiota and understanding the important microbiota—microalgae interactions in the context of the complexity of the studied ecosystem.

MATERIALS AND METHODS

Algal Cultures and Experimental Design

Artificial microcosms of *N. salina* (CCMP, 1776) and the microbiota were generated by acclimating *N. salina* culture together with seawater microbiota from the coast of Santa Cruz, CA (Geng et al., 2016). After 1:10 culture dilution with fresh sterile artificial seawater media (ESAW) (Berges et al., 2001), algal cultures were grown to exponential phase. For the community restructuring experiments, triplicates were generated by splitting the algal cultures into 8 ml/well in 6-well Corning Costar® cell culture plates. The aliquoted exponential phase *N. salina* cultures (day 4 post-inoculation) were immediately spiked with two separate doses of sterile-filtered organic compounds (dosage were chosen based on the typical working concentrations for each chemical and a reference concentration (500 nM) for all chemicals; **Table 1**): (i) mixtures of common forms of bacterial quorum-sensing signaling molecules (Atkinson and Williams, 2009), including acyl-homoserine lactones (AHLs) [Sigma Aldrich (St. Louis, MO)] composed of N-butyryl-DL-homoserine lactone, N-hexanoyl-DL-homoserine lactone, N-octanoyl-DL-homoserine lactone, N-(β-Ketocaproyl)-L-homoserine lactone [31 nM (Wagner-Dobler et al., 2005) and 500 nM]; (ii) tetracycline (500 nM and 104 μM; Sambrook et al., 1989); (iii) ampicillin (500 nM and 134 μM; Sambrook et al., 1989); (iv) tropodithietic acid (TDA), an antibacterial and chemical signaling compound (31 nM and 500 nM; D'Alvise et al., 2012; Enzo Scientific, Farmingdale, NY); (v) D-glucose (500 nM and 300 μM) [Sigma Aldrich (St. Louis, MO)]. Low doses of D-glucose (500 nM) were treated as negative controls, as the effect of glucose on the bacterial community has been found to be minimal compared to antibiotic treatment (Dandekar et al., 2012). The incubation continued at 21°C under constant light conditions (100 μmol photons $m^{-2}s^{-1}$). An initial 4 ml was taken from each sample after 3 h and centrifuged 10,000 g for 5 min to pellet the bacterial community. The remaining 4 ml in each well were harvested after 24 h. Bacterial community pellets were stored at −80°C prior to DNA extraction.

TABLE 1 | Chemical treatments in algal microcosms.

Sample name	Chemicals[a]	Treatment time (hours)	Number of sequences	Observed OTUs[b]
starth0	Blank	0	81,967	3731
AHLL3	AHLs (31 nM)	3	114,404	3711
AMPL3	Ampicillin (500 nM)	3	103,175	3774
GLUCOSEL3	Glucose (500 nm)	3	159,219	3550
TDAL3	TDA (31 nm)	3	121,794	3698
TETL3	Tetracycline (500 nm)	3	138,805	3615
AHLH3	AHLs (500 nm)	3	114,275	4029
AMPH3	Ampicillin (134 μM)	3	121,688	4208
BLANK3	Blank	3	110,341	3759
GLUCOSEH3	Glucose (300 μM)	3	137,209	3778
TDAH3	TDA (500 nm)	3	122,655	4176
TETH3	Tetracycline (104 μM)	3	146,511	4104
AHLL24	AHLs (31 nm)	24	223,733	3036
AMPL24	Ampicillin (500 nm)	24	135,886	3857
GLUCOSEL24	Glucose (500 nm)	24	138,265	3360
TDAL24	TDA (31 nm)	24	245,234	3320
TETL24	Tetracycline (500 nm)	24	242,666	4100
AHLH24	AHLs (500 nm)	24	180,657	3606
AMPH24	Ampicillin (134 μM)	24	130,815	3732
BLANK24	Blank	24	128,023	3704
GLUCOSEH24	Glucose (300 μM)	24	242,402	2892
TDAH24	TDA (500 nm)	24	203,911	4130
TETH24	Tet (104 μM)	24	311,800	2875

[a] *Chemical name (final concentration).*
[b] *Observed OTUs/sample rarefied at 80,000 sequences per sample.*

Samples and 16S rRNA Gene Sequencing

Genomic DNA was extracted from algal culture samples with associated microbiota using a ZR Fungal/Bacterial DNA MiniPrep (ZYMO Research, Irvine, CA) following the manufacturer's protocol. 16S gene PCR preparation with standard procedures with barcoded primer set 341F forward and 518R reverse primer as previously described (Bartram et al., 2011). The triplicate PCR products from each sample were pooled and purified using QIAquick PCR purification kit (Qiagen, Valencia, CA) followed by quantification on a Nanodrop ND spectrophotometer (Thermo Science, Wilmington, DE). Twenty-three samples in equal amount with unique index sequence were mixed and further subjected to 2% gel purification using QIAquick gel extraction kit (Qiagen) following by quantification with a Bioanalyser DNA 7500 chip (Agilent Technologies, Santa Clara, CA). The prepared 16S rRNA gene library with addition of 30% PhiX was sequenced for 151-nucleotide paired-end multiplex sequence on MiSeq (Illumina, Hayward, CA) with a loading concentration of 8 pM following manufacturer's protocol.

Sequence Processing

Sequence reads were filtered to remove sequences of poor quality (e.g., two or more continuous base calls below 30 and length <75 bases). Forward and reverse sequences of paired-end sequences were assembled by aligning 3′ ends using SHE-RA software (Rodrigue et al., 2010). Stitched sequences were then clustered using the UCLUST algorithm with 97% similarity and assigned to operational taxonomic units (OTUs) above a 0.80 confidence threshold, which is a homology cutoff value above which typically denotes bacterial species, and taxonomic classifications were assigned in reference to Greengenes taxonomy (RDP-Classifier) in QIIME (DeSantis et al., 2006; Caporaso et al., 2010; Sul et al., 2011). OTUs ascribed to chloroplasts were then excluded from the pre-trimmed OTU table. Differences between samples (beta diversities) were performed using QIIME rarefied at depth 80,000 sequences/sample in post-trimmed OTUs table (DeSantis et al.,

2006; Caporaso et al., 2010). To obtain relative abundances of OTUs per sample, the post-trimmed OTU reads were divided by the sum of usable reads. Principal coordinate analysis (PCoA) was applied based on their between-samples weighted UniFrac distances metrics. Jackknifing was performed by resampling 1000 times with replacement of 50,000 sequences per sample in post-trimmed OTUs table and was used to build a rooted pairwise similarity tree using the Unweighted Pair Group Method with Arithmetic Mean (UPGMA) in QIIME (Caporaso et al., 2010)

Correlation Network Analysis

To remove poorly represented OTUs and reduce network complexity, we filtered and retained OTUs that were observed in a minimum of 13 out of total 23 samples, resulting in 1766 OTUs out of 27,298 OTUs being selected. Based on this, we calculated all pairwise Pearson correlations between OTUs using the WGCNA module in R (Team, 2015). Rather than focusing on the significance of the correlation, soft thresholding power was applied in WGCNA to dynamically prune branches off the dendrogram depending on clusters shape (DiLeo et al., 2011). To minimize spurious associations during module identification, the adjacency matrix was transformed to a Topological Overlap Matrix, corresponding dissimilarity was then calculated as a robust measure of interconnectedness in a hierarchical cluster analysis (DiLeo et al., 2011). Average linkage hierarchical cluster analysis was used to construct the corresponding dendrogram (DiLeo et al., 2011).

Network Centralities

Networks were explored, analyzed and visualized with Cytoscape based on the pairwise correlations (Smoot et al., 2011). Global measurements (e.g., betweenness, closeness, neighborhood connectivity, and topological coefficient) assessing the topology and centrality of the resulting network were calculated using Cytoscape with the NetworkAnalyzer plugin (Doncheva et al., 2012). To relate modules to chemical treatments, we correlated the eigengene for each module with the chemicals and looked for significant associations based on *p*-values.

RESULTS

Response of the Microbial Community Associated with *N. salina* to Chemical Perturbations

To generate a collection of datasets representing species relative abundance in response to known perturbations, we added a set

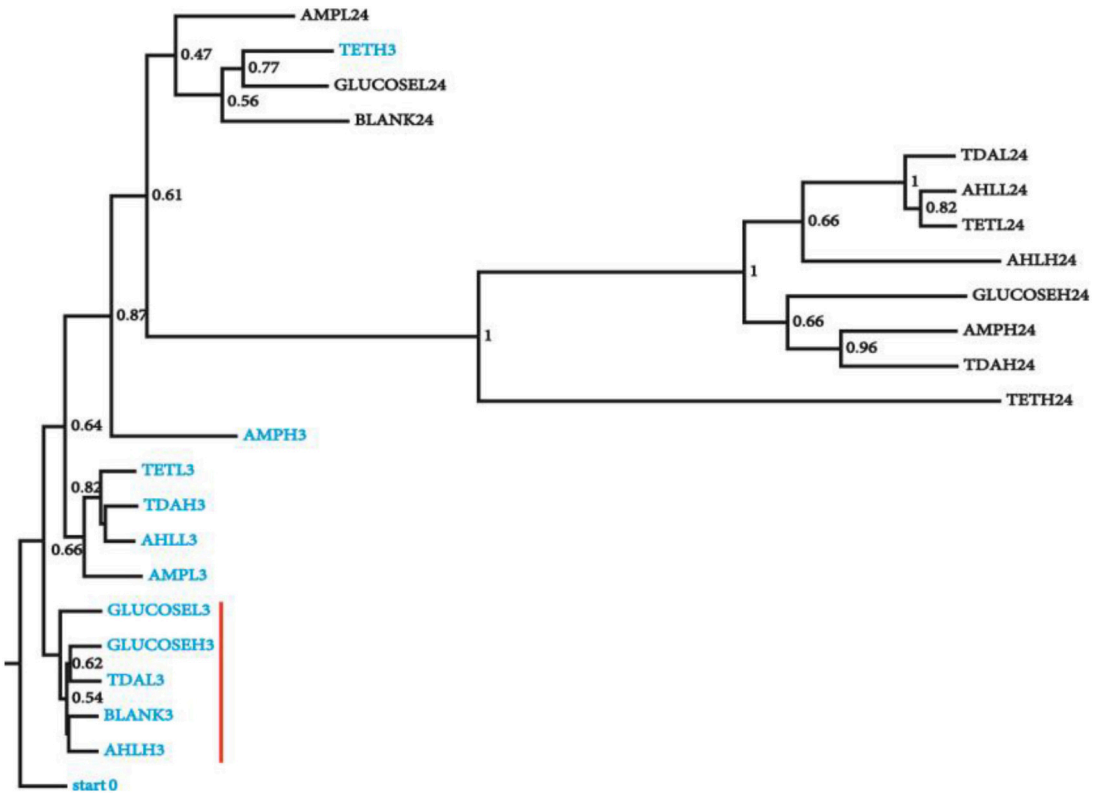

FIGURE 1 | Clustering of microbial diversity (β-diversity) of the starting microbiota with the samples from different chemical treatments at 3 and 24 h. Jackknifing of the UPGMA tree displays the robustness of clustering of the microbiota from the 3 h from 24 h samples. Bootstrap values are shown at the nodes of the tree, indicating percentage of jackknifed data supporting the node. Samples are named as following: chemical name (e.g., GLUCOSE), H/L (high/low concentration, e.g., L) and treatment time (e.g., 3), sample (GLUCOSEL3, treated with low amount of glucose for 3 h). Samples from 3 h (blue) treatment that were most similar to the starting microbiota are highlighted with a red vertical red bar.

of chemicals expected to have pervasive effects on *N. salina* microbial communities to the culture during exponential growth phase. The spiked chemicals include AHLs mixtures, tetracycline, ampicillin, TDA, and D-glucose in low and high concentrations chosen to maximize the likelihood of microbiota perturbations (Section Materials and Methods). The microbial community associated with *N. salina* from one untreated and four treated samples were collected at 3 and 24 h post inoculation, along with one starting microbiota (0 h), collectively generating 23 samples (**Table 1**). A total combined 21,029,577 reads from rRNA 16S gene V3 region of 23 microbiota samples were successfully assigned to individual samples. After filtering out low quality reads and OTU assignments (Section Materials and Methods), we obtained an OTU table of the 23 samples with a mean of 158,931 Seqs/sample (minimum: 81,976; maximum: 311,800; median 137,209 Seqs/sample) (**Table 1**). We assessed inter-sample variability using PCoA based on unweighted Unifrac metric measures in which the distance represents dissimilarity among community structures (**Figure 1**) (Lozupone and Knight, 2005). Among all tested microbiota, the initial microbiota (start0), blank control (3 h) and glucose treated samples (3 h) were found to be most similar in composition, thus clustering to what we call the "early" microbiota group (**Figure 1**, labeled with the red bar). The similarities among these groups reflect glucose and short temporal lags have only marginal effects on the structure of the microbiota. These patterns are expected, as glucose is widely used by many bacteria through the hexose monophosphate pathway in glucose metabolism, thereby having minimal effects in restructuring the microbial assemblage as compared to antibiotics (Dandekar et al., 2012). In contrast, short-term 3-h low concentration antibiotics treated-samples (TETL3 and AMPL3) migrate further away from the starting sample (start0) (**Figure 1**). This shift is further pronounced when comparing the starting microbiota and the high-dose antibiotics-treated samples (TETH3 and AMPH3) at the same 3-h timepoint (**Figure 1**). In addition, the short-term low TDA treatment for 3 h (TDAL3) resulted in a microbiota that coincided with "early" group microbiotas, which are most similar to the starting microbiota, whereas the high TDA imposed pronounced effects on the microbiota.

The microbiotas from the 3 h time points clustered together, while the 24 h treatment microbiotas formed a separate cluster (**Figure 1**), revealing groupings in the bacterial community as a function of treatment time. Collectively, 16S gene profiles displayed both culture age-dependent and chemical-responsive structural rearrangement of algal microbiota.

Structural Modulation of Algal Microbiota upon Chemical Treatments

To assess pairwise Pearson correlations among OTU relative-abundance data, we randomly selected 80,000 sequences per sample, built OTU tables, and filtered OTUs that contributed to at least half of 23 microbiota samples. The 1766 qualified OTUs produced from this process were subsequently fitted to a correlation matrix with scale free topology (power of 6, $R^2 = 0.81$) using WGCNA, which has been shown to be robust for analyzing relative abundance data (DiLeo et al., 2011). WGCNA revealed five major co-abundance modules that were arbitrarily given colors yellow, brown, blue, turquoise, and gray (**Figure S1**). Upon identification of modules in the microbial community associated with *N. salina*, we associated them with external treatment factors. **Figure 2A** shows that OTU membership in the yellow module was positively correlated with culture-age associated OTUs (coefficient $= 0.54$, $P < 0.05$). **Figure 2B** illustrates that treatment time was especially important, as three modules were found to be significantly associated with treatment time, whereas the blue (coefficient $= -0.80$, $P < 0.05$) and turquoise (coefficient $= -0.57$, $P < 0.05$) modules were negatively correlated with treatment time. These data indicate treatment time was a primary factor in contributing to variations in species abundance in these particular studies, which is consistent with beta-diversity analysis using unweighted Unifrac metric measure (**Figure 1**). Neither the glucose treatment nor the untreated microbiota was significantly associated with any of the five identified modules ($P > 0.05$). There were also no modules significantly associated with tetracycline under the studied concentrations. **Figure 2B** shows the brown colored module was selectively correlated with ampicillin treatment ($P < 10^{-7}$). Taxonomy analysis showed the brown chemotype-specific module was enriched by the *Rhodobacteraceae* family (13 out of 14, with only 1 coming from the *Erythrobacteraceae* family, $P < 0.05$, enrichment analysis), whereas the yellow module was

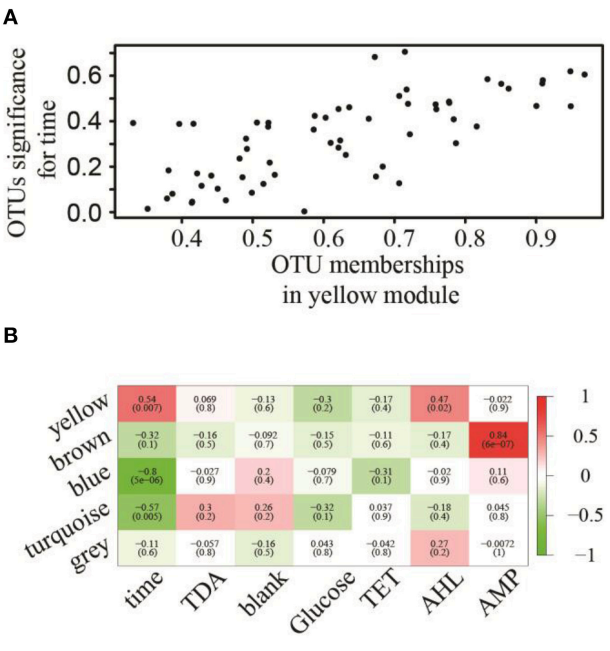

FIGURE 2 | Association of modules with external treatment factors. (A) OTUs associated with treatment–time with respect to their membership significance belonging to the yellow module. **(B)** Eigengene adjacencies heatmap identifying modules (row) that significantly associated with chemical treatments (column). Negative correlations (green) and positive correlations (red) indicate high adjacency (DiLeo et al., 2011), while white (zero) indicates low adjacency.

enriched by the *Alteromonadaceae* family (8 out of 11, $P < 0.05$, enrichment analysis) (**Figure 3**). Therefore, the apparent module substructures were associated with the taxonomical coherence of dominant OTUs.

Network Centralities and Identification of Hubs

To display an empirical base for discovery and to explore specific details of the substructures of the community, associations from the top 1000 OTUs ranked by coefficient were plotted. **Figure 4** shows the resulting microbial network consisting of 1000 nodes and 68,675 edges with average clustering network coefficient of 0.856, suggesting the down-selected OTUs constituted a highly connected network. The average number of network neighbors between all pairs of nodes was 137, and the network centralization was 0.768 as determined using NetworkAnalyzer (Doncheva et al., 2012). Hub nodes within respective modules are often proposed to be critical components for the network (Mayali and Azam, 2004). To identify species that may be acting as hubs, and thus be critically important components of the community network structure, we ranked nodes using various network centrality measures, including betweenness, closeness, neighborhood connectivity and topological coefficient (**Table 2**). Based on these measures, species from the *Alteromonas* and *Rhodobacteraceae* families were hypothesized to be key species influencing the inter-OTU relationships.

TDA Alter the Structure of the Microbial Community Associated with *N. salina*

Correlation network analysis led us to hypothesize that bacterial species from *Rhodobacteraceae* are key species in structuring the microbial community associated with *N. salina*. To gather

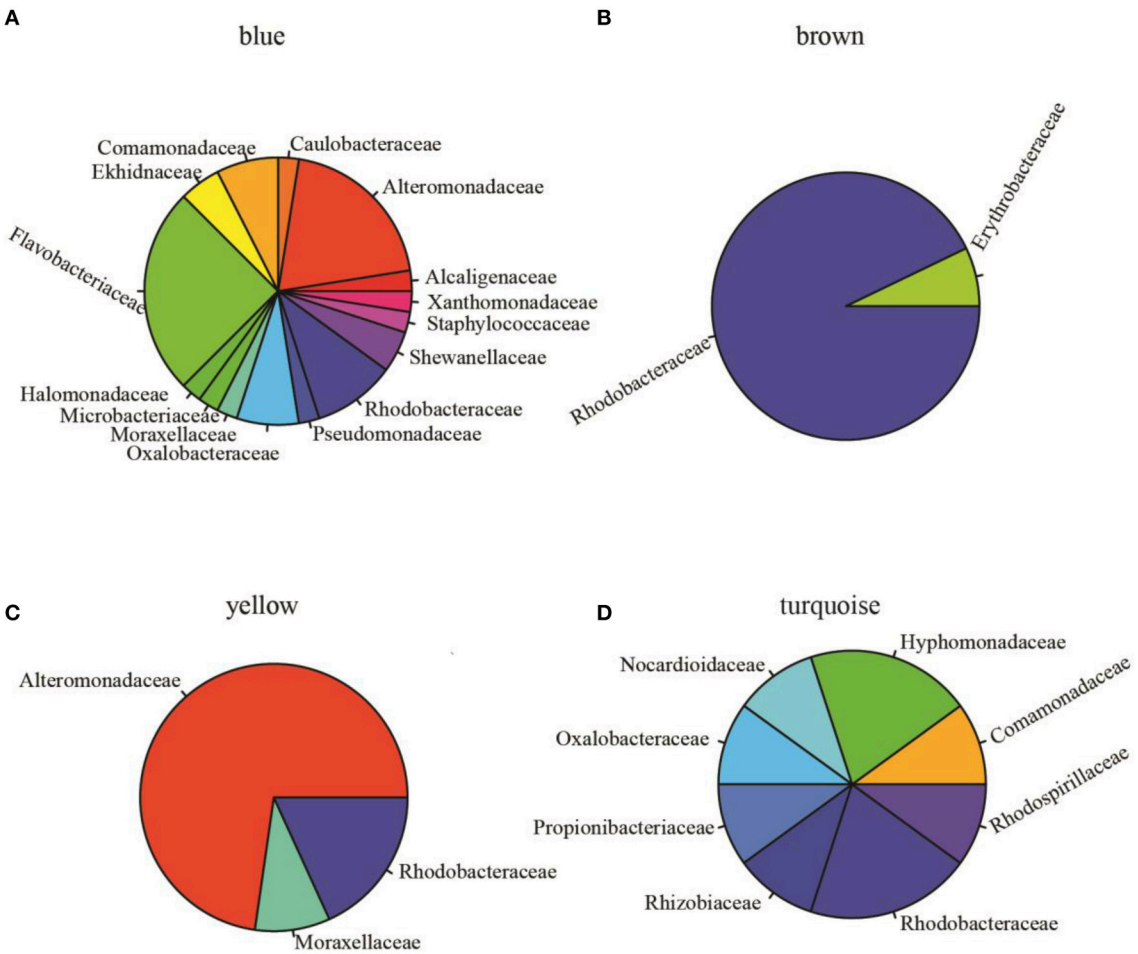

FIGURE 3 | Relative abundance of OTUs at the family level (indicated by different colors) in identified modules. (A) Blue module (total OTUs 40 annotated at family level, 127 OTUs unassigned at family level are not shown) was dominated by *Flavobacteriaceae* (25%, $n = 10$) and *Alteromonadaceae* (20%, $n = 8$). **(B)** Brown module (14 OTUs annotated, 63 unassigned) was dominated by *Rhodobacteraceae* (92%, $n = 13$). **(C)** Yellow module (total OTUs 11 annotated at family level) is comprised of *Alteromonadaceae* (72%, $n = 8$), *Rhodobacteraceae* (9.1%, $n = 1$), and *Moraxellaceae* (9.1%, $n = 1$). **(D)** Turquoise module (10 OTUs assigned to 8 families, 876 unassigned OTUs) is comprised of 8 families. These data showed that *Rhodobacteraceae* was significantly enriched in the brown module (one-sided Fisher's exact test, $P < 0.0001$) and *Alteromonadaceae* was significantly enriched in the yellow module (one-sided Fisher's exact test, $P < 0.05$).

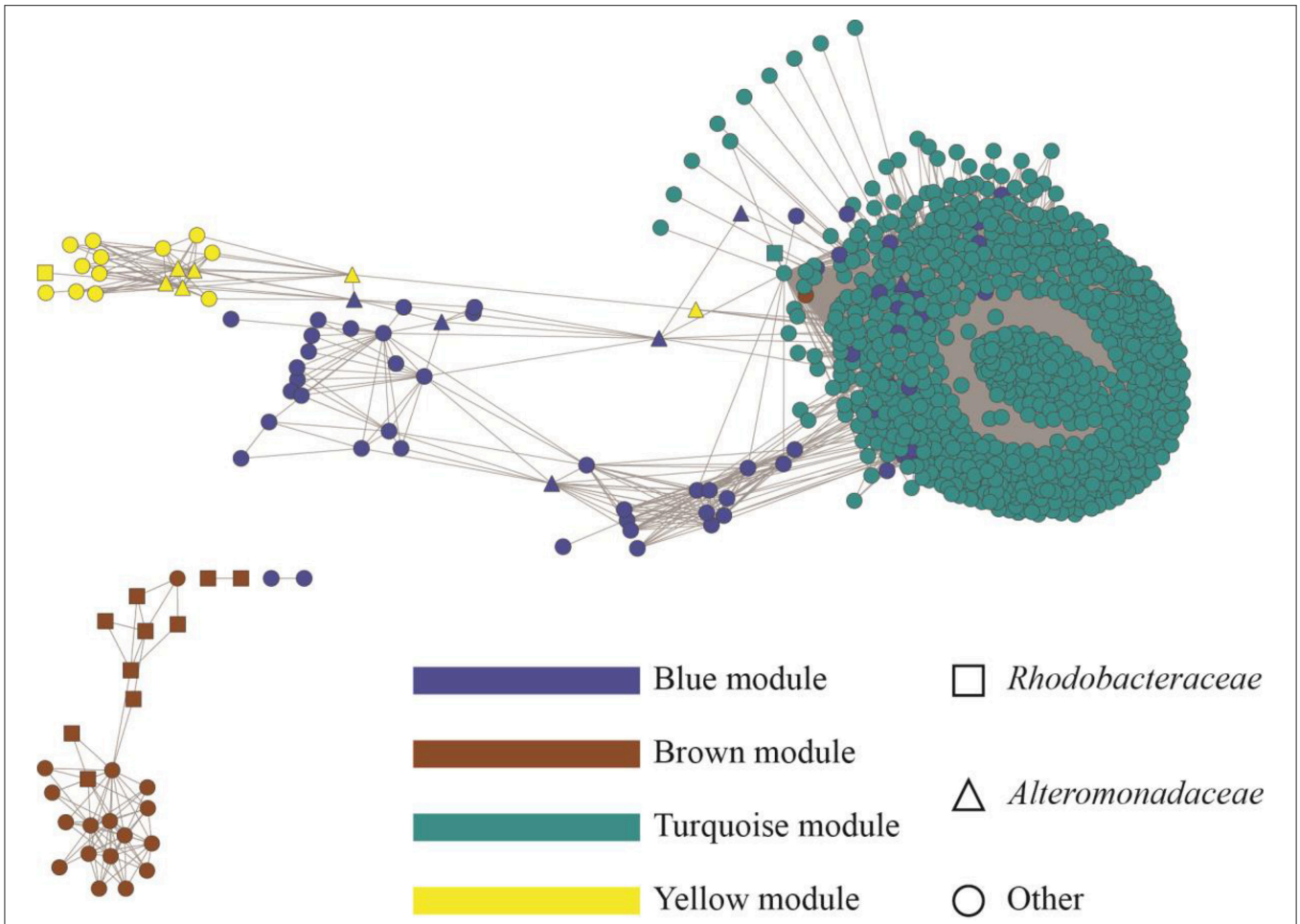

FIGURE 4 | Topology of the microbial community associated with *N. salina*. The identified modules were colored according to module names (Blue, Brown, Turquoise, and Yellow). The whole network contains 1000 nodes representing bacterial OTUs and 68,675 edges, showing correlations between the OTUs with an edge weight cutoff of 0.20 in the WGCNA network (DiLeo et al., 2011). OTUs were annotated at the family level. *Rhodobacteraceae* and *Alteromonadaceae* are shown as squares and triangles, respectively. OTUs from families other than *Rhodobacteraceae* and *Alteromonadaceae* are displayed as circle.

evidence for this hypothesis, we treated *N. salina* containing microbial communities with varying concentrations of TDA, a hallmark antibiotic in many species of the *Roseobacteria* clade in *Rhodobacteraceae,* and sampled the microbiota at 3 and 24 h time periods. Taxonomic distributions at the family-level across TDA-perturbed samples, grouped by exposure time, are illustrated in **Figure 5**. The largest taxa in all microbiota were populations of *Flavobacteriia*, *Alphaproteobacteria,* and *Gammaproteobacteria* bacterial classes. **Figure 5** also shows that the 24 h microbiota decreased in relative abundance of *Flavobacteriia* (23 ± 4%) and *Alphaproteobacteria* (14 ± 4%), comparted to 3 h (excluding TDA, 500 nM, 3 h) *Flavobacteriia* (39 ± 2%) and *Alphaproteobacteria* (32 ± 2%). Meanwhile, *Gammaproteobacteria* relative abundance at 24 h increased to 60 ± 9% compared to 3 h (excluding TDA, 500 nM, 3 h) *Gammaproteobacteria* (25 ± 9%). Of particular note, the microbiota (TDA, 500 nM, 3 h) was composed of *Flavobacteriia* (31 ± 1%), *Alphaproteobacteria* (21 ± 0%), and *Gammaproteobacteria* (45 ± 2%), suggesting it exhibits some compositional similarities to 24 h microbiota (**Figure 5**). PCoA of the data revealed patterns of beta-diversity (unweighted UniFrac distance metric) primarily forming two clusters differentiated by the time point at which the microbiota was sampled (**Figure 6**). Specifically, without TDA treatment, the microbiota at the 3-h time point were similar in structure to the starting microbiota (Unifrac distance, 0.03 ± 0.01). The addition of low doses of TDA (31.25 nM) slightly shifted the microbial composition over the 3-h time period (Unifrac distance, 0.05 ± 0.02). In contrast, treatment with higher TDA doses (500 nM) markedly shifted the composition away from the initial microbiota (Unifrac, 0.14 ± 0.02), and at the 3-h time point clustered with the samples obtained after 24 h. Hence, the data imply that microbiota exposed to 500 nM TDA will not only drastically restructure (as compared to the unperturbed community), but also hasten the progression of microbial community structure in a dose-dependent manner toward the more mature microbiota.

TABLE 2 | Identified "keystone" OTUs in co-abundance networks.

OTU ID[a]	Family[b]	Betweenness	Closeness	Neighborhood Connectivity	Topological Coefficient	Module Membership
268	NA[c]	0.51	0.71	8	0.36	Brown
179[d]	***Rhodobacteraceae***	**0.29**	**0.51**	**5**	**0.28**	**Brown**
1070	NA	0.14	0.9	151	0.16	Turquoise
264	*Erythrobacteraceae*	0.11	0.63	8	0.41	Brown
265	NA	0.08	0.62	8	0.43	Brown
267	NA	0.07	0.6	9	0.45	Brown
1057	NA	0.06	0.85	161	0.17	Turquoise
176	***Rhodobacteraceae***	**0.05**	**0.38**	**3**	**0.47**	**Brown**
91	***Alteromonadaceae***	**0.05**	**0.49**	**276**	**0.3**	**Blue**
126	***Rhodobacteraceae***	**0.05**	**0.47**	**10**	**0.53**	**Brown**
1040	NA	0.04	0.82	165	0.18	Turquoise
1009	NA	0.03	0.81	163	0.18	Turquoise
1066	NA	0.03	0.8	165	0.18	Turquoise
266	NA	0.03	0.56	10	0.51	Brown
1087	NA	0.02	0.79	168	0.18	Turquoise
1048	NA	0.02	0.8	167	0.18	Turquoise
131	***Rhodobacteraceae***	**0.02**	**0.52**	**10**	**0.5**	**Brown**
257	NA	0.02	0.55	10	0.54	Brown
89	***Alteromonadaceae***	**0.02**	**0.48**	**643**	**0.7**	**Yellow**
92	***Alteromonadaceae***	**0.02**	**0.33**	**11**	**0.44**	**Yellow**

[a] *Assigned OTU identity.*
[b] *OTU taxonomy at family level.*
[c] *NA, OTU taxonomic assignment not available at family level.*
[d] *Proposed "keystone" OTUs Rhodobacteraceae and Alteromonadaceae are highlighted in bold.*

DISCUSSION

Among the efforts to understand the complexity of microalgae microbiota, this current study is unique in that it aimed to chart multispecies relationships underpinning the substructure of microalgae microbiota. To achieve this aim, we experimentally perturbed a multispecies algal microbiota with various chemical treatments, quantified the changes to taxa profiles, and applied network analysis for modeling of interspecies relationship which provided a cohesive overview of the microbial community associated with *N. salina* structure.

It is well established that antibiotics can cause major disturbances within the ecological balance of microbiomes (Mayali and Azam, 2004). Thus, we postulated that antibiotic treatment provides an inferable means to introduce variations among bacterial species due to differential antibiotic susceptibility among them. Indeed, chemical treatments introduced major variations among the microbial communities within the same treatment time. High doses of antibiotic treatment noticeably shifted the overall microbiota structure. Thus, the generated 16S gene metagenomics profiles generally reflected microbiota changes in response to chemical perturbations.

These observations highlight two strengths of correlation network approach. First, rather than listing pair-wise correlations, all correlations were integrated into a unified network of interacting species, making it possible to identify small substructures within the microbiota. While this model is generated only by first-order correlations among species, it presents rich, albeit indirect, information on microbiota community structure, allowing us to explore and test species interactions and prioritize hypotheses. Specifically, the bacterial OTU variations resulting from a set of time-series chemical treatments allowed us to identify five modules emerging out of the complex *N. salina* microbial community. We demonstrated that members of *Rhodobacteraceae* dominated the brown OTUs module, which was significantly associated with ampicillin treatment (**Figure 3**). Reports have shown that species of the *Roseobacter* clade encode intrinsic β-lactamases and are resistant to β-lactam antibiotics such as ampicillin, with tolerance up to 500 μg/ml (Peng et al., 2011; Treangen et al., 2013). This is 10-fold greater than our high dose ampicillin treatment of 50 μg/ml. Meanwhile, bacteriostatic tetracycline, which inhibits bacteria from reproducing (Peng et al., 2011), surprisingly did not result in the formation of modules. Lack of module formation from tetracycline treatment in our experiments can be explained by the possibility of tetracycline activities being compromised by the formation of complexes with divalent cations (such as Mg^{2+}) prevalent in F/2 medium (Lambs et al., 1988; Treangen et al., 2013). In comparison, general metabolites such as glucose did not perturb the network significantly as evidenced by the absence of modules emerging from glucose-supplemented

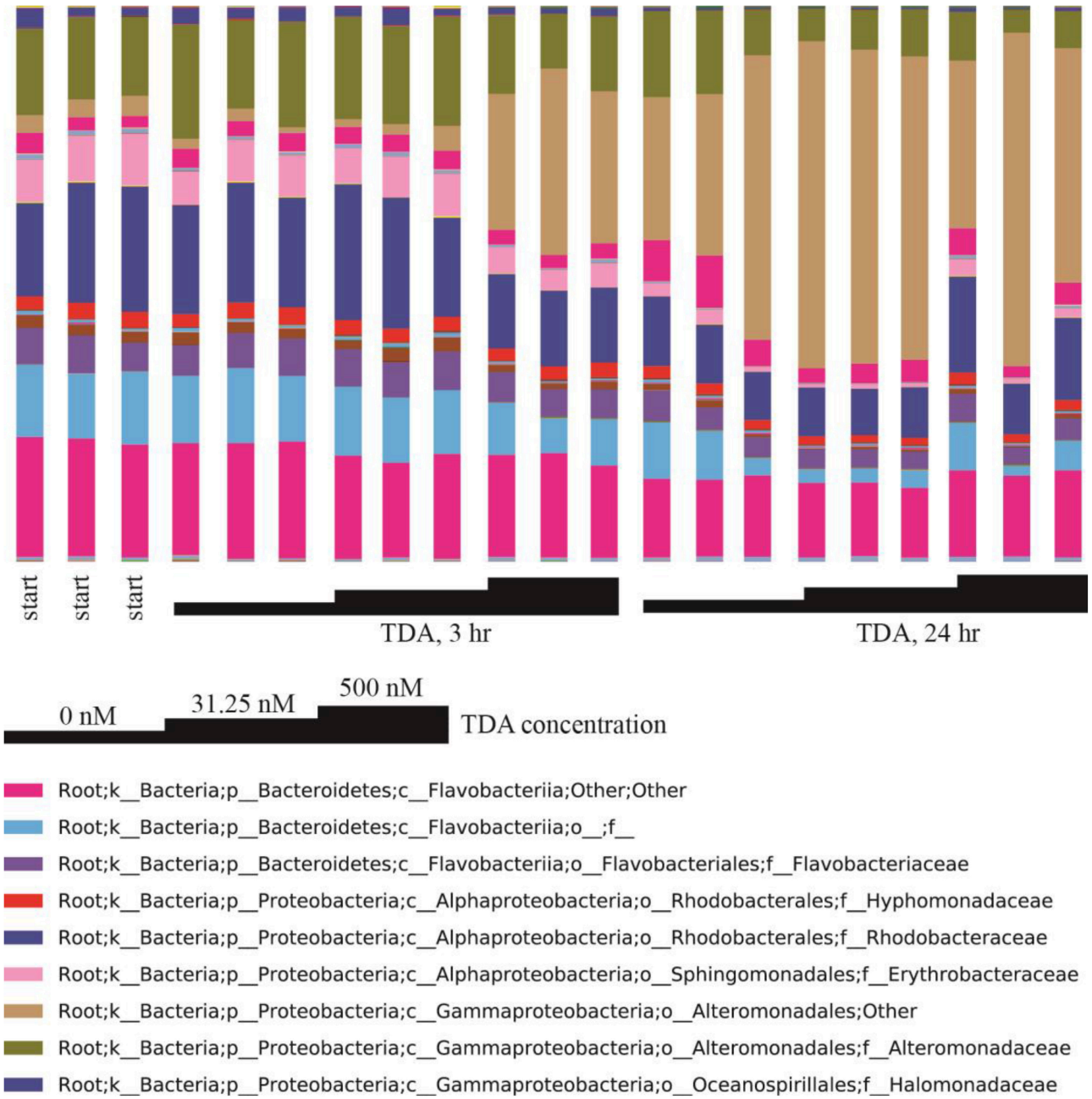

FIGURE 5 | Family-level taxonomic composition of TDA-perturbed microbiota. Triplicate samples are grouped by TDA concentration and exposure time. Taxonomic affiliations of OTUs are shown at the family level (see legend colors) and TDA treatment concentrations are indicated.

cultures. Overall, these results reflect that an OTU co-abundance network generated correlated associations from empirical data that recapitulates biological information, and therefore has value for further inference analysis.

While correlation analyses do not offer direct mechanistic interpretations, the formation of modules might stem from, for example, between-bacteria metabolic cross-feedings, biofilm formation of aggregated sub-communities, species couplings via chemical signaling or toxic compounds, which could result in bacterial species-species abundance correlations in 16S gene profile data sets. With our data sets, it appears the correlation network has applicability in mining subsets of microbial lineages that share common responsiveness to acute perturbation such as antibiotic treatment and is perhaps less applicable to those stemming from treatments (such as with ubiquitous metabolites) that do not significantly perturb bacterial abundance. Nevertheless, the integration of correlations into interconnected networks may be applied in

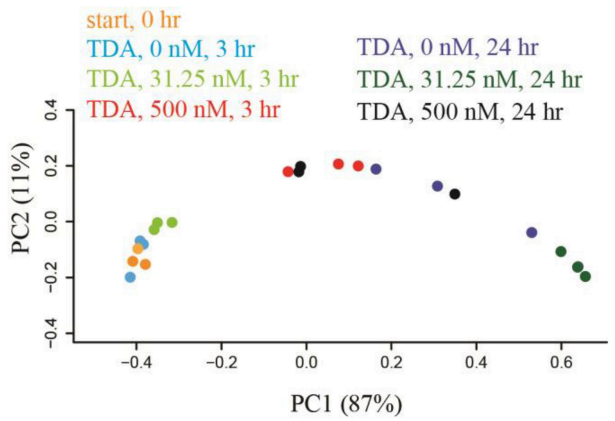

FIGURE 6 | Microbiota were shifted by TDA addition in a dose-dependent manner within 3 h treatment based on weight-Unifrac PCoA with respect to treatment time and TDA concentration. TDA (500 nM)-treated microbiota shifted the microbiota structure away from 3 h-microbiota cluster toward the 24 h-group.

bridging from bacterial species' activity to microbial community functionality.

Network centrality analysis has been successfully applied in multiple fields (Jeong et al., 2001; Rho et al., 2010; Duran-Pinedo et al., 2011), and we used it to mine influential bacterial species underpinning the interaction network of the microbial community associated with *N. salina*. The top *Rhodobacteraceae* OTU has low connectivity, suggesting it has few interaction with other OTUs in the network. Meanwhile, it has higher betweenness values compared to other OTUs. This pattern suggests modular organization of the network via a minimal number of connections required for information flow. These high-betweenness, low-connectivity OTUs may be conceptually thought of as "bridges" in the non-redundant shortest paths, the observation of which resembles previously reported properties of other biological networks (Joy et al., 2005). In comparison, the high-connectivity, low-betweenness case of *Alteromonadacea* suggests it lies on a large number of redundant shortest paths between other vertices. The difference between the network inferences of *Rhodobacteraceae* and *Alteromonadacea* is likely linked to distinct biological and ecological roles of these two groups. *Rhodobacteraceae*, which contains the *Roseobacter* clade, are one of the most ubiquitous and abundant bacterial lineages associated with phytoplankton both in environmental and laboratory cultures (Geng and Belas, 2010b; Amin et al., 2012) and has been shown to form close relationships with microalgae (Treangen et al., 2013; Kelder et al., 2014). The interactions among members of the *Roseobacter* clade (*Alphaproteobacteria*) and microalgae may occur through physical attachment (Miller and Belas, 2006; Mayali et al., 2008; Krohn-Molt et al., 2013), exchange of nutrients and metabolites (Keshtacher-Liebso et al., 1995; Howard et al., 2006), or antibiotics and signaling molecules (Brinkhoff et al., 2004; Seyedsayamdost et al., 2011; Amin et al., 2015). On the other hand, the marine bacteria from *Alteromonadaceae* are dominant phylotypes among microbial communities in response to the flux of organic matter in phytoplankton blooms, demonstrating how species of *Alteromonadaceae* could participate in structuring microalgae bacterial communities (McCarren et al., 2010; Tada et al., 2011).

To explore the possibility of the key species having influential effects on the overall configuration of the microbiota, we looked for evidence of microbiota responsiveness to the proposed key species. We subjected the *N. salina* microbial communities to varying doses of TDA, which is secreted as a hallmark bioactive compound in many species of the *Roseobacter* clade from *Rhodobacteraceae* family (Berger et al., 2011). TDA has both antibiotic and transcription induction activity in a subgroup of algae-associated bacterial genera that include *Phaeobacter*, *Silicibacter*, *Ruegeria*, and *Pseudovibrio* (Berger et al., 2011). Interestingly, we found that in general the relative abundance of *Rhodobacteraceae* decreased, while bacteria in *Alteromonadales* order of unclassified family increased in composition (**Figure 5**). These observed patterns between TDA and taxa composition are less clear since TDA activity to *Alteromonadales* has not been documented. Meanwhile the large total number of bacterial populations and differential bacterial growth rates in microbiota might have compounded the observed relative abundance. In terms of community structure, we observed shifting of microalgae microbiota induced by TDA dosage, and a 3 h 500 nM TDA treatment sufficiently skewed the original microbiota structure toward the 24 h unperturbed microbiota. This suggests that, given the myriad complexity in microbiota, microbial community associated with *N. salina* potentially harbors a dynamic property that responds to the presence of infochemicals exemplified by TDA. While the concentration of TDA produced naturally in either sea water or within the phycosphere is not documented, the involvement of bioactive compounds such as TDA in modulating microbiota structure has profound implications for bacterial community assemblages. Indeed, multiple bioactive compounds with various activities and specificities, such as indole-3-acetic acid (Amin et al., 2015) and indigoidine (Cude et al., 2012), have been characterized in many *Roseobacter* strains from microalgae microbiota (Buchan et al., 2005; Cude et al., 2012; Leiman et al., 2013; Treangen et al., 2013). In this context, the chemical composition and quantities of bioactive compounds from key species in microbiota may play a role in fine tuning of microbiota to different microbiota compositions and structures.

Our finding from network analysis therefore offers a tangible experimental metagenomics framework to tackle the following question: what is the structure of microbial community associated with *N. salina* if modeled from the species-species correlation network? Module formation in the microbiota network helps bridge the gap between deep knowledge of individual keystone OTUs and a systems-level view of the microbial community. But such application will have to tackle several issues. Given the connectivity of the correlation network, the correlation network model does not provide detailed mechanisms nor offer regulatory ramification of such variations. While accurate inter-OTU correlation analysis remains an area of active research, methods developed recently such as

CoNet (Faust et al., 2012), SparCC (Friedman and Alm, 2012), SPIEC-EASI (Kurtz et al., 2015), and MENA (Deng et al., 2012) could potentially be used to analyze inter-OTUs relationships in microalgae microbiota to improve association accuracy. Meanwhile, many of the remaining OTUs in modules have limited functional annotations due to the nature of 16S amplicon method. Such limitation, however, could be solved using metagenomics combined with metatranscriptomics to better understand microbiota roles in the ecosystem. In the long term, delineation of the substructure of the microbial community associated with *N. salina* may help us detect, investigate, and assess practical responsiveness of "key" species or probiotic species introduced into the microbiome to withstand environmental perturbations and improve microalgae production.

AUTHOR CONTRIBUTIONS

KS, TL, EY designed experiments. HG, EY, MT performed experiments. HG, KS analyzed and modeled data. HG, TD, EY, KS wrote manuscript.

ACKNOWLEDGMENTS

This work was supported by the Laboratory Directed Research and Development Program at Sandia National Laboratories, which is a multiprogram laboratory operated by Sandia Corporation, a Lockheed Martin Company, for the US Department of Energy's National Nuclear Security Administration under Contract DE-AC04-94AL85000. Additional funding was provided by the U.S. Department of Energy (DOE) Genomic Science Program under contract SCW1039.

SUPPLEMENTARY MATERIAL

The Supplementary Material for this article can be found online at: http://journal.frontiersin.org/article/10.3389/fmicb.2016.01155

Figure S1 | Modules of OTUs in chemical treated microbiotas network. Hierarchical clustering dendrogram of OTUs was built based on dissimilarity based on nodes topological overlap. Modules have been colored by module membership.

REFERENCES

Alavi, M., Miller, T., Erlandson, K., Schneider, R., and Belas, R. (2001). Bacterial community associated with *Pfiesteria*-like dinoflagellate cultures. *Environ. Microbiol.* 3, 380–396. doi: 10.1046/j.1462-2920.2001.00207.x

Amin, S. A., Hmelo, L. R., Van Tol, H. M., Durham, B. P., Carlson, L. T., Heal, K. R., et al. (2015). Interaction and signalling between a cosmopolitan phytoplankton and associated bacteria. *Nature* 522, 98–101. doi: 10.1038/nature14488

Amin, S. A., Parker, M. S., and Armbrust, E. V. (2012). Interactions between diatoms and bacteria. *Microbiol. Mol. Biol. Rev.* 76, 667–684. doi: 10.1128/MMBR.00007-12

Atkinson, S., and Williams, P. (2009). Quorum sensing and social networking in the microbial world. *J. R. Soc. Interface* 6, 959–978. doi: 10.1098/rsif.2009.0203

Bartram, A. K., Lynch, M. D. J., Stearns, J. C., Moreno-Hagelsieb, G., and Neufeld, J. D. (2011). Generation of multimillion-sequence 16S rRNA gene libraries from complex microbial communities by assembling paired-end Illumina reads. *Appl. Environ. Microbiol.* 77, 3846–3852. doi: 10.1128/AEM.02772-10

Berger, M., Neumann, A., Schulz, S., Simon, M., and Brinkhoff, T. (2011). Tropodithietic acid production in *Phaeobacter gallaeciensis* is regulated by N-acyl homoserine lactone-mediated quorum sensing. *J. Bacteriol.* 193, 6576–6585. doi: 10.1128/JB.05818-11

Berges, J. A., Franklin, D. J., and Harrison, P. J. (2001). Evolution of an artificial seawater medium: improvements in enriched seawater, artificial water over the last two decades. *J. Phycol.* 37, 1138–1145. doi: 10.1046/j.1529-8817.2001.01052.x

Brinkhoff, T., Bach, G., Heidorn, T., Liang, L., Schlingloff, A., and Simon, M. (2004). Antibiotic production by a Roseobacter clade-affiliated species from the German Wadden Sea and its antagonistic effects on indigenous isolates. *Appl. Environ. Microbiol.* 70, 2560–2565. doi: 10.1128/AEM.70.4.2560-2565.2003

Bruhn, J. B., Gram, L., and Belas, R. (2007). Production of antibacterial compounds and biofilm formation by *Roseobacter* species are influenced by culture conditions. *Appl. Environ. Microbiol.* 73, 442–450. doi: 10.1128/AEM.02238-06

Buchan, A., Gonzalez, J. M., and Moran, M. A. (2005). Overview of the marine *Roseobacter* lineage. *Appl. Environ. Microbiol.* 71, 5665–5677. doi: 10.1128/AEM.71.10.5665-5677.2005

Caporaso, J. G., Kuczynski, J., Stombaugh, J., Bittinger, K., Bushman, F. D., Costello, E. K., et al. (2010). QIIME allows analysis of high-throughput community sequencing data. *Nat. Methods* 7, 335–336. doi: 10.1038/nmeth.f.303

Carney, L. T., Reinsch, S. S., Lane, P. D., Solberg, O. D., Jansen, L. S., Williams, K. P., et al. (2014). Microbiome analysis of a microalgal mass culture growing in municipal wastewater in a prototype OMEGA photobioreactor. *Algal Res.* 4, 52–61. doi: 10.1016/j.algal.2013.11.006

Choi, J. K., Yu, U., Yoo, O. J., and Kim, S. (2005). Differential coexpression analysis using microarray data and its application to human cancer. *Bioinformatics* 21, 4348–4355. doi: 10.1093/bioinformatics/bti722

Cole, J. J. (1982). Interactions between bacteria and algae in aquatic ecosystems. *Annu. Rev. Ecol. Syst.* 13, 291–314. doi: 10.1146/annurev.es.13.110182.001451

Costello, E. K., Lauber, C. L., Hamady, M., Fierer, N., Gordon, J. I., and Knight, R. (2009). Bacterial community variation in human body habitats across space and time. *Science* 326, 1694–1697. doi: 10.1126/science.1177486

Cude, W. N., Mooney, J., Tavanaei, A. A., Hadden, M. K., Frank, A. M., Gulvik, C. A., et al. (2012). Production of the antimicrobial secondary metabolite indigoidine contributes to competitive surface colonization by the marine roseobacter Phaeobacter sp. Strain Y4I. *Appl. Environ. Microbiol.* 78, 4771–4780. doi: 10.1128/AEM.00297-12

D'Alvise, P. W., Lillebo, S., Prol-Garcia, M. J., Wergeland, H. I., Nielsen, K. F., Bergh, O., et al. (2012). Phaeobacter gallaeciensis reduces *Vibrio anguillarum* in cultures of microalgae and rotifers, and prevents vibriosis in cod larvae. *PLoS ONE* 7:e43996. doi: 10.1371/journal.pone.0043996

Dandekar, A. A., Chugani, S., and Greenberg, E. P. (2012). Bacterial quorum sensing and metabolic incentives to cooperate. *Science* 338, 264–266. doi: 10.1126/science.1227289

Deng, Y., Jiang, Y. H., Yang, Y., He, Z., Luo, F., and Zhou, J. (2012). Molecular ecological network analyses. *BMC Bioinformatics* 13:113. doi: 10.1186/1471-2105-13-113

DeSantis, T. Z., Hugenholtz, P., Larsen, N., Rojas, M., Brodie, E. L., Keller, K., et al. (2006). Greengenes, a chimera-checked 16S rRNA gene database and workbench compatible with ARB. *Appl. Environ. Microbiol.* 72, 5069–5072. doi: 10.1128/AEM.03006-05

DiLeo, M. V., Strahan, G. D., Den Bakker, M., and Hoekenga, O. A. (2011). Weighted correlation network analysis (WGCNA) applied to the tomato fruit metabolome. *PLoS ONE* 6:e26683. doi: 10.1371/journal.pone.0026683

Doncheva, N. T., Assenov, Y., Domingues, F. S., and Albrecht, M. (2012). Topological analysis and interactive visualization of biological networks and protein structures. *Nat. Protoc.* 7, 670–685. doi: 10.1038/nprot.2012.004

Duran-Pinedo, A. E., Paster, B., Teles, R., and Frias-Lopez, J. (2011). Correlation network analysis applied to complex biofilm communities. *PLoS ONE* 6:e28438. doi: 10.1371/journal.pone.0028438

Faust, K., Sathirapongsasuti, J. F., Izard, J., Segata, N., Gevers, D., Raes, J., et al. (2012). Microbial co-occurrence relationships in the human microbiome. *PLoS Comput. Biol.* 8:e1002606. doi: 10.1371/journal.pcbi.1002606

Friedman, J., and Alm, E. J. (2012). Inferring correlation networks from genomic survey data. *PLoS Comput. Biol.* 8:e1002687. doi: 10.1371/journal.pcbi.1002687

Ge, H., Liu, Z., Church, G. M., and Vidal, M. (2001). Correlation between transcriptome and interactome mapping data from *Saccharomyces cerevisiae*. *Nat. Genet.* 29, 482–486. doi: 10.1038/ng776

Geng, H., and Belas, R. (2010a). Expression of tropodithietic acid biosynthesis is controlled by a novel autoinducer. *J. Bacteriol.* 192, 4377–4387. doi: 10.1128/JB.00410-10

Geng, H., and Belas, R. (2010b). Molecular mechanisms underlying roseobacter-phytoplankton symbioses. *Curr. Opin. Biotechnol.* 21, 332–338. doi: 10.1016/j.copbio.2010.03.013

Geng, H., Sale, K. L., Tran-Gyamfi, M. B., Lane, T. W., and Yu, E. T. (2016). Longitudinal analysis of microbiota in microalga *Nannochloropsis salina* cultures. *Microb. Ecol.* 72, 14–24. doi: 10.1007/s00248-016-0746-4

Gilbert, J. A., Steele, J. A., Caporaso, J. G., Steinbruck, L., Reeder, J., Temperton, B., et al. (2012). Defining seasonal marine microbial community dynamics. *ISME J.* 6, 298–308. doi: 10.1038/ismej.2011.107

Gonzalez, A., King, A., Robeson Ii, M. S., Song, S., Shade, A., Metcalf, J. L., et al. (2012). Characterizing microbial communities through space and time. *Curr. Opin. Biotechnol.* 23, 431–436. doi: 10.1016/j.copbio.2011.11.017

Gonzalez, J. M., and Moran, M. A. (1997). Numerical dominance of a group of marine bacteria in the alpha-subclass of the class Proteobacteria in coastal seawater. *Appl. Environ. Microbiol.* 63, 4237–4242.

Hold, G. L., Smith, E. A., Birkbeck, T. H., and Gallacher, S. (2001). Comparison of paralytic shellfish toxin (PST) production by the dinoflagellates *Alexandrium lusitanicum* NEPCC 253 and *Alexandrium tamarense* NEPCC 407 in the presence and absence of bacteria. *FEMS Microbiol. Ecol.* 36, 223–234. doi: 10.1111/j.1574-6941.2001.tb00843.x

Howard, E. C., Henriksen, J. R., Buchan, A., Reisch, C. R., Bürgmann, H., Welsh, R., et al. (2006). Bacterial taxa that limit sulfur flux from the Ocean. *Science* 314, 649–652. doi: 10.1126/science.1130657

Jeong, H., Mason, S. P., Barabasi, A. L., and Oltvai, Z. N. (2001). Lethality and centrality in protein networks. *Nature* 411, 41–42. doi: 10.1038/35075138

Joy, M. P., Brock, A., Ingber, D. E., and Huang, S. (2005). High-betweenness proteins in the yeast protein interaction network. *J. Biomed. Biotechnol.* 2005, 96–103. doi: 10.1155/JBB.2005.96

Kayser, H. (1979). Growth interactions between marine dinoflagellates in multispecies culture experiments. *Mar. Biol.* 52, 357–369. doi: 10.1007/BF00389077

Kelder, T., Stroeve, J. H. M., Bijlsma, S., Radonjic, M., and Roeselers, G. (2014). Correlation network analysis reveals relationships between diet-induced changes in human gut microbiota and metabolic health. *Nutr. Diabetes* 4, e122. doi: 10.1038/nutd.2014.18

Keshtacher-Liebso, E., Hadar, Y., and Chen, Y. (1995). Oligotrophic bacteria enhance algal growth under iron-deficient conditions. *Appl. Environ. Microbiol.* 61, 2439–2441.

Krohn-Molt, I., Wemheuer, B., Alawi, M., Poehlein, A., Gullert, S., Schmeisser, C., et al. (2013). Metagenome survey of a multispecies and alga-associated biofilm revealed key elements of bacterial-algal interactions in photobioreactors. *Appl. Environ. Microbiol.* 79, 6196–6206. doi: 10.1128/AEM.01641-13

Kurtz, Z. D., Muller, C. L., Miraldi, E. R., Littman, D. R., Blaser, M. J., and Bonneau, R. A. (2015). Sparse and compositionally robust inference of microbial ecological networks. *PLoS Comput. Biol.* 11:e1004226. doi: 10.1371/journal.pcbi.1004226

Lambs, L., Venturini, M., Decock-Le Reverend, B., Kozlowski, H., and Berthon, G. (1988). Metal ion-tetracycline interactions in biological fluids. Part 8. Potentiometric and spectroscopic studies on the formation of Ca(II) and Mg(II) complexes with 4-dedimethylamino-tetracycline and 6-desoxy-6-demethyl-tetracycline. *J. Inorg. Biochem.* 33, 193–210. doi: 10.1016/0162-0134(88)80049-7

Lee, S.-O., Kato, J., Takiguchi, N., Kuroda, A., Ikeda, T., Mitsutani, A., et al. (2000). Involvement of an extracellular protease in algicidal activity of the marine bacterium *Pseudoalteromonas* sp. strain A28. *Appl. Environ. Microbiol.* 66, 4334–4339. doi: 10.1128/AEM.66.10.4334-4339.2000

Leiman, S. A., May, J. M., Lebar, M. D., Kahne, D., Kolter, R., and Losick, R. (2013). D-amino acids indirectly inhibit biofilm formation in *Bacillus subtilis* by interfering with protein synthesis. *J. Bacteriol.* 195, 5391–5395. doi: 10.1128/JB.00975-13

Lovejoy, C., Bowman, J. P., and Hallegraeff, G. M. (1998). Algicidal effects of a novel marine pseudoalteromonas isolate (class Proteobacteria, gamma subdivision) on harmful algal bloom species of the genera Chattonella, Gymnodinium, and Heterosigma. *Appl. Environ. Microbiol.* 64, 2806–2813.

Lozupone, C., and Knight, R. (2005). UniFrac: a new phylogenetic method for comparing microbial communities. *Appl. Environ. Microbiol.* 71, 8228–8235. doi: 10.1128/AEM.71.12.8228-8235.2005

Mayali, X., and Azam, F. (2004). Algicidal bacteria in the Sea and their impact on algal blooms1. *J. Eukaryot. Microbiol.* 51, 139–144. doi: 10.1111/j.1550-7408.2004.tb00538.x

Mayali, X., Franks, P. J. S., and Azam, F. (2008). Cultivation and ecosystem role of a marine roseobacter clade-affiliated cluster bacterium. *Appl. Environ. Microbiol.* 74, 2595–2603. doi: 10.1128/AEM.02191-07

McCarren, J., Becker, J. W., Repeta, D. J., Shi, Y., Young, C. R., Malmstrom, R. R., et al. (2010). Microbial community transcriptomes reveal microbes and metabolic pathways associated with dissolved organic matter turnover in the sea. *Proc. Natl. Acad. Sci. U.S.A.* 107, 16420–16427. doi: 10.1073/pnas.1010732107

Miller, T. R., and Belas, R. (2006). Motility is involved in Silicibacter sp. TM1040 interaction with dinoflagellates. *Environ. Microbiol.* 8, 1648–1659. doi: 10.1111/j.1462-2920.2006.01071.x

Peng, Y., Leung, H. C., Yiu, S. M., and Chin, F. Y. (2011). Meta-IDBA: a *de novo* assembler for metagenomic data. *Bioinformatics* 27, i94–i101. doi: 10.1093/bioinformatics/btr216

Porsby, C. H., Webber, M. A., Nielsen, K. F., Piddock, L. J., and Gram, L. (2011). Resistance and tolerance to tropodithietic acid, an antimicrobial in aquaculture, is hard to select. *Antimicrob. Agents Chemother.* 55, 1332–1337. doi: 10.1128/AAC.01222-10

Raes, J., and Bork, P. (2008). Molecular eco-systems biology: towards an understanding of community function. *Nat. Rev. Microbiol.* 6, 693–699. doi: 10.1038/nrmicro1935

Rho, M., Tang, H., and Ye, Y. (2010). FragGeneScan: predicting genes in short and error-prone reads. *Nucleic Acids Res.* 38, e191. doi: 10.1093/nar/gkq747

Rodrigue, S., Materna, A. C., Timberlake, S. C., Blackburn, M. C., Malmstrom, R. R., Alm, E. J., et al. (2010). Unlocking short read sequencing for metagenomics. *PLoS ONE* 5:e11840. doi: 10.1371/journal.pone.0011840

Sambrook, J., Fritsch, E. F., and Maniatis., T. (1989). *Molecular Cloning: A Laboratory Manual*. Cold Spring Harbor, NY: Cold Spring Harbor Laboratory Press.

Seyedsayamdost, M. R., Case, R. J., Kolter, R., and Clardy, J. (2011). The Jekyll-and-Hyde chemistry of *Phaeobacter gallaeciensis*. *Nat. Chem.* 3, 331–335. doi: 10.1038/nchem.1002

Sison-Mangus, M. P., Jiang, S., Tran, K. N., and Kudela, R. M. (2014). Host-specific adaptation governs the interaction of the marine diatom, Pseudo-nitzschia and their microbiota. *ISME J.* 8, 63–76. doi: 10.1038/ismej.2013.138

Smoot, M. E., Ono, K., Ruscheinski, J., Wang, P. L., and Ideker, T. (2011). Cytoscape 2.8: new features for data integration and network visualization. *Bioinformatics* 27, 431–432. doi: 10.1093/bioinformatics/btq675

Sul, W. J., Cole, J. R., Jesus Eda, C., Wang, Q., Farris, R. J., Fish, J. A., et al. (2011). Bacterial community comparisons by taxonomy-supervised analysis independent of sequence alignment and clustering. *Proc. Natl. Acad. Sci. U.S.A.* 108, 14637–14642. doi: 10.1073/pnas.1111435108

Tada, Y., Taniguchi, A., Nagao, I., Miki, T., Uematsu, M., Tsuda, A., et al. (2011). Differing growth responses of major phylogenetic groups of marine bacteria to natural phytoplankton blooms in the western North Pacific Ocean. *Appl. Environ. Microbiol.* 77, 4055–4065. doi: 10.1128/AEM.02952-10

Team, R. C. (2015). *R: A Language and Environment for Statistical Computing*. Vienna: R Foundation for Statistical Computing.

Treangen, T. J., Koren, S., Sommer, D. D., Liu, B., Astrovskaya, I., Ondov, B., et al. (2013). MetAMOS: a modular and open source metagenomic

assembly and analysis pipeline. *Genome Biol.* 14:R2. doi: 10.1186/gb-2013-14-1-r2

Wagner-Dobler, I., Thiel, V., Eberl, L., Allgaier, M., Bodor, A., Meyer, S., et al. (2005). Discovery of complex mixtures of novel long-chain quorum sensing signals in free-living and host-associated marine alphaproteobacteria. *Chembiochem* 6, 2195–2206. doi: 10.1002/cbic.200500189

Yoon, J., Blumer, A., and Lee, K. (2006). An algorithm for modularity analysis of directed and weighted biological networks based on edge-betweenness centrality. *Bioinformatics* 22, 3106–3108. doi: 10.1093/bioinformatics/btl533

Conflict of Interest Statement: The authors declare that the research was conducted in the absence of any commercial or financial relationships that could be construed as a potential conflict of interest.

frontiers in Microbiology

REVIEW
published: 18 May 2016
doi: 10.3389/fmicb.2016.00673

Metabolic Network Modeling of Microbial Interactions in Natural and Engineered Environmental Systems

Octavio Perez-Garcia[1], Gavin Lear[2] and Naresh Singhal[1]**

[1] Department of Civil and Environmental Engineering, University of Auckland, Auckland, New Zealand, [2] School of Biological Sciences, The University of Auckland, Auckland, New Zealand

We review approaches to characterize metabolic interactions within microbial communities using Stoichiometric Metabolic Network (SMN) models for applications in environmental and industrial biotechnology. SMN models are computational tools used to evaluate the metabolic engineering potential of various organisms. They have successfully been applied to design and optimize the microbial production of antibiotics, alcohols and amino acids by single strains. To date however, such models have been rarely applied to analyze and control the metabolism of more complex microbial communities. This is largely attributed to the diversity of microbial community functions, metabolisms, and interactions. Here, we firstly review different types of microbial interaction and describe their relevance for natural and engineered environmental processes. Next, we provide a general description of the essential methods of the SMN modeling workflow including the steps of network reconstruction, simulation through Flux Balance Analysis (FBA), experimental data gathering, and model calibration. Then we broadly describe and compare four approaches to model microbial interactions using metabolic networks, i.e., (i) lumped networks, (ii) compartment per guild networks, (iii) bi-level optimization simulations, and (iv) dynamic-SMN methods. These approaches can be used to integrate and analyze diverse microbial physiology, ecology and molecular community data. All of them (except the lumped approach) are suitable for incorporating species abundance data but so far they have been used only to model simple communities of two to eight different species. Interactions based on substrate exchange and competition can be directly modeled using the above approaches. However, interactions based on metabolic feedbacks, such as product inhibition and synthropy require extensions to current models, incorporating gene regulation and compounding accumulation mechanisms. SMN models of microbial interactions can be used to analyze complex "omics" data and to infer and optimize metabolic processes. Thereby, SMN models are suitable to capitalize on advances in high-throughput molecular and metabolic data generation. SMN models are starting to be applied to describe microbial interactions during wastewater treatment, *in-situ* bioremediation, microalgae blooms methanogenic fermentation, and bioplastic production. Despite their current challenges, we envisage that SMN models have future potential for the design and development of novel growth media, biochemical pathways and synthetic microbial associations.

Keywords: environmental biotechnology, systems biology, microbial communities, process engineering, metabolic network, genome-scale metabolic model, flux balance analysis, wastewater treatment

OPEN ACCESS

Edited by:
Xavier Mayali, Lawrence Livermore National Laboratory, USA

Reviewed by:
Frank J. Bruggeman, Netherlands Institute for Systems Biology, Netherlands
Ali Navid, Lawrence Livermore National Laboratory, USA

****Correspondence:***
Octavio Perez-Garcia
octavio.perez@auckland.ac.nz;
Naresh Singhal
n.singhal@auckland.ac.nz

Specialty section:
This article was submitted to Aquatic Microbiology, a section of the journal Frontiers in Microbiology

Received: *19 January 2016*
Accepted: *25 April 2016*
Published: *18 May 2016*

Citation:
Perez-Garcia O, Lear G and Singhal N (2016) Metabolic Network Modeling of Microbial Interactions in Natural and Engineered Environmental Systems. Front. Microbiol. 7:673. doi: 10.3389/fmicb.2016.00673

INTRODUCTION

Microbial communities, and the biochemical and ecological interactions occurring in and among them, are ubiquitous in nature. They are vital for human as well as for environmental health, and are manipulated in systems ranging from wastewater treatment plants and agricultural crops to human digestive tracts. Advances in computational tools such as Stoichiometric Metabolic Network (SMN) models and their simulation algorithms [e.g., Flux Balance Analysis (FBA)] are enabling the *in silico* analysis of microbial interactions to enhance desirable metabolic attributes. Community members or metabolic features identified with model predictions can, in theory, be manipulated to control the exchange of metabolic compounds of relevance for environmental protection or industrial applications. Here, we provide an overview of how microbial interactions can be modeled using stoichiometric metabolic networks as well as the main challenges to achieve this. We also describe how such models are starting to be applied to analyze and control natural and engineered environmental systems. Our target audiences are microbiologists, ecologists, and environmental/process engineers who are not currently familiar with metabolic network modeling.

THE BIG PICTURE

Newer technologies for environmental assessment, waste treatment, and valuable chemical generation are required to achieve equilibrium between socio-economic development and the environment. Growing concerns about the lack of sustainability of past economic growth patterns, and increased awareness of a potential future water and climate crisis, have made clear that the environment and the economy can no longer be considered in isolation from one another. For instance, the global population is expected to increase by 13%, from 7.3 billion in 2015 to 8.3 billion by 2030, (OECD, 2009). This will lead to increased needs for clean water, energy, food, animal feed, fiber for clothing, and housing, therefore putting more strain on our natural environment. As noted in a strategic document by the Organization for Economic Cooperation and Development (OECD, 2011), a return to sustained and sustainable growth will depend upon innovation that delivers a much greener growth model. In this context, environmental and industrial applications of biotechnology, and in particular, applications involving microbial communities, are expected to underpin future innovation. Indeed microbial communities are already developed, used and controlled for the treatment of contaminated environments (land, air, water) and for sustainable manufacturing of valuable chemicals (Kleerebezem and van Loosdrecht, 2007; Miller et al., 2010; Vallero, 2010; Agler et al., 2011; Marshall et al., 2013). SMN modeling, in addition to microbial ecology, fermentation technology, "omics" technologies and process engineering, can assist the development and optimization of many critical microbial processes.

ENVIRONMENTAL PROCESSES INVOLVING MICROBIAL INTERACTIONS

Members of microbial communities interact with one another by trading metabolites or by exchanging dedicated molecular signals to detect and respond to each other's presence (Brenner et al., 2008). These interactions enable the division of labor whereby the overall output of the community results from the combination of tasks performed by constituent individuals or sub-populations (Teague and Weiss, 2015). Microbial guilds (also called ecological functional groups) are groups of organisms within the community that exploit a class of environmental resource in a similar way. A particular microbial community can be dominated by one or many guilds (Begon et al., 2005). The overall chemical conversions resulting from guilds' metabolic activity (e.g., compound or biomass formation) are termed bioprocesses (Miller et al., 2010). Environmental bioprocesses of human interest are catalyzed by a wide variety of microbial guilds (**Table 1**) and can be categorized as those involved in major biogeochemical cycles (which are generally applied to remove pollutants from water, soil, and air) and those involved in the production of organic compounds (which are applied for the production of valuable chemicals such as alcohols, methane, or lipids). By interacting with each other, the microbial guilds act as "functional bricks" by which both natural and artificial microbial communities are assembled. Thus, the diversity of environmental bioprocesses is largely defined by the diversity of microbial guilds.

Definition of Microbial Interactions

Guilds or species interactions in microbial communities can be either metabolism-based or be driven by ecological traits. Several good reviews have summarized the study of ecological interactions among microbes in synthetic as well as in natural microbial communities (Faust and Raes, 2012; Mitri and Richard Foster, 2013). Here, we emphasize the role of metabolism in driving species interactions and *vice versa*, since metabolism-based views allow the creation of both theoretical mechanistic models and experimental manipulation.

The net effect of the metabolic interaction between species/guild A on a second species/guild B can be positive (+), negative (−) or neutral (0, no impact on the species involved) (Faust and Raes, 2012; Großkopf and Soyer, 2014). The possible combinations of win, lose, or neutral outcomes for two interaction partners allow the classification of nine interaction types. However, if interaction directionality is neglected (i.e., +/− is considered the same as −/+), there are six basal interaction patterns. **Figure 1** depicts these interaction patterns by ecological and a corresponding metabolic representation (i.e., the communication between species via their metabolic products). Since, the combinatorial explosion of possible interaction states quickly reaches large numbers with only a few species, the challenge is to find key interactions that are over-represented in nature or that can have significant percolating effects at the community level (e.g., stabilizing or de-stabilizing interactions) (Großkopf and Soyer, 2014). Indeed, microbial interaction networks, like human social networks, generally imply the presence of many taxa with only a few links and a few

TABLE 1 | Common environmental processes catalyzed by microbial guilds.

Catalytic microbial guild	Catalyzed environmental process	Service/Application	Guild's model species	References
Aerobic heterotrophic bacteria	Organic carbon degradation (breakdown of suspended carbon to soluble carbon)	Organic matter removal from wastewater	Bacteroidetes α- and β- proteobacteria, *Acidovorax* spp., *Fermicutes* spp.	Wagner and Loy, 2002; Wagner et al., 2002; Das et al., 2011
	Organic carbon oxidation (soluble carbon to CO_2)	Organic matter removal from wastewater	Bacteroidetes α- and β- proteobacteria, *Acidovorax* spp., *Fermicutes* spp.	Wagner and Loy, 2002; Wagner et al., 2002; Das et al., 2011
	Proteolysis (organic nitrogen to NH_4^+)	Global nitrogen cycle, organic matter removal from wastewater	Bacteroidetes α- and β- proteobacteria, *Acidovorax* spp., *Fermicutes* spp.	Wagner and Loy, 2002; Wagner et al., 2002; Das et al., 2011; Schreiber et al., 2012
Heterotrophic denitrifiers	Denitrification (NO_3^-/NO_2^- reduction to N_2)	Global nitrogen cycle, biological nitrogen removal from wastewater	*Paracoccus denitrifican, Pseudomonas aeruginosa, Acidovorax* spp., α-, and β-Proteobacteria	Ferguson, 1998; Brown, 2010; Kraft et al., 2011; Schreiber et al., 2012
Autotrophic nitrifiers, including both, ammonia oxidizing bacteria (AOB) and nitrite oxidizing bacteria (NOB)	Nitritation (NH_4^+ oxidation to NO_2^-)	Global nitrogen cycle, nitrogen removal from wastewater	*Nitrosomonas europaea, Nitrosomonas eutropha, Nitrosospira* spp.	Hooper, 1991; Arp et al., 2002; Chain et al., 2003; Ferguson et al., 2007; Perez-Garcia et al., 2014b
	Nitratation (NO_2^- oxidation to NO_3^-)	Global nitrogen cycle, nitrogen removal from wastewater	*Nitrospira defluvii, Nitrobacter* spp.	Freitag and Bock, 1990; Ferguson et al., 2007; Lücker et al., 2010; Schreiber et al., 2012
	Nitrifier denitrification and hydroxylamine incomplete oxidation (production of NO and N_2O)	Production and emission green house and ozone depleting gases	*Nitrosomonas europaea, Nitrosomonas eutropha*	Shaw et al., 2006; Yu et al., 2010; Chandran et al., 2011; Schreiber et al., 2012
Anaerobic ammonium oxidizers (ANAMMOX)	Ammonium oxidation to di-nitrogen gas (NH_4^+ oxidation to N_2)	Global nitrogen cycle, nitrogen removal from wastewater	*Kuenenia stuttgartiensis*, *Candidatus* Jettenia asiatica, *Brocardia anammoxidans*	Kuypers et al., 2003; Kuenen, 2008; Hu et al., 2012
Glycogen accumulating organisms (GAOs)	Anaerobic glycogen formation (carbon uptake and storage compound formation without phosphorus release)	Phosphorus removal from wastewater	*Micropruina glycogenica, Tetrasphaera* spp., *Amaricoccus* spp.	Seviour et al., 2003; de-Bashan and Bashan, 2004; Martín et al., 2006; Wilmes et al., 2008
Phosphate accumulating organisms (PAOs)	Anaerobic phosphorus release (hydrolysis of intracellular polyphosphates for carbon uptake and storage compound formation)	Phosphorus removal from wastewater	*Acinetobacter* spp., *Microlunatus phosphovorus, Clostridium* spp., *Candidatus* Accumulibacter phosphatis	Seviour et al., 2003; de-Bashan and Bashan, 2004; Martín et al., 2006; Wilmes et al., 2008
	Aerobic phosphorus uptake (storage compound degradation accompanied by soluble phosphorus uptake)	Phosphorus removal from wastewater	*Acinetobacter* spp., *Microlunatus phosphovorus, Candidatus* Accumulibacter phosphatis	Seviour et al., 2003; de-Bashan and Bashan, 2004; Martín et al., 2006; Wilmes et al., 2008
Polyhydroxyalkanoates (PHA) accumulating bacteria	Anaerobic formation of carbon storage compounds in form of polymers of the PHA family	Polyhydroxybutyrate (PHB) base bioplastic production	*Pseudomonas oleovorans, Alcaligenes eutrophus, Azotobacter vinelandii, Alcaligenes latus*	Batstone et al., 2003; Patnaik, 2005; Dias et al., 2008
Hydrogen producing acetogenic bacteria/archea	Fermentation of higher organic acids to produce acetate, H_2, and CO_2	Hydrogen and methane production	*Clostridium* spp., *Syntrophomonadaceae* spp., Bacteriodetes	Hatamoto et al., 2007; Rittmann et al., 2008; Khanal, 2009a,b

(Continued)

TABLE 1 | Continued

Catalytic microbial guild	Catalyzed environmental process	Service/Application	Guild's model species	References
Autotrophic homoacetogenic bacteria	Syngas fermentation (use of hydrogen carbon monoxide and dioxide as carbon and energy source)	Ethanol, butanol, methane and small chain fatty acid production	*Clostridium ljungdahlii*	Khanal, 2009b; Abubackar et al., 2011
Heterotrophic homoacetogenic bacteria	Fermentation of higher organic acids and alcohols to produce acetate and CO_2	Methane production	Streptococcaceae and Enterobacteriaceae families, *Clostridium aceticum, Acetobacterium woodii,* and *Bacteroidetes* spp., *Clostridium* spp., *Lactobacillus* spp.	Hatamoto et al., 2007; Rittmann et al., 2008; Khanal, 2009a,b
Anaerobic methanogenic archea	Acetotrophic conversion of acetate to methane	Methane production	*Methanosarcina* spp. and *Methanosaeta* spp.	(Hatamoto et al., 2007; Rittmann et al., 2008; Khanal, 2009a,b)
	Hydrogenotrophic conversion of carbon dioxide to methane	Methane production	*Methanosarcina* spp	Hatamoto et al., 2007; Rittmann et al., 2008; Khanal, 2009a,b
Photo-autotrophs (Microalgae/Cyanobacteria)	Nutrient assimilation (soluble N & P assimilation to organic molecules)	Eutrophication of water bodies, nutrient removal from wastewater	*Clamydomonas reinhardtii, Chlorella vulgaris, Spirulina platensi, Microcystis aeruginosa*, *Anabaena* spp., *Oscilatoria* spp., *Nostoc* spp.	de-Bashan and Bashan, 2004, 2010; Perez-Garcia et al., 2010
	Autotrophic CO_2 fixation (CO_2 fixation to biomass)	Global carbon cycle, biomass formation, CO_2 sequestration	*Clamydomonas reinhardtii, Chlorella* spp., *Spirulina platensi, Microcystis aeruginosa*, *Scenedesmus obliquus, Nanochloropsis* spp.	Das et al., 2011; Cheirsilp and Torpee, 2012; Girard et al., 2014; Wu et al., 2015
	Autotrophic and heterotrophic lipid, starch and pigments production	Biofuels and valuable chemical production	*Chlorella vulgaris, Chlorella prototecoides*	de-Bashan et al., 2002; Perez-Garcia et al., 2011; Choix et al., 2012a,b; Perez-Garcia and Bashan, 2015
	Production of nitrous and nitrous oxides	Production and emission green house and ozone depleting gases	*Chlorella vulgaris*	Guieysse et al., 2013; Alcántara et al., 2015
	Synthesis of exo-polymers	Bio-absorption of organic compounds and pollutants	*Clamydomonas reinhardtii, Chlorella vulgaris, Spirulina platensis.*	Markou and Georgakakis, 2011; Subashchandrabose et al., 2013
Cyanobacteria	Production and realize of secondary metabolites and toxic organic compounds (microcystin, nodularin, cylindrospermopsin, among others)	Self-population an grazer organism control	*Microcystis aeruginosa*, *Anabaena* spp., *Oscilatoria* spp., *Nostoc* spp.	Welker and Von Döhren, 2006; Yadav et al., 2009; Kaplan et al., 2012; Dittmann et al., 2013; Neilan et al., 2013
Dissimilatory metal-reducing bacteria.	Anaerobic Fe^{3+} reduction to Fe^{2+} (reduction of insoluble iron to soluble form)	Global iron cycle, bioremediation of metallic pollutants in soil and groundwater	*Geobacter metallireducens*, *Geobacter sulfurreducens, Albidoferax ferrireducens, Shewanella putrefaciens*	Lovley and Coates, 1997; Malik, 2004; Gadd, 2010; Melton et al., 2014
	Anaerobic Mn^{4+} reduction to Mn^{2+} (reduction of insoluble iron to soluble form)	Global iron cycle, bioremediation of metallic pollutants in soil and groundwater	*Geobacter metallireducens*, *Geobacter sulfurreducens, Albidoferax ferrireducens, Shewanella putrefaciens*	Lovley and Coates, 1997; Malik, 2004; Gadd, 2010; Melton et al., 2014
	Anaerobic As^{5+} reduction to As^{3+} (reduction of insoluble arsenic to soluble)	Bioremediation of metallic pollutants in soil	*Geospirillum arsenophilus, Geospirillum barnseii, Chrysiogenes arsenatis, Sulfurospirillum* strain NP4	Lovley and Coates, 1997; Malik, 2004; Lear et al., 2007; Gadd, 2010

(Continued)

TABLE 1 | Continued

Catalytic microbial guild	Catalyzed environmental process	Service/Application	Guild's model species	References
	Aerobic Hg^{2+} reduction to Hg^0 (reduction of soluble mercury to volatile form)	Bioremediation of metallic pollutants in soil and water	*Pseudomonas* spp.	Lovley and Coates, 1997
	Anaerobic U^{6+} reduction to U^{4+} (reduction of soluble uranium to insoluble form)	Soil bioremediation of radioactive pollutants	*Thiobacillus thiooxidan, Rhodoferax ferrireducens, Geobacter sulfurreducens, Shewanella putrefaciens, Desulfotomaculum reducens*	Lovley and Coates, 1997; Malik, 2004; Gadd, 2010
	Anaerobic Tc^{4+} reduction to Tc^{7+} (reduction of soluble technecium to poorly soluble form)	Soil bioremediation of radioactive pollutants	*Geobacter* spp.	Lear et al., 2010
	Anaerobic and aerobic Cr^{6+} reduction to Cr^{3+} (reduction of soluble chromium to insoluble form)	Bioremediation of metallic pollutants in soil and water	*Pseudomonas* spp., *Achromobacter Eurydice, Desulfovibrio vulgaris, Bacillus* spp., *Desulfotomaculum reducens*	Wang and Shen, 1995; Lovley and Coates, 1997; Malik, 2004; Gadd, 2010
Heavy metal resistant microbes	Heavy metal (Cu, Zn, Ni, Cd, Pb, Hg) immobilization by biosorption, bioaccumulation, biochelation	Bioremediation of metallic pollutants in soil and water	*Alcaligenes eutrophus, Alcaligenes xylosoxidans, Stenotrophomonas* sp., *Ralstonia eutropha, Staphylococcus* sp., *Pseudomonas syringae*	Lovley and Coates, 1997; Diels et al., 1999; Malik, 2004; Gadd, 2010; Edwards and Kjellerup, 2013
Dissimilatory sulfate reducing bacteria	Anaerobic SO_4^{2-} reduction to H_2S (reduction of soluble and insoluble sulfur to volatile form)	Global sulfur cycle, treatment of sulfur and sulfate contaminated groundwater and industrial wastewater	*Desulfovibrio* spp., *Thermodesulfovibrio yellowstonii, Archaeoglobus* spp., *Desulfatibacillum* spp. *Desulfothermus* spp., *Desulfotomaculum reducens*	Lovley and Coates, 1997; Malik, 2004; Gadd, 2010; Pereira et al., 2011; Hao et al., 2014
Sulfur oxidizing bacteria	Chemiolitotrophic H_2S, S^0 oxidation to SO_4^{2-} (reduction of soluble and insoluble sulfur to volatile form)	Global sulfur cycle, bioremediation of sulfur pollutants in water	*Beggiatoa* spp., *Thiobacillus novellus, Sulfolobus* spp., Purple and green sulfur-oxidizing bacteria	Lovley and Coates, 1997; Kappler et al., 2000; Malik, 2004; Gadd, 2010; Pokorna and Zabranska, 2015
Iron oxidizing bacteria	Chemiolitotrophic Fe^{2+} oxidation to Fe^{3+} (oxidation of soluble iron to insoluble form)	Global iron cycle, bioremediation of metallic pollutants in water	*Leptospirillum ferrooxidans, Acidithiobacillus ferrooxidans, Sulfobacillus thermosulfidooxidans*	Lovley and Coates, 1997; Malik, 2004; Gadd, 2010
Ectomycorrhizal fungi	Filamentous (hyphae) extension of plant root systems (do not penetrate plant root cells)	Enhance plant acquisition of nitrogen, minerals and water	*Russula xerampelina, Amanita francheti, Suillus bovinus*	Gardes and Bruns, 1996; Chalot and Brun, 1998; Reid and Greene, 2012
Arbuscular mycorrhizae fungi	Filamentous (hyphae) extension of plant root systems (penetrate plant root cells)	Enhance plant acquisition of nutrients, minerals and water	*Rhizophagus Irregularis, Piriformospora indica*	Reid and Greene, 2012
Endophytic fungi	Fungi-plant symbiotic production of bioactive compounds	Pathogen and predator resistance	Clavicipitaceae family	Reid and Greene, 2012

(Continued)

TABLE 1 | Continued

Catalytic microbial guild	Catalyzed environmental process	Service/Application	Guild's model species	References
Lignocellulosic fungi	Lignin degradation to soluble carbohydrates mediated by peroxidases and laccase	Global carbon cycle, lignocellulosic biomass degradation, biofuel production, bio-refining of valuable chemicals	*Phanerochaete chrysosporium*, *Pleurotus* spp., *Trametes versicolor*, *Phanerochaete chrysosporium*	Bugg et al., 2011; Harms et al., 2011
	Organic pollutant degradation to harmless compounds mediated by peroxidase, laccase and cytochromes	Organic pollutant degradation, bioremediation	*Gloeophyllum* spp., *Trabeum* spp., *Gilocladium virens*, *Trametes versicolor*, *Phanerochaete chrysosporium*, *Candida* spp.	Keller et al., 2005; Bugg et al., 2011; Harms et al., 2011; Lah et al., 2011; Margot et al., 2013
Recalcitrant pollutant degrading bacteria	Organic pollutant degradation to harmless compounds mediated by peroxidase, laccase, and cytochromes	Organic pollutant degradation (pesticides, pharmaceuticals, agrochemicals, industrial waste chemicals, oil, and petrochemicals)	*Pseudomonas* spp., *Streptomyces* spp., *Desulfovibrio* spp., *Brevundimonas diminuta*,	Díaz, 2004; Head et al., 2006; Singh, 2009; Guazzaroni and Ferrer, 2011; Nikel et al., 2014
Plant growth promoting bacteria (PGPB)	Diazotrophic nitrogen fixation (di-nitrogen gas conversion to ammonia, which is available for plant assimilation)	Global nitrogen cycle, increase biomass production yields of plants or microalgae	*Azospirillum brasilense*, *Azospirillum lipoferum*, *Bacillus pumilus*, *Azoarcus* sp., *Rhizobium leguminosarum*	Hartmann and Bashan, 2009; Hernandez et al., 2009; Reid and Greene, 2012
Plant and microalgae promoting bacteria	Phytohormone production (indole-3-acetic acid and gibberellin production)	Increase of starch formation, and ammonium and phosphate uptake by microalgae	*Azospirillum brasilense*, *Bacillus pumilus*	de-Bashan et al., 2002, 2005, 2011; Choix et al., 2012a, 2014; Meza et al., 2015a,b

Communities' microbial guilds can be modeled using metabolic networks by rendering genomic data of model species enlisted in the fourth column.

highly connected (hub) taxa (Faust and Raes, 2012; Großkopf and Soyer, 2014). The definitions of these microbial interactions are important, allowing them to be formally described for use in SMN modeling frameworks.

Use of Microbial Interactions in Engineered Processes

Engineered processes relying on microbial communities have been around for nearly a century. Microbial interactions are intentionally stabilized by selecting the source of the microbial inoculum and by controlling environmental conditions to promote the selection of favorable microbial taxa and processes (Rodríguez et al., 2006; Kleerebezem and van Loosdrecht, 2007). The use and stabilization of microbial communities for bioprocessing can have clear advantages over the use of traditional pure cultures (Rodríguez et al., 2006; Kleerebezem and van Loosdrecht, 2007; de-Bashan et al., 2011; Marshall et al., 2013). Such advantages are: (i) no sterilization requirement, reducing operational costs; (ii) the capacity to use cheap, mixed, or complex substrates; (iii) greater adaptive capacity (a larger pool of genes allows different processes to be performed depending on the environmental conditions); (iv) increased process robustness; (v) performance of complicated tasks (division of labor and metabolic modularity allow several processes to occur in a single culture); and (vi) that controlling interactions allows process regulation. The above advantages confirm cultures of microbial communities (a.k.a. mixed microbial cultures) are an attractive platform for the discovery and development of new bioprocesses. For instance, the use of open mixed microbial cultures (MMC) and less-pure or waste materials as substrate can substantially decrease the cost of polyhydroxyalkanoates (PHA) or microalgae based products and therefore increase their market potential and positive environmental outcomes (Dias et al., 2005; Rodríguez et al., 2006; Pardelha et al., 2012; Perez-Garcia and Bashan, 2015). Anaerobic digestion is a classic example of a process that combines the objectives of elimination of organic compounds from a waste stream with the generation of a valuable product in the form of methane-containing biogas (Kleerebezem and van Loosdrecht, 2007). Bioprocesses based on MMC exhibit robustness and reproducibility, which is highly desirable in industrial applications (Allison and Martiny, 2008; Werner et al., 2011). Additionally, The physicochemical properties of bioreactor feed may select the most efficient and effective microbial catalysts and even lead to the evolution of more stable and productive microbial communities (Marshall et al., 2013). For instance, biological wastewater treatment by activated sludge and bioreactors for PHA production can operate continuously for years.

Limitations of Processes Based on Microbial Interactions

Despite the above-mentioned advantages, environmental processes based on microbial communities are currently not widely applied at industrial scale—except for wastewater treatment and anaerobic biodigesters—as this technology

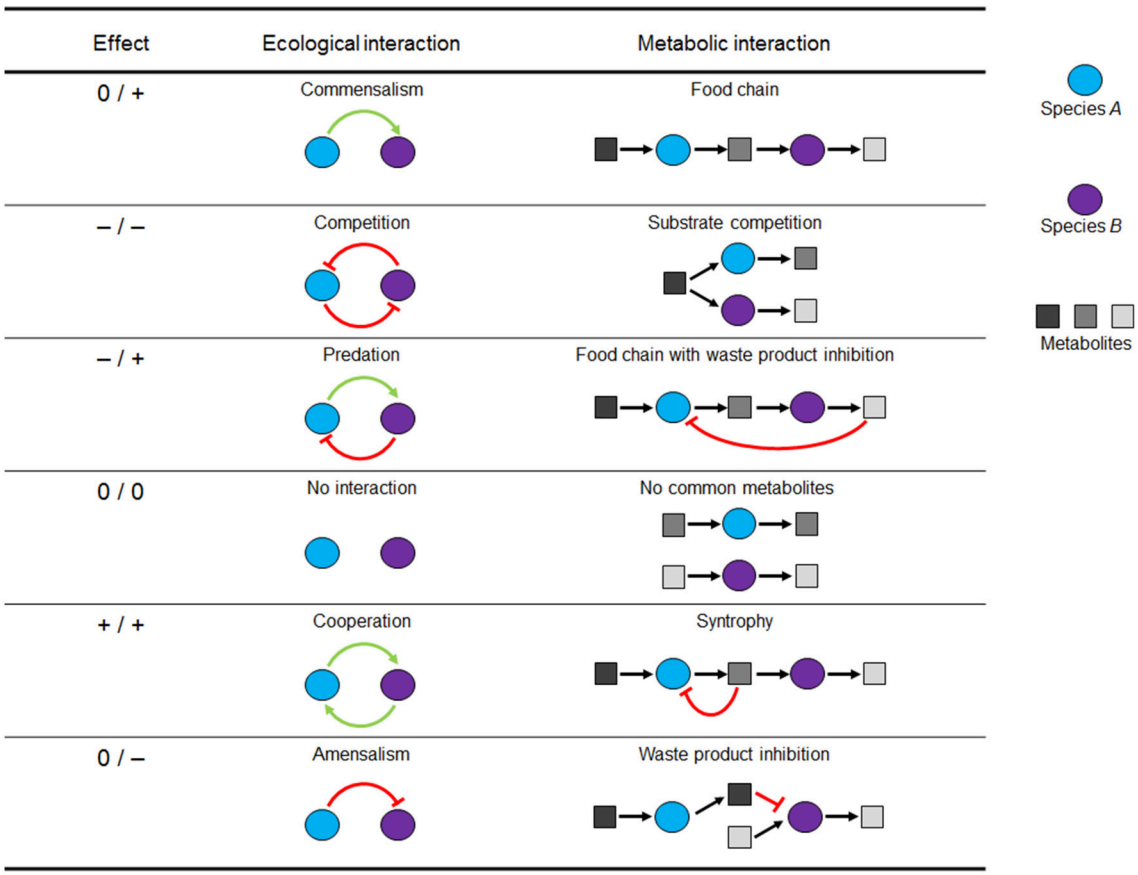

FIGURE 1 | Pairwise microbial interactions in environmental processes. For each interaction partner, there are three possible outcomes: positive (+), negative (–), or neutral (0). Metabolic but not ecological interactions can be modeled using metabolic networks. Figure adapted from Großkopf and Soyer (2014).

still presents significant difficulties. The products formed by microbial communities vary in amount and composition and can have low market value (Kleerebezem and van Loosdrecht, 2007; Agler et al., 2011). Control of the optimum balance among the microorganisms is not straightforward and requires a better understanding of microbial community behavior (Agler et al., 2011). In some MMC processes, the observed yields are much lower than the ones observed from pure cultures or expected from the theoretical process reaction stoichiometry. For example, in anaerobic bio-hydrogen production from carbohydrates, the measured hydrogen production per mole of glucose is much lower (two moles) than the theoretical four mol-H/mol-Glucose yield expected from the bioprocess reaction stoichiometry (Li and Fang, 2007). Another disadvantage is that metabolic routes for waste degradation or product formation can be undefined, therefore complicating the implementation of operation strategies (Rodríguez et al., 2006; Li and Fang, 2007). Therefore, even though mixed microbial cultures are attractive for bioprocessing, the above negative aspects challenge their wider application. In this context, mathematical modeling of metabolic conversions, and interactions can assist to overcome these limitations.

STOICHIOMETRIC METABOLIC NETWORK (SMN) MODELS

Bioprocess Modeling and Metabolic Modeling

Natural and engineered environmental processes are complex systems that depend on external chemical and physical factors. The problem of complexity can be addressed with mathematical models that enable simulation (prediction) of process behavior. So that it is possible to estimate the impact that changing independent variables (e.g., biomass retention time, key nutrient concentrations, pH or temperature) will have on the service or product of interest (Makinia, 2010). Mathematical modeling of bioprocesses is a common practice in environmental engineering. For instance, the International Water Association's Activated Sludge Models (ASM) are a family of bioprocess models widely used by researchers and wastewater treatment facility operators (Kaelin et al., 2009; Makinia, 2010). The main applications of ASM models are, according to van Loosdrecht et al. (2008): to gain insight into process performance and to evaluate possible scenarios for process and plant upgrading. Given such applications, mathematical modeling is a powerful tool to address

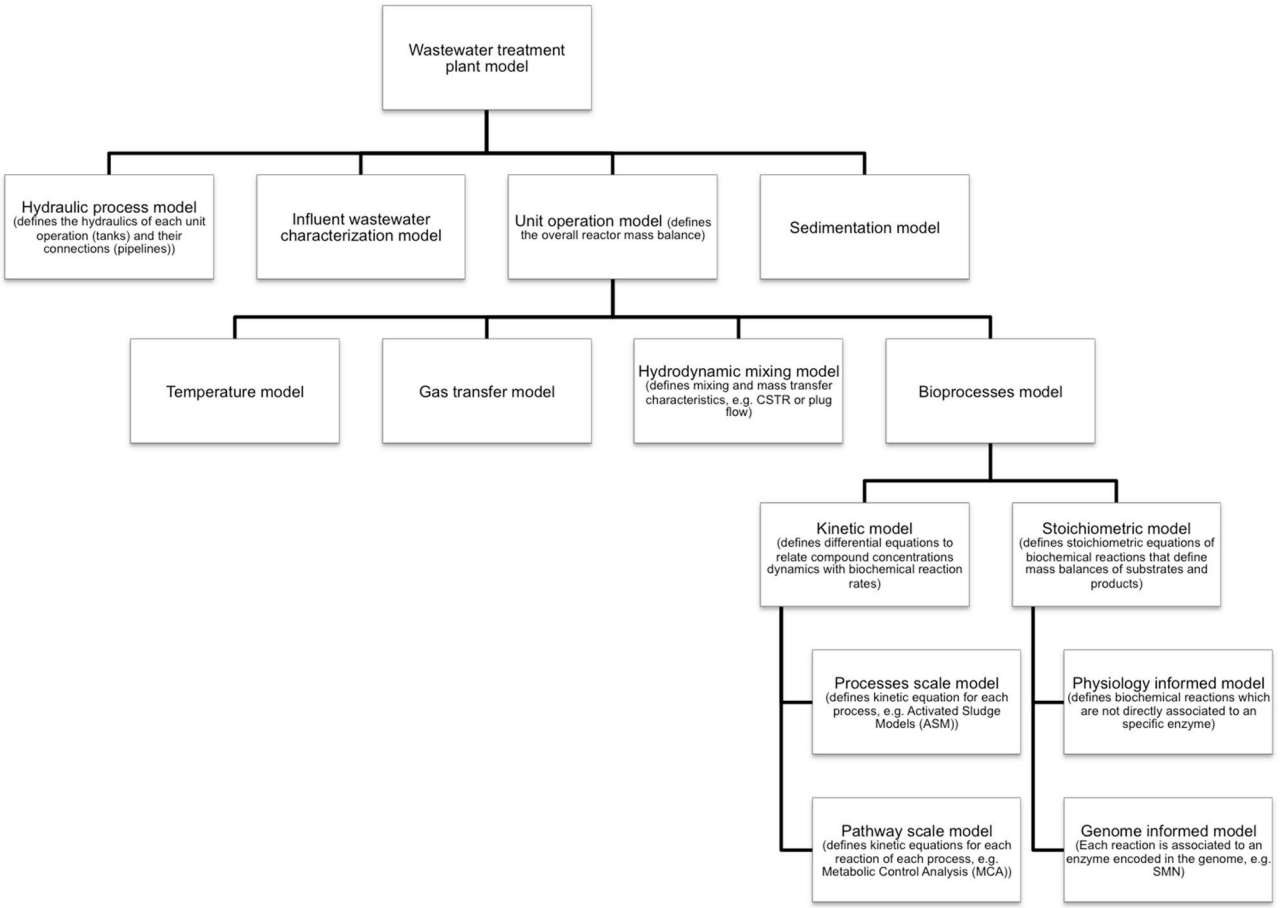

FIGURE 2 | Sub-models of an environmental system (e.g., a full scale wastewater treatment plant). SMN models are genome informed stoichiometric models of biological processes. Inherently, SMN is not a kinetic model therefore does not capture process dynamics. Nevertheless, SMN and kinetic models can be integrated in a common modeling framework.

the complexity and poor reproducibility of environmental processes.

Metabolic models are developed and applied when is necessary to account for detailed microbial physiology (Ishii et al., 2004). These models capture metabolic pathways as sequences of specific enzyme-catalyzed reaction steps converting substrates into cell products. Given this level of detail, metabolic models are commonly applied to (Oehmen *et al.*, 2010): (i) generate mechanistic hypotheses from experimental observations; (ii) improve process efficiency by providing a quantitative basis for process design, control and optimization; (iii) estimate the activity of a specific microbial guild; and (iv) investigate the involvement of a specific metabolic pathway in observed processes. However, metabolic models capture only the molecular/biochemical aspect the whole environmental system. For example, a model of a full-scale wastewater treatment system implementing a biological treatment operation (e.g., activated sludge) has a hierarchy of sub models as shown in **Figure 2** (Makinia, 2010). The diagram shows that metabolic models are extensions of bioprocess models and that also physical and chemical phenomenon such as hydrodynamics, mixing, temperature, and gas transfer have to be modeled in order to capture the full complexity of an environmental process. Nevertheless, each sub-model can operate as a standalone mathematical tool. In this sense, the inclusion of metabolic information is essential for deeper bioprocess understanding and operation improvement.

As shown in **Figure 3**, metabolic models serve as a bridge between molecular/biochemical research and environmental engineering practice, functioning as a tool that can better link the work of microbiologists and engineers in understanding and optimizing a particular environmental bioprocess (Oehmen *et al.*, 2010). Several culture dependent and independent techniques can be applied to analyze community physiology (yields, growth rates, and metabolite consumption/production rates), ecology (species presence/absence and abundance) and molecular properties (functional gene, enzyme, and metabolite presence/absence and abundance). Data generated through these analyses can be encoded and integrated into a metabolic model of the original microbial community. The model is calibrated

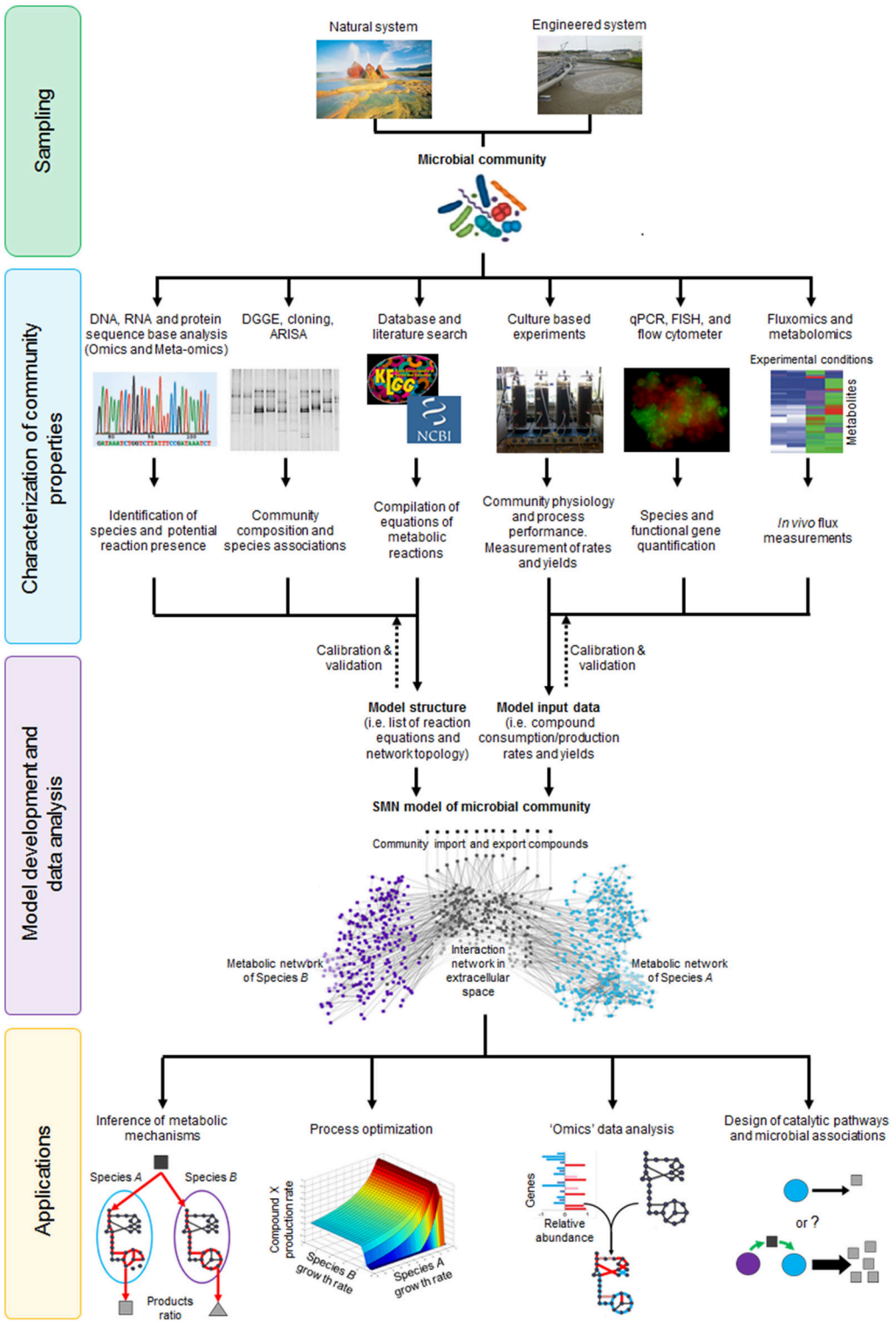

FIGURE 3 | The stoichiometric metabolic network modeling approach for analysis of microbial interactions and communities in natural and engineered environmental systems. The approach is subdivided in four main stages (i) sampling of microbial communities from environmental systems; (ii) characterization of community properties and species interactions through culture dependent and culture independent techniques; (iii) integration of experimental data through model development and analysis; and (iv) application of SMN model as tool to study basic mechanisms or design processes. DGGE, Denaturing Gradient Gel Electrophoresis; ARISA, Automated Ribosomal Intergenic Spacer Analysis; qPCR, quantitative Polymerase Chain Reaction; FISH, Fluorescence *In-situ* Hybridization. Dotted lines represent rounds of model calibration and validation against experimental data. The artwork representing the "Microbial community" was taken from Vanwonterghem et al. (2014).

and validated by iteratively comparing model generated data against experimental data, which is a critical step to establish model reliability. Once that model accuracy is satisfactory, it can be applied to infer metabolic mechanisms, optimize processes, analyze high-throughput "omic" data or design novel catalytic pathways or microbial associations (**Figure 3**). Given that metabolic models both describe and quantify biological mechanisms, they are used as state-of-the-art research tools and for practical applications through linkages with bioprocess models.

Introduction to SMN Models

Stoichiometric metabolic network (SMN) models—also known in the literature as genome-scale or genome-informed metabolic (GEM or GIM) models—are mathematical representations of cell biochemistry used to quantify metabolic reaction rates and therefore describe cell phenotypes (Varma and Palsson, 1994b; Kitano, 2002; Ishii et al., 2004; Palsson, 2009). SMN models are data analysis tools particular to bioinformatics and systems biology disciplines. The aim of these disciplines is to investigate and understand the systematic relationships between genes, molecules, and organisms through computational modeling (Kitano, 2002; Kell, 2006; Park et al., 2008; Endler et al., 2009). SMN models have become an important tool for characterizing the metabolic activity of cells in biotechnological processes and have promising potential to assist in the analysis and understanding of microbial interactions (Lovley, 2003; Zengler and Palsson, 2012). The explosion in the number of new SMN models for up to 200 different organisms over the last few years highlights the increasing popularity of this approach, particularly in pharmaceutical and chemical industries (Feist and Palsson, 2008; Park et al., 2008; Milne et al., 2009; Kim et al., 2012; O'Brien et al., 2015). Although the method has inherent drawbacks and presents important challenges (please consult Section Applications of SMN Modeling of Microbial Interactions for further details), it continues to provide a fertile research field, as demonstrated by the recent growth of model analysis methods and tools (Durot et al., 2009; Kim et al., 2012; Lewis et al., 2012).

Reconstruction of the Metabolic Network

Metabolic network are formulated using genomic information of the species to be modeled. For each microbial species or guild to be modeled, an initial metabolic network has to be formulated from gene-annotation data found in the scientific literature and online biochemical databases (e.g., KEGG, Model SEED, and NCBI, please consult **Table 2** for details). These databases are used to obtain complete sets of stoichiometric equations to "map" or "reconstruct" complete biochemical pathways. Specialized biochemistry literature is also used to obtain details of reaction stoichiometry, cofactors and by-products. Usually information in the databases and the literature is incomplete (e.g., unknown reaction co-factors or compound synthesis steps). Therefore, therefore manual curation of the metabolic network—adding and balancing all equations to fill network gaps—is commonly necessary. The reader is referred to the excellent protocol by Thiele and Palsson (2010) for details of how to reconstruct metabolic networks for each species/guild to be modeled. Here, we provide a general description of the essential elements of the reconstruction process.

A metabolic network consists of a list of mass and charge-balanced stoichiometric biochemical reactions that are classified as either reversible or irreversible (Savinell and Palsson, 1992; Thiele and Palsson, 2010). As illustrated in **Figure 4**, networks of biochemical reactions are reconstructed from existing knowledge of which genes are present in each species, as well as the function of genes. **Figure 4** depicts the SMN reconstruction process as follows: the organism's DNA encodes information to synthesize specific proteins with enzymatic activities (A and B); proteins catalyze specific reactions where metabolites are used as substrates (x, a, y) to be transformed into products (z, b, c); subsequent reactions form metabolic pathways, which constitute cell metabolism; each reaction is represented as a stoichiometric equation (A and B); the equations are then compiled in an extensive list of reactions involved in the modeled pathways. The network topology concept refers to the web structure formed by metabolites interconnected through biochemical reactions, the biochemical pathway formed through these connections and how metabolites are distributed in different intracellular compartments (Varma and Palsson, 1994b; Orth et al., 2010).

Depending of the number of reactions they contain, SMN models may be classified as pathway-scale or genome-scale. Pathway-scale models contain reaction equations for specific and essential metabolic pathways. The size of this model ranges from 10 or 20 to 100 of equations, so they are easily developed, calibrated, and validated. In contrast, GEMs contain reaction equations for all metabolic pathways occurring in an organism, according to the catalytic enzymes encoded in its genome. The size of genome-scale models can go from a few hundred, for models of bacteria, and archaea with small genomes, to a couple of thousand for models of eukaryotic organisms (Kim et al., 2012). Although expansion of the model may improve the fitness to experimental data, it also presents important additional difficulties, such as: (a) the tendency to overestimate the rate of reactions in pathways that may only have a low flow of metabolites as SMN models assume that all enzymes in a pathway are present and active (unless explicit experimental evidence to the contrary); (b) the uncertainty of incomplete pathways or unknown reaction stoichiometry details, particularly in secondary metabolic pathways (Feist et al., 2009).

Compartmentalization and Reaction Equations of the Metabolic Network

The reactions can be modeled as occurring in different cellular compartments such as the periplasm, chloroplast, cytoplasmic and extracellular spaces (Chain et al., 2003). To do this, labels such as [e], [p], and [c] are assigned to metabolic compounds to indicate their occurrence in a particular compartment. The metabolite "x[e]" is thereby differentiated from "x[p]"and their diffusion between two different compartments is defined as "x[e] ↔ x[p]." By using compartmentalization, the reconstructed networks can have stoichiometric equations to represent three types of biochemical reaction (Thiele and Palsson, 2010): (i) Exchange reactions, which define the composition of the "synthetic growth medium." They do not represent a biochemical

TABLE 2 | Examples of useful internet databases of biochemical reactions, metabolic pathways, and microbial genomes.

Database	Application	Internet URL
KEGG. Kyoto Encyclopedia of Genes and Genomes	Very useful database with detailed information of enzymes, pathway reactions and compounds	http://www.genome.jp/kegg/
The Model SEED	Very useful database where complete genome scale models can be downloaded	http://seed-viewer.theseed.org/seedviewer.cgi?page=ModelView
NCBI. National Center for Biotechnology Information	Detailed information about literature, genomes, genes, proteins and compounds	http://www.ncbi.nlm.nih.gov/
BRENDA	Specific detailed information on enzymes and reactions	http://www.brenda-enzymes.info/
Metacyc	Specific detailed information of pathways and reactions	http://metacyc.org/
GOLD, Genomes On Line Database	Specific detailed information of genomes, genes	http://www.genomesonline.org/
BioModels database	Curated models of biological systems	http://www.ebi.ac.uk/biomodels-main/
BiGG database	Curated genome scale models	http://bigg.ucsd.edu/

Please refer to Durot et al. (2009) or Thiele and Palsson (2010) for extensive lists of databases.

conversion but rather define which chemical compounds are consumed into or exported from the metabolic system; (ii) Transport or diffusion reactions, which define a compounds flow of mass from one compartment to another; and (iii) True metabolic reactions (inferred from organism genomes), which define biochemical transformations of compounds to form other compounds catalyzed by an enzyme. Network reactions can be defined as reversible or irreversible reactions depending on the catalytic enzyme properties. Additionally, identical or similar reactions—including reversible and irreversible versions of the same reaction—can be included in the network because each version might be associated with a different enzyme or set of genes.

Conversion of Reconstructed SMN into a Mathematical Model

The conversion of an organism or microbial guild SMN reconstruction into a model requires transformation of the reaction list into a mathematical matrix format. Thus, the equations' stoichiometric coefficients are arranged in the stoichiometric matrix (S), of size m per n. Every row of this matrix represents a unique compound i (for a system with m number of compounds); and every column represents a reaction j (for a system with n number of reactions) (**Figure 4**). So that, an entry s_{ij} in the matrix S is a stoichiometric coefficient of metabolite i in reaction j. A negative entry on the S matrix indicates that the corresponding compound is consumed in the reaction. Conversely, a positive entry indicates that the corresponding compound is produced in the reaction. A stoichiometric coefficient of zero is used for every metabolite that does not participate in a particular reaction. The S matrix contains all the information relating to the reactions modeled for a particular organism (Varma and Palsson, 1994a; Orth et al., 2010). The modeled system boundaries are defined using physicochemical and environmental data as network input data (constraints) (Varma and Palsson, 1994a). The constraints can be grouped into any one of five categories (Price et al., 2003; Oberhardt et al., 2009): (i) physicochemical (e.g., conservation of mass defined in the S matrix); (ii) topological (e.g., compartmentalization and spatial restrictions associated with metabolites/enzymes defined in the S matrix); (iii) genotypical (defined by the profile of functional genes expressed by the organisms under a given environmental condition which in turn defines which reactions allow the flow of metabolites) (iv) environmental (i.e., media composition; these constraints are captured in the model as lower (α_j) and upper (β_j) bounds of substrate consumption rates; and (v) thermodynamic (defined by the observed compounds concentration and fluxes as well as Gibbs energy of reaction, then captured in the model as reaction reversibility). As shown in **Figure 3**, physicochemical, topological, and genotype constraints generally define the structure of the model (i.e., the list of equations and network topology), while environmental and thermodynamic constraints generally define model input data. In the same way that a cell is unique in having one genome and many phenotypes, a metabolic reconstruction is unique for its target organism but context-specific models can be derived by changing the constraint values, therefore representing cellular functions under different environmental or state conditions (Thiele, 2009).

Model Simulation

Once the metabolic network is captured in a matrix format, different mathematical analyses can be performed. These computational methods have been reviewed in recent publications such as Durot et al. (2009), Kim et al. (2012), and Lewis et al. (2012). Lewis et al. (2012) presents a comprehensive overview of the different methods and their applications. In general, the methods (algorithms) to simulate SMN models follow two main categories, biased methods formulated as optimization problems and unbiased methods formulated to characterize all possible solution able to be obtained given

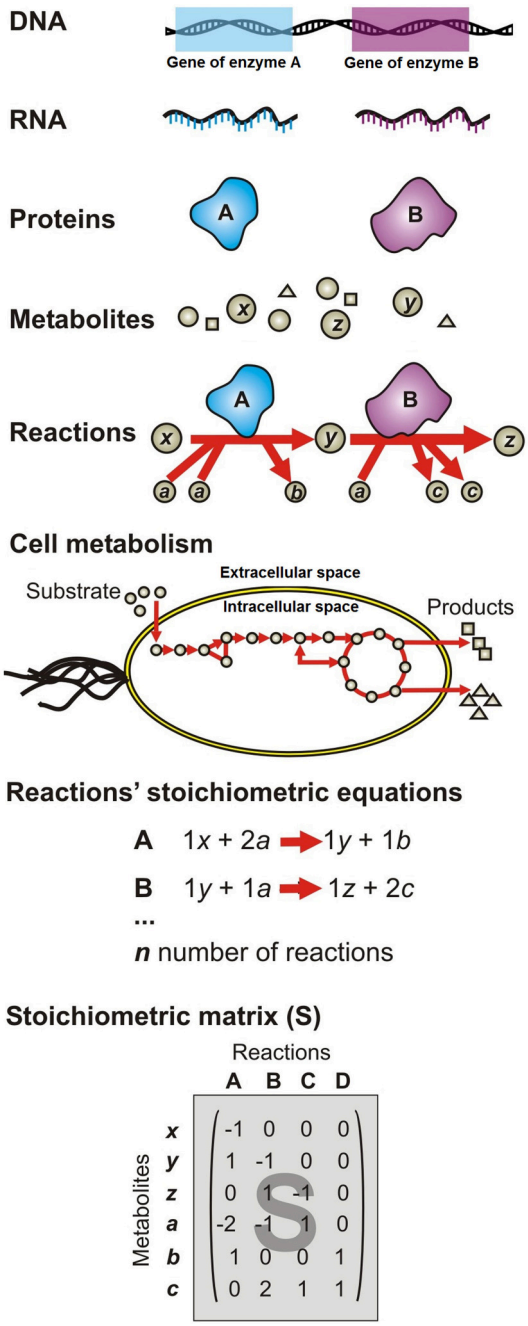

FIGURE 4 | Formulation of the stoichiometric metabolic network (SMN) of a single species (or microbial guild) using genomic information. DNA encodes information to synthesize specific proteins with enzymatic activities (A and B); proteins catalyze specific reactions where metabolites are used as substrates (*x*, *a*, *y*) to be transformed into products (z, b, c); subsequent reactions form metabolic pathways, which constitute cell metabolism; each reaction is represented as a stoichiometric equation (A and B); the equations are then compiled in an extensive list of reactions involved in the modeled pathways.

the network topology (characterize network's solution space) (Schellenberger and Palsson, 2009). Hence, biased methods include the optimization of an objective function to identify physiologically relevant flux distributions; and unbiased methods describe all possible network's flux distributions. FBA is the most basic and commonly-used biased method for simulating SMN models. It is effective in making quantitative predictions of flux distributions using a few governing constraints on the model (Edwards et al., 2001; Oberhardt et al., 2009; Orth et al., 2010). A complete description of the plethora of these methods and their applications is beyond the scope of this review and will not be discussed further. Nevertheless, an introductory description of FBA is provided below to illustrate how metabolic reaction rates (a.k.a. fluxes) are predicted using SMN models.

Flux Balance Analysis (FBA)

FBA and their related methods are used to predict steady state fluxes (i.e., reaction rates) in the metabolic network, rather than time-dependent metabolite concentrations (Varma and Palsson, 1994a). FBA provides a "snapshot" estimation of the rates of all network reactions simultaneously operating under a specific environmental or physiological state (Varma and Palsson, 1994b; Orth et al., 2010). A set of specific reaction rates estimated at a specific steady state is called flux distribution (v) (Varma and Palsson, 1994b; Orth et al., 2010). All reaction rates are generally expressed in units of millimoles (mmol) of compound produced or consumed per unit of biomass per hour (h). Biomass is commonly expressed as grams of dry weight (gDW)—although, for microbial community models can also be expressed as grams of volatile suspended solids (gVSS) or chemical oxygen demand (gCOD)—so that the reaction rates have the following units:

$$\text{mmol gDW}^{-1}\,\text{h}^{-1}$$

In FBA the dynamic mass-balance for each compound in the network is represented by the equation:

$$\frac{dX}{dt} = S \bullet v \tag{1}$$

where X is the vector of metabolite concentrations, t is time, S is the stoichiometric matrix with size $m \times n$ and v is the vector of metabolic fluxes through all network's reactions (Savinell and Palsson, 1992). Transitions of metabolic activity are typically on the order of a few minutes, which is much faster than cellular growth rates and other changes in the microorganisms' environment. So that metabolic changes are considered to be in a steady-state relative to growth and environmental transients (Varma and Palsson, 1994a). In a system at steady-state the change in concentration of metabolites over time is equal to zero so that:

$$\frac{dX}{dt} = S \bullet v = 0 \tag{2}$$

Equation (2) implies that the fluxes of metabolic compound formation i are balanced with its degradation fluxes so that the sum of fluxes equals zero. In other words, metabolite accumulation is disregarded and all the flux of mass entering into the network goes out.

A precise definition of the boundary of the system to be modeled is also needed to formulate an explicit mathematical

representation. Consequently, a specific environmental or phenotypic condition (described in Section Conversion of Reconstructed SMN into a Mathematical Model) is modeled by defining specific values of reaction rates using the following form:

$$\alpha_j \leq v_j \leq \beta_j \tag{3}$$

where α_j and β_j represent the lower and upper bounds for reaction rate v_j. A lower bound (α) and an upper bound (β) are in fact set to every reaction. Bounds for exchange reactions represent the flow of nutrients into and out of the biochemical system; while bounds for transport reactions (occurring across cell and subcellular compartment membranes) and metabolic reactions (occurring within the confines of the cell membrane) represent physicochemical constraints on reaction rates due to thermodynamics or catalytic enzyme availability (Orth et al., 2010). The set rates define a given environmental condition and physiological state, and reduce (or "constraint") the number of possible solutions for v (Edwards et al., 2001; Oberhardt et al., 2009; Orth et al., 2010).

As SMNs (represented as S) are underdetermined systems, meaning that there are more reactions than there are compounds ($n > m$), there is no unique flux distribution (v) solution. An optimization algorithm [linear programing (LP) for FBA] is therefore used to find the optimal v that minimizes or maximizes a particular objective function (Z) defined by the user (Varma and Palsson, 1994a). Typically, the objective function is set to maximize the rate of the biomass production reaction ($Z = v_{biomass}$), although other objective functions, such as minimization of resource utilization and maximization of ATP production can be used depending on the simulation condition (Schuetz et al., 2007). The output of FBA is a particular vector v that maximizes or minimizes Z (Oberhardt et al., 2009; Orth et al., 2010). The mathematical formalism for FBA's optimization problems is as follows:

$$max\,(v_{Biomass})$$
$$s.t. \left\{ \begin{array}{l} S \bullet v = 0 \\ \alpha_j \leq v_j \leq \beta_j \\ v_{Substrate\ Uptake} = Substrate\ uptake \\ measured\ experimentally \end{array} \right\}$$

Biomass production is mathematically represented by adding an artificial "biomass formation equation." The equation defines precursor metabolites at a stoichiometry that simulates the production of one gram of biomass dry weight (DW) (Pramanik and Keasling, 1997). To formulate an equation for biomass production, the dry weight cellular composition of the organism of interest, and its energetic requirements for biomass synthesis need to be obtained experimentally, from the literature, or estimated using data from phylogenetically related organisms (Feist and Palsson, 2010). Cellular composition refers to the fraction of proteins, RNA, DNA, carbohydrate, lipids, polyamines, and other biomass constituents. These components are enlisted in the biomass reaction as constituent metabolites such as amino acids, nucleic acids, etc. Stoichiometric coefficients of enlisted metabolites are scaled to satisfy the required mass to form one gram of biomass dry weight. As a result, the flux through the biomass reaction (in mmol gDW^{-1} h^{-1} units) is equivalent to the growth rate (μ, in h^{-1} units) of the organism as gDW and mmol units can be eliminated (Oberhardt et al., 2009; Feist and Palsson, 2010).

Computational Tools and Software

Several software packages are used to build and simulate SMN models. **Table 3** lists some of these software packages and provides details of their application. The reader is referred to Medema et al. (2012) for an extensive review of computational tools and software packages for metabolic network modeling. The majority of these packages are available in the internet as freeware. **Figure 5** illustrates the research workflow that we, the authors, commonly adopt to perform modeling studies. The corresponding data resources and the software packages used for each step are also shown. In step (i), searches of scientific literature and biochemical databases are undertaken to acquire stoichiometric equations of biochemical reactions forming specific metabolic pathways. The network is reconstructed in a spreadsheet as this format is easy to use and the data can easily be transferred among different simulation software. The list of equations is loaded into MATLAB® (The MathWorks, Inc., Natick, Massachusetts, United States.) using the COBRA toolbox. Model loading and simulation can be also done in software packages such as Optflux (Rocha et al., 2010). In the following step, (ii), Excel and R software are used to record the metabolite concentration curves observed in experimental cultures and then calculate specific rates for the production and consumption of culture substrate and products. Acquisition of experimental data characterizing the microbial community properties (step ii, also shown as stage ii in **Figure 3**) is crucial as such data is required to compare all model generated predictions. In step (iii), specific rates of substrate consumption measured in experimental cultures are used as SMN model input data (constraints) in the MATLAB-COBRA toolbox. The model is simulated (e.g., via FBA) and fitted (calibrated) to datasets observed from cultures (Perez-Garcia et al., 2014a). In step (iv), once the model is calibrated, the COBRA toolbox is used to perform a second round of model analysis to estimate metabolic rates; and the effect of operational parameters of experimental cultures on metabolic pathways is inferred from these estimated metabolic rates (stage "Applications" of **Figure 3**). Finally network visualization and network topology analysis can be performed using Cytoscape, CellDesigner, and Optflux (consult **Table 3** for further software information). It is important to recognize that SMN models are not stand alone tools but rather support tools to be used to analyze data, generate hypotheses and design new "wet" experiments.

APPROACHES TO MODELING MICROBIAL INTERACTIONS USING SMN MODELS

While several aspects of microbial metabolism can be fruitfully addressed by studying pure cultures of individual

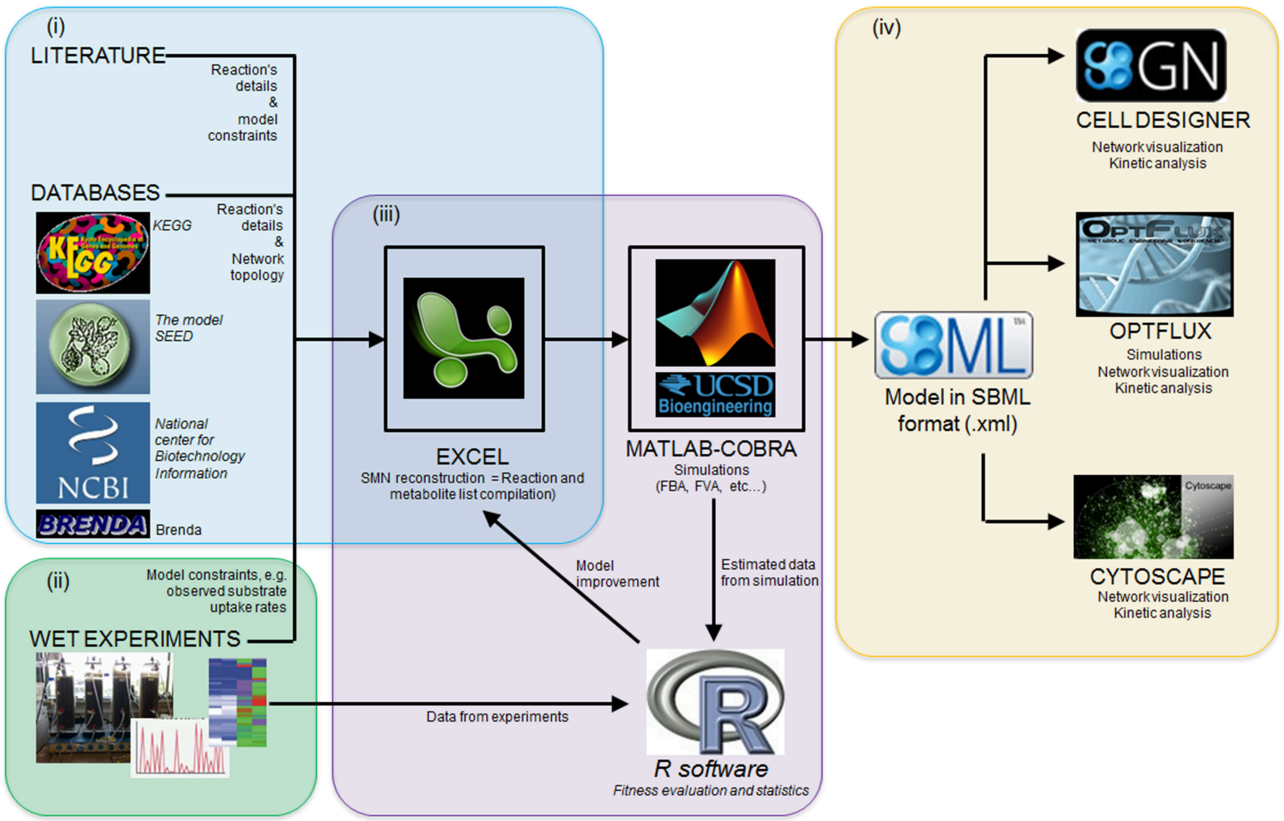

FIGURE 5 | A research workflow to model microbial interactions using SMN models. (i) network reconstruction step; (ii) acquisition of experimental data; (iii) the model calibration step, which involves the statistical comparison of model estimated data against experimentally observed data and further model parameter adjustment to improve predictions; (iv) the calibrated model can be used to perform further analysis in other software platforms. See Section Computational Tools and Software for details.

microbial species, many environmental bioprocesses require an understanding of how microbes interact with each other (Lovley, 2003; Klitgord and Segrè, 2010; Zengler and Palsson, 2012). A lack of information about environmental factors controlling the growth and metabolism of microorganisms in natural and polluted environments often limits the implementation of monitoring or management strategies (Lovley, 2003). Within this context, SMN modeling can be a relevant computational approach to underpin the analysis of microbial interactions in such processes (Miller et al., 2010; Vilchez-Vargas et al., 2010). The development of SMN modeling methods capturing species interactions enables increasingly realistic predictions of whole community phenotypes (Stolyar et al., 2007; Oberhardt et al., 2009) and quantification of rates of exchange of compounds between different populations (Lovley, 2003; Stolyar et al., 2007). An important advantage of using SMNs is that many different types of metabolic interaction occurring simultaneously can be modeled. For instance, it is possible to model two species simultaneously competing for several nutrients (e.g., oxygen, phosphate, and carbon dioxide in nitrification systems) but having a commensal interaction through other compounds (e.g., nitrite in nitrification systems). In addition, a relevant feature of SMN models is that they can be applied to simulate the cellular metabolism of homogenous mixtures of suspended cells such as those in stirred tank reactors, as well as in biofilms or stratified systems by implementing appropriate reaction–diffusion equations (Rodríguez et al., 2006). Given that SMN models contain extensive details of many metabolic pathways and intermediates, the exchange of multiple metabolites between different species can be analyzed.

SMN modeling approaches have been used since 1999 to understand the behavior of biological systems in complex environments and to model organisms relevant to environmental bioprocesses, when Pramanik et al. (1999) first developed a SMN model of phosphate accumulating organisms. This was the first attempt to adapt SMN's to model microbial communities. Later Lovley (2003) presented a coherent framework to combine omic techniques, computational biology, and metabolic network modeling to study environmental processes. As shown in **Table 4**, the literature to date indicates that SMN modeling has been applied to quantify metabolic rates in environmental bioprocesses in only a few studies. Generally, in these studies the number of species in the modeled community is referred to as N while each modeled species is referred to as k (Zomorrodi and Maranas, 2012). **Table 4**

TABLE 3 | Examples of software packages used to develop and simulate SMN models.

Software package	Application and software type	Internet URL for download
Microsoft Excel	Build-up of SMN reconstruction file. Standalone software	http://office.microsoft.com/en-us/excel/
MATLAB®	Software and computing environment	http://www.mathworks.com/
	Standalone software	
COBRA toolbox	SMN modeling and simulation in MATLAB	http://opencobra.sourceforge.net/openCOBRA/Welcome.html
	Free MATLAB toolbox	
Optflux	SMN modeling and simulation. Standalone and free software	http://www.optflux.org/
FASIMU	SMN modeling and simulation. Standalone and free software	http://www.bioinformatics.org/fasimu/
SBML toolbox	Functions allowing SBML models to be used in different modeling software	http://sbml.org/Software/SBMLToolbox
	Free toolbox for modeling software	
libSBML 5.5.0	Programming library to manipulate SBML files	http://sbml.org/Software/libSBML
	Software library	
GLPK solver	Optimization problem solver	http://www.gnu.org/s/glpk/
Tomlab solver	Optimization problem solver	http://tomopt.com/tomlab/
Gurobi solver	Optimization problem solver	http://www.gurobi.com/
Cytoscape	Network visualization	http://www.cytoscape.org/
	Stand alone and free software	
CellDesigner	Pathway graphic reconstruction. Standalone and free software	http://www.celldesigner.org/
anNET	Analysis of metabolites concentrations with SMN models. Free MATLAB toolbox	http://www.imsb.ethz.ch/researchgroup/nzamboni/research

also shows that four approaches have been developed to model microbial interactions in environmental processes using SMNs. We define these approaches as: (i) lumped networks, (ii) compartment per guild networks (also known as multi-compartment networks), (iii) dynamic-SMN (also known as hybrid SMN), and (iv) bi-level optimization simulation. These approaches are described in the following sections; a conceptual scheme for each modeling approach is illustrated in **Figure 6**.

Lumped Network Approach

Here, the community is modeled as a single entity in which all metabolic reactions and metabolites from the species/guilds are combined into a single set of reactions (i.e., a single S matrix) (**Figure 6**). A metabolic network of the whole mixed microbial population is built up by inventorying the most common catabolic reactions, i.e., electron transport chain, glycolysis, tricarboxylic acid cycle (TCA), and amino acid synthesis; and later adding reactions of pathways unique to specific species. For instance, **Figure 6** depicts that reactions from the species A, B, and C belong to a single set of equations (system), where overlapped blocks represent common reactions. Reactions of discrete pathways can be lumped into a single reaction that represents the overall pathway (Rodríguez et al., 2006). Reactions catalyzed by more than one species/guild are only considered once, therefore pathway redundancy is disregarded. The spectrum of compounds produced by the community is generally obtained by maximizing the rate of the reaction that represents the overall production of biomass by the community, which sums all biomass precursors (i) with stoichiometric coefficients (s) synthetized by N number community members (k) (i.e., $Z = max\left(v_{biomass}^{community}\right)$ where $v_{biomass}^{community} = \sum_{k=1}^{N} s_i^k$). The lumped approach models the community metabolic potential by treating all enzymatic activities and metabolites as residents of the same physical space, therefore intracellular compartments are commonly neglected.

The approach is based on the assumption that all the organisms in the community have reactions in common and exploit the environment in a similar way (**Table 4**). It treats the microbial community as a single virtual microorganism catalyzing common biochemical pathways (Rodríguez et al., 2006). The virtual microorganism should be regarded as a representation of the different microbial strains involved in the bioprocess. This assumption brings both advantages and disadvantages. Ignoring microbial diversity and assuming a virtual microorganism able to carry out the most common biological conversions is acceptable in steady state and completely mixed conditions (Rodríguez et al., 2006) thus, simplifying the processes of model development and calibration. The metabolic potential based on community functional gene annotations can be directly investigated, as the assignment of each reaction to a constituent guild is unnecessary. The approach is quite flexible, can be scaled to different levels of detail and has low computational burden. With these advantages, the method is uniquely suited for initial and exploratory analyses of poorly understood communities (Taffs et al., 2009). Nevertheless, a minimum knowledge of community metabolism and physiology is required. In other hand, a major disadvantage is that microbial diversity and the dynamics of the process are neglected using the lumped approach (Rodríguez et al., 2006). Consequently, lumped networks capture the overall matter and energy transformations catalyzed by the community without providing detailed information of individual guilds and their interactions (Taffs et al., 2009). This method also neglects the logistics associated with transferring metabolites between organisms, including conversion of the relevant metabolite into one for which transporters are available (Taffs et al., 2009). Consequently, the lumped network approach is not strictly suitable to model microbial interactions but rather to analyze the overall behavior of a given community.

TABLE 4 | Approaches and applications for SMN modeling of environmental bioprocesses.

Modeling approach	Environmental bioprocess	Modeled organisms/guilds	Model application	References
Lumped network	Enhanced biological phosphorus removal (EBPR)	Mixed population of Phosphate accumulating organisms	Description of how carbon, energy, and redox potential are channeled through metabolic pathways	Pramanik et al., 1999
	Nitrification	*Nitrosomonas* sp. and *Nitrobacter* sp.	Description the redox reactions of the electron transport chain	Poughon et al., 2001
		Nitrosomonas europaea	Quantification of rates of N_2O production through diverse pathways	Perez-Garcia et al., 2014a
	Anaerobic fermentation of carbohydrates to alcohols and carboxylic acids	Mixed population of anaerobic fermentative organisms	Link of operation parameters (feeding composition, gas partial pressure and pH) to product formation	Rodríguez et al., 2006
	Photoautotrophic growth of planktonic/suspended cells	*Synechocystis* sp. PCC 680, single species model	Description of functional properties of phototrophic growth	Knoop et al., 2010, 2013; Maarleveld et al., 2014
			Description of photosynthetic process under different lights and inorganic carbon concentrations	Nogales et al., 2012
		Cyanothece sp. ATCC 51142 single species model	Study of photosynthesis activity in the electron transport chain	Vu et al., 2012
		Chlamydomonas reinhardtii, single species model	Study of biological photosynthesis and phototaxis processes	Chang et al., 2011; Hong and Lee, 2015
			Description of metabolic regulation of mixotrophic growth,	Chapman et al., 2015
	Phototropic growth of microbial mat and toxin production	*Synechococcus* spp., *Chloroflexus* spp, and sulfate reducing bacteria	Description of metabolic mechanism behind the observed biomass productivity, relative abundance and toxin productivity	Taffs et al., 2009
	Subsurface anaerobic fermentation of organic matter	*Clostridium cellulolyticum*, *Desulfovibrio vulgaris*, and *Geobacter sulfurreducens*	Description of substrate consumption routes in microbial community	Miller et al., 2010
	Fermentative anaerobic production of H_2 and acetate	Community enriched with *Clostridium* sp., *Lactobacillus* sp., and *Seleomanas* sp.	Description of metabolic routes for product degradation	Chaganti et al., 2011
	Waste sugars fermentation to PHA	Mixed population of PHA producing organisms, Lumped-dynamic model	Linking operation parameters (feeding regime) to product formation	Dias et al., 2008
			Linking operation parameters (feed composition) to product formation	Pardelha et al., 2012
			Assessing single population contribution to process performance	Pardelha et al., 2013
Compartment per guild network	Methanogenic fermentation	*Desulfovibrio vulgaris* and *Methanococcus maripaludis*	Description of metabolic mechanism behind the association of organisms	Stolyar et al., 2007
		Geobacter metallireducens and *Geobacter sulfurreducens*	Investigation of synthrophic associations for direct interspecies electron transfers	Nagarajan et al., 2013

(Continued)

TABLE 4 | Continued

Modeling approach	Environmental bioprocess	Modeled organisms/guilds	Model application	References
	Growth of phototropic microbial mat	*Synechococcus* spp, *Chloroflexus* spp, and sulfate reducing bacteria	Description of metabolic mechanism behind the observed biomass productivity, relative abundance, and toxin productivity	Taffs et al., 2009
	Commensalism and mutualism between pairs of organisms	Pairs of seven different bacteria[+]	Novel process development. Identifying new environmental conditions that support specific ecological interactions	Klitgord and Segrè, 2010
	Nitrification	Four AOB species together with four NOB species[*]	Description of metabolic mechanisms of NO and N_2O turnovers during biological nitrogen removal	Perez-Garcia et al., 2016
	Syntrophic consortium	*Escherichia coli* strains consortium	Prediction of species abundances and metabolic activities. Analysis of global responses to metabolic limitations	Khandelwal et al., 2013
Dynamic-SMN	*In situ* uranium bioremediation by microbial reduction and precipitation	*Geobacter sulfurreducens*	Description of metabolic mechanisms in ground water bodies, Hydrodynamic-SMN model	Scheibe et al., 2009
	In situ uranium bioremediation by microbial reduction and precipitation	*Geobacter sulfurreducens* and *Rhodoferax ferrireducens*	Description of metabolic mechanisms in ground water, Monod-SMN	Zhuang et al., 2011
	Nitrification	An AOB species together with an AOB species	Investigation of mechanisms causing discrepancies between functional and composition changes in communities	Louca and Doebeli, 2015
Bi-level simulation	Phototropic growth of microbial mat	*Synechococcus* spp, *Chloroflexus* spp, and sulfate reducing bacteria	Description of metabolic mechanism behind the observed biomass productivity, relative abundance and toxin productivity	Taffs et al., 2009
		Synechococcus spp, *Chloroflexus* spp, and sulfate reducing bacteria	Assessing the effect microbial community structure on the total community biomass	Zomorrodi and Maranas, 2012
	Methanogenic fermentation	*Desulfovibrio vulgaris* and *Methanococcus maripaludis* synthorphic association	Linking the effect of microbial community composition to process performance.	Zomorrodi and Maranas, 2012
		Simithella spp., *Desulfovibrio* spp, *Methanocalculus* spp., *Methanoculleus* spp., *and Methanosaeta* spp.	Assessing the impacts of metabolic redundancy in microbial communities. "Meta-omics" data analysis	Embree et al., 2015
	Subsurface anaerobic fermentation of organic matter	*Clostridium cellulolyticum*, *Desulfovibrio vulgaris*, and *Geobacter sulfurreducens*	Description of substrate consumption routes in microbial community	Zomorrodi and Maranas, 2012

[+]*Genome scale models of Escherichia coli, Helicobacter pylori, Salmonella typhimurium, Bacillus subtilis, Shewanella oneidensis, Methylobacterium extorquens, and Methanosarcina barkeri.*

[*]*AOB, ammonia oxidizing bacteria: Nitrosomonas europaea, Nitrosomonas eutropha, Nitrosospira multiformis, and Nitrosococcus oceani. NOB, nitrite oxidizing bacteria: Candidatus Nitrospira defluvii, Nitrobacter winogradskyi, Nitrobacter hamburgensis, Nitrospina gracilis.*

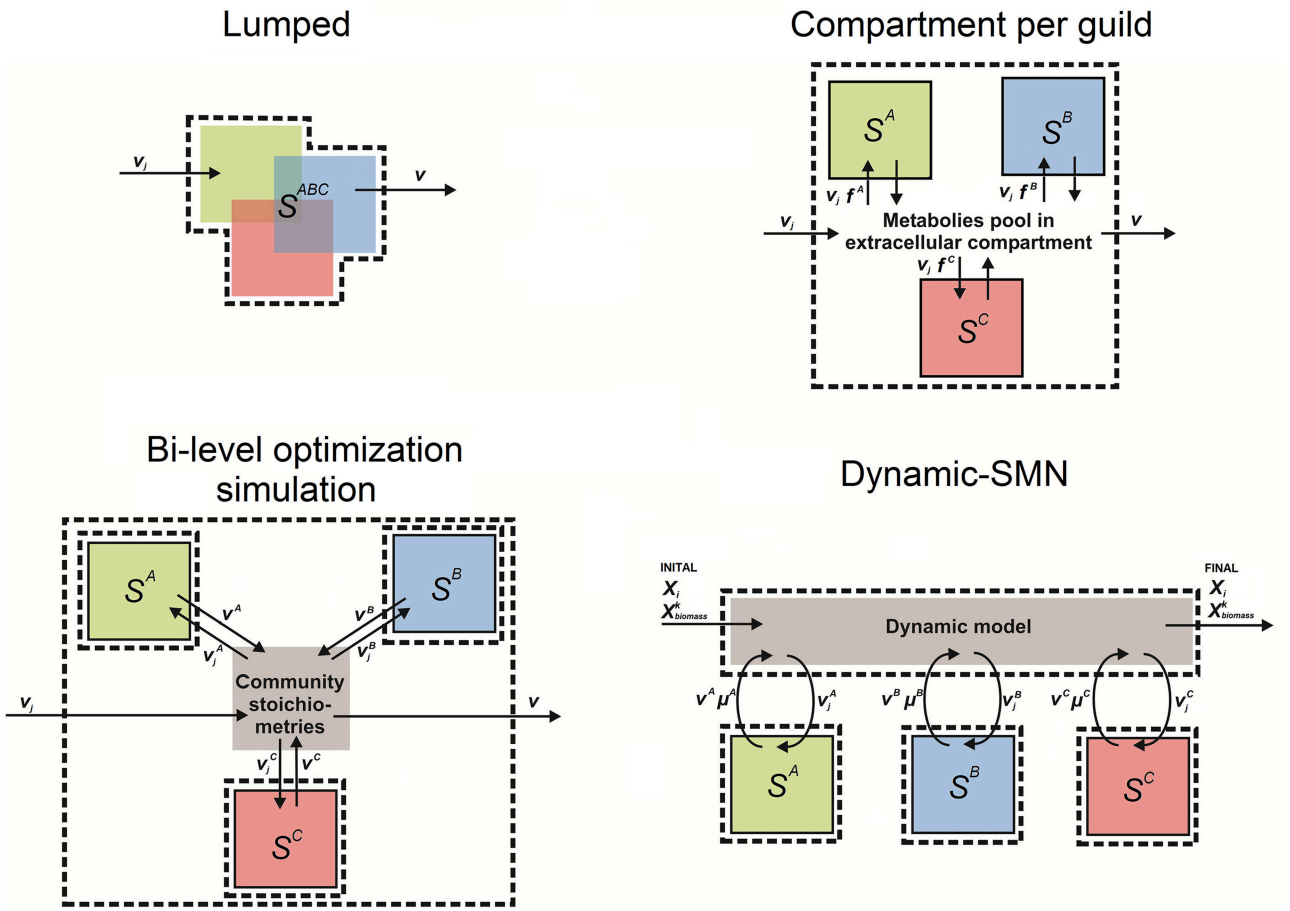

FIGURE 6 | Conceptual scheme of the four approaches to model mixed microbial cultures using stoichiometric metabolic networks. In all figures boxes S^A, S^B, S^C represent sets of equations (captured as an *S* matrix) of metabolic reactions occurring in organisms/guilds *A*, *B*, and *C*, respectively. S^{ABC} is a matrix lumping metabolic reactions occurring in organisms/guilds *A*, *B*, and *C*. These sets of reactions can have any number of sub compartments to model reactions occurring in the extracellular space and organelles; boxes with dashed lines indicate model (system) boundaries; boxes with solid lines indicate guild boundaries; v_j is the flux of metabolite in reaction *j*; *V* is the vector of fluxes estimated by the model; V^k is the vector of fluxes estimated by the model of species/guild *k* (*A*, *B*, or *C*) ; X_i is the concentration of metabolite *i*; μ^k (a.k.a. $v^k_{biomass}$) is the growth rate (biomass production rate) of species *k*; f^k is the fraction of species *k* in community's biomass; and $X^k_{biomass}$ is the biomass concentration of modeled species/guild *k* (*A*, *B*, or *C*). Figure inspired in Taffs et al. (2009) modeling approaches diagrams.

Compartment Per Guild Approach (Multi-Compartment)

In a compartment per guild network, each organism or guild is modeled as a distinct compartment of the network and exchangeable metabolites are transferred through an extra compartment representing the extracellular environment (Stolyar et al., 2007; Taffs et al., 2009; Klitgord and Segrè, 2010) (**Figure 6**). This fictitious extra compartment represents the extracellular environment shared by the microbial species/guilds so that they are modeled as being spatially separated by the extracellular medium (Klitgord and Segrè, 2010). The approach is implemented by assigning reactions and metabolites to a network representing each guild, with suffixes on metabolite identifiers preventing sharing of compounds common to the metabolism of multiple guilds. For instance, ammonium (NH_4^+) is a metabolite for species/guilds A and B, so that in the model the ammonium entity is defined three times, one for each species [e.g., NH_4^+(a) for species/guild A and NH_4^+(b) for species/guild B] and an extra one for the shared extracellular environment [e.g., NH_4^+(e)]. Explicit transport reactions are defined to account for the exchange of metabolites between species/guild members and the extracellular environment (Taffs et al., 2009). This allows interactions such as the commensalism and competition to be captured (**Figure 1**). Biomass formation reactions are defined for each modeled species/guild. The optimization problem is generally solved by maximizing the production rate of the community biomass, which sums the rates of biomass production of all modeled species (i.e., $Z = \max\left(v^{community}_{biomass}\right)$, where $v^{community}_{biomass} = \sum_{k=1}^{N} v^k_{biomass}$). Species abundances can be captured by scaling the overall community substrate uptake rates with a vector containing the fractions of species *k* in the biomass (f^k), $v^k_{substrate\ uptake} = v^{community}_{substrate\ uptake} * f^k$. Consequently species

substrate uptake rates are proportional to species biomass abundance.

The compartment per guild approach allows tracing of the metabolic behavior of each modeled species/guild. Dividing the community into species/guild-level compartments linked by transferred metabolites, e.g., oxygen, is an intuitive way to represent interactions within a community. This approach is optimal to analyze pairwise interactions in communities of only two different microbial guilds. Examples of such small communities are the ones formed by ammonia and nitrite oxidizing bacteria in nitrification processes (Ferguson at al., 2007) or the ones formed by microalgae and plant growth promoting bacteria (de-Bashan et al., 2005; de-Bashan and Bashan, 2010). It is also an ideal method for understanding which guild performs a particular metabolic transformation. For example, it is easy to estimate the fraction of total biomass or ATP produced by each guild (Taffs et al., 2009). Also, the approach allows the capturing species abundance profiles, as observed in experiments (Perez-Garcia et al., 2016). Separating species/guild metabolism in different compartments makes it possible to verify potential microbial interactions, or to formulating new growth media on basis of each species metabolic requirements (Klitgord and Segrè, 2010). A drawback of this approach is that the size of the resulting network can lead to a "combinatorial explosion" of new pathways composed by reactions from different guilds (Klamt and Stelling, 2002). To address this limitation, the models for each guild member can be constructed to only capture the necessary metabolic capabilities while maintaining computational tractability (Taffs et al., 2009). A second drawback of this approach is the requirement for significant *a priori* information or assumptions, as specific transport reactions must be assigned to each individual species/guild (Stolyar et al., 2007).

Bi-Level Optimization Approach

The approaches described above rely on either a single objective function to describe the entire community (Stolyar et al., 2007) or separate optimization problems for each microorganism (Tzamali et al., 2011). Bi-level optimization integrates both species and community-level fitness criteria into a multi-level/objective framework. The bi-level optimization approach is based on the assumption that a universal community-specific fitness criterion does not exist (Zomorrodi and Maranas, 2012). This approach uses successive rounds of simulations to analyze potential interactions within a community. A first round of optimization simulations (e.g., flux balance analysis) is applied to each modeled guild in isolation. Then the output data is mined for ecologically relevant interactions, compiled and used to define new stoichiometric reactions that are used in a second round of optimization simulations to examine the potential for interactions between guilds (**Figure 6**). Conceptually, the first round of simulations provides guild-level compound production rates, then proportions between estimated rates define new community stoichiometry's which are then used to define inter-guild interactions (Taffs et al., 2009). The bi-level optimization approach, like that developed as the OptCom algorithm (Zomorrodi and Maranas, 2012), postulates a separate biomass maximization problem for each species as initial (inner) optimization problems, consequently capturing driving forces of species-level fitness. Inter-guild interactions (**Figure 1**) are modeled with interaction constraints in the second (outer) optimization problem capturing the exchange of metabolites among different species and using maximization of overall community biomass as objective function (Zomorrodi and Maranas, 2012).

Bi-level optimization algorithms such as OptCom can capture metabolic interactions among members of a microbial community (**Table 4**). It is possible to incorporate ecological data of the community (i.e., species or guild presence/absence and abundance) as constraints in the second optimization problem. The observed growth rates of individual species can be used to define (constrain) the biomass flux of internal guild models. Food chains, substrate competition, syntrophy, and product inhibition can be modeled using bi-level optimization approaches. For instance, OptCom can be used for assessing the optimal growth rate for different members in a microbial community and subsequently making predictions regarding metabolic exchange given the identified optimal levels (Zomorrodi and Maranas, 2012). An advantage of the bi-level optimization approach is that it can also be coupled with differential equations to generate dynamic models (Zomorrodi et al., 2014). Theoretically, it is possible to include metabolic and species abundance data for an indefinite number of species or guilds. However, this remains challenging given the gaps in knowledge of species identities and metabolic details of complex communities. The bi-level simulation approach has the disadvantage of requiring two rounds of data processing and simulation, which can be computationally burdensome. In addition, using two types of data processing introduces some rounding error (Taffs et al., 2009). Finally, manual selection of ecologically interesting modes from individual models requires a priori knowledge and can significantly influence the solution.

Dynamic-SMN (Hybrid)

This approach couples the rate predictions of SMN models with differential equations that capture the dynamic response of the biological process with respect to compounds concentration, temperature, or pH. The main attribute of hybrid models is that they can predict reaction rates together with compound concentrations across a time period, which is a major advantage in applications such as process optimization. Consequently, interactions that depend on changes in substrate concentration or species abundance can be modeled with this approach. Dynamic-SMNs have been applied to model single species (Mahadevan et al., 2002; Hjersted et al., 2005; Çalik et al., 2011) as well as multiple species (Scheibe et al., 2009; Zhuang et al., 2011). This hybrid approach has been previously referred to as dynamic FBA (dFBA) (Mahadevan et al., 2002). Here, we refer to this method as dynamic-SMN rather than dFBA to avoid the assumption that the intracellular flux distribution can only be obtained via FBA and not other simulation algorithms such as flux variability analysis or random sampling.

Dynamic-SMN models are formed by three types of equations: (i) kinetic and (ii) differential equations, both capturing the process dynamics; and (iii) stoichiometric reaction equations of

each modeled species/guild (S^k), which capture the biochemical transformations (**Figure 6**). Initial conditions of the simulated system must be defined a priory (i.e., initial concentration of substrates (X_i) and species biomass ($X^k_{biomass}$)). Also the analyzed time period is subdivided into discrete time intervals so that simulation length and the number of intervals must be defined (e.g., a simulation of 2 h using 7200 time intervals of 1 s each). During the simulation, the following four subroutines are executed for each time interval: (i) the substrates and biomass concentrations are used in the kinetic equations to estimate the uptake rate of substrates ($v^k_{Substrate\ uptake}$) for each species k. A kinetic equation (e.g., Monod or Logistic) is used for each substrate of interest related to each modeled species. For instance, two Monod equations are included in a model that capture the consumption of one substrate by two species; (ii) the obtained $v^k_{Substrate\ uptake}$ values are used as constraints of the respective S^k to solve the optimization problem (e.g., via FBA); (iii) the predicted production rates for compounds of interest and biomass (v^k_i and $v^k_{biomass}$) are used in differential equations to obtain the change of concentrations ΔX_i and $\Delta X^k_{biomass}$; (iv) new concentrations at the end of the simulation step (X^{NEW}_i and $X^{k\ NEW}_{biomass}$) are calculated by adding $\Delta X^k_{biomass}$ and ΔX_i to the initial concentrations X_i and $X^k_{biomass}$. The new concentrations are used as a starting point for the next itineration of subroutines executed for the next time interval. This continues until the simulation length is reached. At each time interval, the flux constraints for each organism vary based on the substrate concentration at that particular time, leading to dynamic variations. The underlying assumption of this approach is that the speed of processes inside the cell are faster than the changes in the surrounding environment, which allows the kinetics of environmental factors to be defined (e.g., substrate concentration change), without defining intracellular kinetic processes (Mahadevan et al., 2002).

Dynamic-SMN models captures both metabolic complexity and metabolic dynamism. The approach is particularly well suited to model microbial interactions in heterogeneous environments (e.g., batch cultures), as it does not assume constant yield coefficients (Schuetz et al., 2007). Because the majority of environmental bioprocesses (e.g., wastewater biotreatment and soil bioremediation) display time dependent dynamics, this approach has the potential to truly capture their behavior (**Table 4**). For instance, dynamic-SMN has been applied successfully to study bioremediation processes with mixed microbial populations (Zhuang et al., 2011; Embree et al., 2015). Scheibe et al. (2009) coupled a genome-scale SMN model of *Geobacter sulfurreducens* to a soil reactive transport model (HYDROGEOCHEM) to define *in situ* bioremediation strategies for uranium spills in soil. By representing an aquifer as a numeric grid, the hybrid model simulates time and space dependent hydrological, geochemical, and metabolic processes in the spill area. Another innovative tool based on SMN models is the Computation of Microbial Ecosystems in Time and Space (COMETS) (Harcombe et al., 2014). The approach couples dynamic-FBA simulations with extracellular-compounds diffusion models, which makes it possible to track not only the temporal but also spatial dynamics of multiple microbial species in complex environments with a complete genome scale resolution (Zomorrodi and Segrè, 2015). The COMETS approach has been applied successfully to identify the spatial arrangements of different species colonies in engineered microbial communities. Another novel tool is the Microbial Community Modeller (MCM) which combines genome-based model construction with statistical analysis and calibration to experimental data in a single platform (Louca and Doebeli, 2015). MCM has been used to simulate successional dynamics in single-species evolution experiments, and pathway activation patterns observed in microarray transcript profiles (Louca and Doebeli, 2015).

As a drawback, this approach is computationally demanding as several SMN simulations have to be performed to analyze the entire time period. Additionally, model calibration can be tedious because of the need to adjust many kinetic parameters including maximum reaction rates v_{max} and affinity constants K_m of kinetic equations (Makinia, 2010). Also, the maximum number of microbial and metabolic species depends on the computational hardware capacity. Nevertheless, given the complexity of defining kinetic equations for each modeled guild, this approach is best suited to simulated interactions within small communities of two to five guilds.

Comparing Approaches

Advantages and disadvantages of the approaches can be compared in terms of their required input data, their generated output data and their implementation (**Table 5**). In terms of input data, all the approaches except the lumped approach require extensive information about metabolic reactions and pathways from different species/guilds. Species presence/absence and abundance data can be used as model input for all approaches except for the lumped approach because the community is analyzed as a whole and the metabolism of individual species is not captured. Metabolic information from systems with a large number of species or guilds is better captured using lumped and bi-level optimization approaches because each species is modeled independently. Nevertheless, the computational requirement to run bi-level optimization simulations with multiple SMN can be significant. Presence/absence data of functional genes, enzymes or metabolites can be captured using all the approaches by defining gene-protein-reaction associations with Boolean rules (Thiele and Palsson, 2010; Lewis et al., 2012). Different approaches yield different output data and information. In general all the approaches are appropriate to obtain metabolic fluxes at the community level (i.e., overall production and consumption rates of compounds) but the dynamic-SMN additionally provides compound concentration profiles across time. Quantification of physiological attributes (fluxes) at the species/guild level (i.e., intracellular fluxes) can be generated with all the approaches except with lumped models. Similarly, microbial interactions among community species and guilds (i.e., exchange and competition of metabolites) can be quantified using all the approaches except the lumped approach as this does not contemplate the exchange of compounds between

species. The temporal and spatial dynamics of compound concentrations can only been captured with the dynamic-SMN approach. In contrast, the lumped, multi-compartment and bi-level optimization approaches provide rates of metabolic reactions at a specific steady state.

The best approach for use depends on the system under analysis (**Table 5**). Natural and engineered systems without well-defined species populations are best modeled with lumped models. The lumped approach represents the coarsest methodology, requires the least *a priori* information and is easier to implement than alternative approaches. It can be used when other approaches cannot (due to complexity) or should not (due to lack of detailed data). These advantages are balanced against its tendency to overestimate the metabolic potential. This is unsurprising, as real communities are not super-organisms. Individuals are membrane-separated and must contend with the logistics associated with matter and energy transport. Consequently, the lumped technique is best for initial work on "poorly" characterized systems (Taffs et al., 2009). Natural and engineered systems with low species richness are best characterized using the compartment per guild approach. The compartmentalized community analysis method has the advantage of intuitive tractability and separates activity and function by guild, but requires substantially more knowledge of the community than the pooled reactions approach. The compartmentalized method also lends itself uniquely to investigation of the robustness of specific consortium interaction types (Taffs et al., 2009). Natural and engineered systems with high species richness are best characterized using the bi-level optimization approach. This approach has properties very similar to the compartment per guild approach, but with the important advantage of easy scalability, achieved by solving each species' SMN separately. The approach also provides additional ecological insight into the competitive strategies underlying each guilds function. The bi-level simulation approach also easily captures interactions between different guilds as well as between members of the same guild expressing different physiologies. Finally, engineered systems with low species/guild richness are best analyzed using dynamic-SMN models as this approach is the only one that estimates concentrations of compound across temporal and spatial gradients.

APPLICATIONS OF SMN MODELING OF MICROBIAL INTERACTIONS

As more metabolic models of different organisms become available, the modeling of microbial communities becomes more feasible and relevant. SMN modeling has multiple applications for the analysis of microbial interactions and environmental bioprocesses (**Table 4** and **Figure 3**), which are described in the following sections.

Inference of Metabolic Mechanisms from Observed Data

In this application, experimental data is acquired and used as model input to generate estimations of intracellular metabolic rates and inter-species compound exchange rates. Experimental observations of community metabolism are then contrasted and interpreted under the light of model predictions (Pramanik et al., 1999; Chaganti et al., 2011). Because the SMN model includes detailed information of metabolic pathways, a mechanistic interpretation of the results obtained from experiments is possible (Rodríguez et al., 2006). In addition, SMN modeling can be used to infer ecological relationships in complex microbial communities, especially with regard to mechanisms of mass and energy transfer between guilds, and the relationship between species presence and its function in the community (Stolyar et al., 2007; Taffs et al., 2009). For example, in the Stolyar et al. (2007) study simulations helped reveal and clarify essential substrate assimilatory pathways and reaction stoichiometry by comparing simulation results with growth rates of experimental data.

Process Optimization

SMN models can be used to predict the likely outcome of new operation and management strategies for experiments or environmental processes (Scheibe et al., 2009). It is recognized that the investigation of the optimal process operation can be most effectively performed by adopting a model-based methodology (Dias et al., 2005). The model is used to develop experimental designs and hypotheses about relevant metabolic pathway or points of metabolic regulation and modulation (Pramanik et al., 1999). Intracellular flux distributions for different environmental scenarios can be calculated and culture feeding scenarios can be optimized with simulations targeting maximal compound productivity and/or desired composition (Dias et al., 2008). This is particularly useful for linking specific operational parameters to bioprocess product formation. For instance, Dias et al. (2005) and Pardelha et al. (2012) developed a process model based on SMN modeling to optimize the PHB productivity by mixed cultures. These studies aimed to explore optimal carbon sources and ammonia-feeding strategies that maximize both the final intracellular PHB content as well as the volumetric productivity (Dias et al., 2005). Computational tools such as the Search for Interaction-Inducing Media (SIM) algorithm identifies the set of media that support the growth of multi-species cultures and predicts the class of interaction they induce (Klitgord and Segrè, 2010). In summary, the inclusion of genome information in SMN models can be used to select optimal combinations of microbial taxa or genes to promote more efficient substrate degradation and/or production.

Analysis of High-Throughput "Omic" Data

Metabolic network models have successfully helped in the interpretation of transcriptomic, proteomic and metabolomic data from single-species cultures. As mentioned before there is a plethora of published computational methods to analyze SMN models (Durot et al., 2009; Kim et al., 2012; Lewis et al., 2012) including omic data mining. For instance, proteomic and transcriptomic data have been successfully used as constraints of SMN models and interpreted through the Parsimonious FBA (pFBA) (Lewis et al., 2010) and the ME-modeling framework (Lerman et al., 2012) among others. In a similar way, metabolomics data can be interpreted in the light of SMN models

TABLE 5 | SMN approaches to model microbial communities and their capabilities.

	Model capability	Lumped	Compartment per guild	Bi-level optimization simulation	Dynamic-SMN
Required Input data	Requires extensive metabolic pathway information from different species	Not required	Required	Required	Required
	Captures species presence/absence	Limited	Optimal	Appropriate	Optimal
	Captures species abundance	Limited	Appropriate	Appropriate	Optimal
	Captures information from large number of species/guilds	Appropriate	Limited	Appropriate	Limited
	Captures functional gene, enzyme or metabolite presence/absence	Appropriate	Appropriate	Appropriate	Appropriate
	Captures gene-protein-reaction association	Appropriate	Appropriate	Appropriate	Appropriate
Generated output data	Quantifies physiology at community level	Appropriate	Appropriate	Appropriate	Optimal
	Quantifies physiology at species/guild level	Limited	Appropriate	Appropriate	Appropriate
	Quantifies inter species interactions	Limited	Appropriate	Optimal	Optimal
	Describes temporal and spatial changes of compound concentration (capturing process dynamic)	Possible	Possible	Limited	Optimal
Implementation	Easy to develop (network reconstruction)	Easy	Moderate	Challenging	Challenging
	Easy to calibrate	Easy	Moderate	Moderate	Challenging
	Computationally demanding	Low	Low	High	High
	Optimal environmental system to be described	Natural and engineered systems without well-defined species populations	Natural and engineered systems with low species richness	Natural and engineered systems with high species richness	Engineered systems with low species richness

using Network Embedded Thermodynamic (NET; Kümmel et al., 2006), network topology (Çakir et al., 2006), or shadow price (Reznik et al., 2013) analyses. Depending on the intended application, proper method selection is important as results from the same model can differ significantly depending on the method used. For example, Machado and Herrgård (2014) systematically evaluated eight SMN methods for analysis of transcriptomic data and concluded that none of the methods outperform the other for all the tested cases. Recent advances in the use of high-throughput sequencing and whole-community analysis techniques, such as meta-genomics and meta-transcriptomics, are making genomic information available from microbial communities. However, due to the complexity or low reliability of the information generated in many studies, "meta-omic" data may remain without meaning or usefulness. In principle, SMN models can be used to analyze and interpret "meta-omics" data by extending the computational methods developed for "omic" data analysis. However, as best of authors knowledge, SMN models have only been used for metagenomics and other "meta-omics" data analysis in very few studies (i.e., Pérez-Pantoja et al., 2008; Nagarajan et al., 2013; Embree et al., 2015). This gap in the research field opens a promising research opportunities for groups specialized in developing systems biology and bioinformatics tools.

Design of Novel Catalytic Pathways and Microbial Associations

The most innovative application of metabolic network modeling of mixed-microbial communities is to discover and design novel microbial associations and catalytic pathways. The real power of computational biology techniques relies on their ability to rapidly test thousands of metabolic variations or combinations without developing wet experiments or generating mutants. For instance, it is possible to computationally generate artificial microbial ecosystems without re-engineering microbes themselves, but rather by predicting their growth on appropriately designed media. This approach is of particular relevance to environmental biotechnology, given the restrictions on the use of genetically modified organisms in bioremediation strategies. SMN models can be used to identify novel environmental conditions to co-cultivate two or more species by inducing mutualistic or commensal interaction interactions (Stolyar et al., 2007; Klitgord and Segrè, 2010). For example, in the study done by Klitgord and Segrè (2010) 21 models were generated using paired combinations of seven SMN models of different species. From the simulations of these paired models, several putative growth media formulations were identified to induce novel commensal or mutualistic relationships between the species. Naturally, further experimentation is required to confirm model's predictions, but these experiments would be based on a robust hypothesis generated *a priori*. In another relevant *in silico* study by Taffs et al. (2009), three SMN models were used to map the novel pathways generated by the metabolic networks of three species connected to each other via the exchange of substrate and products.

SMN models can help to explore community enzymatic potential to assemble novel interspecies catalytic pathways. Novel pathways can be formed by inducing interactions between different organisms rather than—or in addition to—genetically modified organisms (Chiu et al., 2014). This is beneficial as firstly one could use the metabolic potential of organisms that may be hard to genetically manipulate. Secondly, communities may have a more robust metabolic performance than individual modified species, in which specific mutations can revert the genetic modification. In this sense, symbiotic interactions, e.g., to biodegrade a pollutant, may arise more readily through environmental fluctuations than genetic modifications (Klitgord and Segrè, 2010; Zomorrodi and Segrè, 2015). Using a multi-compartment approach, Klitgord and Segrè (2010) developed the Search for Exchanged Metabolites (SEM) algorithm to verify potential interactions between a pair of organisms by generating lists of metabolites able to be exchanged by a defined pair of species/guilds. This approach has huge potential for discovering and designing novel microbial interactions.

CHALLENGES OF MODELING MICROBIAL COMMUNITIES USING METABOLIC NETWORKS

Whether developed for individual species or microbial communities, SMN models have inherent and important challenges that must be considered, including: (i) valid metabolic networks are difficult to develop as details of many metabolic reactions and pathways are unknown, this is especially true for secondary metabolic pathways (Durot et al., 2009; Thiele and Palsson, 2010; Kim et al., 2012); (ii) model outputs (e.g., intracellular flux estimations) can be uncertain as model predictions do not necessarily reflect real fluxes, also models can provide multiple solutions to a single problem. Given these features, extensive model curation and calibration against experimental data is required (Varma and Palsson, 1995; Edwards et al., 2001; Kumar and Maranas, 2009; Perez-Garcia et al., 2014a); (iii) in principle SMN models and their analysis methods simulate cellular systems at steady state and do not consider the accumulation of metabolic compounds, which limits their application to study dynamic systems (Savinell and Palsson, 1992; Varma and Palsson, 1994a); (iv) generally SMN models and their analysis methods have to employ artificial assumptions that can bias the model outputs (i.e., selection of artificial objective functions for model solving) (Segrè et al., 2002; Schuetz et al., 2007; Feist and Palsson, 2010); and (v) in principle SMN models and their analysis methods disregard gene regulatory processes, gene expression profiles, and do not consider enzyme accumulation and kinetics (Pramanik and Keasling, 1997; Price et al., 2003). On top of these challenges, modeling of microbial interactions and communities adds significant layers of complexity which are described below.

The starting point for SMN models is the information on species genome and gene functions. However, it is important to keep in mind that genome annotations in databases may have errors, and that identifying genes that encode for catalytic

enzymes it is not always straight forward. Furthermore, any genome will contain a good portion of genes of unknown function, and large parts of the genome encode proteins involved in non-metabolic processes (Zengler and Palsson, 2012). Knowledge of the most important microbial guilds involved in the performance of a given mixed microbial culture is a prerequisite. Once the functional guild or species is identified, whole-genome sequences in conjunction with detailed physiological experiments enable SMN models to be generated. De novo genome annotation is a challenge by itself.

Also, determining the abundance of individual microbial species/guilds in the system of interest is essential to develop more realistic SMN models for microbial communities. This is because metabolic fluxes for each species can be scaled to the amount of species abundance, which makes it possible to evaluate the contribution of each species to the whole community performance (Khandelwal et al., 2013; Perez-Garcia et al., 2016). Biological abundance can be quantified directly with techniques like fluorescent *in situ* hybridization (FISH), quantitative polymerase chain reaction data (qPCR), reverse transcription qPCR (RT-qPCR) and flow cytometry (Wagner and Loy, 2002; Daims et al., 2006). Cultivation-independent approaches, such as metagenomics, metatranscriptomics, and metaproteomics, target the community as a whole and can also provide insights into species/guild abundance, but they have limited resolution at the species or strain level (Zengler and Palsson, 2012). An outstanding question is whether SMN models can be applied to the much larger number of interacting species present in most ecosystems, and whether large modular stoichiometric models are going to be useful and necessary.

SMN modeling efforts of microbial communities should also focus on identifying suitable objective functions. The solution space of a given model is not entirely a feature of network structure, but also a function of the chosen objective function (Z) and constraints ($\alpha_j \leq v_j \leq \beta_j$). SMN modeling uses optimization principles to estimate reaction rates of a given metabolic network. As mentioned before, generally maximization of biomass production per unit of substrate is the most suitable objective function for single-species metabolic networks (Segrè et al., 2002; Schuetz et al., 2007; Feist and Palsson, 2010). This seems to also hold true for multi-species metabolic networks (Klitgord and Segrè, 2010; Perez-Garcia et al., 2016). However, it is important to acknowledge that no single objective can be used to predict experimental data under all conditions of a given biological system. Thus, it is necessary to identify the most relevant objective for each condition. To do this, formal studies investigating the use of different objective functions to model a given microbial community under different environmental conditions are required. Under nutrient scarcity, cell metabolism normally supports efficient biomass formation with respect to the limiting nutrient. This operational state appears to have evolved under the objective to maximize either the ATP or biomass yield (synonymous to the frequently used maximization of growth rate objective). For cultures under conditions that allow unlimited growth, in contrast, energy production is clearly not optimized *per se* because cells secrete or accumulate large amounts of organic compounds, instead of using them for energy generation (Schuetz et al., 2007). Investigations of different objective functions on models' predictive capabilities will enhance the reliability and robustness of SMN models of microbial interactions.

An appropriate and rigorous model calibration is required to achieve a high level of confidence that the estimated rates of metabolic reactions are a valid representation of the metabolic activity of real cells. Surprisingly there is no many methods available to compare experimental versus predicted data. Although SMN model calibration involves: (a) an accurate definition of stoichiometric equations based strictly on proven biochemical data by which the chemical compounds and capabilities of mass transformations of the system are defined; (b) correct definition of objective function(s) and the solving method of the optimization problem; and (c) obtaining high fitness (e.g., high correlation) between experimental data and model predictions—the model must mimic at least the consumption and production rates of compounds observed in cultures. Most estimated rates of metabolic reactions cannot be measured experimentally and therefore cannot be validated directly. Nonetheless, data from microarray transcript profiles, transcriptomics, proteomics, metabolomics, and fluxomics [13C-based metabolic flux analysis (13C-MFA)] methods can be used to reduce uncertainty and increase the accuracy of the model's predictions (**Figure 3**).

Finally, it is important to recognize the different dynamics scales of biological system. At least four scales can be pointed: evolutionary, environmental, population and cell regulatory. For instance it is suggested that while community's organism lineages fluctuate extensively through time and conditions, the functional content of microbial communities displays stability and correlations with environmental parameters (Klitgord and Segrè, 2011). As asked by Klitgord and Segrè (2011): "Will the often large fluctuations in population dynamics dwarf the importance of regulatory dynamics within individual species? How can one model and understand the interplay between these two types of dynamic phenomena and their role in shaping microbial ecosystems?" Answering these important questions can significantly impact both, basic biological and evolutionary concepts as well as practical community culturing applications. None of our current computational tools can simultaneously capture the dynamics in all the mentioned scales. However, modeling approaches such as COMETS, HYDROGEOCHEM, OptCom, and MCM are pioneering tools to integrate different scale dynamics.

CONCLUSIONS

SMN modeling and systems biology can contribute to a comprehensive understanding of microorganisms, their interaction with other species in a community and their interplay with their environment. Understanding how interaction among cells enables the spread of information and leads to dynamic population behaviors is a fundamental problem in biology (Xavier, 2011). Meaningful insight into the interaction of microorganisms with other organisms and the environment has

often been hampered by the fact that microbial communities are extremely complex (Zengler and Palsson, 2012). Nowadays, realistic microbial community models are long way off, because our knowledge of microbial interactions is still incomplete. Even if all this knowledge were available, microbial community modeling faces daunting challenges as microbiomes are highly complex, nonlinear, evolving systems that can be chaotic and therefore unpredictable (Faust and Raes, 2012). SMN modeling approaches can help to address such complexity because most interactions between different microorganisms influence their metabolism. Identification of the most important microbial guilds involved in the analyzed environmental system is a prerequisite to characterizing it using an SMN model. Once the functional guild or species is identified, whole-genome sequences, in conjunction with detailed physiological experiments, enable SMN models to be generated for the identified organisms. Species-specific SMN models are then used to build up community models using one of the four modeling approaches. Modeling of microbial communities requires the description of molecular mechanisms that describe species interactions, such as competition, food chains, and inhibition (**Figure 1**). Nevertheless, it is important to recognize the SMN models do not capture strict ecological interaction (e.g., predation, parasitism) but rather metabolic interactions that can have ecological repercussions within the community (**Figure 1**).

The successful application of SMN modeling to characterize microbial interactions in natural and engineered environmental systems requires recognizing and modeling several abiotic factors influencing process performance (**Figure 2**). The chemical factors of the process include carbon source availability, nutrient availability, electron donor/acceptor availability, pH, and chemical stressors. The physical factors are those imposed by the micro/macrogeography of the organisms location and include, for example, humidity, conductivity, temperature, pressure, diffusion, and texture and density of the extracellular matrix (de Lorenzo, 2008). As this complexity increases, there is a need to develop a new set of fundamental principles, concepts and algorithms that will further reveal the secrets of microbial and cellular communities (Zengler and Palsson, 2012). SMN modeling of microbial communities and subsequent computer simulations are tools that can lead to a better understanding of the microbial cell and will undoubtedly contribute significantly to the field of environmental biotechnology. Microbial ecology and environmental biotechnology are inherently tied to each other. The concepts and tools of microbial ecology are the basis for managing processes in environmental biotechnology; and these processes provide interesting ecosystems to advance the concepts and tools of microbial ecology (Rittmann, 2006). Revolutionary advancements in molecular tools to understand the structure and function of microbial communities are strengthening the power of microbial ecology. A push from advances in modern materials along with a pull from a societal need to become more sustainable is enabling environmental biotechnology to create novel processes (Rittmann, 2006).

Systems biology tools such as SMN modeling have created the opportunity to develop the next generation of models of environmental process involving biological transformations. Nowadays, cheaper molecular biology and genomics, proteomics, and metabolomic techniques allow us to identify and quantify specific microbial species, full genome sequences, gene expression activity and metabolic compounds (Lovley, 2003). In addition, metabolomics can be applied to elucidate the biodegradation pathways of pollutants by identifying and quantifying dozens or even hundreds of compounds in a single sample (Villas-Bôas and Bruheim, 2007). Powerful computers are becoming cheaper, and new computation algorithms for data mining and model simulation are generated more readily (Lewis et al., 2012). The significant advantage of SMN models in this context is that they can incorporate the data generated with these new techniques and tools to produce a more accurate and realistic quantification of microbial processes. Therefore advanced metabolic models like these can serve as a bridge between molecular/biochemical research and environmental engineering practices, effectively functioning as a tool that can better link the work of microbiologists and engineers (Oehmen et al., 2010). SMN models are tools with potential to be used not only in research but also in applications such as biogeochemical cycle analysis and techno-economics, through linkages with hydrodynamic and geochemical models. The methods and applications detailed in this review and future developments in this area will help to decipher patterns of compounds and energy flow in environmental systems; these capabilities must be employed for the sustainable and integral development of human socio-economic activities within nature.

AUTHOR CONTRIBUTIONS

OP: Main literature revision and initial manuscript preparation. GL: Revision of sections focusing in microbial ecology and interactions and editorial improvement. NS: Revision of sections focusing in mathematical modeling and main paper editor.

ACKNOWLEDGMENTS

The valuable scientific and intellectual feedback from Professors Bart Smets and Benoit Guieysse substantially improved the quality of this article. We thank the Reviewer's for their valuable feedback which helped to significantly improve the overall quality of the document. OP was supported by doctoral scholarships from The University of Auckland and The Mexican National Council for Science and Technology (CONACyT). OP thanks Dr. Diana Spratt Casas for editorial improvement.

REFERENCES

Abubackar, H. N., Veiga, M. C., and Kennes, C. (2011). Biological conversion of carbon monoxide: rich syngas or waste gases to bioethanol. *Biofuel Bioprod. Biorefin.* 5, 93–114. doi: 10.1002/bbb.256

Agler, M. T., Wrenn, B. A., Zinder, S. H., and Angenent, L. T. (2011). Waste to bioproduct conversion with undefined mixed cultures: the carboxylate platform. *Trends Biotechnol.* 29, 70–78. doi: 10.1016/j.tibtech.2010.11.006

Alcántara, C., Muñoz, R., Norvill, Z., Plouviez, M., and Guieysse, B. (2015). Nitrous oxide emissions from high rate algal ponds treating domestic wastewater. *Bioresour. Technol.* 177, 110–117. doi: 10.1016/j.biortech.2014.10.134

Allison, S. D., and Martiny, J. B. H. (2008). Resistance, resilience, and redundancy in microbial communities. *Proc. Natl. Acad. Sci. U.S.A.* 105, 11512–11519. doi: 10.1073/pnas.0801925105

Arp, D. J., Sayavedra-Soto, L. A., and Hommes, N. G. (2002). Molecular biology and biochemistry of ammonia oxidation by *Nitrosomonas europaea*. *Arch. Microbiol.* 178, 250–255. doi: 10.1007/s00203-002-0452-0

Batstone, D. J., Pind, P. F., and Angelidaki, I. (2003). Kinetics of thermophilic, anaerobic oxidation of straight and branched chain butyrate and valerate. *Biotechnol. Bioeng.* 84, 195–204. doi: 10.1002/bit.10753

Begon, M., Townsend, C. R., and Harper, J. L. (2005). E*cology: From Individuals to Ecosystems*. Oxford: Blackwell Publishing Ltd.

Brenner, K., You, L., and Arnold, F. H. (2008). Engineering microbial consortia: a new frontier in synthetic biology. *Trends Biotechnol.* 26, 483–489. doi: 10.1016/j.tibtech.2008.05.004

Brown, C. E. (2010). *The Microbial Ecology of Acidovorax Temperansin Activated Sludge*. Ph.D. thesis, The University of Auckland.

Bugg, T. D. H., Ahmad, M., Hardiman, E. M., and Rahmanpour, R. (2011). Pathways for degradation of lignin in bacteria and fungi. *Nat. Prod. Rep.* 28, 1883–1896. doi: 10.1039/c1np00042j

Çakir, T., Patil K. R., Önsan, Z. I., Ülgen, K. Ö., Kirdar, B., and Nielsen, J. (2006). Integration of metabolome data with metabolic networks reveals reporter reactions. *Mol. Syst. Biol.* 2, 50. doi: 10.1038/msb4100085

Çalik, P., Sahin, M., Taspinar, H., Soyaslan, E. S., and Inankur, B. (2011). Dynamic flux balance analysis for pharmaceutical protein production by *Pichia pastoris*: Human growth hormone. *Enzyme Microb. Technol.* 48, 209–216. doi: 10.1016/j.enzmictec.2010.09.016

Chaganti, S. R., Kim, D.-H., and Lalman, J. A. (2011). Flux balance analysis of mixed anaerobic microbial communities: effects of linoleic acid (LA) and pH on biohydrogen production. *Int. J. Hydrogen Energy* 36, 14141–14152. doi: 10.1016/j.ijhydene.2011.04.161

Chain, P., Lamerdin, J., Larimer, F., Regala, W., Lao, V., Land, M., et al. (2003). Complete genome sequence of the ammonia-oxidizing bacterium and obligate chemolithoautotroph *Nitrosomonas europaea*. *J. Bacteriol.* 185, 2759–2773. doi: 10.1128/JB.185.9.2759-2773.2003

Chalot, M., and Brun, A. (1998). Physiology of organic nitrogen acquisition by ectomycorrhizal fungi and ectomycorrhizas. *FEMS Microbiol. Rev.* 22, 21–44. doi: 10.1111/j.1574-6976.1998.tb00359.x

Chandran, K., Stein, L. Y., Klotz, M. G., and Van Loosdrecht, M. C. M. (2011). Nitrous oxide production by lithotrophic ammonia-oxidizing bacteria and implications for engineered nitrogen-removal systems. *Biochem. Soc. Trans.* 39, 1832–1837. doi: 10.1042/BST20110717

Chang, R. L., Ghamsari, L., Manichaikul, A., Hom, E. F. Y., Balaji, S., Fu, W., et al. (2011). Metabolic network reconstruction of *Chlamydomon*as offers insight into light-driven algal metabolism. *Mol. Syst. Biol.* 7, 518. doi: 10.1038/msb.2011.52

Chapman, S. P., Paget, C. M., Johnson, G. N., and Schwartz, J. M. (2015). Flux balance analysis reveals acetate metabolism modulates cyclic electron flow and alternative glycolytic pathways in *Chlamydomonas reinhardtii*. *Front. Plant Sci.* 6:474. doi: 10.3389/fpls.2015.00474

Cheirsilp, B., and Torpee, S. (2012). Enhanced growth and lipid production of microalgae under mixotrophic culture condition: Effect of light intensity, glucose concentration and fed-batch cultivation. *Bioresour. Technol.* 110, 510–516. doi: 10.1016/j.biortech.2012.01.125

Chiu, H.-C, Levy, R., and Borenstein, E. (2014). Emergent biosynthetic capacity in simple microbial communities. *PLoS Comput. Biol.* 10:e1003695. doi: 10.1371/journal.pcbi.1003695

Choix, F. J., de-Bashan, L. E., and Bashan, Y. (2012a). Enhanced accumulation of starch and total carbohydrates in alginate-immobilized *Chlorella* spp. induced by *Azospirillum brasilense*: I. Autotrophic conditions. *Enzyme Microb. Technol.* 51, 294–299. doi: 10.1016/j.enzmictec.2012.07.013

Choix, F. J., de-Bashan, L. E., and Bashan, Y. (2012b). Enhanced accumulation of starch and total carbohydrates in alginate-immobilized *Chlorella* spp. induced by *Azospirillum brasilense*: II. Heterotrophic conditions. *Enzyme Microb. Technol.* 51, 300–309. doi: 10.1016/j.enzmictec.2012.07.012

Choix, F. J., Bashan, Y., Mendoza, A., and De-Bashan, L. E. (2014). Enhanced activity of ADP glucose pyrophosphorylase and formation of starch induced by *Azospirillum brasilense* in *Chlorella vulgaris*. *J. Biotechnol.* 177, 22–34. doi: 10.1016/j.jbiotec.2014.02.014

Daims, H., Taylor, M. W., and Wagner, M. (2006). Wastewater treatment: a model system for microbial ecology. *Trends Biotechnol.* 24, 483–489. doi: 10.1016/j.tibtech.2006.09.002

Das, P., Lei, W., Aziz, S. S., and Obbard, J. P. (2011). Enhanced algae growth in both phototrophic and mixotrophic culture under blue light. *Bioresour. Technol.* 102, 3883–3887. doi: 10.1016/j.biortech.2010.11.102

de-Bashan, L. E., Antoun, H., and Bashan, Y. (2005). Cultivation factors and population size control the uptake of nitrogen by the microalgae *Chlorella vulgaris* when interacting with the microalgae growth-promoting bacterium *Azospirillum brasilense*. *FEMS Microbiol. Ecol.* 54, 197–203. doi: 10.1016/j.femsec.2005.03.014

de-Bashan, L. E., and Bashan, Y. (2004). Recent advances in removing phosphorus from wastewater and its future use as fertilizer (1997-2003). *Water Res.* 38, 4222–4246. doi: 10.1016/j.watres.2004.07.014

de-Bashan, L. E., and Bashan, Y. (2010). Immobilized microalgae for removing pollutants: review of practical aspects. *Bioresour. Technol.* 101, 1611–1627. doi: 10.1016/j.biortech.2009.09.043

de-Bashan, L. E., Bashan, Y., Moreno, M., Lebsky, V. K., and Bustillos, J. J. (2002). Increased pigment and lipid content, lipid variety, and cell and population size of the microalgae *Chlorella* spp. when co-immobilized in alginate beads with the microalgae-growth-promoting bacterium *Azospirillum brasilense*. *Can. J. Microbiol.* 48, 514–521. doi: 10.1139/w02-051

de-Bashan, L. E., Schmid, M., Rothballer, M., Hartmann, A., and Bashan, Y. (2011). Cell-cell interaction in the eukaryote-prokaryote model of the microalgae *Chlorella vulgaris* and the bacterium *Azospirillum brasilense* immobilized in polymer beads. *J. Phycol.* 47, 1350–1359. doi: 10.1111/j.1529-8817.2011.01062.x

de Lorenzo, V. (2008). Systems biology approaches to bioremediation. *Curr. Opin. Biotechnol.* 19, 579–589. doi: 10.1016/j.copbio.2008.10.004

Dias, J. M. L., Oehmen, A., Serafim, L. S., Lemos, P. C., Reis, M. A. M., and Oliveira, R. (2008). Metabolic modelling of polyhydroxyalkanoate copolymers production by mixed microbial cultures. *BMC Syst. Biol.* 2:59. doi: 10.1186/1752-0509-2-59

Dias, J. M. L., Serafim, L. S., Lemos, P. C., Reis, M. A. M., and Oliveira, R. (2005). Mathematical modelling of a mixed culture cultivation process for the production of polyhydroxybutyrate. *Biotechnol. Bioeng.* 92, 209–222. doi: 10.1002/bit.20598

Díaz, E. (2004). Bacterial degradation of aromatic pollutants: a paradigm of metabolic versatility. *Int. Microbiol.* 7, 173–180.

Diels, L., De Smet, M., Hooyberghs, L., and Corbisier, P. (1999). Heavy metals bioremediation of soil. *Appl. Biochem. Biotechnol. Part B Mol. Biotechnol.* 12, 149–158.

Dittmann, E., Fewer, D. P., and Neilan, B. A. (2013). Cyanobacterial toxins: Biosynthetic routes and evolutionary roots. *FEMS Microbiol. Rev.* 37, 23–43. doi: 10.1111/j.1574-6976.2012.12000.x

Durot, M., Bourguignon, P. Y, and Schachter, V. (2009). Genome-scale models of bacterial metabolism: reconstruction and applications. *FEMS Microbiol. Rev.* 33, 164–190. doi: 10.1111/j.1574-6976.2008.00146.x

Edwards, J. S., Ibarra, R. U., and Palsson, B. O. (2001). *In silico* predictions of *Escherichia coli* metabolic capabilities are consistent with experimental data. *Nat. Biotechnol.* 19, 125–130. doi: 10.1038/84379

Edwards, S. J., and Kjellerup, B. V. (2013). Applications of biofilms in bioremediation and biotransformation of persistent organic pollutants,

pharmaceuticals/personal care products, and heavy metals. *Appl. Microbiol. Biotechnol.* 97, 9909–9921. doi: 10.1007/s00253-013-5216-z

Embree, M., Liu, J. K., Al-Bassam, M. M., and Zengler, K. (2015). Networks of energetic and metabolic interactions define dynamics in microbial communities. *Proc. Natl. Acad. Sci. U.S.A.* 112, 15450–15455. doi: 10.1073/pnas.1506034112

Endler, L., Rodriguez, N., Juty, N., Chelliah, V., Laibe, C., Li, C., et al. (2009). Designing and encoding models for synthetic biology. *J. R. Soc. Interface* 6, S405–S417. doi: 10.1098/rsif.2009.0035.focus

Faust, K., and Raes, J. (2012). Microbial interactions: from networks to models. *Nat. Rev. Microbiol.* 10, 538–550. doi: 10.1038/nrmicro2832

Feist, A. M., Herrgård, M. J., Thiele, I., Reed, J. L., and Palsson, B. ø. (2009). Reconstruction of biochemical networks in microorganisms. *Nat. Rev. Microbiol.* 7, 129–143. doi: 10.1038/nrmicro1949

Feist, A. M., and Palsson, B. O. (2010). The biomass objective function. *Curr. Opin. Microbiol.* 13, 344–349. doi: 10.1016/j.mib.2010.03.003

Feist, A. M., and Palsson, B. ø. (2008). The growing scope of applications of genome-scale metabolic reconstructions using *Escherichia coli*. *Nat. Biotechnol.* 26, 659–667. doi: 10.1038/nbt1401

Ferguson, S. J. (1998). "The *Paracoccus denitrificans* electron transport system: aspects of organisation, structures and biogenesis," in *Biological Electron Transport Chains: Genetics, Composition and Mode of Operation*, eds G. W. Canters and E. Vijgenboom (Dordrecht: Kluwer Academic Publisher), 77–88.

Ferguson, S. J., Richardson, D. J., and van Spanning, R. J. M. (2007). "Biochemistry and molecular biology of nitrification," in *Biology of the Nitrogen Cycle*, eds H. Bothe, S. J. Ferguson, and W. E. Newton (*Elsevier, Amsterdam),* 209–222.

Freitag, A., and Bock, E. (1990). Energy conservation in *Nitrobacter*. *FEMS Microbiol. Lett.* 66, 157–162. doi: 10.1111/j.1574-6968.1990.tb03989.x

Gadd, G. M. (2010). Metals, minerals and microbes: geomicrobiology and bioremediation. *Microbiology* 156, 609–643. doi: 10.1099/mic.0.037143-0

Gardes, M., and Bruns, T. D. (1996). Community structure of ectomycorrhizal fungi in a *Pinus muricata* forest: above- and below-ground views. *Can. J. Bot.* 74, 1572–1583. doi: 10.1139/b96-190

Girard, J.-M., Roy, M.-L., Hafsa, M. B., Gagnon, J., Faucheux, N., Heitz, M., et al. (2014). Mixotrophic. cultivation of green microalgae *Scenedesmus obliquus* on cheese whey permeate for biodiesel production. *Algal Res.* 5, 241–248. doi: 10.1016/j.algal.2014.03.002

Großkopf, T., and Soyer, O. S. (2014). Synthetic microbial communities. *Curr. Opin. Microbiol.* 18, 72–77. doi: 10.1016/j.mib.2014.02.002

Guazzaroni, M.-E., and Ferrer, M. (2011). "Metagenomic Approaches in Systems Biology," in *Handbook of Molecular Microbial Ecology I: Metagenomics and Complementary Approaches*, ed F. J. de Bruijn (New Jersy, NY: *John Wiley & Sons),* 473–489.

Guieysse, B., Plouviez, M., Coilhac, M., and Cazali, L. (2013). Nitrous Oxide (N_2O) production in axenic *Chlorella vulgaris* microalgae cultures: evidence, putative pathways, and potential environmental impacts. *Biogeosciences* 10, 6737–6746. doi: 10.5194/bg-10-6737-2013

Hao., T.-W., Xiang, P.-Y., Mackey, H. R., Chi, K., Lu, H., Chui, H.-K., et al. (2014). A review of biological sulfate conversions in wastewater treatment. *Water Res.* 65, 1–21. doi: 10.1016/j.watres.2014.06.043

Harcombe, W. R., Riehl, W. J., Dukovski, I., Granger, B. R., Betts, A., Lang, A. H., et al. (2014). Metabolic resource allocation in individual microbes determines ecosystem interactions and spatial dynamics. *Cell Rep.* 7, 1104–1115. doi: 10.1016/j.celrep.2014.03.070

Harms, H., Schlosser, D., and Wick, L. Y. (2011). Untapped potential: Exploiting fungi in bioremediation of hazardous chemicals. *Nat. Rev. Microbiol.* 9, 177–192. doi: 10.1038/nrmicro2519

Hartmann, A., and Bashan, Y. (2009). Ecology and application of *Azospirillum* and other plant growth-promoting bacteria (PGPB) - Special Issue. *Eur. J. Soil Biol.* 45, 1–2. doi: 10.1016/j.ejsobi.2008.11.004

Hatamoto, M., Imachi, H., Yashiro, Y., Ohashi, A., and Harada, H. (2007). Diversity of anaerobic microorganisms involved in long-chain fatty acid degradation in methanogenic sludges as revealed by RNA-based stable isotope probing. *Appl. Environ. Microbiol.* 73, 4119–4127. doi: 10.1128/AEM.00362-07

Head, I. M., Jones, D. M., and Röling, W. F. (2006). Marine microorganisms make a meal of oil. *Nat. Rev. Microbiol.* 4, 173–182. doi: 10.1038/nrmicro1348

Hernandez, J.-P., de-Bashan, L. E., Rodriguez, D. J., Rodriguez, Y., and Bashan, Y. (2009). Growth promotion of the freshwater microalga *Chlorella vulgaris* by the nitrogen-fixing, plant growth-promoting bacterium *Bacillus pumilus* from arid zone soils. *Eur. J. Soil Biol.* 45, 88–93. doi: 10.1016/j.ejsobi.2008.08.004

Hjersted, J., Henson, M. A., and Mahadevan, R. (2005). "Dynamic flux balance analysis of yeast primary metabolism in fed-batch culture," in *AIChE Annual Meeting, Conference Proceedings* (Cincinnati, OH), 9169–9170.

Hong, S.-J., and Lee, C. G. (2015). "Microalgal systems biology through genome-scale metabolic reconstructions for industrial applications," in *Handbook of Marine Microalgae: Biotechnology Advances*, ed S. K. Kim (Amsterdam: Academic Press), 353–370.

Hooper, A. B. (1991). Spectroscopic and rapid kinetic studies of reduction of cytochrome c554 by hydroxylamine oxidoreductase from *Nitrosomonas europaea*. *Biochemistry* 30, 11466–11472.

Hu, Z., Speth, D. R., Francoijs, K. J., Quan, Z. X, and Jetten, M. S. (2012). Metagenome analysis of a complex community reveals the metabolic blueprint of anammox bacterium "*Candidatus* Jettenia asiatica". *Front. Microbiol.* 3:366. doi: 10.3389/fmicb.2012.00366

Ishii, N., Robert, M., Nakayama, Y., Kanai, A., and Tomita, M. (2004). Toward large-scale modeling of the microbial cell for computer simulation. *J. Biotechnol.* 113, 281–294. doi: 10.1016/j.jbiotec.2004.04.038

Kaelin, D., Manser, R., Rieger, L., Eugster, J., Rottermann, K., and Siegrist, H. (2009). Extension of ASM3 for two-step nitrification and denitrification and its calibration and validation with batch tests and pilot scale data. *Water Res.* 43, 1680–1692. doi: 10.1016/j.watres.2008.12.039

Kaplan, A., Harel, M., Kaplan-Levy, R. N., Hadas, O., Sukenik, A., and Dittmann, E. (2012). The languages spoken in the water body (or the biological role of cyanobacterial toxins). *Front. Microbiol.* 3:138. doi: 10.3389/fmicb.2012.00138

Kappler, U., Bennett, B., Rethmeier, J., Schwarz, G., Deutzmann, R., McEwan, A. G., et al. (2000). Sulfite:cytochrome c oxidoreductase from *Thiobacillus novellus*. Purification, characterization, and molecular biology of a heterodimeric member of the sulfite oxidase family. *J. Biol. Chem.* 275, 13202–13212. doi: 10.1074/jbc.275.18.13202

Kell, D. B. (2006). Systems biology, metabolic modelling and metabolomics in drug discovery and development. *Drug Discov. Today* 11, 1085–1092. doi: 10.1016/j.drudis.2006.10.004

Keller, N. P., Turner, G., and Bennett, J. W. (2005). Fungal secondary metabolism - From biochemistry to genomics. *Nat. Rev. Microbiol.* 3, 937–947. doi: 10.1038/nrmicro1286

Khanal, S. K. (2009a). "Microbiology and biochemistry of anaerobic biotechnology," in *Anaerobic Biotechnology for Bioenergy Production: Principles and Applications*, ed S. K. Khanal (New Jersey, *NJ: John Wiley & Sons, Inc),* 29–41.

Khanal, S. K. (2009b). "Overview of anaerobic biotechnology," *in Anaerobic Biotechnology for Bioenergy Production: Principles and Applications, ed S. K. Khanal (*New Jersey, *NJ: John Wiley* & *Sons, Inc),* 1–27.

Khandelwal, R. A., Olivier, B. G., Röling, W. F. M., Teusink, B., and Bruggeman, F. J. (2013). Community flux balance analysis for microbial consortia at balanced growth. *PLoS ONE* 8:e64567. doi: 10.1371/journal.pone.0064567

Kim, T. Y., Sohn, S. B., Kim, Y. B., Kim, W. J., and Lee, S. Y. (2012). Recent advances in reconstruction and applications of genome-scale metabolic models. *Curr. Opin. Biotechnol.* 23, 617–623. doi: 10.1016/j.copbio.2011.10.007

Kitano, H. (2002). Computational systems biology. *Nature* 420, 206–210. doi: 10.1038/nature01254

Klamt, S., and Stelling, J. (2002). Combinatorial Complexity of Pathway Analysis in Metabolic Networks. *Mol. Biol. Rep.* 26, 233–236. doi: 10.1023/A:1020390132244

Kleerebezem, R., and van Loosdrecht, M. C. (2007). Mixed culture biotechnology for bioenergy production. *Curr. Opin. Biotechnol.* 18, 207–212. doi: 10.1016/j.copbio.2007.05.001

Klitgord, N., and Segrè, D. (2010). Environments that induce synthetic microbial ecosystems. *PLoS Comput. Biol.* 6:e1001002. doi: 10.1371/journal.pcbi.1001002

Klitgord, N., and Segrè, D. (2011). Ecosystems biology of microbial metabolism. *Curr. Opin. Biotechnol.* 22, 541–546. doi: 10.1016/j.copbio.2011.04.018

Knoop, H., Gründel, M., Zilliges, Y., Lehmann, R., Hoffmann, S., Lockau, W., et al. (2013). Flux balance analysis of cyanobacterial metabolism: the metabolic network of *Synechocystis* sp. PCC 6803. *PLoS Comput. Biol.* 9:e1003081. doi: 10.1371/journal.pcbi.1003081

Knoop, H., Zilliges, Y., Lockau, W., and Steuer, R. (2010). The metabolic network of *Synechocystis* sp. PCC 6803: systemic properties of autotrophic growth. *Plant Physiol.* 154, 410–422. doi: 10.1104/pp.110.157198

Kraft, B., Strous, M., and Tegetmeyer, H. E. (2011). Microbial nitrate respiration - Genes, enzymes and environmental distribution. *J. Biotechnol.* 155, 104–117. doi: 10.1016/j.jbiotec.2010.12.025

Kuenen, J. G. (2008). Anammox bacteria: From discovery to application. *Nat. Rev. Microbiol.* 6, 320–326. doi: 10.1038/nrmicro1857

Kumar, V. S., and Maranas, C. D. (2009). GrowMatch: an automated method for reconciling *in silico/in vivo* growth predictions. *PLoS Comput. Biol.* 5:e1000308. doi: 10.1371/journal.pcbi.1000308

Kümmel, A., Panke, S., and Heinemann, M. (2006). Putative regulatory sites unraveled by network-embedded thermodynamic analysis of metabolome data. *Mol. Syst. Biol.* 2, 2006.0034. doi: 10.1038/msb4100074

Kuypers, M. M. M., Silekers, A. O., Lavik, G., Schmid, M., Jøorgensen, B. B., Kuenen, J. G., et al. (2003). Anaerobic ammonium oxidation by anammox bacteria in the Black Sea. *Nature* 422, 608–611. doi: 10.1038/nature01472

Lah, L., Podobnik, B., Novak, M., Korošec, B., Berne, S., Vogelsang, M., et al. (2011). The versatility of the fungal cytochrome P450 monooxygenase system is instrumental in xenobiotic detoxification. *Mol. Microbiol.* 81, 1374–1389. doi: 10.1111/j.1365-2958.2011.07772.x

Lear, G., Mcbeth, J. M., Boothman, C., Gunning, D. J., Ellis, B. L., Lawson, R. S., et al. (2010). Probing the biogeochemical behavior of technetium using a novel nuclear imaging approach. *Environ. Sci. Technol.* 44, 156–162. doi: 10.1021/es802885r

Lear, G., Song, B., Gault, A. G., Polya, D. A., and Lloyd, J. R. (2007). Molecular analysis of arsenate-reducing bacteria within Cambodian sediments following amendment with acetate. *Appl. Environ. Microbiol.* 73, 1041–1048. doi: 10.1128/AEM.01654-06

Lerman, J. A., Hyduke, D. R., Latif, H., Portnoy, V. A., Lewis, N. E., Orth, J. D., et al. (2012). In silico method for modelling metabolism and gene product expression at genome scale. *Nat. Commun.* 3, 929. doi: 10.1038/ncomms1928

Lewis, N. E., Hixson, K. K., Conrad, T. M., Lerman, J. A., Charusanti, P., Polpitiya, A. D., et al. (2010). Omic data from evolved E. *coli are consistent with computed optimal growth from genome-scale models. Mol. Syst. Biol.* 6, 390. doi: 10.1038/msb.2010.47

Lewis, N. E., Nagarajan, H., and Palsson, B. O. (2012). Constraining the metabolic genotype-phenotype relationship using a phylogeny of *in silico* methods. *Nat. Rev. Microbiol.* 10, 291–305. doi: 10.1038/nrmicro2737

Li, C., and Fang, H. H. P. (2007). Fermentative hydrogen production from wastewater and solid wastes by mixed cultures. *Crit. Rev. Environ. Sci. Technol.* 37, 1–39. doi: 10.1080/10643380600729071

Louca, S., and Doebeli, M. (2015). Calibration and analysis of genome-based models for microbial ecology. *Elife* 4:e08208. doi: 10.7554/eLife.08208

Lovley, D. R. (2003). Cleaning up with genomics: applying molecular biology to bioremediation. *Nat. Rev. Microbiol.* 1, 35–44. doi: 10.1038/nrmicro731

Lovley, D. R., and Coates, J. D. (1997). Bioremediation of metal contamination. *Curr. Opin. Biotechnol.* 8, 285–289. doi: 10.1016/S0958-1669(97)80005-5

Lücker, S., Wagner, M., Maixner, F., Pelletier, E., Koch, H., Vacherie, B., et al. (2010). A *Nitrospira metagenome* illuminates the physiology and evolution of globally important nitrite-oxidizing bacteria. *Proc. Natl. Acad. Sci. U.S.A.* 107, 13479–13484. doi: 10.1073/pnas.1003860107

Maarleveld, T. R., Boele, J., Bruggeman, F. J., and Teusink, B. (2014). A data integration and visualization resource for the metabolic network of *Synechocystis* sp. PCC 6803. *Plant Physiol.* 164, 1111–1121. doi: 10.1104/pp.113.224394

Machado, D., and Herrgård, M. (2014). Systematic evaluation of methods for integration of transcriptomic data into constraint-based models of metabolism. *PLoS Comput. Biol.* 10:e1003580. doi: 10.1371/journal.pcbi.1003580

Mahadevan, R., Edwards, J. S., and Doyle, I. I. I. F. J. (2002). Dynamic flux balance analysis of diauxic growth in *Escherichia coli*. *Biophys. J.* 83, 1331–1340. doi: 10.1016/S0006-3495(02)73903-9

Makinia, J. (2010). *Mathematical Modelling and Computer Simulation of Activated Sludge Systems*. London: IWA publishing.

Malik, A. (2004). Metal bioremediation through growing cells. *Environ. Int.* 30, 261–278. doi: 10.1016/j.envint.2003.08.001

Margot, J., Bennati-Granier, C., Maillard, J., Blánquez, P., Barry, D. A., and Holliger, C. (2013). Bacterial versus fungal laccase: potential for micropollutant degradation. *AMB Express* 3, 1–30. doi: 10.1186/2191-0855-3-63

Markou, G., and Georgakakis, D. (2011). Cultivation of filamentous cyanobacteria (blue-green algae) in agro-industrial wastes and wastewaters: a review. *Appl. Energy* 88, 3389–3401. doi: 10.1016/j.apenergy.2010.12.042

Marshall, C. W., LaBelle, E. V., and May, H. D. (2013). Production of fuels and chemicals from waste by microbiomes. *Curr. Opin. Biotechnol.* 24, 391–397. doi: 10.1016/j.copbio.2013.03.016

Martín, H. G., Ivanova, N., Kunin, V., Warnecke, F., Barry, K. W., McHardy, A. C., et al. (2006). Metagenomic analysis of two enhanced biological phosphorus removal (EBPR) sludge communities. *Nat. Biotechnol.* 24, 1263–1269. doi: 10.1038/nbt1247

Medema, M. H., Van Raaphorst, R., Takano, E., and Breitling, R. (2012). Computational tools for the synthetic design of biochemical pathways. *Nat. Rev. Microbiol.* 10, 191–202. doi: 10.1038/nrmicro2717

Melton, E. D., Swanner, E. D., Behrens, S., Schmidt, C., and Kappler, A. (2014). The interplay of microbially mediated and abiotic reactions in the biogeochemical Fe cycle. *Nat. Rev. Microbiol.* 12, 797–808. doi: 10.1038/nrmicro3347

Meza, B., de-Bashan, L. E., and Bashan, Y. (2015a). Involvement of indole-3-acetic acid produced by *Azospirillum brasilense* in accumulating intracellular ammonium in *Chlorella vulgaris*. *Res. Microbiol.* 166, 72–83. doi: 10.1016/j.resmic.2014.12.010

Meza, B., de-Bashan, L. E., Hernandez, J. P., and Bashan, Y. (2015b). Accumulation of intra-cellular polyphosphate in *Chlorella vulgaris* cells is related to indole-3-acetic acid produced by *Azospirillum brasilense*. *Res. Microbiol.* 166, 399–407. doi: 10.1016/j.resmic.2015.03.001

Miller, L. D., Mosher, J. J., Venkateswaran, A., Yang, Z. K., Palumbo, A. V., Phelps, T. J., et al. (2010). Establishment and metabolic analysis of a model microbial community for understanding trophic and electron accepting interactions of subsurface anaerobic environments. *BMC Microbiol.* 10:149. doi: 10.1186/1471-2180-10-149

Milne, C. B., Kim, P. J., Eddy, J. A., and Price, N. D. (2009). Accomplishments in genome-scale *in silico* modeling for industrial and medical biotechnology. *Biotechnol. J.* 4, 1653–1670. doi: 10.1002/biot.200900234

Mitri, S., and Richard Foster, K. (2013). The genotypic view of social interactions in microbial communities. *Annu. Rev. Genet.* 47, 247–273. doi: 10.1146/annurev-genet-111212-133307

Nagarajan, H., Embree, M., Rotaru, A.-E, Shrestha, P. M., Feist, A. M., Palsson, B. ĂŸ., et al. (2013). Characterization and modelling of interspecies electron transfer mechanisms and microbial community dynamics of a syntrophic association. *Nat. Commun.* 4, 2809. doi: 10.1038/ncomms3809

Neilan, B. A., Pearson, L. A., Muenchhoff, J., Moffitt, M. C., and Dittmann, E. (2013). Environmental conditions that influence toxin biosynthesis in cyanobacteria. *Environ. Microbiol.* 15, 1239–1253. doi:10.1038/ncomms3809

Nikel, P. I., Martínez-García, E., and De Lorenzo, V. (2014). Biotechnological domestication of pseudomonads using synthetic biology. *Nat. Rev. Microbiol.* 12, 368–379. doi: 10.1038/nrmicro3253

Nogales, J., Gudmundsson, S., Knight, E. M., Palsson, B. O., and Thiele, I. (2012). Detailing the optimality of photosynthesis in cyanobacteria through systems biology analysis. *Proc. Natl. Acad. Sci. U.S.A.* 109, 2678–2683. doi: 10.1073/pnas.1117907109

Oberhardt, M. A., Chavali, A. K., and Papin, J. A. (2009). Flux balance analysis: interrogating genome-scale metabolic networks. *Methods Mol. Biol.* 500, 61–80. doi: 10.1007/978-1-59745-525-1_3

O'Brien, E. J., Monk, J. M., and Palsson, B. O. (2015). Using genome-scale models to predict biological capabilities. *Cell* 161, 971–987. doi: 10.1016/j.cell.2015.05.019

OECD (2009). *The Bioeconomy to 2030. Designing a Policy Agenda*. *Paris: OECD Publishing.*

OECD (2011). *Future Prospects for Industrial Biotechnology. Paris: OECD Publishing.*

Oehmen, A., Carvalho, G., Lopez-Vazquez, C. M., van Loosdrecht, M. C. M., and Reis, M. A. M. (2010). Incorporating microbial ecology into the metabolic modelling of polyphosphate accumulating organisms and glycogen accumulating organisms. *Water Res.* 44, 4992–5004. doi: 10.1016/j.watres.2010.06.071

Orth, J. D., Thiele, I., and Palsson, B. O. (2010). What is flux balance analysis? *Nat. Biotechnol.* 28, 245–248. doi: 10.1038/nbt.1614

Palsson, B. (2009). Metabolic systems biology. *FEBS Lett.* 583, 3900–3904. doi: 10.1016/j.febslet.2009.09.031

Pardelha, F., Albuquerque, M. G. E., Carvalho, G., Reis, M. A. M., Dias, J. M. L., and Oliveira, R. (2013). Segregated flux balance analysis constrained by population structure/function data: the case of PHA production by mixed microbial cultures. *Biotechnol. Bioeng.* 110, 2267–2276. doi: 10.1002/bit.24894

Pardelha, F., Albuquerque, M. G. E., Reis, M. A. M., Dias, J. M. L., and Oliveira, R. (2012). Flux balance analysis of mixed microbial cultures: Application to the production of polyhydroxyalkanoates from complex mixtures of volatile fatty acids. *J. Biotechnol.* 162, 336–345. doi: 10.1016/j.jbiotec.2012.08.017

Park, J. H., Lee, S. Y., Kim, T. Y., and Kim, H. U. (2008). Application of systems biology for bioprocess development. *Trends Biotechnol.* 26, 404–412. doi: 10.1016/j.tibtech.2008.05.001

Patnaik, P. R. (2005). Perspectives in the modeling and optimization of PHB production by pure and mixed cultures. *Crit. Rev. Biotechnol.* 25, 153–171. doi: 10.1080/07388550500301438

Pereira, I. A. C., Ramos, A. R., Grein, F., Marques, M. C., da Silva, S. M., and Venceslau, S. S. (2011). A comparative genomic analysis of energy metabolism in sulfate reducing bacteria and archaea. *Front. Microbiol.* 2:69. doi: 10.3389/fmicb.2011.00069

Perez-Garcia, O., de-Bashan, L. E., Hernandez, J., and Bashan, Y. (2010). Efficiency of growth and nutrient uptake from wastewater by heterotrophic, autotrophic, and mixotrophic cultivation of *Chlorella vulgaris* immobilized with *Azospirillum brasilense*. *J. Phycol.* 46, 800–812. doi: 10.1111/j.1529-8817.2010.00862.x

Perez-Garcia, O., and Bashan, Y. (2015). "Microalgal heterotrophic and mixotrophic culturing for bio-refining: From metabolic routes to techno-economics," in *Algal Biorefineries, Vol. 2, Products and Refinery Design*, eds A. Prokop, R. K. Bajpai, M. E. Zappi (Switzerland: Springer International Publishing), 61–131.

Perez-Garcia, O., Chandran, K., Villas-Boas, S. G., and Singhal, N. (2016). Assessment of nitric oxide (NO) redox reactions contribution to nitrous oxide (N2O) formation during nitrification using a multispecies metabolic network model. *Biotechnol. Bioeng.* 113, 1124–1136. doi: 10.1002/bit.25880

Perez-Garcia, O., Escalante, F. M. E., de-Bashan, L. E., and Bashan, Y. (2011). Heterotrophic cultures of microalgae: metabolism and potential products. *Water Res.* 45, 11–36. doi: 10.1016/j.watres.2010.08.037

Perez-Garcia, O., Villas-Boas, S. G., and Singhal, N. (2014a). A method to calibrate metabolic network models with experimental datasets. *Adv. Intell. Syst. Comput.* 294, 183–190. doi: 10.1007/978-3-319-07581-5_22

Perez-Garcia, O., Villas-Boas, S. G., Swift, S., Chandran, K., and Singhal, N. (2014b). Clarifying the regulation of NO/N2O production in *Nitrosomonas europaea* during anoxic–oxic transition via flux balance analysis of a metabolic network model. *Water Res.* 60, 267–277. doi: 10.1016/j.watres.2014.04.049

Pérez-Pantoja, D., De La Iglesia, R., Pieper, D. H., and González, B. (2008). Metabolic reconstruction of aromatic compounds degradation from the genome of the amazing pollutant-degrading bacterium Cupriavidus necator JMP134. *FEMS Microbiol. Rev.* 32, 736–794. doi: 10.1111/j.1574-6976.2008.00122.x

Pokorna, D., and Zabranska, J. (2015). Sulfur-oxidizing bacteria in environmental technology. *Biotechnol. Adv.* 33, 1246–1259. doi: 10.1016/j.biotechadv.2015.02.007

Poughon, L., Dussap, C.-G., and Gros, J.-B. (2001). Energy model and metabolic flux analysis for autotrophic nitrifiers. *Biotechnol. Bioeng.* 72, 416–433. doi: 10.1002/1097-0290(20000220)72:4<416::AID-BIT1004>3.0.CO;2-D

Pramanik, J., and Keasling, J. D. (1997). Stoichiometric model of *Escherichia coli* metabolism: incorporation of growth-rate dependent biomass composition and mechanistic energy requirements. *Biotechnol. Bioeng.* 56, 398–421.

Pramanik, J., Trelstad, P. L., Schuler, A. J., Jenkins, D., and Keasling, J. D. (1999). Development and validation of a flux-based stoichiometric model for enhanced biological phosphorus removal metabolism. *Water Res.* 33, 462–476.

Price, N. D., Papin, J. A., Schilling, C. H., and Palsson, B. O. (2003). Genome-scale microbial *in silico* models: the constraints-based approach. *Trends Biotechnol.* 21, 162–169. doi: 10.1016/S0167-7799(03)00030-1

Reid, A., and Greene, S. E. (2012). *How Microbes Can Help Feed the World.* A report from the American Academy of Microbiology, Washington, DC: American Academy of Microbiology.

Reznik, E., Mehta, P., and Segrè D. (2013). Flux imbalance analysis and the sensitivity of cellular growth to changes in metabolite pools. *PLoS Comput. Biol.* 9:e1003195. doi: 10.1371/journal.pcbi.1003195

Rittmann, B. E. (2006). Microbial ecology to manage processes in environmental biotechnology. *Trends Biotechnol.* 24, 261–266. doi: 10.1016/j.tibtech.2006.04.003

Rittmann, B. E., Krajmalnik-Brown, R., and Halden, R. U. (2008). Pre-genomic, genomic and post-genomic study of microbial communities involved in bioenergy. *Nat. Rev. Microbiol.* 6, 604–612. doi: 10.1038/nrmicro1939

Rocha, I., Maia, P., Evangelista, P., Vilaça, P., Soares, S., Pinto, J. P., et al. (2010). OptFlux: an open-source software platform for *in silico* metabolic engineering. *BMC Syst. Biol.* 4:45. doi: 10.1186/1752-0509-4-45

Rodríguez, J., Kleerebezem, R., Lema, J. M., and Van Loosdrecht, M. C. M. (2006). Modeling product formation in anaerobic mixed culture fermentations. *Biotechnol. Bioeng.* 93, 592–606. doi: 10.1002/bit.20765

Savinell, J. M., and Palsson, B. O. (1992). Optimal selection of metabolic fluxes for *in vivo* measurement. I. Development of mathematical methods. *J. Theor. Biol.* 155, 201–214. doi: 10.1016/S0022-5193(05)80595-8

Scheibe, T. D., Mahadevan, R., Fang, Y., Garg, S., Long, P. E., and Lovley, D. R. (2009). Coupling a genome-scale metabolic model with a reactive transport model to describe *in situ* uranium bioremediation. *Microb. Biotechnol.* 2, 274–286. doi: 10.1111/j.1751-7915.2009.00087.x

Schellenberger, J., and Palsson, B. ø. (2009). Use of randomized sampling for analysis of metabolic networks. *J. Biol. Chem.* 284, 5457–5461. doi: 10.1074/jbc.R800048200

Schreiber, F., Wunderlin, P., Udert, K. M., and Wells, G. F. (2012). Nitric oxide and nitrous oxide turnover in natural and engineered microbial communities: biological pathways, chemical reactions, and novel technologies. *Front. Microbiol.* 3:372. doi: 10.3389/fmicb.2012.00372

Schuetz, R., Kuepfer, L., and Sauer, U. (2007). Systematic evaluation of objective functions for predicting intracellular fluxes in Escherichia coli. *Mol. Syst. Biol.* 3, 119. doi: 10.1038/msb4100162

Segrè D., Vitkup, D., and Church, G. M. (2002). Analysis of optimality in natural and perturbed metabolic networks. *Proc. Natl. Acad. Sci. U.S.A.* 99, 15112–15117. doi: 10.1073/pnas.232349399

Seviour, R. J., Mino, T., and Onuki, M. (2003). The microbiology of biological phosphorus removal in activated sludge systems. *FEMS Microbiol. Rev.* 27, 99–127. doi: 10.1016/S0168-6445(03)00021-4

Shaw, L. J., Nicol, G. W., Smith, Z., Fear, J., Prosser, J. I., and Baggs, E. M. (2006). *Nitrosospira* spp. can produce nitrous oxide via a nitrifier denitrification pathway. *Environ. Microbiol.* 8, 214–222. doi: 10.1111/j.1462-2920.2005.00882.x

Singh, B. K. (2009). Organophosphorus-degrading bacteria: Ecology and industrial applications. *Nat. Rev. Microbiol.* 7, 156–164. doi: 10.1038/nrmicro2050

Stolyar, S., Van Dien, S., Hillesland, K. L., Pinel, N., Lie, T. J., Leigh, J. A., et al. (2007). Metabolic modeling of a mutualistic microbial community. *Mol. Syst. Biol.* 3, 92. doi: 10.1038/msb4100131

Subashchandrabose, S. R., Ramakrishnan, B., Megharaj, M., Venkateswarlu, K., and Naidu, R. (2013). Mixotrophic cyanobacteria and microalgae as distinctive biological agents for organic pollutant degradation. *Environ. Int.* 51, 59–72. doi: 10.1016/j.envint.2012.10.007

Taffs, R., Aston, J. E., Brileya, K., Jay, Z., Klatt, C. G., McGlynn, S., et al. (2009). In Silico approaches to study mass and energy flows in microbial consortia: a syntrophic case study. *BMC Syst. Biol.* 3:114. doi: 10.1186/1752-0509-3-114

Teague, B. P., and Weiss, R. (2015). Synthetic communities, the sum of parts: complex behaviors are engineered from cooperating cell communities. *Science* 349, 924–925. doi: 10.1126/science.aad0876

Thiele, I. (2009). *A Stoichiometric Model of Escherichia coli's Macromolecular Synthesis Machinery and Its Integration with Metabolism*. Electronic Theses and Dissertations, San Diego, CA: University of California.

Thiele, I., and Palsson, B. ø. (2010). A protocol for generating a high-quality genome-scale metabolic reconstruction. *Nat. Prot.* 5, 93–121. doi: 10.1038/nprot.2009.203

Tzamali, E., Poirazi, P., Tollis, I. G., and Reczko, M. (2011). A computational exploration of bacterial metabolic diversity identifying metabolic interactions and growth-efficient strain communities. *BMC Syst. Biol.* 5:167. doi: 10.1186/1752-0509-5-167

Vallero, D. A. (2010). *Environmental Biotechnology: A Biosystems Approach. San Diego,* CA: Academic Press.

van Loosdrecht, M. C. M., Ekama, G. A., Wentzel, M. C., Brdjanovic, D., and Hooijmans, C. M. (2008). "Modelling activated sludge processes," in *Biological Wastewater Treatment. Principles, Modelling and Design*, eds M. Henze, M. C. M. van Loosdrecht, G. A. Ekama, M. C. Wentzel, D. Brdjanovic (ondon: IWA Publishing), 361.

Vanwonterghem, I., Jensen, P. D., Ho, D. P., Batstone, D. J., and Tyson, G. W. (2014). Linking microbial community structure, interactions and function in anaerobic digesters using new molecular techniques. *Curr. Opin. Biotechnol.* 27, 55–64. doi: 10.1016/j.copbio.2013.11.004

Varma, A., and Palsson, B. O. (1994a). Metabolic flux balancing: Basic concepts, scientific and practical use. *Nat. Biotech.* 12, 994–998. doi: 10.1038/nbt1094-994

Varma, A., and Palsson, B. O. (1994b). Stoichiometric flux balance models quantitatively predict growth and metabolic by-product secretion in wild-type *Escherichia coli* W3110. *Appl. Environ. Microbiol.* 60, 3724–3731.

Varma, A., and Palsson, B. O. (1995). Parametric sensitivity of stoichiometric flux balance models applied to wild-type Escherichia coli metabolism. *Biotechnol. Bioeng.* 45, 69–79. doi: 10.1002/bit.260450110

Vilchez-Vargas, R., Junca, H., and Pieper, D. H. (2010). Metabolic networks, microbial ecology and 'omics' technologies: towards understanding *in situ* biodegradation processes. *Environ. Microbiol.* 12:3089–3104. doi: 10.1111/j.1462-2920.2010.02340.x

Villas-Bôas, S. G., and Bruheim, P. (2007). The potential of metabolomics tools in bioremediation studies. *OMICS J. Integr. Biol.* 11, 305–313. doi: 10.1089/omi.2007.0005

Vu, T. T., Stolyar, S. M., Pinchuk, G. E., Hill, E. A., Kucek, L. A., Brown, R. N., et al. (2012). Genome-scale modeling of light-driven reductant partitioning and carbon fluxes in diazotrophic unicellular cyanobacterium *Cyanothece* sp. ATCC 51142. *PLoS Comput. Biol.* 8:e1002460. doi: 10.1371/journal.pcbi.1002460

Wagner, M., and Loy, A. (2002). Bacterial community composition and function in sewage treatment systems. *Curr. Opin. Biotechnol.* 13, 218–227. doi: 10.1016/S0958-1669(02)00315-4

Wagner, M., Loy, A., Nogueira, R., Purkhold, U., Lee, N., and Daims, H. (2002). Microbial community composition and function in wastewater treatment plants. *Antonie Van Leeuwenhoek* 81, 665–680. doi: 10.1023/A:1020586312170

Wang, Y.-T., and Shen, H. (1995). Bacterial reduction of hexavalent chromium. *J. Ind. Microbiol.* 14, 159–163. doi: 10.1007/BF01569898

Welker, M., and Von Döhren, H. (2006). Cyanobacterial peptides - Nature's own combinatorial biosynthesis. *FEMS Microbiol. Rev.* 30, 530–563. doi: 10.1111/j.1574-6976.2006.00022.x

Werner, J. J., Knights, D., Garcia, M. L., Scalfone, N. B., Smith, S., Yarasheski, K., et al. (2011). Bacterial community structures are unique and resilient in full-scale bioenergy systems. *Proc. Natl. Acad. Sci. U.S.A.* 108, 4158–4163. doi: 10.1073/pnas.1015676108

Wilmes, P., Andersson, A. F., Lefsrud, M. G., Wexler, M., Shah, M., Zhang, B., et al. (2008). Community proteogenomics highlights microbial strain-variant protein expression within activated sludge performing enhanced biological phosphorus removal. *ISME J.* 2, 853–864. doi: 10.1038/ismej.2008.38

Wu, X., Ge., T., Wang, W., Yuan, H., Wegner, C. E., Zhu, Z., et al. (2015). Cropping systems modulate the rate and masystems modulate the rate and magnitugnitude of soil microbial autotrophic CO2 fixation in soil. *Front. Microbiol.* 6:379. doi: 10.3389/fmicb.2015.00379

Xavier, J. B. (2011). Social interaction in synthetic and natural microbial communities. *Mol. Syst. Biol.* 7, 483. doi: 10.1038/msb.2011.16

Yadav, G., Gokhale, R. S., and Mohanty, D. (2009). Towards prediction of metabolic products of polyketide synthases: an *in silico* analysis. *PLoS Comput. Biol.* 5:e1000351. doi: 10.1371/journal.pcbi.1000351

Yu, R., Kampschreur, M. J., Van Loosdrecht, M. C. M., and Chandran, K. (2010). Mechanisms and specific directionality of autotrophic nitrous oxide and nitric oxide generation during transient anoxia. *Environ. Sci. Technol.* 44, 1313–1319. doi: 10.1021/es902794a

Zengler, K., and Palsson, B. O. (2012). A road map for the development of community systems (CoSy) biology. *Nat. Rev. Microbiol.* 10, 366–372. doi: 10.1038/nrmicro2763

Zhuang, K., Izallalen, M., Mouser, P., Richter, H., Risso, C., Mahadevan, R., et al. (2011). Genome-scale dynamic modeling of the competition between *Rhodoferax* and *Geobacter* in anoxic subsurface environments. *ISME J.* 5, 305–316. doi: 10.1038/ismej.2010.117

Zomorrodi, A. R., Islam, M. M., and Maranas, C. D. (2014). D-OptCom: dynamic multi-level and multi-objective metabolic modeling of microbial communities. *ACS Synt. Biol.* 3, 247–257. doi: 10.1021/sb4001307

Zomorrodi, A. R., and Maranas, C. D. (2012). OptCom: a multi-level optimization framework for the metabolic modeling and analysis of microbial communities. *PLoS Comput. Biol.* 8:e1002363. doi: 10.1371/journal.pcbi.1002363

Zomorrodi, A. R., and Segrè, D. (2015). Synthetic ecology of microbes: mathematical models and applications. *J. Mol. Biol.* 428, 837–861. doi: 10.1016/j.jmb.2015.10.019

Conflict of Interest Statement: The authors declare that the research was conducted in the absence of any commercial or financial relationships that could be construed as a potential conflict of interest.

Advantages of publishing in Frontiers

OPEN ACCESS
Articles are free to read for greatest visibility and readership

FAST PUBLICATION
Around 90 days from submission to decision

HIGH QUALITY PEER-REVIEW
Rigorous, collaborative, and constructive peer-review

TRANSPARENT PEER-REVIEW
Editors and reviewers acknowledged by name on published articles

Frontiers
Avenue du Tribunal-Fédéral 34
1005 Lausanne | Switzerland

Visit us: www.frontiersin.org
Contact us: info@frontiersin.org | +41 21 510 17 00

REPRODUCIBILITY OF RESEARCH
Support open data and methods to enhance research reproducibility

DIGITAL PUBLISHING
Articles designed for optimal readership across devices

FOLLOW US
@frontiersin

IMPACT METRICS
Advanced article metrics track visibility across digital media

EXTENSIVE PROMOTION
Marketing and promotion of impactful research

LOOP RESEARCH NETWORK
Our network increases your article's readership